Development of a 3D Perfusion System to Monitor Response of Osteoblast-like Cells Incubated on Synthetic Bone Graft Substitute Granules with Varied Hierarchical Porosities under Dynamic Conditions

Navinderpal Kaur Chana

MSc. BEng (Hons)

Submitted in partial fulfilment of the requirements of the Degree of

Doctor of Philosophy

September 2015

Supervision

Dr. Karin A. Hing

Dr. Simon C. F. Rawlinson

School of Engineering and Material Science

Queen Mary University of London

Statement of Originality

I, Navinderpal Kaur Chana, confirm that the research included within this thesis is my own work or that where it has been carried out in collaboration with, or supported by others, that this is duly acknowledged below and my contribution indicated. Previously published material is also acknowledged below.

I attest that I have exercised reasonable care to ensure that the work is original, and does not to the best of my knowledge break any UK law, infringe any third party's copyright or other Intellectual Property Right, or contain any confidential material.

I accept that the College has the right to use plagiarism detection software to check the electronic version of the thesis.

I confirm that this thesis has not been previously submitted for the award of a degree by this or any other university.

The copyright of this thesis rests with the author and no quotation from it or information derived from it may be published without the prior written consent of the author.

Signature: 

Date: Monday 28th September 2015

Abstract

The development of multi-level porous scaffolds with an optimised chemistry of 0.8wt% silicon substituted hydroxyapatite (SA) is an example of the successful contribution of material science to the medical world. The key to the development of next generation synthetic bone graft substitutes (BGS) may be through understanding of the mechanisms behind the structure of a BGS modulating cell response perhaps through alteration of the local environment within the graft material. The aim of this thesis was to develop an *in vitro* system with which to characterise ionic exchange and monitor cell response to real granular synthetic bone graft substitute materials within a truly 3D environment. The purpose of the system being to more closely mimic the 3D environment *in vivo* to enable a more systematic investigation of how scaffold structure can impact on the local physiological environment and subsequent cell behaviour.

Initially, experiments were performed with small volumes of porous scaffold granules (identical in form to those used clinically) exposed to a range of volumes of continuously recirculating cell culture media, without serum protein supplementation. The results obtained demonstrated that the capacity of hydroxyapatite (HA) based porous granules to rapidly deplete calcium and phosphate ions from the local aqueous environment necessitated the use of a fully perfused flow to waste system. Subsequent experiments were performed to uniformly introduce osteoblast-like cells to the granules and to monitor the behaviour of the cells *in situ* on the porous granules within the perfused 3D environment for periods of up to 7 days. The work conducted in this thesis has successfully identified that porous apatite BGS granules interact significantly with the local aqueous environment. A 3D perfusion system has been developed that enables clinically relevant BGS to be seeded with osteoblast-like cells that can then be monitored as they colonise and respond to the various BGS types. With the use of osteoblast-like cells this system corroborates *in vivo* findings within orthotopic defect sites, with respect to a clear response to BGS granule chemistry, but mixed sensitivity to BGS structure.

Acknowledgements

I would like to start by thanking the Almighty Waheguru Ji for providing me with strength and courage to complete this PhD.

I would like to sincerely thank my supervisors and mentors, Dr Karin A. Hing and Dr Simon C.F. Rawlinson for their constant support, persistence and guidance during the development of this research. Their invaluable knowledge and expertise has made the experience even more fruitful and I will forever appreciate the opportunities they have provided me with throughout these four years. Thank you Dr Krystelle Mafina who provided me with most of my training for the characterisation of the materials. She started off as my 'to go to' person for the duration of my postgraduate MSc project and since then has become more of a friend who has seen me through all the happy and emotional times during this PhD. Thank you to Chris Mole and Shafir Iqbal for provided me with comprehensive technical support throughout the four years. Thank you to Rory Wilson for all the XRD data analysis, Dr Zofia Luklinska for training me on the SEM before she left and Russell Bailey who continued to provide technical support during my numerous SEM sessions. Thank you to Filipe Almeida, Viviana Castagna and Alan Parish my PhD colleagues, who put up with me and made every day of my PhD enjoyable. I would also like to thank Anu Solanki and Moh Raja for their constant support, our 9 years of friendship has truly been amazing.

I would like to thank my family. Thank you Daddy Ji, Mummy Ji, Vudi Bhan, Choti Bhan, JJ and AJ for having confidence in me to finish this PhD and always providing me with unconditional love and invaluable support to see this PhD through to the end. Guki, Simi, Rusty, Navi, Gursimi and Jassi my little angels! Without you all life as 'Nini Masi' would not be the same. Thank you to my in laws, the Notay family, for giving me the opportunity to finish my write up after marriage.

Finally, thank you to my best friend and soul partner Rai Bahadur Raman Singh Notay. During this PhD we have gone from being engaged to being married and your support has only increased every day. You have been my rock throughout this journey and without your support I feel I would not have reached my goal. I love you very much and I am very lucky to now call you my husband and spend the rest of my life with you.

This work was funded by the Engineering and Physical Science Research Council. Thank you ApaTech (Baxter Inc.) for supplying samples and Lucideon for ICP and XRF analysis.

Contents

List of Figures

List of Tables

Chapter 1 Literature Review

1.1 Introduction

There was an estimated 1,109,000 clinical procedure in 2010 which were performed in the USA whereby bone grafting techniques were implemented and this figure is projected to reach 1,295,260 in 2015 (BioMedGPS 2012). This increase in demand for bone graft substitutes has led to an increase in clinical interest in synthetic alternatives, such as calcium phosphate ceramics, to allograft and autografts. The efficiency of calcium phosphates has been widely investigated however there still needs to be a better understanding of the mechanisms behind their healing action. There have been many characteristics that have been explored within calcium phosphates *in vitro* in order to understand and explain the amount and level of bone growth within treated defective sites. These characteristics include phase purity, surface area, total porosity, pore size and pore interconnectivity (Hing, Gibson et al. 1998, Hing, Merry et al. 1999, Hing, Annaz et al. 2005, Hing, Revell et al. 2006, Hing, Wilson et al. 2007).

Bone, a naturally occurring material, refers to a family of materials which are all made up of fibrous protein collagen, impregnated with a mineral closely resembling a synthetic calcium phosphate, hydroxyapatite (Currey 2002). Bone has evolved to satisfy a variety of mechanical functions, for which the structures are fine-tuned which in itself is a challenge. The make-up of bone is dependent on its location and function in the body (Weiner and Wagner 1998). This is in turn means its composition varies immensely across the skeletal system. There is also a difference in the structure of bone between individuals as genetics, age, diet and health are important factors. As well as acting as a framework for the attachment of muscles, bone also protects vital organs such as the heart, lungs and brain from external impacts (Boyne 1970).

Bone has the ability to constantly remodel itself and heal very small fractures without any scar tissue being formed. However in some cases where there has been a great deal of bone lost due to traumatic events or disease, there is an increasing demand for materials which can be used to replace the lost bone substance in the human body. There have been attempts made to develop synthetic hydroxyapatite (HA) bone substitute materials which provide a porous mineral scaffold through which the surrounding bone can vascularise, then infiltrate

and finally regain mechanical integrity of the lost bone (Gauthier, Bouler et al. 1998, Yuan, Yang et al. 2001, Hing 2004). Having a porous material will also allow the new mineral bone to form within the implant and ultimately replace the substitute material with new bone by the process of chemical resorption or cellular remodelling. Remodelling is a process which bone undergoes in response to mechanical loading according to Wolff's law. However the underlying mechanism by which bone cells respond to the change in environment, which can be the strain in the load-bearing matrix or fluid flow through the porous network, has not been fully understood or resolved. These materials are generally used to treat patients whom have suffered bone diseases, bone fracture and other bone defects (Hing 2004). The progression in this field has helped many patients improve their quality therefore it has been found that the life expectancy has risen to be twice as high as it had been at the beginning of the 20^{th} century (Hench 1998).

This research thesis aims to investigate the influence of ionic exchange in the physiological environment on cell development using a 3D perfusion system. Cellular response is believed to be sensitive to ionic exchange between the bone graft substitute (BGS) and the surrounding medium. However, to date these effects have not been studied extensively using a dynamic perfusion system in order to more closely try and mimic the *in vivo* environment and understand whether a change in graft chemistry has an impact on cellular response under more physiologically relevant dynamic perfusion conditions.

This chapter of the thesis will endeavour to give a critical overview of bone biology, BGS used in bone repair, ionic exchange between BGS and surrounding medium and finally current perfusion systems being used for bone repair.

1.2 Bone Structure

Bone is an exceptionally dynamic material. It has the ability to cope with extreme environments which are forced upon it throughout its lifetime. It is a highly organised and specialised connective tissue which undergoes continuous remodelling in response to structural stresses or the bodies need for calcium. From day to day, bone adapts itself with regards to structure, composition and its interactions with the surroundings in order to manage the physical and chemical demands that are placed upon it.

The five main functions of bone are; facilitate locomotion, support and protect the body’s vital organs, produce blood cells and mineral homeostasis. The tissues that are found within bone are osseous tissue, marrow, periosteum, nerves, blood vessels and cartilage (Currey

2002). The typical structure of bone is usually analysed macroscopically as shown in Figure 1.1, using the partially sectioned humerus (arm bone) and femur (thigh bone). The structure consists of the following parts;

- ***Diaphysis*** - bone's shaft also known as the body
- ***Epiphysis*** - ends of the bone known as proximal and distal parts of the humerus
- ***Metaphysis*** - connection area between the diaphysis and epiphysis
- ***Articular cartilage*** - thin layer covering the epiphysis
- ***Periosteum*** - thin layer covering the outer surface of the bone
- ***Medullary cavity*** - space within the daiphysis
- ***Endosteum*** - thin membrane lining the marrow cavity.

The outer surface of bone is covered with a layer of periosteum which is made up of dense connective tissue containing collagenous fibres and many cells. However where there is an interaction of bone through joints, the bone is lined with cartilage. The periosteum has an outer layer that is fibrous and an inner layer that is osteogenic. Through the Sharpey's fibres, the bone attaches to the outer cortical surface of bone which extends into the underlying bone tissue. The primary tissue in bone is called osseous tissue which is a hard but a light weight material. It is composed mainly of calcium phosphate which is known as the bone mineral. The mineral gives the bone its strength but it is also very brittle. Collagen provides the elasticity for bone and is found to be the main constituent of bone. All of the osseous tissue found in bone has cells that are embedded in its matrix of mineral and collagen.

Macroscopically, it is possible to identify the two different types of bone: compact and spongy bone. The existence of these forms of bone depends on the location and function of the osseous tissue (Tortora and Derrickson 2008). Compact bone, or cortical bone as it is also known, is always found at the surface of bone. Here it forms a protective and sturdy layer. Compact bone can be distinguished from spongy bone by the spatial orientation of its mineral and organic elements and also by its locations in the skeleton (Figure 1.2).

Compact bone is the strongest form of bone. It is found beneath the periosteum and also makes up most of the diaphysis. The compact bone provides support, protection and resistance to the stresses which are produced by weight and movement. The blood vessels, lymphatic vessels and nerves from the periosteum go through the compact bone through canals called *'Volkmann's canals'*, which extend perpendicular to the osteons and supply blood to the deeper osteons in the bone and to the marrow cavity tissues. These canals later connect with the canals from the marrow cavity, periosteum and Haversian canals. These are

also known as the *central canals* which are all part of the basic functional unit of compact bone known as the osteon or the *Haversian system*. The central canals within this system are surrounded by concentric rings of mineralised lamellar bone in which bone cells (osteocytes) are found between layers of calcified matrix (lamellae) in small spaces called lacunae (as can be observed in (Figure 1.2) (Currey 2002).

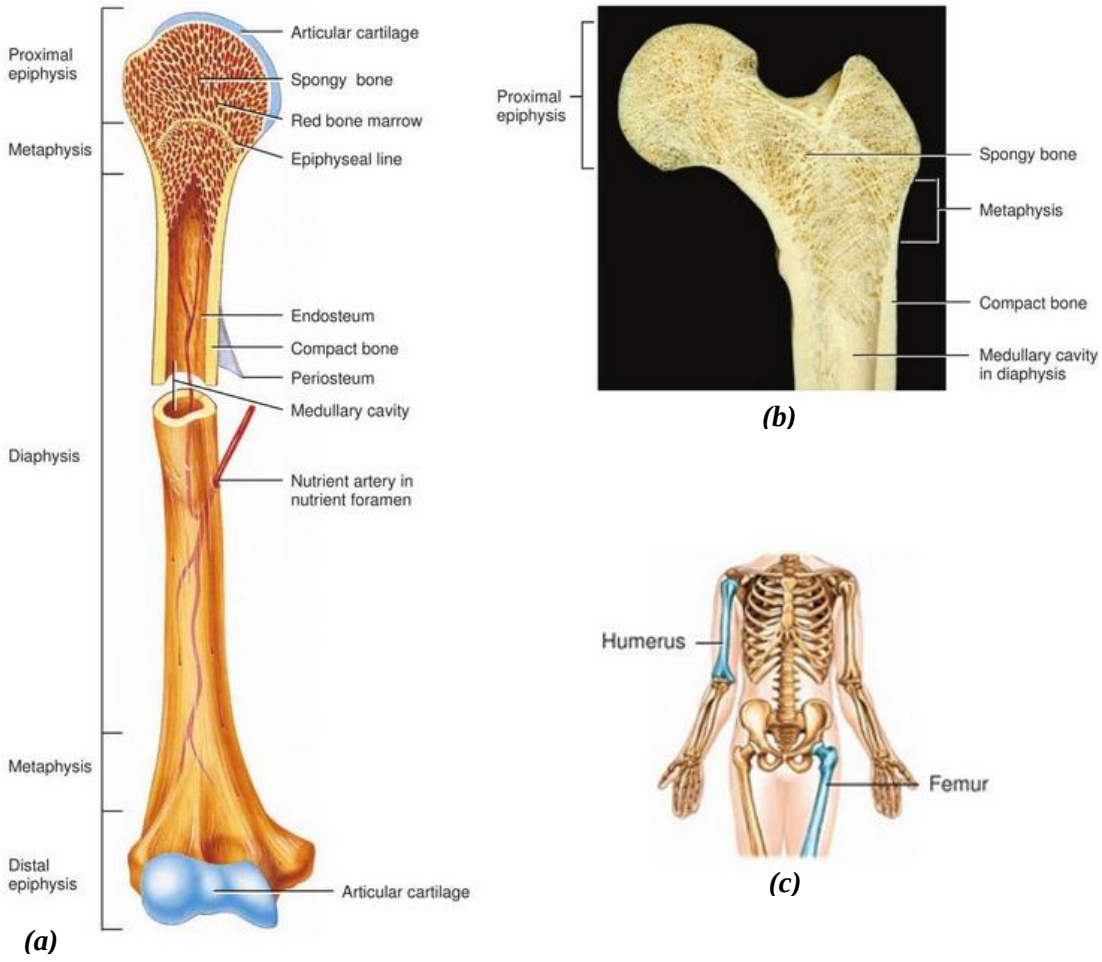

Figure 1.1: Structure of (a) partially sectioned humerus (arm bone), (b) partially sectioned femur (thigh bone) and (c) skeletal image showing humerus and femur. Adapted from Tortora and Derrickson (Tortora and Derrickson 2008)

In comparison, the spongy bone (also known as cancellous bone) does not contain osteons. In appearance, the spongy bone is very porous. The matrix within this form of bone forms struts and plates which are called trabeculae. These then branch out into an open structure with an interconnected network of pores which may be filled with red bone marrow (or yellow in adults) and help make bone lighter. Found within each trabeculae are lacunae that contain osteocytes. Small canaliculi filled with extra cellular matrix (ECM) are found in all

directions from these lacunae, as can be seen in Figure 1.3 (Tortora and Derrickson 2006). Trabeculae have a thickness of approximately 100-300µm with spacing's of 300-1500µm between neighbouring trabeculae. This mean 75-95% of the total volume of spongy bone is porous (Athanasiou, Zhu et al. 2000).

Apparent density and trabecular architecture strongly influence the mechanical properties of cancellous bone tissue, while changes in mineralisation do not have a significant effect (Hodgskinson and Currey 1990). The strength of cancellous bone varies over the range of observed densities as it is related to the square of the apparent density. The modulus of cancellous bone varies as either the square or cube of the apparent density. The mid-range values for the strength and modulus of cancellous bone are 2-5MPa and 90-400MPa respectively (Rohl, Larsen et al. 1991).

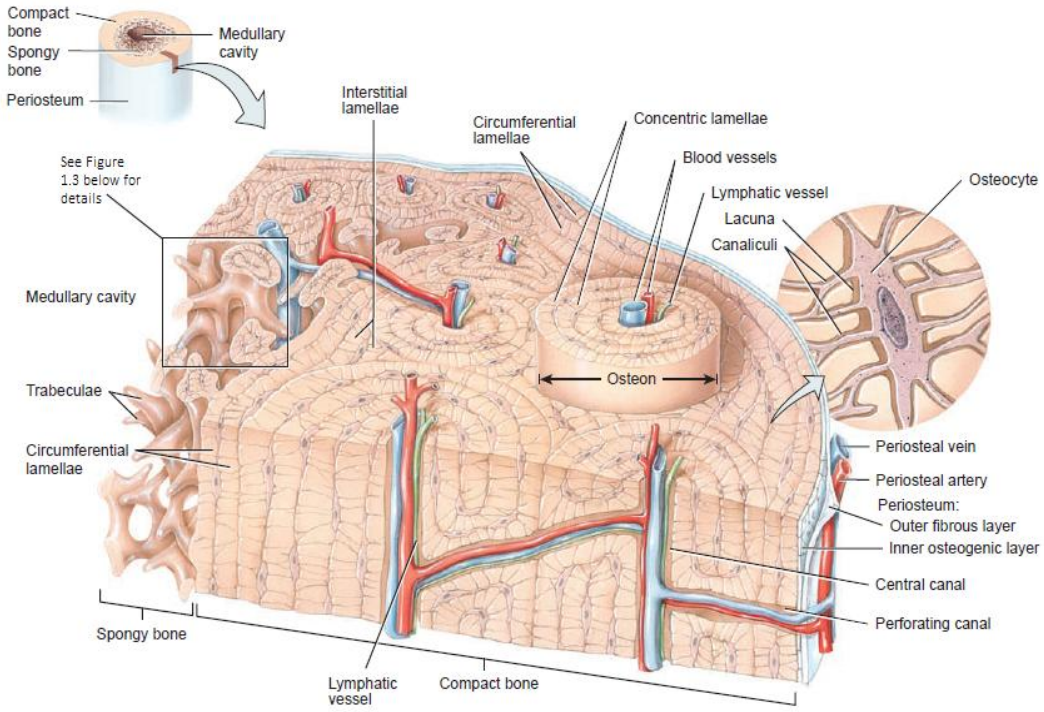

Figure 1.2: Microscopic structure of a bone showing the osteons in compact bone and trabeculae in spongy bone. Adapted from Tortora and Derrickson (Tortora and Derrickson 2008)

Compact bone is anisotropic and the direction of the osteons determine the mechanical properties to a great extent. The strength of compact bone has been reported to be between 78.8 and 151 MPa in the longitudinal orientation in tension. In compression the strength of compact bone has been stated to be between 131 and 224 MPa. It has been said that compact

bone is weaker in the transverse direction, perpendicular to the osteons direction showing strengths of 51-56 MPa in tension and 106-133 MPa in compression. The shear modulus is reported as being 3.30 GPa and the elastic moduli is stated to be 17-20 GPa in tension and compression in the longitudinal direction (Yaszemski, Payne et al. 1996).

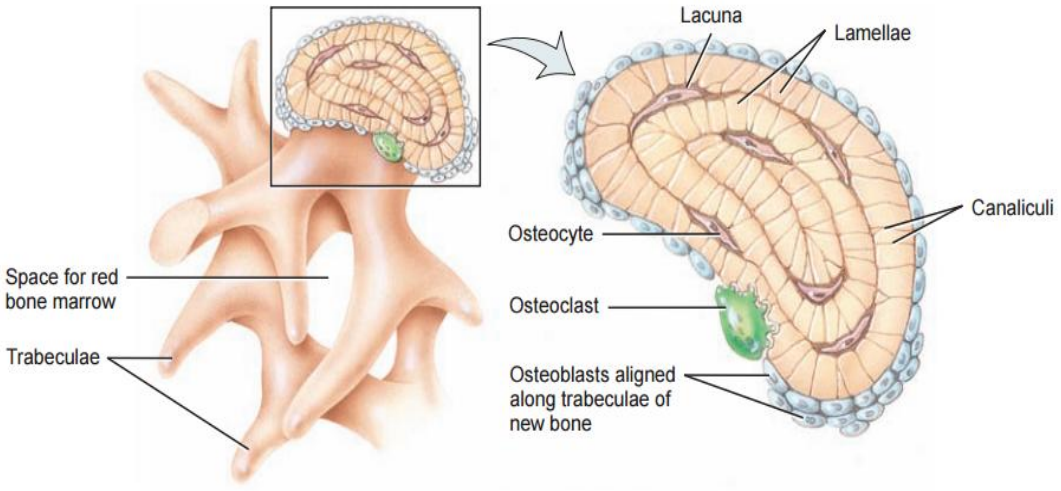

Figure 1.3: Enlarged aspect and details of spongy bone trabeculae. Adapted from Tortora and Derrickson (Tortora and Derrickson 2008)

1.2.1 Bone Composition

Bone can be divided in to two/three main components when looking at it histologically; the matrix, bone cells and the bone marrow.

- ***Matrix*** **-** Provides a framework to support other components of bone. It also contains majority of the minerals which are reserved in bone, and protects against compressive, tensile, flexural and torsional stresses applied across bone.

- ***Bone Cells*** - There are three main cell types that are found in bone, which help in supporting the framework of bone and release minerals from the matrix. This allows the bone to adapt should there be any changes that occur within bone.

- ***Bone Marrow*** - This contains stem cells along with other cells and allows the bone to be supplied with adequate oxygen and nutrients in order to maintain an interaction with the nervous system.

1.2.1.1 Bone Matrix

The bone matrix can be divided into two parts; inorganic and organic parts. The inorganic part of the matrix is composed of poorly crystalline salts and bone mineral crystals whilst the organic part is composed of collagen fibrils and non-collagenous proteins. The make-up of the matrix gives it a unique composition where it is able to provide bone with great mechanical strength in all directions whilst maintaining a minimal weight.

1.2.1.1.1 Inorganic Part

The mineral content of bone is mainly calcium phosphate $Ca_3(PO)_4$ and it accounts for almost two-thirds of the weight of bone. The mineral content has a similar structure to HA, $Ca_{10}(PO_4)_6(OH)_2$, with trace amounts of other ions such as carbonate, magnesium, sodium or potassium (Robinson 1952). Bone mineral consists of platelets which are irregular in shape. They are of varying lengths, with widths of 30-45nm and thickness of approximately 5nm. These platelets are parallel to one another and lie along the collagen fibrils (Landis 1995, Landis, Hodgens et al. 1996).

1.2.1.1.2 Organic Part

The organic part of the bone matrix is made up of the collagen fibrils and non-collagenous proteins which contribute in determining the structure of bone in varying ways.

1.2.1.1.2.1 *Collagen*

Collagen is the most abundant protein found in the body, making up more than half of the proteins found. Collagen compromises about 85-90% of the proteins found in bone (Miller 1984, Currey 2002). Collagen is formed of 3 α-chains known as polypeptide chains. There are 25 different chains that have been identified which form 15 different collagen types. Table 1.1 highlights the main collagen types and which tissue type they are found in.

The major collagen type found in bone is Type I (collagen-I). This can be found in random network arrangements; coarse bundles, parallel fibre sheets and helical bundles which are supported by collagen cross-linkers (Alberts, Bray et al. 1994, Hing 2004). However collagen-I in bone is weakly cross-linked and has a high degree of mineralisation. Due to these properties collagen-I provides elasticity and toughness in bone tissue.

Table 1.1: Major types of collagen and their main properties. Adapted from Alberts et al (Alberts, Bray et al. 1994)

Type	Form	Tissue Distribution
I	Fibril	Bone, Skin, Tendon, Ligaments, Cornea, Internal organs (amounts to 90% of the body collagen)
II	Fibril	Cartilage, Intervertebral disc, Notochord, Vitreous humour of eye
III	Fibril	Skin, Blood vessels, internal organs
V	Fibril (with type I)	Same as Type I
XI	Fibril (with type II)	Same as Type II
IX	Lateral association	Cartilage
XII	Lateral association	Tendon, Ligaments
IV	Sheet-like network	Basal laminae
X	Sheet-like network	Deep calcified layer of cartilage
VII	Anchoring fibrils	Beneath stratified squamous epithelia

1.2.1.1.2.2 *Non-collagenous proteins*

There is a vast array of non-collagenous proteins found in the body, however four of them are of particular interest as they regulate mineralisation and remodelling of bone. These are Osteocalcin (OC), Osteopontin (OP), Osteonectin (ON) and Bone-sialoprotein (BSP).

Proteins such as Fibronectin (FN) and Vitronectin (VN) are important in bone development and bone healing as well as growth factors (Table 1.2)

Table 1.2: Important non-collagenous proteins in bone and their main functions. Adapted from Guth (Guth 2007)

Group	Name	Function and Property
Matrix Proteins	Osteocalcin	Binds calcium; involved in homeostasis; inhibits crystal growth
	Osteopontin	Inhibits crystal growth
	Osteonectin	Binds to calcium and bone mineral; involved in control of cell spreading
	Bone-sailprotein	Binds bone mineral; promotes nucleation
Attachment Proteins	Fibronectin	Promotes attachment of cells to extracellular matrix
	Vitronectin	Promotes attachment of cells to extracellular matrix
Growth Factors	Bone Morphogenic Protein	Induce differentiation of mesenchymal stem cells into osteoblasts
	Insulin-like growth factor	Stimulate proliferation and differentiation of osteoblasts
	Transforming growth factor β-I/II	Stimulate proliferation and differentiation of osteoblasts
	Vascular endothelial growth factor	Important in vasculogenensis and angiogenensis

Osteocalcin (OC) - OC is the most abundant protein of the non-collagenous proteins found in bone. Due to its moderate affinity for calcium, it strongly binds to bone apatite or HA allowing it to regulate calcium homeostasis. It is believed that through this mechanism, OC has the ability to influence bone mineralisation. The concentration of OC in serum is linked to bone metabolism therefore serving as a biological marker for *in vivo* assessments of bone disease (Hoang, Sicheri et al. 2003). The synthesis of OC is by mature osteoblasts only during mineralisation.

Osteopontin (OP) - OP is an acidic phosphorylated glycoprotein which acts as a potent inhibitor of bone mineral formation. It has been suggested that OP acts as a trigger for early differentiation of osteoblasts and that it may also be involved in the local communication between osteoblasts and osteoclasts (Uemura, Nemoto et al. 2001).

Osteonectin (ON) - ON is a glycoprotein which gives it a high affinity to bind with calcium and HA. It has also been demonstrated that ON has the ability to bind with collagen-I and collagen-V (Sasaki, Hohenester et al. 1998). ON can be found in pre-osteoblasts, osteoblasts, osteocytes, and also newly formed osteoids in bone matrix

Bone-sailprotein (BSP) - BSP is the second most common non-collagenous protein in bone. It displays a high affinity for the bone mineral phase and promotes attachment and differentiation of osteoblasts. An increase in bone resorption has been demonstrated with an increase in BSPs (Cutler and Garcia 2003). It has also been demonstrated that BSPs have the ability to promote the nucleation of bone mineral formation (Wuttke, Muller et al. 2001).

Fibronectin (FN) - FN is a high molecular weight glycoprotein. In bone FN links the extracellular matrix to the cells by translating the matrix environment into cellular signals. FN has binding sites for extracellular matrix proteins and also integrin receptors. Many proteins can be bound to FN binding sites. The integrin $\alpha 5\beta 1$ is only specific to FN however other integrins such as integrin-$\alpha 1\beta 8$ and integrin-$\alpha v\beta 3$ are not exclusively bound to FN. This in turn means that FN selectively promotes the adhesion of proteins and thereafter cells. It is only FN that requires integrins in order for cell attachment, whereas other proteins such as ON do not need integrins for cell attachment (Cowles, Brailey et al. 2000). It has also been shown that HA allows FN to readily be absorbed onto its surface thus inducing the proliferation of osteoblasts on the HA surface (Garcia, Ducheyne et al. 1998).

Vitronectin (VN) - In comparison to FN, VN is a smaller glycoprotein, also termed spreading factor which is found in plasma and extracellular matrix (Ayad, Boot-Handford et al. 1998). Like FN, VN also plays an important role in cell attachment to their surrounding

matrix (Kim, Arakawa et al. 2003) and also in cell migration (McKeownLongo and Panetti 1996). FN and VN seem to undertake similar roles in the interaction between the extracellular matrix and cells. However the adsorption behaviour of both proteins is not similar (Steele, Dalton et al. 1995). It has also been shown that both FN and VN can be absorbed on HA in favourable conformations to the integrin mediated cell adhesion (Kilpadi, Chang et al. 2001).

Bone Morphogenic Proteins (BMP) - BMPs are a family of cytokines that have demonstrated stimulation and differentiation of mesenchymal stem cells down the osteogenic cell linage (Wozney and Rosen 1998). They are secreted from osteoprogenitor cells and mature osteoblasts. As bone formation begins through the adhesion of cells in clusters, BMPs regulate bone growth. BMPs have been used in clinical applications for their use in orthopaedic reconstruction, however not all BMPs show the same effectiveness in bone formation. BMP-2 and BMP-7 have shown interest for use in clinical applications (Wozney and Rosen 1998, Koch, Jadlowiec et al. 2005, Pluhar, Turner et al. 2006)

Insulin-like growth factors (IGF) - These are growth factors that stimulate the proliferation of already committed differentiated osteoblasts and chondrocytes. They also induce the secretion of matrix from both of these types of cells (Buckwalter, Glimcher et al. 1996).

Transforming growth factor (TGF) - It causes differentiation of MSCs to chondrocytes. It is also known to induce proliferation of chondrocytes and osteoblasts. Bone resorption has been seen to be enhanced at certain concentrations (Buckwalter, Glimcher et al. 1996).

Vascular endothelial growth factor (VEGF) - It is a fundamental regulator of angiogenesis. VEGF is needed for the proliferation of blood vessels, longitudinal bone growth and also the formation of endochondral bone (Ferrara 2004).

1.2.1.2 Bone Cells

Bone contains a very large range of cells as it is a vascular tissue however, for the formation, maintenance and resorption of bone, three cell types are of particular interest; osteocytes, osteoclasts and osteoblasts. Osteocytes and osteoblasts differentiate from MSCs and osteoclasts form from mononuclear monocytes which come from hematopoietic stem cells.

1.2.1.2.1 Osteocytes

Osteocytes are the most abundant cell type in mature bone. When approximately 10% of the osteoblastic cell population become enclosed in to the developing matrix, the cell type is

then referred to as osteocytes. Within this embedded bone matrix, they form a network, where they transport nutrients and waste. Osteocytes are found in the lacunae within the bone matrix connected with other neighbouring osteocytes through gap junctions by means of long processes housed in canaliculi channels with diameters of 0.2 - 0.3µm. within these gap junctions small molecules are allowed through easily in order to help regulate the flow of minerals and ions from the matrix to the cells (Currey 2002). Osteocytes have a very low metabolic rate however they are actively involved in maintaining bone which can further lead to other cell types being stimulated or inhibited (Alberts, Bray et al. 1994).

1.2.1.2.2 Osteoclasts

Osteoclasts are responsible for the resorption of bone, they are better known as bone-resorbing cells. They are very large, multinucleated cells which are derived from precursor cells which are found to circulate in the blood (Currey 2002). The aggressive nature of these cells make them clamp to the surface of the bone and leave a space underneath a ruffled border which is found to be very mobile. Under this border the bone can be seen dissolving. Above this border, organic and mineral debris are found packed in to little vesicles which then pass through the cell body of the osteoclasts (Nesbitt and Horton 1997, Salo, Lehenkari et al. 1997, Currey 2002). They are constantly remodelling bone tissue and are critical in controlling and maintaining calcium homeostasis (Alberts, Bray et al. 1994). These cells are very aggressive in the way they are able to attach to the bone surface and resorb the bone (Currey 2002).

1.2.1.2.3 Osteoblasts

Osteoblasts are derived from bone-lining cells. These bone-lining cells cover all surfaces of bone forming a continuous sheet that controls the transfer of ions from the body to the bone (Miller, Saintgeorges et al. 1989). Osteoblasts are responsible for the formation of new bone. They are small mononucleated cells about 10µm in diameter. There is an initial collagenous matrix (osteoids) that the cells lay down in which mineral is later deposited. Osteoblasts help in the mineralisation of bone by secreting matrix vesicles. These vesicles are calcium rich and bud off the osteoblast membrane. In addition to being calcium rich, the vesicles also contain a high concentration of lipids and alkaline phosphatase (ALP). ALP is an enzyme which has been associated with the mineralisation of bone. It is found to be localised in the outer plasma membrane and connected to the inositol membrane by a phosphatidyl-glycan bridge. ALP is then synthesised by osteoblasts in vesicles which also contain inorganic phosphate which are then anchored in the areas favourable to bone growth (Anderson 2003). ALP is considered an early marker for differentiation in bone formation. The other proteins

that are produced, secreted and embedded in to the bone matrix by osteoblasts are the non-collagenous proteins; OP, ON, OC, BSP as well as the growth factors (Guth 2007).

In vitro work that has been carried out, is either on primary osteoblast-like cells or osteoblasts-like cell lines. The primary cells are extracted from bone that has been sacrificed whereas, cell lines are osteoblasts that have been immortalised often from carcinogenic origins. Examples of human osteoblast-like cell lines include, MG63, HOB-TE85, Saos-2 and G-292 cells. The activity of osteoblast -like cells has been investigated for many years and they have shown a positive involvement in bone in growth in to graft materials. In 1912, Macewen classed osteoblast-like cells as 'bone forming cells' and further saw that they responded to a range of different stimuli (Macewen 1912). Since then studies into osteoblast-like cells has advanced and become ever more complex. It is found that there is variability in the results that are obtained from *in vitro* work on cell lines however it has been accepted that the cell lines are more consistent with reactions to stimuli in comparison to primary cells (Guth 2007).

1.2.2 Bone Growth, Repair and Remodelling

Bone growth occurs during two stages of life; childhood and adolescence. It occurs in longitudinal and radial growth patterns. During longitudinal growth, cartilage proliferates at the growth plates in the piphyseal and metaphyseal areas on long bones. Subsequently the cartilage then undergoes mineralisation which then forms primary new bone. It is well known that bone has the ability to change shape which in turn allows the skeleton to respond to biological or mechanical stimuli. These stresses have the ability to activate the actions of osteoblasts and osteoclasts which then cause a change in the bone axis. Wolff's Law explains how bone changes shape in order to adapt to the stresses placed on them.

The mechanism behind bone repair is different in adults in comparison to embryos. There are two main bone repair mechanisms in developing bone.

- *Intramembranous Ossification*. This occurs more so in flat bones such as the skull. During this process, the bone is formed from the condensation of the mesenchymal tissue. This is known as the ossification centre. The cells within this tissue differentiate into osteoblasts which then synthesise osteoids leading to mineralisation (Alberts, Bray et al. 1994).
- *Endochondral Ossification*. This occurs in long and short bones and has an initial formation of cartilage which is later replaced by new bone. During fracture of

mature bone, it is only endrochondral ossification that takes place, where mesenchymal stem cells transform in to chondroblasts which lay down collagen followed by ossification by osteoblasts (Alberts, Bray et al. 1994).

A traumatic injury, such as a fracture in bone, results in a number of process occurring; inflammation, repair and remodelling. In response to this, there is a sequence of cellular, hormonal and vascular events which take place. It starts with the release of inflammatory mediators and ends when the remodelling of the repair tissue reaches a homeostatic state (Alberts, Bray et al. 1994, Buckwalter, Einhorn et al. 1996).

Inflammation is *'the cellular and vascular response to injury, including release of inflammatory mediators, vasodilation, exudation of plasma and migration of inflammatory cells to the injury site*' (Buckwalter, Einhorn et al. 1996).

The process of inflammation then causes swelling, erythema, increased tissue temperature, pain and/or impaired tissue function. Inflammatory response in injured vascularised tissue is almost immediate, however in non-vascularised tissue such as cortical bone this process is delayed or sometimes does not occur at all. The injured tissue releases vasoactive mediators which cause vasodilation and increased permeability of the blood vessels. At the site of injury, a haematoma appears which allows fibrin to form and allows platelets to bind to collagen. This achieves homeostasis. The aggregation of platelets releases vasoactive mediators as well as growth factors and cytokines. This process is then followed by the migration of mesenchymal cells leading to their differentiation and beginning the repair process. Figure 1.4 highlights the mesengenic process for bone repair (Caplan and Bruder 2001). At the same time new capillaries form in to the site of injury from endothelial cells which then undergo proliferation near the injury (Buckwalter, Einhorn et al. 1996).

Remodelling is the reorganisation and reshaping of the repaired tissue and is completes successful healing. The process involves the removing, replacing and reorganising of cells and matrix. More importantly this process helps in the removal of excessive repair matrix as well as the reduction of cell and capillary density. The reorganisation of the collagen fibrils facilitates inorganic deposition in alignment with the chemical and mechanical stimuli placed upon the bone (Buckwalter, Einhorn et al. 1996).

Cortical and cancellous bone have different remodelling process which occur. In cortical bone, osteonal tunnelling occurs where the osteoclasts excavate a Haversian canal which is then refilled by osteoblastic matrix deposition. Cancellous bone is remodelled by osteoclasts

eroding the surface of the bone. This forms a Howship's lacunae followed by osteoblasts refilling the Howship's lacunae (Cowles, DeRome et al. 1998).

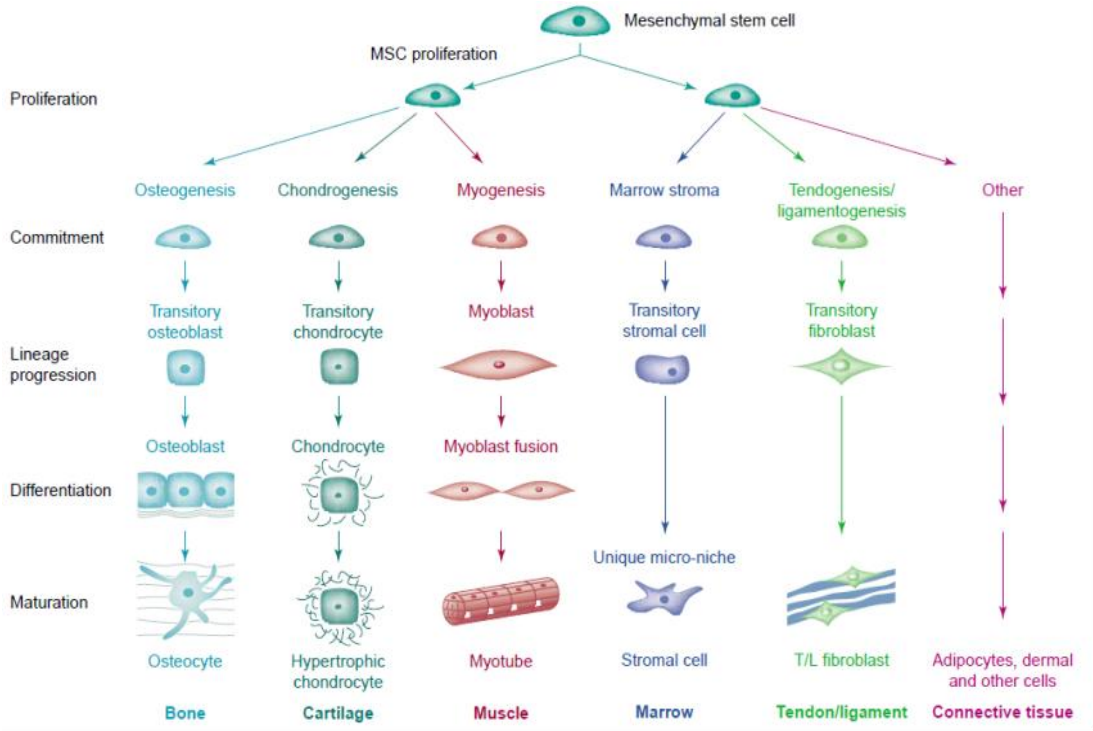

Figure 1.4: The Mesengenic Process (Caplan and Bruder 2001)

There is still dispute regarding bone healing around implants in the body and how the repair process occurs. There are many researchers who believe that the incorporation of porous bone graft substitutes uses a bone appositional process in order to heal the bone around the implant (Carlsson, Regner et al. 1994, Hofmann, Bloebaum et al. 1997, Bloebaum, Willie et al. 2007). While other researchers (Galante, Rostoker et al. 1971, Bobyn, Pilliar et al. 1980) believe that the bone healing around the implant occurs through a mechanism that is similar to the endochondral fracture healing model which involves the periosteum.

1.3 Bone Grafting

It is important to focus on bone graft materials as bone fractures and osteoporosis is a worldwide clinical issue which is increasing with time. Osteoporosis has been recognised as an established, well known disease that affects 75 million people in the United States, Europe and Japan. It is estimated to affect 200 million women worldwide of which two-tenths are aged 60, one-fifth are aged 70, two-fifths are aged 80 and one-fifth are aged 90. Osteoporosis causes more than 8.9 million fractures annually worldwide, of which 4.5 million occur in America and Europe alone. (Kanis 2007).

Bone grafting as a technique was first established and successfully documented in the 1800s by replacing missing bone with either material from the patients' own body (autograft) or from a donor (allograft) (Pountos, Jones et al. 2006). Along with autografts and allografts, there are also xenografts that are in use. The 'Gold Standard' in bone grafting is said to be the use of autografts. This is when the graft is taken from the patient in order for it to be put back into the same patient. This in turn would reduce the immunogenic response and also provide a structural scaffolding material. However disadvantages such as, limited volume, donor site morbidity, increased pain and risk of infection due to an additional operation site, this type of graft is becoming increasing less popular (Guth, Buckland et al. 2006).

An alternative to the autografts would be to use allograft materials. Such grafts are taken from a donor and inserted into the patients' defective site. A clear risk of using autografts is that there will be some form of risk of contamination therefore causing an immunological response eventually leading to rejection of the graft. The use of xenografts is a method by which the graft is taken from another species. The first attempt of such a graft was made in 1668 by a Dutch surgeon who described filling a bone defect in a soldiers cranium with a piece of skull from a dog (De Long, Einhorn et al. 2007). There have been some claims that they cause antigenic responses, it was then found that these grafts were not suitable for bone grafting applications (Younger and Chapman 1989).

Bone grafting now uses BGS materials which are made of biomaterials. Biomaterials are materials that are used to replace or make a device to replace a part of function of the body (Hench 1998). As well as replacing missing bone, these biomaterials are being used to augment the defect site by encouraging new bone growth into the actual defective site. This new bone should eventually replace the graft material within the site and maintain an optimal balance between its form and function (Hing, Wilson et al. 2007). Depending on its application, the bone graft material must have some important characteristics, one of which is being biocompatible. For a material to be biocompatible it is said to have the ability to perform with an appropriate response for a specific application. Another characteristic to be considered is the bioactivity of the material.

Metals and alloys have also been used as bone replacement materials. Due to their toughness and bioinert nature, metals and alloys are often used in load bearing applications, for example the hip. The advantage of metals used as bone fixation devices is that they provide an instant support load however the major drawback to these materials is that there is a need for secondary surgery in order to remove the metal pin or plate once the fracture site has healed. If these materials are not removed there is a danger of the bone resorbing itself due to

the lack of mechanical stimulation that is available (Schmalzried, Szuszczewicz et al. 1998). As these materials are tougher and stronger than the surrounding bone, they are able to absorb most of the mechanical impacts to the bone. This however leads to the surrounding bone not being mechanically stimulated therefore leading to the degeneration of the tissue over time. As this occurs the implanted material will being to loosen causing the need of secondary surgery to rectify the problem.

Bone graft materials that are in use today are polymers, bioglass and calcium phosphate based ceramics. The incorporation of a graft material is very sensitive and dynamic process. The equilibrium between the osteoprogenitor cells, differentiation of osteoblast cells, osteoinduction, osteoconduction and the biochemical properties of the graft material are essential for the successful integration of the graft material in to the body (Burchardt 1983, Burchardt 1987). An *osteoconductive material* is one that supports the formation of bone on its surface by osteoblast cells and an *osteoinductive material* is when it has the ability to induce bone formation by influencing the differentiation of stem cells into bone forming cells (Hing 2004).

1.3.1 Natural Bone Grafts

There are two main types of natural biomaterials; Demineralised Bone Matrix (DMB) and Collagen. DMB is produced by an acid extraction of banked allograft bone. This biomaterials is able to provide a vast array of osteoconductive scaffolds which have minimal structural strength. The efficiency of DMB rests on its ability to promote new bone which is affected by many parameters. Osteotech Inc., (Eatontown, NJ) were the first to make DMB commercially available; Grafton Gel (Betz 2002).

Collagen, as mentioned previously is the most abundant protein found in the extracellular bone matrix. Like DMB, collagen provides very little structural support and can cause an immunogenic response. Even though collagen has its positive attributes, it is not being used clinically as a standalone bone substitute material, but has found application as a sponge for the delivery of BMP-2 (Betz 2002).

Coralline hydroxyapatite (CHA) is manufactured from marine coral, which has a natural trabecular structure similar to that of bone. While some studies have demonstrated the biocompatible properties and osteogenic results (Kuehne, Bartl et al. 1994, Wei, Cai et al. 2003, Mygind, Stiehler et al. 2007, Fu, Xu et al. 2013), as a BGS and a bone void filler the

use of CHA maybe limited due to its inherent mechanical weakness and reduced biodegradation (Damien and Revell 2004).

1.3.2 Synthetic Bone Grafts

The advantages of using synthetic biomaterials as bone graft substitutes (BGS) are that there is a great availability of the materials, there is no need for a secondary surgical procedure, reduced risk of an immunogenic response, and an elimination of disease transfer. As mentioned before, there are many biomaterials that are being used as synthetic BGS; ceramics, such as apatites and bioglasses (Hench 1991, Heikkila, Aho et al. 1993, Knowles 2003, Hing, Wilson et al. 2007) and polymers or copolymers (Fabriziushoman and Cooper 1991, Kowalczynska, Nowak-Wyrzykowska et al. 2005).

With the development of a biomaterial, there are factors that need to be taken in to consideration in order to design and make a bioactive biomaterial. The first parameter that is important is the mechanical strength of the material as this will then allow the patient to start applying pressure to the defect site and therefore be able to use the operated site as soon as possible. Another parameter that is vital to consider is the porosity of the biomaterial. The greater the porosity of the material, the greater interconnectivity the material has therefore allowing better conditions for vascularisation and incorporation of the material into the defective site. It has previously been shown that the osteoconductivity and osteoinductivity of the biomaterial is very important however the degree of them is still under debate. Nevertheless there are biological and also synthetic elements that are being designed and utilised to enhance these properties (Vanblitterswijk, Bakker et al. 1991, Hunter, Archer et al. 1995, Ozawa and Kasugai 1996).

1.3.2.1 Calcium Regulation in the Body

Within the body, the levels of free calcium and phosphate are maintained in the extracellular fluid and intracellular compartments whilst they are 'stored' within the skeleton (Favus, Bushinsky et al. 2006).

The total body calcium and phosphate content in adults is about 1000g and 542g of which 99% and 85% exists as the hydroxyapatite crystal in the mineral phase of bone respectively. The crystal contributes to the mechanical weight bearing properties of bone. It also serves as a calcium and phosphate reservoir that can be mobilised rapidly in order to support the many biological systems in which calcium and phosphate are regulators and cofactors (Favus, Bushinsky et al. 2006).

Calcium homeostasis is controlled by three major hormones: parathyroid hormone (PTH), calcitonin, and 1,25-dihydroxyvitamin D [$1,25(OH)_2D_3$]. The extracellular fluid calcium concentration is tightly controlled by a complex homeostatic mechanism involving fluxes of calcium between the extracellular fluid and the kidney, bone, and gut. These fluxes are carefully regulated by the three major hormones. Important cellular functions are dependent on the maintenance of the extracellular calcium concentration within a narrow range. Disturbances of this tightly regulated homeostatic system leads to disorders of calcium metabolism that have predictable effects, which can be ascribed to effects on these cellular functions. The regulation of blood calcium concentrations is important for muscle contractions and nerve impulses, which are electrically stimulated. If calcium levels are too high, the membrane permeability to sodium decreases and membranes become less responsive. However, if calcium levels fall too low, membrane permeability to sodium increases and may cause muscle spasms as a result. PTH which is produced by the parathyroid glands is released in response to low calcium levels in the blood. Calcium levels are increased by targeting the skeleton, kidneys and the intestine. In the skeleton, PTH stimulates osteoclasts which cause bone to be resorbed, releasing calcium from the bone to the blood. PTH can inhibit osteoblasts, reducing calcium deposition in bone. PTH increases dietary calcium absorption in the intestines and stimulates re-absorption of the calcium in the kidneys. PTH also initiates the formation of calcitriol, an active form of vitamin D and acts on the intestines to increase absorption of dietary calcium. The release of PTH is inhibited by consequent elevation of blood calcium levels. An overproduction of PTH causes *Hyperparathyroidism*, which leads to excessive amounts of calcium being removed from bones and introduced into blood circulation. This produces structural weakness of the bones, leading to bone fractures and nervous system impairment due to high blood calcium levels. *Hypoparathyroidism*, results from the underproduction of PTH, causing extremely low levels of blood calcium, leading to impaired muscle function (Favus, Bushinsky et al. 2006).

1.3.2.1.1 Calcium Phosphate Bone Grafts

There has been a vast amount of research carried out on calcium phosphate based ceramics. The first time calcium phosphates were used for bone repair was in the 1920s. Tricalcium phosphate (TCP) was implanted in to rabbit forelegs. This study was successful in demonstrating improved osteogenesis (Albee 1920). Calcium phosphates have been divided in to two categories; bioresorbable and bioactive biomaterials. β- tricalcium phosphates and α-tricalcium phosphates are amongst the bioresorbable calcium phosphates being used clinically. These materials have the ability to degrade and allow the formation of new bone. However these materials may not always bond directly with the bone tissue causing

inhibition of cell attachment which will eventually lead to an increased inflammatory response and graft failure (Lu, Blary et al. 2004, Hing, Wilson et al. 2007). Calcium phosphates that are bioactive, such as HA promote bone formation directly on the materials surface (Patel, Best et al. 2002, Hing 2004). Bioactive materials interact with the surrounding tissue directly which forms a chemical bond with the surrounding bone tissue (Hing 2004).

1.3.2.1.2 Hydroxyapatite (HA)

Amongst all the different types of calcium phosphates that are available, HA $Ca_{10}(PO_4)_6(OH)_2$, is the most commonly used within the fields of dentistry and orthopaedic surgery. HA was first commercialised in the mid-seventies independently by Jarcho, Groot and Aoki (Hench and Wilson 1993). The term apatite is given to a family of compounds, all of which have similar structures but not the same composition.

Crystalline HA is a synthetic material and is chemically similar to the mineral component found in bone and teeth. The structure of HA can be described as a hexagonal unit cell (Figure 1.5). It has space groups of $P6_3/m$ and has lattice parameters a = 9.432Å and c = 6.881Å. There are four hydroxyl ions with four calcium ions that lie parallel to the c-axis and the remaining six calcium ions associate with two hydroxyl groups within the unit cell. The phosphate tetrahedral forms the basic remaining structure of the HA unit cell (Vallet-Regi and Arcos 2005).

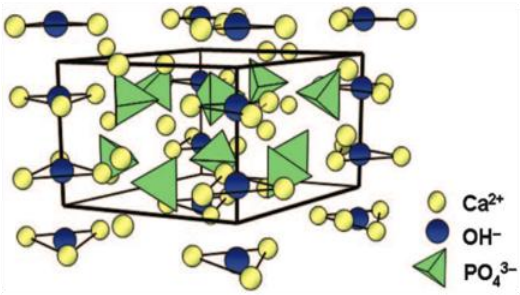

Figure 1.5: Crystal structure of Hydroxyapatite (HA) (Vallet-Regi and Arcos 2005)

The main advantage of HA is that it is chemically similar to the mineral found within human bone. It has a good stiffness of 80-85GPa (Brown and Constantz 1994). HA is a highly cytocompatible material that has been considered for use in many applications; coatings for metallic implants (Gross and Berndt 1998), a porous ceramic facilitating bone in growth (Kobayashi, Shingaki et al. 1993), granulate to fill small defects (Sari, Yavuzer et al. 2003) and also for tissue engineering purposes (Kruyt, Dhert et al. 2004).

HA allows for a specific biological response within the tissue and implant interface. This then leads to the formation of bonds between the bone and the grafting material. The formation of this chemically bonding interface takes place as part of the bone remodelling phenomenon (Haibo Wang 2004). Due to this interface, HA has a much higher bonding strength in comparison to other implants like metals, which allows micro movement between the implant and the surrounding bone. This is most useful in the early period after implantation and for rapid fixation.

With its good biocompatibility properties, HA still however has its drawbacks. The brittle behaviour of HA gives it an increased risk of fracture. Being a ceramic material, it has a low impact resistance therefore failing easily when loaded at a high velocity and it also has a low strain to failure (<0.3%). HA has a lower Young's Modulus than cortical bone therefore making it stiffer (Brown and Constantz 1994). Unfortunately HA also has low reliability especially in wet conditions which prevents it from being used in heavy load bearing applications by itself (Suchanek and Yoshimura 1998).

Even though HA is a bioactive material, the actual bioactive process shows some drawbacks when compared to other bioactive materials. For example, the apatite formation in silica-based glasses occur within a few minutes (Zhong and Greenspan 2000), whereas the apatite formation in HA can take place over several days (Oonishi, Hench et al. 2000). It has also been shown that minute changes in the phase purity of HA causes drastic effects in the biological response of the materials. For example the presence of calcium oxide (CaO) causes enhance inflammation or cause cytotoxic response (Hing 2004).

Moreover it is desirable to have a graft material, which will eventually resorb therefore leaving space for new bone formation. Influenced by its porous structure, HA has a low resorption rate, which is considered by many to be a limiting factor. This would in turn mean that longer rehabilitation times would be required for the patient with the subsequent probability increase of failure due to the deficient implant fixation (Vallet-Regi and Arcos 2005). The bioactive behaviour of HA can be improved by introducing substitutions within the structure of the HA unit cell (Gibson, Best et al. 1999, Ergun, Webster et al. 2002).

The apatite lattice has the ability to incorporate a wide range of ionic substitutions. Cations and anions can easily be substituted for cations and anions of the same oxidative states within the HA lattice. These include lead (Pb^{2+}), magnesium (Mg^{2+}) or strontium (Sr^{2+}) being substituted for calcium (Ca^{2+}) and fluoride (F^-) or chloride (Cl^-) being substituted for the hydroxyl group (OH^-). Substitutions of differing oxidative states can also take place,

particularly substituting phosphate (PO_4^{3-}) group by silicate (SiO_4^{4+}) (Demaeyer, Verbeeck et al. 1993). Depending on what substitution take place, many changes take place; these include changes in crystal morphology, crystallinity, thermal stability and also solubility.

Examples of the likely substitutions in biological carbonate substituted apatites are usually classified by two types: type A, where hydroxyl groups (OH^-) are substituted by carbonate groups (CO_3^{2-}) and type B where phosphate (PO_4^{3-}) groups are substituted by CO_3^{2-} (Wilson, Elliott et al. 1999). When considering the type B carbonated apatites, single valence cations such as Na^+ or K^+ are incorporated in the Ca^{2+} positions to reach neutrality (Verbeeck, Demaeyer et al. 1995). Upon substitution, Type B carbonated apatites show a decrease in the a axis and an increase in the c axis. They also increase the solubility of the apatite. Other substitutions include, fluoride (F^-) and chloride (Cl^-), both of which can replace the OH^- or PO_4^{3-} ions from their site within the lattice. Incorporation of these ions can bring about vital changes in the HA lattice structure. Fluoride has the ability to promote mineral formation *in vivo*, increase the structural stability, induce a higher crystallinity and also enhance the mineralisation and calcification process *in vitro*. Chloride can expand the a axis and decrease the c axis and it has the ability to stabilise HA when it is exposed to sintering (Demaeyer, Verbeeck et al. 1993).

HA can also incorporate cations with the same oxidation state as Ca^{2+}, such as Sr^{2+}, Pb^{2+}, Mg^{2+} etc. These substitutions again bring about changes in HA. Strontium increases the dissolution rate and both the a and c axis. Lead can increase the lattice parameters, whereas magnesium increases the dissolution rate but decreases the crystallinity and finally aluminium can also decreases the crystallinity of HA (Bigi, Falini et al. 1996).

Ionic substitutions with different oxidation states are also very common, which in turn play an important role in the chemical, structural and microstructural properties. The change in valence gives rise to charge imbalance and therefore is compensated by means of some mechanism, for example creating new anionic vacancies (Deboer, Sakthivel et al. 1991).

Many authors have studied the incorporation of Si as SiO_4^{4-}, into the apatite structure at the PO_4^{3-} position. Through the Rietveld structural refinement of the x-ray diffraction, it was demonstrated that the incorporation of silicate ions decreased and increased the a and c axis respectively of the HA unit cell (Porter, Patel et al. 2004). Moreover it has also been seen that substituting silicate ions into the HA structure increased the solubility and also enhanced osteoblast like cells activity (Gibson, Huang et al. 1999). It has also been proven that silicate

group substitutions enhance bone regeneration (Patel, Best et al. 2002, Botelho 2005, Hing, Revell et al. 2006, Guth, Campion et al. 2010, Castagna 2014).

1.3.2.1.3 Silicon in Bone Development

Carlisle in 1970 was the first to show the importance of silicon in the formation and mineralisation of bone. She reported the detection of silicon *in vivo* within the active calcification regions (unmineralised osteoid region) of the young bone in mice and rats. Silicon levels of up to 0.5wt% were seen in these areas, which in turn suggested that Si had an important role in the bone calcification process (Carlisle 1970).

In 1972, Schwarz and Milne demonstrated that a silicon deficient diet in rats retarded the growth and disturbed the development of bone structures. They particularly saw a change in the skull size and also the architecture of the bone within these rats. It was suggested that silicon plays an important role in the binding of structures due to the stability of the Si-O-Si bonds present. Therefore there was a successful attachment of cells (Schwarz and Milne 1972). However one of the most important findings of Schwarz was in 1978 when he discovered an enzyme, which had the capability to remove silicic acid from a synthetic bond form, Silicase. The enzyme is membrane bound and is found in the pancreas, stomach and in the kidneys but at a lower concentration. The enzyme is stable and can be heated to temperatures of 100^{o}C without losing activity for at least 10 minutes. Schwarz also proposed a correlation between the effects of silicon and bone disease along with wound healing and atherosclerosis (Schwarz 1978).

Earlier in 1972, Carlisle presented a study on chicks, which concluded that there is an importance of silicon in the mineralisation of bone. She was successful in showing that silicon plays a role in the growth and development of bone, connective tissue metabolism and bone calcification process. She showed that the chicks, with a silicon deficiency, had distorted skeletal development, less flexible legs, smaller skull and also flatter bones (Carlisle 1972). Using electron microprobe, Carlisle also demonstrated that silicon is concentrated in the cytoplasm of osteoblast cells in young bones. Therefore there is a direct relation between the concentration of silicon and the amount of calcification taking place. The study showed that after an increase in calcium there is a decrease in silicon, especially when the levels of calcium reach the values that are seen in bone apatite. The maximum amount of silicon was seen when there was a Ca/P ratio of 0.7, however this very quickly decreased when the Ca/P ratio increased to 1.67 (Carlisle 1972). There have been many studies that have shown the importance of binding calcium in calcification, and this study also suggested that silicon plays an important role in the process as well. The abnormalities

that were seen with the bone skull are related to a deficiency in collagen of the connective tissue matrix. The chicks that were silicon deficient, showed lower amounts of cartilage, glycoaminoglycans (GAG) and collagen within their articular cartilage. This further led Carlisle to show that the site of action of silicon in connective tissue metabolism is on the GAG-protein complexes of the ground substance. It was found that silicon is bound to GAG and associated with polysaccharides and small proteins in 'higher animals' (Carlisle 1974).

It was suggested that silicon incorporated into apatites would improve the *in vivo* bioactive performance. New apatite layers are formed on the surface of many glasses and also glass ceramics after a few hours in simulated body fluids (SBF). The silanol group (Si -OH) formation was proposed as the catalyst for the apatite phase nucleation. Such events suggested the idea of incorporating Si in to the HA structure (Arcos, Greenspan et al. 2002, Arcos, Greenspan et al. 2003)

In vivo and *in vitro* testing have given evidence of the important improvement of the bioactive behaviour with the respect to non-substituted apatites (Hing 2004). Silicon containing calcium phosphates, such as silicon substituted hydroxyapatite (SA) has been shown to have the potential to increase the rate of bone apposition significantly to HA bioceramic implants (Porter, Buckland et al. 2006). Most of the work conducted on SA has shown to be very promising with corresponding data supporting its effectiveness within the bone grafting sector. Studies by Porter et al have examined the *in vivo* dissolution process in phase pure HA and SA. It was found that there was an increased number of triple junctions in SA compared to the phase pure HA and that this may have a significant role in the increasing solubility of the material and the subsequent that the bone apposes these ceramics (Porter, Patel et al. 2003, Porter, Botelho et al. 2004, Porter, Patel et al. 2004, Porter, Buckland et al. 2006). The amount of Si that can be incorporated into the apatite lattice is limited as previous studies have collected values ranging from 0.1 to 1.5wt% in Si (Best, Bonfield et al. 2001, Harding, Rashid et al. 2005). Small amount of Si between 0.5 – 1% is enough to yield bioactive improvements (Hing, Annaz et al. 2005). High-resolution transmission electron microscopy has been used to observed dissolution from HA, 0.8wt% SA and 1.5wt% SA after 6 and 12 weeks *in vivo*.

Many methods have been conducted to synthesis SA. Ruys described a sol gel procedure (Ruys 1993). Tanizawa and Suzuki tried using hydrothermal methods to obtain materials with higher Ca/(P+Si) ratios (Tanizawa and Suzuki 1995). The synthesis of SA by solid state reaction was performed however, in this case there was a need to also add secondary ions such as La^{3+}, Nd^{3+} or SO^{4-} (Boyer, Carpena et al. 1997, Boyer, Savariault et al. 1998, Serret,

Cabanas et al. 2000). Aqueous precipitation is a novel method of synthesising SA as it produces a one-phase product when sintered at the optimum temperature for research or clinical applications. This process involves an acid-base neutralisation reaction utilising calcium hydroxide ($Ca(OH)_2$) and orthophosphoric acid (H_3PO_4) in the presence of a Si containing compound.

XPS has been used to determine that the silicon exists as a tetrahedral silicate SiO_4 group rather than in a polymeric form of SiO_2 for silicon amounts of up to 1.2wt% (Botelho, Lopes et al. 2002). Balas, in 2003 achieved similar results and reported the polymerisation of the silicate species at the surface for silicon contents higher than 1.6wt% (Balas, Perez-Pariente et al. 2003). The ZP measurements showed that at physiological pH =7.4 surface charge was significantly lowered by the presence of silicate groups; therefore a faster apatite layer formation would follow. However the presence of polymeric species seems to decrease the bioactive behaviour of SA (Botelho, Lopes et al. 2002). It was also reported that the incorporation of silicon in to the HA lattice induced a more negative surface charge and changes in surface silicate ion group with the 0.8 wt% material showing higher bioactivity (Rashid, Buckland et al. 2005).

1.3.2.2 Protein Adhesion

On the implantation of a biomaterial, protein adsorption on to the foreign surface occurs within seconds of implantation. The rapid protein adsorption means that the cells arriving at the biomaterials surface interact to this layer rather than directly with the material itself. Therefore this layer of protein is considered vital in the control of the reactions that occur with the implanted material. The adsorption of proteins on to the surface on biomaterials does not occur randomly or sequentially. The binding of these proteins is found to be competitive and very much dependant on the adhesive protein present, the molecular weight, concentration and the time the proteins have to absorb on to the surface (Sawyer, Hennessy et al. 2005). Proteins are found to have an interesting nature of altering their conformations in order to maximise the energy they gain from adsorption. If a particular protein conformation is energetically unfavourable, the adsorption will be irreversible (Horbett 2004).

Some proteins can also be desorbed from the surface by other molecules in the solution. This effect is described by the ‘Vroman effect’. The theory states that smaller proteins from the blood plasma have the ability to be displaced by fewer larger proteins that have higher affinities for the surface. Proteins have the ability to induce two types of effects: tendency to

induce apatite formation (eg.fibronectin) or inhibit apatite nucleation (eg.albumin) (Daculsi, Pilet et al. 1999, Green, Davies et al. 1999, Gugala and Gogolewski 2004).

Several factors can alter the behaviour of proteins, these include: supersaturation ratio of the solution, the local concentration of the co-precipitating ions, the presence of other proteins and finally whether the proteins are free or whether they have been immobilised. Adsorption of proteins can be promoted or opposed by a number of factors, including; dehydration of proteins or the surfaces, conformational changes of the proteins themselves and whether there are charged groups present at the interface (Wilson, Clegg et al. 2005).

There have been many studies conducted investigated the adhesion and influence of proteins on HA and SA. It has been proposed that the presence of a protein layer on HA and SA acts as a dissolution barrier, this in turn prevents ions from diffusing directly from the SA surface to the solution. Botelho found that the dissolution of SA in the presence of serum free SBF started at earlier time points and from AFM images, the dissolution on the grain boundaries and grains are clear, therefore forming an apatite layer in a shorter period of time (Botelho, Brooks et al. 2011). However, research by Guth et al, looked at similar affects using serum containing and serum free MEM and found that under physiological conditions the reservoir for exchangeable ions in both HA and SA in the absence of serum proteins facilitated greater ionic exchange particularly with 0.8wt% SA. This supported previous findings that substituting silicon into the HA lattice facilitates a number of ionic interactions between the medium and surrounding physiological environment, including but not limited to silicate ion release, which may play a crucial role in determining the overall bioactivity of the material. The study also showed that there was not a significant net release of calcium and phosphate was not observed, therefore a rapid or significant net dissolution of the material is not necessarily a prerequisite for the bioactivity in these materials (Guth, Campion et al. 2011).

Adsorption and protein concentration is seen to increase over time until a monolayer coverage is obtained on the material surface. This may be true of the adsorption of individual proteins therefore it can be suggested this is also expected for the adsorption of multiple proteins on the surface of a biomaterial (Noh, Yohe et al. 2008). It has also been shown that adsorption of proteins is confined to the number of binding sites that are available on the surface of the material specific to each individual proteins. As a result the rate at which adsorption takes place would be affected over time. Therefore it can be concluded that it is difficult to define the relation between adsorption rate and proteins as there are many different proteins that are present.

Findings by Guth et al in 2011 were in agreement with earlier work conducted by Rashid et al in 2005 whereby, different levels of silicon (0.4, 0.8 and 1.5wt%) and how they directly influenced protein adsorption were studied. Complete DMEM with 10% FCS was used to incubate the materials for a certain period of time. It was found that the proteins from the serum were absorbed within 10 minutes of incubation time. The amount of protein that was absorbed by the 0.8wt% SA was significantly higher at 12 and 24 hours of incubation than any of the other materials used. In addition to this the percentage of cell coverage was also seen to be higher at 0.8wt% SA than on the other materials studied. These results in turn demonstrated that the capacity for a surface to absorb proteins is reflected by its potential to support quick cellular response at the surface (Rashid, Buckland et al. 2005).

Castagna, conducted a study assessing fibronectin behaviour on bone scaffolds. Protein adsorption experiments were performed on dense discs (HA and SA) and porous granules (HA80/20, SA80/20 and SA80/30). Each of the samples were incubated in two different concentrations of fibronectin, Fn1:0.1mg/ml and Fn2: 0.25mg/ml. Samples were taken at 1, 5, 10, 15, 30 & 60 minutes. It was found that the incorporation of silicon along with the porous structure enhanced Fn absorption using the higher Fn concentration (Castagna 2014). These findings were in agreement with previous work conducted by Guth et al whereby microporous HA and SA discs were developed with matched porosity and surface morphology in order to identity whether porosity and silicate substitution effect protein adsorption. Adhesion proteins such as fibronectin and vitronectin were used. It was confirmed that the microporous SA discs had a greater affinity for both proteins compared with HA, suggesting differences in the mechanism behind the surface affinity to SA (Guth, Campion et al. 2010).

1.3.2.3 Ion Release

The dissolution and re-precipitation of ions was first introduced to explain the behaviour of the highly soluble bioglasses. It has been found that bioactive glasses are a good candidate for bone repair and regeneration because when immersed in a physiological solution, bioglass can form an amorphous CaP layer which then crystallises to hydroxyl carbonate apatite which has a similar chemical composition and structure to the mineral phase of human bone (Mami, Lucas-Girot et al. 2008, Dietrich, Oudadesse et al. 2009, Bui, Oudadesse et al. 2012).

It is accepted that when bioglass comes into contact with any growth medium, it causes bioglass to dissolve by the action of hydrolysis. Phosphate and calcium ions are released

from the surface of the material. This then causes the concentration of ions to increase around the implant. This area becomes favourable for the precipitation of an apatite layer, which in turn makes the implant bioactive (Bagambisa, Joos et al. 1993). There is an increase in the phosphate and calcium ions in the spaces found between the bone and implant. Precipitation of HA within these spaces will incorporate the existing bone and the implant and ensure the osteointegration of the implant (Weng, Liu et al. 1997). Proteins are readily absorbed onto the formed apatite layer and have the ability to signal and promote cell adhesion. Osteoblasts in particular are associated with bone bonding. It has been stated that three main changes occur when looking at the effects of dissolution. These are as follows: (LeGeros, Parsons et al. 1988)

1. Physical changes: porosity, crystallinity, grain size, crystal size and surface area.
2. Chemical changes: ion substitutions and therefore a change in composition.
3. Biological changes: degree of bone contact, type of bone, changes in cell mediating factors such as osteoclasts, macrophages etc.

Habibovic proposed a mechanism flow chart by which osteoinduction occurs by biomaterials. The flow chart takes into consideration all biomaterials whether or not they are CaP containing biomaterials. Figure 1.6 summarises the dissolution and protein adhesion process by which new bone is formed (Habibovic, Yuan et al. 2005).

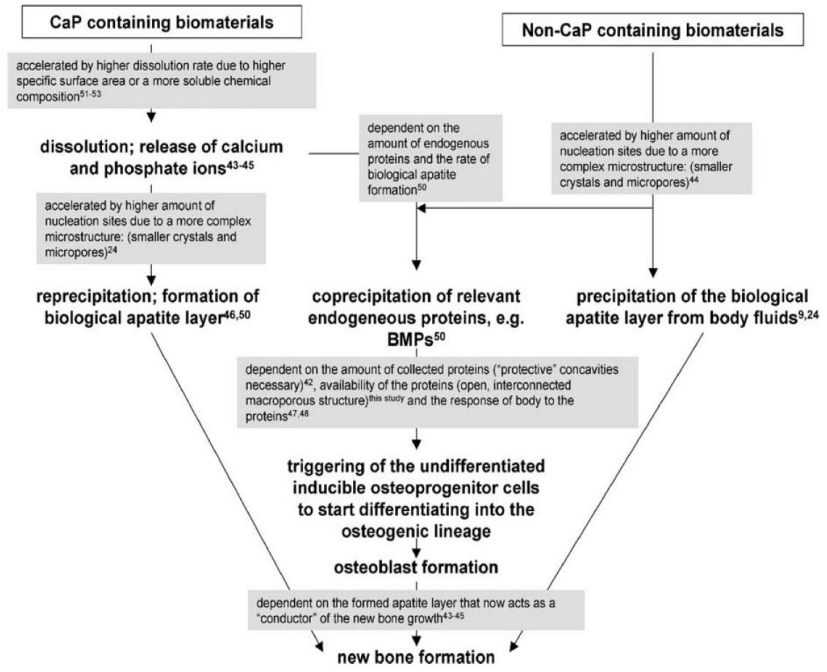

Figure 1.6: Flow chart of the proposed mechanism of osteoinduction by biomaterials (Habibovic, Yuan et al. 2005)

Studies conducted on the dissolution behaviour regarding HA and SA calcium phosphate implants, suggest that there are many proposed mechanism underlying the phenomenon of the osteoinductive nature of these materials. Many intrinsic properties such as, pore size, pore connectivity and pore volume along with functional characteristics such as, permeability and dissolution of materials affect many components of the bone formation process, suggesting that the mechanisms behind osteoinductivity are very complex and have not yet been fully understood (Barradas, Yuan et al. 2011, Campion 2015).

It was found that Ca, P and Si ions diffuse through the bioceramic grains to the HA and bone interface, which is driven by a concentration gradient. The increased concentration of ions speeds up the precipitation of the apatite, which in turn will induce bone apposition at the surface of the implant. Further, these observations may explain the mechanism by which bioactivity is increased with the incorporation of silicate ions. However there still needs to be further work to determine the rate at which silicon was released.

Porter conducted an *in vivo* study observing the dissolution behaviour from HA, 0.8 and 1.5wt% SA implants after 6 and 12 weeks. The study used high-resolution transmission electron microscopy (HR-TEM) to compare dissolution at defect structures within the samples used. They hypothesised that the incorporation of silicate ions into the HA lattice would increase its bioreactivity by increasing the number of defect structures present. The defect structures are site specific within the HA ceramic, therefore by increasing the number of defect structures the solubility of the HA ceramic is increased and so is its rate of osseointegration. The observations confirmed that defects, in particular those involving grain boundaries were the starting point of the dissolution process *in vivo*. Dissolution was first seen in the 1.5wt% SA, 0.8wt% SA and finally HA implants, therefore suggesting that there is a higher rate of dissolution with an increase in Si content. The dissolution was found to be most prevalent at grain boundaries and also triple junctions (Porter, Patel et al. 2003).

Many studies have shown that the bioactivity of HA bioceramics is dependent on the microstructure and on the number and type of defect structures that are present (Nelson, McLean et al. 1983, Daculsi, Legeros et al. 1989). Daculsi compared the dissolution of phosphate and calcium ions from HA and also bone apatite. Like Porter, the study showed that the process of dissolution was initiated at grain boundaries and dislocations present *in vivo*. It has also been highlighted that defects play a role in the dissolution behaviour of HA and SA bioceramic implants. The defect type is found to be an important factor which in turn influences the rate of dissolution. Grain boundaries that are incoherent and are without lattice continuity may be more sensitive to dissolution (Wen and Liu 1998).

Porter et al also used ovine models to implant HA and SA grafts of 1-2mm in size. It was revealed that the SA and bone interface showed organised collagen fibrils at 6 weeks, whereas the same effect was seen at 12 weeks with the HA and bone interface. This suggests that SA is able to develop a new apatite phase on the surface, which is in contact with the physiological fluids faster than HA does. This study showed the increased bone apposition with the use of SA, therefore an increased bioactive behaviour. They also suggested that this fact was related to the higher dissolution rates of the SA implants compared to the pure HA implants. This is because there is an increase in the number of defects in SA, which help the osteoconductive properties. Therefore the authors suggest the use of SA implants in comparison to HA implants (Porter, Patel et al. 2004).

It has been shown that the dissolution of silicon in to tissue culture medium is at detectable levels with in semi-dynamic condition. Following investigations using HOB cells within the same set up, showed that an increase in the collagen I production was immediate with the presence of silicon in the medium (Guth, Buckland et al. 2006). The study confirmed that there is an importance of silicon with the stimulation of osteoblastic development. Higher silicon content appears to promote rapid bone mineralisation and have great HOB cell growth, since large amounts of phosphate mineral development has been observed in some studies (Balamurugan, Rebelo et al. 2008).

It has been found that grain size plays an important role in bone apposition due to the difference in size between the silicate and phosphate ions, which in turn cause a decrease in grain size. Observations have demonstrated that the dissolution of the smallest grains of triple junctions have suggested that a decrease in grain size can increase the solubility of the material. Scanning electron microscopy (SEM) results have showed a significant decrease in grain size in SA when compared to HA. This decrease the grain size, could therefore present another potential mechanism by which the silicate ions increase the *in vivo* bioactivity of SA implants (Patel, Follon et al. 2003). Grain boundary structures have been shown to have an influence on the dissolution behaviour of many biological apatites. A mass exchange between inorganic ions and protein molecules have also observed (Wen and Liu 1998).

Rapid dissolution and a net release of calcium and phosphate ions from the apatite matrix acts as a precursor to subsequent re-precipitation on bone-like apatite at the surface in order to facilitate ion exchange in biochemical processes. It has been shown that under physiological conditions the exchangeable ions available within HA and SA in the absence of serum proteins is limited however, the presence of serum proteins facilitates greater ionic exchange particularly with SA (Chana 2010, Guth, Campion et al. 2011). This in turn

supports observations that the dissolution and re-precipitation of ions play a key role in determining the bioactivity and osteoconductivity of biomaterials. A recent study using bioactive bioglass showed that a change in media characteristics affects glass dissolution and apatite formation therefore these factors need to be taken in to consideration when interpreting results from ionic dissolution or cell culture studies (Shah, Brauer et al. 2014).

1.3.2.4 Macro and Microporosity

For over 30 years, porous ceramics have been used as synthetic bone graft substitutes. Many studies have shown that with an increased macroporosity there is a greater and faster degree of bone penetration (Kuehne, Bartl et al. 1994). This can be related to the volume available for bone ingrowth and the interconnectivity of the structure. Bone is a mineralised tissue which requires an internal blood supply. Formation of new bone or any repair must be followed by the formation of a vascular network also present between pores (Rubin, Popham et al. 1994). This statement has been demonstrated by the penetration of bone in porous implants, which have larger pore interconnection sizes. It has also been observed that there is improved integration within the porous scaffolds which have smaller, well connected porosity in comparison to scaffolds with larger and more isolate pores (Kilpadi, Sawyer et al. 2004).

Bone functionality responds to external mechanical stimuli which regulates many cell types including osteoblasts and osteocytes, they have also been shown to mediate osteoblastic differentiation. Therefore it is possible to see whether local strain within the scaffolds struts induce or inhibit bone formation. This in turn would mean that scaffold porosity could be responsible for regulating bioactivity. However the volume of bone regeneration maybe dependant on features of macroporosity (Hing, Annaz et al. 2005). There have been some recent studies *in vivo* and *in vitro* that have seen biological sensitivity to the level of microporosity (Annaz, Hing et al. 2004, Hing, Saeed et al. 2004). This would suggest that in the long term there is an influence of both macroporosity and microporosity on bone adaption (Hing, Annaz et al. 2005). Annaz et al showed that cells are able to sense the microporosity and respond to this by orienting protruded filipodia towards the micropores (Annaz, Hing et al. 2004).

Porous materials help in forming the interlock between the material and the bone. It is able to reduce the amount of motion between the tissue and the implant; therefore studies have shown that increasing the porosity means higher level of bone apposition (Hing, Annaz et al. 2005). Interconnections between pores are necessary in order to promote body fluid

circulation and also cell migration. Most of the time interconnectivity of commercial bone substitutes is not quantified. High porosity content seems to favour bone ingrowth as macropores can be colonised immediately. However it must be remembered that increasing the porosity or size of pores will affect the mechanical properties drastically (Bignon, Chouteau et al. 2003). Some studies have shown there to be an increase in bioactivity whereas in some cases it has led to improved osteointegration. The main concern with porosity is controlling the extent of porosity needed for the application.

Micropores expose more material with a higher surface area to volume ratio; this in turn influences protein adhesion. In an *in vivo* study, Holmes demonstrated that HA microporous implants are able to act successfully as a BGS (Holmes and Hagler 1988) and increased the bioactive behaviour of materials (Rouahi, Gallet et al. 2006). A study conducted by Hing et al (2005), looked at whether or not microporosity enhances bioactivity of synthetic bone graft substitutes. The research described an investigation into the influence of microporosity on early osseointegration and final bone volume with porous HA. Four samples were used HA70-1, HA70-2, HA80-1 and HA80-2. Two of the samples had a nominal total porosity of 70% and the other two of 80%. Within each of the total porosity paired grades the microporosity within the HA struts was varied with HA70-1 and HA80-1 having 10% and HA70-2 and HA80-2 having 20% strut porosity. Cylindrical specimens were implanted in the femoral condyle of New Zealand white rabbits. The specimens were then retrieved for analysis at 1, 3, 12 and 24 weeks. The distribution of porosity had a significant effect on the pattern of osseointegration. Together the results indicated that manipulation of the levels of microporosity within a substitute can be used to increase osseointegration and elevate the equilibrium volume of bone (Hing, Annaz et al. 2005).

When investigating the differences in the levels of microporosity, there have been some *in vivo* studies which have found that with a greater level of microporosity, osteointegration is enhanced (Hing, Saeed et al. 2004, Campion, Chander et al. 2011). However, in a recent study, Castagna found that having a lower microporosity (SA80/20) enhanced a better proliferation response compared to the higher strut porosity (SA80/30) (Castagna 2014).

A higher osteogenic potential of SA with a greater strut porosity has been previously demonstrated with *in vivo* studies (Hing, Saeed et al. 2004, Campion, Chander et al. 2011, Coathup, Samizadeh et al. 2011, Chan, Coathup et al. 2012, Coathup, Hing et al. 2012). Findings by Castagna showed that a change in strut porosity has a significant effect on ALP activity. SA with 30% strut porosity showed increase cell differentiation irrespective of either being pre-treated with fibronectin or not being pre-treated (Castagna 2014).

In vivo studies have showed that a dense collagenous cellular region is found in the centre of some micropores and it appeared that these specific regions gradually got replaced by bone (Coathup, Samizadeh et al. 2011, Coathup, Hing et al. 2012). However the study reported that this was occurring commonly on CaP specimens used in comparison to silicon containing CaP specimens with greater strut porosities.

1.4 *In Vitro* Testing Environments

For many years, *in vitro* testing has consisted of many techniques exploring varying dynamic environments to achieve positive results for bone repair. The three main environments which have been used are; static, semi-dynamic and dynamic environments however, the differentiation between some of these environments has led to misleading interpretations as to what actually is happening during testing within the individual environments.

1.4.1 Static and Semi-Dynamic Environments

It has generally been accepted that experimentation utilising static environments means culturing cells in tissue culture plates for an extended length of time without media changes. A famous example of this type of testing involves SBF testing by Kokubu et al whereby the SBF was not replenished for the duration of the study of over 15 days (Kokubo, Ito et al. 1990, Kokubo, Kushitani et al. 1990). Since then there have been other studies which have also taken this approach in the interest of allowing for cross-comparison of their tests with historical studies. Recently Campion conducted tests in order to understand the effect of strut porosity on the bioactivity of calcium phosphate materials in order to determine the likely impact on the process of osteointegration when implanted into bone. The test materials (SA-23, SA-32 and SA-46) were submerged in SBF for up to 30 days without replenishing the SBF (Campion 2015). The results indicated that the strut porosity of a material substrate should be increased to maximise the potential for the formation of a precursor to bone like apatite after implantation. SA-32 and SA-46 showed a quicker formation of an apatite layer followed by SA-32. The results were also able to confirm that TCP is much less bioactive than SA and therefore likely to facilitate successful osteointegration when implanted in bone.

It is believed that testing under 2D cultures systems, for example on tissue culture plates whereby the media is refreshed periodically is described as a semi-dynamic environment. It is interesting to note that a system using media under static flow conditions whereby the media is not circulating within a system is termed semi-dynamic. There are many studies which perform their tests under these conditions. For example, SBF has been refreshed by

investigators every 12 hours (Lin, Li et al. 2009), every 2 days (Ning and Zhou 2002, Wang, Qu et al. 2008), weekly (Cortes, Medina et al. 2004) or every two weeks (Pirhonen, Niiranen et al. 2006) and has been termed semi-dynamic tests on 2D culture plates. In comparison, a study conducted by Chana in 2010, termed her experiment semi-dynamic whereby, a large volume of media was static however the BGS granules cased in a mesh basket were being rotated using overhead stirrers at a constant rate of 70rpm for the duration of the experiment. It must be noted that due to the shear effects of the stirring mechanism, the fluid that was local to the rotating BGS granules was at a greater rate of velocity than the fluid towards the beaker walls. Therefore the term, semi-dynamic is more suited for this type of experiment (Chana 2010).

Table 1.3 highlights work that has been conducted in order to compare research using static and semi-dynamic environments within *in vitro* testing. From the table it is evident that similar terminology is being used for completely different experimental set-ups. Regardless of whether there is a refreshment of media during a static experimental setup using culture plates, the fluid is not under any movement suggesting a static environment. However within a semi-dynamic environment because there is movement of the sample this creates fluid shear creating movement of the surrounding immediate fluid.

For the duration of this current work, the term semi-dynamic will be used for experiments whereby there is sample movement and the term static will be used for cell culture experiments conducted with regular media refreshments.

Table 1.3: A representative review of *in vitro* studies using static and semi-dynamic environments

Author	Media Refresh	Media/Sample Movement	Authors Description
(Im, Qureshi et al. 2004)	Single media refresh at 24 hours	-	24h, 48h and 72h static study incubating MG63 seeded bisphosphonate in DMEM containing serum in culture plates. Increase in cell proliferation and maturation by the end of the study.
(Porter, Botelho et al. 2004)	-	It was assumed that convection would be sufficient to stir the SBF solutions	5 day static study incubating HA, 0.8wt% & 1.5wt% SA powders in SBF. The site at which dissolution nucleates was at crystal surfaces in SBF. EDX mapping of the SA after 5 days of immersion in SBF demonstrated a preferential loss of silicon in dissolving regions if the ceramic.
(Kim, Lee et al. 2005)	-	-	2hr, 8hr and 4 day static study incubating MG63 cell seeded fluroapatite-polycaprolactone discs in DMEM in culture plates. Regulation of gene expression of both ALP and OC when culturing MG63 cells on fluorine based apatite compared to a non-fluorine based apatite.
(Guth, Buckland et al. 2006)	-	-	14 day static study incubating MG63 seeded 0.8wt% SA microporous discs in DMEM containing serum in culture plates. Silicon release detected within first 24 hours, however levels decreased at 3 and 7 days and subsequently rose again after day 10.
(Guth, Buckland et al. 2006)	Refreshed every 3 days	-	14 day semi-dynamic study incubating MG63 seeded 0.8wt% SA microporous discs in DMEM containing serum in culture plates. Silicon release detected in the surrounding medium within the first 24 hours, but

			subsequently reduced with each change in medium, reaching minimal levels at day 10.
(Raja 2010)	-	SA BGS granules rotating in basket at 70rpm placed in 750ml of static media	9 day semi-dynamic study incubating SA80/20 and SA80/30 in SBF with and without serum. Results showed apatite formation on the SA80/30. Dissolution rate was twice as high for SA80/30 than SA80/20 in serum free SBF. In SBF containing serum dissolution rate of SA80/30 was slower.
(Botelho, Brooks et al. 2011)	-	-	5 day static study incubating 0.8wt% % 1.5wt% SA in serum free and serum containing SBF in culture plates. Slower dissolution observed with serum containing SBF. Dissolution observed at the grain boundaries and also on grains.
(Samy 2011)	-	SA BGS granules rotating in basket at 70rpm placed in 750ml of static media	9 day semi-dynamic study incubating SA80/30 and SA80/45 in EMEM containing serum. The dissolution studies were found to increase the pore size in both samples. The sample with 45% microporosity was also found to dissolve at a higher rate. There was no change to the phase composition of either silicon substituted hydroxyapatite sample after dissolution testing.
(Gyorgyey, Ungvari et al. 2013)	-	-	24hour cell attachment, 72 hour cell proliferation and 3 and 7 days ALP activity static study. MG63 cells seeded on Ti discs laser and not laser treated in DMEM containing serum. It was found that laser treating the Ti discs did not affect cell attachment and proliferation significantly.
(Adams, Mostafa	Refreshed at 72	-	5 day semi-dynamic study incubating HA and carbonate containing HA

et al. 2014)	hours		discs in DMEM containing serum in culture plates. The study saw calcium phosphate rations increase monotonically with an increase in carbonate content however this saw a decrease in differentiating MG63 cells.
(Shah, Brauer et al. 2014)	-	Polystyrene container with glass powder and dissolution medium placed in a temperature controlled shaking incubator at 60rpm	3 & 7 day semi-dynamic study incubating fluoride containing glass BG powder in 4 different media; acetate MEM, HEPES MEM, HEPES carbonate MEM and HEPES serum MEM. Faster apatite formation in acetate buffered MEM. Presence of carbonate resulted in formation of calcite. Presence of serum proteins delayed apatite formation. Results showed that dissolution medium composition is an important factor to consider during *in vitro* experiments.
(Chan, Chang et al. 2015)	Not mentioned	Not mentioned	9 day semi-dynamic study incubating MG63 seeded bicalcium phosphate bioceramic and HA in DMEM containing serum in culture plates. The results showed MG63 cells 'spreading faster' on the surface of the bioceramic in comparison to the surface of the commercially available HA. It was also suggested that the bioceramic can enhance osteoinductivity *in vivo*.
(Meredith and Mallick 2015)	Not mentioned	Not mentioned	13 day semi-dynamic study incubating MG63 cell seeded HA pellets in MEM containing serum in culture plates. Increase in proliferation of MG63 cells observed when seeded in five different HA samples which were produced with varying wall thickness in order to create high-strength scaffolds for bone regeneration.

1.4.2 Dynamic *In Vitro* Environments

The biological environment within the bone tissue is known to be a very dynamic interaction between active cells that experience mechanical forces and a three dimensional matrix that is in continuous change. Therefore, in order to engineer bone tissue constructs *in vitro* it is important to develop culture systems that mimic the *in vivo* biological environment (Kale, Biermann et al. 2000, Lanza, Langer et al. 2000).

The current standard tissue culture techniques that are available are not sufficient for bone tissue engineering purposes. This is due to a lack of efficient transport of nutrients and removal of waste products. This therefore results in a lack of nutrients towards the centre of the scaffold; this in turn leads to cell migration to the surface where fresh nutrients are more available. In the end an uneven distribution of cells throughout the scaffold is obtained. (Bancroft, Sikavitsas et al. 2003, Martin, Wendt et al. 2004).

In order to overcome these problems, the design and development of bioreactor systems is important. A bioreactor can be defined as a device in which biological and/or biochemical processes take place under controlled environmental and operating conditions (Martin, Wendt et al. 2004, Salgado, Coutinho et al. 2004, Ikada 2006). Many bioreactor systems have been developed in order to perfuse cell seeded constructs/ scaffolds (Goldstein 2002, Gomes, Holtorf et al. 2006). Figure 1.7 represents all the bioreactors available for tissue engineering as stated in a review by Martin et al 2004 (Martin, Wendt et al. 2004).

Spinner flasks are very basic bioreactors where by scaffolds which are seeded with cells are attached to needles hanging from the lid of the flask (Figure 1.7a). The scaffolds are then covered by the medium that is mixed with a magnetic stirrer at the bottom of the flask (Bancroft, Sikavitsas et al. 2003, Martin, Wendt et al. 2004). Recently Mygind found that dynamic culture of human MSCs on coralline HA scaffolds using a spinner flask resulted in increased proliferation, differentiation and distribution of cells in scaffolds (Mygind, Stiehler et al. 2007).

Rotating wall vessels (Figure 1.7b) provide a dynamic culture environment to the constructs with low shear stresses and high rates of mass transfer. The walls of the vessel rotate such that they enable the drag force (F_d), centrifugal force (F_c) and net gravitational force (F_g) on the construct to be balanced. The construct is said to be in a state of free-fall through the culture medium (Martin, Wendt et al. 2004). The most common rotating wall vessel bioreactor is composed of two concentric cylinders. The cell seeded scaffolds are placed in

the annular space between the cylinders. The outer cylinder is impermeable and rotates in a controlled manner while through the inner stationery cylinder gas exchange is allowed. Having selected the appropriate rotational rates, the free falling of the scaffolds inside can be balanced by the centrifugal forces due to the rotation of the outer cylinder. This therefore creates a microgravity-like culturing condition with laminar rotational flow fields and a low fluid shear stress (Bancroft, Sikavitsas et al. 2003, Martin, Wendt et al. 2004).

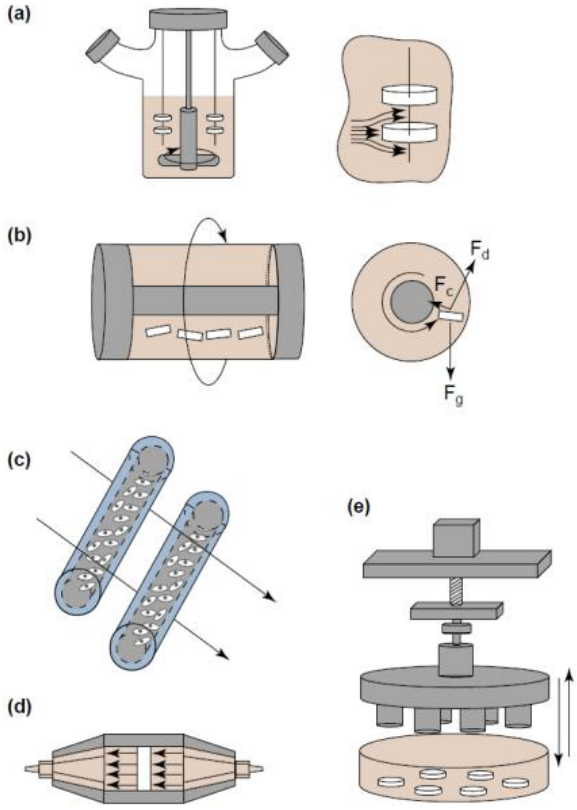

Figure 1.7: Representative bioreactors for tissue engineering applications. (a) Spinner-flask bioreactors, (b) Rotating-wall vessels, (c) Hollow-fiber bioreactors, (d) Direct perfusion bioreactors and (e) Bioreactors that apply controlled mechanical forces. (Martin, Wendt et al. 2004)

A study was conducted by Sikavitsas and team which directly compared the performance of spinner flasks and rotating wall vessel bioreactors to static cultures (Figure 1.8). PLGA scaffolds were seeded with MSCs from rats and cultured in six-well plates (static culture), spinner flasks and rotating wall vessel bioreactors for up to 21 days. The results showed that the constructs cultured in spinner flasks obtained higher proliferation rates and increased osteogenic differentiation. On the other hand, constructs cultured in the rotating wall vessel displayed minimal osteogenic differentiation which the authors attributed to collisions of the constructs with the walls of the rotating bioreactor. In all three culture systems, a dense

cellular layer on the surface of the scaffolds and a considerably lower cell distribution in the inside of the scaffold was revealed by histology, suggesting that the transport of nutrients to the interior of the scaffolds was limited to diffusion in all the cultures. It was concluded that improved tissue culture conditions were needed in order to permit cellular growth throughout tissue-engineered constructs (Sikavitsas, Bancroft et al. 2002).

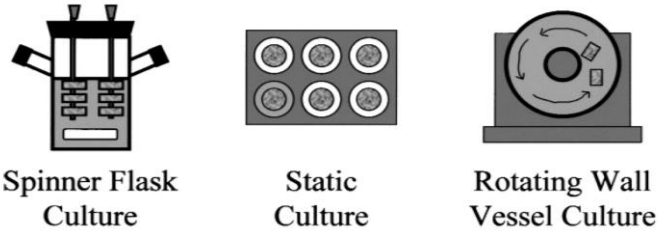

Figure 1.8: Types of bioreactors being used in bone tissue engineering (Sikavitsas, Bancroft et al. 2002)

Hollow- fiber bioreactors can be used in order to enhance mass transfer during the culture of highly metabolic and sensitive cell types, such as hepatocytes (Figure 1.7c). Cells are embedded within a gel inside the lumen of permeable hollow fibers and then the medium is perfused over the exterior surface of the fibers (Jasmund and Bader 2002).

Direct perfusion bioreactors in which medium flows directly through the pores of the scaffold type can be used for either seeding and/or culturing 3D constructs (Figure 1.7d). This type of bioreactor is used for bone tissue engineering applications as it offers an improved as well as enhanced transport of nutrients to the interior of 3D scaffolds. This advantage comes from the fact that this bioreactor delivers medium through the interconnected pores of the scaffold. In these bioreactors, the seeded scaffolds are confined inside a chamber with the appropriate dimensions in order to force the continuously pumped culture medium flow through the interconnected porous network and not around it, as illustrated in (Xu, Du et al. 2008) resulting in an improved cellular distribution.

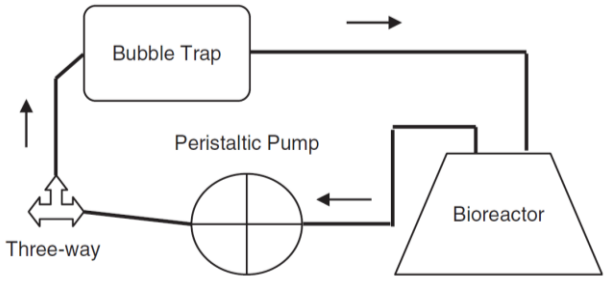

Figure 1.9: Schematic of a perfusion system used by Xu et al for media through cylindrical scaffolds (Xu, Du et al. 2008)

Another advantage of perfusion systems is that they provide mechanical stimulation to the cells by way of fluid shear stress. This is a very important advantage as it can have the ability to mimic the mechanical environment in which bone cells live. Different designs can be found in the literature. However, all of perfusion systems present the same components: a pump to deliver the flow of culture medium, a bioreactor chamber in which the construct is fitted, media containers and a tubing system (Bancroft, Sikavitsas et al. 2003). Some of them incorporate a seeding loop for dynamic cell seeding of the scaffolds (Zhao and Ma 2005). Several types of scaffolds have been seeded with different cell types and cultured in flow perfusion systems for bone tissue engineering purposes. Zhao and Ma used non-woven poly(ethylene terepthalate) fibrous matrices with human MSCs, the same cells that Bjerre et al. seeded on silicate-substitute tricalcium phosphate scaffolds (Zhao and Ma 2005, Bjerre, Bunger et al. 2008). Both these studies were successful in showing the increased proliferation, osteogenic differentiation and cell distribution under flow perfusion culture. Perfusion bioreactor systems are also being used in intestinal tissue engineering (Kim, Penkala et al. 2007), maxillofacial tissue engineering (Depprich, Handschel et al. 2008) and cardiac tissue regeneration (Dvir, Benishti et al. 2006).

Bioreactors that apply controlled mechanical forces are also being used within tissue engineering (Figure 1.7e). These type of bioreactors can apply forces such as dynamic compression to the engineered constructs. They can also be used in order to model systems of tissue development under physiological loading conditions and to generate functional tissue grafts. Compressive forces can also be applied by a computer controlled micro-stepper motor. This allows the constructs to be loaded and the stress on the constructs can be measured using a load cell (Demarteau, Jakob et al. 2003, Demarteau, Wendt et al. 2003).

There is a significant barrier in our understanding of bone physiology at the cellular level because there is alack in methodology in order to study bone cells in their native environment. There is a vast amount of work that has been carried out focussing on the empirical responses of individual cell types to mechanical and chemical stimuli but there are only a few studies that have taken this further in order to understand and determine material specific responses driven by cellular response. There needs to be further research that integrates the influence of substrate chemistry and osteoinductivity in order to understand cell behaviour within the *in vivo* environment. Table 1.4 highlights work that has been conducted in order to look at fluid flow using bioreactor systems and the effect on cellular behaviour.

Table 1.4: A representative review of *in vitro* studies of fluid flow within bioreactor systems and their effect on cellular behaviour

Author(s)	Cell Type	Scaffold Used	Bioreactor / Stimuli	Monitored Response	Observations
(VunjakNovakovic, Freed et al. 1996)	Isolated chondrocytes	Biodegradable polymer scaffolds made of fibrous polyglycolic acid discs	Spinner flasks used as bioreactor	Cell proliferation, total collagen, GAG	Turbulent mixing significantly improved the biochemical compositions and altered morphologies of the constructs. Mixed constructs contained up to 70% more cells, 60% more GAG and 125% more total collagen in comparison to static cultures.
(Botchwey, Pollack et al. 2001)	Human osteoblast-like cells, SaOs-2	Hollow, 'light-than-water' mocrocarriers of degradable poly(lactic-co-glycolic acid)	Rotating bioreactor with velocity of 98mm/s	ALP activity, DNA content, SEM and calcium quantification	Cell proliferation was not significantly increased in comparison to non-rotating static controls. In fact there was a significant decrease in cell number by day 7 of the bioreactor culture. In contrast the development of osteoblastic phenotype was enhanced in the cells as determined by ALP expression accompanied by an elevation in early stage mineralised matrix production by cells by day 3.
(Bancroft, Sikavitsast et al. 2002)	Rat marrow stromal osteoblasts	Titanium fiber mesh scaffolds	Flow perfusion systems using 0.3, 1 and 3ml/min flow	DNA content, ALP activity, Osteopontin measurement,	Mineralised matrix production increased with static cultures with total calcium content of cultured scaffolds increasing with an increase

			rates	Osteocalcin, Calcium content, SEM and light microscopy	in flow rates. Flow perfusion induced *de novo* tissue modelling with the formation of pore like structures in scaffolds and enhanced the distribution of cells and matrix throughout the scaffolds.
(Sikavitsas, Bancroft et al. 2002)	Rat marrow stromal osteoblasts	75:25 poly(D,L-lactic-co-glycolic acid)	Spinner flask and Rotating wall vessel Bioreactors	ALP activity, DNA content, Osteocalcin, calcium deposition and histology.	Spinner flask culture demonstrated a 60% enhanced cell proliferation. At day 14 all cell/polymer constructs exhibited their maximum ALP activity. Total osteocalcin secretion in spinner flasks was 3.5 times higher than static cultures. There was no considerable ALP activity and osteocalcin secretion detected in the rotating wall vessel culture throughout 21 day study.
(Cartmell, Porter et al. 2003)	MC3T3-E1 osteoblast-like cells	Human trabecular bone scaffolds	Flow perfusion system using 0.01,0.1,0.2 and 1ml/min flow rates	ALP activity, DNA content, Osteocalcin, and osteoblastic gene expression	Confocal microscopy indicated that 1ml/min flow rate resulted in substantial cell death. Increase in cell proliferation using 0.01ml/min flow rate relative to 0.2ml/min and static controls. ALP, osteocalcin, mRNA and Runx2 were upregulated at 0.2ml/min compared to the lower flow rates.

(Sikavitsas, Bancroft et al. 2003)	Rat marrow stromal osteoblasts	Titanium fiber meshes with 86% porosity.	Flow perfusion system at 0.3ml/min	DNA content, ALP activity, calcium deposition, SEM	Increase in the media viscosity resulted in an increase in mineralised matrix deposition. An increase in ALP activity was observed under perfusion culture in comparison to static controls. An increase in fluid shear forces led to an increase in mineral deposition suggesting that mechanical stimulation provided by fluid shear forces within 3D perfusion culture can enhance expression of osteoblastic phenotype.
(Wang, Uemura et al. 2003)	Rat marrow stromal osteoblasts	β-TCP blocks with 75% porosity	Flow perfusion system at 2ml/h flow rate	ALP activity, osteocalcin, histology	Significantly higher ALP activity and osteocalcin levels observed in the perfusion group than in the control group both *in vitro* and *in vivo* Histomorphometric analysis revealed higher average ratio of bone to pore in the cell seeded scaffolds in the perfusion group at 4weeks and 8 weeks of implantation.
(Holtorf, Sheffield et al. 2005)	Rat marrow stromal osteoblasts	Porous CaP cylindrical scaffolds: 60% HA/40% β-TCP	Flow perfusion system at an initial ~0.3ml/min flow rate to allow for good cell	ALP activity, osteopontin, histology and SEM	Good cell distribution throughout entire scaffold by 16 days of perfusion culture in comparison to static controls. Greater osteoblastic differentiation and osteopontin

			attachment for 1 day thereafter increased to 1ml/min for the duration of culture		secretion observed in scaffolds within perfusion culture in comparison to static cultures.
(Zhao and Ma 2005)	Human MSCs	Non-woven PET fibrous matrices	Flow perfusion system at 0.1ml/min flow rate	DNA content, lactate and glucose measurements, histology,	Increase in cell density observed over 40 days culture in comparison to static cultures. Increase in differentiated cells within perfusion cultures over study.
(Gomes, Holtorf et al. 2006)	Rat marrow stromal osteoblasts	30:70wt% blend of strach with poly(ε-caprolactone) fiber meshes	Flow perfusion system at 1ml/min flow rate	DNA content, ALP activity, calcium content, SEM, FTIR and thin-film XRD	ALP activity higher in flow cultures but only for the cells cultured on to the higher porosity scaffolds. Calcium deposition patterns were found to very similar for all scaffolds showing greater calcium deposition on cell/scaffold constructs under flow perfusion in comparison to static cultures. Thin-film XRD showed presence of mineralised matrix similar to that of bone on the cell/scaffold constructs after 15 days of culture under flow perfusion.
(Janssen, Oostra et al. 2006)	Goat bone marrow	Biphasic calcium phosphate scaffolds	Flow perfusion system at 4ml/min	MTT assay, SEM, EDX,	After 19 days of cultivation the scaffolds were covered in a viable, homogeneous cell

	stromal cells		flow rate		layer. On line oxygen measurements during cultivation were correlated with proliferating cells therefore showing that oxygen consumption can be used to estimate cell population doubling times during growth within the bioreactor systems created.
(Mygind, Stiehler et al. 2007)	Human MSCs	Coralline HA scaffolds of 200 and 500µm pore sizes	Spinner flasks	DNA content, ALP activity, histology, SEM and total RNA extraction	Faster rate of osteogenic differentiation observed with 200µm pore scaffolds. 500µm showed increase proliferation rates and accommodated higher number of cells.
(Zhao, Chella et al. 2007)	Human MSCs	Porous 3D PET matrices	Flow perfusion system at 0.1 and 1.5ml/min flow rates	DNA content, ALP activity, calcium deposition and western blot analysis	Higher flow rate up regulated osteogenic differentiation potential at day 20 along with greater calcium deposition in the matrix.
(Xu, Du et al. 2008)	Sheep MSCs	Porous β-TCP scaffolds	Flow perfusion system at 3ml/min flow rate	Cell growth, histology and computational fluid dynamics (CFD)	Fluid velocity and shear stress were found to correspond to increased cell proliferation within cell seeded constructs. Histological data shows cell proliferation rates are different throughout the whole scaffolds.
(da Silva, Mateescu et al.	Human osteoblast-	Pure HA and SiHA tablets	Flow perfusion system, at 2ml/h flow	ALP activity, MTT assay	Faster adhesion of cells under dynamic conditions on SiHA samples. Increase in cell

2010)	like cells, SaOs-2		rate		proliferation and ALP activity on both samples under dynamic conditions.
(Janssen, van Dijkhuizen-Radersma et al. 2010)	Human bone marrow stem cells	Biphasic calcium phosphate scaffolds	Flow perfusion system at 4ml/min flow rate	MTT assay, ALP activity, collage-I assay, SEM and EDX	Cell differentiation towards osteogenic lineage observed by collagen-I production and ALP expression. There were no significant differences in osteogenic gene expression profiles between static and dynamic conditions.
(Bjerre, Bunger et al. 2011)	Telomerase-elongated human MSC	Pro Osteon scaffolds (Coralline HA scaffolds)	Flow perfusion system, 16 parallel flow chambers, each supplied with medium via peristaltic pump at 0.1ml/min flow rate	ALP activity, live/dead staining, SEM, Histology	Adhesion and proliferation of cells observed during perfusion culture. In comparison to previous study using spinner flasks as bioreactor systems, perfusion study did not enhance osteogenic properties of cell/scaffold constructs.
(Kim and Ma 2012)	Human MSC	PET discs	Flow perfusion system at 0.2ml/min flow rate	ELISA and immustaining, DNA content, ALP activity, calcium deposition, RT-PCR, CFU-F	Looked into configuring flow patterns of the media flow within the perfusion system in order to investigate characteristics of hMSCs cellular environment. Parallel flow preserved hMSC proliferation and progenicity potential whereas transverse flow induced hMSC

					osteogenic differentiation with higher ALP activity and calcium deposition and up-regulation of osteogenic bone markers.
(Wang, Ma et al. 2014)	Osteoblasts from calvaria 1 day old New Zealand White Rabbits	β-TCP scaffolds	Flow perfusion system with cell seeding at 1ml/min then 0.5ml/min for 1 day to allow better attachment of cells and finally 2ml/min flow rate for the duration of culture	MTT assay, ALP activity, histology, glucose consumption	Better biological properties seen with cell seeded scaffolds within flow perfusion system with higher daily D-glucose consumption, increased cell proliferation and differentiation and cell distribution.
(Schmelzer, Finoli et al. 2015)	Human bone marrow mononuclear cells	HA coated porous polyurethane scaffolds	Flow perfusion system at 15ml/min flow rate then fresh media continuously fed into system at 2ml/h.	Immuno-histochemistry, SEM, flow cytometry, colony forming unit assay, cell viability assay and lactate and glucose measurements.	Cells in bioreactor were metabolically active during long-term culture and improved colony formation unit capacity of hematopoietic progenitors. HA scaffolds did not influence colony formation capacity, percentages of cell type specific fractions, gene expression, cell viability or metabolic turnover in comparison to control cells cultured in bioreactors without scaffolds.

1.5 Direction of Study

SA has proven to be a clear and successful contribution of material science to the medical world. These changes in HA have led to an improvement in the properties and the structure of SA has helped in understanding the mechanism that makes SA a better implant than pure HA. However, the mechanism by which the bioactivity is increased with SA has not yet been fully understood. It also needs to be highlighted that not all bone defects can be treated with the same material. More or less reactive implants will be required for these purposes and this depends on the type and kind of bone defect with regards to the age of patient and anatomical site. By understanding and also controlling the silicon incorporation, there is a chance to tailor specific CaP based implants for each individual scenario. The various groups that have been working on silicon substituted calcium phosphates have given rise to many mechanisms by which bioactivity of these materials has tried to be explained. Some authors have looked into the formation of apatite layers and how fast they form whilst others have looked into the release of Si ions and protein adhesion.

The key to the development of next generation BGS is to understand mechanisms behind both substrate chemistry and strut-porosity modulation of cell response through alteration of niche chemistry within the graft porosity. This will therefore help in trying to unlock the mechanisms behind osteoinductivity in the *in vivo* environment.

This project aims to develop a system in order to monitor cell response and ionic exchange within a 3D flow perfusion environment. This will enable informed interpretation of the *in vitro* performance of 3D culture of cells on HA and SA granules packed into a perfusion chamber with altered chemistry and strut porosity. In order to study this a series of sequential experiments have been carried out and are presented in this thesis in the following chapters.

Chapter 2 - Material Characterisation

Chapter 3 - Ionic Dissolution

Chapter 4 - Dynamic Ionic Exchange within a 3D Perfusion System and its Effect on Osteoblast-like Cell Response

Chapter 5 - Influence of Media Replenishment and Media Stirring on Dynamic Ion Exchange and Subsequent Cell Response

Chapter 6 - Effect of Complete Media Replenishment on Dynamic Ion Exchange and subsequent Osteoblast-like Cell Response

Chapter 7 - Effects of a 'to waste' Flow Perfusion System with Different Media Compositions on Dynamic Ion Exchange and Subsequent Cell Response

Chapter 8 - Effects of Serum Containing Media on Dynamic Ion Exchange and Subsequent Cell Response with HA and SA

Chapter 9 - Investigating Cell Seeding Density and Seeding Methods

Chapter 10 - Influence of dynamic fluid flow on ion exchange and cell response within a 3D perfusion culture system.

Chapter 11 - Summary of Findings and Future work.

Chapter 2 Materials Characterisation

Many studies have shown the importance of the physical and chemical properties of biomaterials and their ability to influence cellular behaviour both *in vitro* and *in vivo*. These materials properties include porosity, topography and surface chemistry (Gibson, Best et al. 2002, Annaz, Hing et al. 2004, Hing, Annaz et al. 2005, Coathup, Hing et al. 2012, Chan, Chang et al. 2015). Therefore it is of great importance to fully characterise any test scaffold, to enable the systematic study of *in vitro* behaviour and any materials characteristics. Hydroxyapatite (HA) has been used as a biomaterial since the early 1970's in order to repair, augment and replace bone. In 1971, HA was first used in bulk for dental restorative surgery (Monroe, Votava et al. 1971). Since the first medical application of HA, the importance of structure and chemistry of synthetic calcium phosphate based biomaterials has been extensively researched. Porous HA scaffolds have also been successful in showing full integration and exhibiting bony ingrowth, vascularisation and bone marrow stroma within the internal pores when implanted in to the femoral condyle of New Zealand white rabbits at 3 months after implantation (Hing, Best et al. 1997). When investigating the differences in the levels of microporosity especially between SA80/20 and SA80/30, there have been some *in vivo* studies which have found that with a greater level of microporosity, osteointegration is enhanced (Hing, Saeed et al. 2004, Campion, Chander et al. 2011, Coathup, Samizadeh et al. 2011, Chan, Coathup et al. 2012, Coathup, Hing et al. 2012).

Stoichiometric Hydroxyapatite (HA) and Silicon Substituted Hydroxyapatite (SA) granules were provided by ApaTech Limited, UK. The SA granules provided were of two different strut porosities. The materials used are highlighted in Table 2.1.

The synthesis of SA is based on the preparation of a stoichiometric HA using an aqueous acid-base neutralisation precipitation reaction between calcium hydroxide, $Ca(OH)_2$, and orthophosphoric acid, H_3PO_4. The orthophosphoric acid is added drop wise to an aqueous solution of calcium hydroxide at a greater pH. In this reaction the silicates replace the phosphates from HA. The reaction is carried out at room temperature with the pH maintained at 10.5. When the reactants have completely mixed, the suspension is left overnight to age. The resulting precipitate is filtered and dried at 80^{o}C overnight. The filtered substance is then ground up, milled and finally sieved to give silicon apatite powder. The material is then further processed and sintered at 1200-1300^{o}C for 2 hours.

Table 2.1: Summary of BGS used in this thesis

BGS granules	Description and Granule Size	Nominal total porosity (%)	Nominal strut-porosity (%)
HA80/20	Stoichiometric hydroxyapatite granules (1-2mm)	80	20
SA80/20	0.8wt% Silicon, Silicate-substituted hydroxyapatite granules (1-2mm)	80	20
SA80/30	0.8wt% Silicon, Silicate-substituted hydroxyapatite granules (1-2mm)	80	30

Figure 2.1: Images of granules received & tested a) HA80/20, b) SA80/20 & c) SA80/30

2.1 Materials Characterisation

X-Ray Diffraction (XRD)

XRD is a technique which is used to characterise crystallographic structure, grain size and also look into the preferred orientation in polycrystalline or powdered solid samples. It is commonly used to identify unknown substances and may also be used to characterise heterogeneous solid mixtures to determine the relative abundance of crystalline compounds in order to provide structural information on materials. The technique works on the basis of Braggs Law which was derived by Bragg in 1913. XRD diffractometer, Siemens Xpert-Pro was used (Queen Mary, University of London, UK). The samples were required to be <1mm and were placed in a sampling holder and were scanned continuously by a graphite detector from 20° to 70° 2θ, at a scanning speed of 1°/min 2θ at a minimum step size of 0.02° 2θ and a count time of 2.5 seconds. Monochromatic Cu-Ka radiation was used at wavelengths of Ka_1 = 1.540598 nm and Ka_2 = 1.544426 nm with an intensity ratio of 0.5.

X-ray fluorescence (XRF)

XRF is the emission of x-rays from a material that has been excited with high energy x-rays. This technique is widely used for elemental analysis and chemical analysis particularly to investigate metals, glasses and ceramics. As well as being used in biomaterials research, XRF is also employed within geochemistry, forensic science and archaeology. Calcium, phosphorus and silicon content of all BGS was determined by the quantification of a range of metal oxides using XRF. XRF spectrometer, Philips PW1606 was used at a UKAS (United Kingdom Accreditation Service) accredited laboratory (Lucideon Ltd, UK). The analysis was conducted by methods C201 based on BSEN ISO 12677:2011.

Fourier Transform Infrared Spectroscopy (FTIR)

FTIR comes from infrared spectroscopy (IR). In this study a Thermo Nicolet 8700 FTIR spectrometer with a PA cell-MTEC Photoacoustic cell with a KRS-5 sample chamber window was used (Queen Mary, University of London, UK). Photoacoustic Spectroscopy (PAS) was first invented by Bell in 1880. PAS depends on radiation absorption and also thermal diffusion. The amount of IR energy that is absorbed corresponds to the distribution of the IR functional groups in the specimen. PAS is a fast process, because of the fast conversion of energy to heat. This in turn means that the absorbed energy is released quickly as heat, which is then transferred to the surface of the sample. The samples used in this techniques need to be of a small size, therefore the HA and SA granules used were ground to <1mm in size. A resolution of $4cm^{-1}$ was used and the spectra were produced over 128 scans.

Scanning Electron Microscopy (SEM)

SEM is a type of electron microscope which has the ability to image sample surfaces by scanning with high energy beams of electrons. It characterises samples by, allowing you to see morphology of the specimen, and view the grain size and the shape of the crystal. A sample is placed inside the vacuum column within the microscope. This is because if the air particles were to react to the sample, this would give rise to different compounds being formed and condensing on the surface of the sample and would therefore lower the quality of the final image. Air is then pumped out of the column and an electron gun, which is located at the top of the microscope, releases a beam of electrons at a high energy state. The beam follows a vertical path through the column. It passes the electromagnetic lens which directs and focuses the beam on to the sample. Once the beam of electrons hits the sample, secondary or backscattered electrons are ejected from the sample. Detectors then collect these signals and convert them into a signal that is sent to the viewing screen, producing an

image. For this study a FEI Inspect F high – resolution SEM was used (Figure 2.2). Before testing, HA and SA samples were coated in gold by a sputter coater. A range of magnifications were used; 6000, 12000 and 24000. A spot level of 3.5 was utilised with an aperture of 3. The chamber pressure was 1.36 x 10^{-4} Torr, the gun pressure was 2.62 x 10^{-9} Torr and finally the emission current was 146µA.

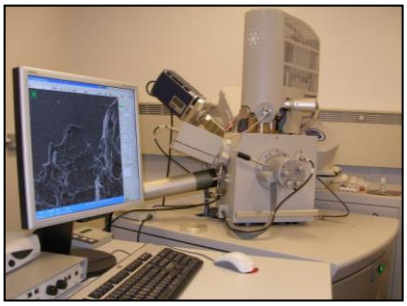

Figure 2.2: FEI Inspect F instrument used for SEM and EDS at Nanovision Centre, Queen Mary, University of London, UK

Energy Dispersive x-ray spectroscopy (EDS)

For EDS analysis the same equipment was used as in SEM (FEI Inspect F), however this time samples of HA and SA were coated in carbon and were again analysed before and after the experiments took place for comparison. EDS is regarded as a semi-quantitative analytical technique for the elemental analysis or mapping of samples. The technique looks at interactions between the electromagnetic radiation and the sample in response to being hit by charged particles. High energy beam of electrons is focused onto a sample surface. Electrons from this beam have the ability to knock out existing electrons from the actual sample surface. An electron from an outer higher energy shell fills this space on the sample surface and the difference in energy shells is released in the form of x-rays. The number and the energy of the x-rays released from a sample have the potential to be measured by an energy dispersive spectrometer. A magnification of 24000 and a spot level of 5 with an aperture of 6 was utilised. The SEM machine was used to carry out EDS (Figure 2.2) the chamber pressure used was 1.36 x 10^{-4} Torr, the gun pressure was 2.62 x 10^{-9} Torr and finally the emission current was 146µA. All the analysis has been done over an area covering the grain and a grain boundary and these have been presented in the results section.

Archimedes Density Measurements

The density of HA and SA samples were measured before experiments using a similar method to the one used by Hing et al based on the Archimedes principle (Hing, Best et al.

1999). Samples were firstly weighed in a dry condition (W_{dry}) in triplicates using an analytical plus electronic balance (Ohaus, Leicester, UK). The samples were then placed into boiling water for one hour; this was to make sure that all the pores present within the samples were completely saturated with water and left to cool still submerged in water. After an hour, the samples were weighed whilst still being submerged in water (W_{sub}) using a density AP solids kit (Ohaus, Leicester, UK) and finally the samples were removed from the water and weighed wet in a saturated state (W_{sat}). The apparent and real densities were calculated using Equation 2.1 and Equation 2.2 respectively where, ρH_2O is the density of deionised water at a given temperature. The former equation takes in to consideration both the open and closed porosity of the materials whereas, the later equation only considers the closed porosity. Equation 2.3 and Equation 2.4 were used to determine the closed porosity and total porosity respectively with an accepted value of 3.156 g/cm^3 used for the theoretical density of hydroxyapatite (ρHA). Although due to the silicate substitution within HA there is a slight shift expected in density of SA, equal values were used for both materials.

$$D_{apparent} = \left(\frac{W_{dry}}{W_{sat} - W_{sub}} \right) \rho H_2O$$

Equation 2.1

$$D_{real} = \left(\frac{W_{dry}}{W_{dry} - W_{sub}} \right) \rho H_2O$$

Equation 2.2

$$CS\mu = \left(1 - \frac{D_{real}}{\rho HA} \right) \times 100$$

Equation 2.3

$$TP = \left(1 - \frac{D_{apparent}}{\rho HA} \right) \times 100$$

Equation 2.4

D = Density, W = Weight, ρH_2O = density of deionised water at a given temperature, $CS\mu$ = Closed strut porosity and ρHA = theoretical density of hydroxyapatite (3.156 g/cm^3).

Brunauer Emmett Teller (BET) and Strut Porosity measure

BET is a common method used to determine the surface area of a material. It allows you to calculate the surface area of powders or particles by analysing the physical adsorption of a gas on the surface of the sample. As a result, this technique is widely used within research and industry. In this study a micromeritrics FlowPrep060 degaser, multiopoint analyser (Micrometrics, UK) was used to measure the surface area of <1mm granular samples. The samples were firstly dried out at 200^{o}C overnight with nitrogen at 15psi. The surface area values were obtained using helium at 15psi with an evacuation rate of 300 mmHg/min.

Figure 2.3: BET instrument set up at Queen Mary University of London

Strut porosity of the porous granules was confirmed by embedding the samples in resin mix with a 5:2 ration of resin and hardener respectively (EpoFix, Struers, UK). Once embedded, the samples were left to set for 8 hours. The specimens were then polished on diamond paper ranging from P500 to P4000 and then imaged using SEM. The strut porosity was determined using ImageJ 1.44i (National Institution of Health, USA) following the method below;

1. Select a SEM image, containing the region of interest, in this case the strut porosity.
2. Select an area within the image with the box tool, such that the area only contains the strut pores and not any pores which would be considered as part of the normal porosity and no overlays on the image such as the scale bar.
3. In Image J, click 'analyse' and 'histogram' to create a histogram of the area, now referred to as the area of interest.
4. List the histogram in a table format and export to excel.
5. Using a pre-defined intensity boundary point (in this case it was at an intensity of 126), such that all intensities between the boundary points are strut porosity and anything above in not.
6. Divide the number of pixels of the strut porosity by the total number of pixels in the area of interest. Repeat this process over a number of images and take the average in order to calculate the strut porosity.

2.2 Results

2.2.1 XRD Analysis

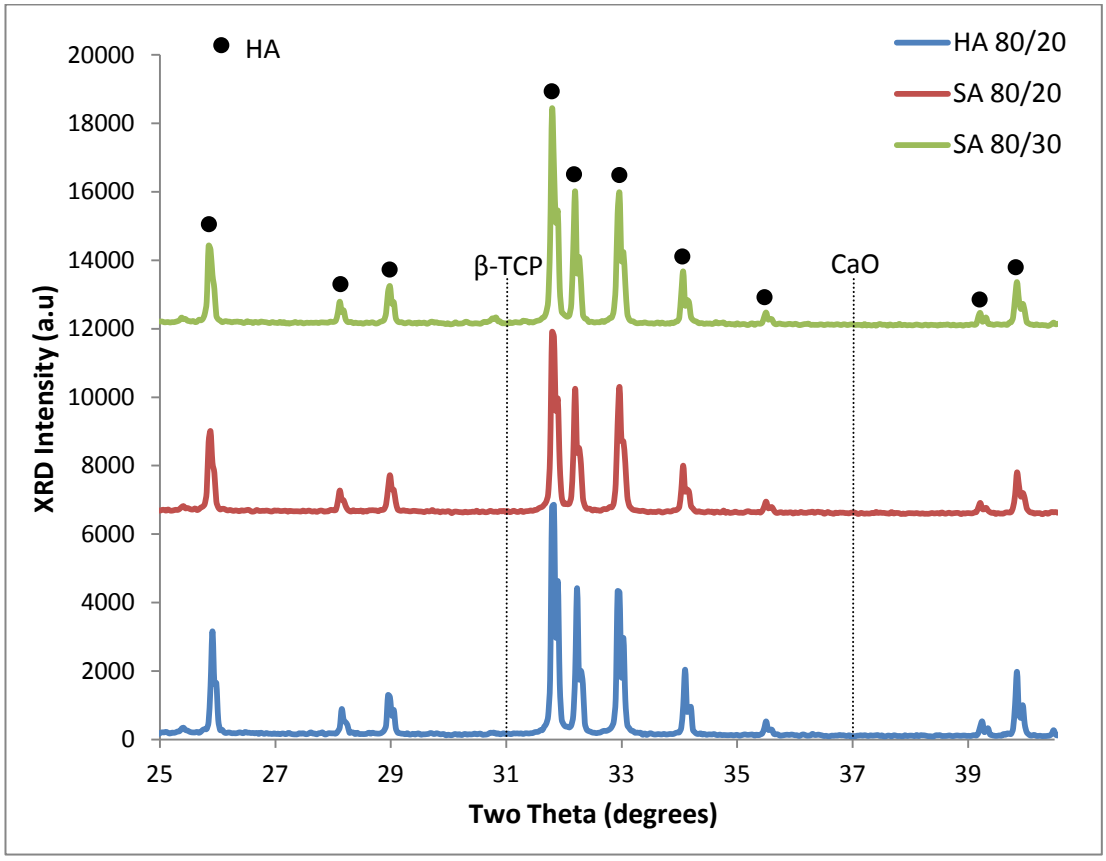

Figure 2.4: XRD patterns of HA80/20, SA80/20 and SA80/30 porous granular samples

XRD of the HA and SA samples was found to be consistent between all the samples (Figure 2.4) No other phases were detected. As indicated on the graph, there was no detection of β tricalcium phosphate (β-TCP) and calcium oxide (CaO) as these are found to be impurities within the samples which may be present either as deliberate additions or as a result of decomposition during the sintering process which makes the Ca/P ratio either greater or less than the stoichiometric molar ratio of 1.67 for HA and SA (Hing, Gibson et al. 1998, Gibson, Huang et al. 1999). The peaks shown are narrow and sharp which indicate a high level of crystallinity for all the compositions. There was no peak intensity observed with the addition of silicate ions or the increasing strut porosity (Hing, Revell et al. 2006).

2.2.2 XRF Analysis

Table 2.2: XRF data for HA and SA granules with calculated atomic ratios

	wt%			Atomic Ratios	
Sample	**CaO**	**P_2O_5**	**SiO_2**	**Ca/P ratio**	**Ca/(P+Si)**
HA 80/20	55.95	42.15	0.16	1.67	1.67
SA 80/20	56.23	40.33	1.84	1.76	1.67
SA 80/30	56.2	40.4	1.75	1.76	1.67

XRF data of the granular samples was able to show that any substitution that did occur was due to the presence of 0.8wt% silicon for the SA samples. The HA samples showed a trace level of silicon present which calculated to be 0.07wt% . Full data sheets are presented in APPENDIX 1 of this thesis.

2.2.3 FTIR Analysis

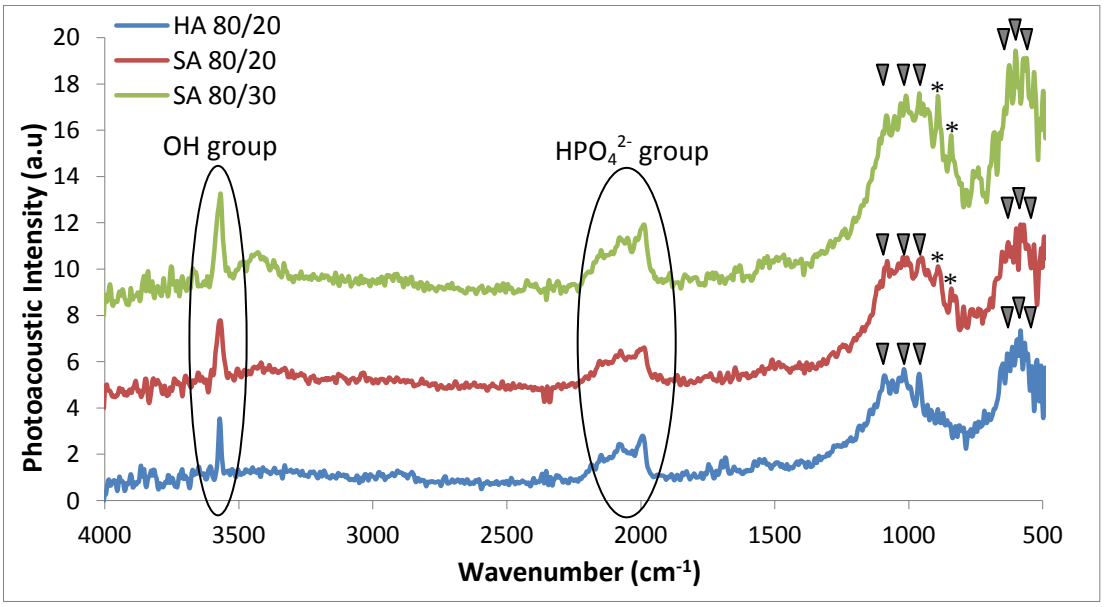

Figure 2.5: FTIR spectra of HA and SA porous granular samples

Using this technique allowed observations to be made about the function groups present within the HA and SA samples structures. In both HA and SA samples there is a noticeable sharp peak present at 3570cm^{-1} which corresponds to the presence of OH groups. The band heights of the peak is found to be slightly higher at ~6PA (photoacoustic) in SA 80/30 than SA 80/20 and HA 80/20 where it is found to be ~4PA.

All the spectrums show a broad peak ~1100cm^{-1}, which indicates the presence of phosphate groups. Phosphate symmetric stretching vibration (ν_3 and ν_1 bands) are characterised by 3 peaks present at 1089cm^{-1}, 1032cm^{-1} and 962cm^{-1}, which again are more defined and intense in sample SA80/30. The phosphate bending vibration (ν_4 bands) is again characterised by 3 peaks present at 631cm^{-1}, 606cm^{-1} and 559cm^{-1} (highlighted ▼). In the two SA samples spectrums two peaks present at ~880cm^{-1} determine the presence of SiO_4^{4-} groups with the Si-O vibration (highlighted *). Finally the spectra for the HA and SA samples show broad peaks present between 2000cm^{-1} – 2200cm^{-1} these peaks may correspond to surface absorbed HPO_4^{2-} groups (Gibson, Best et al. 1999, Hing, Revell et al. 2006).

2.2.4 SEM Analysis

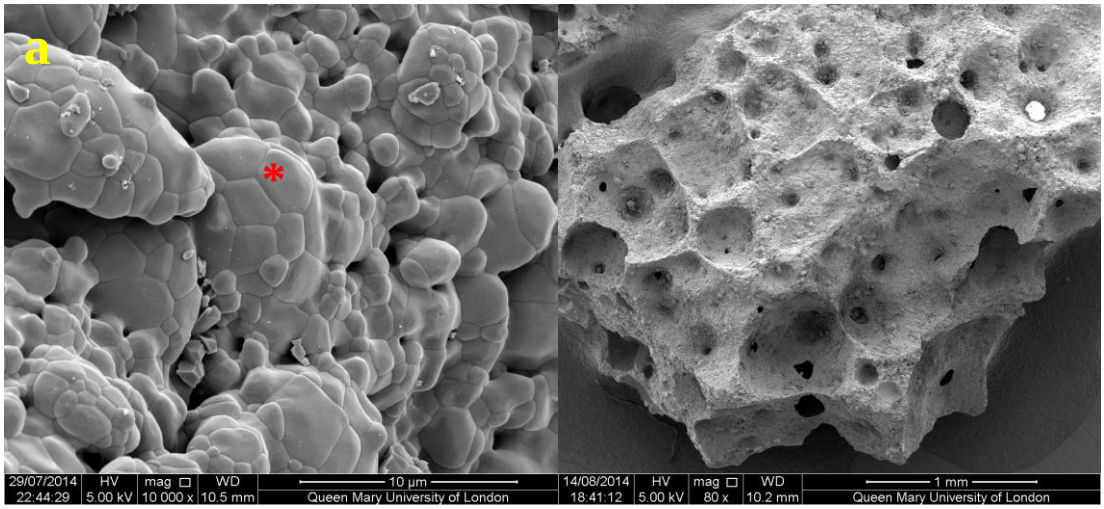

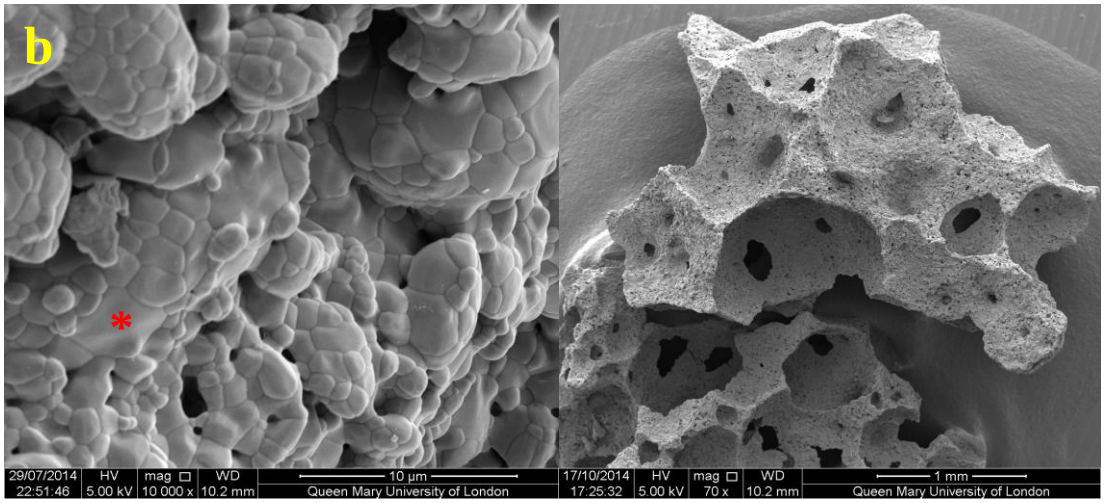

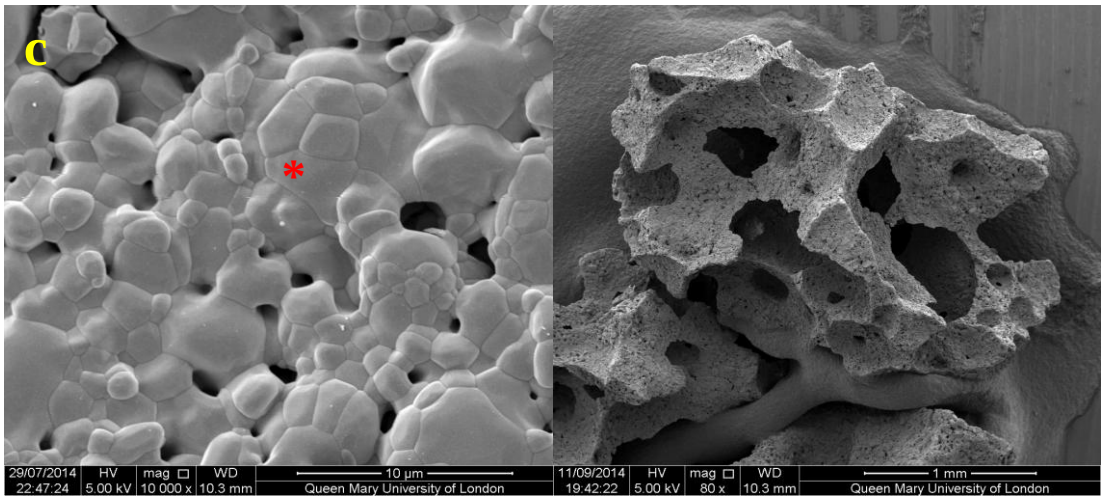

Figure 2.6: SEM images of as received granular samples used, a) HA80/20 at 10000x & 80x, b) SA80/20 at 10000x & 70x and c) SA80/30 at 10000x & 80x

The SEM images in Figure 2.6 were obtained from the samples as they were received from ApaTech Ltd. It is evident from the images above that the sample were not contaminated with no signs of any sample degradation and there is a clear presence of grain boundaries. The above images were taken at a magnification of 10000, HV = 10.00Kv and 5µm.

2.2.5 EDS Analysis

EDS spot analysis was conducted on the samples in order to compare the elemental analysis of the HA and SA structures. These areas have been individually highlighted for all three BGS used above in Figure 2.6 (*) as these SEM images were used in order to obtain the EDS results. Below are the graphical results from the EDS analysis and also respective tables showing the percentage of ion content analysed at certain points on the sample surfaces.

	HA80/20	
Element	Weight %	Atomic %
C	9.74	16.57
O	45.84	58.52
Si	-	-
P	15.15	9.99
Ca	29.27	14.92

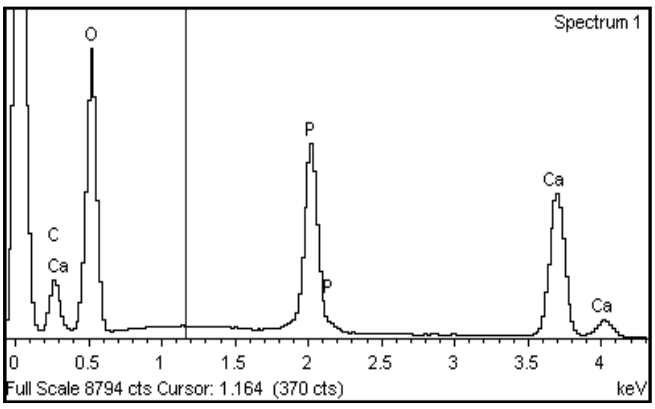

Figure 2.7: EDS spectra and numerical analysis of HA80/20 granular sample

	SA80/20	
Element	Weight %	Atomic %
C	10.08	17.25
O	44.42	57.09
Si	0.76	0.40
P	14.54	9.65
Ca	30.41	15.6

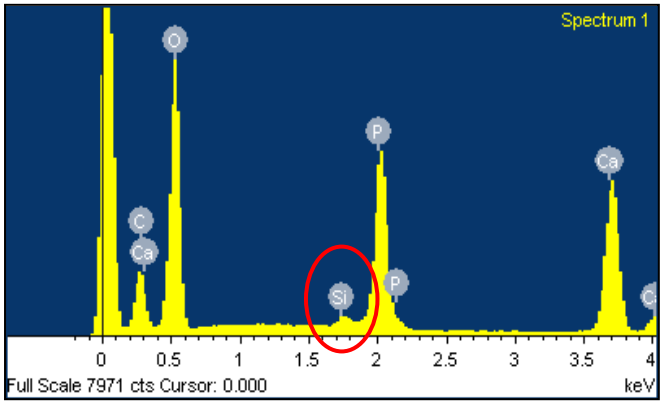

Figure 2.8: EDS spectra and numerical analysis of SA80/20 granular sample

	SA80/30	
Element	Weight %	Atomic %
C	10.35	18.96
O	34.89	48.00
Si	0.78	0.53
P	17.3	12.29
Ca	36.8	20.21

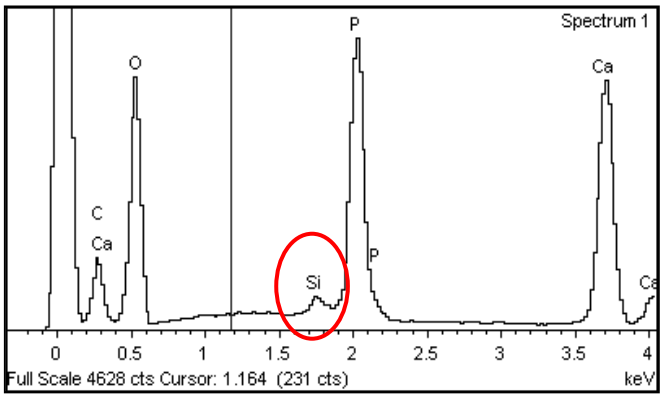

Figure 2.9: EDS spectra and numerical analysis of SA80/30 granular sample

EDS analysis shows that in SA 80/20 (Figure 2.8) and SA 80/30 (Figure 2.9) samples there was a detection of silicon and it was reassuring to see no silicon peak within the HA80/20 sample analysis (Figure 2.7). However with both SA samples there was an expected 0.8wt% of Silicon to be present as this was the specification of the material that was being used.

2.2.6 Archimedes Density Measure

Table 2.3: Archimedes density data for HA and SA porous granular samples

Sample	Apparent Density (gcm^{-3}) (Nominal)	Real Density (gcm^{-3}) (Nominal)	Total Porosity (%)
HA 80/20	0.57 ±0.04	2.80 ± 0.05	80.13
SA 80/20	0.59 ± 0.01	2.96 ± 0.02	80.58
SA 80/30	0.66 ± 0.05	3.08 ± 0.04	80.59

The table above gives an outline of the total porosity of the samples used. These were expected to be ~80%. The readings were conducted in triplicates.

2.2.7 BET Analysis and Strut Porosity Measure

Table 2.4: Surface area data for HA and SA samples obtained using BET

Sample	Sample Weight (g)	Surface Area (m^2/g)
HA 80/20	1.98 ± 0.01	0.25 ± 0.05
SA 80/20	2.15 ± 0.02	0.26 ± 0.05
SA 80/30	2.09 ± 0.01	0.28 ± 0.1

The results obtained above were as expected for the porous SA samples in comparison to HA due to the presence of silicon. Also the surface area for SA80/30 was increased and this is a clear indication that more interconnective pores are present within this particular sample.

Strut porosity analysis also known as the pore interconnectivity was determined by embedding samples in resin and imagining then using SEM. Table 2.5 below quantifies the strut porosity observed in the SEM images for the individual samples embedded in resin. Figure 2.10, Figure 2.11 and Figure 2.12 show SEM images of the three different BGS used in this study at two magnifications; 300 and 1000 magnification, where the images taken at 1000 magnification were used to calculated the strut porosity using ImageJ as explained in section 2.1 above.

Table 2.5: Calculated strut porosities of all samples using ImageJ

Sample	Strut Porosity (%), (±σ)
HA 80/20	19.4 (±0.8)
SA 80/20	19.8 (± 0.5)
SA 80/30	29.5 (± 0.2)

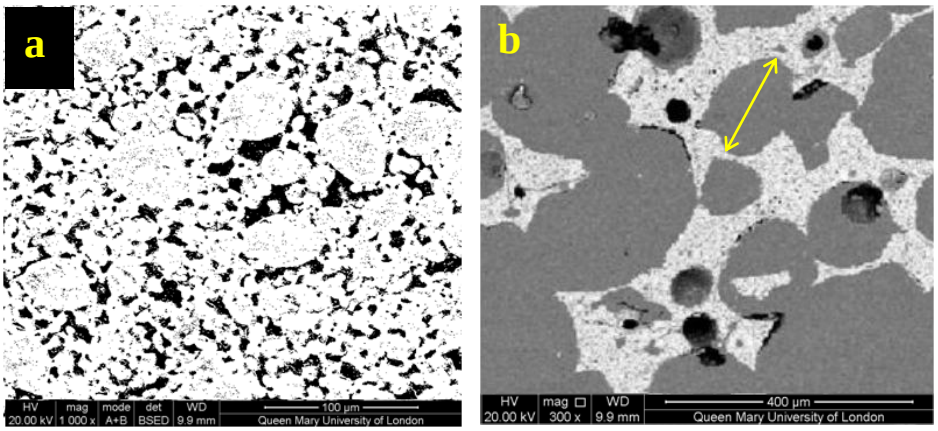

Figure 2.10: SEM images of HA80/20 embedded in resin used for strut porosity analysis at, a) 1000 and b) 300 magnification

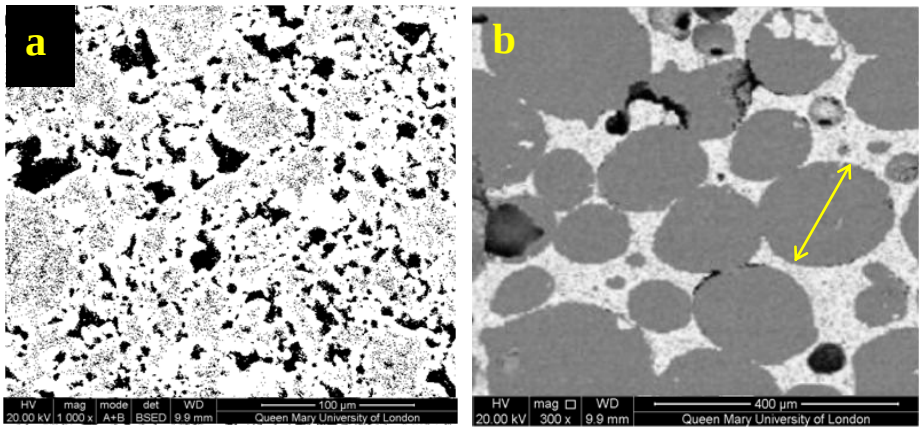

Figure 2.11: SEM images of SA80/20 embedded in resin used for strut porosity analysis at, a) 1000 and b) 300 magnification

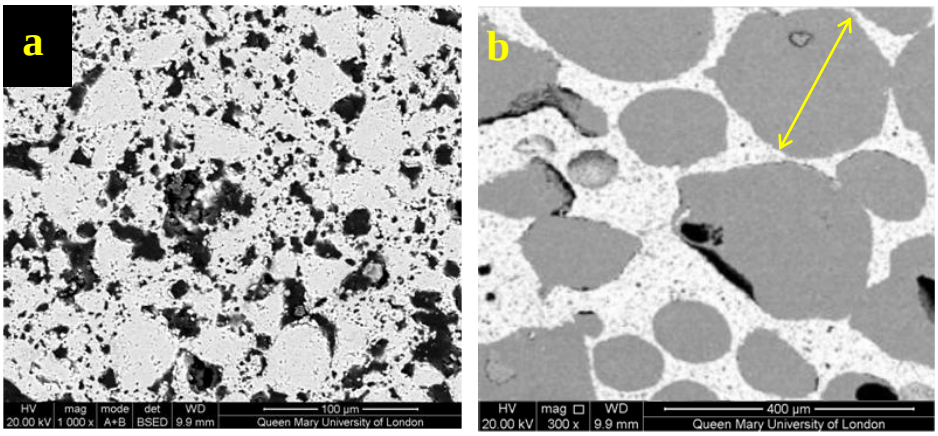

Figure 2.12: SEM images of SA80/30 embedded in resin used for strut porosity analysis at, a) 1000 and b) 300 magnification

2.3 Discussion

From the results obtained in this chapter it has been confirmed that the chemical and physical characteristics of all three BGS used in this study matched their chemical and structural specifications.

Chemical analysis of HA80/20 as received by ApaTech showed that the it was phase pure and highly crystalline with a Ca/P ratio of 1.67. However the sample also showed a 0.07wt% contamination of silicon. The chemical analysis for SA80/20 and SA80/30 showed the BGS to be again highly crystalline, phase pure and silicate substituted hydroxyapatite with a Ca/(P+Si) ratio of 1.67 and 0.8wt% silicon by weight substituted in to the crystal lattice. The findings from SA80/20 and SA80/30 were consistent with previous research for materials which were manufactured by the same aqueous precipitation and foaming method. The results obtained from XRF were able to confirm the absence of any metal contaminants in the form of metal oxides. Full data sheet is available in Appendix 1. The differences in intensities of the XRD patterns from HA80/20, SA80/20 and SA80/30 are known to be due to the incorporation of silicon into the HA lattice. Silicon is known to act as a sintering aid which in turn results in them having a lower crystallinity at the same calcination temperature than that of HA, hence the lower intensity was observed (Gibson, Best et al. 2002). By looking at the XRD and XRF data it is evident that silicon is present within the HA lattice as there is an increase in the Ca/P ratio. An increase in Ca/P ratio would mean the presence of CaO, however the results form XRD show no presence of a CaO peak which confirms that there was something else stabilising the structure and in this case it was silicon within HA.

FTIR analysis was able to confirm all BGS to be free of impurities which is consistent with previously reported results by researchers. Phosphate peaks of ν_3, ν_1 and ν_4 bands in HA and both SA samples and the presence of silicon in the SA samples which were more intense for the SA80/30 BGS were demonstrated. These exact peaks were later observed by Gibson et al in 1999 within 0.4wt% SA and then in 2006 by Hing et al in other wt% SA BGS including 0.8wt% SA which is being used in this study (Gibson, Best et al. 1999, Hing, Revell et al. 2006). Therefore the FTIR spectrum acquired here are in agreement with previous findings.

It is important to analyse a materials surface roughness by looking at its pore structure, interconnectivity and shape. SEM images (see Figure 2.6), taken of all three BGS confirmed the similarity in the grain structure and boundaries. There were no prior depositions on the surface of the materials, such as CaP layer, protein deposition, and precipitation of any contaminants and even the degradation of the sample surfaces. The SEM images showing

the granules set within resin to allow for strut porosity analysis clearly show that as the resin has impregnated the granules suggesting the presence of strut porosity. The strut porosity analysis obtained by Image J are in good agreement with the nominal values.

EDS analysis was conducted on the granules before any experimentation took place. It was encouraging to see a high wt% of calcium and phosphate in all samples. As 0.8wt% of SA was being used in this study with varying strut porosities, it was assumed that before experimentation, both SA samples would contain the full 0.8wt% of silicon. However the wt% of silicon that was detected in SA80/20 and SA80/30 was 0.76wt% and 0.78wt% respectively.

Archimedes principle allowed for the confirmation of the total porosity of all three BGS used in this study as the expected total porosity was to be 80% for all samples and this is what was observed. The strut porosity for HA80/20 and SA80/20 was observed to be very similar at 19.4% and 19.8% respectively, even though they were lower than the expected value of 20%. The strut porosity for SA80/30 was calculated to be 29.5% ± 0.2%. See Table 2.5 for the calculated strut porosities for all samples. The introduction of porosity should not change the surface chemistry within porous granular materials compared to powder or dense disc specimen, as in principle only interconnectivity of the material would increase (Shors and Holmes 2013) which has been demonstrated in these results as the surface chemistry has not changed between SA80/20 and SA80/30 samples.

The surface area of the samples was determined by BET analysis which is shown in Table 2.4. The surface area was seen to greater for the SA80/30 in comparison to HA80/20 and SA80/20 as expected due to the increase in strut porosity. There was no significant difference observed in surface area between HA80/20 and SA80/20.

2.4 Summary

HA and SA samples demonstrated characteristics which corresponded to properties observed previously in literature. There was a confirmation of phase purity along with key functional groups being present within all samples tested. XRF and EDS analysis was able to corroborate the presence of silicon within both SA samples with BET showing a greater surface area also confirming the substitution of silicon within SA80/20 and SA80/30.

Porosity measures for both macro and microporosities confirmed that all three samples had a total porosity of 80% with HA80/20, SA80/20 and SA80/30 either having 20% or 30% strut porosity respectively.

The results obtained confirm the chemical and physical characteristics of the three BGS, therefore further experimentation can be conducted to study the effects that these features play in dynamic ion exchange along with cell response on the BGS.

Chapter 3 Ionic Dissolution

3.1 Background

Bone plays a critical role in mineral homeostasis and maintenance of ion concentrations to very high levels of tolerance. This is critical for normal tissue function and whole organism health and survival. Therefore when assessing performance of a bone graft *in vitro* every effort should be made to replicate the physiological environment in terms of physical properties and chemical composition and not just pH and temperature. From previous studies it has been found that the calcium and phosphate ion concentration are very important when it comes to the bone mineralisation process by osteoblasts (Anderson, Downes et al. 1998, Reffitt, Jugdaohsingh et al. 1999). In 1970 Carlisle was successful in showing the positive effect of silicon on bone mineralisation. Previous research has established that the substitution of silicate ions into HA significantly increases the rate at which bone apposition occurs in comparison to HA and the enhanced bioactivity of SA over HA has been attributed to the effect of the silicate ions in accelerating dissolution. It is believed that the dissolution and re-precipitation of apatite crystallites promote the incorporation of biological molecules (Schepers, Declercq et al. 1991, Weng, Liu et al. 1997, Ducheyne and Qiu 1999).

In blood, the total calcium concentration is maintained at ~0.09mg/ml. The ~0.09mg/ml in the body fluids only comprises about 0.1% of the body's total calcium. Further 0.9% calcium is in use interacellularly, whilst the bulk of 99% of the total calcium of the body is stored in the bone in a mineralised state. The extracellular levels of phosphate are adequate between ~0.08mg/ml - 0.13mg/ml and its homeostasis is not as tightly regulated as that of calcium. Silicon levels however, are not homeostatically regulated in the body. Only traces of this element are found in the human body. Silicate ion release and pH change is well characterised from bioglasses that undergo significant levels of dissolution under physiological conditions. However there is some disagreement in the literature as to whether or not HA and SA undergo any significant levels of ion exchange with the surrounding media. Also these experiments have been conducted under static conditions which do not mimic the *in vivo* environment.

The aim of the work in this chapter was to monitor the pH, calcium, phosphate and silicate ion levels in media incubated with synthetic bone graft substitute granules using a semi-

dynamic system. The objective being to identify if the presence of the granules impacted on the levels of these essential ions. Three different forms of granules were used, all with 80% total porosity. However, two had matched levels of strut porosity (20%) but differing chemistries of stoichiometric hydroxyapatite (HA) and 0.8wt% Si Silicate substituted apatite (SA), while two had matched SA chemistry but different strut porosity levels of 20% and 30%. These different granules were denoted as HA80/20, SA80/20 and SA80/30, their full chemical and structural characterisation is detailed in Chapter 2.

3.2 Methodology

3.2.1 Sample Preparation

HA80/20, SA80/20 and SA80/30 samples were provided by ApaTech Ltd (UK) and characterised as detailed in Chapter 2. Upon receiving the samples, they were of varying granule size; therefore they had to be sieved using sieves of different aperture size (1mm and 5mm) in order to obtain the required granule size (2-5mm) for the dissolution testing.

Figure 3.1: 1mm & 5mm sieves used to separate granules in to the required sizes

3.2.2 Media Preparation

The basic culture medium that was used was serum containing medium (SCM) which was made up from Dulbecco's Modified Eagle Medium (DMEM) supplemented with 10% Fetal Bovine Serum (FBS) and 1% penicillin-streptomycin (Pen/Strep). All products used for the preparation of SCM were of the same batch purchased from Sigma Aldrich (Dorset, UK).

Table 3.1: Summary of SCM compositions

Medium	Components	Volume Used
Serum Containing Media (SCM)	Dulbecco's Modified Eagle Medium (DMEM)	500ml
	Fetal Bovine Serum (FBS)	50ml
	Penicillin-Streptomycin (Pen/Strep)	5ml

3.2.3 Investigation of Ion Exchange under semi-dynamic conditions

As mentioned previously most of the experimentation on ion exchange of apatite base specimens under physiological conditions has to date been performed under static – non-motile conditions. Given the porous nature of most synthetic bone graft substitute granules and the dynamic conditions postulated to occur *in vivo* this appears to be a significant simplification. Figure 3.2 below shows a schematic of the semi-dynamic test rig that was used in this study, based on the equipment used in the pharmaceutical industry for analysis

of tablet dissolution behaviour. Experiments were carried out in replicates of 6 (n=6) for each form of granule type.

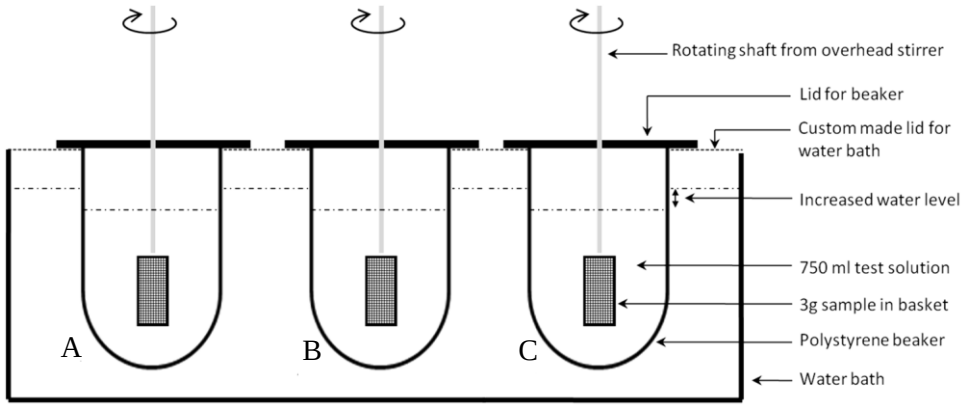

Figure 3.2: Schematic of semi-dynamic dissolution set-up

For every experimental repeat, 3 stations were set up which were distinguished by the following system:

- Station A - HA80/20 immersed in SCM
- Station B - SA80/20 immersed in SCM
- Station C - SA80/30 immersed in SCM

The water baths were set at 37^{o}C a day before the experiments were conducted to ensure that the water had stabilized at a temperature of 37^{o}C ± 0.5^{o}C. It was very important to have the water bath water level higher than the beaker medium level to ensure equal heat transfer to the medium in the beakers. All three 1000ml round bottomed polystyrene beakers were filled with 750ml of SCM and allowed to equilibrate in the water baths for 2 hours before the running of the experiments to ensure the SCM was at 37^{o}C before the experiments begun, at this time 20ml of the bulk media was also transferred to a 25ml polystyrene tube and stored at -20^{o}C. To reduce evaporation of the water and bulk media to an acceptable level throughout the duration of the experiments the water baths were fitted with custom made metal lids and the individual beakers were also lidded.

3 grams of each granular sample was needed per experimental repeat. All the samples were weighed and placed in their respective polytetrafluoroethylene (PTFE) baskets. As shown in the schematic (Figure 3.2) the baskets were then attached to over-head stirrers (Heidolp^{TM} RZR 2021).

Once the SCM had reached 37°C, the filled baskets were immersed into the SCM. The overhead stirrers were switched on and set to a speed of 70rpm providing a semi dynamic environment with each individual BGS basket rotating in their respective round bottom beaker.

Samples of 20ml of test media were extracted from each individual station at time intervals of 15mins, 30mins, 60mins, 120mins, 240mins, 420mins, 24 hours, 48 hours, 120 hours (5 days) and finally 216 hours (9 days). The solutions were extracted into 25ml polystyrene tubes using 60ml pipettes. Upon extraction, the media in the round bottomed beakers were brought back to the full volume (750ml) by the addition of 20ml of fresh bulk SCM. After extraction, the samples were stored at -20ºC and on completion of the 9 day experimental repeat all the frozen samples, including the sample of bulk media taken at the beginning of the experiment/when a new batch of bulk media was made up were sent to NRM Laboratory for ion concentration analysis (see section 3.2.4). After 9 days of incubation in media, the three types of HA and SA granules were removed from the baskets and rinsed with deionised water and allowed to dry on filter paper at room temperature. After drying 0.5g of each type of granule was kept for SEM analysis, whilst the rest of each type of granule was ground down between 1-2mm for chemical analysis.

3.2.4 Elemental Analysis

After the completion of each experimental repeat the frozen media samples were sent to NRM Laboratory, UK for ion concentration analysis using a Perkin-Elmer Optima 3300V ICP-OES spectrometer. The machine was able to detect ion content analysis of calcium (Ca^{2+}), phosphorous (PO_4^{3-}), and dissolved silicon (Si). The detection level of silicate was 0.5mg/l whereas calcium and phosphorus had a detection level of 0.1mg/l.

3.2.5 pH Measurements

The pH was recorded of every 20ml media sample immediately after extraction. The pH was recorded using a Hanna Instrument 9024 combined with both pH and temperature sensor (HI 1230 B and HI 7669/2W respectively). Between 0 - 100°C the effective range of the pH sensor was 0.00 to 14.00 ± 0.01pH and at 20°C the temperature accuracy was ± 0.1°C. Before any readings were taken, the pH metre was calibrated at three points using buffer solutions of pH 10.01, pH 7.01 and pH 4.01. The buffer solutions were made up by dissolving one buffer capsule (BDH Laboratory supplies, UK) with 100ml of deionised water. In between each reading the pH probe was rinsed thoroughly with deionised water.

pH measurements were also taken of the bulk SCM before any experimental work was carried out.

3.2.6 Sample Characterisation

XRD, FTIR and SEM was conducted on all three types of BGS after experimentation, using the methodologies as described in Chapter 2, and compared to the data previously obtained for each of the 'as-received' granule types.

3.2.7 Statistical Analysis

Collected data was analysed and expressed in terms of mean ± standard deviation. Statistical significance was evaluated using ANOVA, Post Hoc test: Tukey HSD with $\alpha=0.05$, (where $*p<0.05$, $**p<0.01$ and $***p<0.005$).

3.3 Results

3.3.1 Ion Concentration Analysis

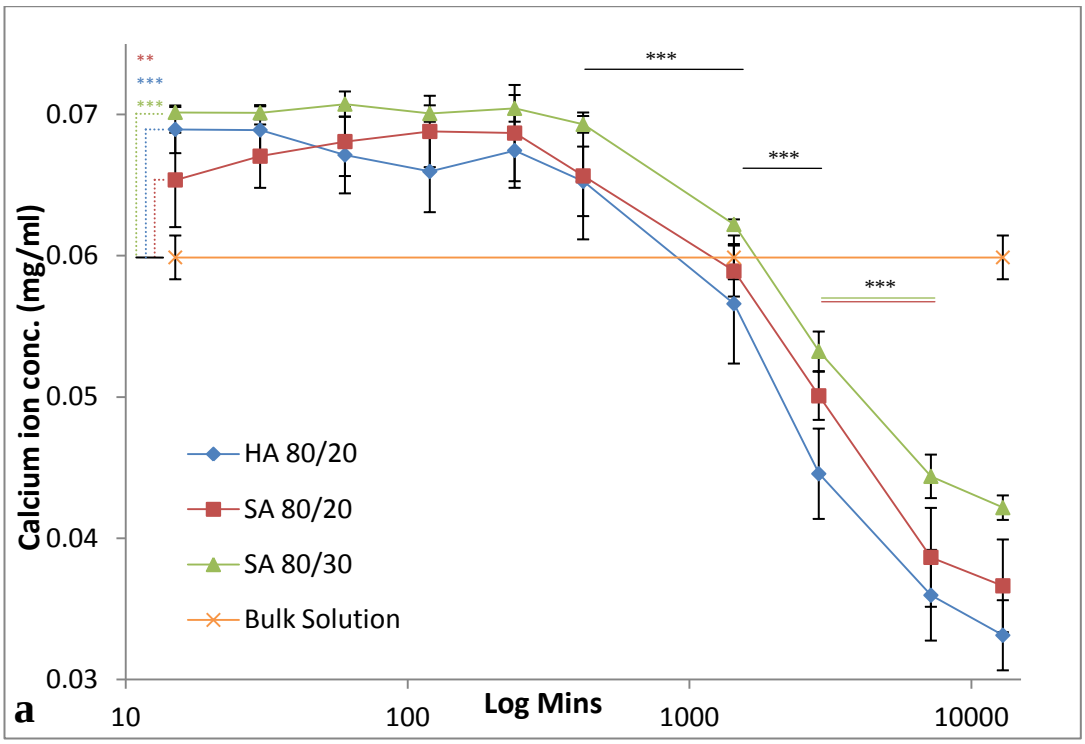

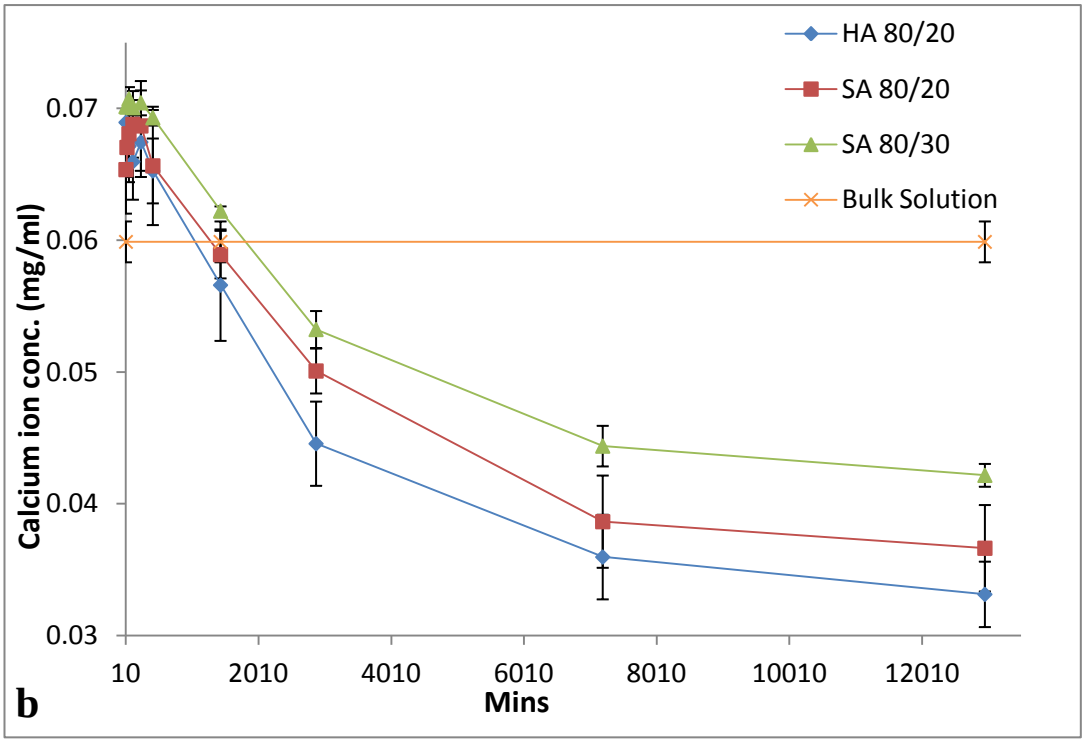

Figure 3.3: Calcium ion dissolution profile for HA80/20, SA80/20 and SA80/30, a) log minutes scale & b) minutes scale (n=6)

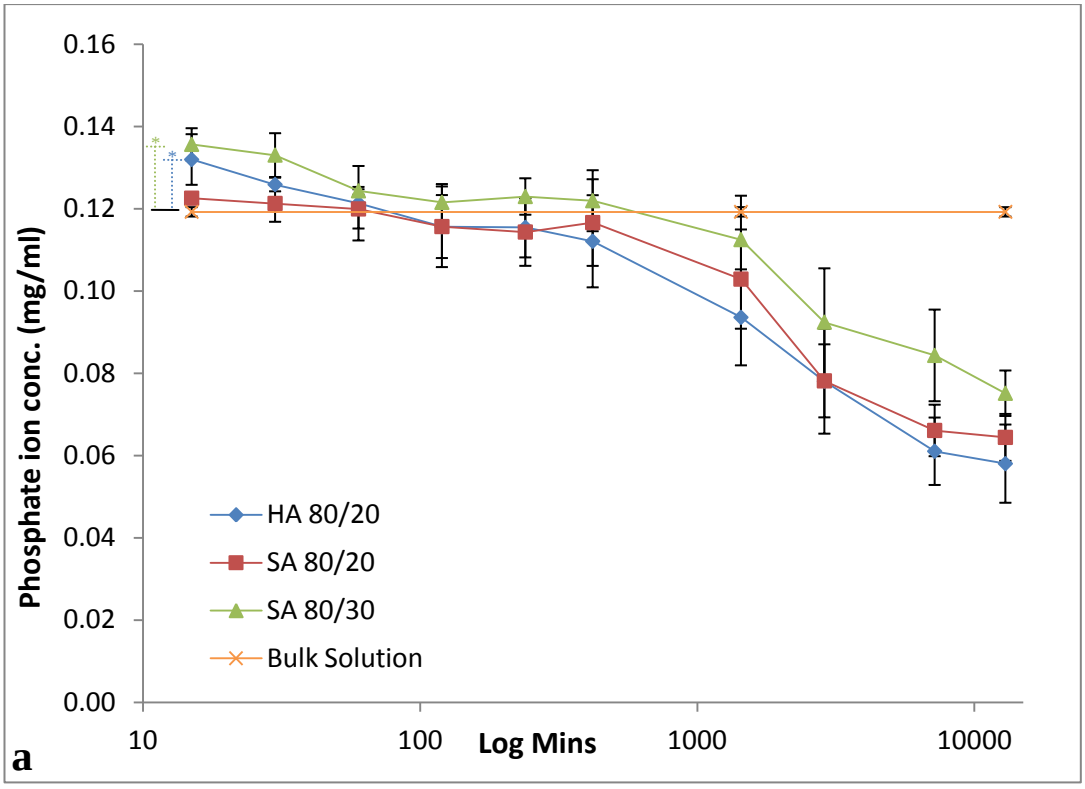

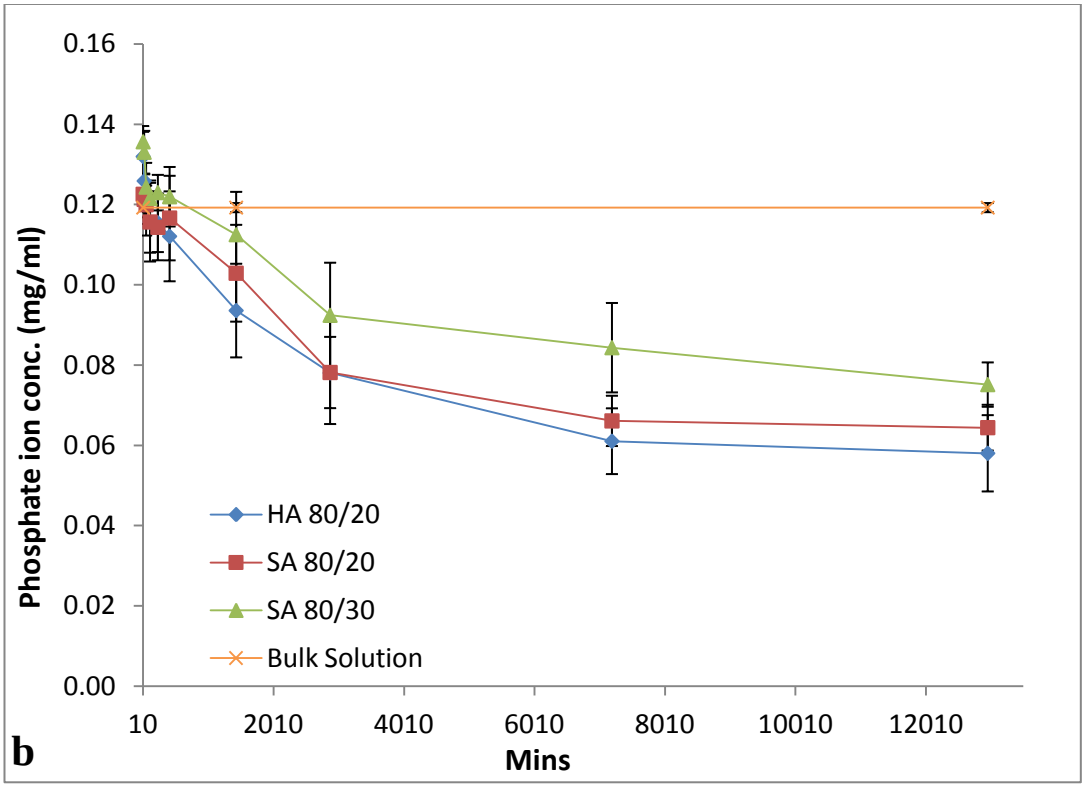

Figure 3.4: Phosphate ion dissolution profile for HA80/20, SA80/20 and SA80/30, a) log minutes scale & b) minutes scale (n=6)

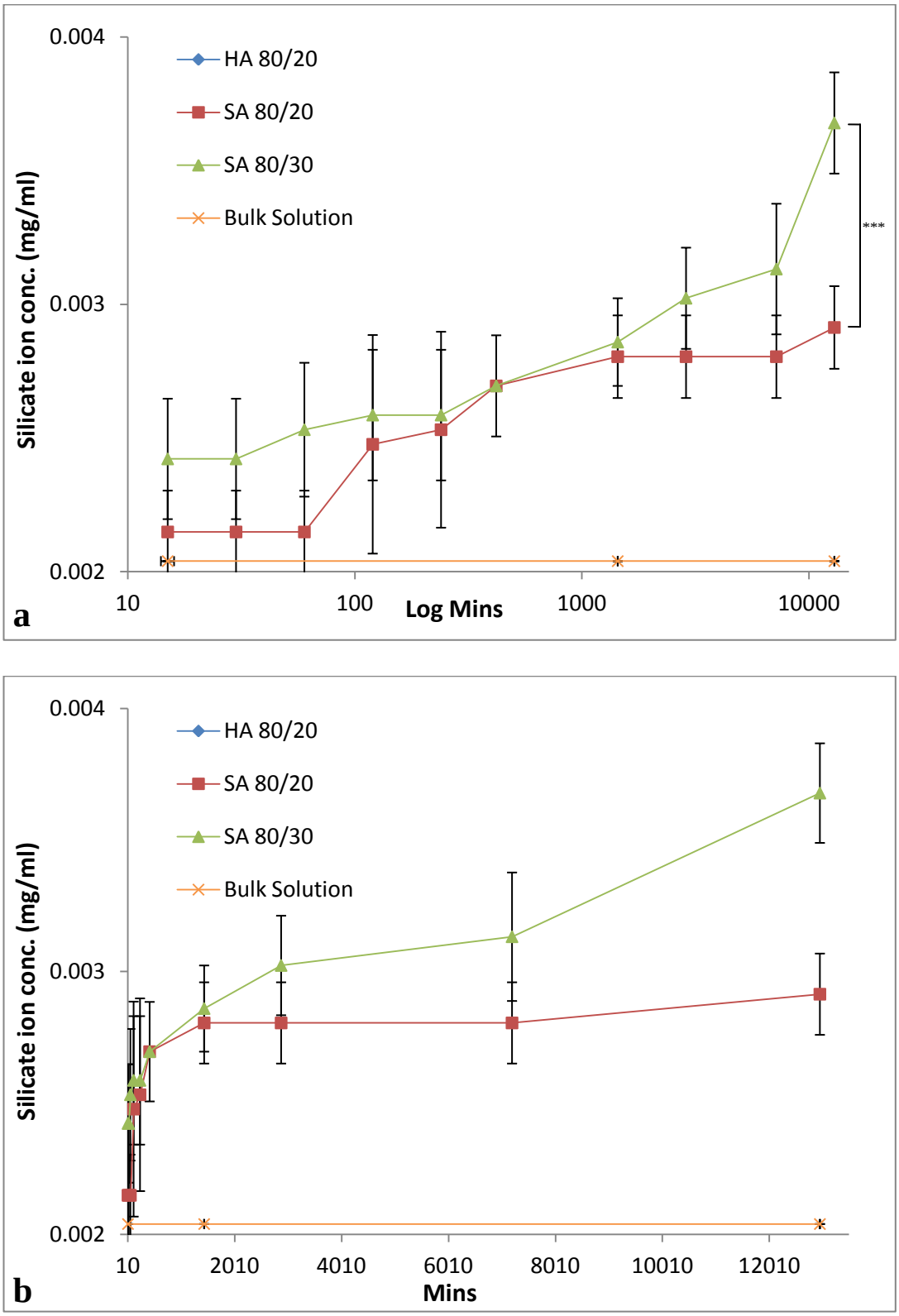

Figure 3.5: Silicate ion dissolution profile for HA80/20, SA80/20 and SA80/30, a) log minutes scale & b) minutes scale (n=6)

Figure 3.3 demonstrates that after only 15 minutes there was a significant increase in the calcium ion concentration irrespective of granule type ($P<0.05$). Calcium levels were not significantly different until 24 hours after which significant depletion occurred for all types although calcium ion concentration was significantly higher in media incubated with SA80/30 as compared to the other two test groups. A similar trend was observed with the dissolution and precipitation of phosphate ions with SA 80/30 showing phosphate levels to be higher throughout the experiment in comparison to HA80/20 and SA80/20 (Figure 3.4). By 1 hour, phosphate levels were not significantly different to the bulk solution irrespective of granule type.

There was an initial bolus release of silicate ions at 15 minutes with both types of SA BGS (Figure 3.5). However while the level of Si ion release was initially greater for SA80/30, although this did not vary significantly for the first 7 hours, whereas at 2 hours there was a significant increase in the level of silicate ions detected in media incubated with SA80/20 granules bringing it to the same level as that in SA80/30 exposed media, the silicate ion levels were not significantly different for SA80/30 and SA80/20 granules until 9 days, when the silicate ion concentration was significantly higher in the media exposed to SA80/30 granules. No silicate ion release was detected from the HA80/20 sample.

The pH increased rapidly to a more basic pH of 8 within the first 7 hours of incubation, approaching a pH of 8.5 by 24 hours and then increasing at a relatively constant rate to a pH of 9.5 by day 9, irrespective of granule type (Figure 3.6).

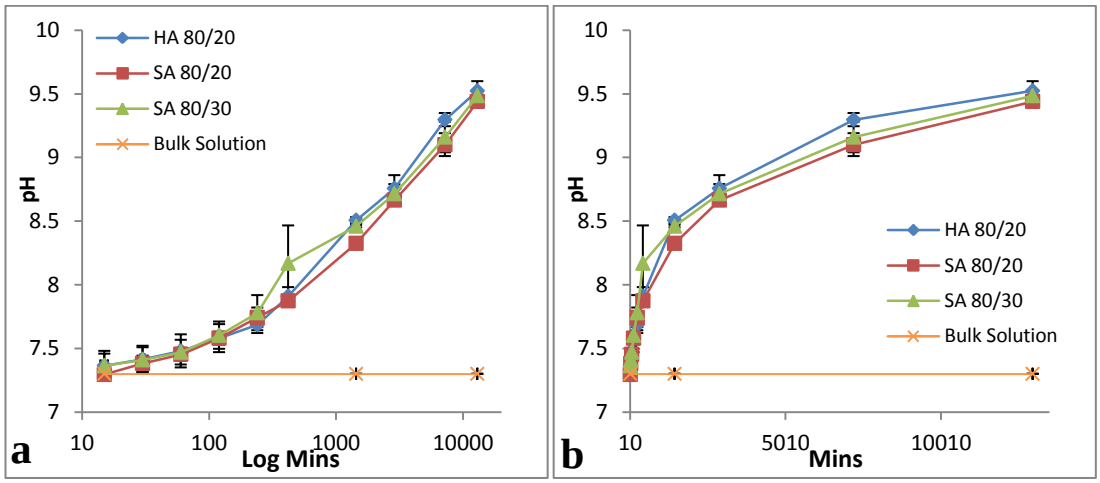

Figure 3.6: pH of SCM upon incubation with HA80/20, SA80/20 and SA80/30, a) log minutes scale & b) minutes scale (n=6)

3.3.2 XRD Analysis

From the XRD patterns it was evident that no other phases were detected and the intensities of the post-incubation patterns for both SA granules were slightly reduced compared to the as received patterns.

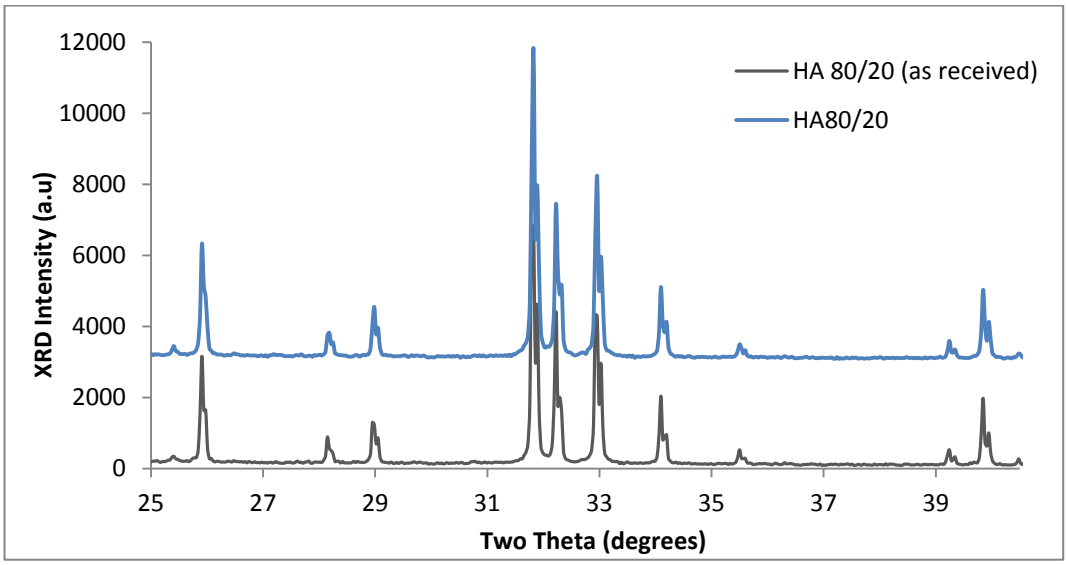

Figure 3.7: XRD patterns for HA80/20, as received and after experimentation

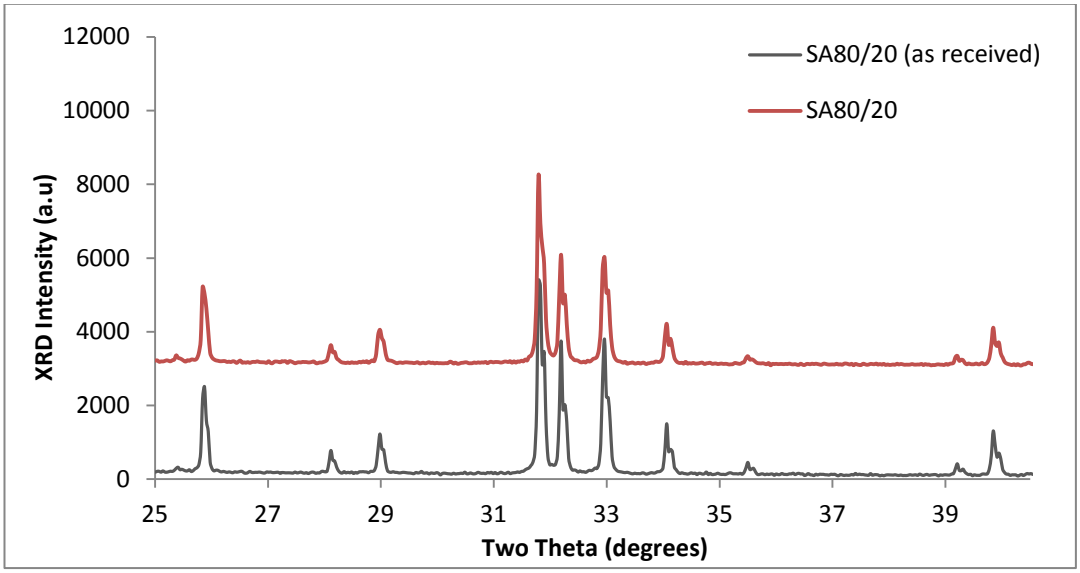

Figure 3.8: XRD patterns for SA80/20, as received and after experimentation

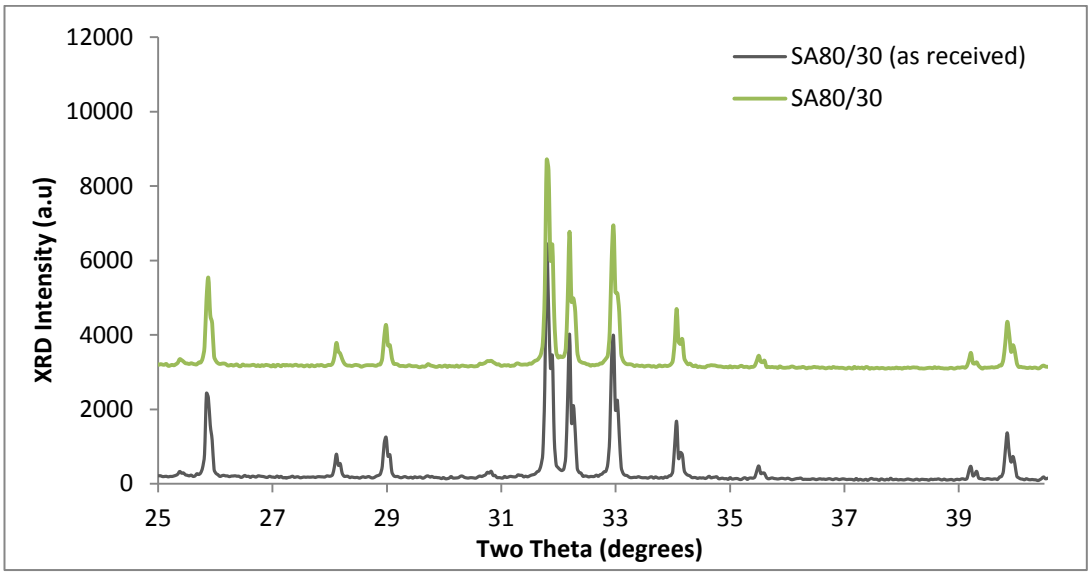

Figure 3.9: XRD patterns for SA80/30, as received and after experimentation

3.3.3 FTIR Analysis

From the FTIR analysis, there was a distinctive difference in that there was a decrease observed in band heights with all the peaks present after experimentation. Looking at the spectra carefully, on both SA samples a new peak between 1550cm^{-1} – 1410cm^{-1} has been highlighted which is associated with carbonate group ν_3 vibration mode but appears as a weak peak in HA80/20 (Hing, Revell et al. 2006).

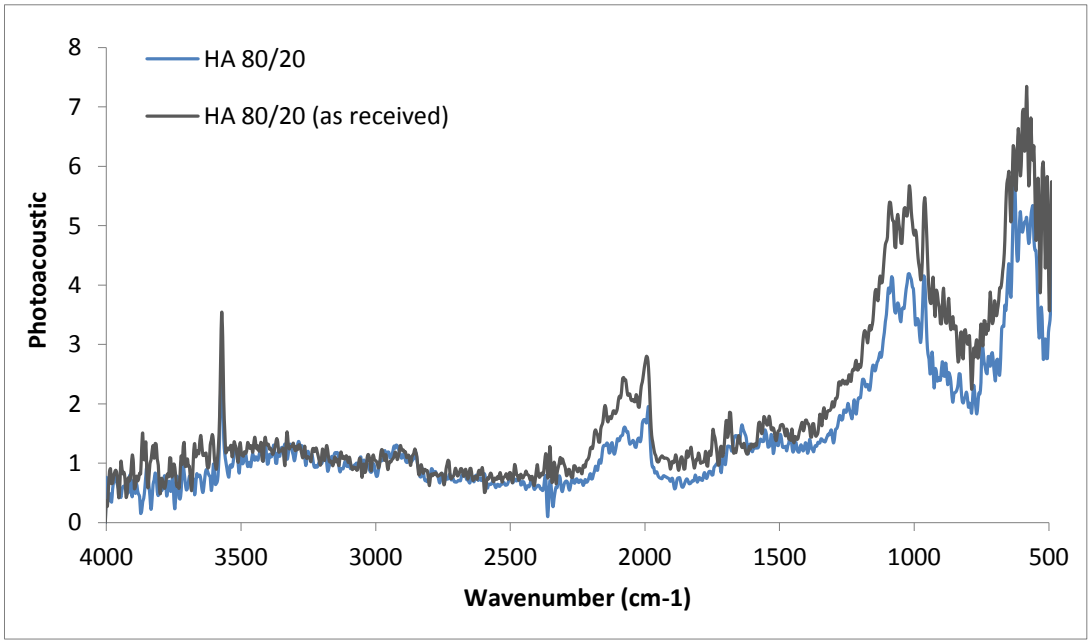

Figure 3.10: FTIR spectra of HA80/20

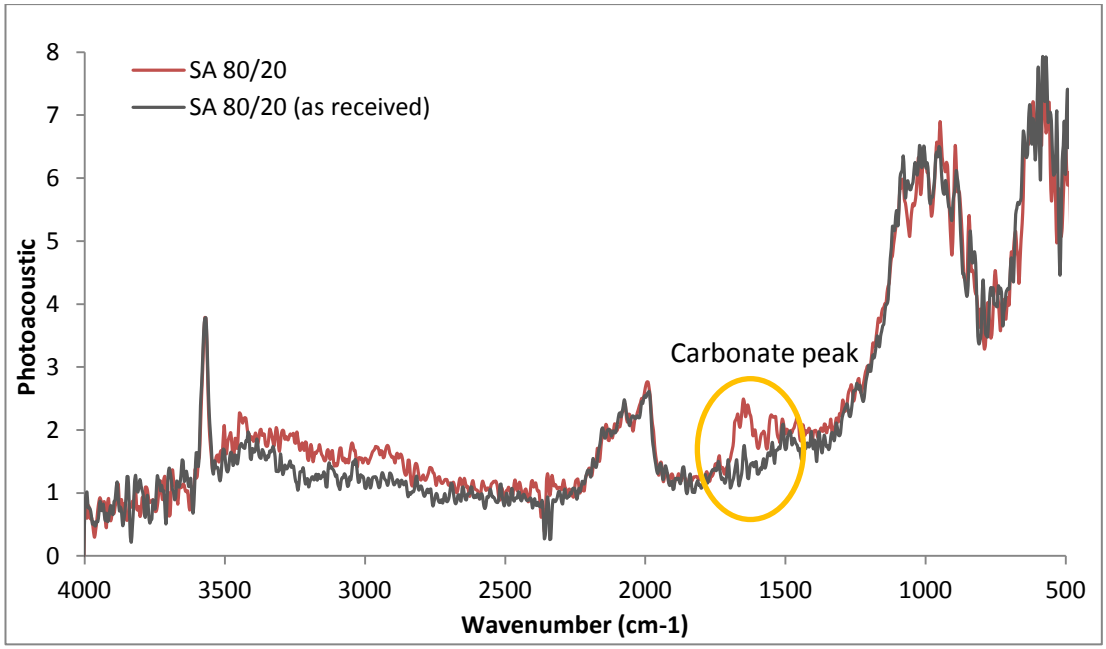

Figure 3.11: FTIR spectra of SA80/20

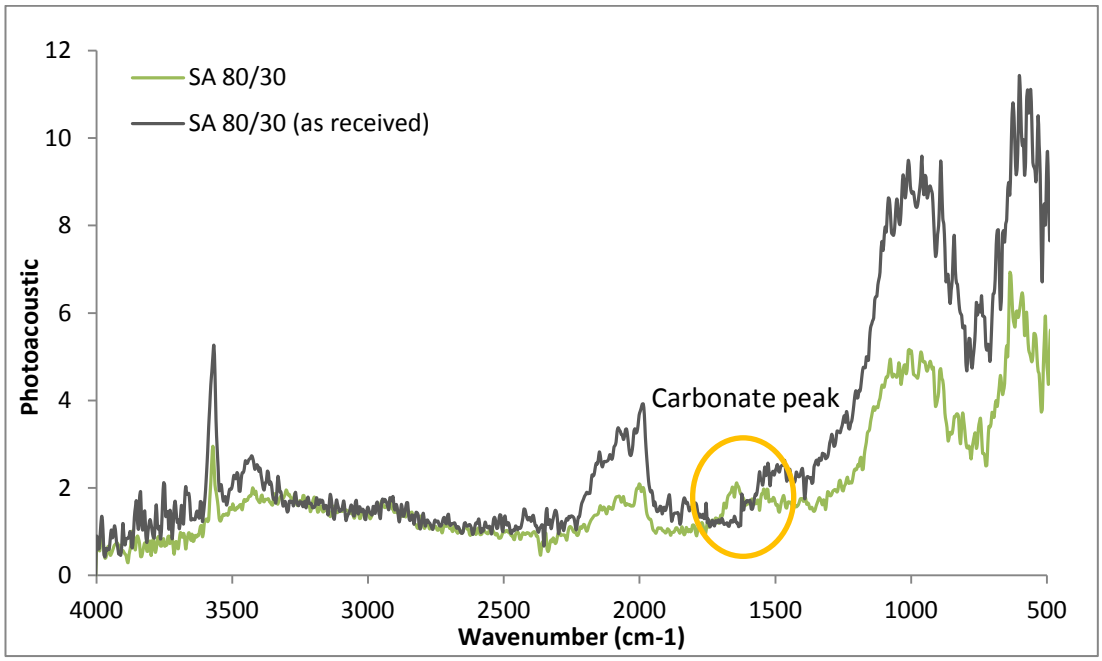

Figure 3.12: FTIR spectra of SA80/30

3.3.4 SEM Analysis

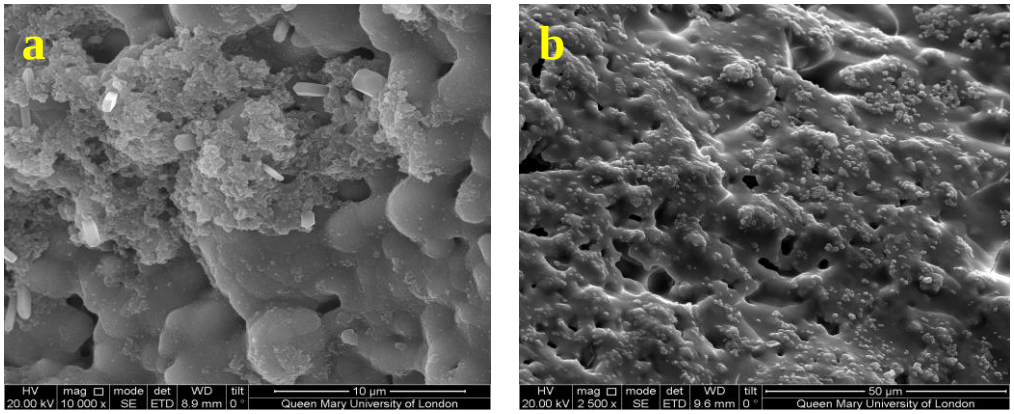

Figure 3.13: SEM images of HA80/20, a) CaP precipitated layer & b) protein deposition as determined by EDS analysis

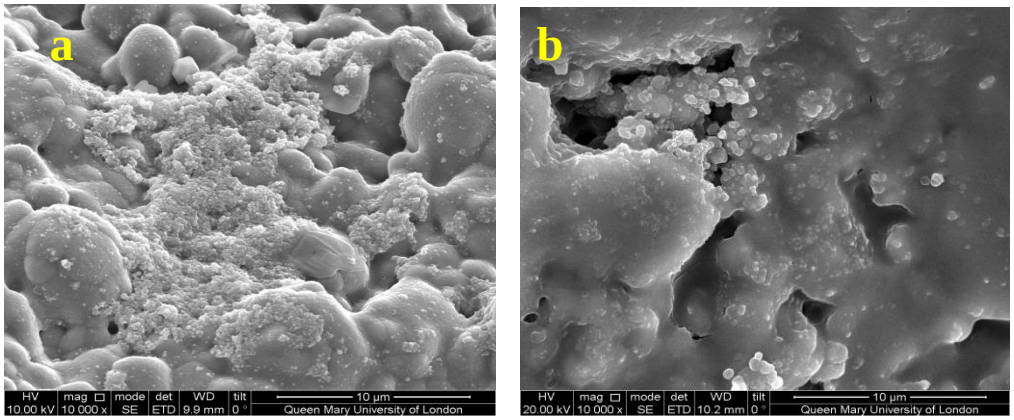

Figure 3.14: SEM images of SA80/20, a) CaP precipitated layer & b) protein deposition as determined by EDS analysis

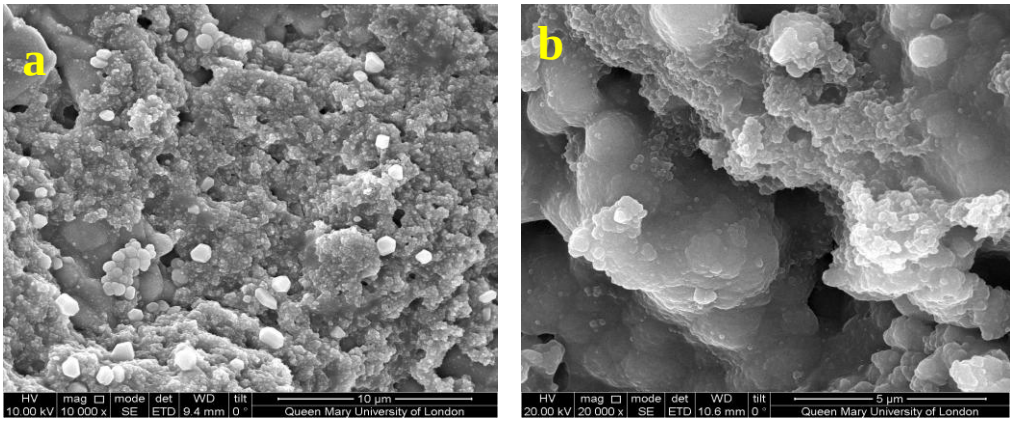

Figure 3.15: SEM images of SA80/30, a) CaP precipitated layer & b) protein deposition as determined by EDS analysis

From Figure 3.13a, Figure 3.14a & Figure 3.15a, it is evident that there is a presence of a CaP precipitated layer on all three BGS surfaces. Figure 3.15 showed a vast spread of the CaP layer on the SA80/30 surface in comparison to HA80/20 and SA80/20.

Also from Figure 3.13b, Figure 3.14b and Figure 3.15b, there was an observed organic layer present on the surface of all the BGS samples, suggesting a deposition of proteins on the surface. In comparison, there was a lesser amount of deposition visible on the SA80/30 sample than on SA80/20 and HA80/20 samples with a greater coverage observed on HA80/20.

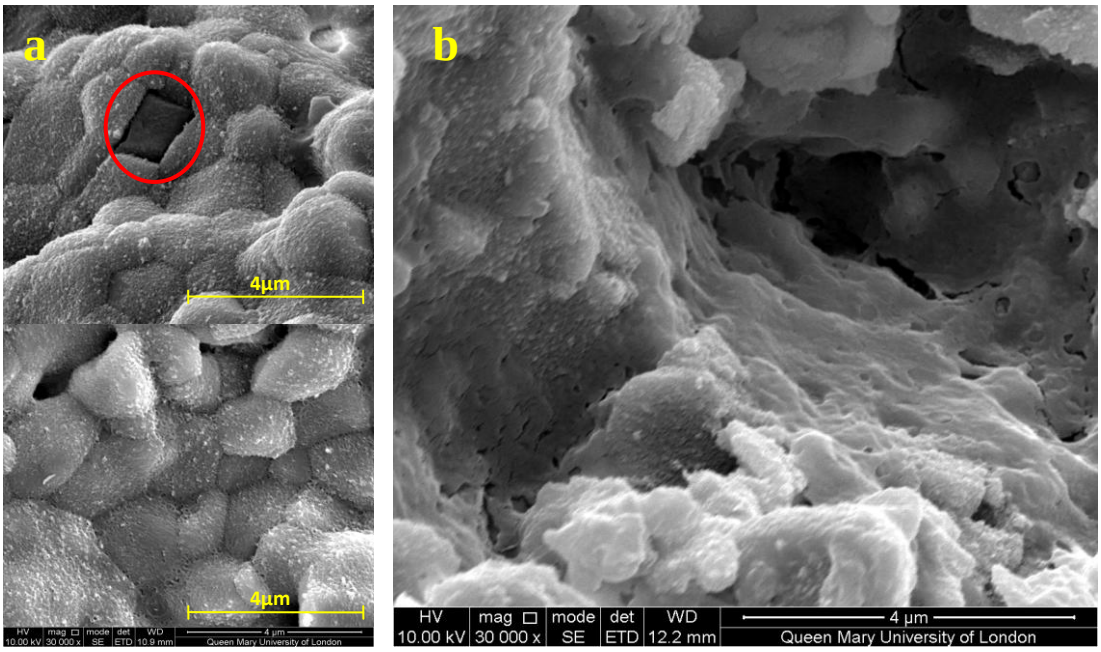

Figure 3.16: a) SEM image showing preferential dissolution (circled) taking place on SA80/20 in comparison to another site on the same sample where preferential dissolution did not occur and b) greater protein deposition observed within deeper pores in SA80/30

SEM images were also conducted within deeper pores found within the respective samples. There was an interesting observation whereby there was greater and more extensive protein deposition and less precipitated calcium phosphate layer seen on the surface of the SA samples and particularly on the SA 80/30 sample as can be seen in Figure 3.16b.

3.4 Discussion

From previous studies it has been shown that immersing the sample in media leads to changes in the physical and chemical properties of the samples along with variations in ionic concentrations of the surrounding media. There was a significant decrease in calcium and phosphate ions observed from all BGS in comparison to the bulk media suggesting the precipitation of a calcium phosphate (CaP) layer on the surface of the samples which was further supported by the results obtained from the SEM analysis conducted.

Macropores are believed to be a vital parameter for osteoinduction for which the mechanism is still under thorough investigation. Interconnected macropores have the ability to make available a sustainable pathway for the supply of blood and other bodily fluids to and from the implanted graft material. Habibovic et al in 2005 suggested that within these well interconnected macropores there is the transfer of calcium and phosphorus ions which are components in the precipitated apatite or apatite like layers making the graft bioactive however, this was for TCP and TCP/HA grafts (Habibovic, Yuan et al. 2005). It has also been shown how increased rate of dissolution leads to the greater release of calcium, phosphate and silicate ions in the surrounding medium therefore a quicker apatite layer formation (Campion, Ball et al. 2013). This is consistent with the findings from this study as SA80/30 showed a greater capacity to resist calcium and phosphorus ion depletion in comparison to HA80/20 and SA80/20 (see Figure 3.3 and Figure 3.4) and showed relatively faster dissolution of silicon ions in media (Figure 3.5)

XRD and FTIR analysis conducted on the BGS after experimentation showed that there was no detection of secondary phases and that there was a carbonate peak introduced in the SA BGS which suggest a carbonate apaitie being preceiptated on the surface of the granules and this is corrobborated with the SEM images taken along with showing the presence of an organic proteinaceous layer on the surface of the BGS.

It was interesting to note that the CaP layer precipitated on all the samples was not of a needle like structure, in fact it was more spread and of a blunt nature. It was seen both on the surface of the samples and within deeper pores. The results from the FTIR analysis suggest that the formation of this CaP layer was in fact bone like apatite favoured by the presence of carbonate peak after immersion in SCM for both SA80/20 and SA80/30 granules. As there was a greater apatite like layer observed on the SA80/30 this suggests that the increase in strut porosity in fact accerlerated ion exchange within this sample despite supporting significant levels of protein adsorption (Figure 3.15). In previous studies it has been demonstrated that the presence of serum proteins regulated the release of calcium, phosphate

and silicate ions which in turn allowed for the deposition of a CaP rich layer on the surface of HA and SA BGS. However the media without serum proteins onbserved an irregular release of these ions and showed no deposition of a CaP layer on the surface of the BGS (Chana 2010).

Protein deposition was seen in all three samples surfaces and along the grain boundaries. However the extent of deposition was greater within deeper pores and generally more of the protein deposition was seen on SA80/20 and HA80/20 samples in comparison to SA80/30. It could be suggested that as these deeper pores were within the bulk of the granules, they were hidden from the fluid shear caused by the rotating motion of the overhead stirrers holding the granules. Therefore the level of protein deposition was greater due to less shear being present. These findings may also be relevant to what happens *in vivo* as, in ectopic studies, osteoinduction is always occurs within the bulk of the granule masses and never at the edges where one might find growth factors present. It was also observed that there was an either or situation whereby many grains were covered with a protein layer but the CaP precipitate could not be seen or the precipitate could be seen but there was no sign of protein deposition. This evidence supported findings by Botelho (2005) whereby it was found that protein attachment occurs before the precipitation of a rich apatite like layer (Botelho, Brooks et al. 2005). An explanation for the greater protein deposition within deeper pores within SA80/30 is that when under semi dynamic conditions there is a high flow of medium around the granulated samples therefore allowing greater precipitation of a CaP layer. However within deeper pores the flow of the medium is a lot lower and the area becomes shear protected therefore the precipitation of a CaP layer becomes more difficult and would require more time in order to fully precipitate a CaP layer within these deep pores.

The SEM imaging was conducted on a single large granule (n=6) respective to the samples used, therefore it also depends which granule is being characterised as the granules present deep within the mesh basket would have been exposed to less shear in comparison to the granules present along the outer surface which would have been exposed to greater shear and flow of medium therefore allowing quick protein attachment to the surface followed by a quicker precipitation of the CaP layer on these specific granules.

3.4.1 Observed trends

There was a significant initial release of calcium ions from all BGS samples when compared to the bulk solutions. All the samples showed an increase in the amount of calcium release which began to decrease by 2 hours of the study. This decrease in calcium ions marked the

precipitation of calcium. A greater increase in the amount of calcium released from the SA80/30 was observed whereas SA80/20 and HA80/20 did not show an as intense release of the ions. Therefore, suggesting that a higher and more favoured dissolution of calcium ions from the SA80/30 sample was occurring.

A similar trend was observed with the release of phosphate ions with a significant initial steady release of the ions with all the samples, however there was not a great release as observed with the initial calcium ion release from all samples. The decrease in phosphate ions also occured alot sooner in comparison to the calcium ion release at 30 minutes in to the experiment. With SA80/30 releasing an increased amount of phosphate ions this would suggest they are helping in desorption of albumin proteins and therefore showing an increase in the amount of calcium ions released as well. As proteins have a lower affinity for the negatively charged phosphate ions, the decrease in the ion concentration at 30 minutes can be put down to the precipitation of the phosphate ions. Finally it has been established that dissolution profiles involving calcium and phosphate ions show similar trends, this therefore suggests that the decrease in calcium and phosphorus ion concentration is attributed to the formation of a CaP layer which is consuming the calcium and phosphate ions from the surrounding media.

The release of silicate ions from both SA80/20 and SA80/30 samples were not significantly different. There was no release of silicate ions in to the media from the HA80/20 samples detected. By day 9 of the study the silicon dissolution was significantly greater in media from the SA80/30 sample in comparison to the SA80/20 sample. Looking at the dissolution profile closly, at 1 hour a greater release of silicon ions is detected from SA80/20 whereas from SA80/30 a greater release is observed from 7 hours. These particular time points mark the decrease in phosphorus ions suggesting a re-precipitation of the phosphorus ions on to the respective sample surfaces. This increase is attributed to the dissolution of silicon ions from the SA80/30 and SA80/20 samples used leading to an increase of Si-OH groups being present within the surrounding media. Leonor et al looked at growing a bone like apatite layer on chitosan microparticles after they had been treated with calcium silicate and later soaked in SBF solution. The authors also found that an increase of silicon concentration was due to the dissolution of silicate ions from the calcium silicate coatings they applied which further lead to the presence of Si-OH groups on their specimens (Leonor, Baran et al. 2008).

As stated by Daculsi et al 1989 dissolution is initiated at grain boundaries and dislocations present *in vivo* (Daculsi, Legeros et al. 1989) and many studies have shown that the bioactivity of HA bioceramics is dependant on the microstructure and on the number and

type of defect structures that are present as they are able to provide the activation energy required to overcome the energy barrier in order to initiate nucleation (Nelson, McLean et al. 1983). Porter et al (2004) postulated that the incorporation of silicon into the HA lattice increased the number of grain boundaries and triple junctions present (Porter, Botelho et al. 2004). The findings from this current work were not in agreement with the findingd from Porter et al as from the SEM images, it is evident that there is CaP layer formation on the actual grains as well as at the grain boundaries and also within the deeper pores there is also visible protein deposition that has occurred as can be seen in Figure 3.16.

The SCM used in this experiment was a pre-buffered medium therefore the bulk solutions of SCM was 7.2. The medium was buffered with sodium bicarbonate. In *in vivo* the pH of blood is usually 7.4. If this value drops below 7.0 or above 7.7 the results could be fatal, as many of the proteins and enzymes become denatured which would affect many metabolic reactions. Fortunately the pH of the blood is controlled by a bicarbonate buffer system. When the pH gets too low (high H^+ concentration.) the flowing occurs:

$$H^+ + HCO3^- \longleftrightarrow H_2CO_3$$

Equation 5

Because H_2CO_3 is a weak acid, the H^+ has the ability to stay associated with the H_2CO_3. This reaction would effectively lower the pH. On the other hand when the pH gets too high (high OH concentration.) the following occurs:

$$OH + H_2CO_3 \longleftrightarrow CO_3^- + H_2O$$

Equation 6

Many other *in vitro* studies that have been conducted have used SBF as their medium which was designed by Kokubu in 1990 which also has the addition of a buffer solution in order to mimic *in vivo* pH conditions (Kokubo, Kushitani et al. 1990). Tris hydroxymethylaminomethan with the addition of hydrochloric acid is well known as a Tris buffering solution which is used within SBF to help maintain the pH. There is also the addition of sodium bicarbonate which also acts as a buffering agent. Table 3.2 highlights the composition of SBF and blood plasma.

Table 3.2: Ionic composition (mmol L^{-1}) of human plasma and SBF (Kokubo, Kushitani et al. 1990)

	Na^+	K^+	Mg^{2+}	Ca^{2+}	Cl^-	HPO_4^{2-}	HCO_3^-	SO_4^{2-}
SBF	142.0	5.0	1.5	2.5	147.8	4.2	1.0	0.5
Plasma	142.0	5.0	1.5	2.5	103	27.0	1.0	0.5

The pH plot seen with this medium showed an increase in the pH with time making the pH more basic (Figure 3.6). This meant that the media was taking up free H^+ ions therefore showing a decrease in the amount available. This is a viable explanation as there are many proteins present in the SCM used. Previously it has been shown that without the addition of serum in media, the pH become more acidic with time (Chana 2010). It was surprising to see that silicon showed no direct effect on the pH, however the pH for all three samples immersed in SCM showed a continuous and steady increase with time. It is generally accepted that as silicon is released it degrades into silicic acid ($SiOH_4$) (Reffitt, Ogston et al. 2003) *In vivo* human blood plasma contains silicic acid at levels of less than 1mg/l. It is supposed to be the most natural form of an element within the environment and is readily removed by the function of kidneys (Canham, Reeves et al. 1999). Taking this into consideration as the silicon degrades into an acid form the pH should have decreased and become more acidic as it was being released from SA used. This did not occur in this study therefore suggesting the pH was not sensitive to silicon release.

3.4.2 Protein Adsorption

When calcium phosphate ceramics are implanted into the body there are a number of events that occur which subsequently affect cell attachment and behaviour. These can include apatite layer formation by dissolution and re-precipitation and protein deposition. Proteins become absorbed onto the substrate surface from the surrounding bodily fluids present within seconds or minutes after immersion (Norde 1995). The factors which determine what protein will be absorbed on to what surface are of a complex nature, however it is accepted that the ionic composition, strength of solution, pH of solution and the functional groups present on the protein and substrate all in turn affect the kinetics of protein adsorption.

In vivo the situation is far more complex with various proteins competing for specific binding spaces in dynamic processes. Proteins initially bound to the substrate maybe replaced by other competing proteins.

The principle forces that cause the non-covalent bonding of the protein to the substrate surface are polar hydrogen bonding forces. These are known to be the main driving force of hydrophobic interactions. Exposed chemical functional groups determine the distribution and also the density of these forces which in turn will affect the hydrophobicity of a substrate. This hydrophobic nature of the substrate had a direct effect upon protein adsorption and further cell adhesion (Sharpe, Sammons et al. 1997).

On adsorption or binding the proteins themselves undergo conformational changes which are thought to also play an active role on the adsorptions of proteins to substrates. It is found that both albumin and fibrinogen proteins exhibit strong adsorption to either hydrophobic or hydrophilic surfaces and to apatite growth sites which in turn would inhibit crystallisation. The difference between the two proteins is that fibrinogen when absorbed onto silicates assumes a conformation which in turn exposes sites for calcium phosphate nucleation (Areva, Peltola et al. 2002). As the SA80/30 samples in SCM showed a greater and higher release of silicate ions it could be suggested that fibrinogen formed a particular conformation in order to promote the nucleation of the CaP layer at the surface.

From SA80/30 there was a greater release and re-precipitation of calcium and phosphorus ions in media along with and increased release of silicon ions (Figure 3.3, Figure 3.4 &

Figure **3.5**) in comparison to HA80/20 and SA80/20. A suggested route for CaP precipitation in the SA samples could be that once proteins have attached to the surface of both SA samples, the calcium ions that are being release would be taken up by the proteins present at the surface of the samples. As SA80/30 has a higher strut porosity, more calcium ions would in theory be covering the surface however there was on the other hand a lot more protein was present on this particular surface in comparison to the SA80/20. Before a CaP layer could be precipitated on the surface, the proteins had to be saturated with calcium ions. This in turn meant that the calcium ions that were being released after the proteins had been saturated were being precipitated onto the sample surface. The same process would be occurring with both SA80/20 and HA80/20 but as the strut porosities for both BGS is less than SA80/30, the time required to release enough calcium ions in order to show more protein deposition on their surfaces is increased therefore less CaP deposition is observed.

Some proteins have a low affinity for the negatively charged phosphate ions; this in turn increases the concentration of phosphate ion in the surrounding medium. After the proteins become saturated with calcium ions, the ‘free’ calcium ions begin to attract the negatively charged silicate ions present on the SA samples.

3.4.3 Role of Silicate Ions

This study has reported results which help in confirming that the presence of silicate ions plays an important role in the CaP precipitate layer. The differences observed in the release and uptake of phosphate ions, especially at later time points between HA and both SA samples were most likely due to the change in mineral structure as a result of the silicate substitution. Gibson et al in 1999 reported that the increased biological reactivity of SA compared to HA was associated with the distortion of the mineral structure (Gibson, Huang et al. 1999). The work reported that 0.4wt% silicate substitution resulted in an increase from 1.85 to 2.75 in the distortion index of HA and SA respectively. This therefore increased the distortion in the mineral structure and is thought to result in the increased activity of SA and it is further enhanced by increasing the wt% of silicate substitution within the HA lattice.

The incorporation of silicon ions distorts the HA structure making it energetically favourable for silicate ions to dissolve. At grain boundaries silicate ions when released leave behind empty defective sites which increase the dissolution of calcium and phosphate ion in the SA structure. This can clearly be seen with the release of these ions as both SA structures show greater dissolution of calcium and phosphate ions in comparison to the HA sample. Silicate ions also help in decreasing the time required for spontaneous precipitation of HA. The SEM images obtained for the SA samples showed a greater CaP layer in comparison to the HA sample. The micropores within the SA samples increased the surface area for an increase in protein deposition which led to ion exchange for a successful CaP precipitated layer. It has been shown that the precipitation of an apatite layer has the ability to further facilitate bone formation leading to enhanced cell attachment, proliferation and finally differentiation (Guth, Buckland et al. 2006).

3.5 Summary and Conclusions

The work that has been presented in this chapter demonstrated the changes in calcium, phosphate and silicate ion concentration in media under semi dynamic conditions for up to 9 days as a result of incubation in HA80/20, SA80/20 and SA80/30.

The study was able to provide results showing changes in ion concentration with changes in material chemistry and strut porosity, however further works that can be suggested in order to clarify pending results and expand on the knowledge gained from this experiment. There characterisation techniques that were conducted in this experiment were successful in showing that changes in dissolution and precipitation, protein deposition and finally CaP precipitation was purely down to chemical changes and strut porosity variation and not any pre-compositional deviations.

Overall SA80/30 showed a greater dissolution of calcium and phosphate ions in comparison to SA80/20 and HA80/20 in the SCM. There was also a superior release of silicate ions from SA80/30 in comparison to SA80/20 causing this surface to become more electronegative. This was due to the higher strut porosity within the SA80/30 sample which further gave an increased surface area for protein deposition and therefore an increase CaP precipitation at the surface. The SA80/30 sample showed a greater amount of CaP layer present at the surface whereas the SA80/20 and HA80/20 showed greater protein deposition with the initiation of CaP layers. This was due to the quicker precipitation of a CaP layer at the SA80/30 surface in comparison to the other two samples. This would suggest that increasing the immersion time for the other two samples would finally show a greater and vast amount of CaP layer covering nearly all of the respective sample surfaces.

The ionic interactions with the surrounding media and the materials surface have shown that material chemistry and increased strut porosity have a positive effect on the dissolution and re-precipitation of a successful CaP layer in order to allow bone in growth. Even though experimental data gained by using a semi dynamic system has been positive, the use of this particular system is not a real depiction of what happens *in vivo* once the BGS has been inserted in to the bone defect site. In order to understand the complexity of interactions between BGS and the surrounding environment *in vivo*, a system which investigates the dynamic exchange of these specific ions between different BGS needs to be established.

Chapter 4 will endeavour to explore the set-up of a dynamic perfusion system which will look at ion exchange between BGS and the surrounding media and what affect this has on osteoblast -like cell response.

Chapter 4 Dynamic ionic exchange within a 3D perfusion system and its effect on osteoblast-like cell response

4.1 Background

There is a significant barrier in our understanding of BGS integration within defect sites at the cellular level because there is a lack in methodology in order to study bone cells in their native environment. There has been a lot of work conducted focussing on the empirical responses of individual cell types to mechanical and chemical stimuli but there are only a few studies that have taken this further in order to understand and determine material specific responses driven by cellular response in their native environments.

There needs to be further research conducted in order to create 3D environments that integrate the influence of substrate chemistry and osteoinductivity in order to understand cell behaviour within the *in vivo* environment, *in vitro*.

Therefore, as a result of the findings in Chapter 3, indicating that in a 'closed' system the presence of porous apatite granules results in a significant depletion in calcium and phosphate ions this next chapter is concerned with the investigation of the effect of media volume on the rate and extent of ion depletion on exposure to a fixed mass of granules.

Additionally, cell culture experiments were performed to investigate any potentially confounding sensitivity to ion depletion under standard 2D (seeded on tissue culture plastic) and 3D (seeded on porous granules), static (no fluid motion/media circulation) conditions with periodic refreshment of pre-conditioned media.

Furthermore, the results of the SEM conducted in Chapter 3 suggested that the spinning basket system lead to different regions of the granule masses being exposed to varying degrees of media circulation, making it unsuitable for future cell culture investigations and that therefore a 3D perfusion system with a more uniform profile of media circulation should be developed.

SA80/20 granules were used in order to investigate whether this new 3D perfusion system would be sensitive to silicate ion concentrations levels. *In vivo* studies have shown that there is a difference in osteoinductivity between SA80/20 and SA80/30 BGS, however the greater strut porosity of SA promoted the formation of more highly mineralised bone at 8 weeks (Coathup, Hing et al. 2012). As the current experiments in this and following chapters are short term *in vitro* studies, it was more favoured to use SA80/20 granules.

In order to conduct these investigations the work was broken down into three distinct steps:

- **STEP 1** – Commissioning of a 3D perfusion system to study the effects of media reservoir volume on the rate and extent of ion exchange with a fixed mass of BGS granules over a period of 7 days, and to prepare sufficient pre-conditioned media (PCM) for experiments in steps 2 and 3.
- **STEP 2** – 2D cell culture studies using MG63 human osteoblast like cells seeded directly into 24 well plates and then exposed to PCM, to study the effect of calcium and phosphate ion depletion from media as a result of exposure to BGS granules.
- **STEP 3** – 3D culture studies using MG63 human osteoblast like cells seeded directly on HA80/20 granules and then exposed to PCM, to study the effect of calcium and phosphate ion depletion from media.

4.2 Methodology

4.2.1 STEP 1 – Commissioning of a 3D - PERFUSION system and investigation of the influence of reservoir volume on ion exchange.

As a result of the investigations conducted in Chapter 3 the decision was made to set up a 3D perfusion system for all further investigations and the following criteria established

- The system should be easy to use to aid repeatability/reliability
- The components of the system must be readily sterilisable
- Granule masses must be presented in chambers that facilitate as uniform a circulation of media as possible
- The system should have multiple chambers to facilitate multiple replicate/multiple granule type testing at the same time
- Each chamber should be independently supplied with media from a distinct reservoir at a controlled flow rate to eliminate cross contamination between replicates/granule types
- The chambers should be designed so that load may be introduced to the individual granule masses using a suitable test rig in future experiments.

With these criteria in mind the following system was developed (Figure 4.1):

- ISMATEC ICP-8 multichannel peristaltic pump (VWR International) - to provide individual flow rate control for media circulation
- Silicone tubing with 1mm inner diameter and 0.75mm wall thickness in order to allow circulation of the media through the system (VWR International)
- Large autoclavable bottles to hold media reservoirs (VWR International)
- Autoclavable 3mm - 3mm small straight push on connectors (small connectors), (Trecarn Engineering, UK)
- Parafilm, in order to secure all connection points to stop any leaking of media whilst circulating (Sigma-Aldrich, UK)
- Hot plates, to heat and maintain media reservoirs to 37^{o}C before and during experimentation.

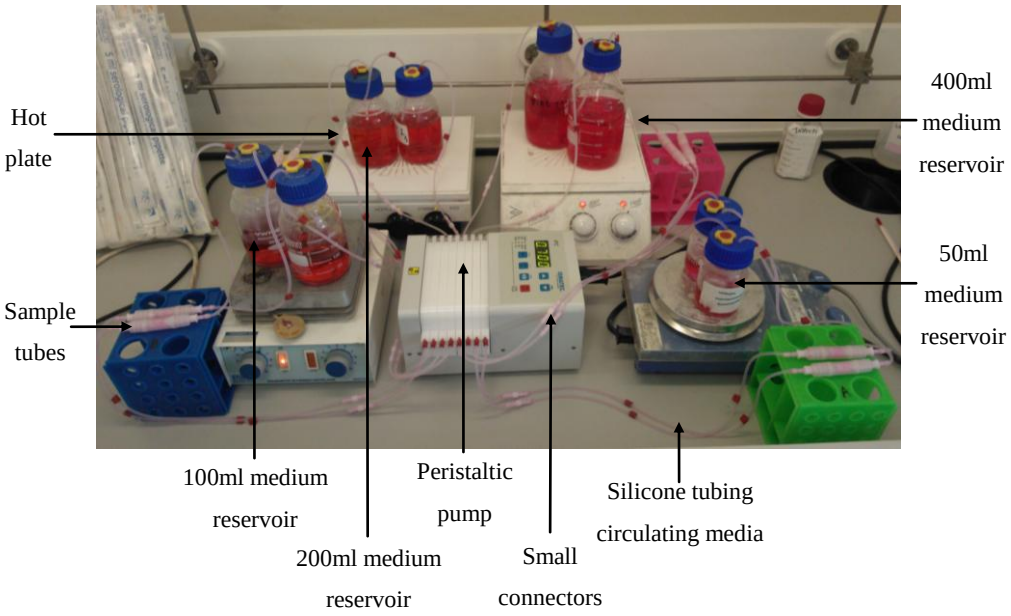

Figure 4.1: 3D- perfusion system for study of media reservoir volumes on ion exchange

Sample chambers were fabricated from the following components:

- 8mm inner diameter, 3mm wall thickness silicone tube (VWR International)
- 8mm diameter high density polyethylene mesh discs of 950 x 700 micros (mesh discs), (Sigma-Aldrich, UK)
- 8mm - 4mm large reducing straight push on connectors (large connectors), (Trecarn Engineering, UK)

For all reservoir volume experiments 0.45g (~ 0.75ml) of SA80/20 granules 1-2mm in size were used and UV sterilised under a sterile laminar hood for 2 hours.

After sterilisation, 0.45 ± 0.02 g granules were weighed out and packed in an 8mm diameter, 15mm length silicone tube, with 8mm diameter mesh discs at either end in order to stop granules falling out. Finally large connectors were put on both ends of the sample tube in order to provide attachment points for silicon tubing to deliver the medium.

Figure 4.2 illustrates the steps taken in order to prepare the sample tubes. For each run of experiments conducted, sample tubes were prepared in duplicates for each of the four reservoir volumes tested. All sample preparation took place under a sterile hood to minimise any contamination from occurring within the sample tubes.

Once all sample chambers were connected to their individual media reservoirs media was circulated at a flow rate of 0.7ml/min.

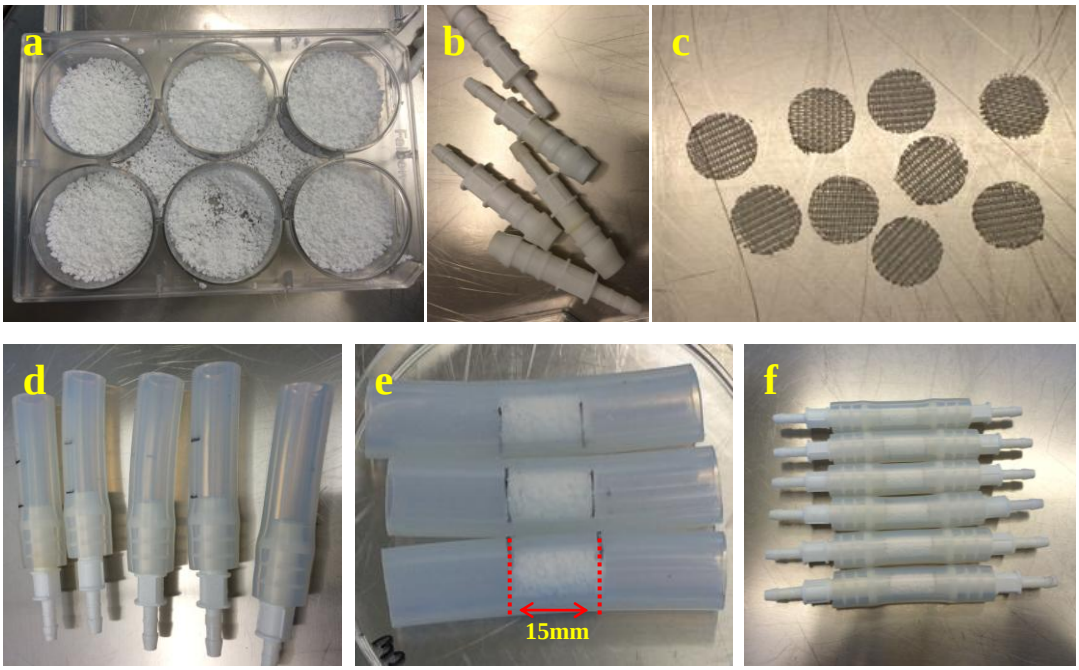

Figure 4.2: Images showing sample preparation steps, a) UV sterilised SA80/20 granules, b) large reducing straight push on connectors, c) 8mm mesh discs, d) large connectors pushed on to silicon tube, e) 0.45g SA80/20 packed into 8mm diameter, 15mm length silicon tube with mesh discs at either end to stop granules from falling out and f) final sample tubes ready containing packed SA80/20 granules

4.2.1.1 Media Preparation and sampling for investigation of the effect of reservoir volume on ion exchange

The base culture media used for this study was Dulbecco's Modified Eagle Medium (DMEM) supplemented with 1% penicillin-streptomycin (Pen/Strep). Although from previous work within our laboratory it was well known that the presence of serum proteins has a significant impact on the pattern of ion exchange the decision was made to conduct further experiments with serum free media to avoid the potentially confounding influence of serum degradation when comparing cell response to pre-conditioned media with fresh media in later studies.

Four different media reservoir volumes (Table 4.1) were selected based around the sample mass:reservoir volume used in the previous spinning basket experiments in Chapter 3 (3.0g granules:750ml media, ~ 1g:250ml).

Table 4.1: Media volumes and sample mass ratios used to investigate effect of reservoir volume on ion exchange

Designation	50PCM	100PCM	200PCM	400PCM
Media Volume (ml)	50	100	200	400
Sample mass (g):Media Volume (ml)	1:111	1:222	1:444	1:888

5 ml of solution was extracted at time intervals of 30 minutes, 1, 2, 4, 24, 72, 120 and 168 hours and replaced with 5ml fresh DMEM+1% Pen/strep The calcium, phosphate and silicate ion concentration of the extracted solutions were analysed using colorimetric assays (detailed in following Section) which had been previously been used within our lab and allowed use of smaller sample volumes (Guth, Campion et al. 2011). At 168 hours the four different volumes of conditioned media were collected and individually sterile filtered and supplemented with 10% FBS for use in cell culture experiments as preconditioned media (PCM).

4.2.1.2 Colorimetric Assays used to determine Ionic Concentration

4.2.1.2.1 Calcium Assay

Calcium ion concentrations were determined by using a QuantiChrom™ calcium assay kit, DICA-500 (BioAssay Systems, USA) used according to the manufactures instructions. Calcium standards (Std) were prepared from the stock solution provided in the kit plus the addition of deionised water (d.H_2O) to obtain 8 concentrations ranging from 0mg/dL to 20mg/dL, highlighted in Table 4.2. The calcium concentrations were calculated from the calibration curve (presented in APPENDIX 2) if the R^2 value was ≥0.99. Final calcium ion concentrations for standards and samples were converted from mg/dL to mg/ml.

All reagents and standards had to be equilibrated to room temperature before use. All standards and samples were tested in triplicate. Sufficient working reagent was prepared by combining reagent A and B (provided in the kit) in equal volumes. The assay procedure was as follows:

- Dilute standards as indicated in Table 4.2 above
- Transfer 5µl of the standards and samples into wells of a clear bottom 96 well plate
- Add 200µl of the working reagent to standards and samples

- Incubate plate at room temperature for 3 minutes and read optical density at 570nm using MultiScan Ascent^{TM} and its associated software (Labsystems, UK).

Table 4.2: Calcium standard solution dilutions provided in kit

Std.	Std + d.$H_2$0 (µl)	Final Vol. (µl)	Ca conc. (mg/dL)	Ca conc. (mg/ml)
1	100 + 0	100	20	0.2
2	80 + 20	100	16	0.16
3	60 + 40	100	12	0.12
4	40 + 60	100	8	0.08
5	30 + 70	100	6	0.06
6	20 + 80	100	4	0.04
7	10 + 90	100	2	0.02
8	0 + 100	100	0	0

4.2.1.2.2 Phosphate Assay

For the determination of phosphate ion concentration, the assay protocol has been followed as previously described in worked conducted by Guth et al (Guth, Campion et al. 2011) and was originally adapted from Chen et al (Chen, Toribara et al. 1956). All reagents used for this assay were purchased from Sigma-Aldrich, UK unless otherwise stated.

A 16 point dilution was prepared ranging between 0mM to 9mM (0mg/ml to 3.22mg/ml respectively). The standards were made from a stock solution of 100mM sodium dibasic dodecahydrate (SDD) in d.H_2O which was prepared dissolving 1.79g of SDD in 50ml d.H_2O to obtain a volume of 50ml standard solution. The standard solution concentrations used are listed in Table 4.3 below.

The concentrations of phosphate present in the sample were calculated using the calibration curve (presented in APPENDIX 2) if the R^2 value was $\geq$ 0.99. Final phosphate ion concentrations for standards and samples were converted from mM to mg/ml.

The solutions that were required and used in order to prepare the phosphate reagent for the assay are listed in Table 4.4. The phosphate reagent was prepared by mixing together one volume 6M sulphuric acid, 2 volumes of d.H_2O, one volume of 2.5% (wt/v) ammonium molybdate and one volume of 10% (wt/v) ascorbic acid.

Table 4.3: Phosphate standard solutions prepared

Std	100mM SDD (µl) + d.H_2O (µl)	Final Vol (µl)	P conc.(mM)	P conc.(mg/ml)
1	0 + 100	100	0	0
2	0.25 + 99.75	100	0.25	0.0895
3	0.5 + 99.25	100	0.5	0.179
4	0.75 + 99.25	100	0.75	0.2685
5	1.0 + 99	100	1.0	0.358
6	1.25 + 98.75	100	1.25	0.4475
7	1.5 + 98.5	100	1.5	0.537
8	1.75 + 98.25	100	1.75	0.6265
9	2 + 98	100	2	0.716
10	3 + 97	100	3	1.074
11	4 + 96	100	4	1.432
12	5 + 95	100	5	1.79
13	6 + 94	100	6	2.148
14	7 + 93	100	7	2.506
15	8 + 92	100	8	2.864
16	9 + 91	100	9	3.222

Table 4.4: Solutions required for phosphate reagent

Volumes	Solution	Composition	Storage
1	6M Sulphuric Acid	17.4M sulphuric acid + d.H_2O	Room Temperature for 6 months
2	d.H_2O	-	-
1	2.5% (wt/v) Ammonium Molybdate	Ammonium Molybdate + d.H_2O	Room Temperature for 6 months
1	10% (wt/v) Ascorbic Acid	Ascorbic Acid + d.H_2O	Make on the day

All solutions and samples had to be equilibrated to room temperature before use. All standards and samples were tested in triplicates. The assay procedure was as follows:

- Make up standards as indicated in Table 4.3.
- Transfer 20µl of standards and samples in to wells of a clear bottom 96 well plate
- Add 80µl of d.H_2O to all wells containing standards and samples

- Add 100µl of prepared phosphate reagent as described in Table 4.4
- Lightly shake plate for 10 seconds before sealing it
- Incubate plate at 37^{o}C for 2 hours
- Let plate return to room temperature and read optical density at 805nm using MultiScan Ascent^{TM} and its associated software (Labsystems, UK).

4.2.1.2.3 Silicate Assay

For the determination of silicate ion concentration, the assay protocol has been adapted as previously described in worked conducted by Guth et al (Guth, Campion et al. 2011) and was originally adapted from Raggi et al (Raggi, Sabbioni et al. 1999). All reagents used for this assay were purchased from Sigma-Aldrich, UK unless otherwise stated.

The standards were made from sodium silicate solution (SSS). In order to obtain a 1.7mM standard solution, 30µl of SSS was mixed with 2970µl of d.H_2O. From this stock, 870µl was mixed with 30µl of DMEM + 1% pen/strep. From this stock solution a serial dilution of 8 points was prepared ranging between 0mM to 1.36mM (0mg/ml to 0.32mg/ml respectively) using d.H_2O. Final silicate ion concentrations for standards and samples were converted from mM to mg/ml. The concentrations of silicate present in the sample were calculated using the calibration curve (presented in APPENDIX 2) if the R^2 value was $\geq$ 0.99. The standard solution concentrations used are listed in Table 4.5.

Table 4.5: Silicate standard solutions prepared

Std	Serial Dilutions	Silicate conc.(mM)	Silicate conc.(mg/ml)
1	400µl of d.H_2O	0	0
2	400µl	0.02	0.005
3	400µl	0.04	0.01
4	400µl ÷ 2 each time to obtain serial dilutions	0.08	0.02
5	400µl	0.17	0.04
6	400µl	0.34	0.08
7	400µl	0.68	0.16
8	800µl of 1.36mM	1.36	0.32

There were two silicate reagents that needed to be made and used for this assay. The solutions that were required and used in order to prepare the two silicate reagents for the assay are listed in Table 4.6. Silicate reagent A was prepared by mixing together one volume of 4.5M sulphuric acid with one volume of 0.1M ammonium molybdate. Silicate reagent B was prepared by mixing 2 volumes of 10% (wt/v) oxalic acid with one volume of 3% (wt/v) ascorbic acid.

Table 4.6: Solutions required for silicate reagents

Reagent	Volumes	Solutions	Composition	Storage
A	1	4.5M Sulphuric Acid	17.4M sulphuric acid + d.H_2O	Room Temperature for 6 months
	1	0.1M Ammonium Molybdate	Ammonium Molybdate + d.H_2O	Room Temperature for 6 months
B	2	10% (wt/v) Oxalic Acid	Oxalic Acid + d.H_2O	Make on the day
	1	3% (wt/v) Ascorbic Acid	Ascorbic Acid + d.H_2O	Make on the day

All solutions and samples had to be equilibrated to room temperature before use. All standards and samples were tested in triplicates. The assay procedure was as follows:

- Make up standards as indicated in Table 4.5.
- Transfer 100µl of standards and samples in to wells of a clear bottom 96 well plate
- Add 100µl of Reagent A to all wells containing standards and samples, gently shake and seal plate
- Incubate plate at room temperature for 1 hour 30 minutes.
- Add 60µl of Reagent B to all wells containing standards and samples, gently shake and seal plate
- Incubate plate at room temperature for 10 minutes
- Read optical density at 805nm using MultiScan Ascent^{TM} and its associated software (Labsystems, UK).

4.2.1.3 pH Measurements

The pH was measured, as previously described in chapter 3 of each batch of freshly prepared DMEM+1% pen/strep and of all the samples collected during the reservoir volume experiments.

4.2.1.4 SEM Analysis

SEM analysis was conducted on the SA80/20 BGS after experimentation had been conducted. The protocol and equipment used is stated in Chapter 2 section 2.1.

4.2.2 STEP 2 – STATIC 2D CELL CULTURE EXPERIMENTS

4.2.2.1 Cell thawing, expansion and seeding

All cell culture work was conducted under a sterile laminar flow hood. The cells used in this study were human osteosarcoma MG63 cells and were initially cultured using serum containing medium (SCM), comprised of DMEM supplemented with 10% FBS and 1% Pen/strep. Prior to seeding, the cells were thawed and expanded as follows. MG63 cells were thawed at 37^{o}C by placing the 1.5ml cryovial stored in liquid nitrogen in a water bath. SCM was also warmed in the water bath. 1ml of SCM was added very gently to the thawed cells. The cells were then transferred to a 10ml centrifuge tube and 8ml of SCM was added. This suspension was then centrifuged at 1800rpm for 5 minutes. The supernatant was discarded and the pellet of cells was re-suspended in 1ml of SCM. After gently mixing the suspension in order to obtain a homogeneous mix of cells and solution, the suspension was then transferred to a T75flask (75cm^2 of growth area) with the addition of 10ml SCM. The cells were then left to incubate at 37^{o}C and 5% CO_2 and labelled as passage 1. The flask was regularly observed under a light microscope and media was changed every 2 days until the flask was 80% confluent with cells.

When the culture had reached 80% confluency, the cells were passaged. 10ml of SCM in the T75 flask was discarded and the cell layer was washed with sterile phosphate buffered saline solution (PBS). After the wash with PBS the cells were trypsinised in order to detach the cells from the surface of the flask. 2ml of trypsin-EDTA solution was added to the flask and then incubated at 37^{o}C, 5% CO_2 for 5 minutes. The cells were then checked under a light microscope to see whether they had detached from the surface of the flask. 2ml of SCM was

then added to the flask and then the resultant cells/trypsin/SCM solution was transferred to a centrifuge tube and spun down at 1800rpm for 5 minutes.

After centrifugation the supernatant was removed and the pellet of cells was resuspended in fresh SCM and transferred to new T75 flasks in order to obtain a 1:2 dilution of the cells in SCM. The flasks were then left to incubate at 37^{o}C and 5% CO_2 and labelled passage 2. This passaging process was continued until passage 4 (P4) was reached when static cell culture experiments could take place.

4.2.2.1.1 Cell Counting

Upon reaching P4, the cells again were trypsinised and centrifuged in order to attain the pellet of cells. This pellet was then resuspended in fresh SCM. A very small volume of this new cell suspension was taken in order to count the cells so the desired cell concentration could be achieved.

20µl of the cell suspension was homogeneously mixed with 20µl of trypan blue solution. 20µl of this solution was then pipetted on to a haemocytometer under a cover slip which was then placed under a light microscope. Viable cells were bright and round in shape while round, blue cells were considered to be non-viable. The viable cells were counted and the desired cell concentration was calculated.

4.2.2.1.2 Cell Density Optimisation

The desired cell concentration was chosen after doing a static cell density experiment which looked at $2x10^4$ cells/ml, $3x10^4$ cells/ml and $4x10^4$ cell/ml. The individual cell concentrations where seeded in 24 well plates in SCM and incubated for 1, 3 and 5 days at 37^{o}C and 5% CO_2. The SCM was changed after 24 hours and 48 hours thereafter. DNA and ALP quantification was conducted and the results obtained are presented in APPENDIX 3. From the obtained results, $4x10^4$ cells/ml was chosen as the cell density to use in this study as this particular cell density was successful in showing an increase in cell proliferation over 5 days when seeded on 24 well plate.

4.2.2.1.3 Cell Seeding, incubation and harvesting

Having reached P4 and optimised the cell density the cells were then seeded in to 24 well plates in SCM at a density of $4x10^4$ cells/ml and allowed to attach for 2 hours at 37^{o}C and 5% CO_2. From previous studies is has been shown that between 1.5 and 2 hours is the optimum time for MG63 cells to attach to a scaffold surface (Guth 2007). Therefore, the cells were left to attach to the plate surface for 2 hours. After 2 hours the SCM was replaced with either one of four preconditioned media supplemented with 10% FBS (50PCM,

100PCM, 200PCM or 400PCM) obtained from the perfusion study into the effect of reservoir volume or fresh SCM as a control.

The cells were incubated for periods of 1, 3 and 5 days under static conditions (no fluid motion) with periodic refreshment of the media, initially at 24 hours then every 48 hours thereafter. Figure 4.3 illustrate a schematic of the general procedure of the 2D static cell culture experiment with cells seeded directly on 24 well plates.

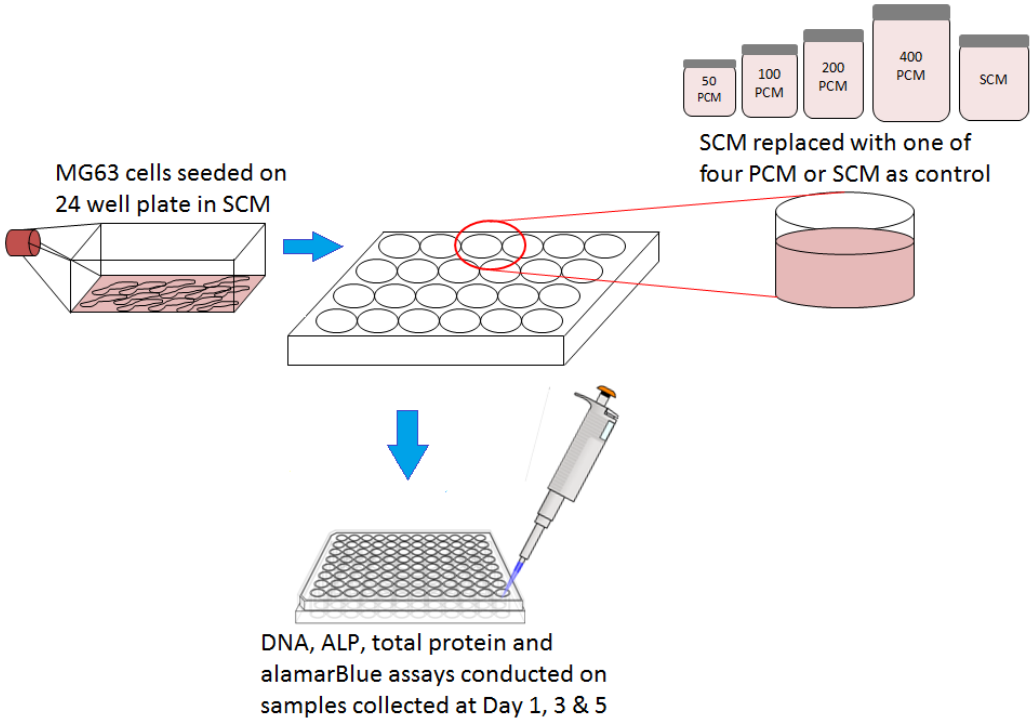

Figure 4.3: Schematic showing general procedure of static cell culture experiment with cells seeded on 24 well plates

After incubation for either 1, 3 or 5 days the media from the wells was collected in 1.5ml eppendorf tubes and stored at -20ºC. Cell lysates were collected for analysis by washing each individual well in the plates twice with 1ml PBS and then treating them each with 1ml 0.05% Triton-X (TX) solution. The plates were then sealed and stored at -20ºC. Prior to analysis the plates were thawed at room temperature and placed in an ultrasonic bath for 5 minutes, the resultant lysate solutions in the individual wells were then collected and stored in 1.5ml eppendorf tubes. Total DNA, alkaline phosphatase (ALP) activity and total protein was then quantified as detailed in sections 4.2.2.2-4.2.2.4. Cell metabolic activity was monitored using the AlamarBlue® assay which was conducted on the same population of cells at several time points over a period of 5 days as detailed in section 4.2.2.5.

4.2.2.2 Total DNA Quantification

Total DNA content was calculated by using a Quant-iT PicoGreen dsDNA Assay kit (Life Technologies, UK). The PicoGreen dye is highly sensitive to double-stranded DNA therefore it is able to bind to DNA in solution. Therefore it is a very good indicator of DNA levels in specific samples.

The kit provided a 100µg/ml lambda DNA solution which was mixed with 735µl of a pre-made TE buffer (1ml TE buffer mixed with 20ml distilled DNAse-free water). A serial dilution of 8 points was made ranging from 1µg/ml to 0.007µg/ml and was tested in triplicates. The concentrations of DNA present in the samples were calculated using the calibration curve (presented in APPENDIX 4) if the R^2 value was $\geq$ 0.99. The standard solution concentrations used are listed in Table 4.7 below.

Table 4.7: DNA standard solution prepared using serial dilutions

Std.	TE Diluent (µl) + DNA stock (µl)	Final DNA conc. (µg/ml)
1	100 + 100	1
2	100	0.5
3	100	0.25
4	100	0.125
5	100	0.0625
6	100	0.03125
7	100	0.015625
8	100	0.0078125

Transfer 100µl each time to obtain serial dilutions

All solutions and samples had to be equilibrated to room temperature before use. The PicoGreen working reagent is light sensitive, so it was very important that the addition of the reagent was done in a dark room to avoid inaccuracies in the fluorescence readings. Individual samples were tested at n=6 for repeatability. The assay procedure was as follows:

- Make up standards as indicated in Table 4.7.

- Transfer 100µl of standards and samples in to wells of a black 96 well plate
- Prepare working reagent by adding 1ml PicoGreen solution to 200ml TE buffer in to a dark container or simply wrap container in foil if it is transparent.
- Add 100µl of PicoGreen working reagent to all wells containing standards and samples, gently shake and seal plate. This step needs to be conducted in a dark room.
- Incubate plate at room temperature for 2 minutes
- Read fluorescence at excitation 485nm and emission 538nm using FLUOstar OPTIMA fluorometer and its associated software (BMG LABTECH, UK).

4.2.2.3 Alkaline Phosphatase (ALP) Activity

Alkaline phosphatase (ALP) activity was measured using a colorimetric assay (Abcam, UK). This allows for the quantification of the activity of the ALP enzyme by indirect measurement of the ALP product.

In order to prepare the standards, the following procedure needed to be followed;

- Dissolve 2 pNPP tablets in 5.4ml of assay buffer to produce a 5mM working solution. (2 tablets allow for 100 tests).
- Add 40µl of the 5mM working solution to 160µl of assay buffer in order to obtain 1mM pNPP Standard solution.

Using the 1mM pNPP standard solution as prepared above, a 6 point dilution was made ranging from 0 nmol/well to 20 nmol/well. The concentrations of ALP present in the samples were calculated using the calibration curve (presented in APPENDIX 4) if the R^2 value was $\geq$ 0.99. The standard solution concentrations used are listed in Table 4.8 below and were directly made in the 96 well plate in triplicates.

Table 4.8: ALP standard solutions prepared

std	1mM pNPP std (µl) + Assay buffer (µl)	Final Vol. (µl)	ALP conc. (nmol/well)
1	0 + 120	120	0
2	4 + 116	120	4
3	8 + 112	120	8
4	12 + 108	120	12
5	16 + 104	120	16
6	20 + 100	120	20

All solutions and samples had to be equilibrated to room temperature before use. Individual samples were tested at n=6 for repeatability. The assay procedure was as follows:

- Make up standards as indicated in Table 4.8
- Transfer 50µl of samples in to wells of a clear bottom 96 well plate
- Add 30µl of assay buffer to wells containing samples
- Add 50µl of the 5mM working solution to well containing samples and gently shake plate to mix contents
- To the standards alone add 10µl of the ALP enzyme prepared by adding 1ml assay buffer to the ALP enzyme tube provided.
- Seal plate and incubate at room temperature for 1 hour
- Add 20µl of stop solution to all wells containing standards and samples and shake
- Read optical density at 405nm using FLUOstar OPTIMA fluorometer and its associated software (BMG LABTECH, UK).

Upon gaining the results from the ALP assay, the amount of ALP found in each well was then normalised by DNA content of the specific wells.

4.2.2.4 Total Protein Assay

The total protein of the samples collected was assessed by using a colorimetric Macro BCA Protein Assay Kit (Thermo Scientific, UK). The presence of proteins in solution causes the reduction of Cu^{2+} to Cu^{+} which is then able to bond with two molecules of bicinchoninic acid (BCA) in the working solution. This gives a water soluble purple solution which exhibits a strong absorbance at 562nm.

The macromolecular structure of protein, the number of peptide bonds and the presence of four particular amino acids (cysteine, cystine, tryptophan and tyrosine) are reported to be responsible for the colour formation with BCA. Further studies have shown that the colour change with BCA is caused by the sum of individual colour producing functional groups (Wiechelman, Braun et al. 1988)

The kit provided a BSA stock standard solution which was used to make up a 8 point dilution ranging from 0µg/ml to 500µg/ml. To start with 325µl of the BSA stock standard solution was mixed with 325µl of 0.05% TX solution which gave a 1000µg/ml BSA solution. From this solution an 8 point serial dilution was made for the standards.

The concentrations of BSA present in the samples were calculated using the calibration curve (presented in APPENDIX 4) if the R^2 value was $\geq$ 0.99. The standard solution concentrations used are listed in Table 4.9 below and were tested in triplicates.

Table 4.9: BSA standards prepared for BCA total protein assay

Std.	TX Vol. (µl) + BSA stock (µl)	Final BSA conc. (µg/ml)
*	325 + 325	1000
1	325	500
2	325	250
3	325	125
4	325	62.5
5	325	31.25
6	325	15.625
7	325	7.8125
8	325	3.90625
9	325 + 0	0

Transfer 325µl each time to obtain serial dilutions

All solutions and samples had to be equilibrated to room temperature before use. Individual samples were tested at n=6 for repeatability. Prior to starting the assay, the BCA working reagent needed to be prepared by mixing 50 parts of reagent A with 1 part reagent B. This working reagent will be green in colour. The assay procedure was as follows:

- Make up standards as indicated in Table 4.9
- Transfer 25µl of standards and samples in to wells of a clear bottom 96 well plate
- Add 200µl of BCA working reagent to wells containing standards and samples
- Gently shake plate to allow for mixing
- Seal plate and incubate at 37^{o}C for 30 minutes
- Let the plate return to room temperature and read optical density at 562nm using MultiScan Ascent^{TM} and its associated software (Labsystems, UK).

4.2.2.5 AlamarBlue® Assay

There are a variety of methods available for the measurement of cell viability and cell proliferation. These include the measurement of total DNA and at early time-points, measurement of cell metabolic activity. The alamarBlue® Assay measures cell metabolic activity through the conversion of the fluorometric/colorimetric REDOX indicator resazurin (oxidised form) to resorufin (reduced form) in the intracellular environment giving rise to colorimetric and fluorescence changes (Figure 4.4).

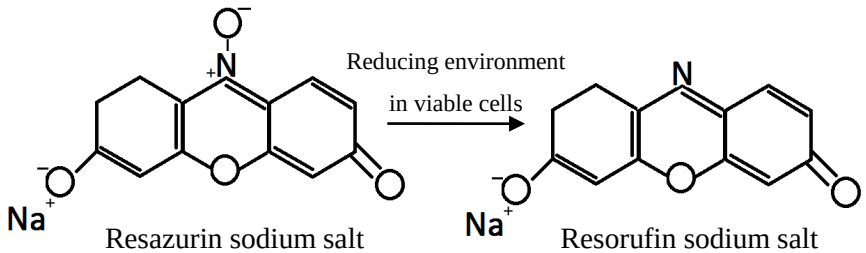

Resazurin sodium salt
weakly fluorescent (blue)

Resorufin sodium salt
strongly fluorescent (red)

Figure 4.4: alamarBlue® assay principle

In order to conduct cell metabolic assays, a phenol free SCM was used made up of DMEM (phenol red free) supplemented with 10% FBS and 1% Pen/strep.

All solutions and samples had to be equilibrated to room temperature before use. Individual samples were tested at n=6 for repeatability. The assay procedure was as follows:

- To the cells seeded on to the 24 well plates, remove SCM and freeze down and add 1ml of phenol free SCM
- Add 10% of alamarBlue® solution (100µl) to the wells containing cells
- From control sample, add 1ml phenol free SCM supplemented with 10% alamarBlue® in an empty well free of cells in a 24 well plate
- Incubate 24 well plate for 6 hours at 37^{o}C and 5%CO_2
- During incubation, prepare 100% reduced alamarBlue® by autoclaving 1ml phenol free SCM supplemented with 10% alamarBlue® at 121^{o}C for 15 minutes. The solution should turn change colour from blue to red.
- After incubation transfer 100µl of each sample, control and 100% reduced solution in to wells of a white 96 well plate.
- Read fluorescence at excitation 560nm and emission 590nm using FLUOstar OPTIMA fluorometer and its associated software (BMG LABTECH, UK).

The % alamarBlue® reduction of the cells was calculated using the following equation:

$$\%\ reduction\ of\ alamarBlue® = \left(\frac{S^{x} - S^{control}}{S^{100\%\ reduced} - S^{control}}\right) \times 100$$

Equation 7

where: S^{x} is the fluorescence value of the tested sample

$S^{100\%\ reduced}$ is fluorescence value of the autoclaved sample

$S^{control}$ is the fluorescence value of the control sample (without cells)

The incubation time was optimised by conducting a time course study against the % reduction of alamarBlue® for the different concentration on cells that were tested prior to the start of the experiment. From the results, it was observed that 6 hours was the optimum incubation time required for measuring cell metabolic activity. These results can be found in APPENDIX 5.

4.2.3 STEP 3 - STATIC 3D CELL CULTURE Experiments

4.2.3.1 Cell thawing, expansion and seeding

Using the techniques detailed in section 4.2.2.1 MG63 cells were thawed, expanded to P4 and seeded onto 0.45g (0.75ml) of UV sterilised HA80/20 granules in 24 well plates in SCM at a density of $4x10^4$ cells/ml. HA80/20 granules were used as the test 3D scaffold material to facilitate any changes detected in cell response to the different types of PCM to be related to changes in silicate ions concentrations in the PCM..

Cells were allowed to attach to the HA80/20 granules for 2 hours at 37°C and 5%CO_2. After 2 hours the SCM was replaced with 1ml of either one of the four PCM or fresh SCM as a control. A second control was also used in which cells were seeded onto SA80/20 scaffolds in fresh SCM. Figure 4.5 illustrate a schematic of the general procedure of the static cell culture experiment with cells seeded on 24 well plates on HA80/20 granules.

On the end point collection days (1, 3 and 5 days), the media from the wells was collected in 1.5ml eppendorf tubes and stored at -20ºC. Cell lysates were collected by washing the HA80/20 granules in the individual wells twice with 1ml PBS and then treating each well with 1ml 0.05% Triton-X (TX) solution before sealing the plates and storing at -20ºC.

Prior to analysis the plates were thawed at room temperature and placed in an ultrasonic bath for 5 minutes. The resultant lysate solutions in the individual wells were then collected and stored in 1.5ml eppendorf tubes.

Total DNA and alkaline phosphatase (ALP) activity was quantified as detailed previously in sections 4.2.2.2 and 4.2.2.3, respectively. Total Protein was quantified using similar methods as described in section 4.2.2.4 but with the modifications detailed in section 4.2.3.2.

Cell metabolic activity was monitored using the AlamarBlue® assay which was conducted on the same population of cells at several time points over a period of 5 days as detailed in section 4.2.3.3.

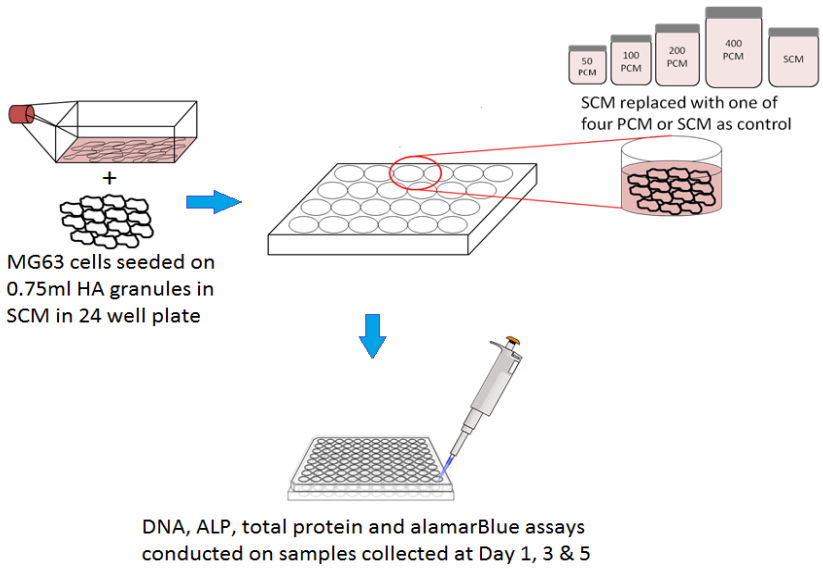

Figure 4.5: Schematic of static cell culture study involving seeding cells on HA80/20 granules and looking at the effects of PCM on cell response

4.2.3.2 Total Protein analysis

As previously described in section 4.2.2.4 the total protein of the lysates collected was assessed using a colorimetric Macro BCA Protein Assay Kit (Thermo Scientific, UK). The standards used to form a calibration curve in order to extrapolate the total protein content in the 3D cell culture samples required a higher concentration of standards.

The kit provided a BSA stock standard solution which was used to make up a 9 point dilution ranging from 0µg/ml to 2000µg/ml as per the manufacturer's instructions. The concentrations of total protein present in the test samples were calculated using the BSA calibration curve (presented in APPENDIX 4) if the R^2 value was $\geq$ 0.99. The standard

solution concentrations used are listed in Table 4.10 and were performed in triplicate. The assay procedure followed was as described in section 4.2.2.4.

Table 4.10: Higher BSA standards prepared for BCA total protein assay as per the manufacturer's instructions

Std.	TX Vol. (µl) + BSA stock (µl)	Final BSA conc. (µg/ml)
A	0 + 300	2000
B	125 + 375	1500
C	325 + 325	1000
D	175 + 175 B	750
E	325 + 325 C	500
F	325 + 325 E	250
G	325 + 325 F	125
H	400 + 100 G	25
I	400 + 0	0

4.2.3.3 AlamarBlue® Assay

The procedure followed in order to obtain results for the % reduction of alamarBlue® was followed as described in section 4.2.2.5. The only difference between the procedures was the control for the assay. The control for the assay for this step in experimentation was adding 1ml of phenol free SCM supplemented with 10% alamarBlue® to 0.45g of HA80/20 granules seeded with cells. The incubation period was still 6 hours and the results for the optimisation of can be found in APPENDIX 5.

4.2.4 Statistical Analysis

Collected data was analysed and expressed in terms of mean ± standard deviation. Statistical significance was evaluated using ANOVA, Post Hoc test: Tukey HSD with $\alpha=0.05$, (where *$p<0.05$, **$p<0.01$ and ***$p<0.001$).

4.2.5 Overall Set-up

In summary there were 3 main steps taken in order to obtain the results presented in this chapter. Step 1 was to set up a 3D perfusion system in order to observe any changes in ion concentrations due to varying the reservoir volume. Step 2 was to carry out static cell culture by seeding cells on 24 well plates and seeing whether the PCM collected from Step 1 had any effects on cell response. Step 3 looked at carrying out a static cell experiment but this time seeding the cells on HA80/20 granules and seeing whether the PCM collected from step 1 had any effect on cell response. Figure 4.6 highlights the main steps taken.

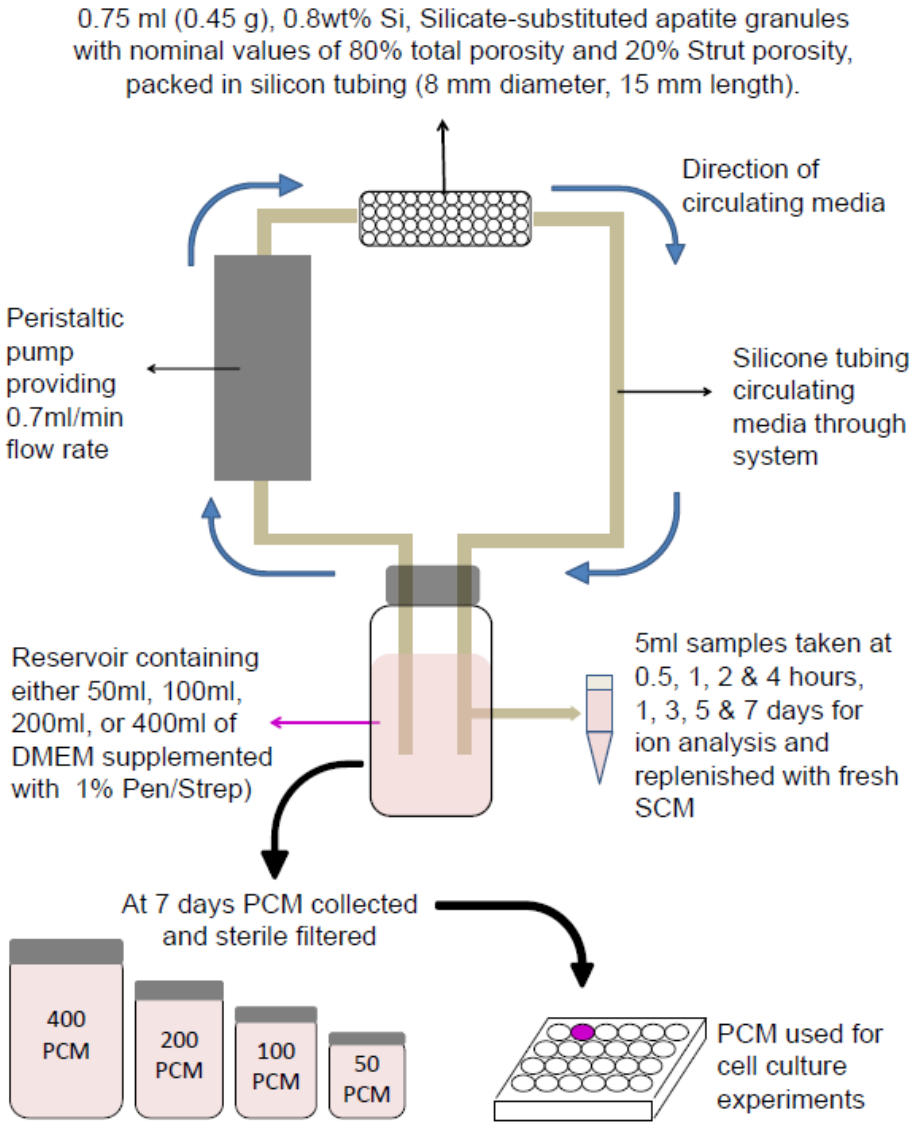

Figure 4.6: Schematic showing experimental set-up using the perfusion system to obtain the four different PCM which were later used for static cell culture experiments with and without incubation on 0.45g of HA80/20 granules

4.3 Results

4.3.1 STEP 1 - Ion Concentration, pH and SEM Analysis

Results of ion concentration analysis are shown in Figure 4.7-Figure 4.9 and clearly demonstrate similar patterns in temporal variation to those obtained in the spinning basket experiments in Chapter 3 (Figures 3.3 - 3.5).

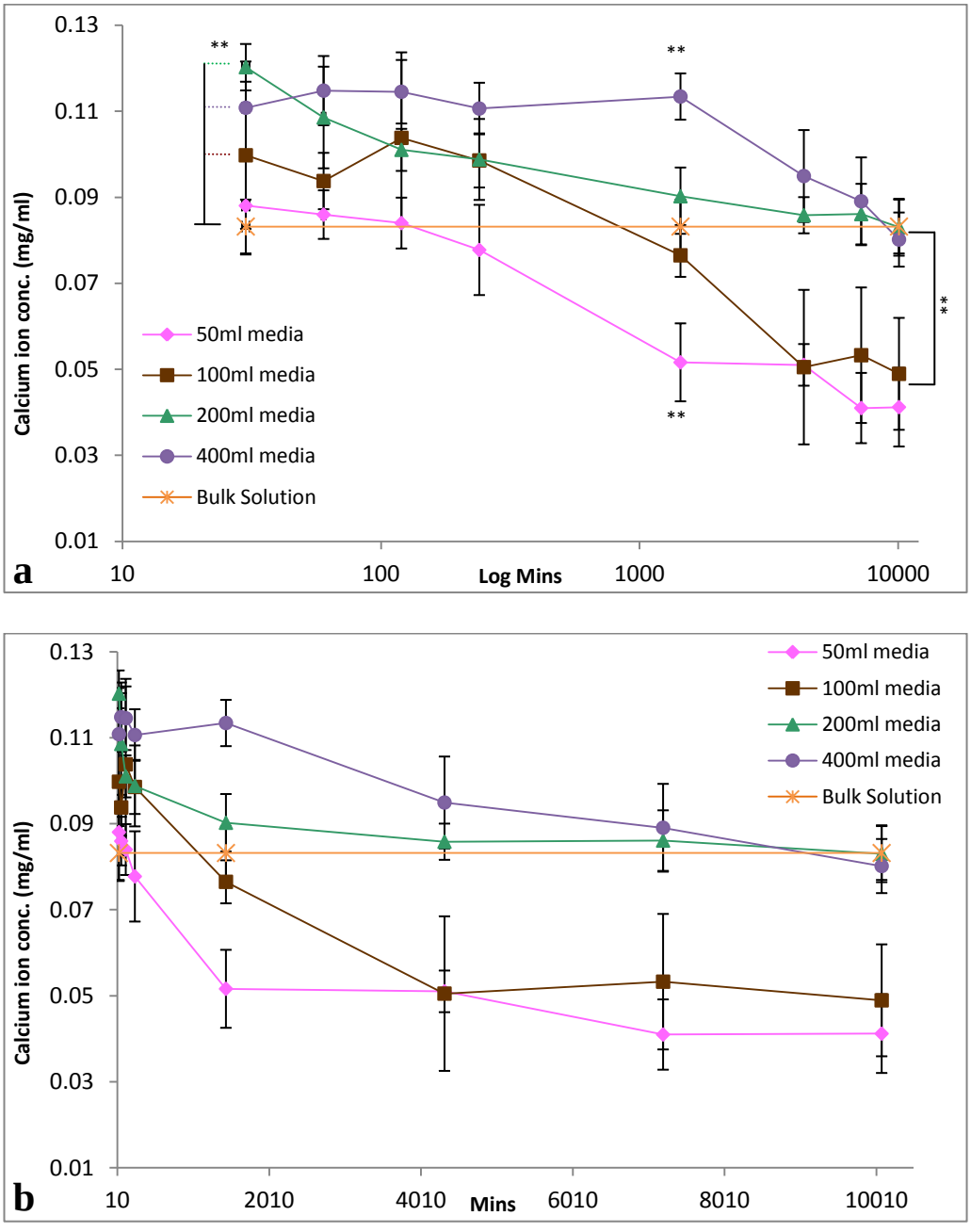

Figure 4.7: Calcium ion concentration for varying reservoir volumes, a) log minutes scale & b) minutes scale (n=6)

Calcium ion concentration (Figure 4.7) was significantly ($p<0.05$) elevated as compared to fresh DMEM after only 30 minutes in the 100, 200 and 400 ml volume reservoirs. These elevated levels were maintained until 4h, for 100 and 200 ml reservoirs, 24h for 400ml reservoir. After these time points the calcium ion concentration levels of 50 and 100ml reservoirs became significantly ($p<0.05$) depleted compared to the base DMEM, while that of the 200 and 400ml reservoirs dropped to levels that were not statistically different as the base DMEM.

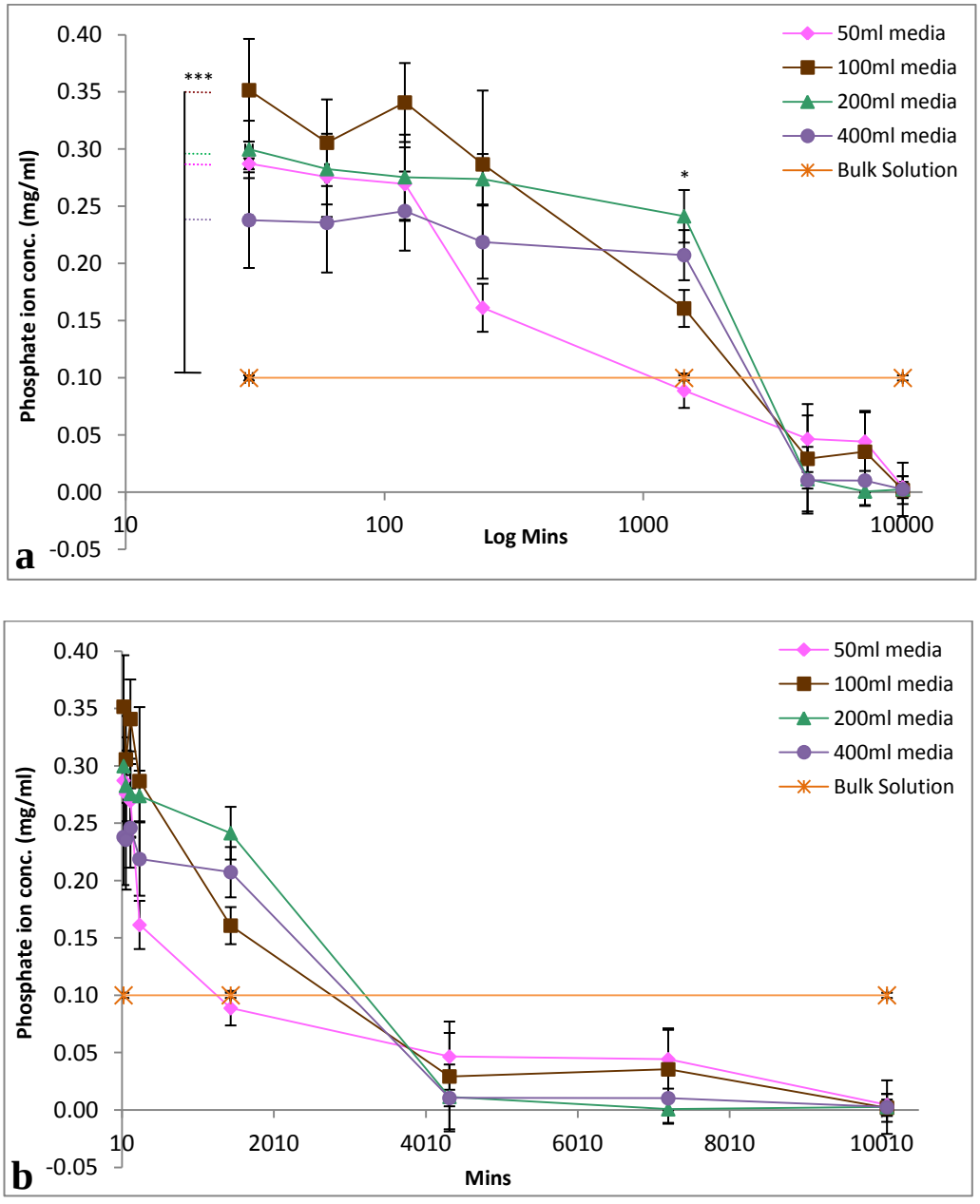

Figure 4.8: Phosphate ion concentration for varying reservoir volumes, a) log minutes scale & b) minutes scale (n=6)

Phosphate ion concentration levels (Figure 4.8) increased significantly ($p<0.005$) as compared to base DMEM by 30 minutes within all reservoir volumes. These elevated levels were maintained for 4 hours for 50 and 100ml reservoirs, 72 hours for 200 and 400ml reservoirs, after which they all dropped to levels of near 0 by 7 days.

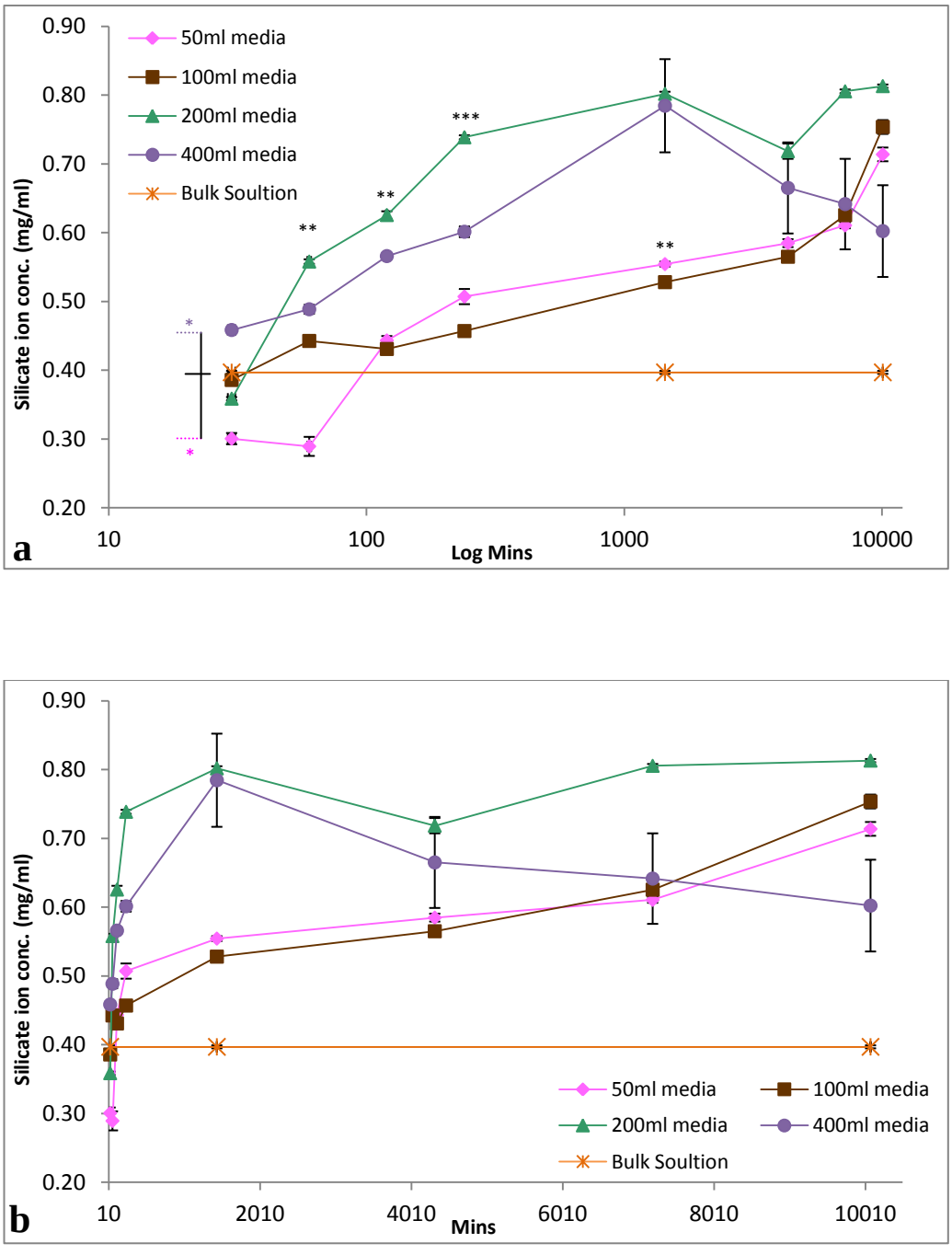

Figure 4.9: Silicate ion concentration for varying reservoir volumes, a) log minutes scale & b) minutes scale (n=6)

Silicate ion concentrations levels (Figure 4.9) also varied with reservoir volume. Initially (by 30 minutes) silicate ion levels dropped significantly ($p<0.01$) in the 50ml reservoir, were not statistically different to base DMEM in the 100 and 200ml reservoirs and was significantly ($p<0.05$) higher in the 400ml reservoir. By 2 hours the level of silicate ion concentration was significantly greater than that of base DMEM within all media volumes. At 24 h silicate levels reached ~ 0.55 and 0.50 mg/ml for 50 and 100ml reservoir volumes, respectively, increasing to 0.70 and 0.75, respectively, by 7 days. While by 24h within the 200 and 400ml reservoirs silicate ion concentration reached maximal levels of around 0.8mg/ml, this level was maintained in 200ml reservoir but dropped to 0.6 mg/ml in 400ml reservoir by 7 days.

As previously observed in Chapter 3 the pH of the 50, 100 reservoirs (Figure 4.10) was observed to increase significantly within the first 30 minutes of exposure to the granules, (within 2h and 4h for the 200 and 400ml reservoirs, respectively), and all were observed to increase almost logarithmically to a pH of ~ 9 over the 7 day period of the experiment.

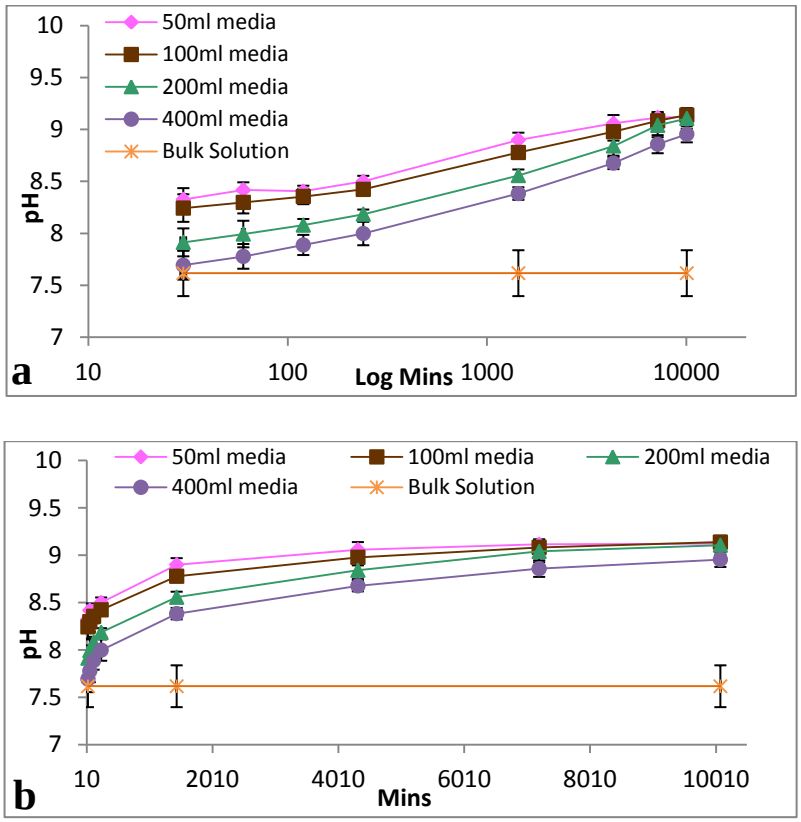

Figure 4.10: pH of varying reservoir volumes, a) log minutes & b) minutes scale (n=6)

From the SEM images in Figure 4.11, it is evident that there was a greater CaP layer precipitated on the surface of the SA80/20 granules circulated with 50ml of media (Figure 4.11a). The 100ml of media also saw a CaP layer precipitated on the surface of SA80/20 granules (Figure 4.11b). However with the increased media volumes, there was either small

amount of scattered CaP precipitation (Figure 4.11c) or no CaP layer (Figure 4.11d) observed on the surface of the granules (200ml and 400ml respectively).

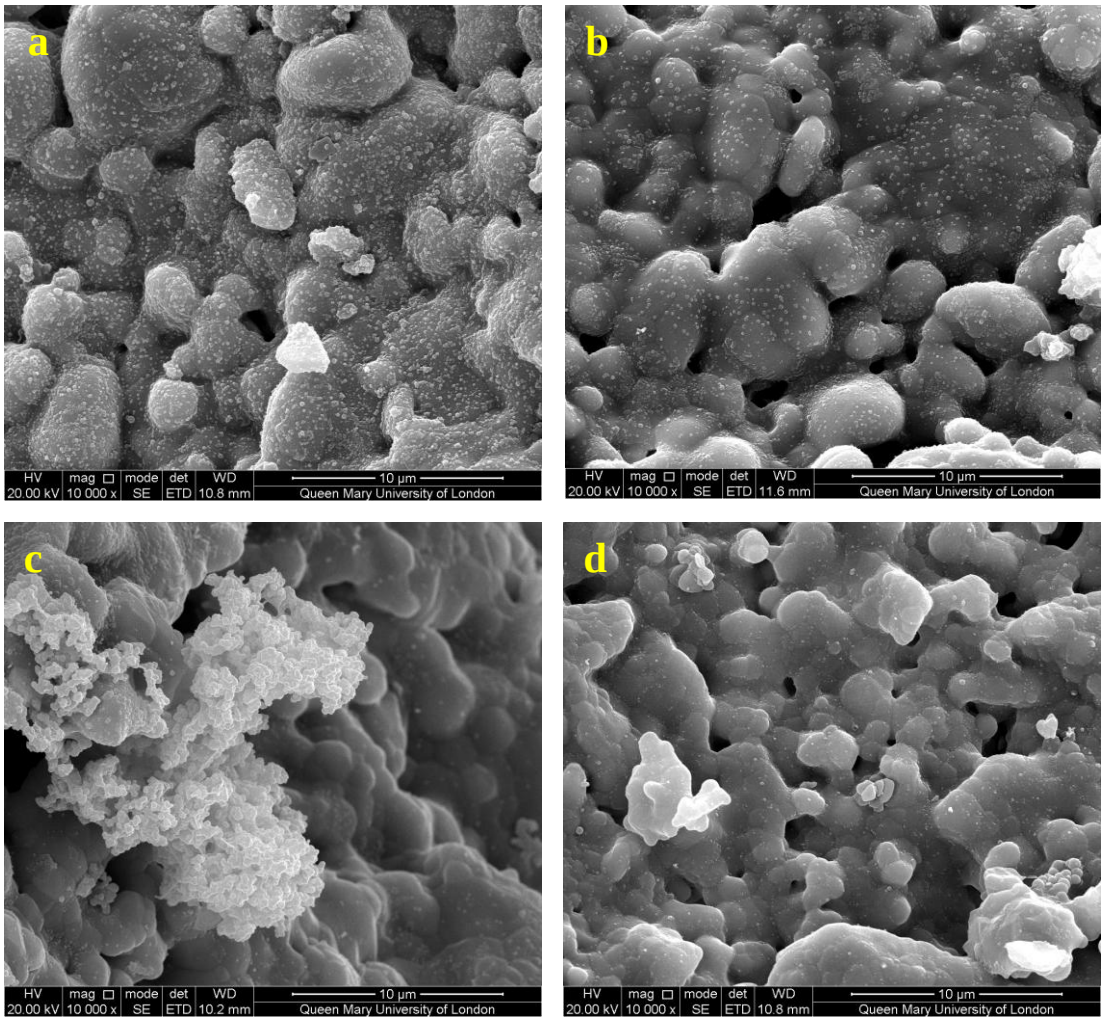

Figure 4.11: SEM images showing precipitation of a CaP layer on the surface of the SA80/20 granules incubated in a) 50PCM, b) 100PCM, c) 200PCM and no CaP layer on d) 400PCM as determined by EDS analysis

4.3.2 STEP 2 - Static 2D cell culture results

Cell response to incubation in the four types of pre-conditioned media, obtained by incubating a fixed mass of SA80/20 granules in differing volumes of DMEM for 7 days clearly demonstrated sensitivity to preconditioning (Figure 4.12). AlamarBlue® data suggested that a higher level of cell metabolic activity was sustained over the 5 day culture period, observed with the 100 PCM in comparison to the other PCM (Figure 4.12a). Relative suppression in protein production in all PCM was seen in comparison to the controls where

cells were incubated in fresh SCM over the 5 days of study (Figure 4.12b). Looking at the Total DNA data - There was a relatively poor level of cell proliferation observed in 50 PCM, 200 PCM and 400 PCM in comparison to 100 PCM and the SCM control (Figure 4.12c). An elevated ALP activity was observed with the 200 PCM over all days in comparison to the other PCM (Figure 4.12d). Overall it can be suggested that 100 PCM was successful in providing a more supportive environment for cell growth and activity (Figure 4.12a & c).

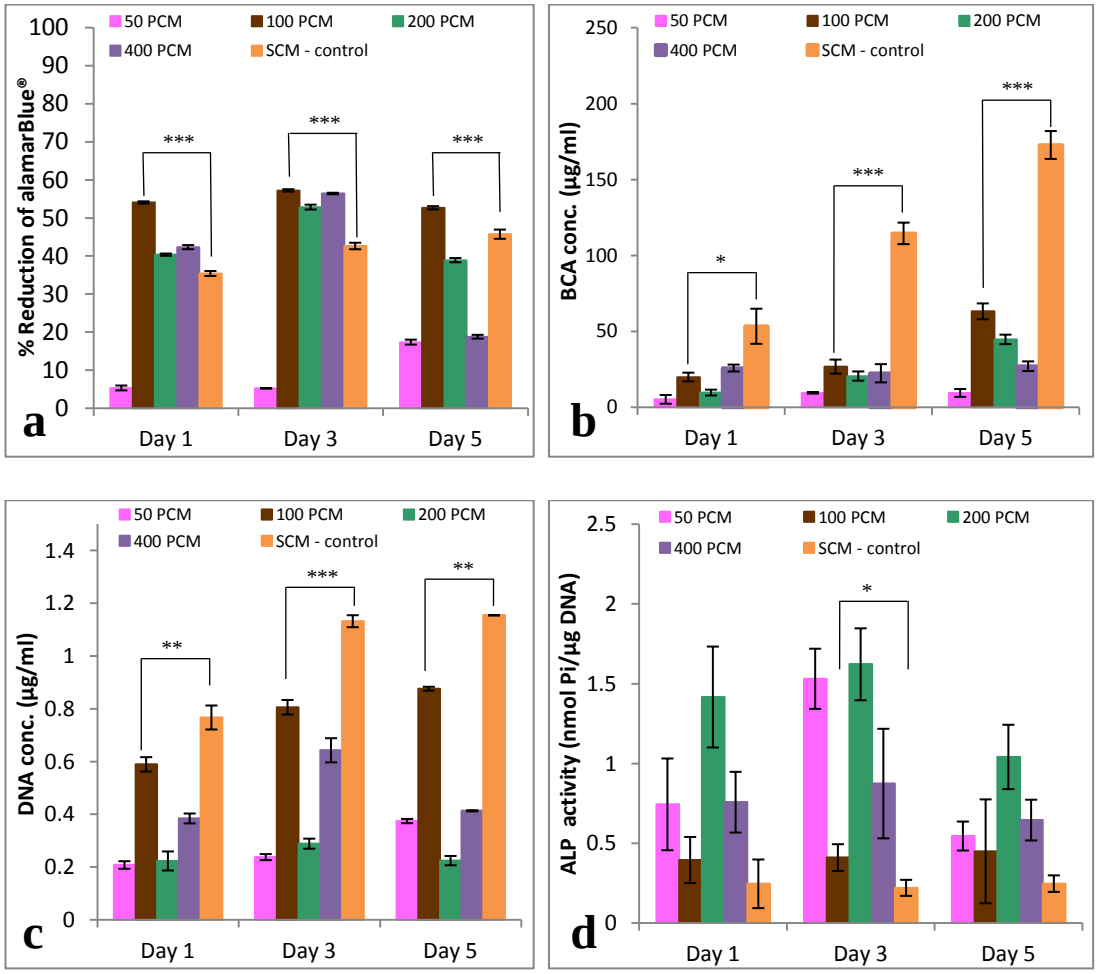

Figure 4.12: a) % reduction of alamarBlue®, b) BCA total protein, c) DNA concentration and d) ALP specific activity for MG63 cells cultured on 24 well plates incubated in PCM over 5 days (n=6)

4.3.3 STEP 3 - Static 3D cell culture results for cells seeded on HA80/20

In this section of the study the cells were seeded on HA80/20 granules incubated with PCM from the four different media volume experiments (50PCM, 100PCM, 200PCM, 400PCM) and SCM for a first control (SCM HA). Additionally a second control of cells incubated on SA80/20 granules in SCM (SCM SA) was also introduced. The results observed were very

different to when the cells were seeded on 24 well plates alone and incubated in the varying 10% FBS supplemented PCM with SCM as a control (Section 4.3.2). There was a significant decrease in the percentage reduction of alamarBlue® observed with all PCM and controls, suggesting an overall decrease in cell activity when incubated in the static 3D environment (Figure 4.13a). Protein production was significantly increase over all PCM in comparison to the PCM when the cells were seeded on 24 well plates alone. Protein production was significantly increase on SCM SA over all days in comparison to the other PCM and SCM HA (Figure 4.13b). Cell proliferation was suppressed in all PCM in comparison to the two controls, with SCM SA showing significantly greater levels than the PCM and SCM HA (Figure 4.13c). In contrast, ALP activity was greater in all PCM and a decrease was observed with the two controls over time (Figure 4.13d).

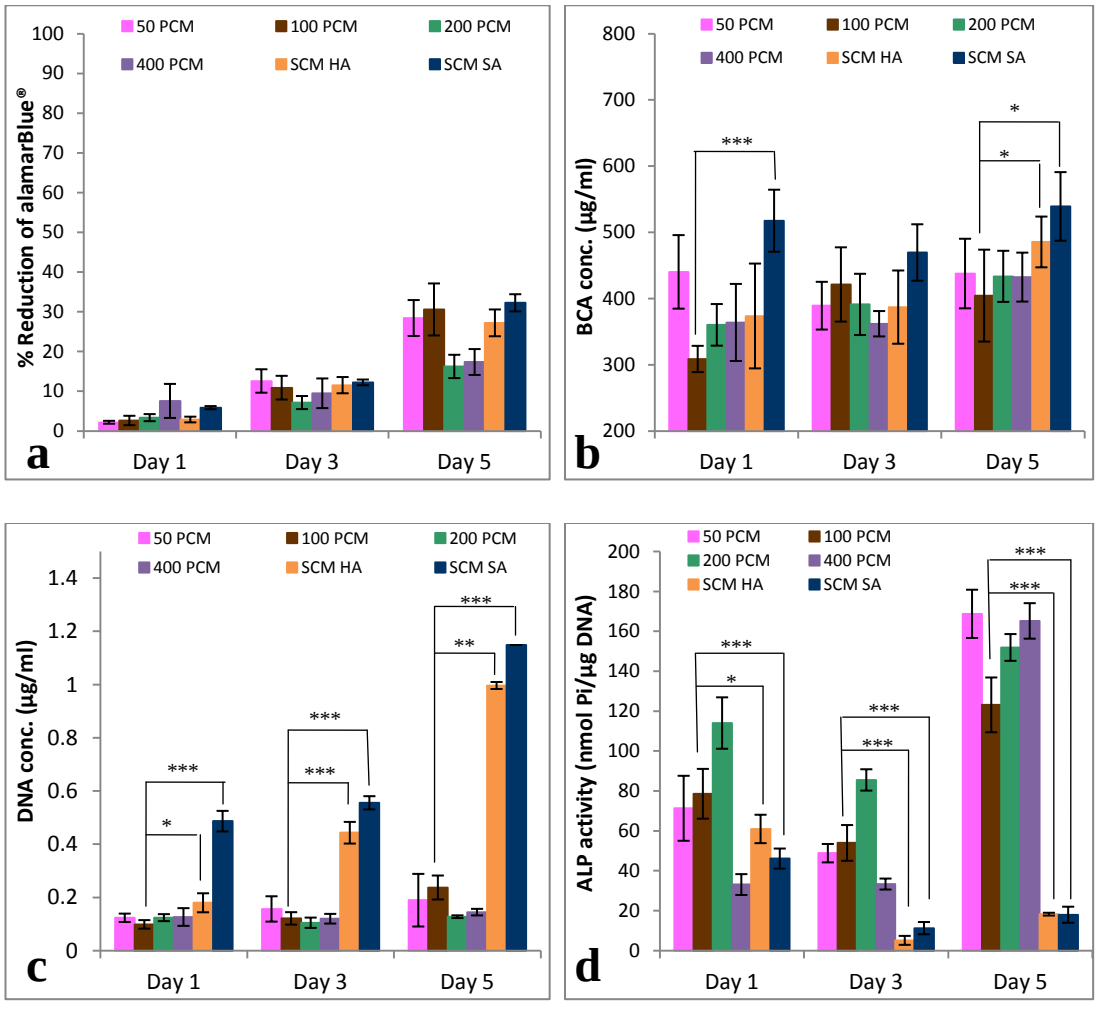

Figure 4.13: a) % reduction of alamarBlue®, b) BCA total protein, c) DNA concentration and d) ALP specific activity for MG63 cells cultured on HA80/20 granules incubated in PCM over 5 days (n=6)

4.4 Discussion

4.4.1 STEP 1 - Perfusion Experiments

The results observed from the conditioning study have clearly demonstrated that there is dependence between the temporal fluctuation in ion concentration and the volume of circulating media under 3D dynamic conditions. It was seen that the higher two volumes (200ml and 400ml) had a greater ability to resists calcium depletion when compared to the two lower volumes of media (50ml and 100ml). At day 7 the two higher volumes had levels of calcium ion which were not statistically different to the basal levels where as a significant depletion in calcium ions was seen with the two lower volumes, with 50ml showing the most depletion in calcium ions by day 7 of the study. Results obtained from the SEM analysis showed a greater and more homogeneous spread of a CaP layer precipitated on the surface of SA80/20 on the two lower media volumes (50ml and 100ml). All the media volumes showed an initial increase in phosphate ions levels to super saturation levels prior to the total depletion of ions by the end of the study in all media volumes. The depleted levels of calcium and phosphate ions from the two lower media volumes would explain the CaP layer observed on the SA80/20 granules. The granules obtained from the 200ml media volume showed a few areas whereby a CaP layer was visible however these specific areas were not representative of the whole surface of the granules seen. The granules obtained from the 400ml media volume showed no CaP layer on the surface of the granules. In comparison to the results observed in chapter 3 whereby the SEM images showed different regions of the granules being covered with a CaP layer, the results obtained from this current work were able to show a more uniform layer of a CaP layer on the surface of the granules which would suggest that the action of media circulation enhanced a better and more consistent coverage of a CaP layer on the surface of the granules. There was a continued steady rise in silicate ion levels for the 50ml and 100ml media. The silicate ion levels appeared to reach a dynamic equilibrium for the 200ml media however the levels dropped after 1 day for the 400ml of media. This dynamic exchange of ions may be linked to the effect of increasing media volume on the capacity of ion exchange with the BGS to either elevate local ion concentrations to super-saturation or to reach a dynamic equilibrium.

Earlier work (Guth 2007) concentrated on ion exchange in static (no media motion) and semi dynamic (static and regular media changes) environments and have shown that over 28 days, calcium and phosphate ion release from SA BGS increased. However, in order for the formation of an apatite layer on the surface of SA from media, a significant drop in calcium

and phosphate ions would have to be expected which Guth was not able to show on the SA samples used under static or semi-dynamic conditions. There was an observed drop in calcium and phosphate ion concentrations in media in the presence of HA after 10 days which then became less pronounced after 10 days. Hing et al in 1999 successfully saw an apatite layer formation on carbonate substituted hydroxyapatite in the presence of human osteoblast-like cells after 24 hours, however this apatite layer did not appear to be as a result of cellular activity and did not see the formation of an apatite layer on HA at all (Hing, Merry et al. 1999). However this particular study did not include any calcium and phosphate ion concentration release data.

The dissolution or even the interactions of ions on material surfaces with the surrounding medium have been described as 'known events' at the surface of a bioactive material and the spontaneous formation of an apatite layer in SBF has been associated with the improved graft incorporation *in vivo* (Kokubo, Kushitani et al. 1990, Wilson, Clegg et al. 2005). A perfect example of this was conducted by Gibson et al in 1999 where the team demonstrated the faster apposition of an apatite layer from SBF on SA compared to HA and this data was then found to be consistent with later studies by Porter and Balas which also successfully showed the increase in bone apatite formation on SA *in vivo* (Gibson, Huang et al. 1999, Balas, Perez-Pariente et al. 2003, Porter, Patel et al. 2003). The results gained from these *in vivo* studies make it more apparent that the current methods employed *in vitro* are not a true reflection of what happens *in vivo* as with many studies the formation of an apatite layer is not observed and there is a limitation in the understanding of the dissolution and re-precipitation of calcium and phosphate ions. The findings in the this chapter however have shown that the use of a 3D perfusion system allows the study of dynamic ion exchange between BGS and the surrounding medium to enable a better understanding of what occurs *in vivo* upon insertion of the BGS to the defective site, as the depletion of calcium and phosphate ions from the two lower volumes of media showed a precipitation of a CaP layer on the surface of the granules.

In addition to the changes in calcium, phosphate and silicate ion concentrations, a shift in the pH of the different volumes of media in the presence of SA80/20 was noted. It is found that due to changes in surface charge and an increase in surface energy of SA leads to more hydrogen ions being absorbed therefore resulting in an increase in pH of the media (Guth 2007). In this study there was a general increase in pH observed for all media volumes used however, the two lower volumes (50ml and 100ml) saw a greater increase in pH in comparison to the higher two volumes (200ml and 400ml). As there was the same volume of SA80/20 granules used for all experiments and there was a difference in the volumes of

media being tested, it can be suggested that with the increase in media volumes there was a greater dilution of hydrogen ions still causing an increase in the pH of the media but a lesser increase in comparison to the lower volumes where the hydrogen ions would have been concentrated. Subsequently an increase in pH would have an effect on ionic interactions between the medium and the materials surface.

The 3D perfusion system set up in the current work used a flow rate on 0.7ml/min which is lower than some flow rates described in other 3D perfusion systems (Bancroft, Sikavitsast et al. 2002, Gomes, Holtorf et al. 2006, Janssen, Oostra et al. 2006, Zhao, Chella et al. 2007, da Silva, Mateescu et al. 2010, Wang, Ma et al. 2014). Modelling the flow rate of medium through a highly porous 3D scaffold in order to estimate the local shear stresses would be ideal however, the complexity of the microarchitecture of these scaffolds make it a very challenging computational problem to solve. A problem that would require a vast amount of time and resources to resolve. The perfusion system in this work was not subjected to rigorous mathematical modelling, as it was primarily designed to test the sustainability of novel grafts for *in vivo* work. Therefore the actual modelling represents a topic for future studies.

Previous studies conducted by Davies have used the paradigm of endothelial cell responses as they represent an admirable model for studies of the effects of fluid flow on cell function (Davies and Dull 1990, Davies and Tripathi 1993, Davies 1995, Barakat and Davies 1998). The endothelium is located at the interface between the vessel wall and blood flow. Due to its location, the endothelium is uniquely exposed to forces that have diverse mechanical characteristics. In addition to pressure, associated stretch and solid mechanical forces, the endothelial cells are continuously exposed to relatively high fluid flow leading to wall shear stresses to which they are known to readily respond. From these previous studies it has also been suggested that flow characteristics rather than the magnitude of the shear stress may play a noticeable role in cell turnover in complex '*chaotic*' flow conditions in comparison to well defined laminar flow when determining cellular response (Davies and Dull 1990). Disturbances to steady laminar flow, for example the endothelium is exposed to changing frequency and direction due to shear stress, may be just as important as the levels of shear interaction. One of the early observations of endothelial response to steady laminar flow was cell alignment and elongation in the direction of fluid flow. On the other hand this does not occur in cells exposed to either during turbulent of oscillatory pulsatile flow (Davies, Remuzzi et al. 1986).

Exploring a simple model of fluid flowing through an empty tube (Figure 4.14), the flow would be laminar, as explained in prior studies, generating predictable wall shear stress. If the fluid viscosity or velocity are increased, then the wall shear stress would also increase.

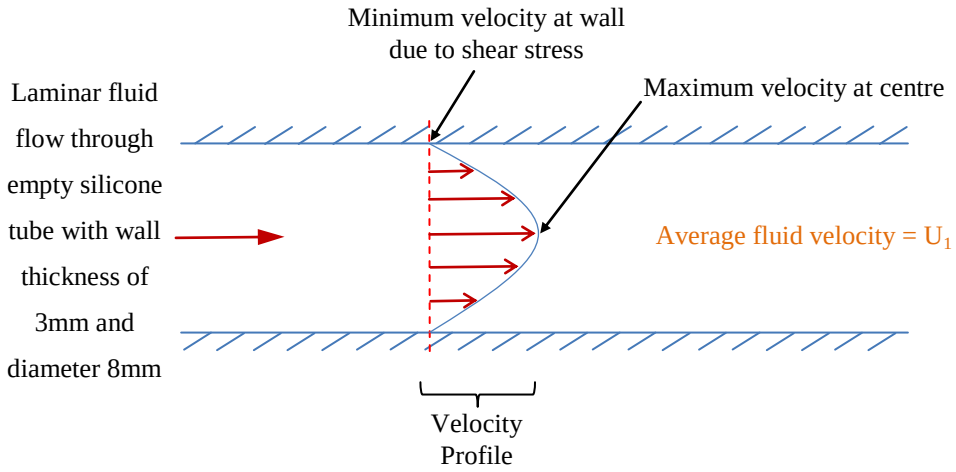

Figure 4.14: Schematic showing simple fluid flow through and empty silicone tube

However, once non-uniform porous granules are introduced in to the tube (Figure 4.15), the assumptions used to describe simple fluid flow through an empty tube would be invalid. The flow would initially be laminar as it entered the tube and then be disturbed by the presence of the porous granules. This would cause fluid molecules to speed up due to the extra distance the molecules have to travel and change direction causing unsteady, non-uniform turbulent flow. The average fluid velocity would therefore be described as being lower with the simple fluid flow in comparison to the disturbed fluid flow ($U_1 < U_2$).

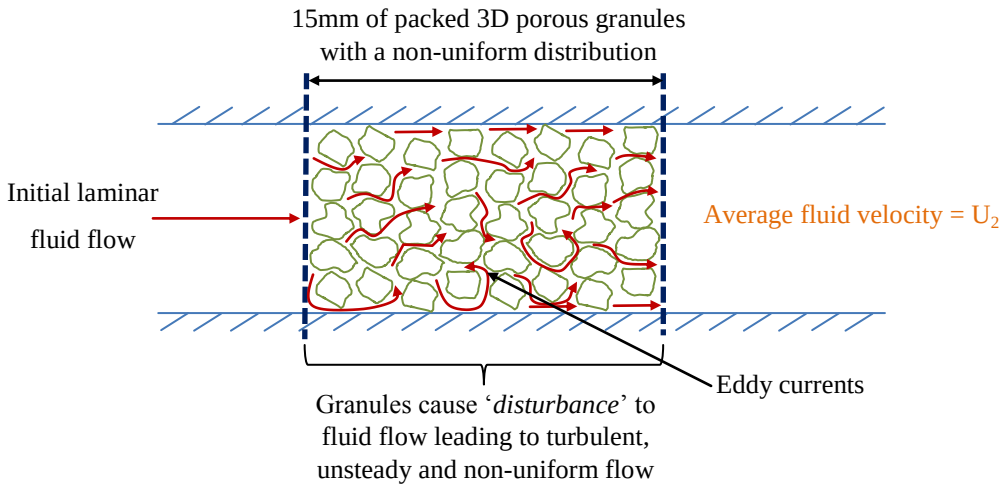

Figure 4.15: Schematic showing disturbed fluid flow upon introducing porous granules

In order to try and model this complicated turbulent flow, the model would have to make reference to Reynolds and Lattice Boltzmann theories, which are used in computational fluid dynamic (CFD) methods for fluid simulation, and consider the effects of fluid velocity and viscosity. Calculating these parameters would involve a great deal of difficulty as the porous granules would be different in size and shape therefore leading to non-uniform fluid flow. Additionally there would be frictional losses associated with the tube wall and even the porous granules surface which would further complicate calculations. This perfusion model aims to replicate the in vivo situation without reference to the consequence of fluid velocities. The maths required to deal with a non-uniform distribution of porous granules is beyond the scope of this current study, therefore data in the literature of the flow rates used in prior studies was used to empirically work out what flow rate would be used to make the current system work.

Although the calcium and phosphate ion concentration in media have been studied, the spontaneous formation of an apatite layer from the medium has not been investigated thoroughly. It is important to note that many studies concentrate on the dissolution of ions from BGS to the surrounding media under static and semi-dynamic conditions, however the work conducted in this chapter demonstrated the dissolution and re-precipitation of calcium and phosphate ions under 3D dynamic perfusion conditions in order for the formation of an apatite layer which would consequently lead on to bone apposition. The fact that ion concentrations continue to fluctuate throughout the 7 day period, and that the phosphate levels drop to levels approaching zero even when a media volume of 400ml was used suggests that there is a significant degree of continued exchange occurring between the SA80/20 granules and the surrounding medium, even after 7 days of continuous circulation.

4.4.2 STEP 2 - Static 2D Cell Culture on 24 Well Plates

The cell response to the four different PCM on 24 well tissue culture plates highlights the sensitivity of cellular behaviour to variation in growth media ion concentrations. The 2D culture data demonstrated elevated DNA content and % reduced alamar blue of the cells incubated in 100PCM which indicate that the 100 PCM provided the most supportive environment for cell growth and activity, as compared to the other PCM, despite depleted levels of calcium and phosphate ions but being enriched with silicate ions, while ALP activity appeared to be promoted over cell growth in 200 PCM where calcium levels were closer to that of SCM and silicate ion levels were maintained suggesting that the 200PCM provided a better environment for cell differentiation. It can be suggested that the low levels

of phosphate ions observed in all PCM media had a detrimental effect on cell proliferation and protein expression.

Previous work has looked in to cell studies were osteoblast-like cells have been cultured for up to 28 days in control conditions, on standard tissue culture plates and on surface of glass reinforced HA composites. It was found that the HA composites presented better surface characterisations for cell growth as the behaviour was closer to that observed in the control cultures. The control cultures had greater total protein content in comparison to the other material tested and the ALP activity was significantly higher with the control cultures over the 28 days on incubation (Ferraz, Fernandes et al. 1999). The results in the present studied showed that there was an increase in cell activity and cell proliferation, especially with 100PCM.

Conducting the work on tissue culture plates first gave a good indication of how the cells would react to PCM with depleted levels of calcium and phosphate but enriched with silicate ions. The results were successful in showing that 100PCM had better cell proliferation in comparison to the other PCM used.

4.4.3 STEP 3 - Static 3D Cell Culture on HA80/20 Granules

This study demonstrated that variation in calcium, phosphate and silicate $_{ion}$ concentration had a clear impact on osteoblast-like cell response after being incubated under static conditions on HA80/20 granules and SA80/20 granules as a control. 100 PCM provided the most supportive environment for cell proliferation on HA granules as compared to the other PCM despite the significantly depleted levels of calcium and phosphate ions as compared to HA80/20 SCM and a similar level of silicate ion enrichment in 100 PCM as in 50 PCM. Furthermore, comparison of response to PCM as compared to controls highlighted that the depletion of calcium and phosphate ions from all PCM seemed to affect cell proliferation (Figure 4.13c) while cell differentiation was stimulated in all PCM (Figure 4.13d).

Previous work has looked at ion concentration analysis in SBF incubated in other BGS materials. Gupta and team in 2007 looked in to analysing the change in ion concentrations in SBF subsequent to incubation in bioglass and silica-calcium phosphate nanocomposites. The work demonstrated that the calcium concentrations in the presence of bioglass remained the same at 85mg/l (0.085mg/ml) whilst the calcium concentration decreased to 60mg/l (0.06mg/ml) in the presence of silica-calcium phosphate nanocomposites. Furthermore the work also showed that the phosphate ion concentration reduced in the presence of bioglass to

15mg/l (0.015mg/ml) from 50mg/l (0.05mg/ml) after 24 hours incubation. Within 24 hours the silicon levels released from bioglass and the nanocomposite were 7mg/l (0.007mg/ml) and 18mg/l (0.018mg/ml) respectively. A rapid precipitation of an apatite layer was observed on the nanocomposite after 2 hours whereas a similar layer was detected after 8 days on the bioglass surface. These changes in ion concentrations revealed that osteopontin and osteocalcin expression by osteoblast-like cells attached to the silicon rich nanocomposite in comparison to HA after 2 days in culture (Gupta, Kirakodu et al. 2007). The PCM in which HA80/20 granules were incubated in the work presented in this chapter, observed greater silicate ion levels reaching 0.65mg/ml in the 50PCM, 0.7mg/ml in the 100PCM, 0.8mg/ml in the 200PCM and 0.55mg/ml in the 400PCM. This increase in the release of silicate ions saw an increase in MG63 cell differentiation over 5 days with all PCM despite depleted levels of calcium and phosphate ions used in comparison to both controls used which agrees with the findings presented by Gupta et al 2007, where it was suggested that there is a role of dissolved silicon in stimulating the differentiation and mineralisation of osteoblast-like cells.

Cell-line osteoblasts have been shown to provide a more homogeneous population of cells which in turn allow for the study of particular stages of osteoblast phenotype. They are very useful at the early stages in assessing cytocompatibility testing or therapeutic agents, however they do not fully reflect the behaviour of primary cells. The advantages and disadvantages of using MG63 cells are listed in the table below (Heremans, Billiau et al. 1978, Clover, Dodds et al. 1992, Kumarasuriyar, Murali et al. 2009, Saldana, Bensiamar et al. 2011, Czekanska, Stoddart et al. 2012).

Table 4.11: Advantages and Disadvantages of MG63 cells

MG63 Cells	
Advantages	*Disadvantages*
Unlimited number of cells available	Inconsistent regarding cell mineralisation
No interspecies differences	Arrested in pre-osteoblast state
Hormonal administration response similar to human osteoblast cells	
Similar to human integrin subunits profile	

The MG63 cell has been derived from a juxtacortical osteosarcoma diagnosed in the distal diaphysis of the left femur of a 14 year old male (Billiau, Edy et al. 1977). These cells displayed a rapid cell growth without exhibiting contact inhibition which resulted in the formation of aggregates (Heremans, Billiau et al. 1978). The cell line also produces high yields of interferon (Billiau, Edy et al. 1977). It has also been shown that the responsiveness of MG63 cells to 1,25-dihydroxyvitamin D [$1,25(OH)_2D_3$] (a major hormone in calcium homeostasis in extracellular fluid in the body as discussed previously; Chapter 1 section 1.3.2.1) as affecting cellular morphology and phenotype by increasing ALP activity. MG63 cells represent an immature osteoblast phenotype and undergo temporal development in long term culture. However there have been some reported inconsistencies in the literature regarding the mineralisation capabilities of monolayer MG63 cells (Kumarasuriyar, Murali et al. 2009, Saldana, Bensiamar et al. 2011). Di Palma et al investigated the mechanical stimulation of MG63 cells and found that the ALP activity was increased when sequentially stimulated but not by continuous mechanical loading. The work was further compared with the reactions of ROS-17/2.8 (a rat osteoblast like cell line) which showed similar responses although the increase in ALP activity was already observed after 3 days in ROS-17/2.8, as opposed to 5 days in MG63 cells (Di Palma, Douet et al. 2003). Kim et al demonstrated the up-regulation of both the gene expression of ALP and osteocalcin when cultured in fluorhydroxyapatite/polycaprolactone (FHA/PCL) composites compared to HA/PCL composites in MG63 cells. However, this study was not able to determine the differences in either ALP activity or protein expression of osteocalcin when cultured on the two materials (Kim, Lee et al. 2005).

In general, even though differences in cell behaviour of cell lines and primary cells have been observed, both of the cell types are responsive to physical, mechanical and chemical stimulations. MG63 cells are commonly used in the investigation of osteoblast-like cell *in vitro*. A further trend that exists in research, which uses MG63 cells more prevalently in the study of osteoblasts over longer periods of time. Although the inconveniences of this cell line cannot be ignored, primary cells are also accompanied by a series of difficulties. Primary cells are famous for showing variable results due to the biological variations of donors, including age, health status and sex. Further, extraction procedures can lead to the change in cellular behaviour and it can also be a problem to ensure that the obtained cultures are purely osteoblast-like cell cultures. Another obstacle to the use of primary cells is their short life span. For the reasons above and the fact that the current experiments explained in this chapter, and further chapters, involve the setting up of a new 3D perfusion system the work was performed using MG63 cells.

Guth in her thesis in 2007 did not find that changes in ionic interactions produce significant effects on cell development and suggested that it is possible that ions have an effect on further developed cells or that the ions act synergistically with other stimulants in order to increase their effect (Guth 2007). In previous work, media has been supplemented in order to stimulate cell growth and differentiation. β-glycerophosphate has been used as it is an organic source of phosphate which is used to stimulate osteoblast-like cells in culture to produce bone nodules (Aubin, Liu et al. 1995, Gough, Jones et al. 2004, Gupta, Kirakodu et al. 2007). Dexamethasone is another stimulant used in cell culture of MSC and osteoblast-like cells in order to encourage cell differentiation (Gough, Jones et al. 2004, Gupta, Kirakodu et al. 2007). Even though these factors were used in the work presented here, it was observed that cell differentiation was promoted over all PCM used which had depleted levels of calcium and phosphate ions however all PCM were enriched with silicate ions.

Calcium and phosphate ion concentrations of medium have been demonstrated to be critical in the development of osteoblast-like cells and other cell types, however the optimum concentration of these ions in order to promote cell proliferation and differentiation have been quarried by different authors demonstrating different values. Increases in calcium concentrations beyond 0.16mg/ml in medium were established to significantly increase the osteocalcin gene expression and as well as nodule formation in monolayer as well as in 3D constructs (Maeno, Niki et al. 2005). The authors also concluded that lower levels of calcium, i.e. between 0.08mg/ml and 0.16mg/ml had the ability to sustain both cell proliferation and differentiation. Lower levels of calcium have also been investigated where the effect of 0.02mg/ml and 0.04mg/ml calcium on osteoblast-like cell proliferation have been tested and have demonstrated that 0.04mg/ml calcium promoted osteoblastic proliferation (Matsuoka, Akiyama et al. 1999). The work presented in this chapter saw calcium levels reach 0.04mg/ml in 50ml of media and 0.05mg/ml in 100ml of media at 7 days, suggested that despite having low levels of calcium present, the 50PCM and 100PCM were successful in enhancing cell proliferation in comparison to the 200 and 400PCM (Figure 4.13c). 100PCM saw a greater cell proliferation over 5 days in comparison to the other PCM tested. These findings have proven to be in agreement with previous work carried out by Matsuoka et al 1999.

Similarly, phosphate concentrations are understood to be vital on the impact of cellular development. The absence of phosphate in the medium and the minimal and maximum levels of phosphate required have not been investigated intensively and are yet to be defined. Guth 2007, saw the at the significant drop in phosphate levels in medium incubated in the presence of HA and SA did not impact cell proliferation or cell differentiation. However the

work presented in this chapter suggests that the significantly depleted levels of phosphate in all PCM have had an effect on suppressing cell metabolism along with cell proliferation when incubated in the presence of HA80/20 (Figure 4.13a and c) in comparison to being incubated on 24 well plates alone (Figure 4.12a and c). These differences in results may be due to Guth (2007) used microporous discs for the experiments conducted compared to the porous granules used in the current work.

A change in geometry and topography has also been shown to exhibit differences in cell response. Castagna (2014) was successful in showing how porous granules of HA and SA had a great affinity for fibronectin adsorption on the surface of the scaffolds in comparison to dense discs of the same scaffold material. The higher level of fibronectin adsorption on the porous granular HA and SA was described to be because of the presence of the microporosity which would increase the surface area of the implant, giving the protein a more favourable surface to conform in order to facilitate the adsorption of the protein. An earlier study by Guth et al investigated cell response to SA discs when cells are grown on the discs as compared to cells grown in the media exposed to the discs. The study showed that when the cells are grown on the SA discs, with time ALP activity is increased which suggested greater cell differentiation of the cells seeded on the discs in comparison to the cells being grown in media exposed to the discs (Guth, Buckland et al. 2006). From these previous studies it can be concluded that having the cells seeded on to the surface of the ceramic material in comparison to having cells seeded on 2D cell culture plates enhances cell response. It has also been shown that cell response is more sensitive to the scaffold topography whereby the granular form of the scaffold has shown an increased cell differentiation in comparison to the solid discs. In this current study, using solid discs as an extra control would be another way to confirm previous results showing greater cell response to the granular samples in comparison to the 2D cell culture plates and solid disc samples.

4.4.4 100PCM - 2D and 3D Cell Cultures

From both static cell culture studies it is evident that the 100PCM provided the most supportive environment for cell proliferation along with an increase in cell metabolism and total protein expression in comparison to the other three PCM tested. It was very interesting to note that dynamic ion exchange using a 3D perfusion system had a great effect on osteoblast-like cell response. Even with totally depleted level of phosphate, 100PCM was able to enhance cell proliferation when incubated with cells on tissue culture plates and in the presence of HA80/20. Another interesting observation was the difference in the results obtained between the cells being cultured on tissue culture plates and on HA80/20 granules.

Figure 4.16 highlights and compares the % reduction of alamarBlue®, total protein expressed, DNA content and ALP specific activity for the MG63 cells seeded on either tissue culture plates or HA80/20 granules incubated in 100PCM over 5 days in culture. The starting cell seeding density was the same for both experimental set-ups, however the surfaces will be greater for the 3D environment, suggesting more cells were required for a better and equal coverage of the surface in order to enhance cell proliferation

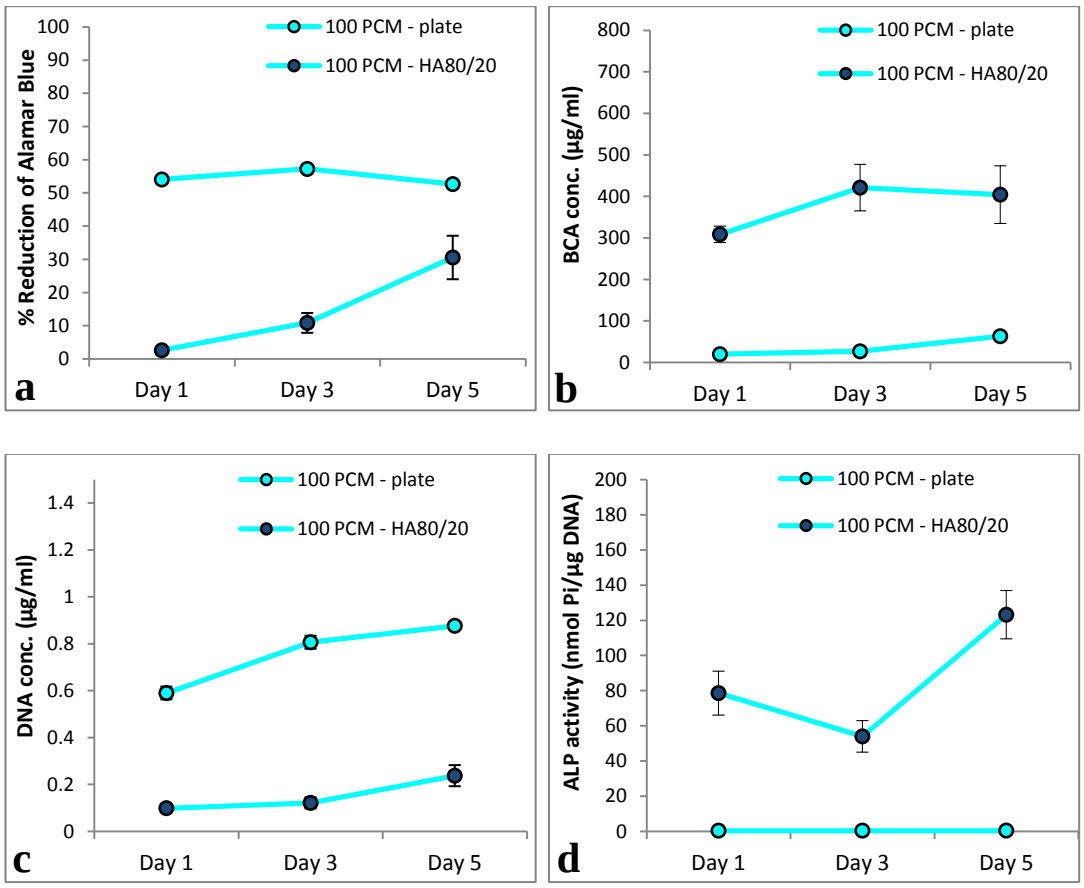

Figure 4.16: a) % reduction of alamarBlue®, b) BCA total protein, c) DNA concentration and d) ALP specific activity for MG63 cells cultured on 24 well plates and HA80/20 incubated in 100PCM over 5 days (n=6)

From both static cell culture studies it is evident that the 100PCM provided the most supportive environment for cell proliferation along with an increase in cell metabolism and total protein expression in comparison to the other three PCM tested. It was very interesting to note that dynamic ion exchange using a 3D perfusion system had a great effect on osteoblast-like cell response. Even with totally depleted level of phosphate, 100PCM was able to enhance cell proliferation when incubated with cells on tissue culture plates and in the presence of HA80/20. Another interesting observation was the difference in the results

obtained between the cells being cultured on tissue culture plates and on HA80/20 granules. Figure 4.16 highlights and compares the % reduction of alamarBlue®, total protein expressed, DNA content and ALP specific activity for the MG63 cells seeded on either tissue culture plates or HA80/20 granules incubated in 100PCM over 5 days in culture. The starting cell seeding density was the same for both experimental set-ups, however the surfaces will be greater for the 3D environment, suggesting more cells were required for a better and equal coverage of the surface in order to enhance cell proliferation

There is a greater reduction in alamarBlue® suggesting greater cell growth and greater cell proliferation (Figure 4.16a and c) observed with the cells cultured on tissue culture plates in 100PCM, however cell differentiation and total protein expressed (Figure 4.16b and d) over 5 days is seen to be greater with the cells seeded on HA80/20 granules. It could be suggested that there was an increase in collagen-I production which would explain the increase in ALP activity. It has been demonstrated that serum proteins significantly alter cell attachment to tissue culture plates. Conditioning the plate surfaces with various extracellular proteins, for example collagen or fibronectin increases cell attachment however conditioning with vitronectin or albumin did not (Carvalho, Kostenuik et al. 2003). When cells are seeded in serum containing media it allows for the protein adsorption to occur simultaneously to cell attachment on the BGS surface. The cells suspended in serum containing medium are able to absorb/anchor/bind the serum proteins to their own cell membrane. Therefore when the cell comes in contact with the materials surface, the cell has the ability to choose between the proteins already bound to their own membrane surface and the proteins that are already absorbed to the materials surface. This therefore explains why total protein expression was observed to be more from the HA80/20 granules in comparison to the tissue culture plates.

Despite 100PCM having totally depleted levels of phosphate ions at 0.01mg/ml, 0.05mg/ml levels of calcium and being enriched with silicate ions at 0.7mg/ml, it still had an effect on cell response however, the depleted levels of calcium and phosphate ions did suppress the proliferation and growth of the cells.

4.5 Summary and Conclusions

The work that has been demonstrated in this chapter has successfully shown that dynamic ion exchange on porous SA BGS granules has an impact on osteoblast-like cell response when seeded on tissue culture plates and on HA80/20 granules. There were many results gained from this work which were positive however there were also many results obtained which would allow for further investigations.

It was interesting to note that the different volumes on media had varying effects on dynamic ion exchange between the BGS and the surrounding media. The two greater volumes of media (200 and 400 ml) were able to avoid total depletion of calcium ions and reach basal levels by the end of the 7 day period however the two lower volumes (50 and 100ml) began to show a decrease in calcium ions by 4 hours in to the experimental work. Another interesting find was the total depletion of phosphate ions in all media volumes by the end of the experimental work. It was expected that the relatively larger volumes would be able to resist total depletions of phosphate ions however this was not the case. By the end of the experiment (day 7) all tested media volumes were enriched with silicate ions ranging from 0.55mg/ml to 0.8mg/ml.

Conditioning the media volumes before the static cell culture experiments showed that a change in ion concentrations of media have an effect on cell response. Even with depleted levels of calcium and phosphate, cells were still proliferating and differentiating however the levels at which this was occurring was limited and suppressed. As 100PCM was able to provide a better environment for cell growth in comparison to the other PCM used and tested, it was selected as a volume of medium to continue testing with in order to investigate other aspects of the 3D perfusion system set up. Critically the ability of SA BGS to deplete a relatively large volume of media of phosphate ions suggests media must be partially refreshed before 24 hours during dynamic 3D perfusion culture experiments. This would in turn reflect the *in vivo* environment more closely and allow mechanisms behind osteoinductivity observed *in vivo* to be fully investigated *in vitro*.

Chapter 5 Influence of Media Replenishment and Media Stirring on Dynamic Ion Exchange and Subsequent Cell Response

5.1 Background

From Chapter 4, it was evident that a change in ion concentration within the media, resulting from the tendency of apatite based bone graft substitute materials to undergo dynamic ion exchange and support precipitation of a bone-like apatite layer on their surfaces, also had an effect on osteoblast-like cell response. As 100PCM was able to provide a better environment for cell growth in comparison to the other PCM investigated, it was selected as a volume of medium to use while investigating other aspects of the 3D perfusion system set up. Critically the ability of SA BGS to deplete a relatively large volume of media of phosphate ions suggests media should be at least partially replenished before 24 hours during the dynamic 3D perfusion culture experiments. This would in turn reflect the *in vivo* environment more closely

Generally, mixing of the media is accepted and used in spinner flask bioreactor models, however the effects of stirring the media within a 3D perfusion system has not been explored. (Bancroft, Sikavitsas et al. 2003, Martin, Wendt et al. 2004). From Chapter 4, it was shown that the calcium ion depletion observed was different to what was expected from the different volumes of reservoirs tested. Therefore in order to make sure all the media in the reservoir is being circulated around the system, introducing a mixing action might be beneficial to keep a good and equal circulation of the reservoir media. Therefore there were two aims to this chapter:

- The first objective was to investigate the dynamic ion exchange between SA80/20 and the surrounding media after partially replenishing the media at 4 hours and identify whether this would have an effect on osteoblast-like cell response when incubated with the pre-conditioned media in the presence of HA80/20 granules for 5 days.
- The second objective was to investigate whether stirring the media during the course of the dynamic perfusion experiment had any effect on the calcium, phosphate and silicate ion concentrations and subsequent cell response.

5.2 Methodology

As in Chapter 4 in order to investigate the two objectives identified for study (Section 5.1) the work was broken down into two distinct steps:

- **STEP 1** – Investigate the effect of partially replenishing media at 4 hours within the closed perfusion system and identify any changes in ion concentrations in media in comparison to media maintained in situ for the full 7 days, and studying the subsequent cell response to this replenished vs. maintained pre-conditioned media under 3D, static (non-motile fluid) conditions for 5 days.
- **STEP 2** - Investigate the effect of stirring the replenished media within the perfusion system and comparing any changes in the ionic concentrations to not stirring the media and still replenishing it at 4 hours. This media would then be used in order to study any changes in osteoblast-like cell response under static conditions for 5 days.

5.2.1 STEP 1 - Partially replenishing the media at 4 hours and investigating ion concentration and subsequent cell response

5.2.1.1 Media and Sample Preparation

Media and sample preparation was the same as described in Chapter 4 sections 4.2.1.1.

5.2.1.2 3D Perfusion System set-up

The set-up of the 3D perfusion system was similar to the set up described previously in Chapter 4 section 4.2.1 however only 100ml volume media reservoirs were used and water baths were used instead of hot plates to keep the temperature of the media constant and stable at 37^{o}C throughout the 7 day circulation period.

PCM in this study was obtained by circulating 100ml of Dulbecco's Modified Eagle Medium containing 1% Penicillin-Streptomycin (DMEM) at a flow rate of 0.7ml/min through 0.45g of SA80/20. 5ml of solution was extracted at time intervals of 0.5, 1, 2 and 4 hours, 1, 3, 5 and 7 days, and replaced with 5ml fresh DMEM for analysis of calcium, phosphate and silicate ion concentrations using colorimetric assays as previously described before in Chapter 4 section 4.2.1.4. Additionally at 4 hours, 50ml of the 100ml circulating media was collected and replenished with fresh DMEM. At 7 days the final 100ml of DMEM was collected and both the 4 hour and 7 day media were individually sterile filtered and supplemented with 10% FBS and stored as 4H-PCM and 7D-PCM. Figure 5.1 shows images

of the perfusion system set-up. pH of all DMEM samples collected was measured during the running of the perfusion study.

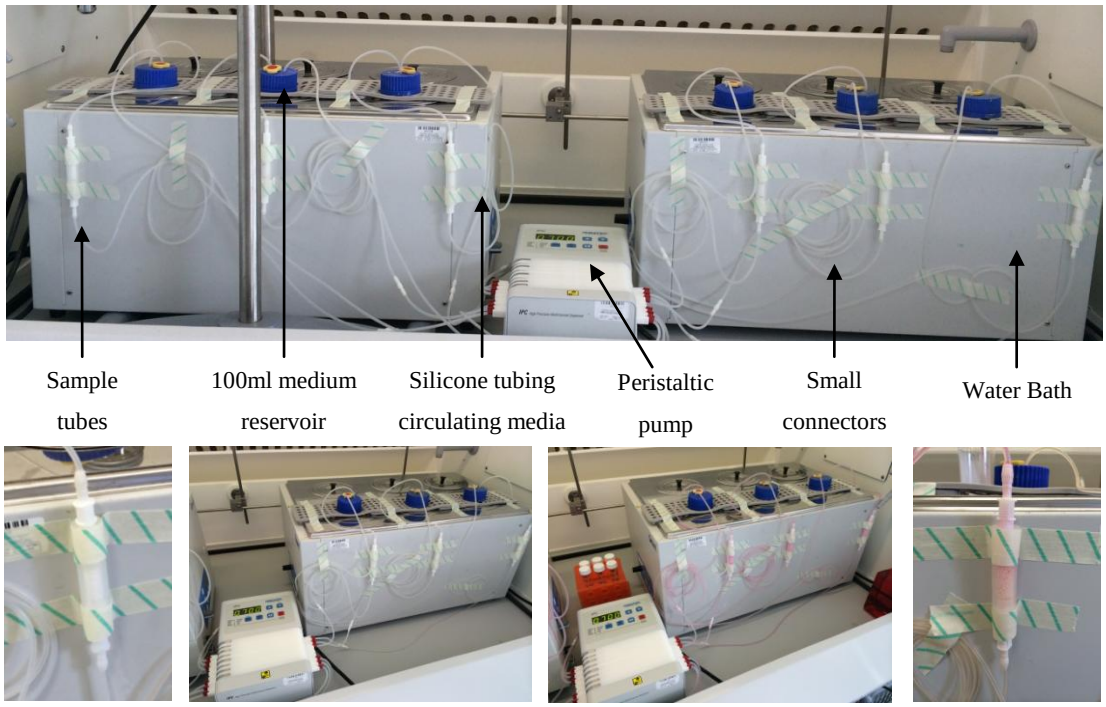

Figure 5.1: Image showing experimental set-up of the perfusion system in order to study whether partially replenishing the media had an effect on ion exchange

SEM analysis was conducted on the SA80/20 granules at 4 hours and at 7 days. The protocol followed can be found in Chapter 2 section 2.1.

5.2.1.3 Static Cell Culture Study on HA80/20

After the perfusion experiments were completed, the collected 4H and 7D PCM was used to conduct static cell culture studies in order to see whether the composition of the media at the different collection points had an effect on osteoblast-like cell response. MG63 cells were grown and expanded as described in Chapter 4 section 4.2.2.1. MG63 osteoblast-like cells (P4) were seeded at a concentration of $4x10^4$ cells/ml on 0.45g of HA80/20 granules in 24 well plates in 1ml of SCM and allowed to attach at 37°C and 5% CO_2. After 2 hours the SCM was replaced with 1ml of either 4H PCM, 7D PCM or fresh SCM as a control. The cells were incubated for periods of 1, 3 and 5 days. The media was refreshed at 24 hours then every 48 hours thereafter. DNA quantification, ALP specific activity, total protein and cell metabolism using alamarBlue® was monitored at each time point. The protocols followed for these assays can be found in Chapter 4 section 4.2.2.2 - 4.2.2.5.

5.2.2 STEP 2 - Stirring the partially replenished media and investigating ion concentration and subsequent cell response

The perfusion studied was conducted as described above in Step 1. The only addition was that the media was stirred using overhead stirrers continuously for the length of the experiment at 70rpm. Again at 4 hours, 50 ml of the 100ml DMEM was collected. At 168 hours (7 days) the 100ml of DMEM was collected and both the 4 hour and 7 day media were individually sterile filtered and supplemented with 10% FBS and stored as 4H-S and 7D-S. Figure 5.2 below highlights the experimental set-up. pH was measured of the DMEM before and of all the samples collected during the running of the perfusion study.

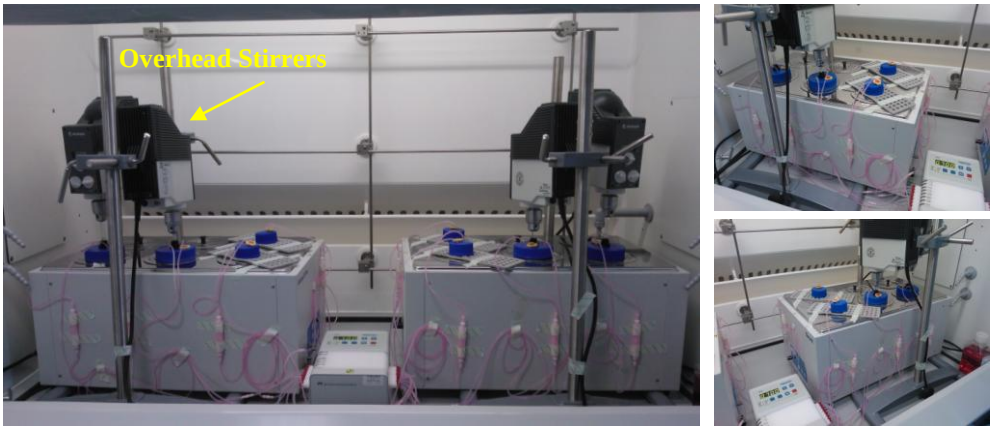

Figure 5.2: Image showing perfusion set-up using overhead stirrers to stir reservoir media continuously for length of perfusion experiment

The collected 4H-S and 7D-S PCM were then used to incubate MG63 cells in the presence of HA80/20 granules and SCM was used as a control along with a second control where SA80/20 granules with SCM where used. The cells were incubated for periods of 1, 3 and 5 days. DNA quantification, ALP specific activity, total protein and cell metabolism was monitored at each time point. SEM analysis was also conducted on the SA80/20 granules at 4 hours and at 7 days. The protocol followed can be found in Chapter 2 section 2.1.

5.2.3 Statistical Analysis

Collected data was analysed and expressed in terms of mean ± standard deviation. Statistical significance was evaluated using ANOVA, Post Hoc test: Tukey HSD with $\alpha=0.05$, (were $*p<0.05$, $**p<0.01$ and $***p<0.005$).

5.3 Results

5.3.1 STEP 1 - Partially Replenishing Media at 4 hours

Results of investigating the effect of partially replenishing media at 4 hours within the closed perfusion system with respect to influence on ion concentration (5.3.1.1) and subsequent cell response to the replenished vs. maintained pre-conditioned media under 3D, static (non-motile fluid) conditions for 5 days (5.3.1.2) are detailed below.

5.3.1.1 Ion Concentration Analysis and pH

On all three ion concentration graphs the points at which the 4 hour media was collected and partially replenished and later used for the static cell culture experiment has been highlighted (♦). The media collected at day 7 and then used for the cell experiment has also been highlighted on all three graphs (♦).

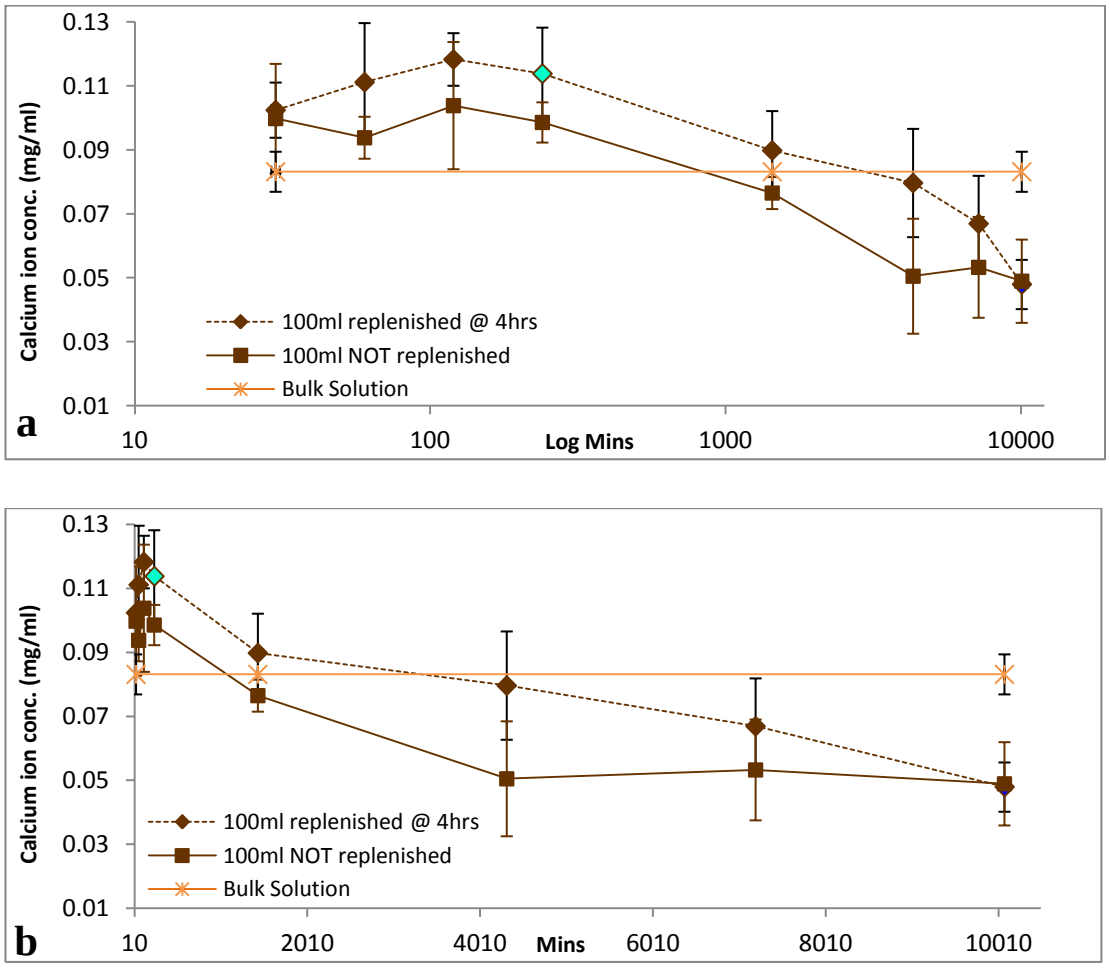

Figure 5.3: Calcium ion concentration for media partially-replenished at 4h and media maintained in situ for 7days, a) log minutes scale & b) minutes scale (n=6)

The general trend in the release and depletion in calcium ions from the partially replenished experiment was not significantly different to the released and depletion of calcium ions from the media that was not partially replenished at 4 hours. The release and depletions of calcium ions from the granules to the surrounding media at 30 minutes and day 7 respectively was statistically identical between the two media types (Figure 5.3).

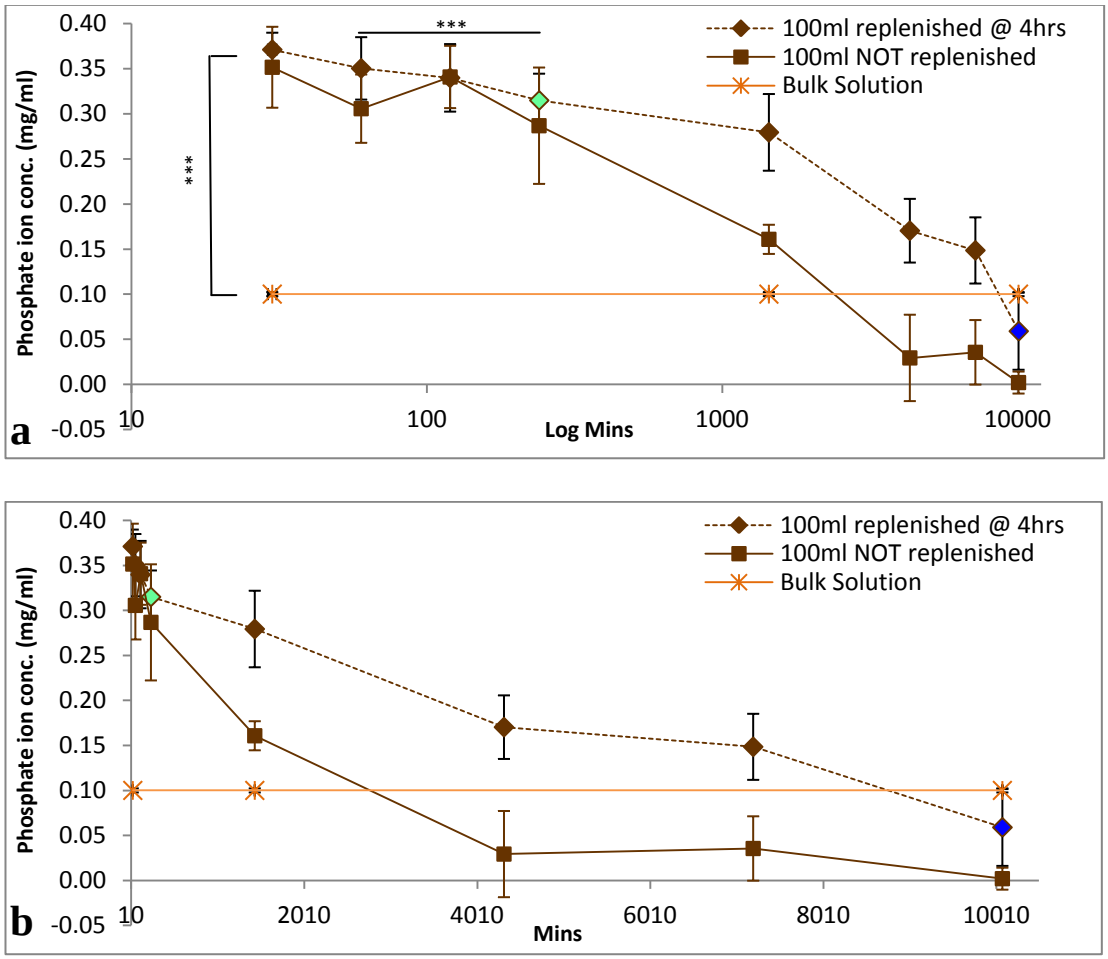

Figure 5.4: Phosphate ion concentration for media partially-replenished at 4h and media maintained in situ for 7days, a) log minutes scale & b) minutes scale (n=6)

The depletion of phosphate ions was significantly delayed from day 1 ($p<0.005$) to day 7 ($p<0.05$) when media was partially replenished in comparison to not replenishing the media. By day 7 the phosphate levels had only just passed basal levels (Figure 5.4).

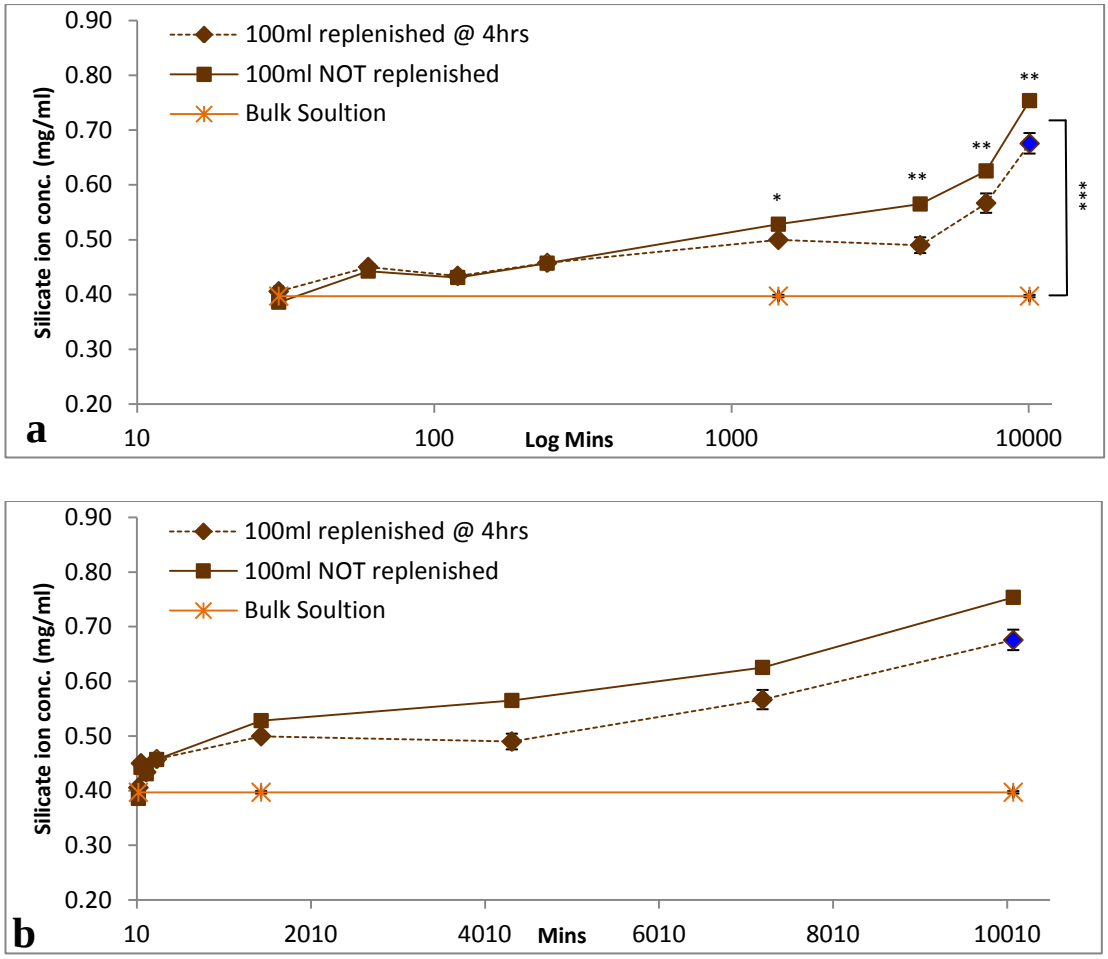

Figure 5.5: Silicate ion concentration for media partially-replenished at 4h and media maintained in situ for 7days, a) log minutes scale & b) minutes scale (n=6)

The release of silicate ions saw a similar trend when compared to media that had not been replenished, showing a sustained release of silicate ions. However there was a significant difference between silicate ion concentration on day 1 ($p<0.05$), day 3 ($p<0.01$), day 5 ($p<0.01$) and day 7 ($p<0.005$) between the replenished media and the not replenished media, with the not replenished media showing a higher release on these particular days. However by the end of the experiment the silicate ion levels in the replenished media were slightly lower than observed in not replenished media (Figure 5.5).

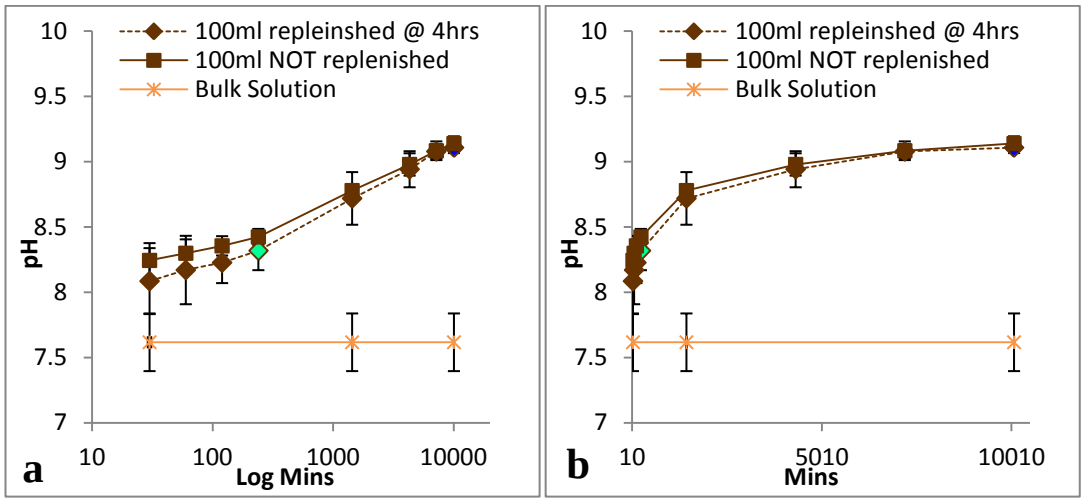

Figure 5.6: pH of media partially-replenished at 4h and media maintained in situ for 7days, a) log minutes scale & b) minutes scale (n=6)

The pH trend observed with the partially-replenished media was not significantly different to that observed with media maintained in situ for 7days. (Figure 5.6).

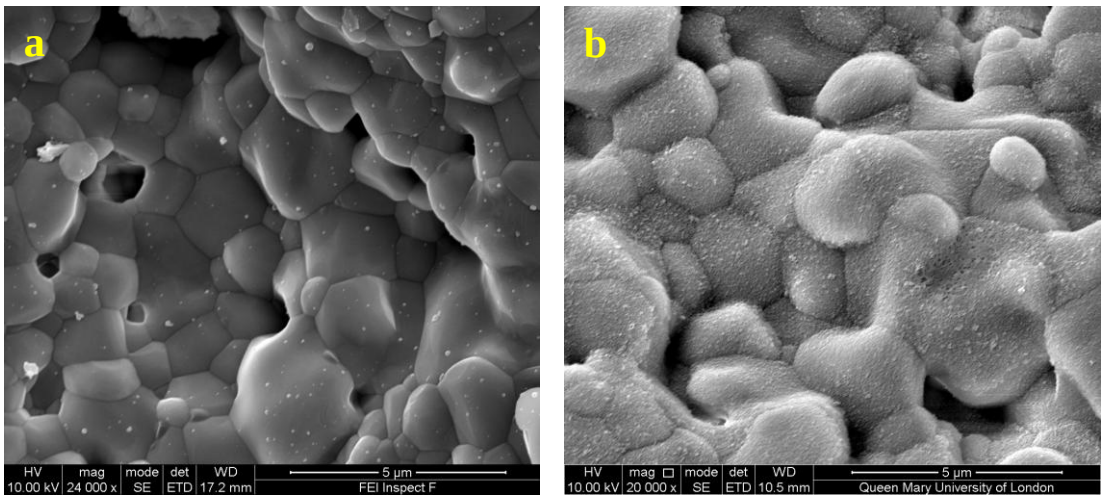

Figure 5.7: SEM images showing SA80/20 granules surfaces circulated with partially replenished media at a) 4 hours & b) day 7

From Figure 5.7, it is evident that there was no CaP layer precipitated on the surface of the granules when imaged at 4 hours. However at day 7 there was a consistent CaP layer precipitated on the surface of the granules.

5.3.1.2 Static Cell Culture on HA80/20

It is important to note that the differences in the media types tested were that 4H PCM was rich in calcium, phosphate and silicate ions however the 7D PCM and the 100PCM not replenished had depleted levels of calcium and phosphate ions but a further enrichment of silicate ions which were not significantly different.

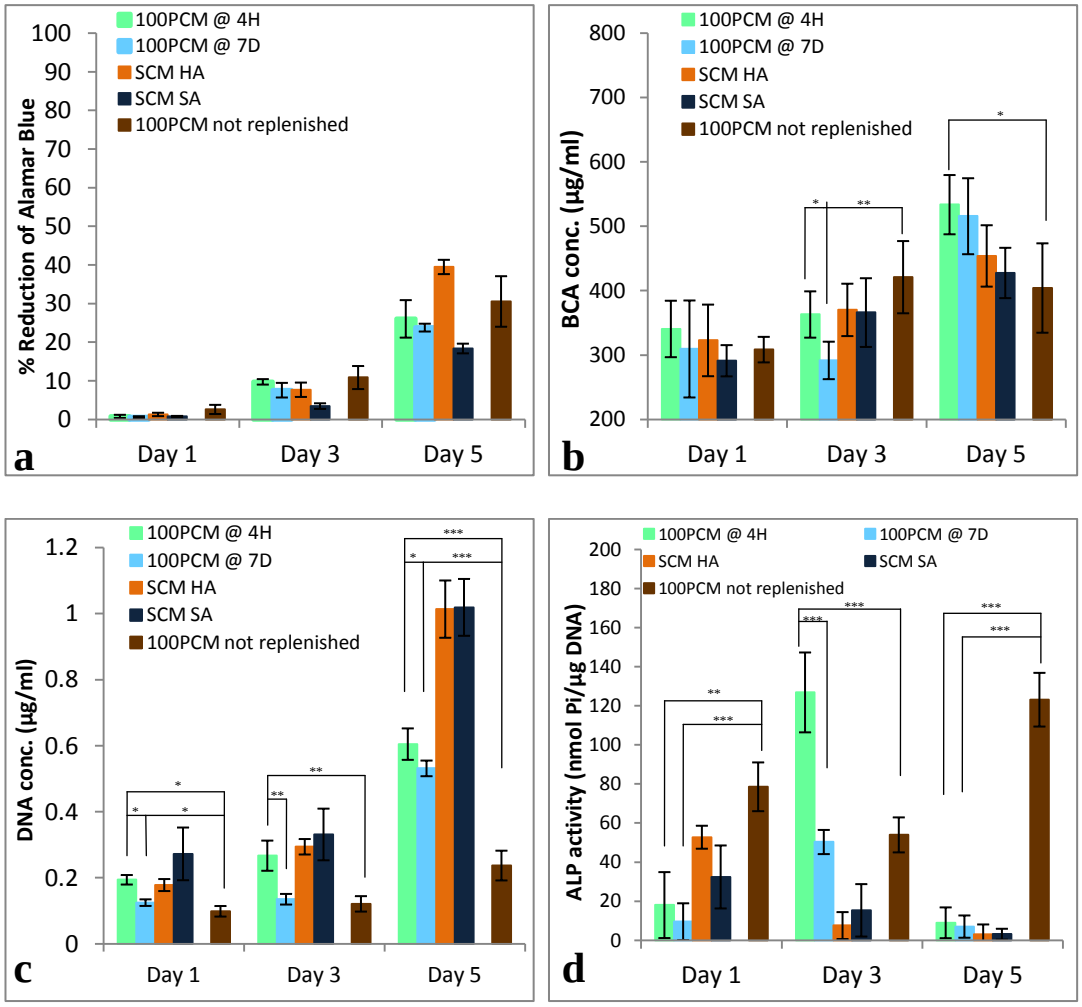

Figure 5.8: a) % reduction of alamarBlue®, b) BCA total protein, c) DNA concentration and d) ALP specific activity for MG63 cells cultured in replenished media (n=6)

Cell metabolic activity was not significantly different between the 4H and 7D PCM as well as the 100PCM not replenished (Figure 5.8a). Protein production at 4H and 7D PCM was significantly increased with time when compared to media that had not been replenished and the two controls (Figure 5.8b). Total DNA was significantly enhanced over time with the 4H and 7D PCM in comparison to media that was not replenished (Figure 5.8c). An elevated ALP activity was observed with the 4H PCM at day 3 however, ALP activity was significantly greater with the 100PCM not replenished over the 5 days (Figure 5.8d).

5.3.2 STEP 2 - Stirring Media

Results of the investigation into the effect of stirring the media within the perfusion system continuously for 7 days and partially-replenishing the media at 4 hours, as compared partially replenishing the media at 4 hours but not stirring throughout the time course, with respect to comparing any changes in the ionic concentrations (section 5.3.2.1) and cell response (5.3.2.2) are detailed below.

5.3.2.1 Ion Concentration Analysis and pH

From Figure 5.9, Figure 5.10 and Figure 5.11, it was evident that stirring the media did not have a significant effect of the calcium, phosphate and silicate ion concentrations. It can also be suggested that that the temporal patterns were smoother for the static reservoirs.

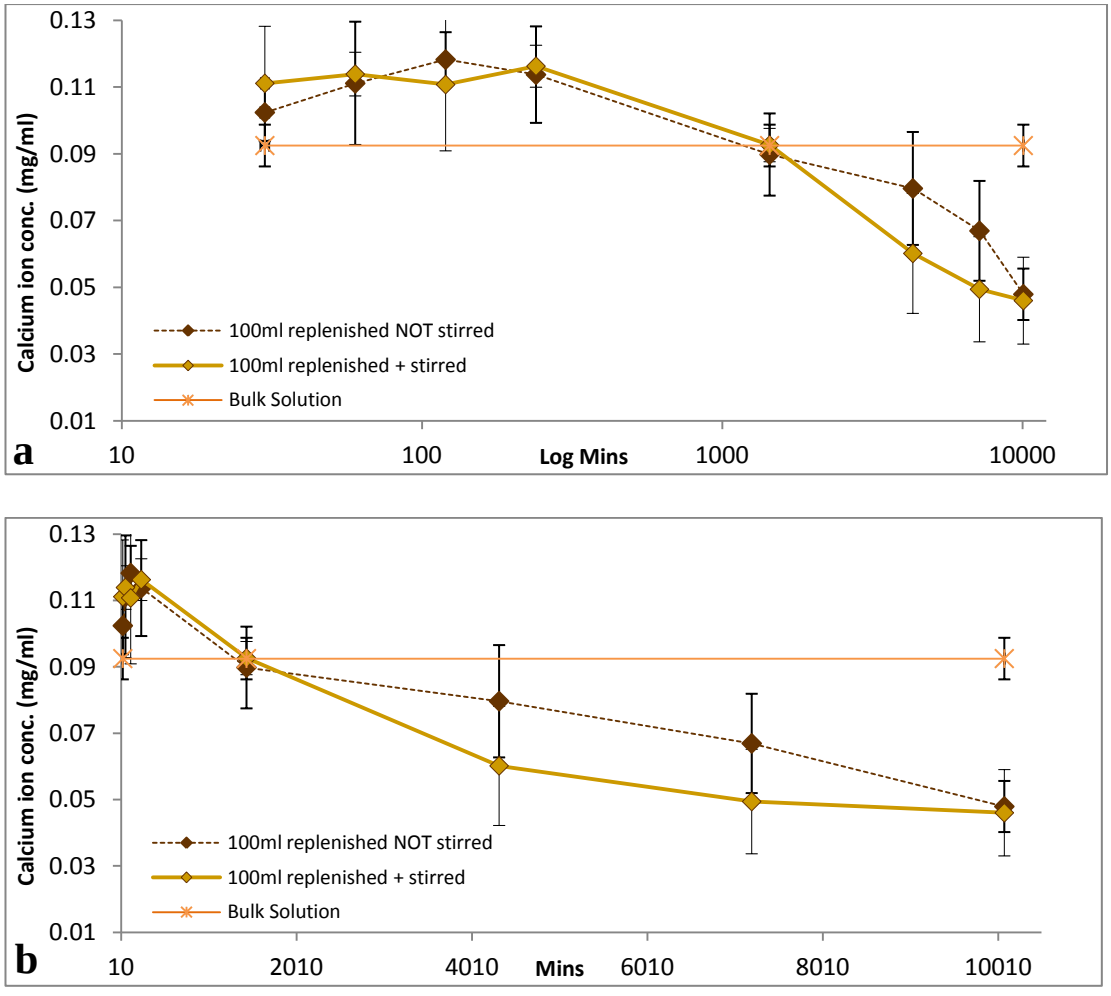

Figure 5.9: Calcium ion concentration of replenished media stirred and not stirred, a) log minutes scale & b) minutes scale (n=6)

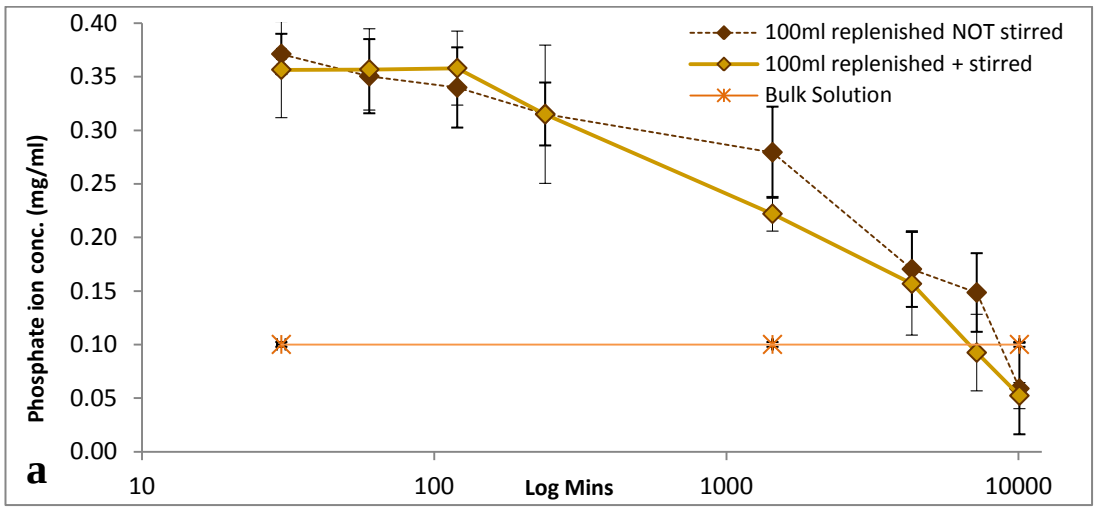

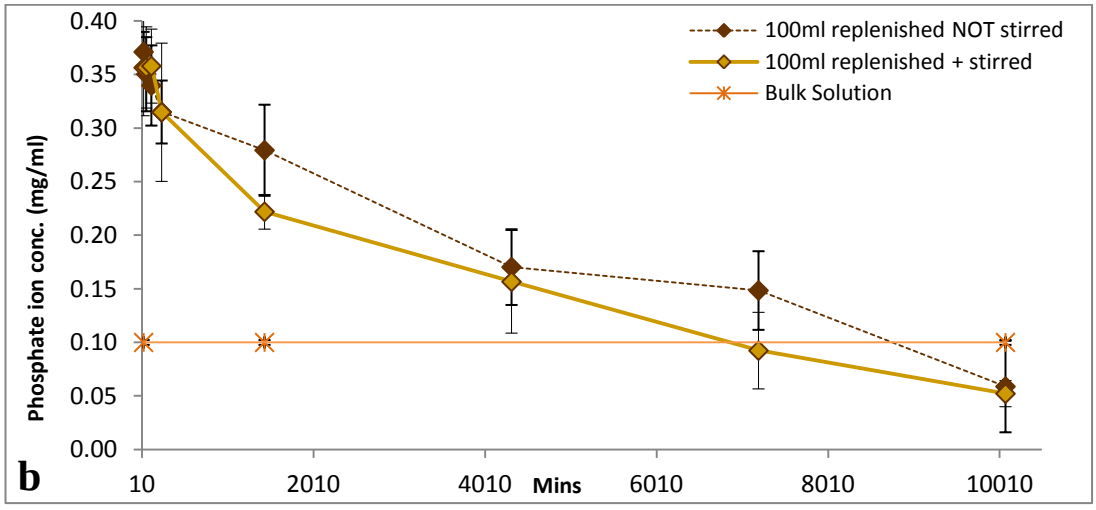

Figure 5.10: Phosphate ion concentration of replenished media stirred and not stirred, a) log minutes scale & b) minutes scale (n=6)

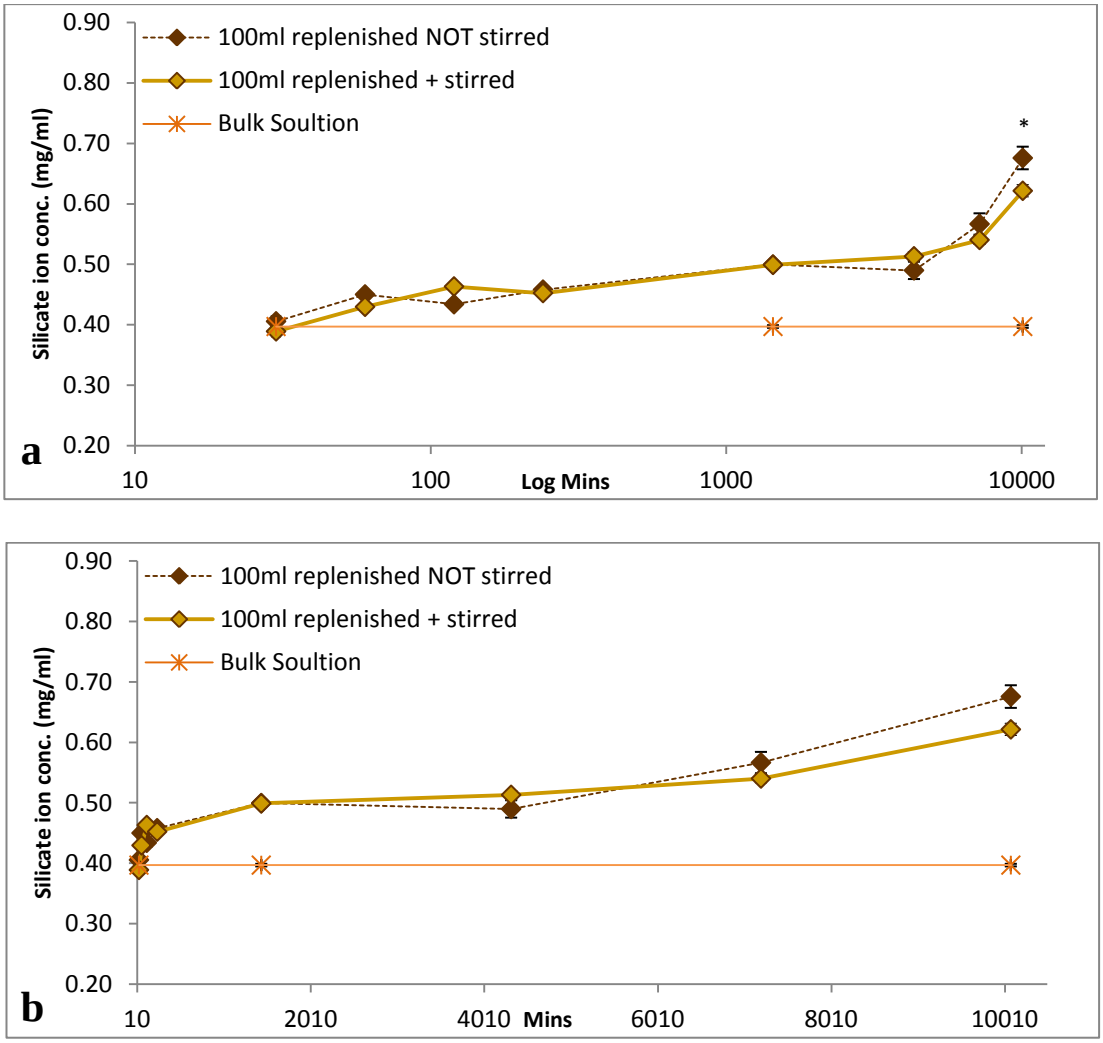

Figure 5.11: Silicate ion concentration of replenished media stirred and not stirred, a) log minutes scale & b) minutes scale (n=6)

No statistical differences in pH were noted between the stirred and unstirred partially-replenished media at any time point of the study, although there was a slight trend towards lower values of pH in the stirred media over the first 3 days of the experiment. (Figure 5.12).

From the SEM images (Figure 5.13) it is evident that at 4 hours during the circulation study there was no CaP precipitated on the surface of the granules however, at day 7 there was a homogeneous CaP layer precipitated on the surface of the SA80/20 granules.

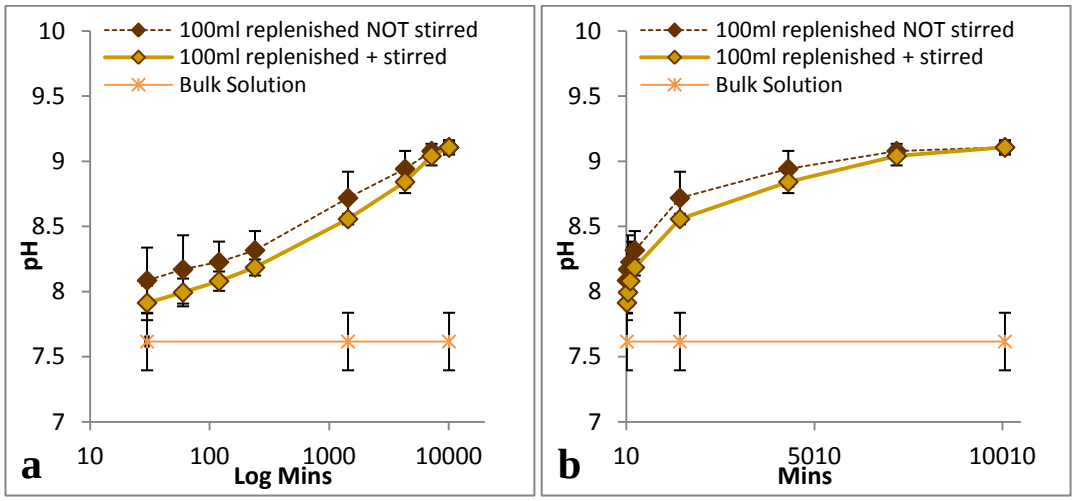

Figure 5.12: pH of replenished media stirred and not stirred, a) log minutes scale & b) minutes scale (n=6)

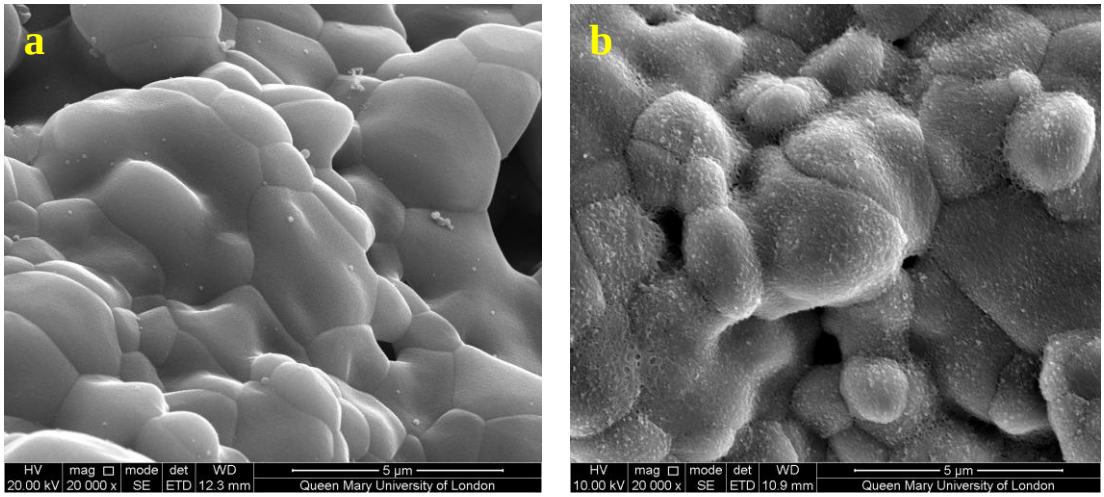

Figure 5.13: SEM images showing SA80/20 granules surfaces circulated with partially replenished stirred media at a) 4 hours & b) day 7

5.3.2.2 3D static Cell Culture on HA80/20

The results gained in this section used four different types of media to incubate HA80/20 granules statically for 5 days along with the two control media SCM HA and SCM SA. The differences between the media types were that 4H and 4H-S (not stirred and stirred) PCM were enriched with levels of calcium, phosphate and silicate ions which were not significantly different. 7D and 7D-S (not stirred and stirred) media had depleted levels of calcium and phosphate levels but there was a further enrichment of silicate ions.

The results obtained from incubating HA80/20 granules in stirred partially replenished, media compared to un-stirred partially replenished media were found to be statistically similar. The increase over time in cell metabolic activity assessed by the alamarBlue® assay showed no significant difference between the stirred and not stirred medium (Figure 5.14a). Protein production increased with time in the stirred media as it did with the media that was not stirred (Figure 5.14b). Total DNA increased with time in all the pre conditioned medium, however the 4 hour media which was not stirred showed a greater total DNA over time in comparison to the stirred media collected at this time point and replenished 7 day stirred and not stirred media (Figure 5.14c). An increased peak was observed at day 3 in ALP activity with both 4 hour medium, stirred and not stirred suggesting greater cell differentiation was taking place when the HA80/20 was incubated in these media types (Figure 5.14d). Overall it can be suggested that stirring the media had no significant effect of cell response.

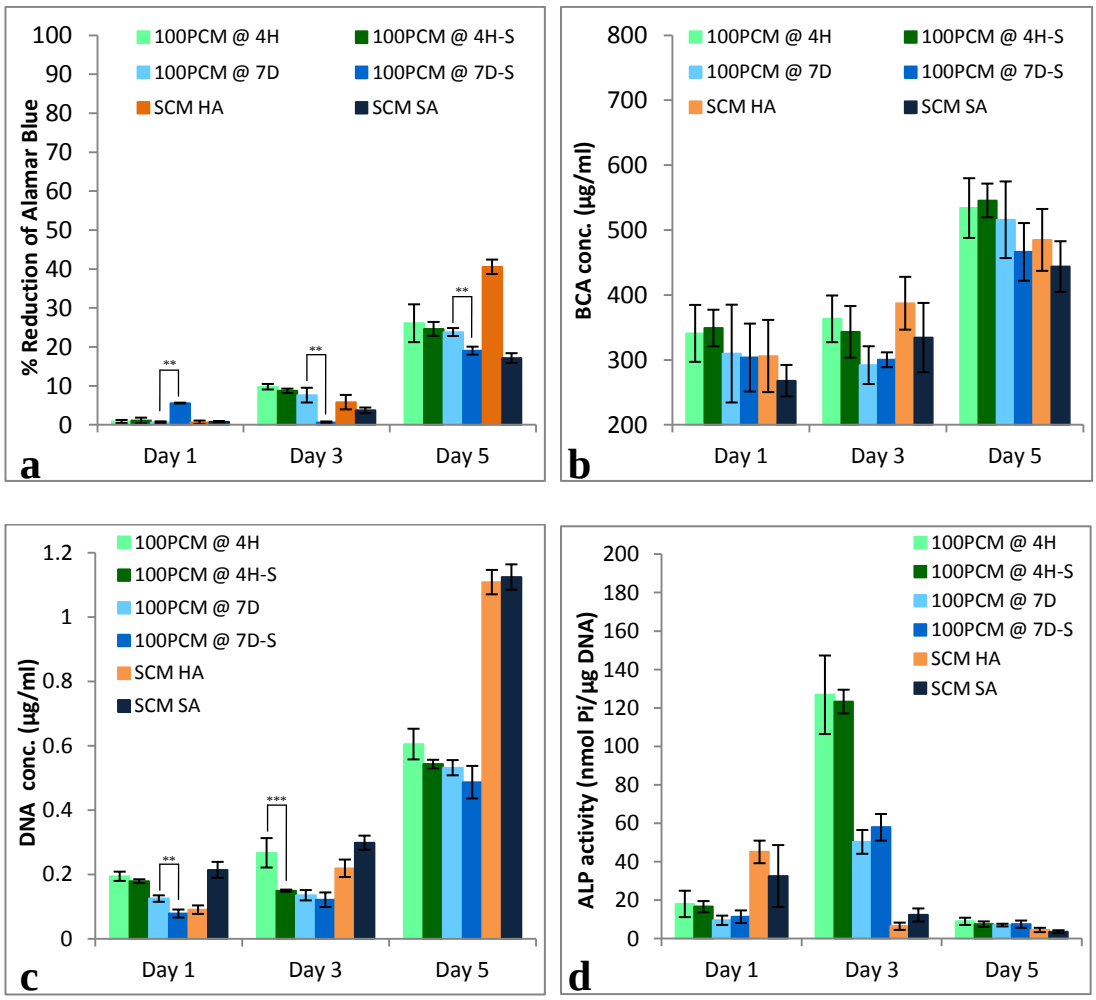

Figure 5.14: a) % reduction of alamarBlue®, b) BCA total protein, c) DNA concentration and d) ALP specific activity for MG63 cells cultured in stirred and not stirred media (n=6)

5.4 Discussion

5.4.1 STEP 1 - Partially Replenishing Media

Figure 5.3, Figure 5.4 and Figure 5.5 clearly demonstrate that even with replenishment at 4H, calcium levels were severely depleted by 3 days (Figure 5.3) while the depletion of phosphate ions was delayed (Figure 5.4) and there was a sustained release of silicate ions (Figure 5.5). Thus 4H PCM was calcium, phosphate and moderately silicate enriched as compared to 7D PCM which was calcium and phosphate depleted, and highly silicate enriched.

After the partial replenishment of the media, the depletion of calcium ion concentration was slowed down however at day 7 the depletion of calcium had reached the same levels in both replenished and not replenished media. There was a significant difference in the release of phosphate ions from the partially replenished media after 4 hours in comparison to the media that had not been replenished at all. There was a gradually decrease in phosphate ion concentration after 4 hours and by day 7 the levels had only just gone past basal levels.

Cell proliferation was significantly reduced in both 4H and 7D PCM as compared to SCM, however the cell proliferation was greater with 4H PCM in comparison to the partially replenished 7D PCM (Figure 5.8c). Results observed from the ALP activity and protein production assays suggest that both 4H and 7D PCM supported differentiation, particularly 4H PCM (Figure 5.8b and d respectively).

Calcium is the most abundant ion in the body, and it is bone that represents the body's calcium reservoir. It has been extensively shown that the presence of calcium ions supports the proliferation and differentiation of cells in bone remodelling, and that this could be an effect both direct and indirect through the activity of monocytes. Moreover, the presence of BGS to support the bone formation process is thought to help bone remodelling through ionic exchange between the surface of the BGS and the physiological environment. The presence of calcium affects the bone remodelling process and many studies have been focused on identifying the role that calcium ions play in directing the bone remodelling process when released from BGS into the surrounding environment. A study from Matsuoka dated 1999 (Matsuoka, Akiyama et al. 1999) showed that increasing concentration of extracellular calcium ions promoted osteogenic differentiation *in vitro* by increasing ALP activity up to 1.6-fold, and ALP, OCN and TGF-β gene expression from osteoblastic cells. Similar results were observed from another study whereby extracellular calcium ions were found to positively stimulate DNA synthesis and ALP activity of osteoblasts in bone

remodelling and osteoblasts proliferation, directly and indirectly via monocytes (Kanatani, Sugimoto et al. 1991). The release of calcium ions from HA and SA discs under static and semi-dynamic conditions, using serum-free media (SFM) or serum-containing media (C-MEM), showed that calcium ions were released only with C-MEM, from SA under both static and semi-dynamic conditions, while on HA there was calcium depletion from the media but only under semi-dynamic conditions. This suggested that serum proteins support this ionic exchange, and that SA more easily facilitates ion exchange between the material and the physiological environment compared to HA. Moreover, a net release of calcium from the materials was not seen, suggesting that the increased bioactivity of these materials is not a result of significant calcium ion dissolution (Guth, Campion et al. 2011).

There have been many other studies which have looked into the dissolution and re-precipitation of calcium and phosphate ions from other varying BGS. It has been suggested that the high rate of TCP degradation produces a localised calcium and phosphate rich environment which maybe favourable for osteogenesis (Frayssinet, Trouillet et al. 1993, Yuan, Zou et al. 1998). Osteoinduction of calcium phosphates is a complex process and it has been found that bone morphogenic proteins (BMP) play an important role along with calcium phosphate ceramics in providing an ideal environment for bone formation. TCP is thought to have a faster rate of dissolution therefore providing greater levels of calcium and phosphate ions within the surrounding media. It has also been suggested that proteins bind to calcium ions within calcium phosphate, therefore this means if there is an abundance of calcium present in the surrounding media, and proteins including BMP bind to this 'extra' calcium and enhance bone formation. *In vivo* there are many proteins that compete for calcium as binding sites, once the proteins have attached to calcium, the remaining calcium is used to precipitate a calcium phosphate rich layer on the surface of the BGS in order to create a bioactive layer to start bone formation (Yuan, Zou et al. 1998). From the results presented in this current study, it is evident that the media collected at 4 hours had elevated levels of calcium and phosphate ions with a small increase in silicate ions which also provided a more supportive environment for cell proliferation in comparison to the 7 day media which had depleted levels of calcium and lower than basal levels of phosphate ions (Figure 5.8c).

The biocompatibility of macroporous calcium phosphate based ceramics make them an ideal material for bone surgery. However their osseointegration is sometimes found to be poor. It is found that ceramics composed of HA and β-TCP induce better osseointergration properties than HA or even TCP alone. Frayssinet et al observed a greater dissolution around grain boundaries within the HA containing β-TCP material. *In vivo* studies found the degradation

of the synthetic material began earlier than the natural sintered bone during the first month of implantation. Again this was down to the incorporation of TCP which has the ability to degrade faster creating a supersaturation of calcium and phosphate ions around the implant. This greater level of calcium and phosphate ions allows for better incorporation of the material allowing faster and better osseointegration (Frayssinet, Trouillet et al. 1993). Again this study agrees with the findings from the results observed in this chapter as greater levels of calcium and phosphate ions present in the surrounding media had a direct effect on increasing cell proliferation in comparison to having depleted levels of these particular ions.

Even though some studies have proven that greater levels of calcium and phosphate ions within the surrounding environment are more favourable for osteogenesis, some authors have shown that TCP had the least amount of bone formation throughout the time points examined which suggested that ion release is not the only factor affecting hMSC induced bone formation (Arinzeh, Tran et al. 2005). Other authors have demonstrated that the slower rates of degradation of calcium phosphate ceramics actually improves the maintenance of the porous macro and microstructure which in turn leads to improved bone formation (Yuan, Zou et al. 1998, Alam, Asahina et al. 2001).

Arinzeh et al were also able to show the expression of osteocalcin of hMSC cultured on 20/80 HA/TCP ceramic material. The osteocalcin expression maybe a result of the increase phosphate levels in the media in the presence of 20/80 HA/TCP as a result of dissolution (Arinzeh, Tran et al. 2005). Other *in vitro* studies have demonstrated that the elevated phosphate levels enhance the expression of osteocalcin in human aortic smooth muscle cells and osteoblasts during osteoblastic differentiation (Giachelli, Jono et al. 2001, Nielsen, Pedersen et al. 2001).

Chemistry of the BGS is also seen to be a factor which influences ionic release. It has been shown that stoichiometric HA is better at releasing calcium ions in comparison to SA at later times points; day 10 and 14 and this increased ALP activity and osteocalcin expression. However when pre-conditioning these materials with fibronectin, the observations are that SA shows a greater release of calcium ions in comparison to HA (Castagna 2014). Moreover, the release of high concentrations of calcium to the microenvironment result is changes in pH, promotes inflammatory response and also favours fibrous tissue formation (Chou, Huang et al. 2005, Hing, Wilson et al. 2007). Furthermore, higher calcium ion concentrations have shown to effect osteoclastic activity, which varies from its inhibition, to its stimulation or having no effect (Berger, Rathod et al. 2001, Zaidi, Moonga et al. 2004). Consequently, a ceramic material which has a lower resorption rate is said to be stable for an

enough period of time in order to allow for the formation of new bone by the host tissue (Currey 2012). In addition, if the release of calcium ions is controlled over time, this favours the formation of an apatite layer, which as mentioned before is crucial for the bioactivity which is displayed in many HA based ceramics (Daculsi, Legeros et al. 1990, Lin, LeGeros et al. 2003, Duan, Zhang et al. 2005). This bioactivity can be responsible for the osteoconductivity and /or osteoinductivity of the ceramic material.

A very recent study attempted to investigate the effects of calcium and phosphate ions independently from one another by preparing composite materials with polylactic acid (PLA) acting as the matrix and calcium carbonate and sodium phosphate salts as matrix fillers. The cells used in this study were hMSC which were cultured on these composite materials and compared with plain PLA particles over time. In parallel the cells were also cultured in tissue culture plates in media supplemented with calcium or phosphate in order to study the effects of these ions independent of the 3D environment created by the composite particles. Calcium was shown to increase proliferation of the cells, whereas both calcium and phosphate positively affected the ALP specific activity. It was also noted that calcium and phosphate had a positive effect on BMP-2 and osteopontin expression. There was also a higher level of mineralisation observed with the incorporation of these ions within the composite particles. Even though the ionic concentrations in the composite cultures were lower, the effects observed were similar for cells cultured on the composite materials and those cultured in supplemented media. This particular study was informative in the sense that it allowed for the testing of the individual ions however the chemical analysis of the media showed that the calcium containing composites did not enrich the medium with calcium as the calcium concentrations found within the media were either comparable or lower than that of plain PLA. It was also interesting to note that the phosphate containing composites enriched the culture media with phosphate ions with the highest release at earlier time points and then slowly decreased with time. This particular composite also saw a depletion in calcium ions. This composite was also more favourable when it came to cell differentiation and it was more notable between days 7 to 14 (Danoux, Bassett et al. 2015).

The partially replenished data presented in this chapter demonstrated that even though there was and an enrichment of calcium and phosphate ions in the media at 4 hours, these levels still dropped to levels below the basal levels observed in DMEM. Previous studies have shown that having an environment which is enriched in these ions promotes osteogenesis, which is obviously crucial when looking at regenerating bone material. The present study was successful in confirming previous findings with the positive effects of increased cell proliferating with HA80/20 incubated in calcium and phosphate rich media.

5.4.2 STEP 2 - Stirring Media

The circulating experiment (Figure 5.9 and Figure 5.10) showed that there were similar trends in the release and depletion of calcium and phosphate ions from both not stirred and stirred media stations. There was a very similar trend in the release of silicate ions observed with both media stations. The cell response to incubating the HA80/20 granules in stirred and not stirred media did not show and significant differences between the two variables. As the media tested was partially replenished at 4 hours either stirred or not stirred, the cell proliferation was still seen to be greater with the 4 hours media in comparison to the media depleted in calcium and phosphate but enriched with silicate ions regardless of whether it was stirred or not (Figure 5.14c). There was an elevated metabolic activity (Figure 5.14a) with the 4 hour stirred media in comparison to the 7 days stirred media. However when comparing all the variables to HA80/20 incubated in SCM, the SCM showed the greatest cell metabolic activity, especially at day 5. There was an increase ALP activity (Figure 5.14d) at day 3 with the 4 hour media again regardless of it being stirred or not stirred in comparison to the 7 day or even the control mediums. For all media types the protein expression was seen to increase with time, however again the 4 hour media stirred and not stirred expressed the most proteins in comparison to the 7 day stirred and not stirred media and the two controls tested (Figure 5.14b). From these results it can be suggested that there was not much difference between the two variables however having the media not stirred during the circulation experiments showed better cell differentiation and cell metabolism making it a more favourable environment.

As mentioned before, mixing of the media is generally accepted and used in spinner flask bioreactor models, however the effects of stirring the media within a 3D perfusion system has not been explored. Previous studies have looked in to seeding hMSC on protein substrates (scaffolds or films) under static conditions, spinner flasks or perfused cartridge. Under static conditions calcium deposition was similar for hMSC grown on collagen scaffolds or films. In spinner flasks, under medium flow, hMSC on collagen scaffolds deposited more calcium and had higher ALP activity in comparison to hMSC grown on collagen films. The medium flow around the constructs resulted in the formation of bone rods which were perpendicular to the construct surface. However in the constructs where the media was perfused through the scaffold, individual bone rods orientated in the direction of fluid flow were formed throughout the constructs, the study was able to show that osteogenesis can be modulated by the flow environment. Therefore without the mixing action of media under perfusion conditions, bone rods were still observed but the only difference was their orientation (Meinel, Karageorgiou et al. 2004).

Spinner flask are found to promote mass transport at construct surfaces due to the action of mixing media, however by having media that is perfusing though the constructs due to the flow rate of the media, this promotes mass transport throughout the construct volume by utilising interstitial flow that is physiological for bone as it provides appropriate nutritional support which is found to be a fundamental requirement of bone formation (Hillsley and Frangos 1994). In order to minimise the diffusion distance and therefore maintain the concentration of nutrients and metabolites at the desired levels, perfusing media through the scaffold exposes the cells to controllable hydrodynamic shear which would in turn create an environment more favourable for bone formation (Meinel, Karageorgiou et al. 2004).

The results from the studies conducted by Bancroft et al indicated that the enhanced media delivery in flow perfusion systems along with mechanical forces may potentially increase cell differentiation. However, while bioreactors such as spinner flasks mitigate external diffusional forces due to the mixing action of the media, the internal diffusional limitation which is the inability of the medium and other nutrients to penetrate within the porous network of the scaffold still remains. In flow perfusion systems the media is pumped through each scaffold continuously, therefore there is no need to mix or stir the bulk media as the fluid shear stresses created by the fluid flow action mitigate the internal and external diffusional limitations which allows for the enhanced delivery of nutrients throughout the entire scaffold and also throughout the internal structure of each scaffold (Bancroft, Sikavitsas et al. 2003).

These findings are in agreement to the results observed in this chapter, as there was no significant difference seen between the media that was stirred and the media that was not stirred. The fluid flow within perfusion systems allows for enhanced media flow to and within scaffolds. Therefore stirring the bulk media makes no difference to the results as the pumping action of the media throughout the whole scaffold already enhances cell response.

5.5 Summary and Conclusions

The first part of the work presented in this chapter has successfully shown that partially replenishing media during the circulation study delays the depletion of calcium and phosphate ions, however by the end of the study a depletion in these ions is still observed. It was also noted that cell response it sensitive to the levels of these particular ions present in the medium, as higher levels of these ions allowed for better and increased cell proliferation and metabolism in comparison to medium with depleted levels of calcium and phosphate. A steady silicate ion release was still observed during the study with partially replenishing the media, but it was very similar to the release observed when the media was not replenished.

The second part of the work presented in this chapter was successful in showing that there was no significant difference in ion release and in cell response when comparing results gained from stirring the bulk media during the circulation study and not stirring the media. The results were able to re-confirm the findings in the first step in this chapter whereby regardless of stirring the bulk media, cell metabolism and proliferation was greater with media with increased levels of calcium and phosphate ions. Looking in to the literature, the stirring action of the bulk medium is not required when studying perfusion systems as the pumping action of the medium provided by a means of the flow rate through the individual scaffolds already allows for a better and enhanced delivery of nutrients and metabolites in to the deeper structure of the porous scaffold. The work presented in this part of the chapter was able to confirm this as no significant difference was observed in the results between stirring and not stirring the media in the circulation study.

The interaction of ions between the materials surface and the surrounding medium have an effect on cellular development around the implant *in vivo* due to the alterations in ionic concentrations presented to the cell. Even though the media was partially replenished at 4 hours in the circulation study, the calcium and phosphate levels still reached depleted levels by day 7 which in turn suppressed the cell response. In order to further study these effects of the increased levels of calcium and phosphate ions on cell response, continuous media refreshment needs to be investigated during the circulation study and see whether this has an effect on cell response on porous BGS in 3D. Also the results gained in the later part of this chapter confirm that there is no need to stir the bulk medium during the circulation study.

Chapter 6 Effect of Complete Media Replenishment on Dynamic Ion Exchange and subsequent Osteoblast-like Cell Response

6.1 Background

From the results obtained in the previous chapter it was observed that partially replenishing the 100ml volume media reservoir with 50ml of fresh DMEM at 4 hours, did not significantly affect the depletion of calcium and phosphate ion levels by the end of the circulation study, at day 7, nor did it significantly affect the rise in pH. However cell proliferation on HA80/20 granules was enhanced when incubated in media that was collected at 4 hours during the circulation study which was enriched in calcium and phosphate ions. Through the comparison of incubation in 4H and 7D partially replenished and maintained in situ media, a sensitivity to cell response to calcium, phosphate and silicate ions in the media incubated on porous granules was demonstrated.

Therefore the objective of this chapter was to investigate the effect that complete replenishment of the media at day 1 and day 5 would have on dynamic ion exchange, pH and cell response.

For complete replenishment of media, day 1 was chosen as the first time point as the results obtained in Chapter 5 section 5.3 marked a decrease in both calcium and phosphate ion concentrations and in order to try and sustain higher levels of these ions, day 5 was chosen to be the next time point, again in order to sustain higher levels of these ions throughout the 7 day circulation period (as ultimately this will be the goal length of a 3D perfusion tissue culture experiment.

6.2 Methodology

6.2.1 Media and Sample Preparation

100ml media and sample preparation was as described in Chapter 4 sections 4.2.1.1.

6.2.2 Perfusion Set-up

The set-up of the 3D perfusion system apparatus was the same as described in Chapter 5 section5.2.1.2.

As in Chapter 5, PCM in this study was obtained by circulating 100ml of Dulbecco's Modified Eagle Medium containing 1% Penicillin-Streptomycin (DMEM) in a closed loop system at a flow rate of 0.7ml/min through 0.45g of SA80/20.

5ml of solution was extracted at time intervals of 0.5, 1, 2 and 4 hours, 1, 3, 5, 6 and 7 days, and replaced with 5ml fresh DMEM for analysis of calcium, phosphate and silicate ion concentrations using colorimetric assays as previously described in Chapter 4 section 4.2.1.2. The length of the experiments was kept the same as stated in previous chapters of 7 days in order to maintain similar testing parameters across all experiments reducing test variability.

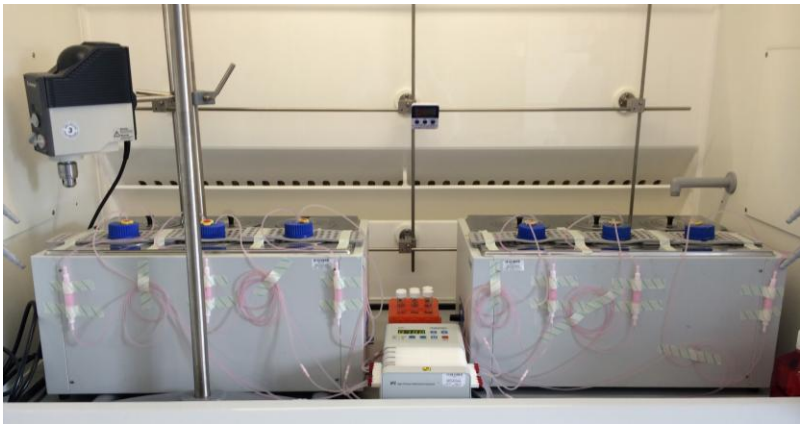

Figure 6.1: Set-up of the perfusion system experiments

Additionally at day 1 and at day 5, the full 100ml of the re-circulating DMEM was collected and completely replenished with 100ml of fresh DMEM. At day 7 the final 100ml of DMEM was collected. The collected day 1, day 5 and day 7 media were individually sterile filtered and supplemented with 10% FBS and stored as 1D PCM, 5D PCM and 7D PCM respectively. The pH of all DMEM samples was measured (as previously described in Chapter 3, Section 3.2.5) on collection throughout the perfusion study. SEM analysis was

also conducted on the granules collected on day1, 5 and 7 of the circulation study. The protocol followed can be found in chapter 2 section 2.1.

6.2.3 Static Cell Culture on HA80/20

After the perfusion experiments were completed, the collected 1D, 5D and 7D PCM were used to conduct static cell culture studies in order to see whether the media types had an effect of osteoblast-like cell response under 3D incubation conditions. MG63 cells were grown and expanded as described in Chapter 4 section 4.2.2.1.

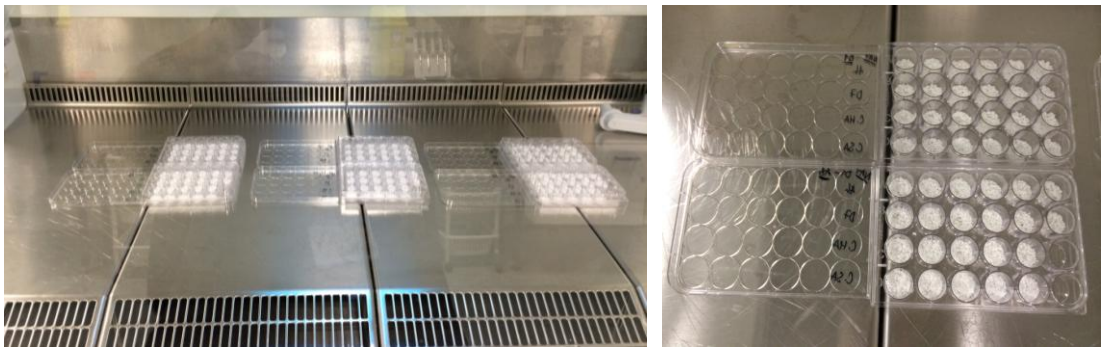

Figure 6.2: Preparation for Static Cell Culture experiments, with cells seeded on HA80/20 granules incubated in either 1D, 5D or 7D PCM over a period of 5 days

MG63 osteoblast-like cells (P4) at a concentration of $4x10^4$ cells/ml were seeded on 0.45g of HA80/20 granules in 24 well plates in 1ml of SCM and allowed to attach at 37°C and 5% CO_2. After 2 hours the SCM was replaced with 1ml of either 1D, 5D, 7D PCM or fresh SCM as a control. Cells incubated on SA80/20 was used as a second control which was incubated in SCM for the duration of the 5 day experiments. The cells were incubated for periods of 1, 3 and 5 days. The media was refreshed at 24 hours then every 48 hours thereafter. DNA quantification, ALP activity, total protein and cell metabolic activity was monitored at each time point. The protocols followed for these assays can be found in Chapter 4 sections 4.2.2.2 - 4.2.2.5.

6.2.4 Statistical Analysis

Collected data was analysed and expressed in terms of mean ± standard deviation. Statistical significance was evaluated using ANOVA, Post Hoc test: Tukey HSD with $\alpha=0.05$, (where *$p<0.05$, **$p<0.01$ and ***$p<0.005$).

6.3 Results

6.3.1 Ion Concentration Analysis and pH

From Figure 6.3, Figure 6.4 and Figure 6.5 it is evident that having a 2 point complete replenishment of the media had an effect on calcium, phosphate and silicate ion concentration over the 7 day period of circulation.

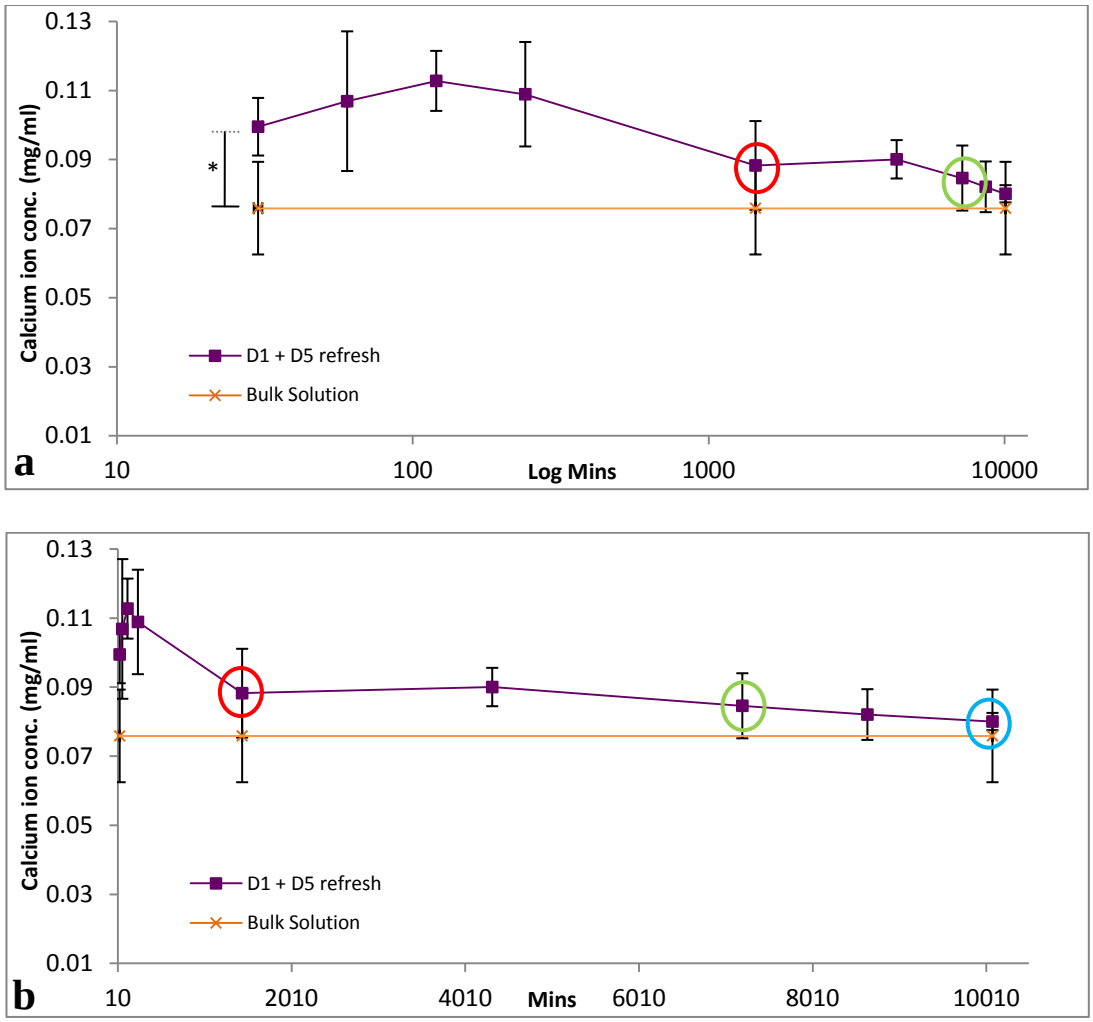

Figure 6.3: Calcium ion concentration for complete replenishment of media at D1 & D5, a) log minutes scale & b) minutes scale (n=6)

There was an initial significant ($p<0.05$) increase in calcium and phosphate concentration as compared to base DMEM at early time points (Figure 6.3 and Figure 6.4). At 24 hours there was a decrease in calcium and phosphate ion concentration observed, and at this time point (circled in red on graphs) the 100ml of media was collected and replaced with 100ml of fresh DMEM. With this complete replenishment at day 1, the calcium and phosphate levels did not

decrease dramatically at day 3 but was maintained. A decrease in both calcium and phosphate ion concentration was seen at D5, however the decrease was only significant with the phosphate ions ($p<0.05$) (circled in green on graphs), and at this point the media was once again completely replenished. At day 6, there was an increase and decrease observed in phosphate and calcium levels respectively compared to day 5 which were not significantly different. By the end of the study at day 7, as a result of the dual step complete replenishment the media contained statistically similar levels of calcium ions to that of the base DMEM, however the phosphate ion concentration was significantly higher ($p<0.005$) than basal levels of DMEM. It is also apparent that from day 1 to day 7 there was no significant difference between the levels of calcium ions in the surrounding media.

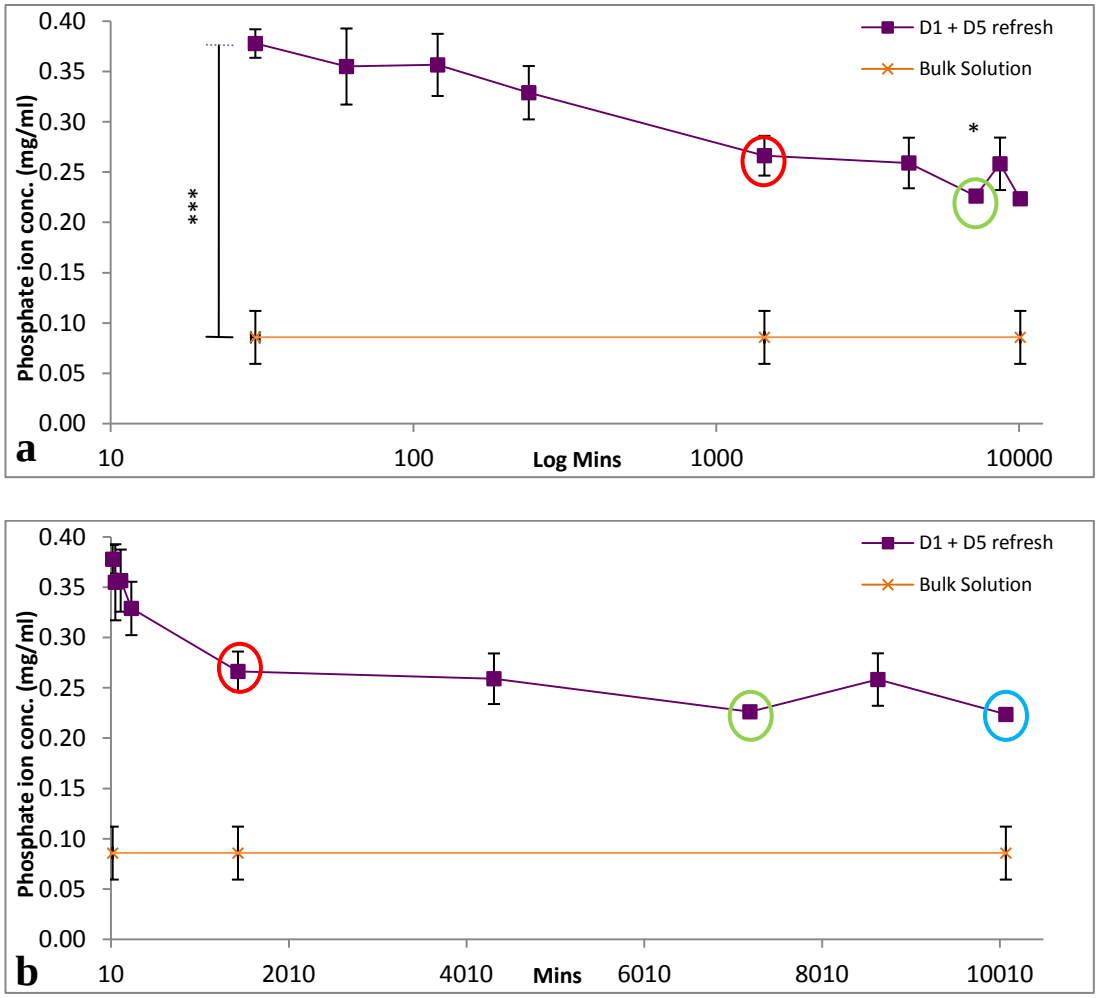

Figure 6.4: Phosphate ion concentration for complete replenishment of media at D1 & D5, a)log minutes scale & b) minutes scale (n=6)

After 1h Silicate ion levels remained statistically ($p<0.05$) increased in comparison to basal levels of DMEM throughout the 7 day period (Figure 6.5). However, there was a significant

difference in the silicate concentrations of the fully-refreshed media at later time points as compared to the non-refreshed media where, after fully refreshing the media at day 1 and day 5, the silicate levels were observed to drop at day 3 and day 6 respectively, and only reaching a level of 0.4 mg/ml by day 7.

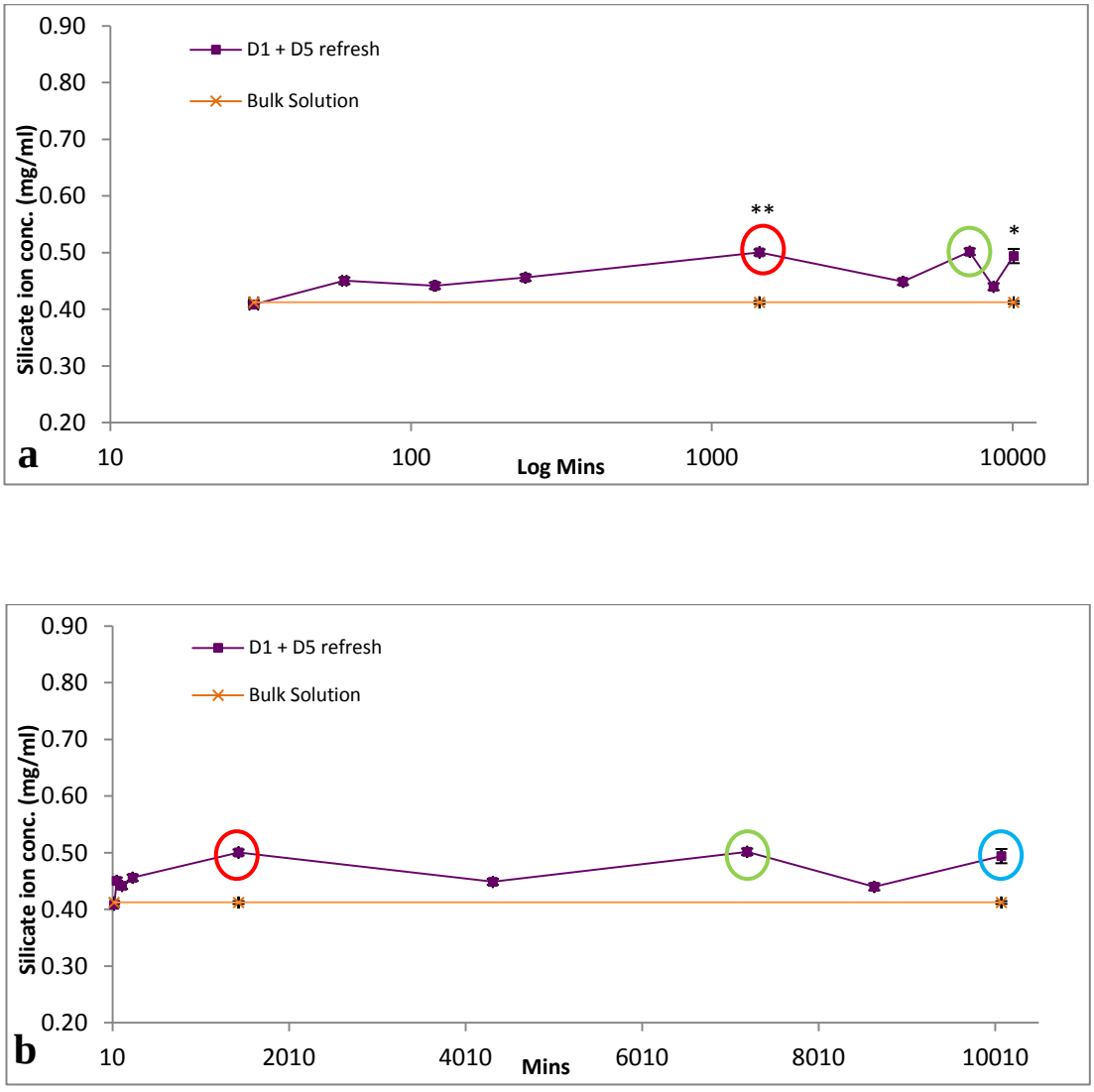

Figure 6.5: Silicate ion concentration for complete replenishment of media at D1 & D5, a)log minutes scale & b) minutes scale (n=6)

As observed previously pH was observed to increase rapidly within the first 24h. Complete replenishment of the media at day 1 and day 5, appeared to have little effect on the magnitude of this elevation as compared to the pH of base DMEM (Figure 6.6).

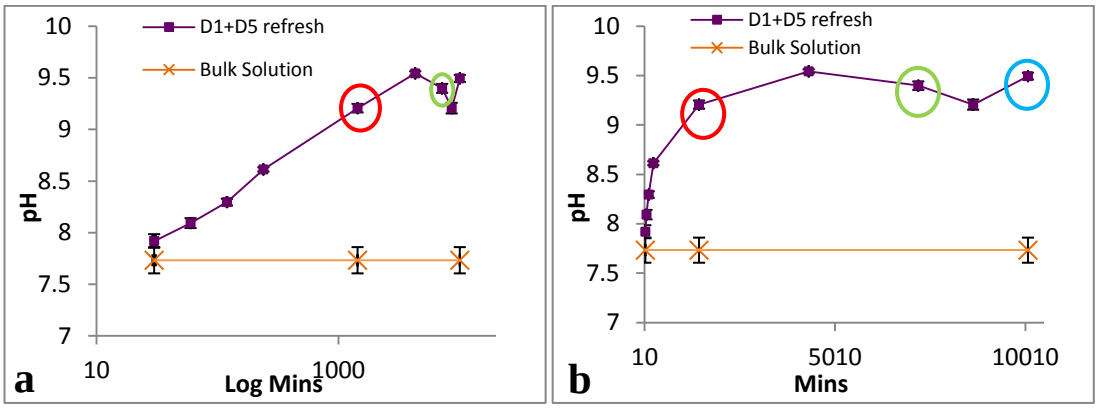

Figure 6.6: pH of complete replenishment of media, a)log minutes scale & b) minutes scale (n=6)

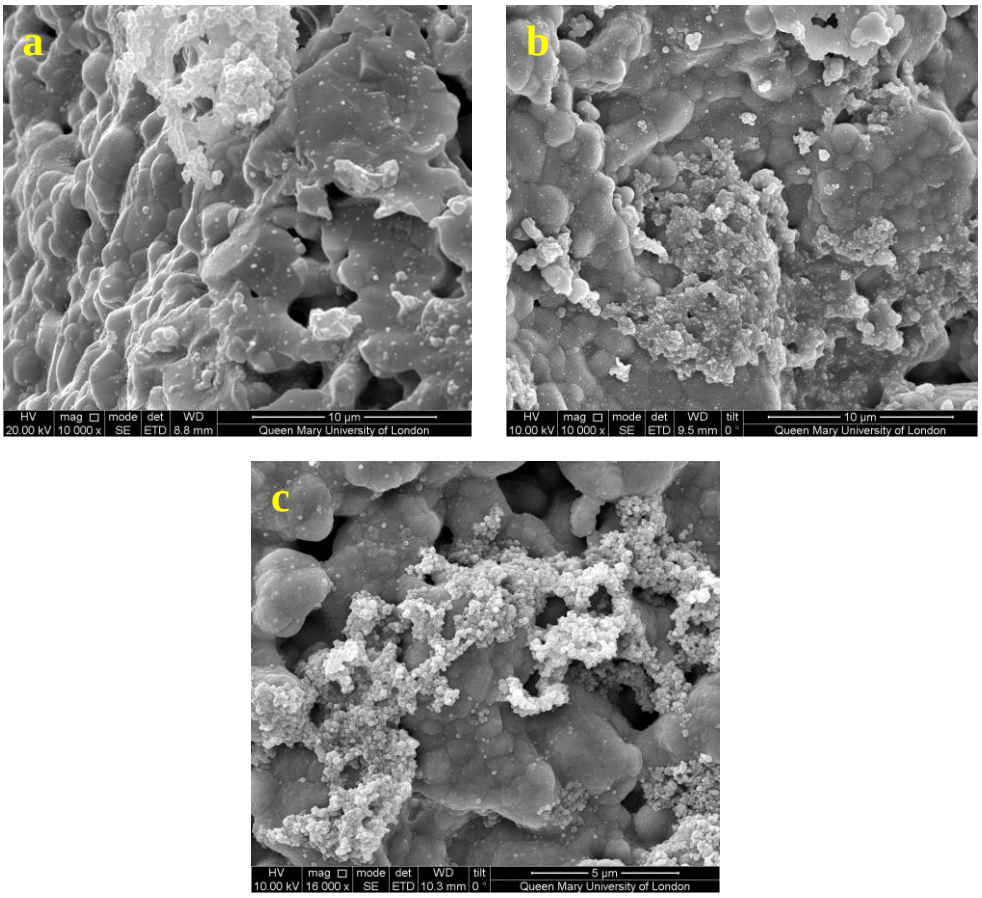

Figure 6.7: SEM images of SA80/20 granules collected at a)day 1, b) day 5 and c) day 7

From the SEM images it is evident that a CaP layer was beginning to be precipitated from day 1. However, it was not a homogeneous layer as seen previously in chapter 4 & 5. There were small areas on the surface of the granules which had apatite crystals present as opposed a uniform layer being deposited.

6.3.2 Static Cell Culture on HA80/20

Cell response was monitored with three different PCM: media collected at 1D, 5D and finally at 7D. The results were compared to the cell response observed with HA80/20 incubated in SCM and SA80/20 incubated in SCM. It is important to note that there were differences in the calcium, phosphate and silicate ion concentrations between the different types of media used as PCM for the 3D static experiments which followed. In comparison to the DMEM, which was the bulk media used for the circulation study, all PCM (1D, 5D and 7D) had statistically similar calcium ion concentrations, statistically higher phosphate and silicate ion concentrations and statistically higher levels of pH. Between 1D, 5D and 7D PCM, the levels of calcium, phosphate and silicate ions were statistically similar.

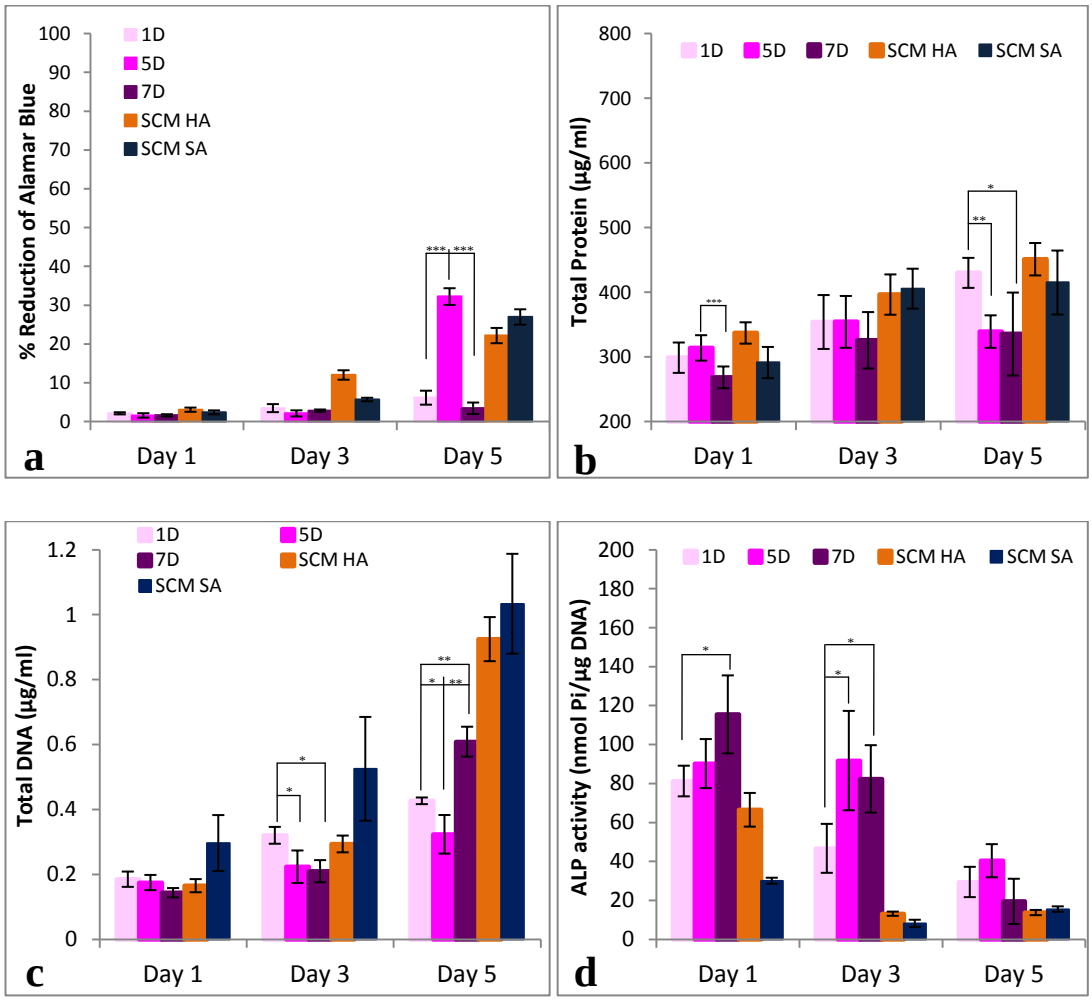

Figure 6.8: a) % reduction of alamarBlue®, b) BCA total protein, c) DNA concentration and d) ALP specific activity for MG63 cells cultured in complete refreshed media (n=6)

Cell metabolic activity was suppressed with all media types, in comparison to the two controls. At day 1 and day 3 there was no significant differences between the PCM. However at day 5, the 5D-PCM had significantly higher levels of cell metabolic activity in comparison to 1D and 7D PCM (Figure 6.8a).

Protein production at day 1 was significantly lower with 7D PCM compared to the other PCM. At day 3 all PCM and both controls were statistically similar. Finally at day 5, 1D PCM had significantly greater protein production in comparison to 5D and 7D PCM, however these levels were statistically similar to the two controls tested (Figure 6.8b).

There was greater cell proliferation observed with the 1D-PCM over time in comparison to the 5D-PCM and 7D-PCM. At day 1, all PCM had statically similar levels of DNA with SCM SA showing statistically greater levels overall ($p<0.05$). At day 3, 1D PCM had statistically greater DNA levels than 5D and 7D PCM. SCM SA again showed statistically greater levels overall ($p<0.05$). At day 5 7D PCM showed statistically greater levels of DNA in comparison to the other PCM. 5D had significantly lower levels in comparison to 1D and 7D PCM. SCM HA and SA showed significantly greater levels overall on day 5 ($p<0.005$). (Figure 6.8c).

Greater levels of ALP activity were observed with the PCM types over the 5 days in comparison to the two controls tested. At day 1, 1D PCM had statistically lower levels than 7D PCM. At day 3, 1D PCM again observed statistically lower levels compared to 5D and 7D PCM. Both SCM had statistically lower levels at day 3 compared to all PCM ($p< 0.005$). At day 5 all PCM and both SCM were statistically similar levels of ALP (Figure 6.8d).

6.4 Discussion

From the results it is evident that having complete replenishments in media at two points delays the depletion of calcium ions however the levels of phosphate and silicate ions are still significantly increased compared to the bulk starting DMEM. During the circulation experiments, there was an initial significant release of calcium and phosphate ions from the granules into the surrounding circulating media and the silicate ion levels were statistically identical to the bulk DMEM. At day 1 the media was significantly enriched in phosphate and silicate ions however the levels of calcium ions were statistically similar to the bulk DMEM. After this first complete replenishment at day 1, the observed calcium and phosphate ion concentrations at day 3 were statistically similar to day 1 before complete replenishment. The silicate ion concentration was significantly decreased in media after the first complete replenishment of media. At day 5, the calcium ion levels were statistically similar to day 3 and phosphate ion concentration was significantly decreased compared to day 3. Silicate ion concentration was significantly increased. After the second complete replenishment at day 5 the calcium levels remained statistically similar with a further decrease, phosphate levels increase significantly and the silicate ion levels decreased significantly. At the end of the circulation experiments (day 7), the media collected had statistically similar levels of calcium ions compared to the bulk DMEM and phosphate and silicate ions were significantly increased compared to the bulk DMEM. From the silicate ion concentration graph it is noted that the drop between day 1 & day 3 and day 5 & day 6 suggests that while silicate ions are still being release in to the media, the rate of release at later time points is not as fast as at early time points. During the complete media replenishments, pH remained statistically increased compared to the bulk DMEM and between the day 1 and day 5 complete replenishment, the pH was significantly increased.

Overall between day 1 and day 7, the levels of calcium, phosphate and silicate ions were not significantly different. Having completely replenished the media, the phosphate and silicate levels remained significantly elevated. This suggests that there is a net loss of phosphate and silicate ions from the BGS granules, however calcium levels remain statistically similar showing a continued decrease. It can be proposed that even though the ions are being released in to the media from the granules, the phosphate and silicate ions are not being used up as fast as the calcium ions for precipitation of a bone like apatite as the SA80/20 granules are carbonate substituted. From the SEM images it is evident that there is a precipitation of bone like apatite at day 1, 5 and 7.

Even though 1D, 5D and 7D PCM collected from the circulation study had statistically similar levels of calcium, phosphate and silicate ions, these observed changes affected cell response when incubated in the three different types of PCM. At day 5 of the static cell culture study cell proliferation was enhanced in comparison to the 1D and 5D media, however SCM still provided the most supportive environment for cell proliferation over time (Figure 6.8c). Peak release of ALP activity was seen to be shifted to day 1 in comparison to previous studies which saw peak release at day 3 with all PCM with 7D PCM observing significantly greater levels (Figure 6.8d).

Looking back and comparing results gained from the current complete replenishment study and the partial replenishment study it is evident that dynamic ion exchange is sensitive to the continuous complete refreshment of media (Figure 6.9). The two point complete replenishment delayed the depletion of calcium ions and maintained elevated phosphate and silicate ion levels in the media (Figure 6.9).

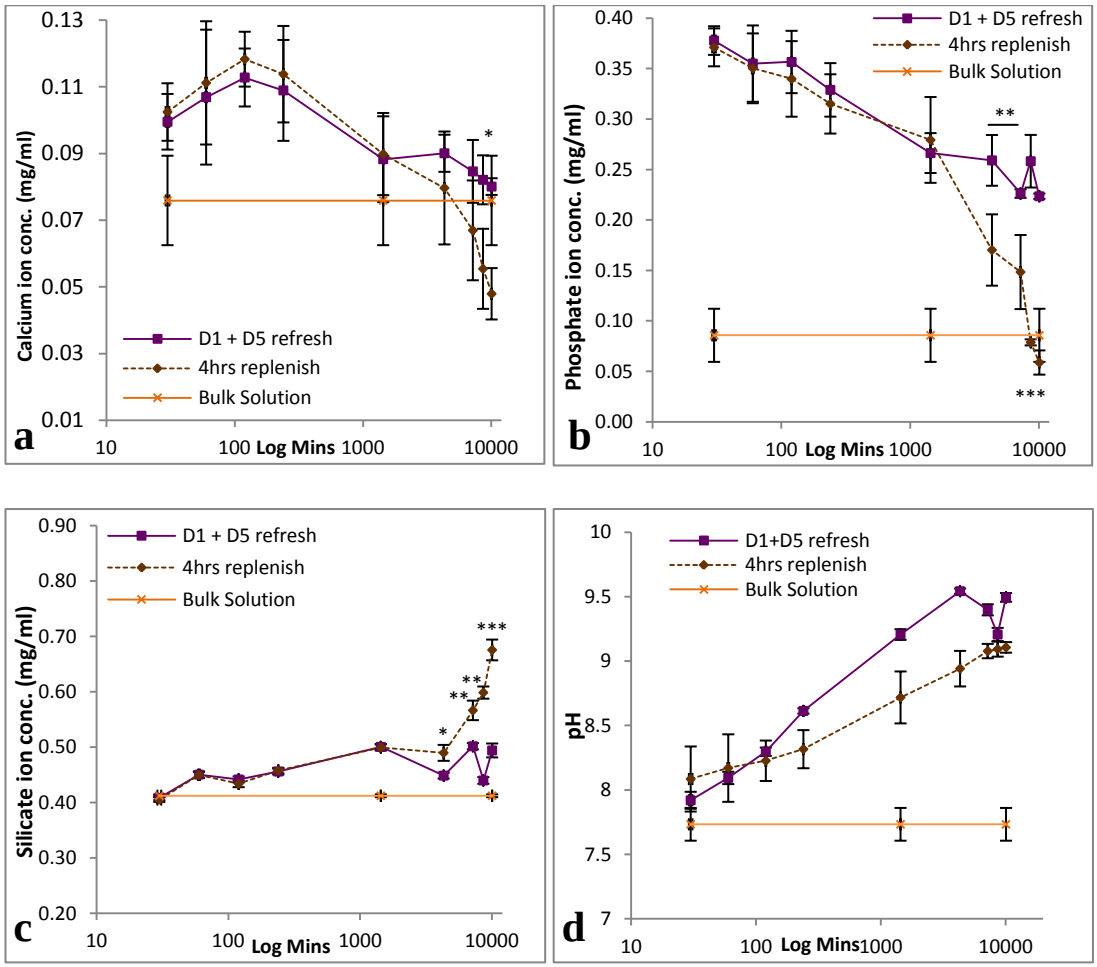

Figure 6.9: a) Calcium ion conc., b) Phosphate ion conc., c) Silicate ion conc. and d) pH graphs for complete replenishment compared to partial replenished media (n=6)

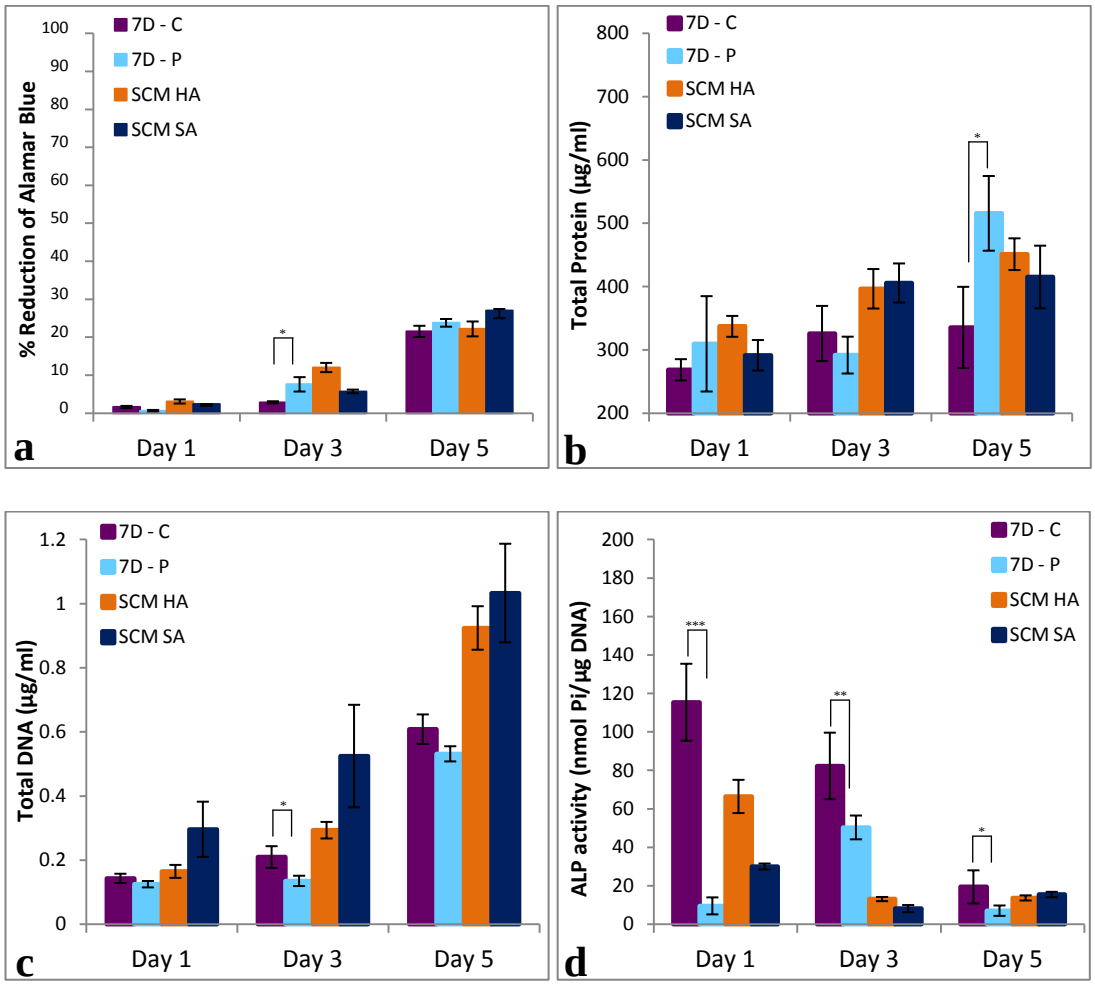

Figure 6.10: a) % reduction of alamarBlue®, b) BCA total protein, c) DNA concentration and d) ALP specific activity for MG63 cells cultured in complete replenished media and partially replenished media for 5 days (n=6)

Further comparison between the 7D media collected in the complete refreshment study and the 7D media collected in the partially replenished study it is evident that the changes in ionic concentration are sensitive cell differentiation (Figure 6.10d). In the graphs displayed above, 7D - C represents the day 7 data gained from the complete replenishment study and 7D - P represents the day 7 data gained from the partially replenished study. There is no significant difference in the cell metabolic activity on day 1 and 5. On day 3, the partially replenished 7D PCM showed a significantly greater increase in cell metabolic activity (Figure 6.10a). Protein production was statistically similar between all PCM and the control SCM for days 1 and 3. On day 5 7D-P showed a significantly greater increase in comparison to 7D-C (Figure 6.10b). Cell proliferation was greater with 7D-C over time however the proliferation was still greater with the controls tested especially with SA80/20 incubated in SCM (Figure 6.10c). At day 1, cell differentiation was significantly greater with 7D-C in

comparison two 7D-P and the two controls, whereas 7D-P showed a significantly increased peak ALP activity at day 3 (Figure 6.10d).

From all these results it is evident that a two point complete replenishment of the media during the circulation study delays the depletion of calcium ions and phosphate and silicate ions remain elevated however at these two points the levels of these ions remain statistically similar and this then in turn enhances cell response. It can be suggested that the change in cell response even though ion concentration levels are similar could be due to the significant increase in pH. At 1D, 5D and 7D PCM from the complete replenishment study, the pH was significantly increase in 5D and 7D PCM where both 5D and 7D PCM had statistically similar pH levels.

When investigating the significant increase in pH with the work presented in this current chapter, further observations found that the makeup of the DMEM used in the circulation studies so far contained high levels of sodium bicarbonate ($NaHCO_3$) at 3.7g/l. The formulation sheet of the DMEM provided by Sigma Aldrich can be found in APPENDIX 6 in this thesis. Sodium bicarbonate is used a buffer in order to maintain the pH of the DMEM. However this buffer is known to have two main disadvantages. The first is that the pKa (the pH of the midpoint of buffering range) of sodium bicarbonate is 6.3 at 37^{o}C, this results in the suboptimal buffering throughout the physiological pH range. Secondly, CO_2 is released in the atmosphere which results in the increase in alkalinity, and the number of hydroxyl ions produced increases in accordance to the amount of sodium bicarbonate added to the medium.

As the circulation experiments were conducted under atmospheric conditions, the presence of high levels of sodium bicarbonate along with the CO_2, forced the pH of the media to become highly alkaline. It is possible to control this by artificially providing CO_2 to the atmosphere and therefore preventing the gas from leaving the liquid which in turn would reduce the hydroxyl ion concentration in solution. However this approach is tricky therefore it is not recommended. Instead it is recommended to use a medium type which contains no sodium bicarbonate and adding N-2-hydroxyethylpiperazine-N'-2-ethanesulfonic acid (HEPES) buffer to the medium to act as the buffering agent.

Many attempts have been made to find the most suitable buffer. The most commonly used alternative to sodium bicarbonate is HEPES buffer which was first described by Good et al in 1966 (Good, Winget et al. 1966). HEPES has proved superior to conventional buffers in comparative biological assays with cell-free preparations. It has many properties which make it an ideal buffering agent to tissue culture media. Principally it does not require an enriched

atmosphere in order to maintain the correct pH and it varies inversely with temperature of the medium, with it approximately having a pH of 7.3 at 37^{o}C.

HEPES is found to be a satisfactory buffering agent for the growth of many different cell types and studies have indicated that 20mM HEPES is the most satisfactory concentration of the buffer to add to tissue culture medium, however it may exhibit toxicity at concentrations higher than 40mM. There is no need for a CO_2 controlled incubator to be used with medium that is solely buffered with HEPES. The addition of HEPES to many powdered mediums containing no sodium bicarbonate should be prepared so that they have a pH of 7.2-7.4 at 37^{o}C at a single strength (1X) solution. HEPES has a pronounced effect on the final pH and it is necessary to measure the pH at the same temperature that the experiments are being conducted at, this is in order to closely monitor any changes if they should occur.

It has been shown that having a system whereby the medium perfusing through BGS is completely replenished enhances cell proliferation (Bjerre, Bunger et al. 2008) however, these media changes occur once a week. Bancroft et al designed a flow perfusion system whereby two medium reservoirs were employed in order to help with the constant and complete refreshment of the medium during the length of the experiments. The results showed that there was an increase in cell proliferation and differentiation when completely refreshing the media (Bancroft, Sikavitsast et al. 2002, Bancroft, Sikavitsas et al. 2003). Even though the current work presented in this chapter was able to show an increase in cell proliferation at day 5 with all PCM, the controls SCM HA and SCM SA were still providing a significantly enhanced environment for cell proliferation to occur. Cell differentiation was significantly increased with PCM in comparison to the control media however this increase was now observed at day 1 instead of at day 3 where it had previously (chapter 4 & 5) been shown to peak suggesting that maybe the cell concentration which is being used is too low for the 3D static cell culture experiments.

The results grained from the work conducted up until this point in the present chapter have fundamentally shown that using a closed system as in chapter 4 is not a good representation of the *in vivo* environment as levels for calcium and phosphate ions are completely depleted. In chapter 5 and this current chapter, it has been shown that arbitrarily picking times to replenish media either partially or completely in order to get some control over calcium ion levels in the media has led to a significant elevation of phosphate and silicate ion levels in the surrounding media as there is still constant ion exchange between the granules and the surrounding DMEM.

A study conducted by Da Silva et al investigated cell response when seeded on HA and SA scaffolds. The authors stated that in order to understand the influence of immersion conditions on ceramic surface transformations, they proposed a new approach based on the use of a flow perfusion bioreactor under constant physiological flow. This means the feeding reservoir is different to the collection reservoir also known as waste medium (da Silva, Mateescu et al. 2010). Investigating cell response under this type of flow is more realistic to what actually happens *in vivo* therefore allowing further research into *in vivo* interactions *in vitro*. The study by Da Silva et al found that cell proliferation was greater under dynamic flow and a higher ALP activity was found for cells under dynamic conditions (da Silva, Mateescu et al. 2010).

Wang et al also used a 'to waste medium' flow perfusion system where at certain time points media was collected from the 'to waste' reservoir. The results gained from this study showed an increase in cell differentiation. After differentiation culture *in vitro* with the perfusion culture system, the osteoblastic cell activity and consequent bone formation were enhance significantly. Holtorf et al showed how the culturing of MSCs on porous CaP scaffolds under flow perfusion systems benefitted from the flow of medium through the scaffold porosity by enhancing the nutrient transport to the scaffold interior which in turn stimulated successful cell differentiation. The constant transport of nutrients was provided by the continuous change of medium. This was achieved by utilising a 'to waste' system which meant that media had to be refreshed every day and therefore a fresh supply of media along with nutrients and metabolites were being received by the cell seeded scaffolds in order to stimulate their growth (Holtorf, Sheffield et al. 2005).

6.5 Summary and Conclusions

The work presented in this chapter was able to demonstrate the sensitivity of dynamic ion exchange to complete replenishment of the media within the closed perfusion system. The study was also able to show that the 3D static cell culture showed sensitivity to changes in ion concentration levels however the assays conducted were not able to register these changes as significant changes.

The most significant finding from the results presented in this chapter were that there were differences in the behaviour of the osteoblast-like cells when incubated in the three different types of PCM in comparison to the controls used. Using a closed system and refreshing the media periodically will put the cells under regular fluctuation with regards to the ionic make-up of the circulating medium. This in turn may have confounding effects on their behaviour. Also it will not be possible to conclude whether the changes in cell behaviour are occurring due to the fluctuation in the dynamic ionic environment, the changes in structure or the changes in chemistry of the BGS granules being used.

Another factor to consider would be changing the media type. It was found that the DMEM being used had high levels of sodium bicarbonate which together with the CO_2 in the air had a negative effect on the maintenance of the pH during the 7 day circulation study. It was therefore suggested that the significant rise in pH may have had an effect on dynamic ion exchange and in turn have an effect on subsequent cell response.

Taking all of these factors in to consideration, the next step would be to set up a system where there is a constant flow of fresh media. The use of a closed system in order to perfuse medium through the circulation experiments is not a true representation of the physiological environment. Even with the complete replenishment of media, the elevated phosphate and silicate ion concentrations in the media are not what is expected physiologically. Once implantation has occur *in vivo*, all bodily fluids are delivered to the site of implantation. In order to mimic this process *in vitro* as closely as possible, the flow perfusion system needs to utilise a 'to waste' system whereby, the medium reservoir delivering the media to the BGS is collected once it has perfused through the BGS. This will provide the constant flow of fresh medium through the system and provide a continuous and fresh supply of nutrients and metabolites to the cell seeded BGS.

Chapter 7 Effects of a 'to waste' Flow Perfusion System with Different Media Compositions on Dynamic Ion Exchange and Subsequent Cell Response

7.1 Background

From the previous Chapter it was evident that osteoblast-like cell response is sensitive to the increase in calcium and phosphate ion concentration in media. From the circulation study, the two time points at which media was collected and completely replenished with fresh DMEM showed the media to be enriched with phosphate ions. Silicate ion release was observed to be statistically higher in comparison to the basal bulk solution levels. Osteoblast-like cell response was found to be sensitive to the changes in ionic concentrations however, even thought there was an increase in total DNA with time, the levels observed were suppressed with all PCM when compared to SCM.

As discussed previously, the use of a closed system in order to perfuse medium through the circulation experiments is not a true representation of the physiological environment. It was also noted that there was a significant rise in pH with time during the 7 days of circulation making the media highly acidic. This could have been due to the formation of bone like apatite combined with the absence of a positive CO_2 atmosphere.

In order to test this theory, the objective of this Chapter was firstly to characterise the ionic concentration and pH behaviour of sodium bicarbonate buffered DMEM and HEPES buffered DMEM when perfused through porous silicate substituted granules, directly to waste, as opposed to into a fixed volume reservoir which was either maintained (Chapter 4), partially refreshed (Chapter 5) or completely refreshed (Chapter 6) over a period of 7 days. Once the ionic behaviour was known the second objective was to investigate osteoblast-like cell response to the two types of collected pre-conditioned media.

7.2 Methodology

In order to meet the objectives set out above the experimental work was performed in two distinct steps:

- **STEP 1** – Use of a to waste (TW) flow perfusion system to investigate ion exchange between SA80/20 granules and two forms of media (a) the sodium-bicarbonate buffered DMEM, as previously used in previous Chapters and (b) 1M HEPES buffered sodium bicarbonate free DMEM

- **STEP 2** – Investigation of cell response to the two types of preconditioned media obtained in step 1.

7.2.1 STEP 1 – Investigation of ion exchange between SA80/20 and DMEM buffered with either sodium-bicarbonate or HEPES in a flow to waste perfusion system

7.2.1.1 Media and Sample Preparation

Sodium bicarbonate buffered DMEM (DMEM) and sample preparation was the same as described in Chapter 4 section 4.2.1.1. Additionally sodium-bicarbonate free DMEM was also prepared supplemented with 1% penicillin-streptomycin and 1M HEPES buffer (DMEM-H) as per detailed in Table 7.1.

Table 7.1: Composition of DMEM-H

Components	Volumes (ml)
Powdered DMEM (13.9g mixed in 1L of dH_2O)	500
Pen/Strep	5
1M HEPES	10

7.2.1.2 TW Flow Perfusion System Set up

The apparatus used for the flow to waste perfusion system was identical to that described in Chapter 5 with one significant modification.

The ‘closed’ medium reservoir was removed and replaced with two separate reservoirs, an ‘input’ reservoir and a ‘waste’ reservoir. The ‘input’ reservoir which was initially filled with 500ml of fresh DMEM or DMEM-H. This reservoir was kept topped up with 500ml of fresh medium at D1 and then an additional 500ml of fresh media every 48h until the end of the experiment.

One other significant change to the methodology was that the flow rate was changed to 0.1ml/min in comparison to 0.7ml/min to reduce the volume of media needed (and frequency of media changes) over a 7 day period to manageable proportions.

Media was sampled by collecting the entire volume of DMEM or DMEM-H present in the waste reservoir at time intervals of 0.5, 1, 2 and 4 hours, 1, 3, 5, 6 and 7 days to give 9 distinct media samples. The pH of these different media samples was then measured (as in chapter 3 section 3.2.5) and the samples were stored at -20^{o}C until they were analysed for calcium, phosphate and silicate ion concentrations using colorimetric assays as previously described in Chapter 4 section 4.2.1.2. SEM analysis was also conducted on the granules collected on day 7. The protocol followed can be found in chapter 2 section 2.1.

PCM for subsequent cell experiments was obtained by sterile filtration and supplementation with 10% FBS of the remaining waste media collected at 1, 3, 5, 6 and 7 days, and stored as 1D, 3D, 5D, 6D and 7D respectively. The earlier time points of 0.5, 1, 2 and 4 hours were not used for production of PCM as the volume of media collected between these time points was not sufficient enough for 5 days of cell culture experiments. Figure 7.1 shows images of the flow to waste perfusion system apparatus.

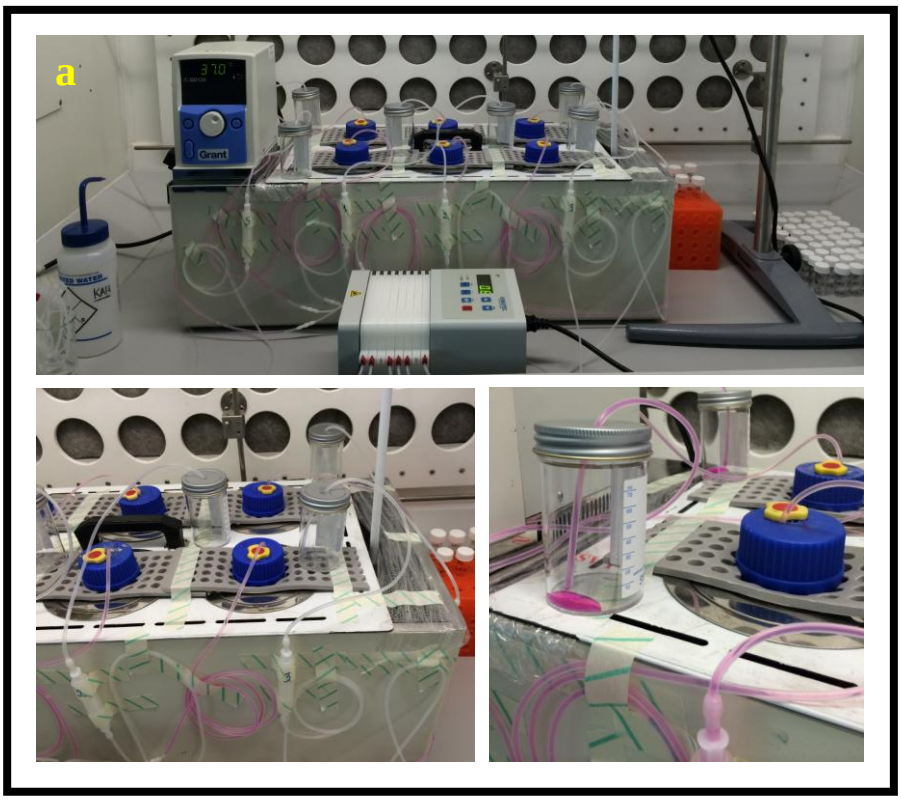

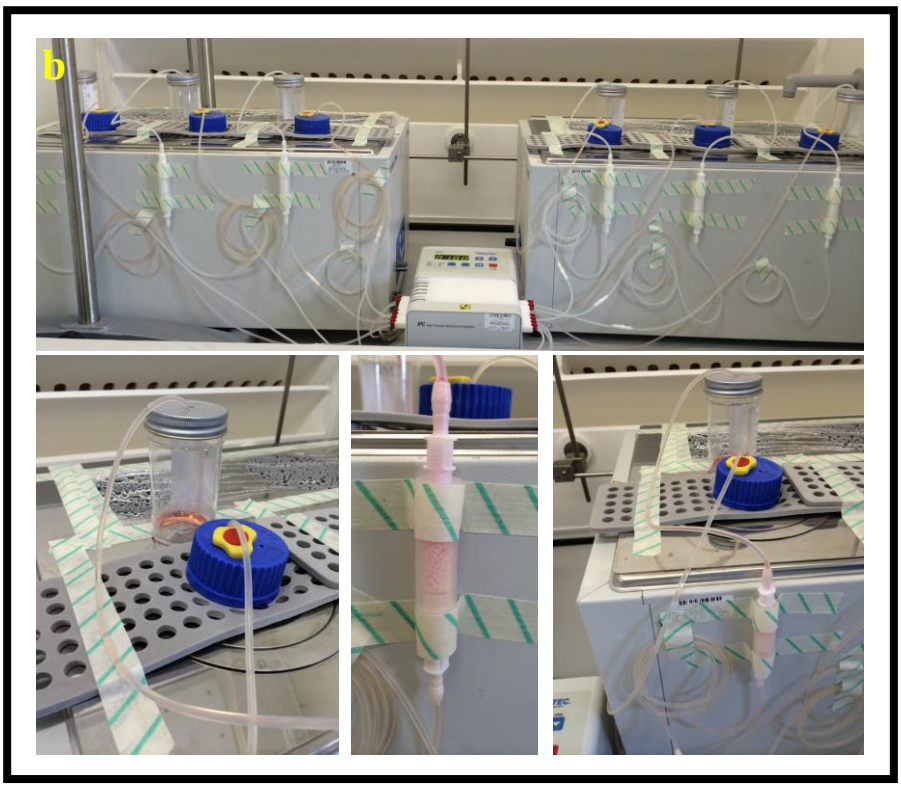

Figure 7.1: Flow to waste perfusion system apparatus (a) with DMEM, (b) with DMEM-H

7.2.2 STEP 2 – Investigation of cell response to flow to waste DMEM buffered with either sodium bicarbonate or HEPES

After the flow to waste perfusion experiments were completed, the collected 1D, 3D, 5D, 6D and 7D PCM from both individual perfusion experiments was used to conduct static 3D cell culture studies to osteoblast-like cell response to the different media types.

MG63 cells were grown and expanded as described in Chapter 4 section 4.2.2.1. MG63 osteoblast-like cells (P4) were seeded at a concentration of $4x10^4$ cells/ml on 0.45g of HA80/20 granules in 24 well plates in 1ml of SCM and allowed to attach at 37°C and 5% CO_2. After 2 hours the SCM was replaced with 1ml of either 1D, 3D, 5D, 6D, 7D or fresh SCM as a control. SA80/20 was used as a second control which was incubated in SCM for the duration of the day 5 experiments. The cells were incubated for periods of 1, 3 and 5 days. The media was refreshed at 24 hours then every 48 hours thereafter using the individual media types being tested. DNA quantification, ALP specific activity, total protein and cell metabolism was monitored at each time point. The protocols followed for these assays can be found in Chapter 4 section 4.2.2.2 - 4.2.2.5.

7.2.3 Statistical Analysis

All collected data was conducted at n=6 and analysed and expressed in terms of mean ± standard deviation. Statistical significance was evaluated using ANOVA, Post Hoc test: Tukey HSD with $\alpha=0.05$, (were *$p<0.05$, **$p<0.01$ and ***$p<0.005$).

7.3 Results

7.3.1 STEP 1 - Investigation of ion exchange between SA80/20 and DMEM buffered with either sodium-bicarbonate or HEPES in a flow to waste perfusion system

7.3.1.1 Ion Concentration Analysis and pH using DMEM

From Figure 7.2, Figure 7.3 and Figure 7.4 it is evident that changing from a closed loop system to a TW flow perfusion system, has had a significant effect on the degree of fluctuation observed in calcium, phosphate and silicate ion concentrations for the duration of the study.

There was an initial significant increase in calcium (1-4h) ion concentrations (Figure 7.2) observed in DMEM as it was circulated through the SA80/20 granules to the waste reservoir, after 1 day there was no significant difference in calcium ion concentration between the base DMEM and the media collected in the flow to waste reservoir.

Phosphate ion concentrations (Figure 7.3) remained significantly elevated in media as it was circulated through the SA80/20 granules to the waste reservoir as compared to the base DMEM for the entire length of the 7 day experiment.

Silicate ion levels throughout the 7 day period remained significantly increased from 4 hours to day 7 ($p<0.05$). At 30 minutes and 2 hours the silicate ion levels were statistically similar to the basal bulk levels slightly increased in comparison to basal levels (Figure 7.4).

Despite the fact that fresh media was being constantly being perfused through the system, the pH was significantly elevated throughout the entire length of the experiment (Figure 7.5).

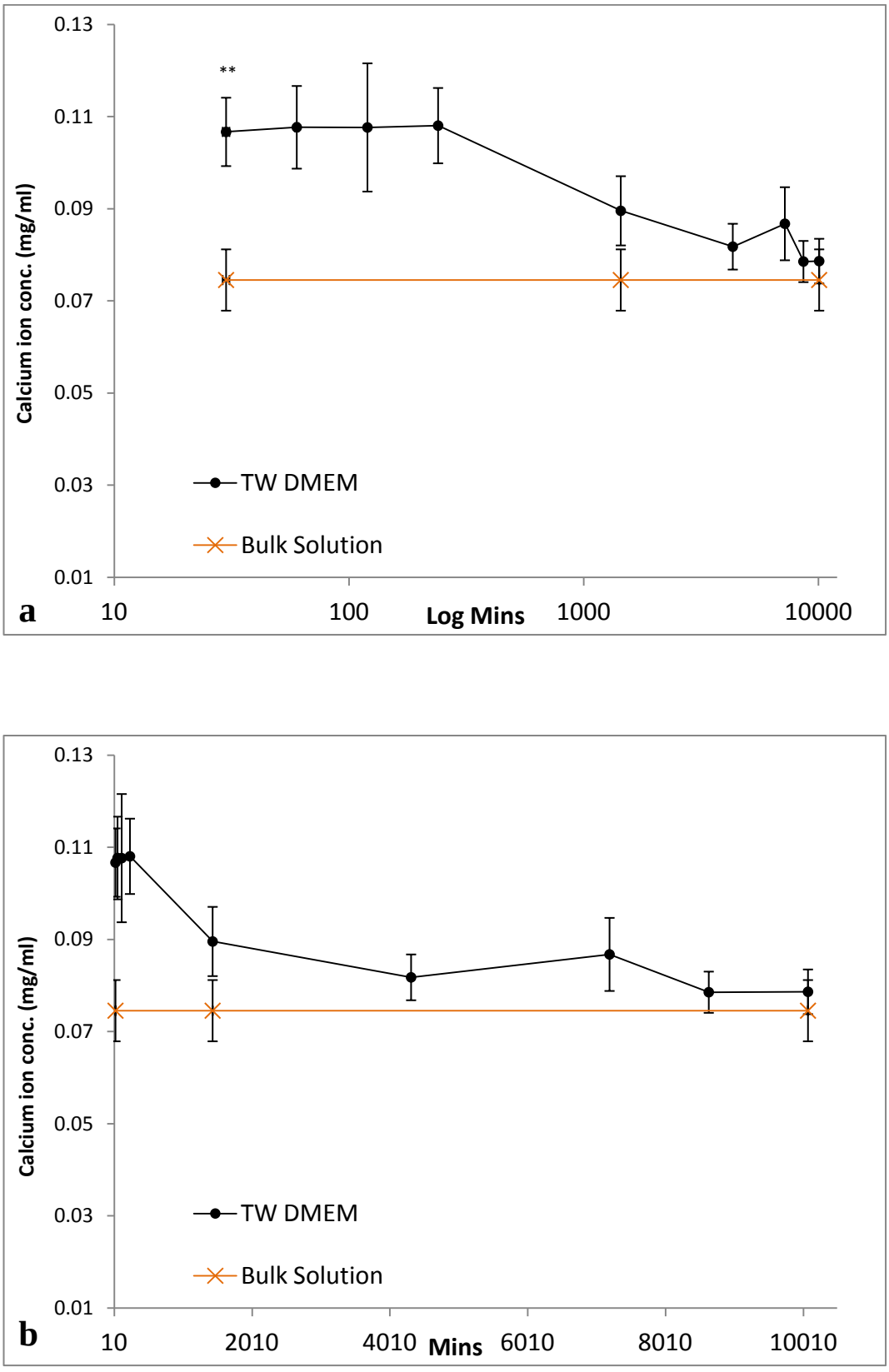

Figure 7.2: Calcium ion concentration of DMEM in flow to waste perfusion system, a) log minutes scale & b) minutes scale (n=6)

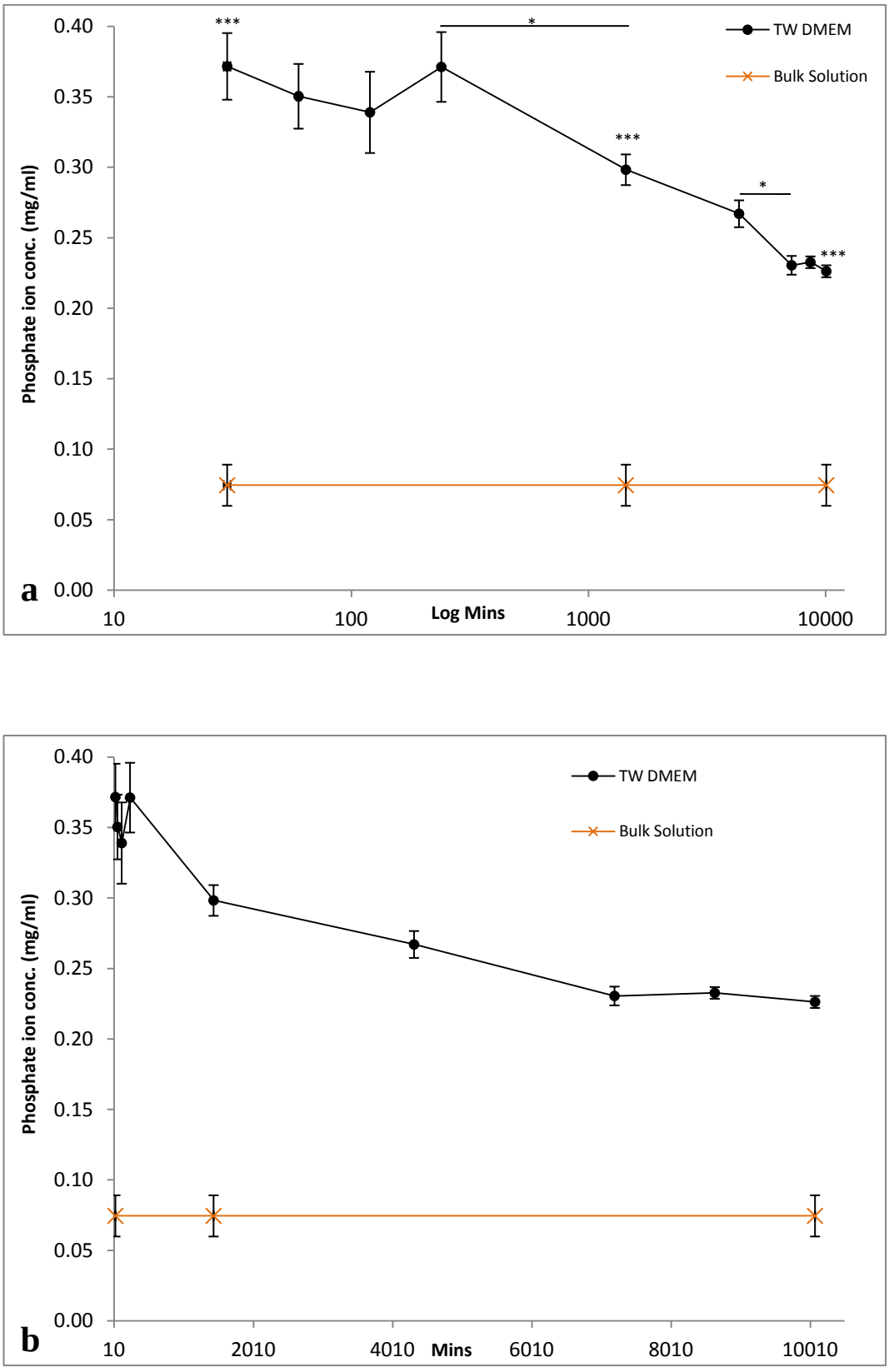

Figure 7.3: Phosphate ion concentration of DMEM in flow to waste perfusion system, a) log minutes scale & b) minutes scale (n=6)

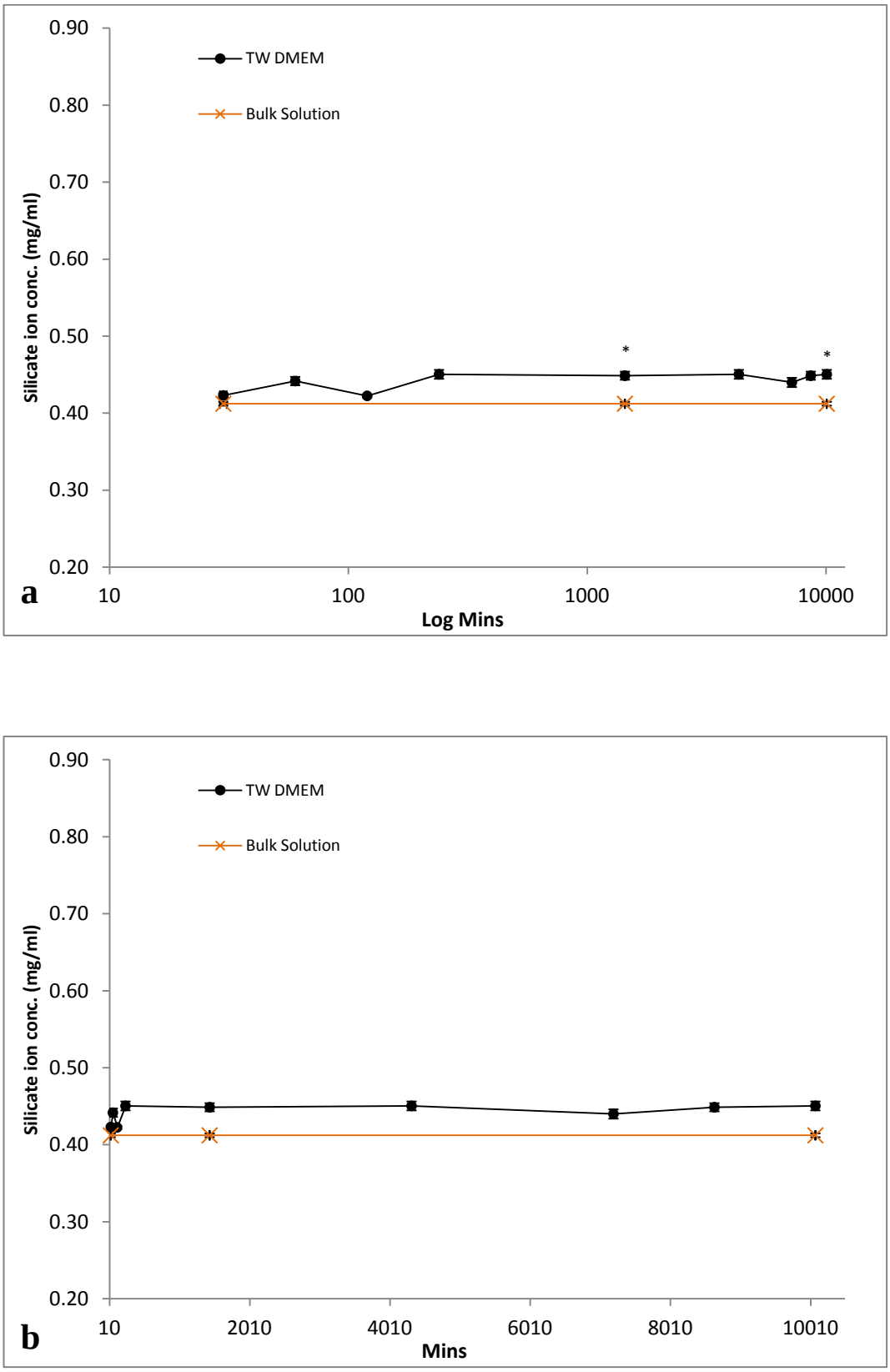

Figure 7.4: Silicate ion concentration of DMEM in flow to waste perfusion system, a)log minutes scale & b) minutes scale (n=6)

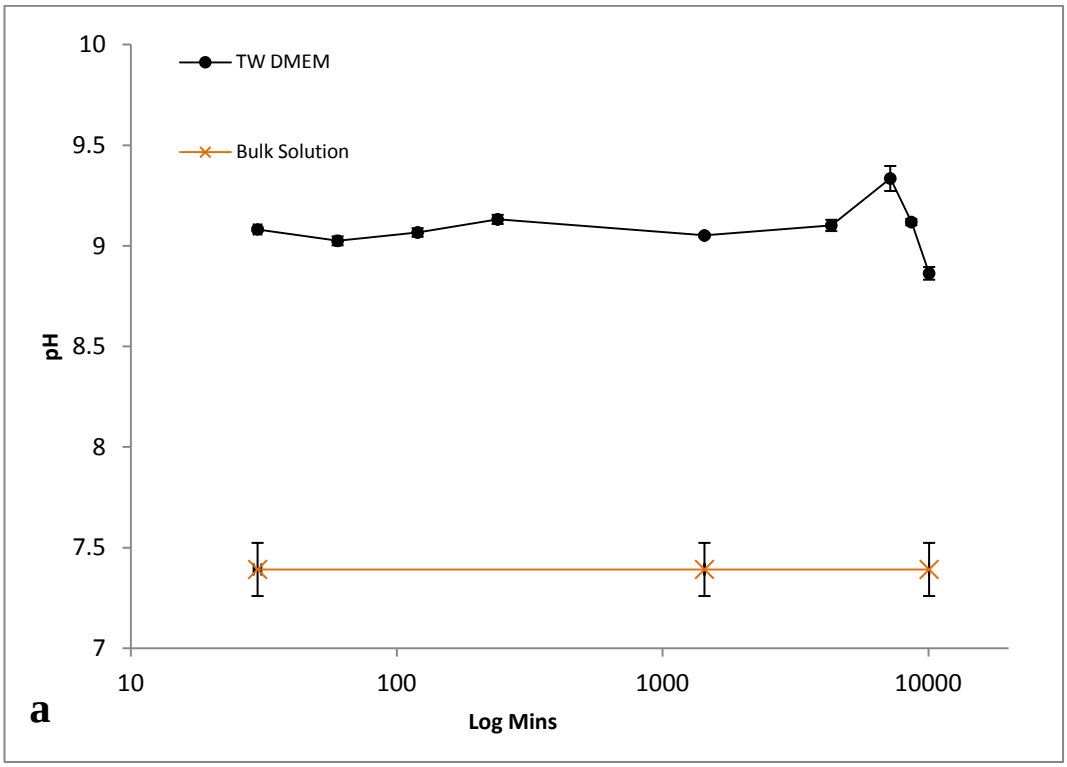

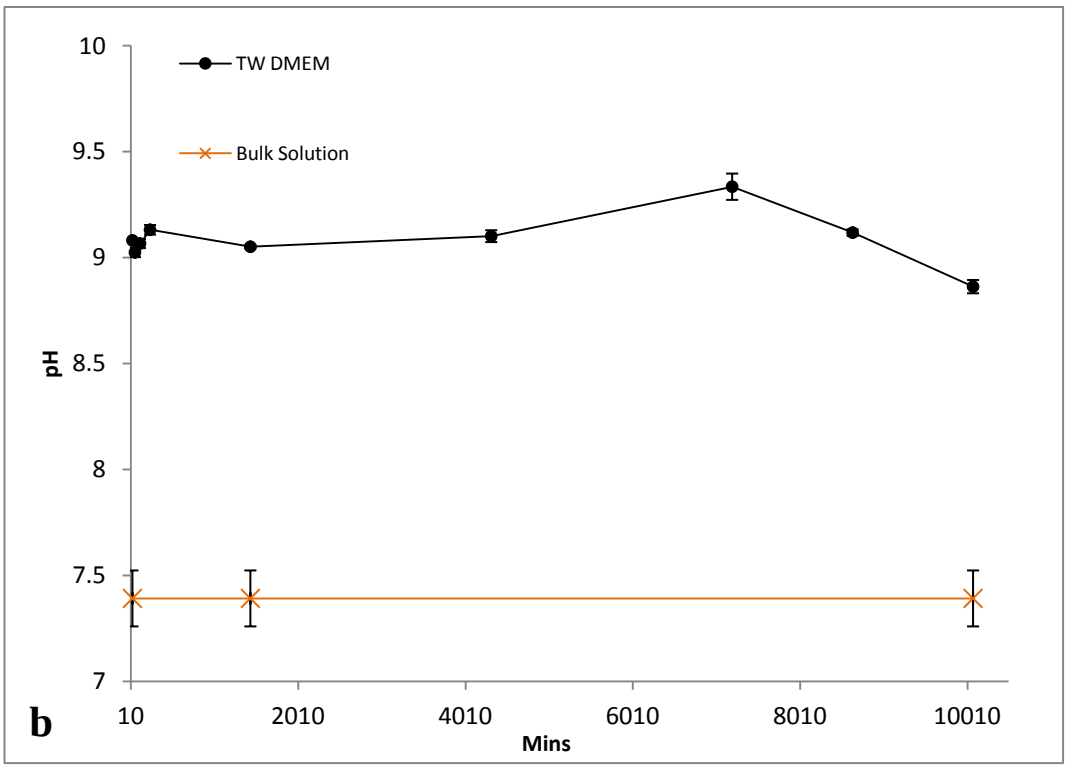

Figure 7.5: pH of DMEM used in TW flow perfusion system, a)log minutes scale & b) minutes scale (n=6)

7.3.1.2 Ion Concentration Analysis and pH using DMEM-H

Comparison of the data observed for DMEM (Figure 7.2 - Figure 7.4) as compared to that observed for DMEM-H (Figure 7.6, Figure 7.7 and Figure 7.8) clearly show how dynamic ion exchange between culture medium and apatite based bone graft substitute porous granules is sensitive to medium composition.

As with DMEM, there was an initial significant increase in calcium (1-4h) ion concentrations (Figure 7.6) observed in DMEM-H as it was circulated through the SA80/20 granules to the waste reservoir, however, unlike DMEM although the after 1 day calcium ion concentration reduced significantly from initial values, calcium concentrations between the base DMEM-H and the DMEM-H collected in the flow to waste reservoir were still significantly different.

Phosphate ion levels remained significantly ($p<0.005$) elevated throughout the 7 day circulation study compared to the base DMEM-H levels (Figure 7.7. From 30 minutes to 4 hours, there was a general increase in phosphate ion concentration in the collected DMEM-H. At 4 hours, there was a significant decrease ($p<0.05$) in phosphate levels. Compared to DMEM, the phosphate levels in the surrounding DMEM-H collected were increased.

Silicate ion levels during the circulation study were found to be significantly greater for the first 4 hours and days 5, 6 & 7 when compared to the bulk levels (Figure 7.8). There was an increase in silicate ions levels in the collected DMEM-H in comparison to DMEM.

The pH of the base DMEM-H was lower than that of the base DMEM, at pH 7.2 as compared to pH 7.4. However, most significantly the pH of the DMEM-H only increased to a maximal level of pH 7.5 after 30 minutes, after which it returned to statically similar levels of pH to the fresh DMEM-H at either 2 or 4 hours (Figure 7.9).

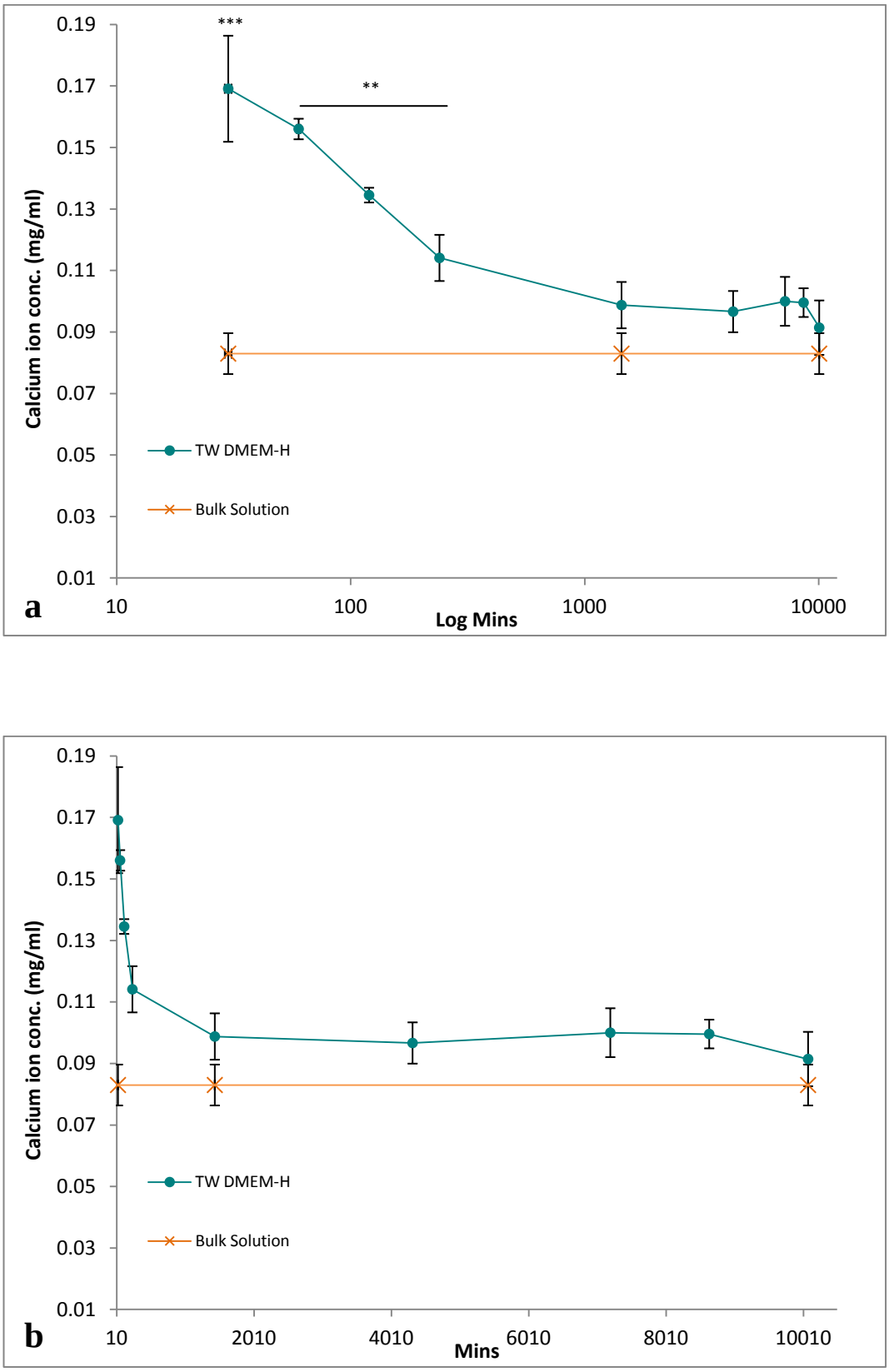

Figure 7.6: Calcium ion concentration of DMEM-H in flow to waste perfusion system, a) log minutes scale & b) minutes scale (n=6)

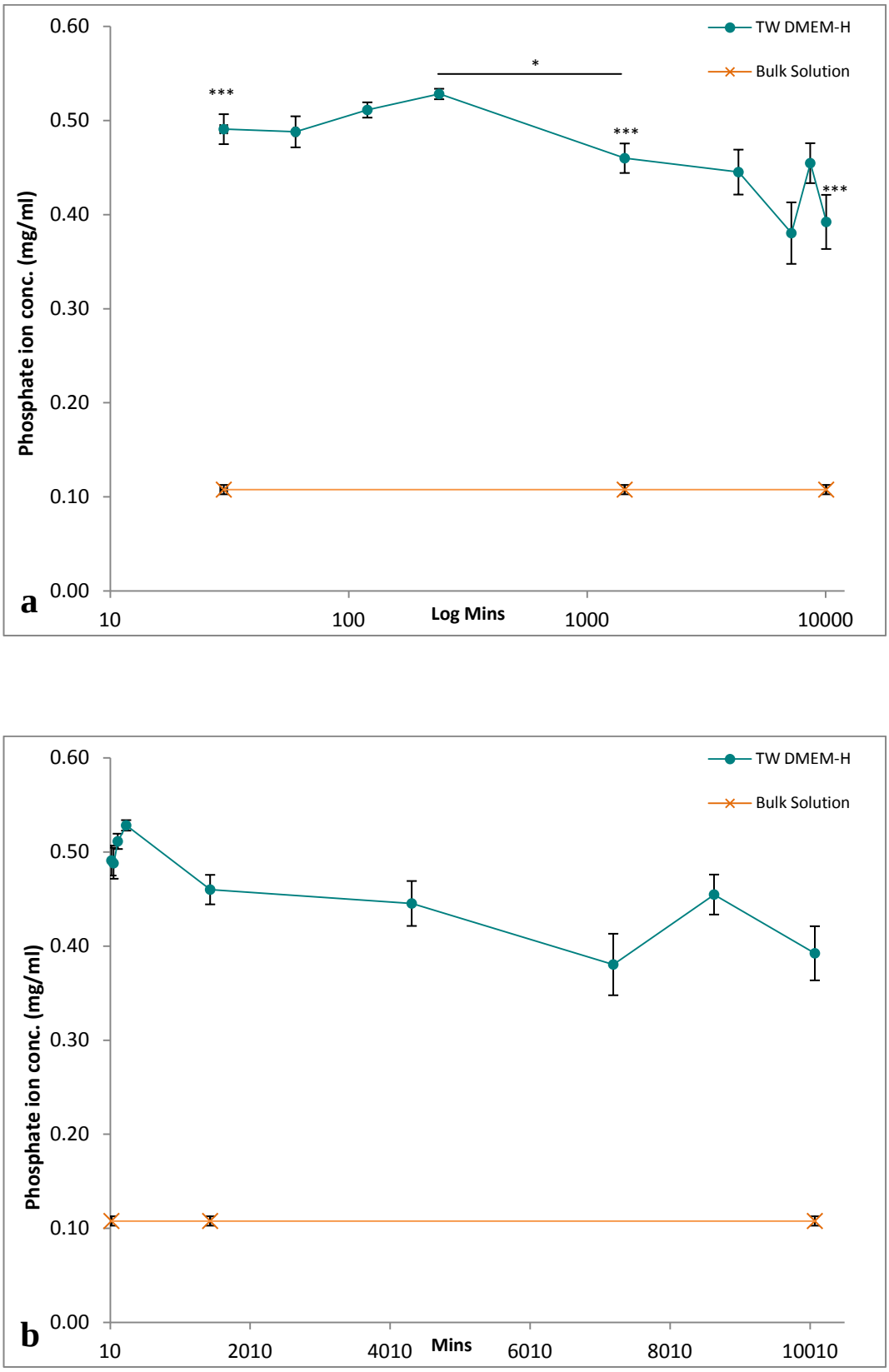

Figure 7.7: Phosphate ion concentration of DMEM-H used in TW perfusion system, a) log minutes scale & b) minutes scale (n=6)

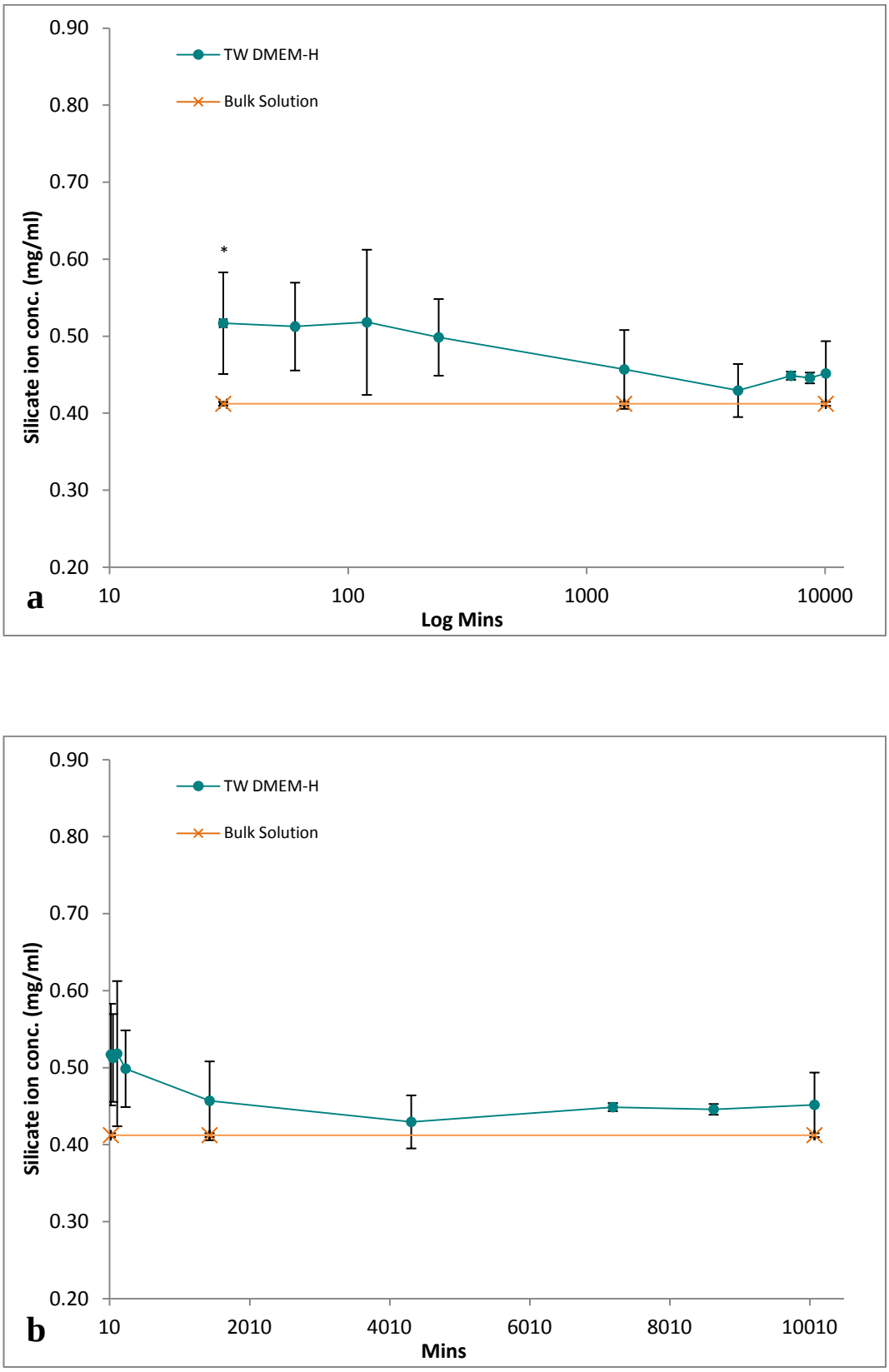

Figure 7.8: Silicate ion concentration of DMEM-H used in TW perfusion system, a) log minutes scale & b) minutes scale (n=6)

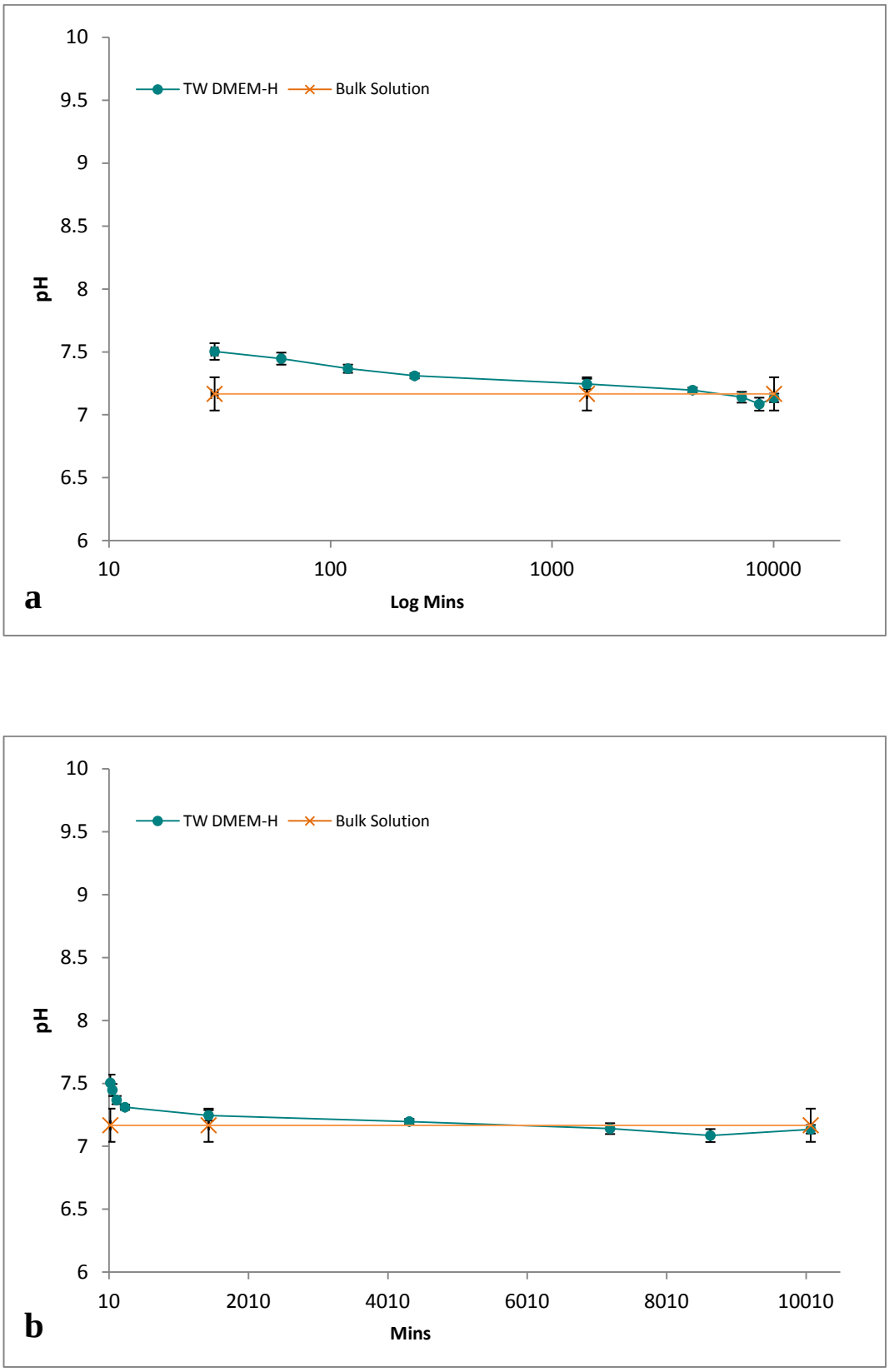

Figure 7.9: pH of DMEM-H used in TW flow perfusion system, a) log minutes scale & b) minutes scale (n=6)

7.3.1.3 SEM Analysis

From the SEM images in Figure 7.10, it is evident that there was an observed CaP layer on the surface of the SA80/20 granules. However, the layer was not found to be homogeneously spread across the surface of the granules. It was found that there was a greater precipitation on the direct surface of the granules in comparison to deeper and more porous areas of the granules.

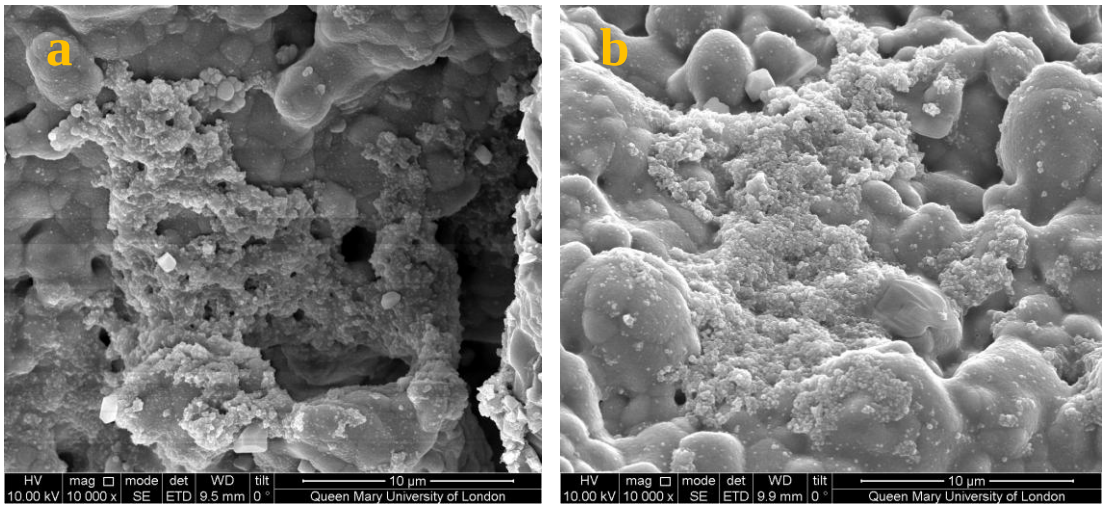

Figure 7.10: SEM images of SA80/20 granules collected at day 7 from the 'to waste' perfusion experiments with a) DMEM and b) DMEM-H

7.3.2 STEP 2 - Investigation of cell response to flow to waste DMEM buffered with either sodium bicarbonate or HEPES

From step 1 of this chapter, similar patterns of behaviour were observed with levels of calcium, phosphate and silicate ion release from the granules to the surrounding collected DMEM or DMEM-H. Calcium concentration initially observed elevated levels which then drop back towards base levels. Phosphate concentration was found to be considerably elevated throughout the study and silicate ion levels were found to be moderately elevated though out study. However degree of elevation was seen to be higher in DMEM-H, particularly for silicate ion concentrations. pH levels between the two different media types were significantly different with, DMEM observing highly acidic pH throughout the 7 days and DMEM-H observing statistically similar pH levels to basal levels.

7.3.2.1 Static Cell Culture on HA80/20

Cell response was monitored by incubating HA80/20 granules in the PCM collected at different time points from the TW flow perfusion study using DMEM. The results show that there is a trend towards earlier time point media supporting greater cell metabolic activity, total protein and total DNA in comparison to the later time point media. It is also evident that none to the pre conditioned environments support peak in ALP activity at day 3 however, 7D-PCM supports it throughout the study.

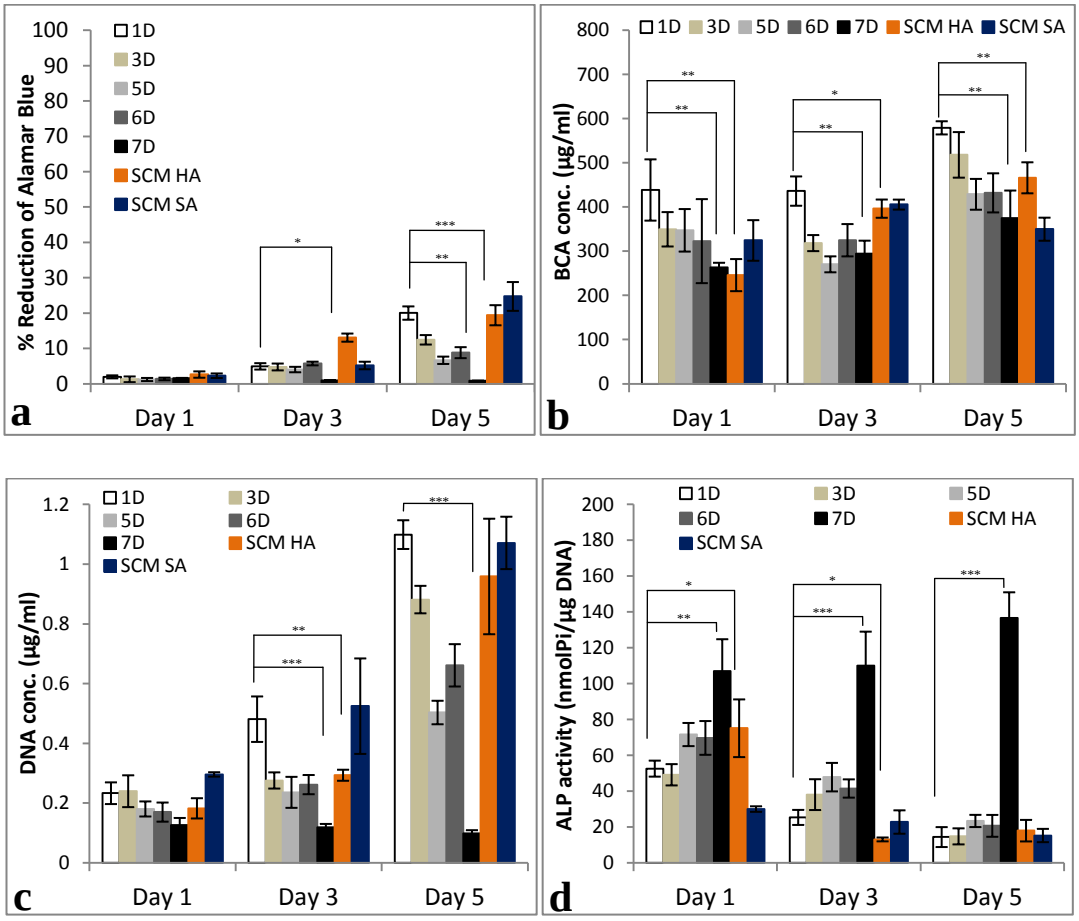

Figure 7.11: a) % reduction of alamarBlue®, b) BCA total protein, c) DNA concentration and d) ALP specific activity for MG63 cells cultured in PCM DMEM for 5 days (n=6)

7.3.2.2 Static Cell Culture on HA80/20

Changes in ion concentrations in the PCM had an effect on cell response. Cell metabolic activity was statistically similar in all PCM over time (Figure 7.12a). Protein expression was greater with 1D PCM at day 1 in comparison to the other media types tested. By day 5 protein was again very similar across all PCM and the two controls that were tested (Figure

7.12b). Total protein and total DNA seem to level off between days 3 - 5 of culture instead of continuing to increase as they do with DMEM. Greater ALP activity was measured in 3D PCM with time ALP activity decreased in all PCM (Figure 7.12d).

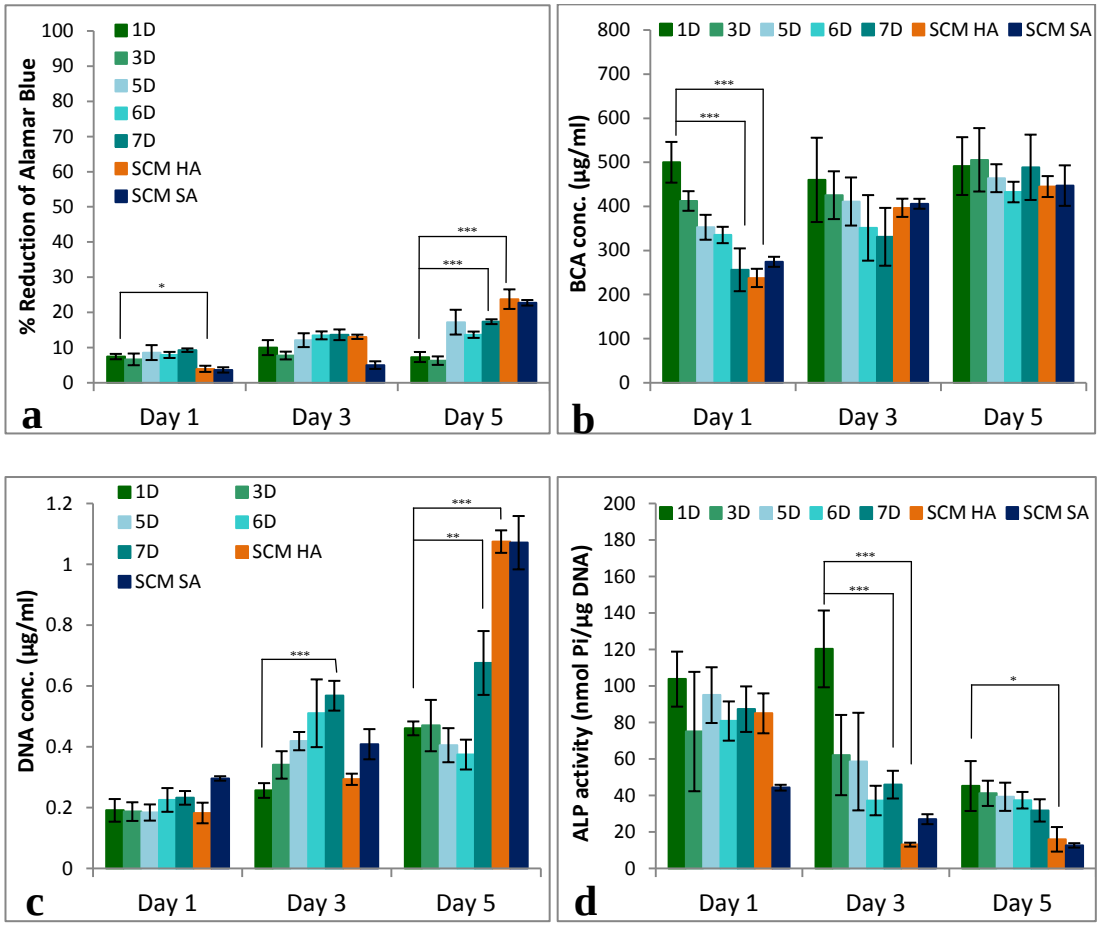

Figure 7.12: a) % reduction of alamarBlue®, b) BCA total protein, c) DNA concentration and d) ALP specific activity for MG63 cells cultured in PCM DMEM-H for 5 days (n=6)

7.4 Discussion

7.4.1 STEP 1 - Investigation of ion exchange between SA80/20 and DMEM buffered with either sodium-bicarbonate or HEPES in a flow to waste perfusion system

The results presented in this Chapter, have made it apparent that changing the flow perfusion system from a closed loop system to a TW flow perfusion system has an effect of dynamic ion exchange. Changing the method of media collection meant that the bulk solution was continuously refreshed. In doing this the results show that there is a continuous change seen in the ion concentrations in comparison to the bulk media throughout the 7 days study. This is evidence that the SA80/20 granules are constantly undergoing ionic exchange with the surrounding medium. It was interesting to see that the levels of phosphate ions remained greatly elevated even by the end of the experimental period, suggesting the DMEM was still enriched with these ions. Over time there was a small release of silicate ions from the SA80/20 granules in to the DMEM however the levels were not significantly different to the levels that were already present in the DMEM before experimentation.

On D1 the levels of calcium and phosphate ions in the collected DMEM were elevated with phosphate ion levels being 3 times greater than the calcium levels. The silicate ion levels detected in the collected DMEM at day 1 were approximately 0.04mg/ml greater than the bulk solution levels. At D3 the levels of calcium and phosphate ions had decreased in comparison to D1 but the release of silicate ion levels remained stable. A similar trend was observed with the following time points. At D5 and D6 there was a further decrease observed with calcium and phosphate levels (Figure 7.2 and Figure 7.3) in the collected DMEM for these specific time points and levels of silicate (Figure 7.4) again remained very similar and stead to the levels detected at previous time points. For the final DMEM collection on D7, the calcium and phosphate ion concentrations in the DMEM were at the lowest levels observed during the circulation study (Figure 7.2 and Figure 7.3), with calcium levels almost reaching basal levels. Phosphate levels were still greatly elevated in comparison to the basal levels. Silicate ion levels were also at the highest by D7, however this increase was not significantly greater than the basal levels (Figure 7.4).

The highly basic nature of the collected DMEM throughout the TW study was a surprising find. It can be suggested that by changing the method of the flow perfusion system from a closed system to a TW system, it has had an effect on the pH. The DMEM contained 3.7g/l

sodium bicarbonate which acted as an internal way for the media to buffer itself. It was found that these levels were far too high and as the circulation experiments were taking place under atmospheric pressure, the CO_2 levels in the surrounding environment would have acted in increasing the alkalinity of the DMEM. Even though a closed system was being utilised for the circulation study, it was not air tight which would have led to the increase in pH. As the DMEM was not being retuned back to the feeding reservoir, this may have had an effect in raising the pH also. Figure 7.13 below shows the colour change in the collected media from when it was initially made before the circulation experiments started to when the first collection of DMEM was made at 30 minutes. It is evident from the colour change that the DMEM has begun to become alkaline. When the DMEM was made up with 1% pen/strep it was deep orange in colour with a pH of 7.4. After 30 minutes of circulation the DMEM became deep pink in colour and the pH went up to 9.1.

Different parts of the body or even different parts of the cell are maintained at different pH, such as the blood is maintained at a pH of 7.4 which is known to be neutral, whereas the stomach can have a pH ranging between 3 and 4 due to the acidic concentrations present. However the pH of cellular fluids remains typically around 7. The effect of a more acidic pH is known to trigger a cascade of immunological response but a more alkaline pH has not yet been investigated thoroughly. When conducting experiments *in vitro*, it is vital to ensure the pH is being kept at a 'normal' pH which is considered to be 7.4. More basic pH levels are known to have an effect on the ionic interactions between the materials surface and the surrounding medium, therefore from the results gained in this step of the current work, it cannot be concluded that the ionic concentrations measured are a true representation of what was actually occurring due to the instability of the pH.

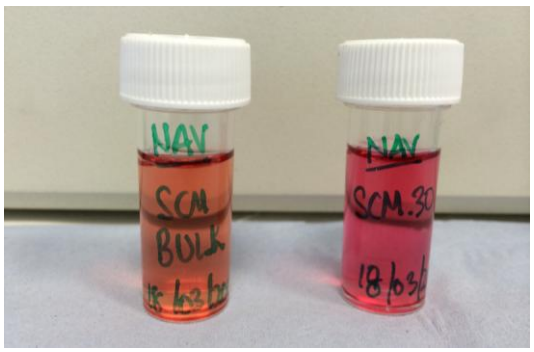

Figure 7.13: Colour change of TW DMEM, a) Bulk solution before experimentation & b) TW DMEM at 30 minutes

When observing the ion concentration results gained from DEMM-H, it is evident that there was an initial increase in calcium and phosphate ion concentration in the collected DMEM-H at 30 minutes (Figure 7.6 and Figure 7.7) with levels reaching 0.16mg/ml and 0.5mg/ml respectively. The levels of calcium in the collected DMEM-H thereafter up to and including 4 hours saw a steep decrease with levels reaching 0.1mg/ml. However, the concentration of phosphate ions in the collected DMEM-H increased to levels reaching 0.53mg/ml. There was also an increase in silicate ion levels for the first 4 hours of the study with an initial release of 0.51mg/ml and by 4 hours the levels had sustained the release of silicate ions with levels remaining at ~0.51mg/ml. The amount of silicate ions released from the SA80/20 granules when perfused with DMEM-H was greater when compared the initial release of silicate ions from work presented in Chapter 5 and Chapter 6. Therefore it can be suggested that using HEPES to buffer the media helped achieve a sustained release of silicate ions from the BGS to the surrounding media.

At D1, the DMEM-H was refreshed with 500ml. The collected DMEM-H saw a further drop of calcium ions reaching ~0.09mg/ml at D1, seeing a 0.02mg/ml drop in 24 hours however, the drop in phosphate ions was greater over 24 hours with levels going from ~0.52mg/ml at 4 hours to ~0.46mg/ml at D1 therefore seeing a difference of 0.06mg/ml. There was also a 0.06mg/ml decrease in silicate ions observed in the collected DMEM-H, going from 0.51mg/ml at 4 hours to 0.45mg/ml at D1.At D3, there was a further ~0.002mg/ml decrease in calcium, phosphate and silicate ion concentrations observed. The finally collection of DMEM-H was on D7 which contained the lowest levels of calcium, phosphate and silicate ion levels with levels at 0.09mg/ml, 0.4mg/ml and 0.45mg/ml respectively. Even though a decrease was observed with all the ion concentrations in the D7 collected DMEM-H, the phosphate levels remained elevated and did not reach basal levels by the end of the circulation study. This means that the media was still enriched with phosphate ions. The calcium and silicate ions however, were close to basal levels.

When comparing the results gained from DMEM buffered either with sodium bicarbonate or HEPES in a flow to waste perfusion system it is evident that the changes in media type have had an effect on osteoblast-like cell response. The graphs presented make the changes in dynamic ion exchange and pH more noticeable between the two different media types used in the TW flow perfusion experiments. There was a greater initial calcium release from the SA80/20 granules into the surrounding media which remained higher for the duration of the circulation study (Figure 7.14a). Overall there was also a greater release of phosphate ions from the granules in to the surrounding media in the TW DMEM-H compared to TW DMEM. The first 4 hours saw an increase in the phosphate ions however in TW DMEM

after the initial release, phosphate ions levels dropped (Figure 7.14b). There was a greater release of silicate ions observed from SA80/20 in to the surrounding DMEM-H in the first 4 hours of the circulation study in comparison to TW DMEM where release of silicate ions throughout the circulation study was not significantly different to the starting basal levels already present in the DMEM (Figure 7.14c).

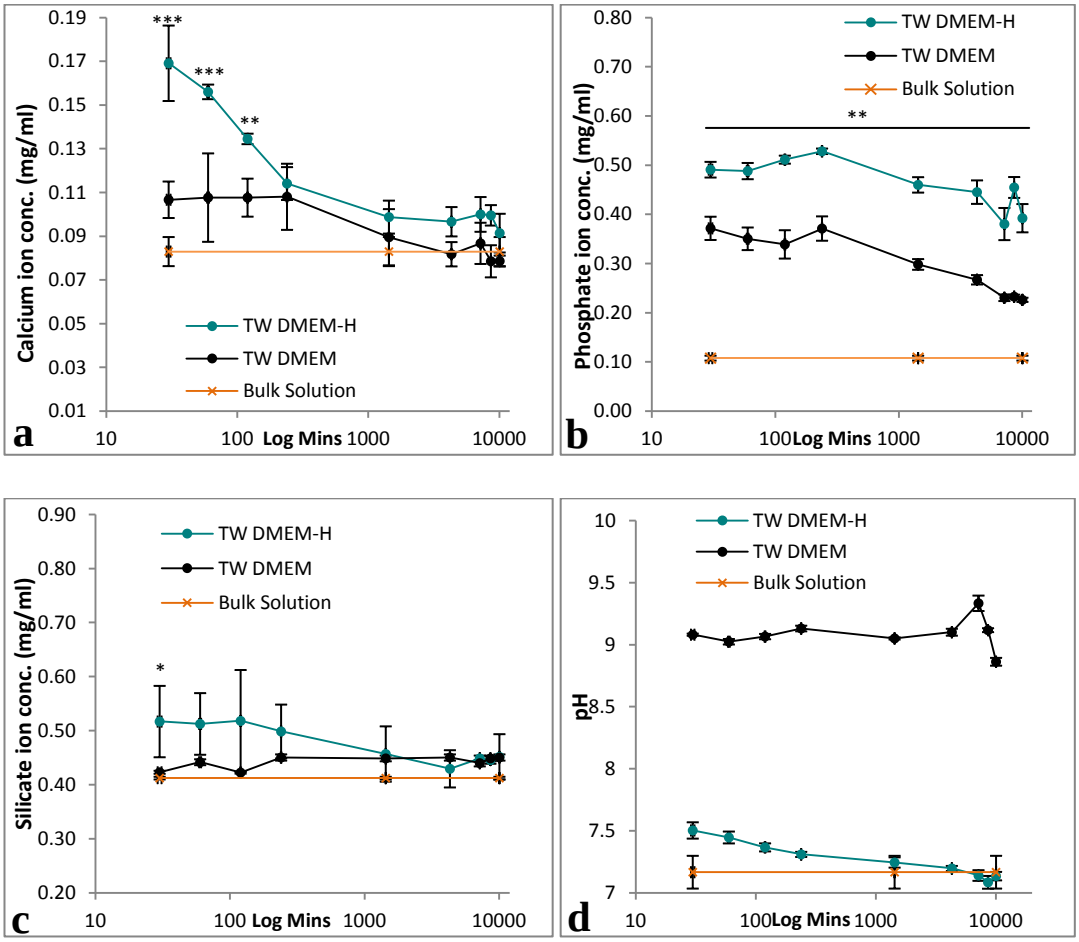

Figure 7.14: a) Calcium ion conc., b) Phosphate ion conc., c) Silicate ion conc. and d) pH graphs for TW DMEM-H compared to TW DMEM (n=6)

By D7 of the TW DMEM-H circulation study the media had greater levels of calcium and phosphate ions compared to the TW DMEM study. Silicate ions levels reached similar levels for both media types which were close to basal levels. It was very interesting to see the dramatic changes in pH trends between the two TW circulation studies using different medium types. It was amazing to see how changing the means by which the medium is buffered can have a striking effect on the pH trend. With the DMEM-H media type the media remained at levels which are considered 'normal' ranging from an initial pH of 7.5 at 30 minutes to 7.1 by D7 of the circulation study.

It has been demonstrated that the extracellular phosphate concentrations are more important in the mineralisation process of osteoblasts than the extracellular calcium concentrations (Lossdorfer, Schwartz et al. 2004, Ketteler and Floege 2006). It has been found that increased extracellular phosphate concentrations are an inducer to bone nodule formation which occurs by osteoblasts. The most commonly used source of extracellular phosphate *in vitro* is β-glycerophosphate. This is known to be an organic source of phosphate which is commonly used in cell culture investigations of bone nodule formation.

The main differences that were observed within the TW DMEM-H circulation study in comparison to the TW DMEM study were that there were elevated levels of calcium, phosphate and silicate ion concentrations observed throughout the circulation study along with a dramatic fall in pH returning it back to 'normal' values (Figure 7.14).

The degree to which an implant can form an apatite layer is influenced by various factors, including changes in pH. Guth et al observed a shift in pH towards higher alkalinity in media free of proteins in the presence of SA (Guth, Campion et al. 2011). It was suggested that this was most likely a result of the release of silicate ions combined with the net negative surface charge of SA which lead to the adsorption of more hydrogen ions and therefore overcoming the buffering capacity of the culture medium (Harding, Rashid et al. 2005).

It is important to maintain pH within the physiological ranges for 'normal' bone repair and function. The effect of variation in pH osteoblast has been under investigation and many studies have confirmed that a variation in pH from the physiological levels cause detrimental effect to cell growth and the expression of proteins. When the pH is not maintained to physiological levels *in vivo*, cellular apoptosis, necrosis and non-specific inflammatory responses have been reported (Furlong, Ascaso et al. 1997). Under a clinical setting it is not expected that there would be such an increase in pH, as it was observed with TW DMEM in this current study. This is because under a clinical setting in the proximity to BGS, there would be highly dynamic fluid exchange that occurs at and around the implantation site. However under static conditions where ~1g of samples is being immersed in 1ml of medium, this effect would be particularly pronounced.

7.4.2 STEP 2 – Investigation of cell response to flow to waste DMEM buffered with either sodium bicarbonate or HEPES

Cell response was also observed to be sensitive to the changes in media type with in a TW flow perfusion system set up (Figure 7.15). From the graphs it is evident that 1D TW

DMEM-H provided a supportive environment for cell differentiation due its enhanced ALP activity measured compared with 1D TW DMEM which observed significantly lower levels of ALP activity (Figure 7.15d). 7D TW DMEM saw enhanced levels of ALP activity over the 5 days in comparison to 7D TW DMEM-H. However, 7D TW DMEM-H observed an increase in cell proliferation in comparison to 7D TW DMEM.

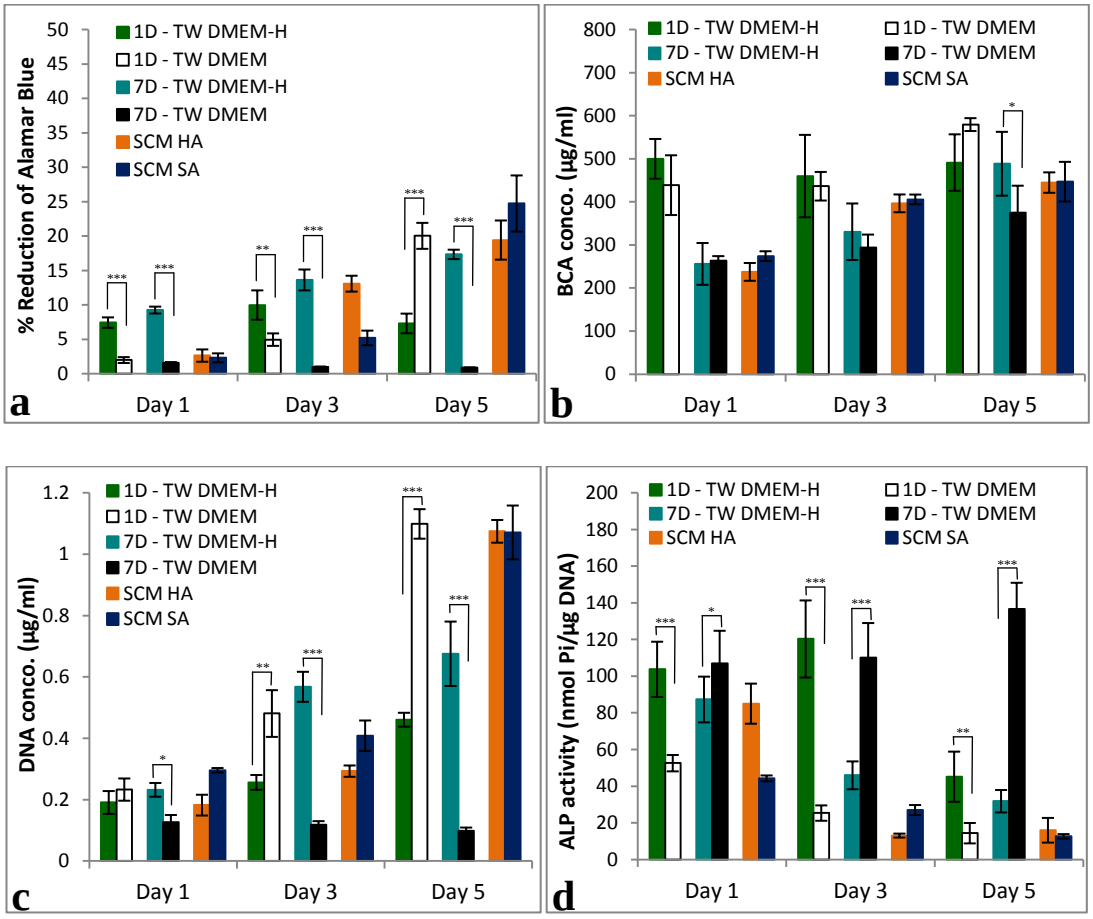

Figure 7.15: a) % reduction of alamarBlue®, b) BCA total protein, c) DNA concentration and d) ALP specific activity for MG63 cells cultured in TW DMEM-H compared to TW DMEM for 5 days with 1D and 7D PCM (n=6)

When investigating cell response to PCM DMEM it was found that 1D-PCM observed significantly enhanced levels of DNA and an increase in metabolic activity. The 1D PCM also expressed significantly more protein over the 5 days of study in comparison to the other PCM and the two controls tested. These findings suggest that the increased levels of these ions in the 1D PCM provided a supportive for cell growth and proliferation. Cell metabolic activity, protein expression along with cell proliferation were decreased at 3D-PCM in comparison to 1D-PCM. However cell differentiation was increased in comparison to 1D at day 3 due to increase ALP activity measured (Figure 7.11d). Cell response to 5D and 6D

collected PCM showed lower levels of protein expression and cell proliferation in comparison to 1D-PCM (Figure 7.11b & c). The levels of ALP expressed were greater with these two PCM in comparison to 1D and 3D PCM (Figure 7.11d). 7D PCM saw a significant drop in cell metabolic activity (Figure 7.11a) along with significantly low levels of cell proliferation in comparison to the other PCM tested and the two controls (Figure 7.11c). However there was enhanced ALP activity observed with the 7D PCM, which was significantly greater than the levels that were observed with the 1D PCM over 5 days of static culture experiments (Figure 7.11d), which suggests that this particular PCM had provided a more suitable environment for cell differentiation. From these results obtained the trend that has been noticed is, as calcium and phosphate ion concentrations decreased in the respective PCM, the MG63 cells started to differentiate as opposed to proliferate.

Cell response to the DMEM-H 1D PCM saw a decrease in cell metabolic activity and cell proliferation (Figure 7.12b & c respectively). However it was interesting to see that the levels of ALP had increased with this particular PCM suggesting that the greater levels of calcium, phosphate and silicate ions provided a positive environment for cell differentiation over 5 days, with day 1 observing the highest ALP activity (Figure 7.12d). Protein expression was greater on day 1 and day 3 with the 1D PCM in comparison to the other PCM tested when collected from the TW DMEM-H circulation study. 3D PCM had a decrease in calcium, phosphate and silicate ions, which in turn showed a decrease in cell metabolic activity, protein expression and cell differentiation (Figure 7.12a, b & d respectively). However, cell proliferation increased in comparison to 1D over 5 day of static cell culture (Figure 7.12c). A similar trend was observed with the 5D and 6D PCM with a decrease in protein expression and cell differentiation in comparison to 1D and 3D. However cell metabolic activity was greater with these two PCM in comparison to 1D and 3D PCM. Cell proliferation was also increased, with 6D PCM observing a significantly greater DNA concentration at day 3 in the static cell culture study in comparison to the other PCM tested. The 5D PCM contained lower levels of calcium, phosphate and silicate ions however the 6D PCM contained lower levels of calcium but increased levels of phosphate and silicate ions in comparison to the 5D PCM. From these results it can be suggested that the decrease in calcium ions and an increase in phosphate and silicate levels provided a favourable environment for cell proliferation (Figure 7.12c).

Cell response showed sensitivity to the decrease in these ions in collected DMEM-H at D7. 7D PCM saw an increase in cell metabolic activity and an increase observed with the DNA concentration over 5 days of culture (Figure 7.12a & c). This suggested that the 7D PCM provided the most supportive environment for cell proliferation. There was a decrease in

ALP activity in comparison to the other PCM tested which suggested that cell differentiation was not supported by this particular PCM (Figure 7.12d). Protein expression was also decreased with the 7D PCM, however at day 5 of the static cell culture study, the protein expression was greater with the 7D PCM in comparison to the other PCM and the SCM controls tested (Figure 7.12b).

From these results it can be seen that there was an inverse effect with the cell response to the all the DMEM-H PCM tested in the cell culture study. A decrease in calcium, phosphate and silicate ion concentrations provided a better environment for osteoblast-like cell growth as opposed to cell differentiation. Whereas an increase in these ions in the respective PCM provided a more supportive environment for cell differentiation over cell proliferation.

An earlier study by Midy et al investigated three CaP powders on osteoblast cells. The three powders used were commercially available HA, nanocrystalline carbonate apatite (CA) and a CaP cement composed of amorphous CaP phase and brushite (CPC-1). The results gained from this study showed that for low levels of calcium, >100μg/ml (>0.1mg/ml), enhanced osteoblast cell proliferation and to a lesser degree differentiation on ALP activity (Midy, Dard et al. 2001). The results found in this particular step of the current study is in agreement with previous findings, as with decreasing levels of calcium cell proliferation was observed to increase. It has also been shown that increasing concentrations of extracellular calcium ions promotes osteogenic differentiation *in vitro* by increasing ALP activity up to 1.6-fold along with OCN and TGF-β gene expression from osteoblastic cells (Matsuoka, Akiyama et al. 1999). Similar results were observed from another study whereby and increase in extracellular calcium ions were found to positively stimulate ALP activity of osteoblasts in bone remodelling and osteoblasts proliferation, directly and indirectly via monocytes (Kanatani, Sugimoto et al. 1991).

It has previously been highlighted that calcium plays a crucial role in directing bone formation and it has been seen that an increase in calcium ions in the extracellular matrix positively stimulate DNA syntheses for bone remodelling (Kanatani, Sugimoto et al. 1991). An increase in phosphate levels has also been shown to enhance osteocalcin expression (Arinzeh, Tran et al. 2005). Osteocalcin is known as a key for the control of bone formation by osteoblasts. The synthesis of osteocalcin is exclusively by osteoblasts and therefore is often used as a bone formation marker *in vivo* (Stein, Lian et al. 1990).

An earlier study by Dvorak et al looked in to the changes in extracellular calcium concentrations on osteoblast function and the involvement of the calcium sensing receptors

in mediating these response. The results they obtained showed that ALP activity was maximal for the calcium concentrations ranging between 1.2mM and 1.8mM (~0.04mg/ml and 0.07mg/ml respectively) (Dvorak, Siddiqua et al. 2004). These specific levels were observed with the results gained in this current study at D7 (Figure 7.2). At the end of the circulation study the levels of calcium ions detected in the collected DMEM were approximately at 0.07mg/ml and this specific PCM saw the greatest ALP levels suggesting it was a favourable environment for the differentiation of the cells (Figure 7.11d).

Taking this in to consideration, as the current work uses a dynamic perfusion system for the delivery of DMEM to the SA80/20 granules and also away from the granules, the increase in alkalinity of the collected DMEM was not expected. This confirms that the DMEM used prior to the TW DMEM-H circulations studies had increased levels of sodium bicarbonate which was together with the CO_2 present in the air causing the pH of the DMEM to rise which suggested the subsequent cell response to the collected PCM from the DMEM experiments may not have been a true representation of what was going on. Under the dynamic flow perfusion system the later investigated DMEM-H stabilised the pH of the DMEM-H which showed a generic increase in calcium, phosphate and silicate ion release along with greater cell differentiation.

7.5 Summary and Conclusions

The work presented in this Chapter has clearly demonstrated that using a TW flow perfusion system is a more realistic method for investigating dynamic ion exchange between BGS and the surrounding media. In doing this it enables a better understanding of the processes taking place *in vivo* therefore allowing for more complex testing to occur *in vitro*. Using a TW flow perfusion system enhanced cell metabolic activity along with protein expression and cell differentiation.

It was also established that by changing the way media was buffered had an effect on dynamic ion exchange within TW flow perfusion system and also effected subsequent osteoblast-like cell response. The DMEM which was previously used had the addition of sodium bicarbonate which acted as the internal buffer for the media. However it was established that these levels were too high which were causing the rise in pH of the media during the circulations studies. The way around this was to use a powdered DMEM without sodium bicarbonate and supplementing the DMEM with 1M HEPES buffering solution. Many studies have confirmed the positive effects of HEPES buffer and the results and the subsequent results gained in the current work showed agreement to this. Previous work has demonstrated the importance of maintaining pH as a reduced pH causes cell death. The effects of a highly alkaline pH have not been investigated fully, but the results from this study showed that an increase in pH causes a suppressed release of calcium and phosphate ion and the release of silicate ions was totally blocked. The enhanced release of these ions caused greater ALP activity which suggested the environment supported cell differentiation.

From this work it can be concluded that the TW flow perfusion system is a better system to be working with and supplementing DMEM with HEPES buffer supports better ion exchange along with positive effects on cell response.

Chapter 8 Effects of Serum Containing Media on Dynamic Ion Exchange and Subsequent Cell Response with HA and SA

8.1 Background

The results from Chapter 7 observed that using a to waste (TW) flow perfusion system was an improved way for investigating dynamic ion exchange between the BGS and surrounding media. It was also established that supplementing the media with HEPES buffer allowed for the pH of the media to remain stable at pH 7.4 which in turn increased the release of calcium, phosphate and silicate ions.

It is commonly accepted that upon implantation a layer of proteins and also other blood components are absorbed on to the surface of the implant. This absorbed layer acts as a mediator between the materials surface and cell. Material properties such as materials chemistry and porosity are influential characteristics in determining the type and quantity of the absorbed protein layer on the materials surface. The absorbed protein layer then influences the cellular development by determining cell attachment, morphology, proliferation and finally cell differentiation. Previously it has been noted that introducing serum proteins to the media type under physiological conditions helps facilitate greater ionic exchange particularly with silicone substituted hydroxyapatite (SA) (Chana 2010).

The objective of the following chapter was to investigate the effects of serum containing media on dynamic ion exchange within a flow to waste perfusion system between 3 grades of bone graft substitute granules, stoichiometric hydroxyapatite of 80% total porosity and 20% strut porosity (HA80/20) and 0.8wt% silicate substituted hydroxyapatite with 80% total porosity and 20% & 30% strut porosity (SA80/20 and SA80/30 respectively) and the surrounding media. Subsequent cell response was also determined by incubating MG63 cells on tissue culture plates with the PCM collected from the TW circulation experiment between HA80/20, SA80/20 and SA80/30 and the surrounding media.

8.2 Methodology

8.2.1 Media and Sample Preparation

The work in this chapter used DMEM-H with the addition of 10% FBS. The medium used was powdered Dulbecco's Modified Eagle Medium supplemented with 1% penicillin-streptomycin, 1M HEPES buffer and 10% FBS. This medium type was now referred to as complete DMEM (C-DMEM). Sample preparation was the same as described in Chapter 4 section 4.2.1.1 however this time as well as SA80/20, HA80/20 and SA80/20 (Chapter 2 & 3) were also being investigated, therefore samples were prepared for all three BGS.

8.2.2 TW Flow Perfusion Set up

PCM in this study was obtained by perfusing an initial 500ml of C-DMEM as the 'input reservoir' at a flow rate of 0.1ml/min through 0.45g of HA80/20, SA80/20 and SA80/30 granules using the TW flow perfusion system. This reservoir was kept topped up with 500ml of fresh medium at D1 and then an additional 500ml of fresh media every 48h until the end of the experiment. Media was sampled by collecting the entire volume of C-DMEM present in the waste reservoir at time intervals of 0.5, 1, 2 and 4 hours, 1, 3, 5, 6 and 7 days to give 9 distinct media samples. The pH of these different media samples was then measured (as in chapter 3 section 3.2.5) and the samples were stored at -20^{o}C until they were analysed for calcium, phosphate and silicate ion concentrations using colorimetric assays as previously described in Chapter 4 section 4.2.1.2. SEM analysis was also conducted on all three types of granules collected on day 7. The protocol followed can be found in chapter 2 section 2.1.

PCM for subsequent cell experiments was obtained by sterile filtration of the remaining waste media collected at 1, 3, 5, 6 and 7 days, and stored as 1D, 3D, 5D, 6D and 7D PCM respectively from all granule types used. The earlier time points of 0.5, 1, 2 and 4 hours were not used for production of PCM as the volume of media collected between these time points was not sufficient enough for 5 days of cell culture experiments. Figure 8.1 shows images of the TW flow perfusion system set-up. pH was also measured of DMEM before and at the individual time intervals during this circulation study.

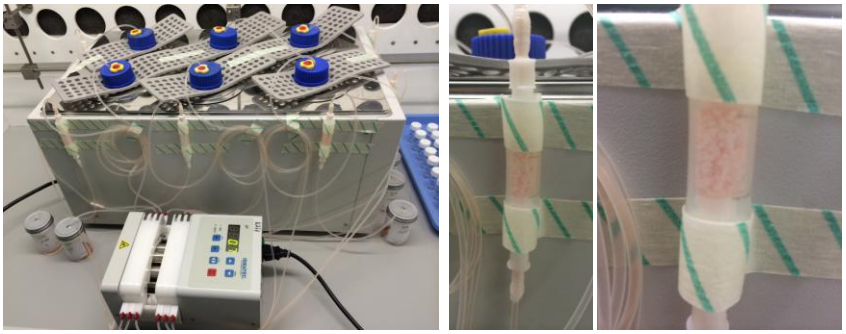

Figure 8.1: Experimental set up for flow to waste perfusion system using HA80/20, SA80/20 and SA80/30 granules perfused with C-DMEM

8.2.3 Static Cell Culture Study on Tissue Culture Plates

After the flow to waste perfusion experiments were completed, all the individually collected PCM from all three BGS were used to conduct static cell culture studies on tissue culture plates in order to investigate whether any differences in dynamic ion exchange between the individual BGS and the perfused media had an effect on osteoblast-like cell response.

MG63 cells were grown and expanded as described previously in Chapter 4 section 4.2.2.1 MG63 osteoblast-like cells (P4) were seeded at a concentration of $4x10^4$ cells/ml SCM in 24 well plates 1ml of cell suspension was add to each well and the cells allowed to attach at 37°C and 5% CO_2. After 2 hours the SCM was replaced with 1ml of either 1D, 3D, 5D, 6D and 7D PCM collected from the three individual BGS or fresh SCM as a control. The cells were incubated for periods of 1, 3 and 5 days. The media was refreshed at 24 hours then every 48 hours thereafter using the individual media types being tested. DNA quantification, ALP specific activity, total protein and cell metabolism using alamarBlue® was monitored at each time point. The protocols followed for these assays can be found in Chapter 4 section 4.2.2.2 and 4.2.2.5.

8.2.4 Statistical Analysis

All collected data was conducted at n=6 and analysed and expressed in terms of mean ± standard deviation. Statistical significance was evaluated using ANOVA, Post Hoc test: Tukey HSD with $\alpha=0.05$, (were *$p<0.05$, **$p<0.01$ and ***$p<0.005$).

8.3 Results

8.3.1 Ion Concentration, pH and SEM Analysis

From the ion concentration analysis results obtained in this chapter it is evident that the presence of serum proteins regulates ion dissolution and re-precipitation from the varying BGS in to the surrounding C-DMEM (Figure 8.2, Figure 8.3 and Figure 8.4).

There is an initial release of calcium, phosphate and silicate ions from all three BGS within the first 30 minutes of perfusion, however the phosphate and silicate ion release is lower with HA80/20 in comparison to SA80/20 and SA80/30.

The release of calcium and phosphate ions is stable for the first 4 hours, after which there is a decrease in calcium levels from HA80/20 and a decrease in phosphate levels from HA80/20 and SA80/20.

From both SA BGS, the calcium levels begin to decrease at D1, after which SA80/30 observes a sustained decrease in calcium ions only just reaching basal levels by the end of the study. D1 also marks the decrease of phosphate ions in the surrounding media from SA80/30.

There is an initial release of silicate ions from all BGS within the first 30 minutes of perfusion, whereby HA80/20 shows only a slight release in comparison to the SA BGS which show greater levels of silicate ion release. After 30 minutes of perfusion there is a decrease in silicate ions within the surrounding media observed (Figure 8.4). The release of silicate ions from HA80/20 returned to basal levels, as these were the levels observed in the C-DMEM before experimentation. Silicate ions remained slightly elevated in comparison to the basal levels from SA80/20 and SA80/30 by the end of the study.

The pH levels observed showed an initial increase in pH for all BGS. Again a lesser increase was observed with theHA80/20 BGS in comparison to both SA BGS. At 4 hours, the pH levels returned to basal levels of 7.3 for the rest of the perfusion study.

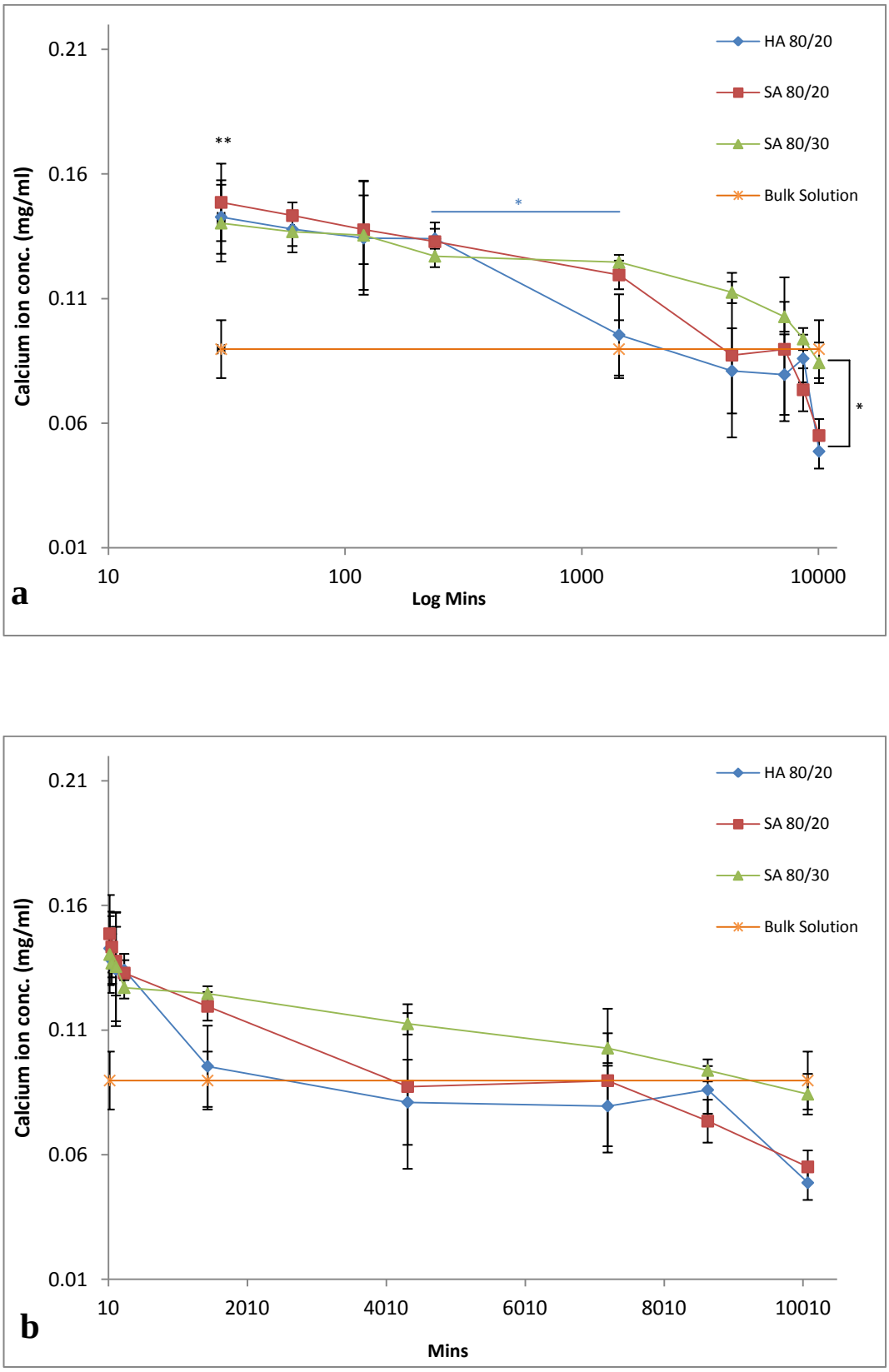

Figure 8.2: Calcium ion concentration of C-DMEM from HA80/20, SA80/20 & SA80/30, a) log minutes scale & b) minutes scale (n=6)

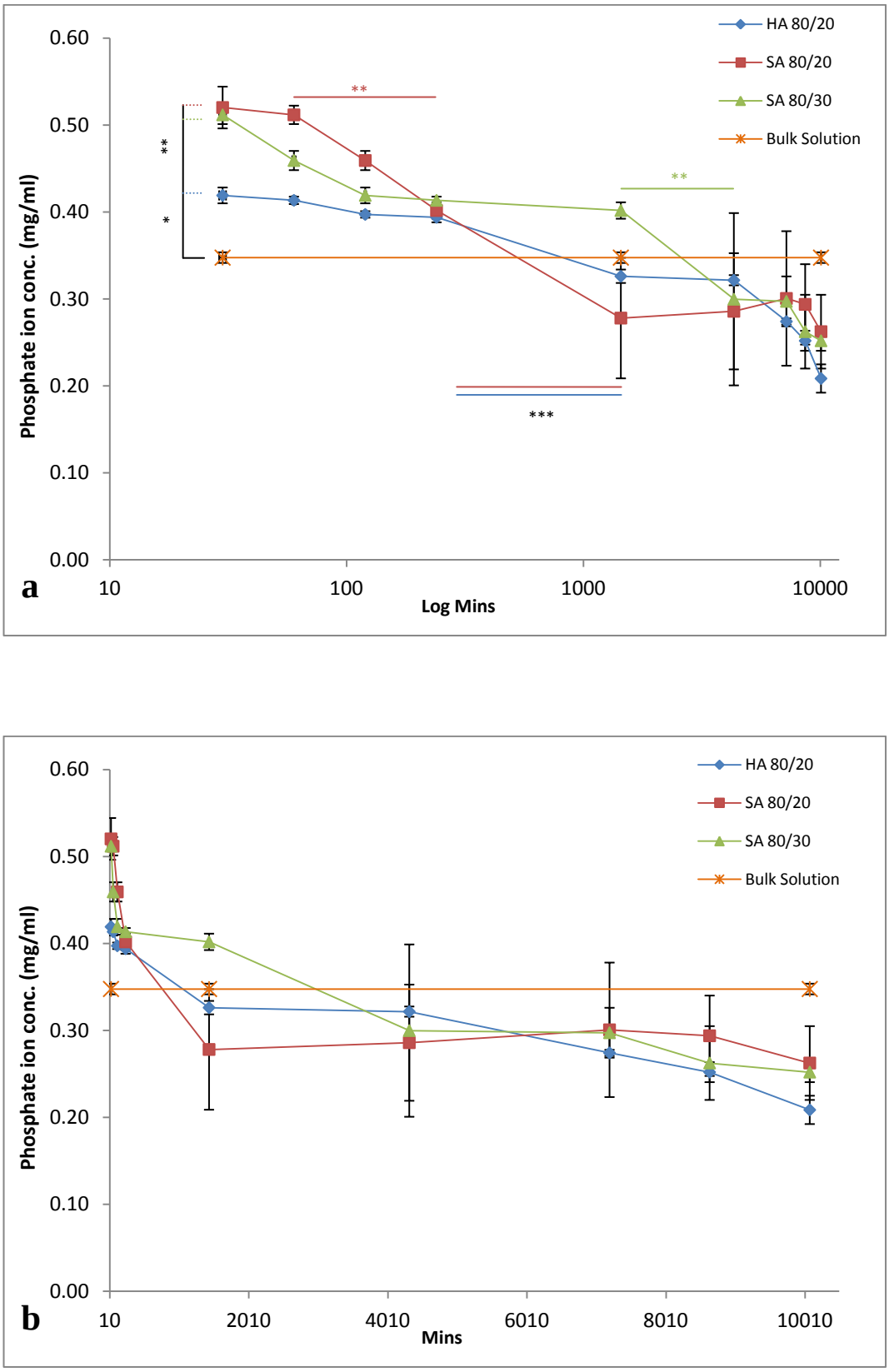

Figure 8.3: Phosphate ion concentration of C-DMEM from HA80/20, SA80/20 & SA80/30, a) log minutes scale & b) minutes scale (n=6)

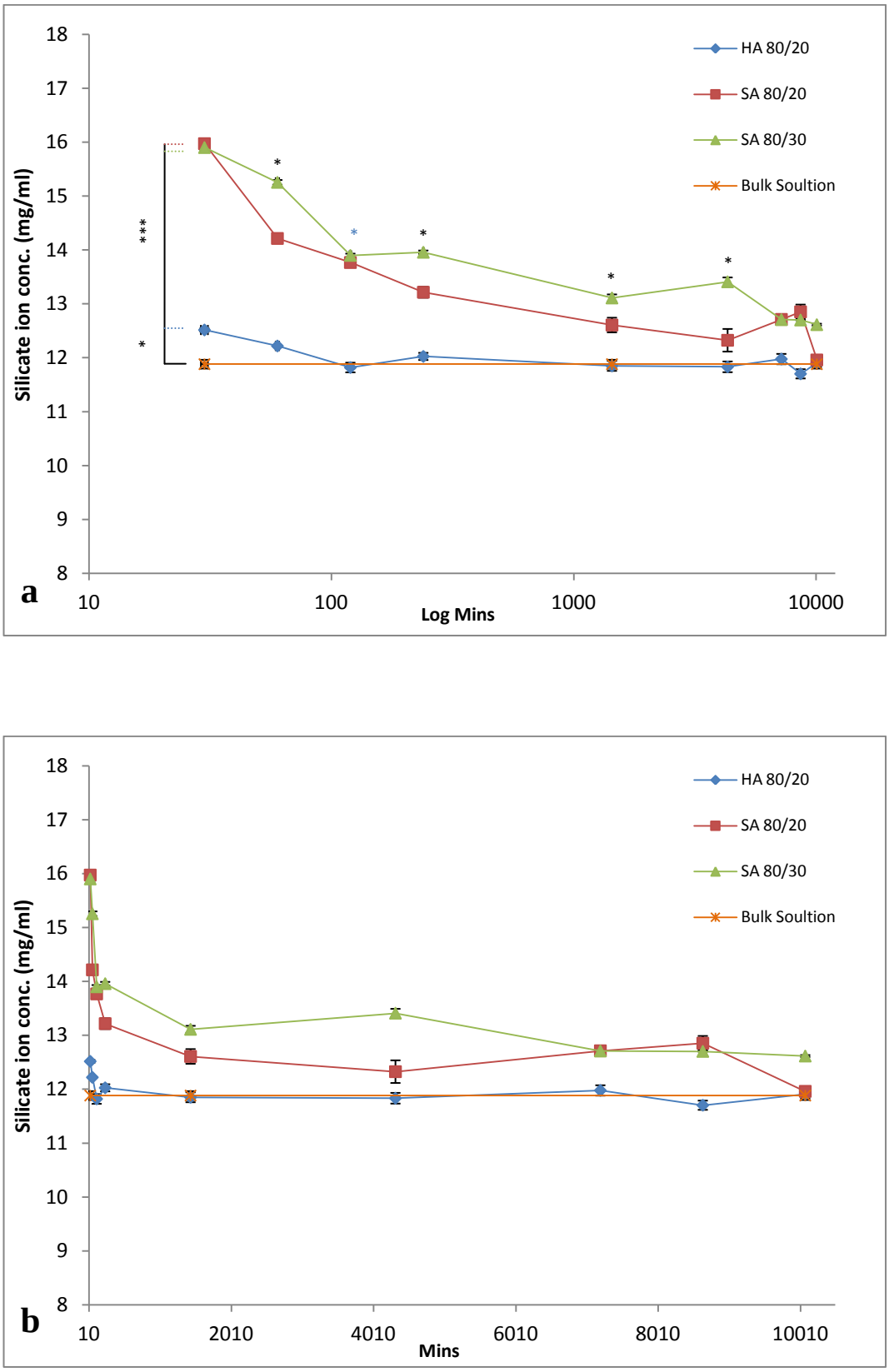

Figure 8.4: Silicate ion concentration of C-DMEM from HA80/20, SA80/20 & SA80/30, a) log minutes scale & b) minutes scale (n=6)

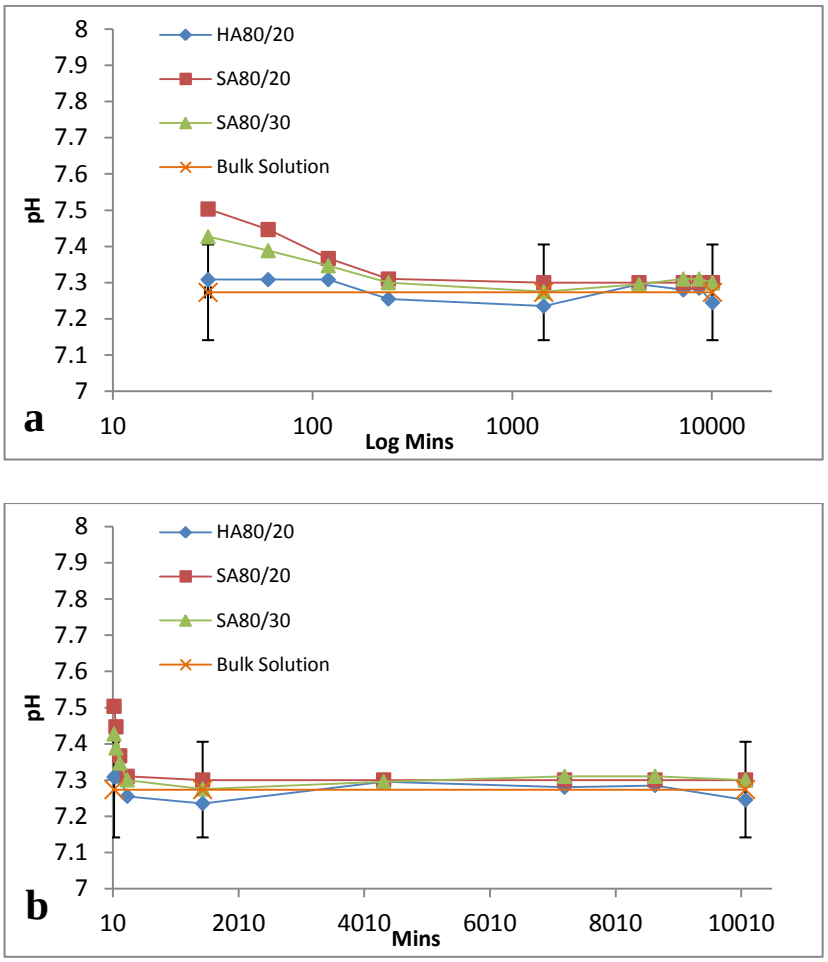

Figure 8.5: pH of C-DMEM from HA80/20, SA80/20 and SA80/30, a) log minutes scale & b) minutes scale (n=6)

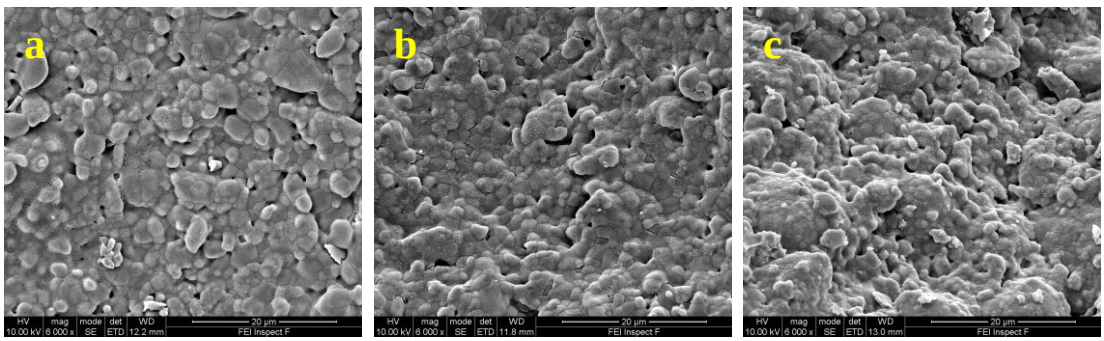

Figure 8.6: SEM images of a) HA80/20, b) SA80/20 & c) SA80/30 granules collected at day 7 from the 'to waste' perfusion experiments with C-DMEM

From the SEM images it is evident that there was a homogenous CaP layer precipitated on the surface of all three granules types tested within the perfusion experiments. All three granules types visually had similar amount of CaP layer precipitation present.

8.3.2 Static Cell Culture on Tissue Culture Plates

Cell response was monitored by incubating MG63 cells in the PCM samples collected after perfusion through one of the three types of BGS. The results for PCM obtained from each type of BGS are presented individually.

8.3.2.1 HA80/20

In Figure 8.7 it is evident that metabolic activity was significantly higher in 7D-PCM and SCM in comparison to the other PCM tested. There was no clear trend observed for the total protein content however all the tested PCM had significantly lower total protein content in comparison to the SCM control. Total DNA did not increase in time for 1D, 3D, 5D or 6D PCM however 7D PCM showed a significant increase in total DNA from day 1-5. There was no clear trend observed for the ALP activity. There lower time point PCM supported higher levels of ALP activity in comparison to the longer time point PCM and SCM control.

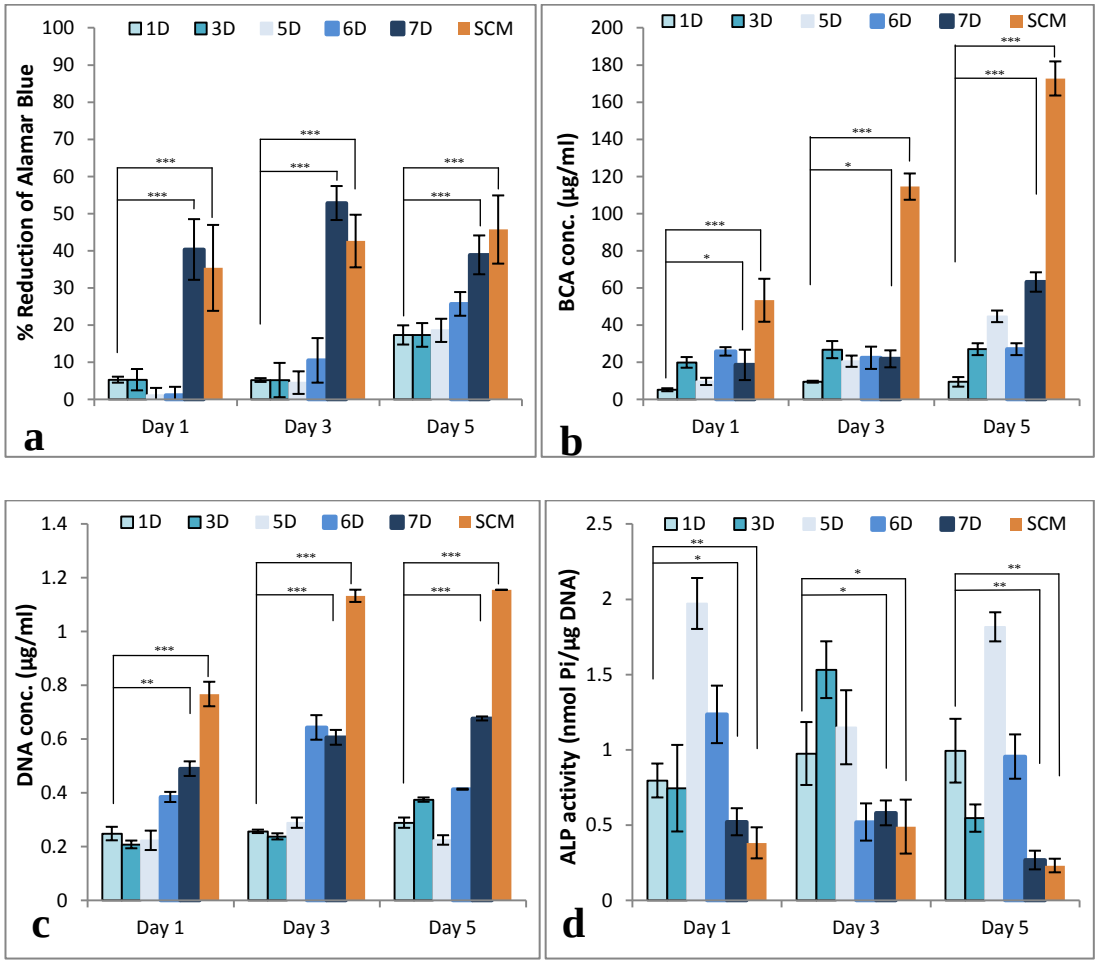

Figure 8.7: a) % reduction of alamarBlue®, b) BCA total protein, c) DNA concentration and d) ALP specific activity for MG63 cells on HA80/20 cultured in PCM for 5 days (n=6)

8.3.2.2 SA80/20

With the PCM obtained from the perfusion study with SA80/20, cell metabolic activity was enhanced over all PCM with time. Cell metabolic activity was the greatest with the 7D PCM (Figure 8.8a). Total protein was also enhanced with all PCM collected from the circulation study with SA80/20 with the release being statistically similar over all PCM tested (Figure 8.8b). DNA concentration was increased with 7D PCM. On day 3, 5D observed enhanced cell proliferation compared to the other PCM tested. Increased ALP activity was observed with 6D PCM on all days. A peak increase in ALP activity was seen with 3D on day 3 of the static cell culture experiments (Figure 8.8d).

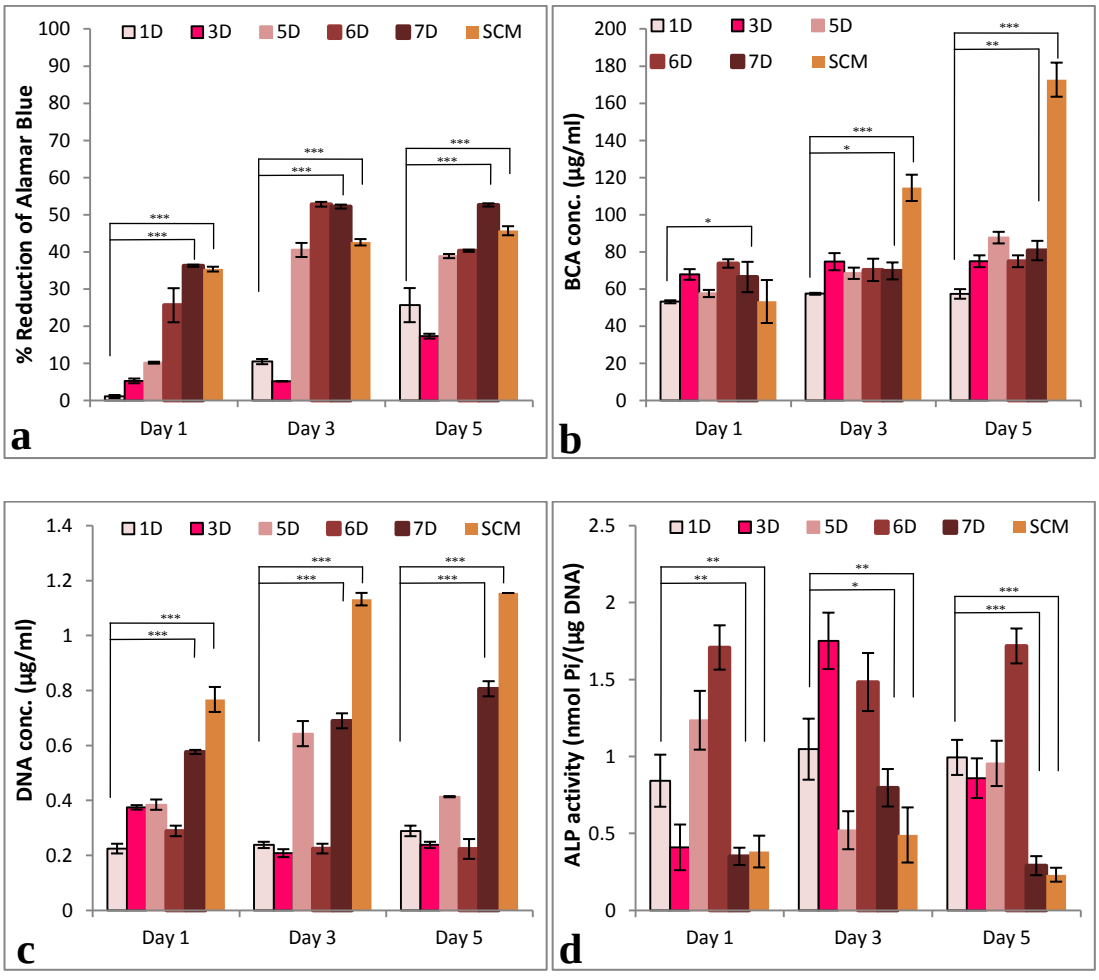

Figure 8.8: a) % reduction of alamarBlue®, b) BCA total protein, c) DNA concentration and d) ALP specific activity for MG63 cells on SA80/20 cultured in PCM for 5 days (n=6)

8.3.2.3 SA80/30

The cell response results obtained from the PCM collected from SA80/30 during the perfusion study were very similar to the results that were obtained with the PCM collected from SA80/20. Cell metabolic activity was more prominent with 7D PCM in comparison to the other PCM tested over time (Figure 8.9a). Total protein was statistically similar among all PCM with time, however total protein was observed to be lesser with 1D over time in comparison to the later PCM collected (Figure 8.9b).

Cell proliferation was enhanced with 7D PCM suggesting it provided a better environment for cell growth. Cell proliferation was observed to be suppressed with the other PCM tested (Figure 8.9c). Finally ALP activity was found to be significantly lower with 5D PCM at day 3 and 5 compared to the other PCM (Figure 8.9d).

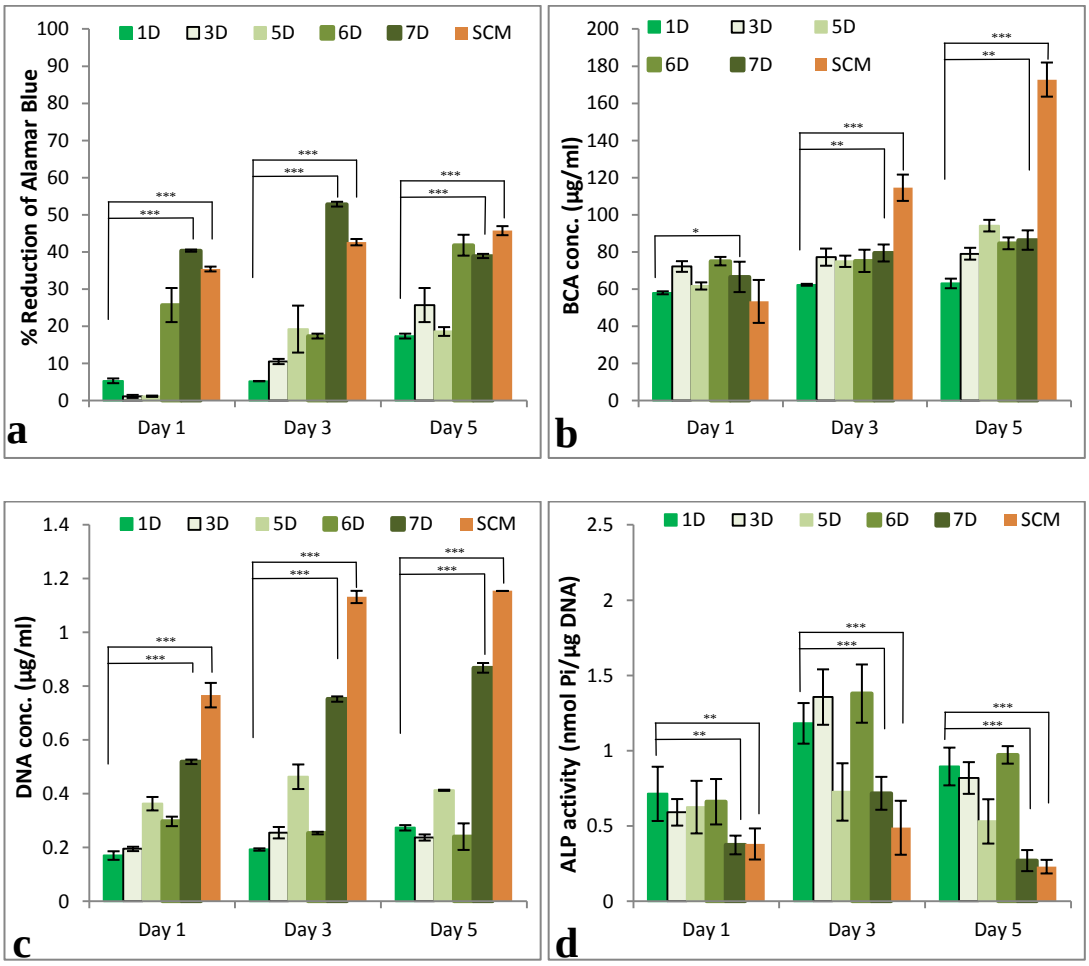

Figure 8.9: a) % reduction of alamarBlue®, b) BCA total protein, c) DNA concentration and d) ALP specific activity for MG63 cells on SA80/30 cultured in PCM for 5 days (n=6)

8.4 Discussion

The results in this Chapter looked in to investigating the changes in dynamic ion concentrations between BGS and the surrounding media in a TW flow perfusion system and the subsequent osteoblast-like cell response to the collected PCM from the individual BGS tested. The results obtained in this work showed that the addition of serum proteins regulated the release on ions in to the surrounding media from the individual BGS tested.

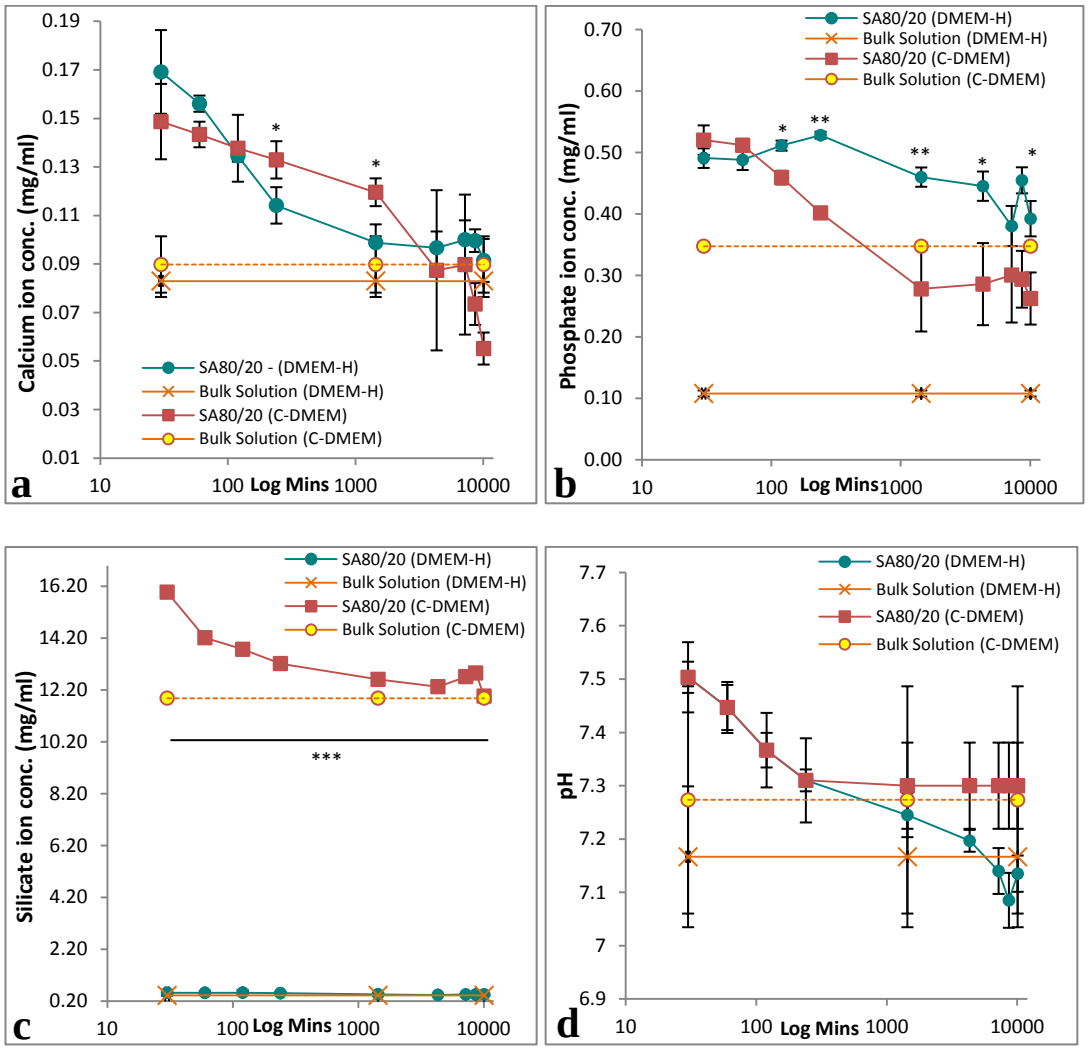

Figure 8.10: a) Calcium ion conc., b) Phosphate ion conc., c) Silicate ion conc. and d) pH graphs for C-DMEM compared to DMEM-H perfused through SA80/20 granules (n=6)

Figure 8.10 shows the effects adding serum to media has on the ion exchange between SA80/20 granules and the surrounding media. It is evident that on the addition of serum to media the calcium, phosphate and silicate ion concentrations in the starting bulk media increases. Calcium and phosphate ion concentrations are regulated and there is a clear trend

in the increase in these ions in the surrounding media at earlier time points and at later time points the concentrations of these particular ions begin to decrease which marks the point of the precipitation of these ions back on the surface of the SA80/20 granules. When comparing the two different types of media, a greater difference was observed with the phosphate ion concentrations. The bulk solution increased to levels 4 times greater with the addition of serum proteins and it was also found that the release and precipitation of phosphate ions over time was regulated. It was interesting to find that the concentration of silicate ions within the bulk solution increased to over 10 fold and that the release pattern of the ions over time were found to decrease to levels significantly greater that the bulk solution up until day 7, where the silicate ions levels reached statistically similar levels to the bulk solution. With the addition of serum to the media, the pH of the media was increased to 7.27 from 7.17 of the starting bulk solution. At 4 hours the pH was maintained at 7.3 up until the end of the experiments at day 7.

Looking at the ion concentration results obtained from the current study in this chapter it was found that at D1 the calcium concentrations were increased in comparison to later time points. HA80/20 had levels reaching basal levels whereas both SA BGS were higher with SA80/30 showing the greatest levels at this particular time point (Figure 8.2). Phosphate ion concentration levels were again greater with SA80/30 at D1, with SA80/20 and HA80/20 showing depleted levels below basal levels of phosphate ions in the surrounding media (Figure 8.3). Silicate ion levels were increased in media with both SA BGS however the media from HA80/20 had the same levels of silicate ions as the bulk solution of C-DMEM (Figure 8.4). The corresponding cell work to the D1 PCM for the individual BGS showed similar trends. With an increase in calcium, phosphate and silicate levels there was an increase in ALP activity observed with all 1D PCM across all three BGS (Figure 8.7d, Figure 8.8d & Figure 8.9d respectively). Cell proliferation was suppressed across all 1D PCM (Figure 8.7c, Figure 8.8c & Figure 8.9 respectively). Total protein was enhanced with the 1D PCM in SA80/20 and SA80/30 in comparison to the 1D PCM obtained from HA80/20 (Figure 8.8b, Figure 8.9b & Figure 8.7b respectively). Cell metabolic activity increased with time across all 1D PCM with all three BGS tested (Figure 8.7a, Figure 8.8a & Figure 8.9a respectively). These results observed suggested that an increase in ionic concentrations provided a more supportive environment for cell differentiation.

On D3 of the perfusion study, there was a decrease observed in calcium and phosphate ions in all BGS, however the drop in calcium levels in the surrounding media from SA80/30 was significantly less compared to HA80/20 and SA80/20 (Figure 8.2). By D3, phosphate levels had dropped below the bulk solution levels (Figure 8.3) with Ha80/20 and Sa80/20,

however, for SA80/30 the levels were significantly above bulk solution levels. Silicate ion levels however were still elevated in both SA BGS with a greater release observed from SA80/30 (Figure 8.4). HA80/20 had statistically similar levels of silicate ions as the bulk solution. Cell proliferation from all the subsequent 3D PCM collected from all three BGS was statistically similar to 1D PCM (Figure 8.7c, Figure 8.8c & Figure 8.9c respectively). At day 3 there was a peak release of ALP with the 3D PCM with HA80/20 and SA80/30 (Figure 8.7d, Figure 8.8d & Figure 8.9d). Total protein was also increased with all the 3D PCM in comparison to the 1D PCM, however cell metabolic activity was statistically similar between all BGS for 1D and 3D PCM.

A similar trend was observed with the following 5D and 6D PCM. As calcium and phosphate ions decreased (Figure 8.2 & Figure 8.3) there was a further increase observed in cell proliferation but the increase was more distinct with the two SA BGS in comparison to the HA80/20 (Figure 8.8c, Figure 8.9c & Figure 8.7c respectively). However this increase was not occurring with time. Silicate ion release at with these two PCM was very similar from both SA BGS and it was at basal levels with HA80/20 (Figure 8.4). Cell differentiation was greater in comparison to cell proliferation for these two respective PCM, with 6D observing greater ALP levels on day 3 from SA80/20 and SA80/30 (Figure 8.8d, Figure 8.9d & Figure 8.7d respectively). Total protein was still seen to be suppressed from the 5D and 6D PCM collected from HA80/20 (Figure 8.7b) in comparison to both SA BGS (Figure 8.8b & Figure 8.9b). Cell metabolic activity was increased with time for 5D and 6D PCM with all BGS over time. The levels of cell metabolic activity that were measured were lower for HA80/20 and SA80/30 when compared to SA80/20.

On D7 there were depleted levels of calcium and phosphate ions in the surrounding media from all BGS, suggesting that these ions had now precipitated back on to the granules surface which is supported by the SEM images obtained which showed CaP layer deposited on the surface of all three BGS granules. There were depleted levels of phosphate in the surrounding media by the end of the study from all BGS (Figure 8.3). Silicate levels in the surrounding media were greater with SA80/30 in comparison to SA80/20 and HA80/20 which had levels which had reached basal levels (Figure 8.4). The subsequent cell response to the 7D PCM collected at the final time point from the circulation study showed that cell metabolic activity and cell proliferation were enhanced with the7D PCM collected from all three BGS (Figure 8.7a, Figure 8.8a, Figure 8.9a & Figure 8.7c, Figure 8.8c, Figure 8.9c respectively). Protein expression was also increased with the 7D PCM however, HA80/20 still showed suppressed levels (Figure 8.7b). Finally ALP activity was decreased over all BGS with the 7D PCM (Figure 8.7d, Figure 8.8d, & Figure 8.9d). From these findings it can

be suggested that a decrease in calcium and phosphate ions provides a more supportive environment for cell proliferation.

➢ 1D PCM - HA80/20, SA80/20 & SA80/30

Comparing the results obtained for all three BGS from the 1D PCM, the differences in cell response become more obvious. From Figure 8.11 it is evident that 1D PCM across all BGS promoted cell differentiation (Figure 8.11d) over cell proliferation (Figure 8.11c). However between the different granule types the differences were not significantly different. Cell metabolic activity was greater with SA80/20 at day 3 and 5 (Figure 8.11a). Total protein was severely suppressed with HA80/20 and elevated with both SA BGS with statistically similar levels (Figure 8.11b). These result clearly indicate that with increased levels of calcium, phosphate and silicate ions, cell differentiation is favoured however the study showed no significant difference between the chemistry and porosities tested. .

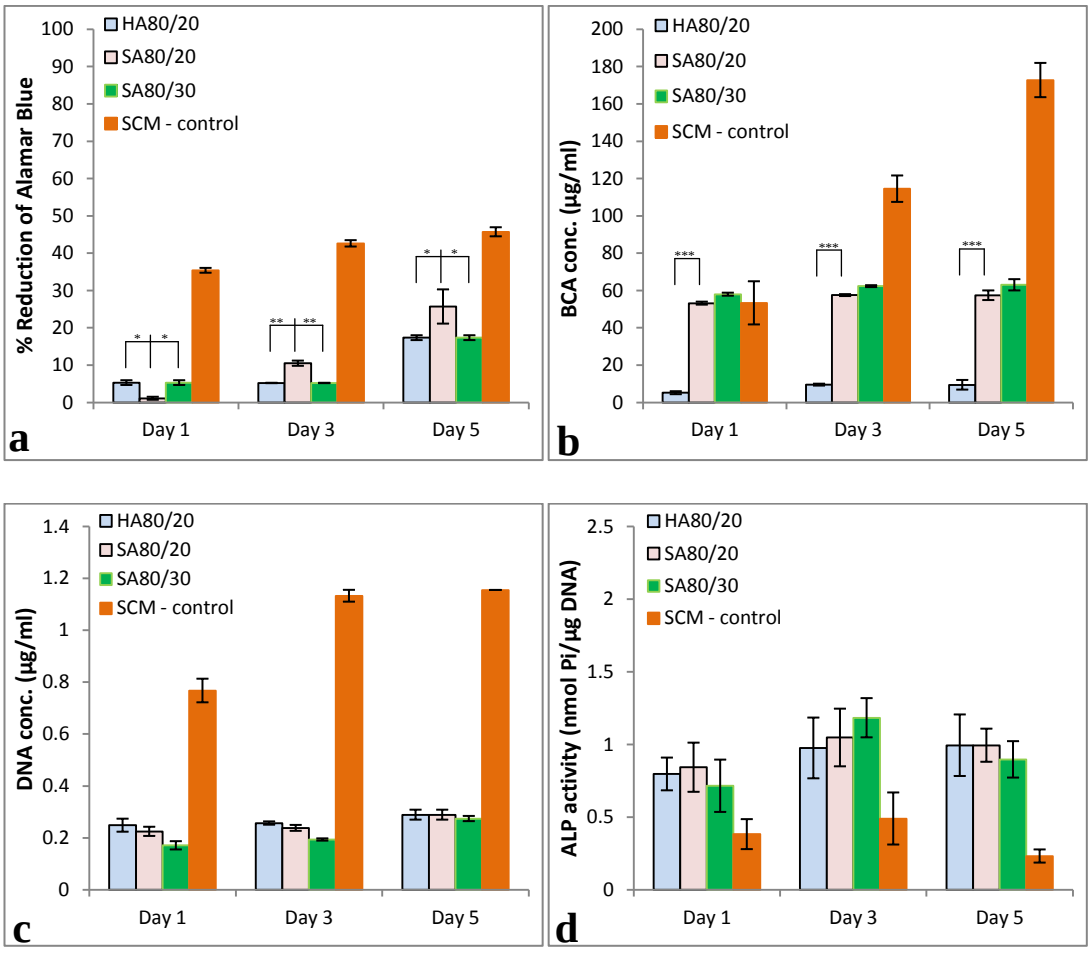

Figure 8.11: a) % reduction of alamarBlue®, b) BCA total protein, c) DNA concentration and d) ALP specific activity for MG63 cells on HA80/20, SA80/20 and SA80/30 cultured in 1D PCM for 5 days (n=6)

➢ 7D PCM - HA80/20, SA80/20 & SA80/30

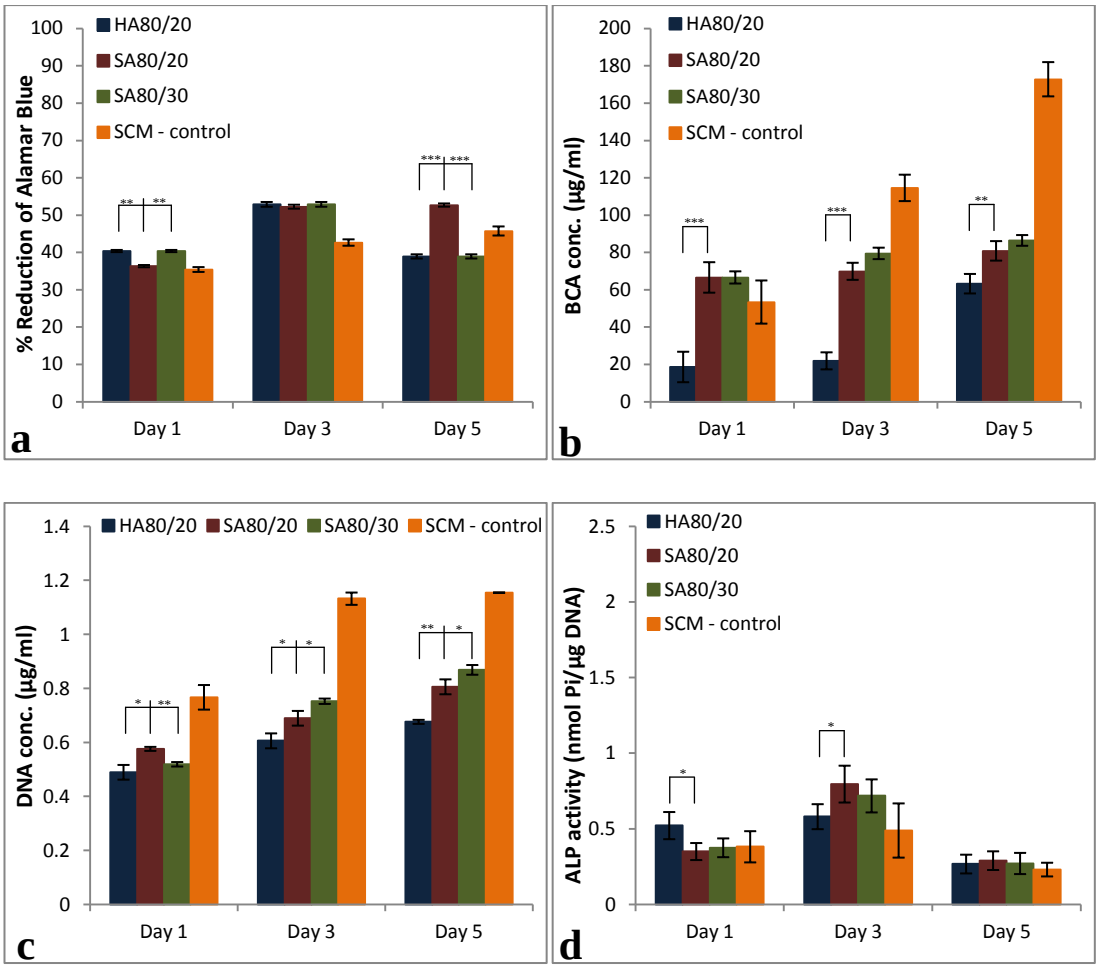

Figure 8.12: a) % reduction of alamarBlue®, b) BCA total protein, c) DNA concentration and d) ALP specific activity for cells on HA80/20, SA80/20 & SA80/30 cultured in 7D PCM (n=6)

Comparing the results obtained from the 7D PCM across all BGS, highlights the differences in cell response. 7D PCM obtained from all BGS during the perfusion study contained depleted levels of calcium and phosphate ions. Silicate ion levels were also depleted in HA80/20 and SA80/20, however they were higher compared to basal levels with SA80/30. Figure 8.12 shows that with depleted levels of calcium and phosphate ions, 7D PCM enhanced cell proliferation (Figure 8.12c). This may be because these ions were precipitated back on to the BGS surface, causing the formation of a bioactive CaP layer which allowed for cell to proliferate. Cell differentiation was suppressed with all BGS with the 7D PCM (Figure 8.12d) and protein expression was increase with the two SA BGS and suppressed with HA80/20 (Figure 8.12b). Compared with 1D PCM, cell metabolic activity was

significantly enhanced, suggesting that the precipitation of an apatite layer allowed for the proliferation of osteoblast-like cells therefore increasing the metabolic activity of the cells.

As mentioned before, previous work has been successful in showing that the release of controlled levels of calcium ions over time favours the formation of an apatite layer, which is found to be necessary for the bioactivity displayed in many ceramic materials (Duan, Zhang et al. 2005). The results presented in this chapter were able to show the controlled release of calcium and phosphate ions in comparison to previous work presented in earlier chapters. It can be assumed that this is due to the addition of serum proteins to the DMEM for the circulation study which were able to control the release of calcium, phosphate and silicate ions from the BGS to the surrounding media.

A study by Valerio et al looked at the effects of ionic products from bioactive glass dissolution on osteoblast proliferation. The study was able to show that osteoblasts in the presence of ionic products from bioglass dissolution showed high proliferation along with collagen secretion when compared to the controls testes. The increased activity was suggested to be related to silicon contents of the bioglass dissolution (Valerio, Pereira et al. 2004). In the present study there was greater silicon release from the SA80/30 sample in comparison to the SA80/20 sample. Also by the end of the circulation study there were still elevated levels of silicate ions in the surrounding medium from SA80/30 whereas silicate ion levels had reached basal levels in the media from SA80/20. As mentioned before the 7D PCM collected from SA80/30 in the circulation experiment showed enhanced levels of cell proliferation. This suggests that this increased activity of SA80/30 7D PCM is related to the silicate ion content observed in this particular media type at the end of the circulation study.

Only trace levels of silicon are found within the human body and are not homeostatically regulated by the body. There is limited literature about silicon as an active element in biology, however Carlisle was the first to demonstrate the impaired development of chick bone under a silicon deficient diet (Carlisle 1972). In cell culture these elements have been studied further. For example, the supplementation of silicic acid to osteoblast--like cell cultures has been shown to increase the collagen-I expression and production (Reffitt, Ogston et al. 2003). Therefore this data was able to suggest that silicon in cell culture medium of osteoblast-like cells stimulates the production of collagen-I, which in turn is accepted as a marker for the production of bone tissue. There has been other research which has been able to further confirm the positive effects of the dissolution products of bioglass, containing high concentrations of silicon on the activity of osteoblast-like cells (Xynos, Edgar et al. 2000, Bielby, Christodoulou et al. 2004, Gough, Jones et al. 2004).

Previous work has demonstrates that the action of proteins present within FBS promotes the dissolution of minerals (Suzuki, Yamamoto et al. 1997). This phenomenon may help in explaining why the dissolution of calcium and phosphate ions is only observed in media containing FBS under static conditions in the presences of the more resorbable SA (Porter, Botelho et al. 2004). There have been other studies where not only serum proteins have been investigate. A study by Combes and Rey looked into the effects of albumin at 5g/l and 40g/l on the apatite formation from SBF on CaP based materials. The study was able to conclude that the proteins have multiple functions on the formation of an apatite layer, ranging from promoting, inhibiting or even both (Combes and Rey 2002). Multiple factors influence specific proteins to have the ability to form or prevent the formation of an apatite layer on the surface of CaP based materials. These factors include, surface charge, solution pH as well as the source of proteins and the purity of them.

The surface properties of both HA and SA have been shown to be significantly different (Chapter 2) and because of this the proteins present in FBS may act in differing ways on the surface of HA and SA. This has also been shown in the dissolution and re-precipitation rate of calcium on HA80/20, SA80/20 and SA80/30 in the presences of proteins whilst the calcium rate was increase in C-DMEM under dynamic flow perfusion conditions in the presence of SA80/30, the calcium concentrations was decreased with HA80/20 and SA80/20 which may indicate the possible formation of an apatite layer. It is important to note that the promotion of inhibition of an apatite layer by proteins *in vitro* may not be directly related to the apatite formation *in vivo* (Combes and Rey 2002).

Earlier work also revealed that there is a significant lag in the formation of an apatite layer from protein containing SBF on well crystallised stoichiometric HA and porous corallines HA. It was also found that the presence of proteins eliminated the apatite formation on β-TCP. Furthermore the presence of the proteins in medium were not able to show a significant effect of the formation of an apatite layer on calcium deficient HA or not well crystallised stoichiometric HA. This work was able to demonstrate the significant effect of proteins in the surrounding medium as well as demonstrating the importance of surface chemistry and the result surface properties in the interaction of ions with the materials surface (Radin and Ducheyne 1996).

The results gained in this chapter were able to show that with the addition of serum proteins the release of calcium, phosphate and silicate ions was regulated and there were clear time points where the depletion of these ions can be seen suggesting the re-precipitation of a successful CaP layer on the surface of the BGS. A quicker depletion of ions was seen with

HA80/20 and SA80/20 BGS. The SA80/30 had a delayed depletion of phosphate ions and silicate ions. By regulating the release of ions form the BGS to the surrounding media, this in turn enhanced cell response. Cell proliferation was enhanced in all BGS with a decrease in calcium and phosphate ions in the PCM. This suggested that a bioactive apatite layer on the surface of the implanted BGS is vital for the attachment and growth of cells for a successful biological response.

Porous ceramics have been considered for over 30 years for use as synthetic BGS (Klawitter and Hulbert 1972). Many reports of a greater and faster rate of bone penetrations with increasing macroporosity in a wide variety of BGS (Kuehne, Bartl et al. 1994, Betz 2002, Hing, Best et al. 2004). This phenomenon has been related to the greater volume available for in growth and the interconnectivity or the openness of the structure. The formation of new bone must be followed by the formation of a vascular network, which is dependent on the degree of structural interconnectivity between pores (Rubin, Popham et al. 1994). This has been demonstrated by a greater penetration of bone in porous implants which have larger pore interconnectivity (Kuehne, Bartl et al. 1994, Kilpadi, Sawyer et al. 2004). It has also be shown that there is improved integration of new bone within constructs that are porous with smaller but well connected porosity in comparison to constructs which have larger more isolated pores (Eggli, Muller et al. 1988). The degree of porosity within a scaffold could be responsible for the regulation of bioactivity of a BGS as a function of its influence on structural permeability (Eggli, Muller et al. 1988) and the local mechanical environment (Hing, Best et al. 2004). However, even though it has been recognised that the rate of integration and the volume of bone regenerated bone maybe dependant on macroporosity, recent studies have shown the biological sensitivity to the levels of microporosity within the struts *in vitro* and *in vivo* (Bignon, Chouteau et al. 2003, Annaz, Hing et al. 2004, Hing, Saeed et al. 2004). Hing et al was successful in showing that the distribution of porosity volume between the macro and micro structure had a significant effect on the early pattern and the dynamics of osseointegration where the increase in either total or strut porosity accelerated osseointegration. It was also found that in the longer term, strut porosity was the dominating factor influencing the mechanics of the scaffold (Hing, Saeed et al. 2004).

These findings in this chapter corroborate with previous work where having a BGS with a greater strut porosity has shown to be biologically sensitive allowing greater cell proliferation.

8.5 Summary and Conclusions

The work presented in this Chapter was able to demonstrate the importance of serum proteins in order to regulate the release of calcium, phosphate and silicate ions from BGS to the surrounding C-DMEM. The presence of serum proteins also allowed for the depletion of calcium and phosphate ions from the surrounding media which in turn meant that these ions were being re-precipitated back on the BGS surfaces forming a homogeneous bioactive CaP layer to allow for further biological responses to take place. Generally there was a greater release and re-precipitation of calcium and phosphate ions from SA80/30 in comparison to HA80/20 and SA80/20. This greater dissolution and re-precipitation lead to sensitivity in cell response which an increase in osteoblast-like cell proliferation over time under static conditions.

Positive effects of greater silicate ions in culture media on osteoblast-like cell response have been demonstrated previously. These findings support the findings in the present work as SA80/30 observed greater levels of silicate ions within the surrounding media by the end of the circulation study. Subsequently this particular PCM provided a more supportive environment for cell growth and metabolic activity. These findings suggest that greater levels of silicate ions in culture media support positive osteoblast-like cell response.

From these findings it is important to consider the activity of osteoblast-like cells within a dynamic flow perfusion system and monitor dynamic ion exchange and see whether this has an effect on osteoblast-like cell response. The current study was able to show that with the 7D PCM where there were depleted levels of calcium, phosphate and silicate ion levels showed a better cell proliferation with increased total DNA content, however the study showed suppressed levels of ALP activity which in turn meant that cell differentiation was suppressed over all BGS types tested. There was no cell differentiation taking place even though fresh SCM was used as controls. This in turn suggests that the cell seeding density of $4x10^4$ cells/ml might have been too low when tested under static conditions. The following Chapter with endeavour to investigate different cell concentrations along with differing methods of seeding MG63 cells on the porous BGS granules in order to allow for an environment to promote cell differentiation within a dynamic flow perfusion system.

Chapter 9 Investigating Cell Seeding Concentration and Seeding Methods

9.1 Background

From the last chapter it was concluded that the addition of serum proteins regulated ion release from the BGS to the surrounding media and subsequently effected static cell response. It is important to note that the work conducted in the previous chapter has seen a new system being set up which has been able to maintain the pH of the media during the perfusion experiments. However it was interesting to note that once the granules had been seeded with cells under static conditions at a cell concentration of $4x10^4$ cells/ml with regular media changes, the cell metabolic activity of these cells was significantly suppressed (results obtained in Chapter 8) in comparison to the results obtained in earlier (Chapter 4) where the pH became acidic. Another point to note was that there was no evidence of cell differentiation by 5 days (Chapter 8). There was only an elevation of ALP activity where the proliferation was suppressed which gave a false positive for specific ALP activity. Even with fresh SCM as a control, the cells show no differentiation even by 5 days as there are proliferating. This in turn suggests that the cell seeding concentration might be too low at $4x\ 10^4$ cells/ml.

The work carried out for this thesis focused on the development of a 3D perfusion system to monitor behaviour of synthetic bone graft substitute granules and osteoblast-like cell response, therefore it was vital to uniformly introduce osteoblast-like cells to the granules surfaces at a sufficiently high cell concentration for normal cell behaviour to be promoted and monitor the behaviour of the cells *in vitro* on the porous granules. However, there is a lack of methods for homogeneously colonising scaffolds. This in turn limits the maximum volume of the bone grafts.

The aim of the work presented in this chapter was to investigate two methods in order to seed cells on to the porous granules and also consider the cell concentration in order to find a suitable cell concentration and seeding method of the MG63 cells on to the porous silicon substitute hydroxyapatite granules (SA80/20) without causing immense cell death before inserting the cell seeded scaffolds in to the 3D flow perfusion environment for periods of up to 7 days.

9.2 Methodology

Two methods were employed to seed the cells on to the porous SA80/20 scaffolds along with testing 3 different cell seeding concentrations.

METHOD 1 - seeding MG63 cells on 0.45g of porous SA80/20 granules of 1-2mm in size statically in 24 well plates for time points of 0, 1 and 3 days at cell concentrations of $4x10^4$cells/ml, $6x10^4$cells/ml and $8x10^4$cells/ml.

METHOD 2 - seeding MG63 cells directly on to 0.45g of porous SA80/20 granules packed into 8mm diameter and 15mm long silicone tubing for time points of 0, 1 and 3 days at cell concentrations of $4x10^4$cells/ml, $6x10^4$cells/ml and $8x10^4$cells/ml.

Table 9.1: Table highlighting seeding methods and cell concentrations tested

Method	Method Description	Cell Concentrations
Method 1	Seeding cells on SA80/20 in 24 well plates	$4x10^4$ cells/ml
		$6x10^4$ cells/ml
		$8x10^4$ cells/ml
Method 2	Seeding cells directly on SA80/20 within silicon tubes	$4x10^4$ cells/ml
		$6x10^4$ cells/ml
		$8x10^4$ cells/ml

9.2.1 METHOD 1

The 3 different cell concentrations tested of MG63 osteoblast-like cells (P4) were seeded on 0.45g (0.75ml) of SA80/20 granules in 24 well plates in 1ml of SCM and allowed to attach for 2 hours at 37°C and 5% CO_2. The different cell concentrations were tested at n=6.

After 2 hours the SCM was collected and stored from all wells. The granules were then transferred to the silicone tubes of 8mm diameter and 15mm length (sample tubes). 1ml of fresh SCM was added to all the sample tubes.

For the day 0 reading, the cells were left for a further 2 hours before the SCM was collected and stored and the granules were transferred back to a 24 well plate.

The cells were then incubated for a further 1 and 3 days in the sample tubes and the SCM was refreshed at 24 hours. At each time point the SCM was collected and stored and the granules were transferred back to a 24 well plate were 3 of the 6 sample repeats were tested for DNA quantification (protocol can be found in Chapter 4 section 4.2.26) and the remaining 3 were then prepared for Scanning Electron Microscopy (SEM).

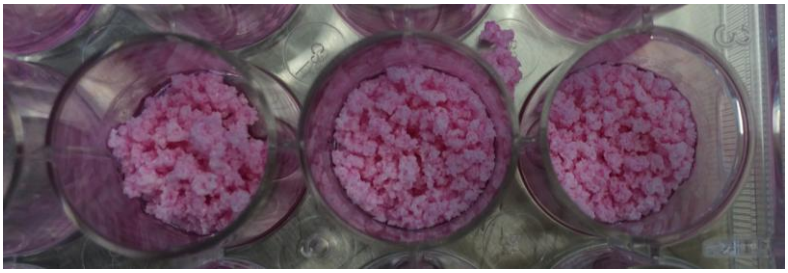

Figure 9.1: SA80/20 granules at day 0, 8x10^4 cell/ml concentration before being transferred to the silicon sample tubes for 2 hours incubation at 37^{o}C, 5% CO_2

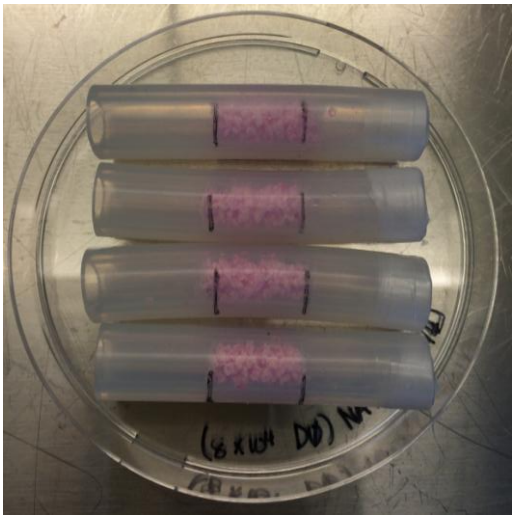

Figure 9.2: SA80/20 granules at day 0, 8x10^4 cell/ml concentration after being transferred to the silicon sample tubes for 2 hours incubation at 37^{o}C, 5% CO_2

9.2.1.1 Scanning Electron Microscopy (SEM)

Following the incubation periods as described above, the samples were transferred from the silicon sample tubes to 24 well plates. The SA80/20 granules were split in to 3 distinctive areas; top, middle and bottom. This was in order to see whether the cells had migrated to the centre of the scaffolds and not just stayed at the top or bottom of the samples tube. Upon collecting the samples in the 24 well plates at the three different section, the samples were

then cooled at 4°C for 30 minutes. The SCM was then removed and stored and the following steps were followed in order to prepare the samples for SEM.

Figure 9.3: SEM preparation set-up under fume hood

SEM preparation should be done under a fume hood due to the carcinogen nature of some of the solvents being used. Lab coats, gloves and goggles should be worn at all times during the SEM preparation process.

- Primarily fix the samples by adding 1ml of 1.5% glutaraldehyde buffered in 0.2M sodium cacodylate (pH 7.2). Keep sample at 4°C for a further 12 hours.
    - Prepare the primary fixative by diluting 1.5ml of 25% glutaraldehyde (Agar, UK) with 11ml of dH_2O to form a 3% solution.
    - Prepare the 0.2M sodium cacodylate buffer (Sigma-Aldrich, UK) by dissolving 4.28g of sodium cacodylate in 100ml of dH_2O. Adjust the pH to be between 7.2 - 7.4 by adding 5M hydrochloric acid (HCL) drop-wise.
    - Mix equal volumes of the 3% glutaraldehyde solution and 0.2M sodium cacodylate buffer to make 1.5 % glutaraldehyde solution and store at 4°C.
    - All waste involving glutaraldehyde should be disposed of separately to other solvents.
- Secondary fix the samples with 1ml of 1% osmium tetroxide buffered in 0.1M sodium cacodylate, and incubate for 60minutes at room temperature.
    - Prepare the secondary fixative by diluting 2% osmium tetroxide (Agar, UK) with an equal volume of 0.2M sodium cacodylate buffer.

- It is vital to handle osmium tetroxide with care as it is a carcinogen solution. Preparation of the 2% solution should be done under a fume hood with all necessary precautions put in place.

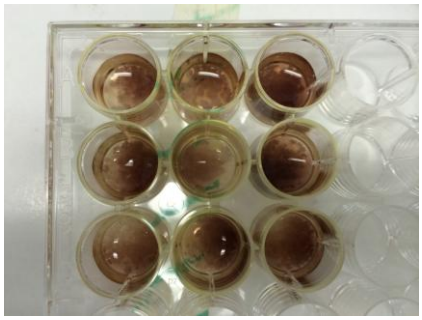

Figure 9.4: Colour change of 2% osmium tetroxide solution once incubated for 60 minutes at room temperature with cell seeded SA80/20 granules

- Wash samples 3 times at 5 minute intervals with 1ml 0.1M sodium cacodylate buffer.
  - All waste involving osmium tetroxide should be disposed of separately to other solvents due to its carcinogenic nature.
- Add 1ml of 1% tannic acid (Sigma-Aldrich, UK) to samples and incubate for 30 minutes at room temperature.
  - Prepare 1% tannic acid by dissolving 0.0255g of tannic acid in 30ml of 0.05M sodium cacodylate buffer (pH7.2-7.4). Tannic acid acts as a mordant which enhances later staining with heavy metals.
- Wash samples twice at 5 minute intervals with 1ml 0.1M sodium cacodylate buffer.
  - All waste involving tannic acid should be disposed of separately to other solvents.
- Carry out dehydration process of the samples by washing the samples twice at 5 minute intervals with 1ml of graded ethyl alcohols (20%, 30%, 40%, 50%, 60%, 70%, 80%, 90%, and 96%).
- Wash samples with 1ml of 100% ethyl alcohol twice at 10minute intervals.
  - All waste involving the different grades of ethyl alcohol should be collected and disposed of separately to other solvents.
- Immerse samples in 1ml hexamethyldisilazane (HMDS), Sigma-Aldrich, UK) for 10 minutes and air dry overnight.
  - All waste involving HMDS should be collected and disposed of separately to other solvents due to its carcinogen nature.
- Finally, mount samples on metal stubs and gold coat samples for SEM imaging.

Figure 9.5: SA80/20 granules mounted on stubs and gold coated ready for SEM imaging

9.2.2 METHOD 2

Before seeding the cell on to the SA80/20 granules, the sample tubes were prepared as previously described in Chapter 4 section 4.2.1.2 but without the addition of the large connectors. These were not needed as the cell seeding concentration and method were being tested.

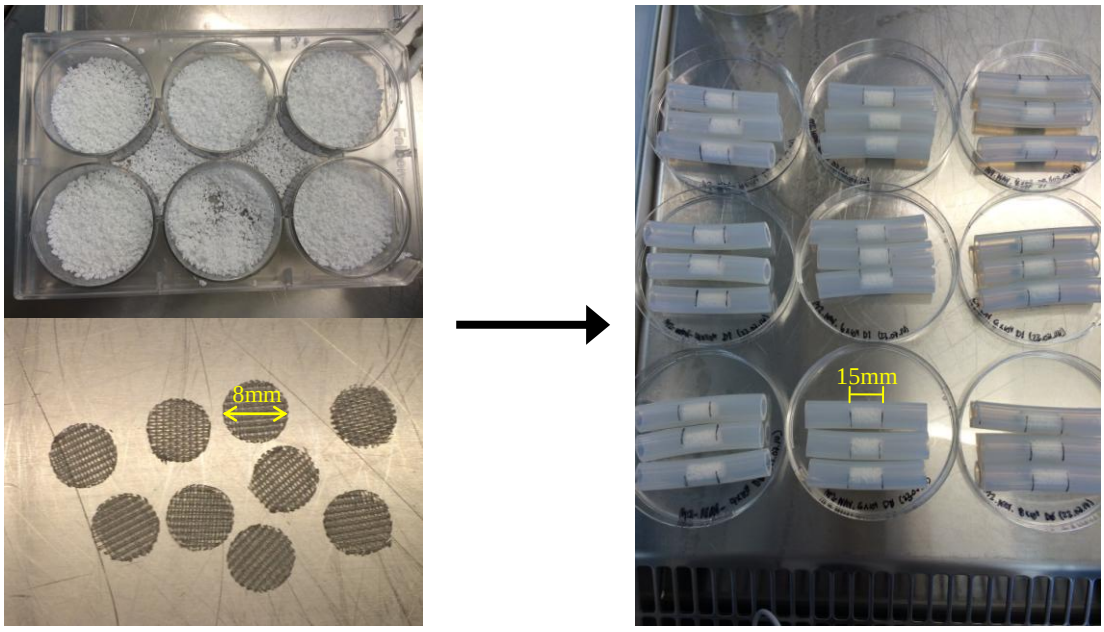

Figure 9.6: Sample tube preparation before seeding them with different cell conc.

The sample tubes were prepared at an n=6. Once the sample tubes had been prepared, the individual tubes containing 0.45g of SA80/20 granules were preconditioned with 200µl of SCM (100µl from either side of the sample tube) for 30 minutes at room temperature.

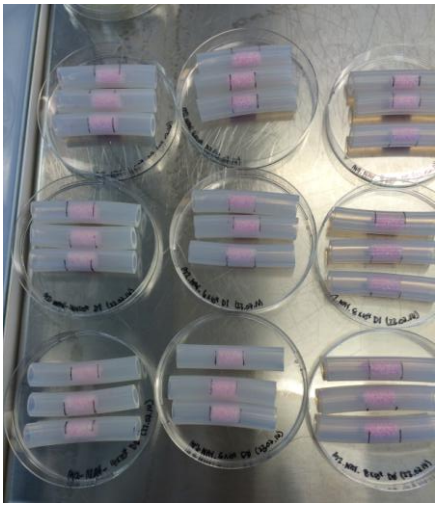

Figure 9.7: SA80/20 sample tubes preconditioned with 200µl of SCM before cell seeding

In the meantime the 3 different cell concentrations tested of MG63 osteoblast-like cells (P4) were made up to the volumes that were needed. It was noted that on a trial run that after preconditioning the granules with 200µl of SCM, the 0.45g of granules could only hold another 500µl of media. Taking this into consideration the 3 different cell concentrations tested were now made up per 500µl and not per 1ml. This in turn meant that the individual cell concentrations were doubled per 1ml so that the maximum cell concentrations of $4x10^4$, $6x10^4$ and $8x10^4$ cells were added to the granule masses.

After 30 minutes, the sample tubes containing the granules were seeded with 500µl of the 3 different cell concentrations and then allowed to attach for 2 hours at 37°C, 5% CO_2. After 2 hours the SCM was collected and stored from the day 0 samples. The granules were then transferred from the sample tubes to a 24 well plate.

The cells were then incubated for a further 1 and 3 days in the sample tubes and the SCM was refreshed at 24 hours. At each time point the SCM was collected and stored and the granules were transferred back to a 24 well plate were 3 of the 6 sample repeats were tested for DNA quantification (protocols found in Chapter 4 section 4.2.26) and the remaining 3 were then prepared for SEM as described above in section 9.2.1.1.

9.2.3 Statistical Analysis

All collected data was conducted at n=6 and analysed and expressed in terms of mean ± standard deviation. Statistical significance was evaluated using ANOVA, Post Hoc test: Tukey HSD with $\alpha=0.05$, (where *$p<0.05$, **$p<0.01$ and ***$p<0.005$).

9.3 Results

9.3.1 METHOD 1

The SEM images obtained from granules seeded using the lower concentration of $4x10^4$ cells/ml, suggest that over 3 days in culture significant levels of osteoblast-like cell attachment and growth was not observed. Day 0, showed no cell attachment on the surface of the SA80/20 granules at either of the sections taken (Figure 9.8, Figure 9.9 and Figure 9.10). This same behaviour was also apparent on day 1 (Figure 9.11, Figure 9.12 and Figure 9.13 respectively) and on day 3 (Figure 9.14, Figure 9.15 and Figure 9.16).

The SEM images observed for the second concentration of cells that was tested; $6x10^4$ cells/ml showed cell attachment on the later days in culture. At day 0, there were no cells observed at the surface of the SA80/20 granules (Figure 9.17, Figure 9.18 and Figure 9.19). However, at day 1 there were cells that were observed at the top and bottom sections collected from the samples tubes. There were no cell observed in the middle section of the SA80/20 sample tube suggesting that the cells had not migrated to the centre of the cylindrical sample tube (Figure 9.20, Figure 9.21 and Figure 9.22). This trend was also observed on day 3 (Figure 9.23, Figure 9.24 and Figure 9.25).

The greatest cell concentration tested was $8x10^4$ cells/ml. There was cell attachment observed on all the days at all the sections taken and tested throughout the SA80/20 sample tubes. At day 0, cells were seen at the lower and higher magnifications (Figure 9.26, Figure 9.27 and Figure 9.28). The same behaviour was seen on day 1 (Figure 9.29, Figure 9.30 and Figure 9.31) and at day 3 (Figure 9.32, Figure 9.33 and Figure 9.34). Even though cells were seen on all days and at all section on the granules, there were not very many cells observed. By day 1 and day 3, cell growth was not seen to increase.

4x10^4 cells/ml (a: 2400/5000 mag & b: 10000 mag)

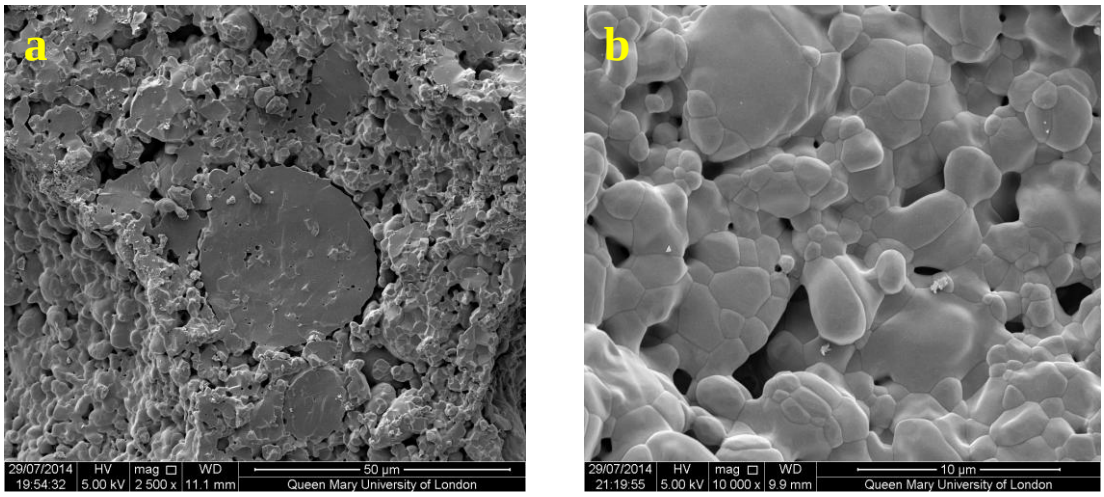

Figure 9.8: MG63 cells seeded at a cell conc. of 4x10^4 cells/ml at DAY 0 (TOP)

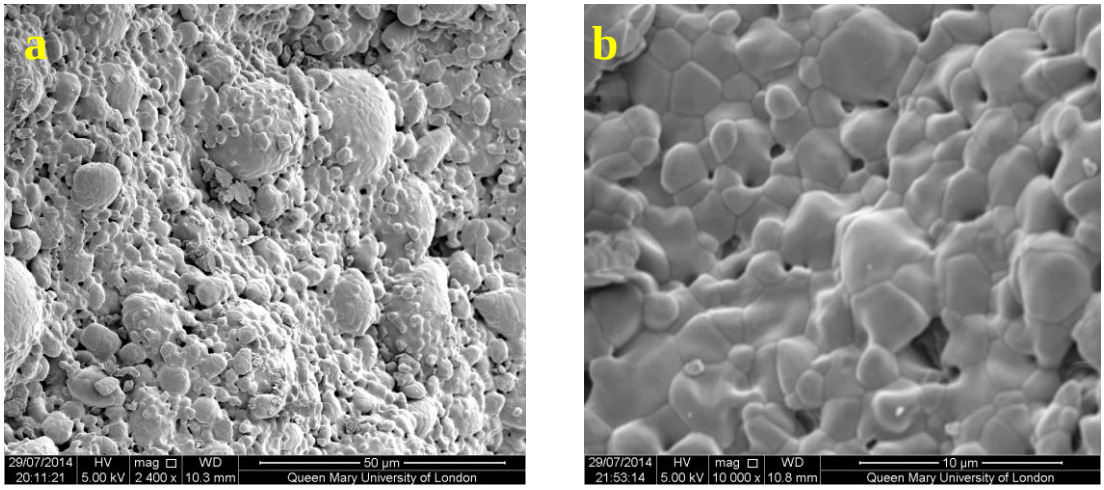

Figure 9.9: MG63 cells seeded at a cell conc. of 4x10^4 cells/ml at DAY 0 (MIDDLE)

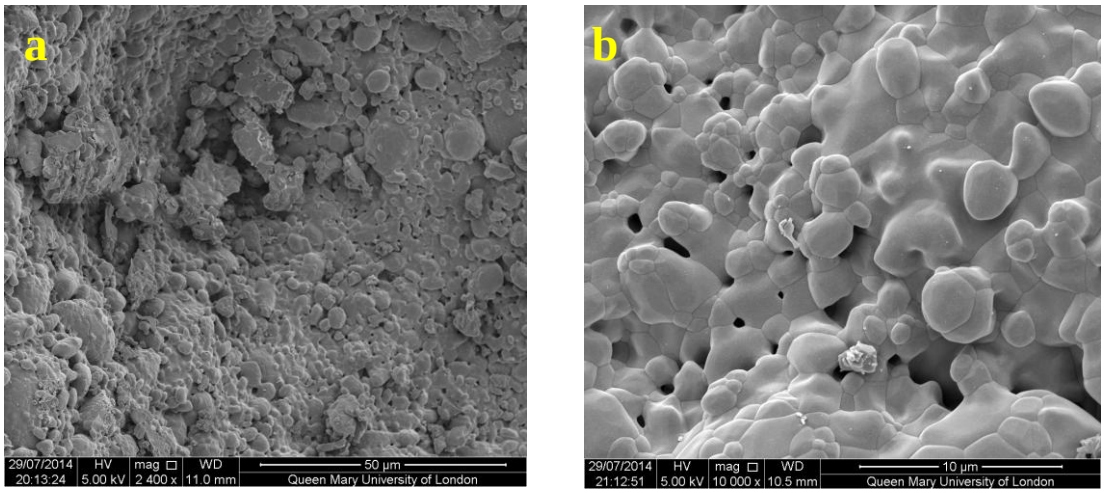

Figure 9.10: MG63 cells seeded at a cell conc. of 4x10^4 cells/ml at DAY 0 (BOTTOM)

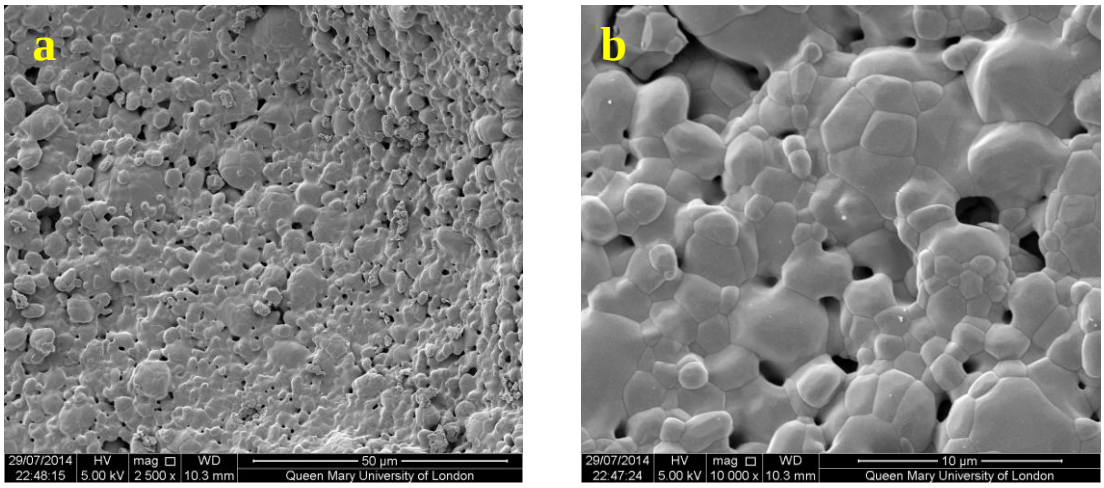

Figure 9.11: MG63 cells seeded at a cell conc. of 4x10^4 cells/ml at DAY 1 (TOP)

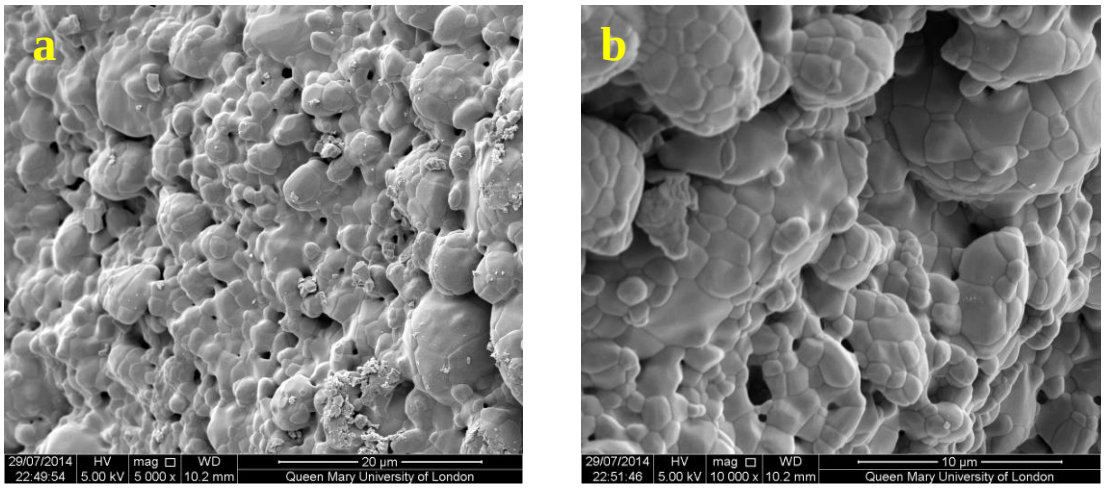

Figure 9.12: MG63 cells seeded at a cell conc. of 4x10^4 cells/ml at DAY 1 (MIDDLE)

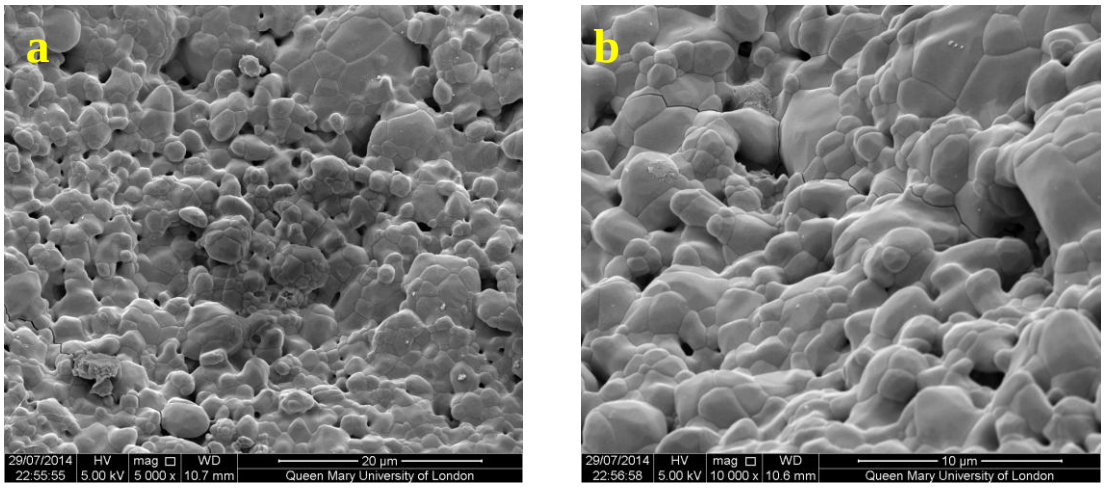

Figure 9.13: MG63 cells seeded at a cell conc. of 4x10^4 cells/ml at DAY 1 (BOTTOM)

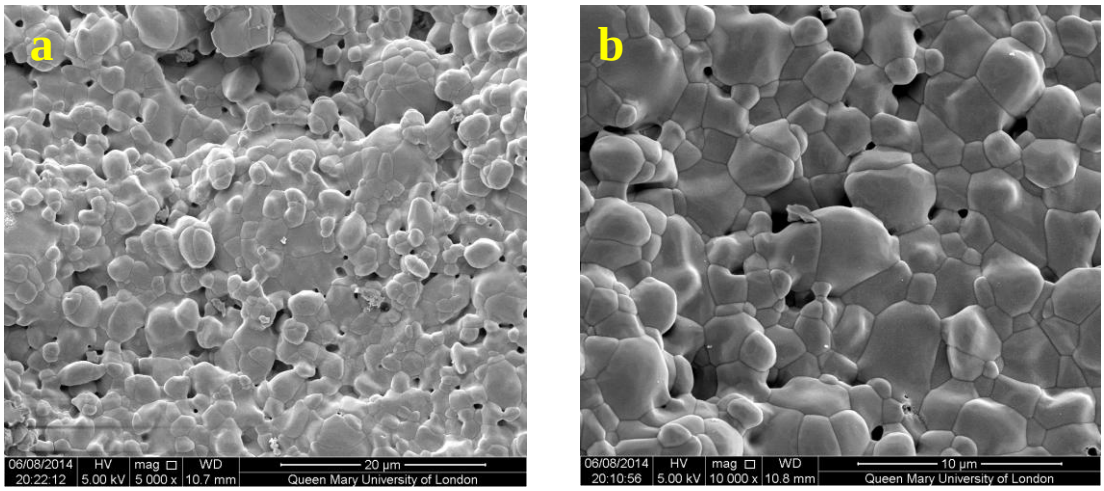

Figure 9.14: MG63 cells seeded at a cell conc. of 4x10^4 cells/ml at DAY 3 (TOP)

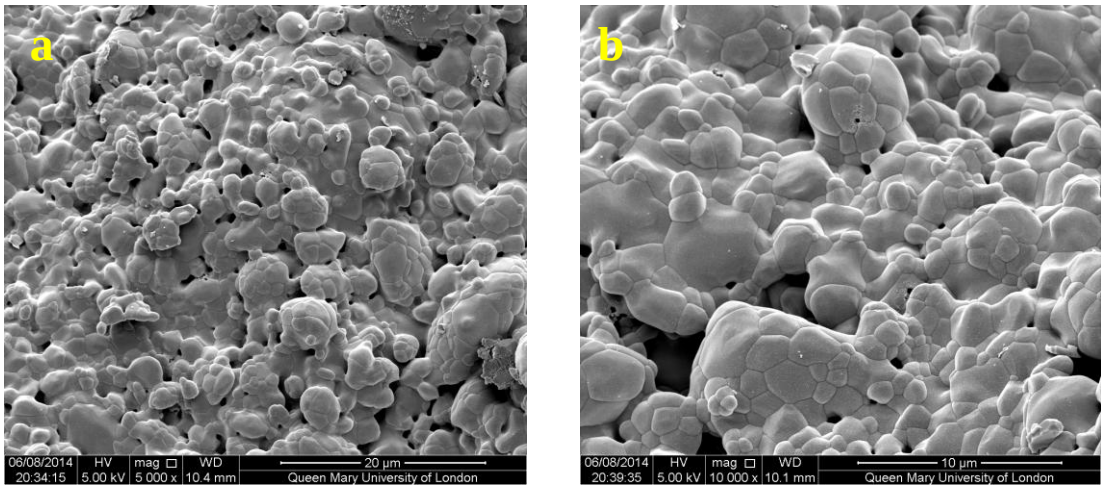

Figure 9.15: MG63 cells seeded at a cell conc. of 4x10^4 cells/ml at DAY 3 (MIDDLE)

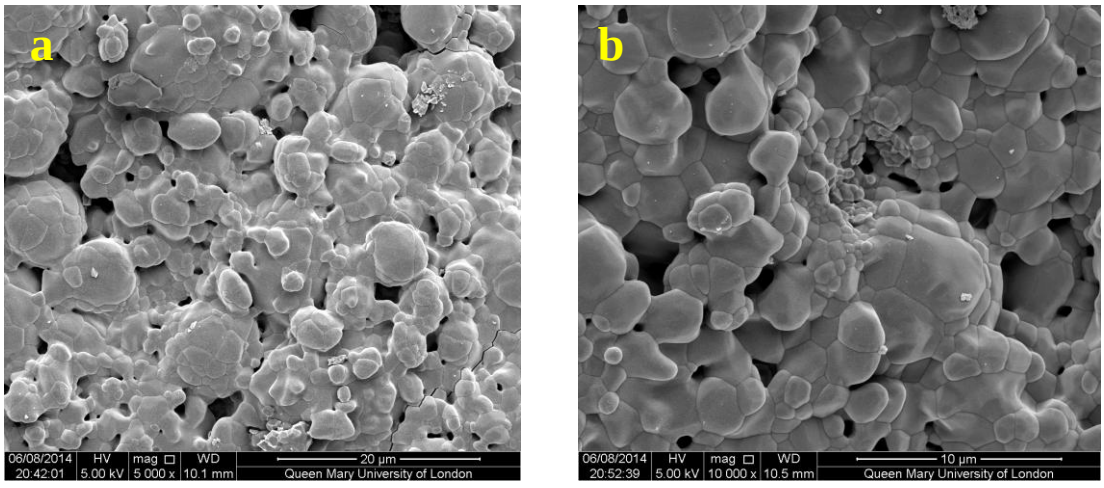

Figure 9.16: MG63 cells seeded at a cell conc. of 4x10^4 cells/ml at DAY 3 (BOTTOM)

6x10^{4}cells/ml (a: 2400/5000mag & b: 10000 mag)

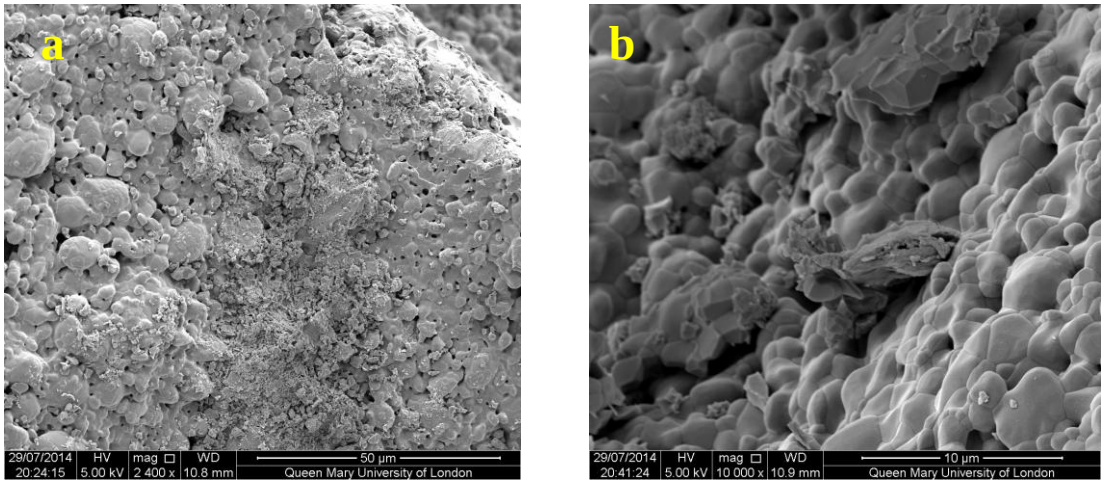

Figure 9.17: MG63 cells seeded at a cell conc. of 6x10^4 cells/ml at DAY 0 (TOP)

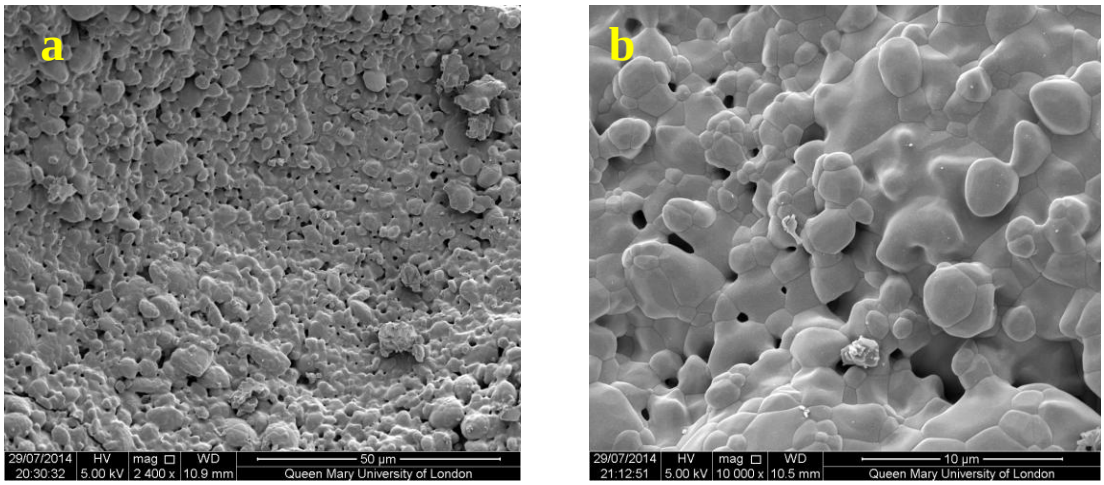

Figure 9.18: MG63 cells seeded at a cell conc. of 6x10^4 cells/ml at DAY 0 (MIDDLE)

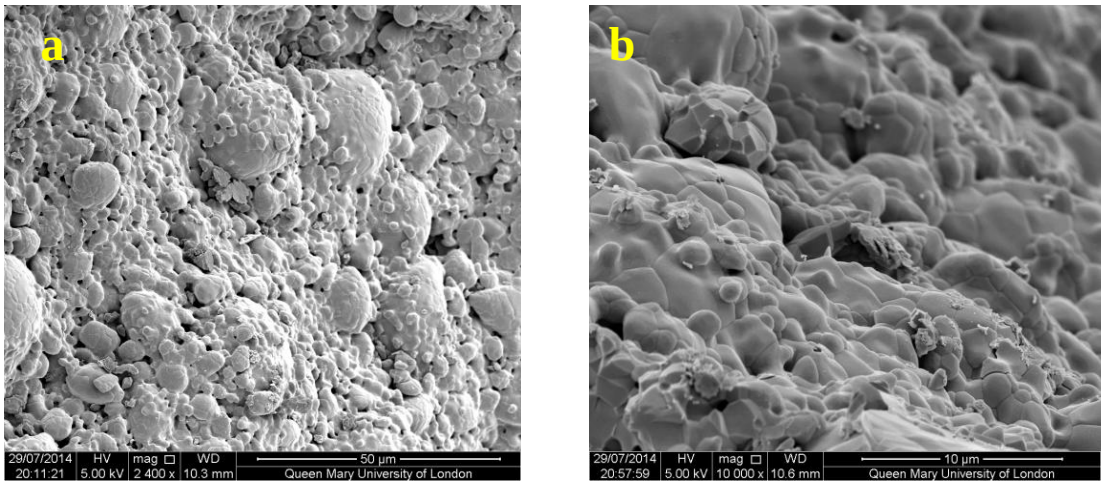

Figure 9.19: MG63 cells seeded at a cell conc. of 6x10^4 cells/ml at DAY 0 (BOTTOM)

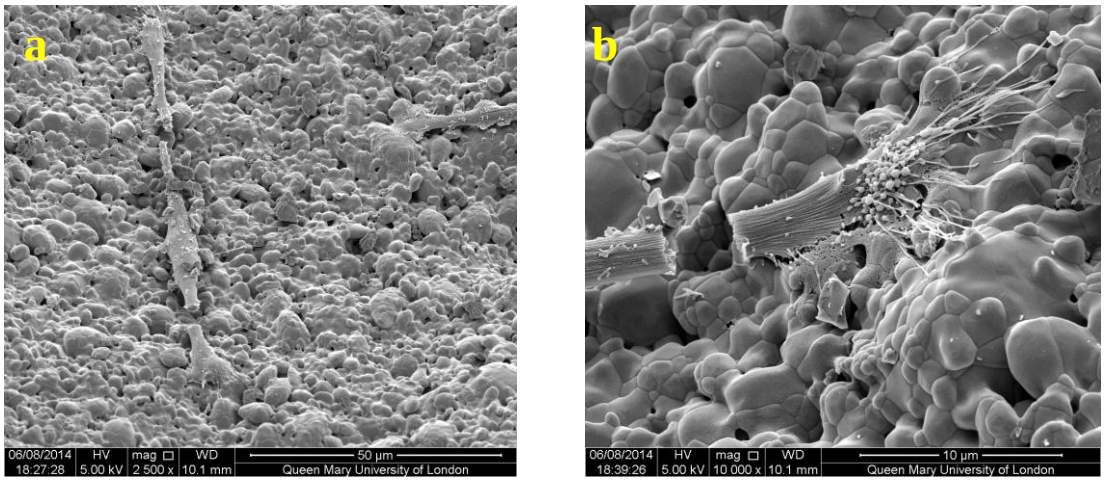

Figure 9.20: MG63 cells seeded at a cell conc. of 6x10^4 cells/ml at DAY 1 (TOP)

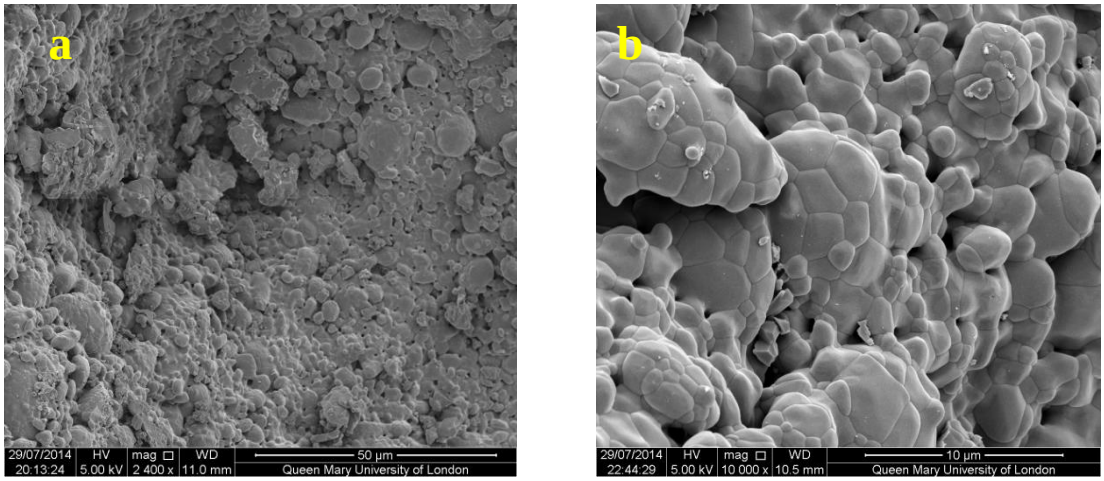

Figure 9.21: MG63 cells seeded at a cell conc. of 6x10^4 cells/ml at DAY 1 (MIDDLE)

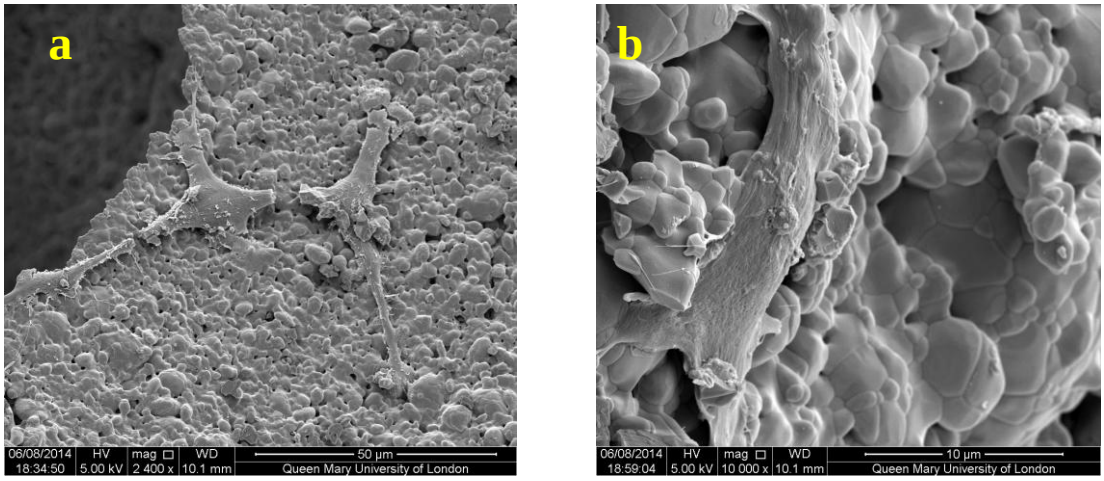

Figure 9.22: MG63 cells seeded at a cell conc. of 6x10^4 cells/ml at DAY 1 (BOTTOM)

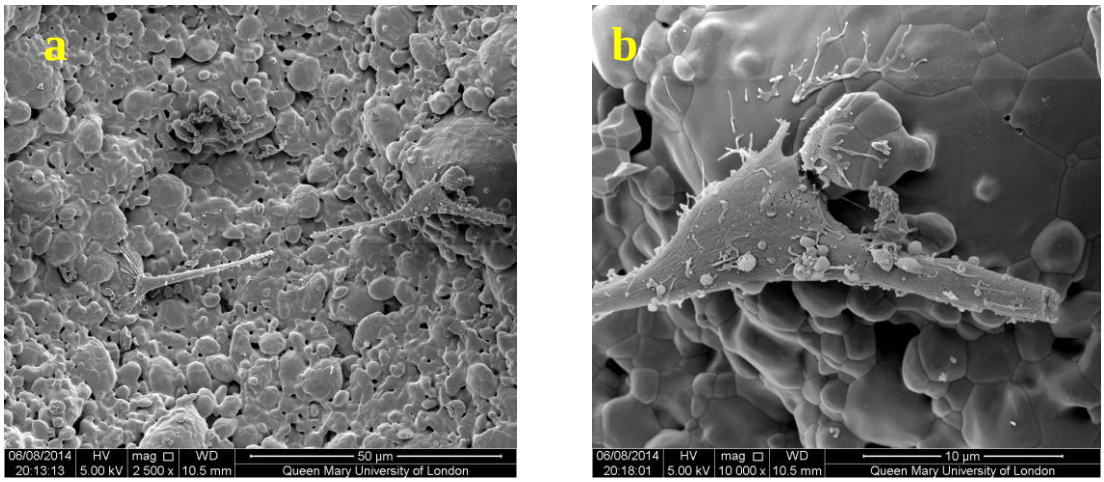

Figure 9.23: MG63 cells seeded at a cell conc. of 6x10^4 cells/ml at DAY 3 (TOP)

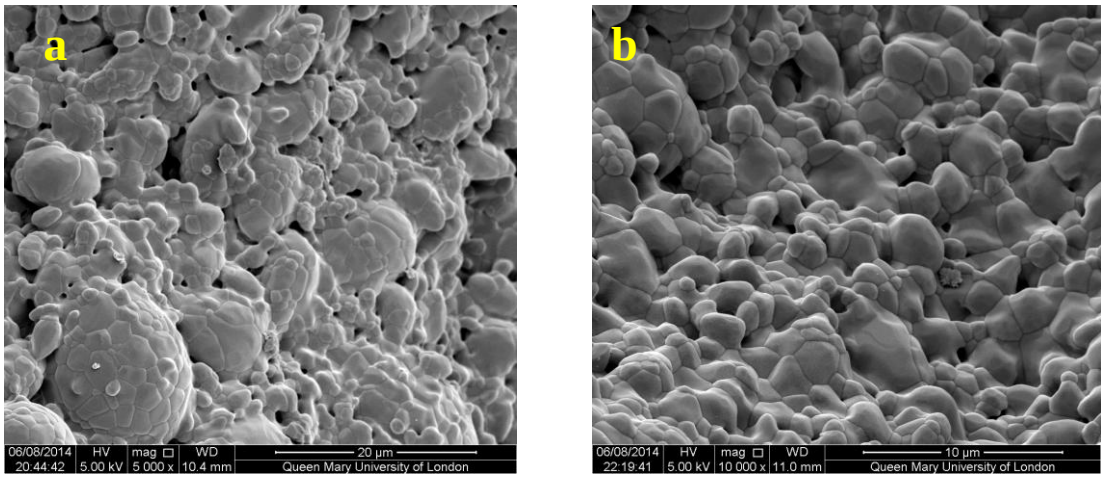

Figure 9.24: MG63 cells seeded at a cell conc. of 6x10^4 cells/ml at DAY 3 (MIDDLE)

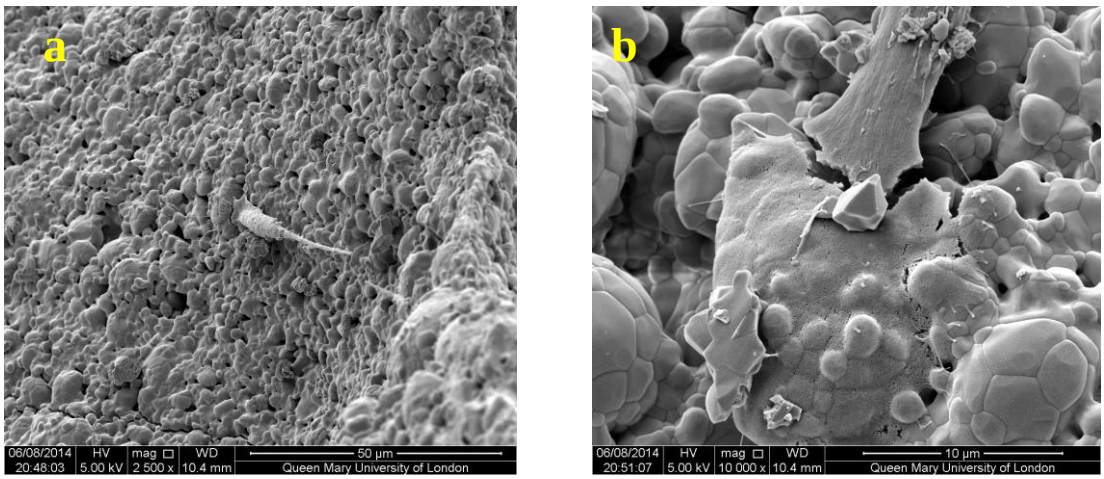

Figure 9.25: MG63 cells seeded at a cell conc. of 6x10^4 cells/ml at DAY 3 (BOTTOM)

8x10^4 cells/ml (a: 2400/5000 mag, b: 10000 mag)

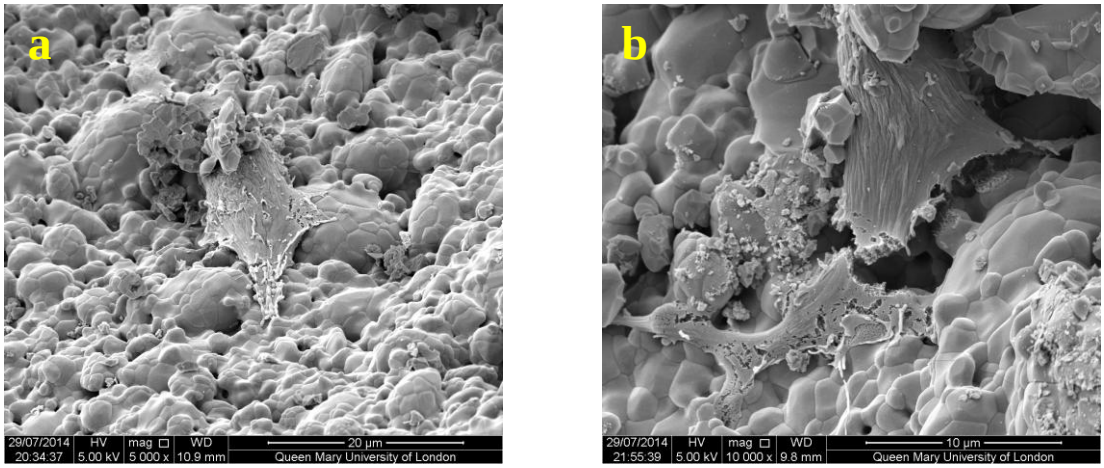

Figure 9.26: MG63 cells seeded at a cell conc. of 8x10^4 cells/ml at DAY 0 (TOP)

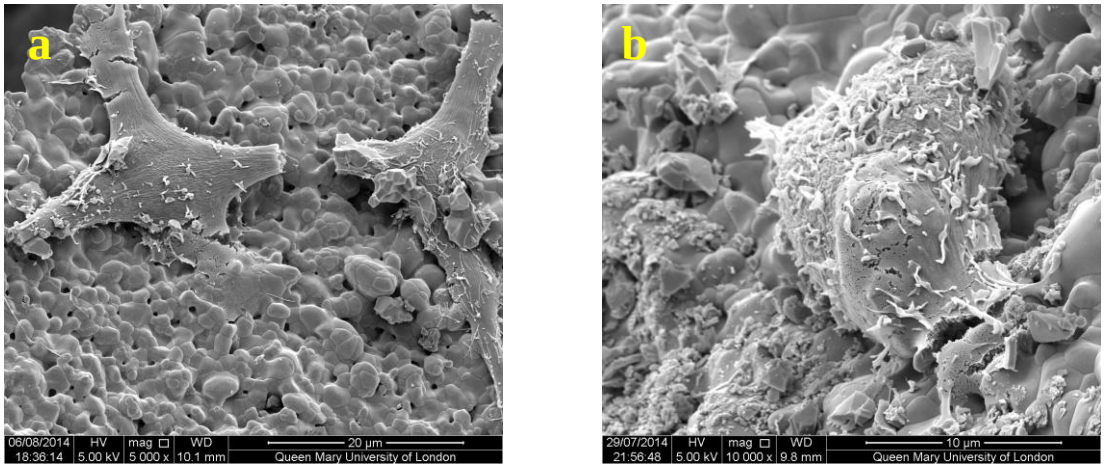

Figure 9.27: MG63 cells seeded at a cell conc. of 8x10^4 cells/ml at DAY 0 (MIDDLE)

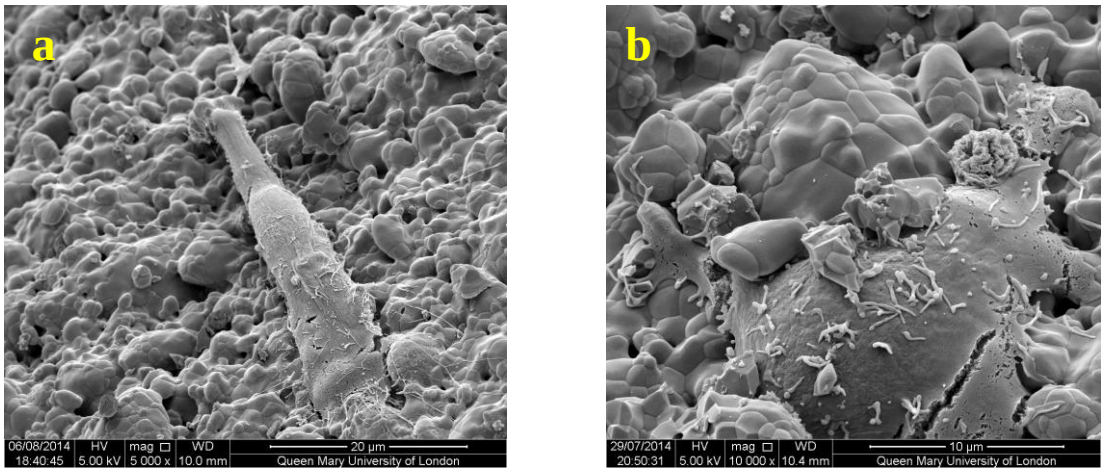

Figure 9.28: MG63 cells seeded at a cell conc. of 8x10^4 cells/ml at DAY 0 (BOTTOM)

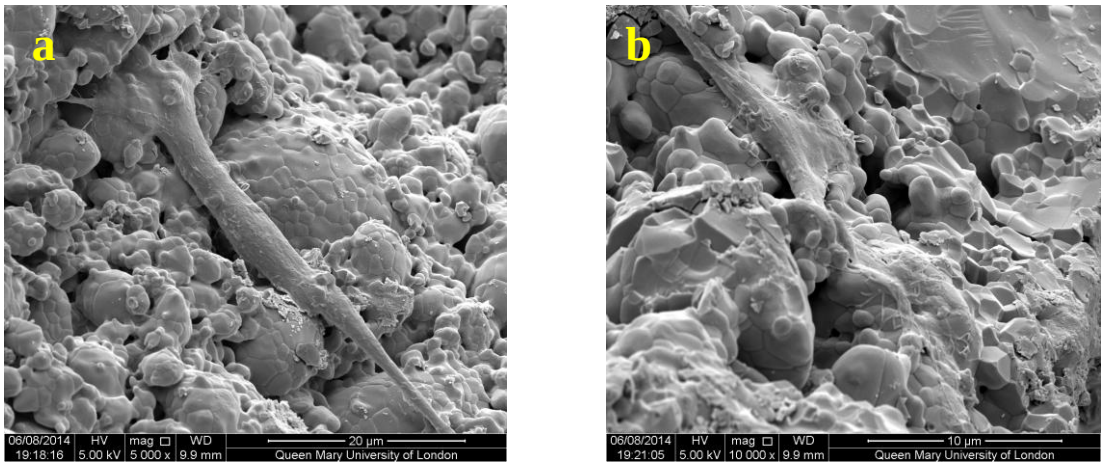

Figure 9.29: MG63 cells seeded at a cell conc. of 8x10^4 cells/ml at DAY 1 (TOP)

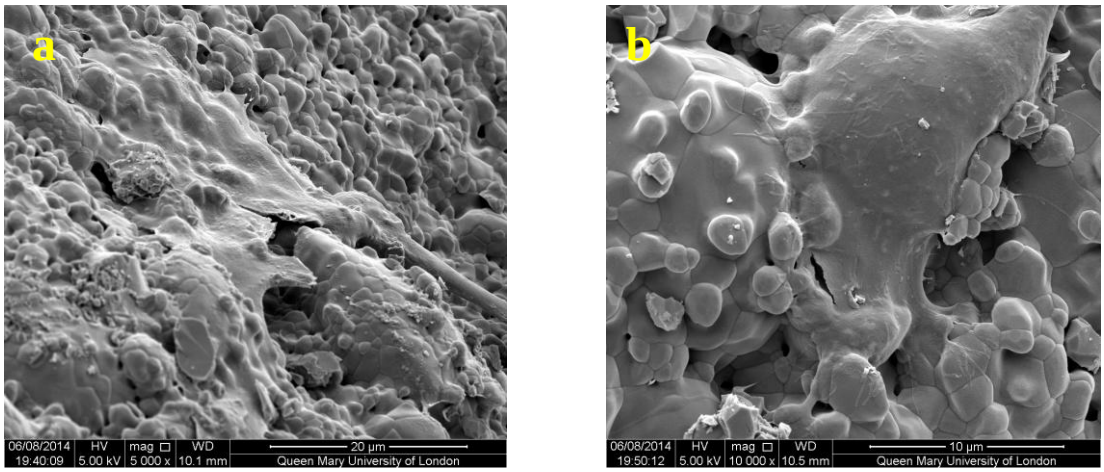

Figure 9.30: MG63 cells seeded at a cell conc. of 8x10^4 cells/ml at DAY 1 (MIDDLE)

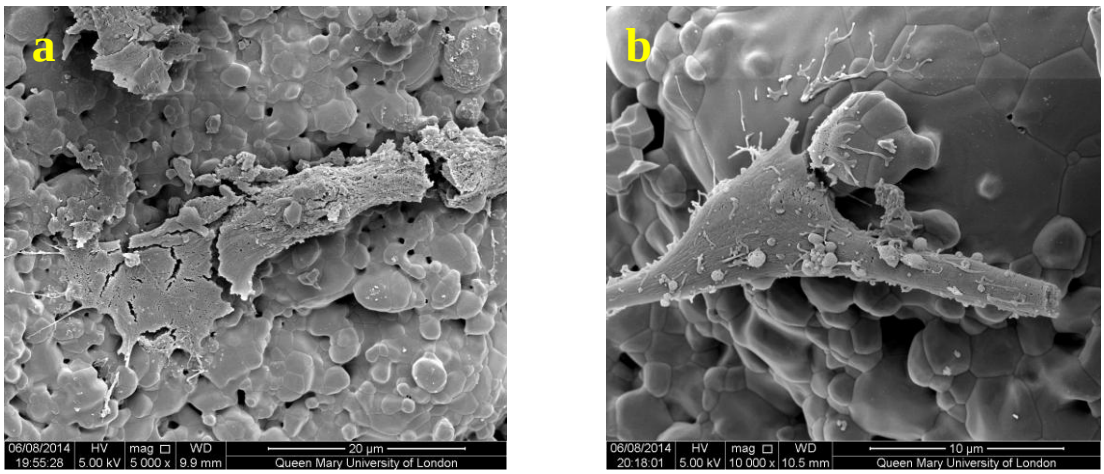

Figure 9.31: MG63 cells seeded at a cell conc. of 8x10^4 cells/ml at DAY 1 (BOTTOM)

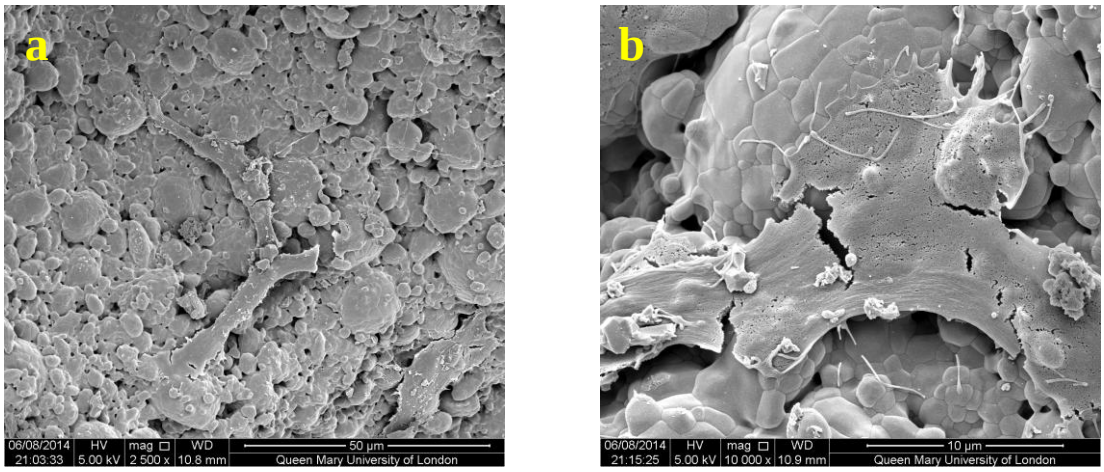

Figure 9.32: MG63 cells seeded at a cell conc. of 8x10^4 cells/ml at DAY 3 (TOP)

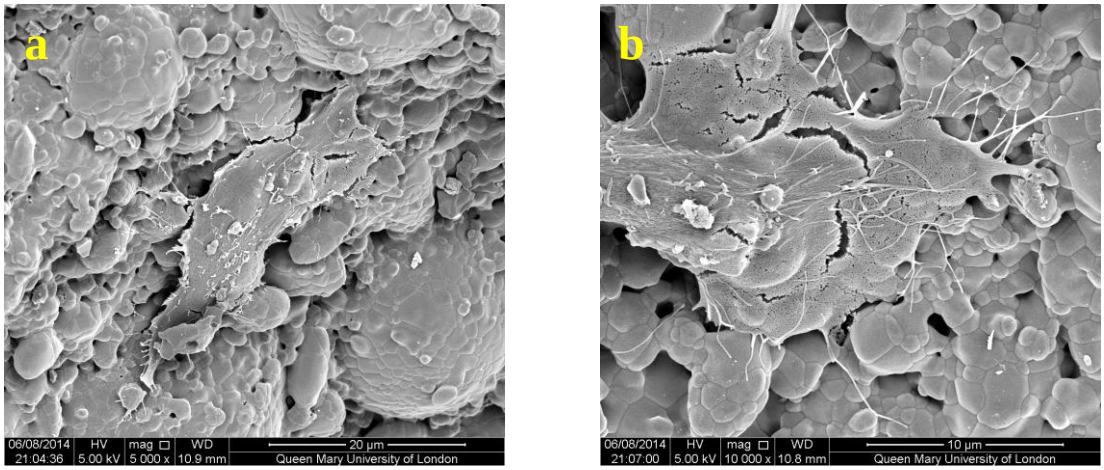

Figure 9.33: MG63 cells seeded at a cell conc. of 8x10^4 cells/ml at DAY 3 (MIDDLE)

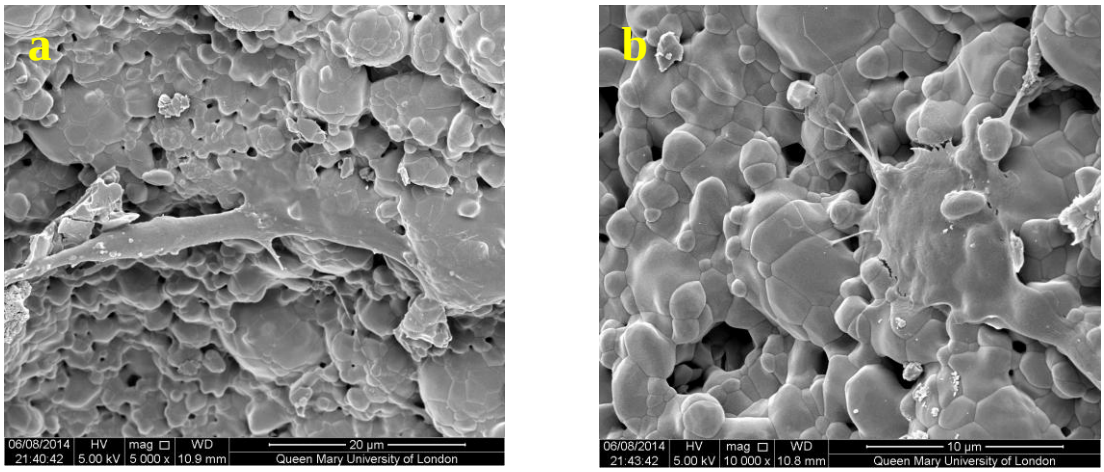

Figure 9.34: MG63 cells seeded at a cell conc. of 8x10^4 cells/ml at DAY 3 (BOTTOM)

The qualitative observations of the SEM analysis was corroborated by the quantitative analysis of total DNA detailed in Figure 9.35. From the DNA results, the highest cell concentration used had a significantly greater level of cell attachment in comparison to the other two lower cell concentrations tested. With the two lower cell concentrations, the total DNA was not significantly different in comparison to one another and over three days the differences between the lower two cell concentrations remained statistically similar.

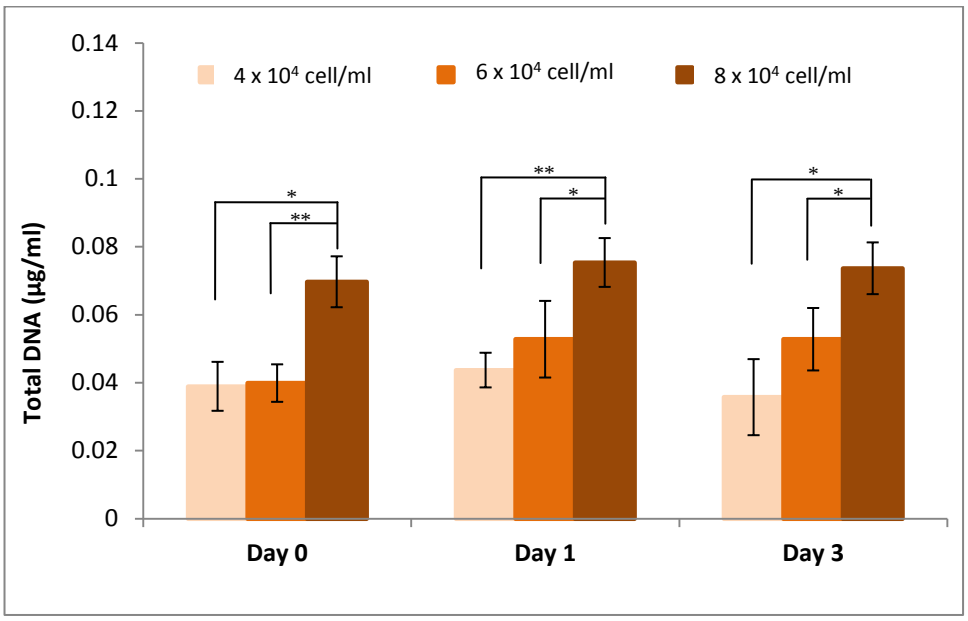

Figure 9.35: DNA conc. observed for all cell concentrations tested for 3 days using Method 1 (n=6)

9.3.2 METHOD 2

The SEM images obtained from the lowest concentration of cells that were used ($4x10^4$ cells/ml), show that at day 0 and day 1 no cells were visible on the surface of the SA80/granules at any of the sections taken from the sample tube (Figure 9.36Figure 9.37Figure 9.38 and Figure 9.39Figure 9.40Figure 9.41 respectively). However by day 3 there were cells seen attached to the surface of the SA80/20 granules. The cells were observed at all the sections taken within the sample tube (Figure 9.42Figure 9.43Figure 9.44).

The second cell concentration tested was $6x10^4$ cells/ml. There was cell attachment observed on all the days at all the sections taken and tested throughout the SA80/20 sample tubes. At day 0, cells were seen at the lower and higher magnifications (Figure 9.45Figure 9.46Figure 9.47). The same behaviour was seen on day 1 (Figure 9.48Figure 9.49Figure 9.50) and at day 3 (Figure 9.51Figure 9.52Figure 9.53). Even though cells were seen on all days and at all section, there were not very many cells observed. By day 1 and even day 3, the cell growth was not seen to increase.

The final cell concentration tested was $8x10^4$ cells/ml. Cell attachment was observed on all days throughout all the sections taken of the SA80/20 granules from the samples tubes. This suggested that there was good migration of the cells to the centre of the sample tubes. At day 0, there were clusters of cells seen at the granules surface (Figure 9.54Figure 9.55Figure 9.56). At day 1, the cells look more spread in shape covering greater surface of the granules (Figure 9.57Figure 9.58Figure 9.59). With an increase in time, cell attachment became more prominent. At day 3 there was a wider spread of confluent cells, almost 'sheet-like' in nature which were observed on the granule surface (Figure 9.60Figure 9.61Figure 9.62).

4x10^4 cells/ml (a: 2400/5000 mag, b: 10000 mag)

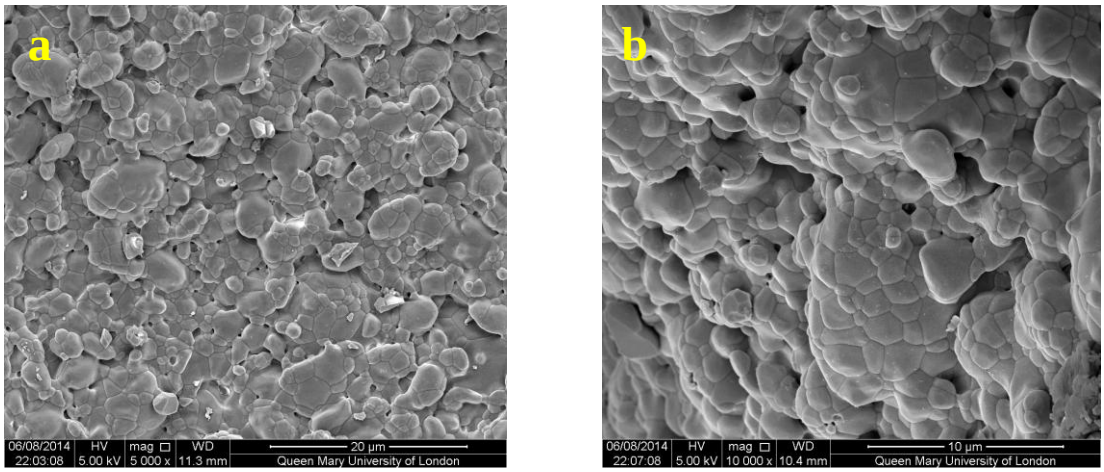

Figure 9.36: MG63 cells seeded at a cell conc. of 4x10^4 cells/ml at DAY 0 (TOP)

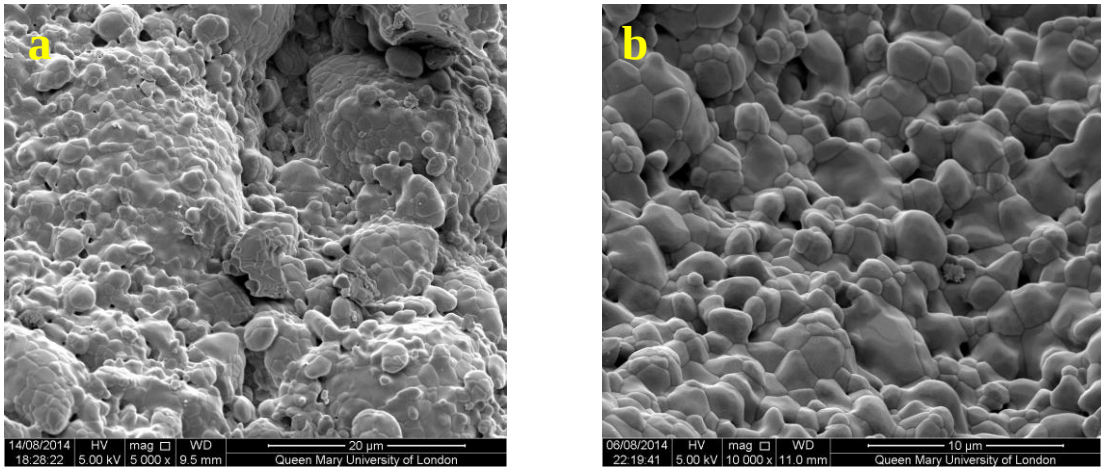

Figure 9.37: MG63 cells seeded at a cell conc. of 4x10^4 cells/ml at DAY 0 (MIDDLE)

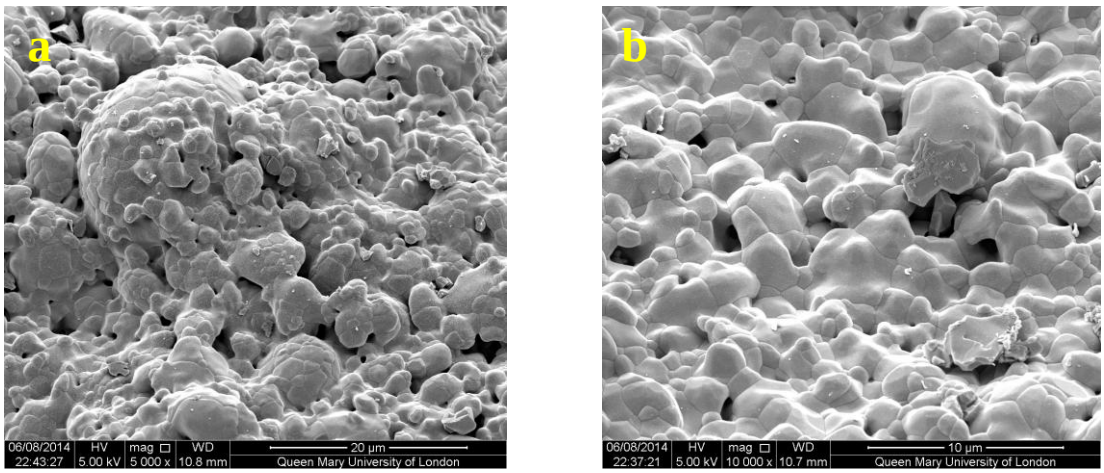

Figure 9.38: MG63 cells seeded at a cell conc. of 4x10^4 cells/ml at DAY 0 (BOTTOM)

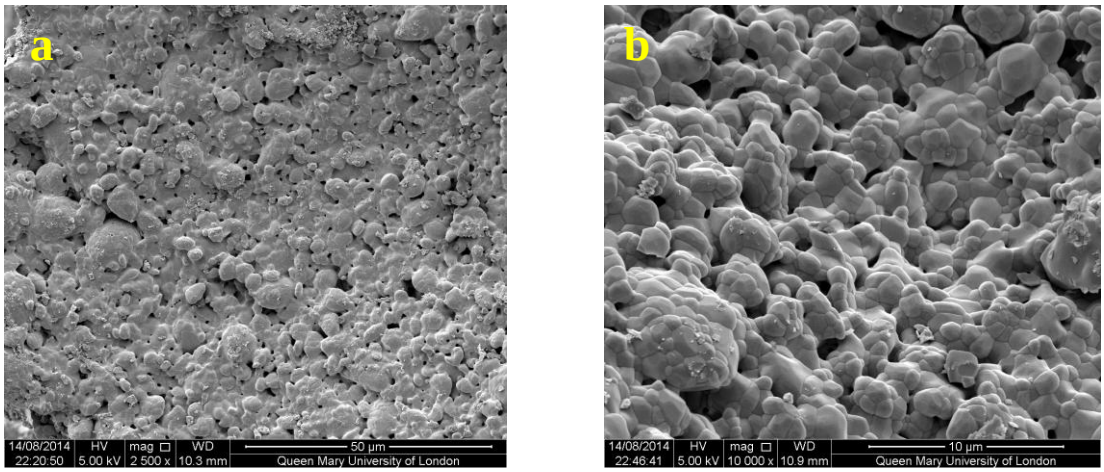

Figure 9.39: MG63 cells seeded at a cell conc. of 4x10^4 cells/ml at DAY 1 (TOP)

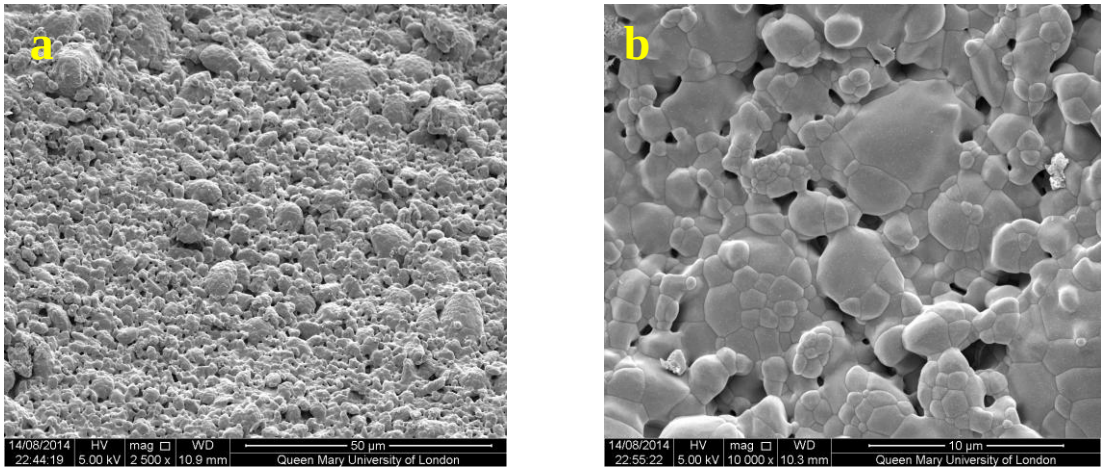

Figure 9.40: MG63 cells seeded at a cell conc. of 4x10^4 cells/ml at DAY 1 (MIDDLE)

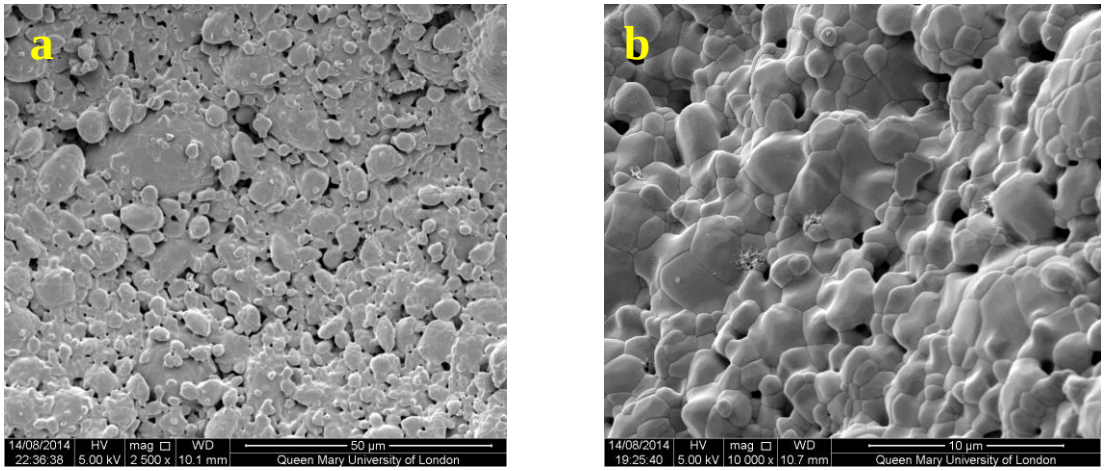

Figure 9.41: MG63 cells seeded at a cell conc. of 4x10^4 cells/ml at DAY 1 (BOTTOM)

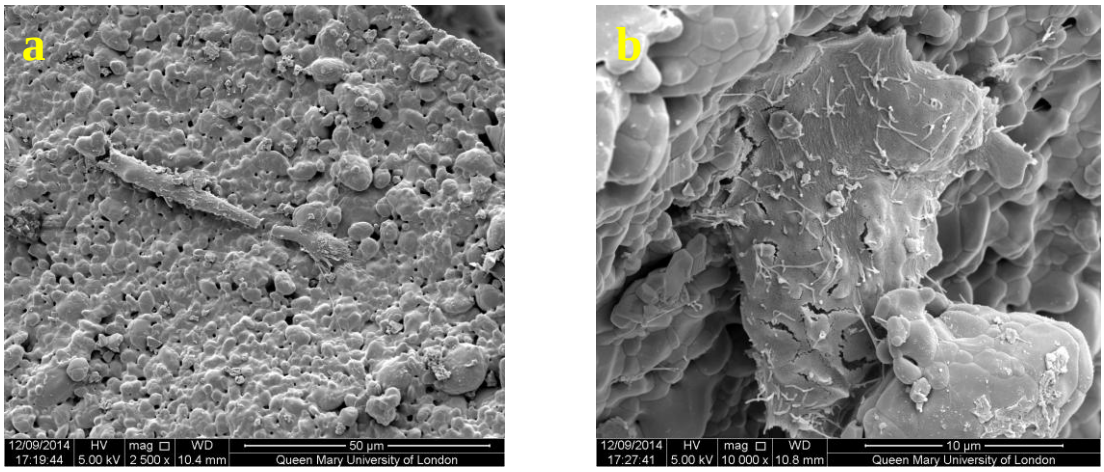

Figure 9.42: MG63 cells seeded at a cell conc. of 4x10^4 cells/ml at DAY 3 (TOP)

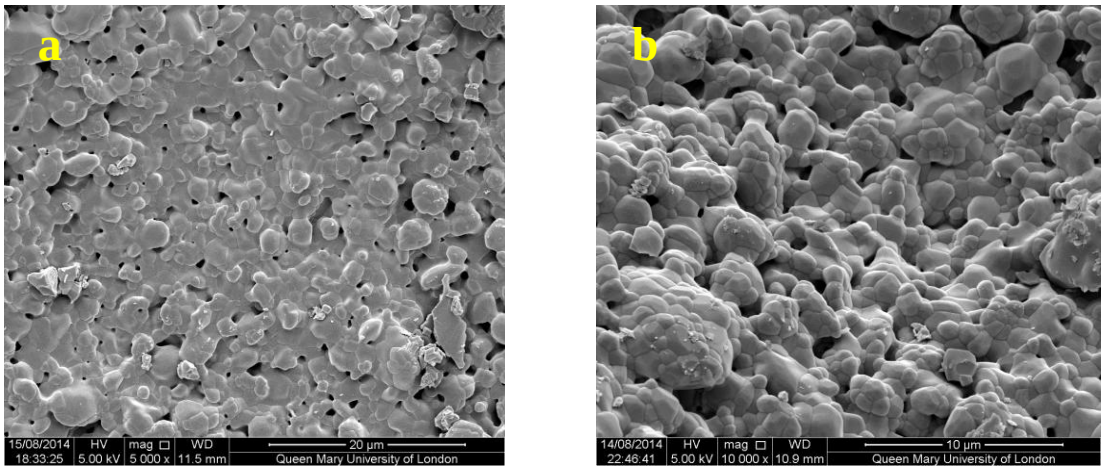

Figure 9.43: MG63 cells seeded at a cell conc. of 4x10^4 cells/ml at DAY 3 (MIDDLE)

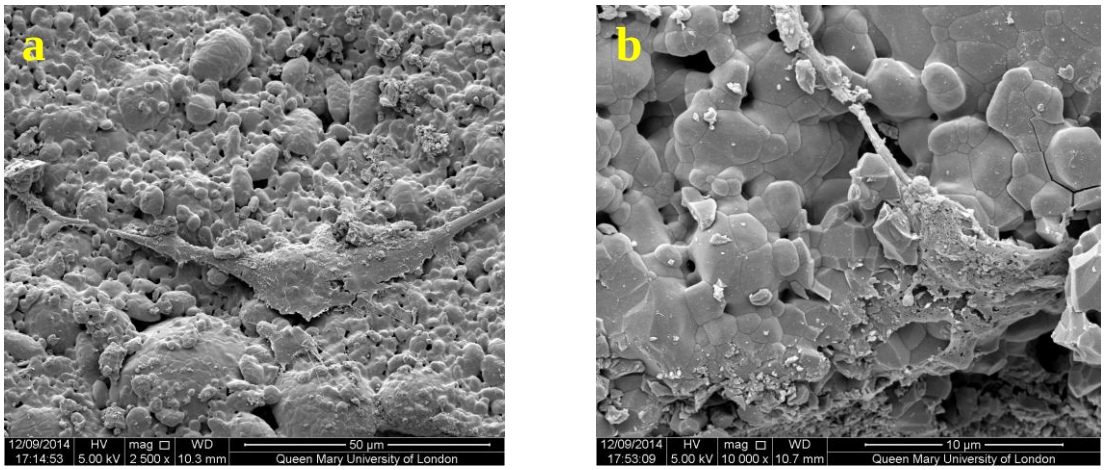

Figure 9.44: MG63 cells seeded at a cell conc. of 4x10^4 cells/ml at DAY 3 (BOTTOM)

6x10^4 cells/ml (a: 2400/5000 mag, b: 10000 mag)

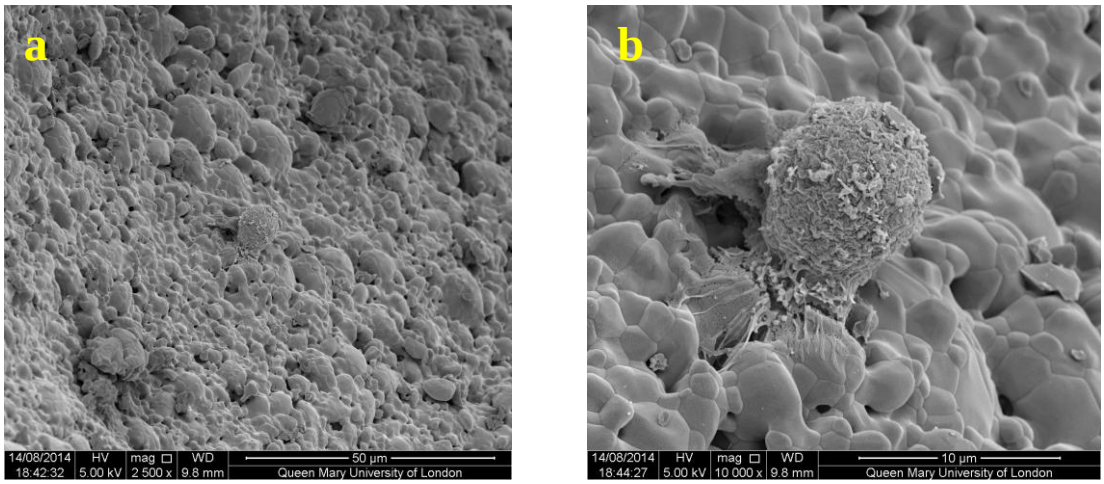

Figure 9.45: MG63 cells seeded at a cell conc. of 6x10^4 cells/ml at DAY 0 (TOP)

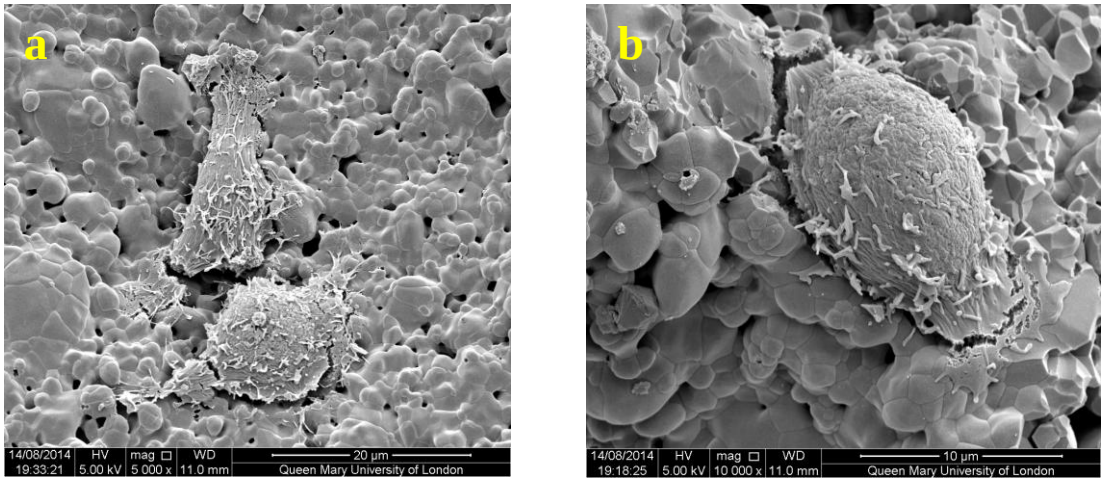

Figure 9.46: MG63 cells seeded at a cell conc. of 6x10^4 cells/ml at DAY 0 (MIDDLE)

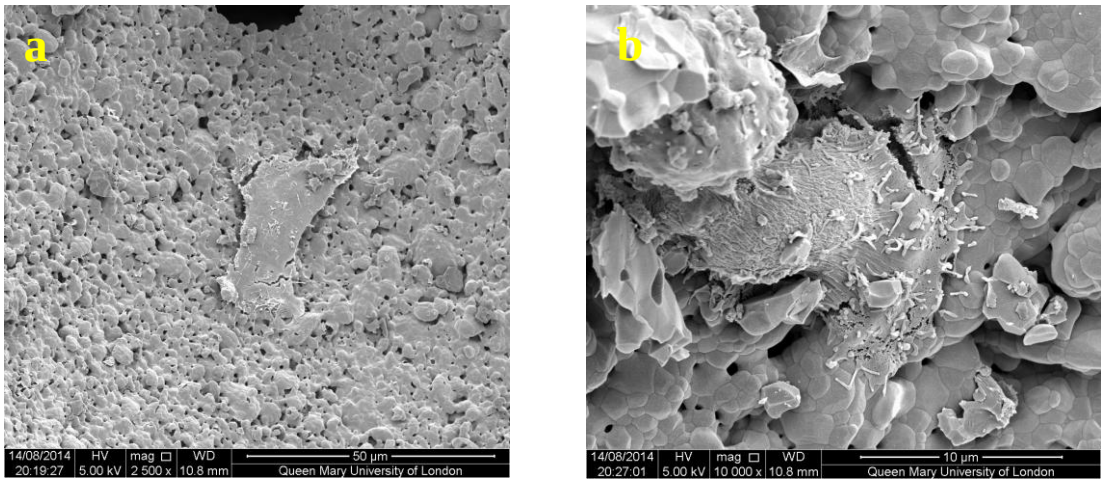

Figure 9.47: MG63 cells seeded at a cell conc. of 6x10^4 cells/ml at DAY 0 (BOTTOM)

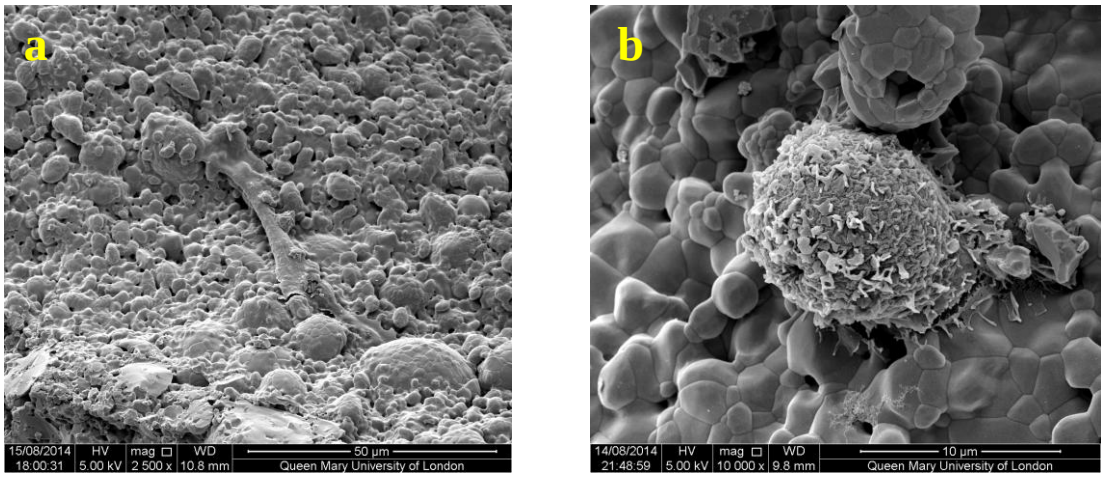

Figure 9.48: MG63 cells seeded at a cell conc. of 6x10^4 cells/ml at DAY 1 (TOP)

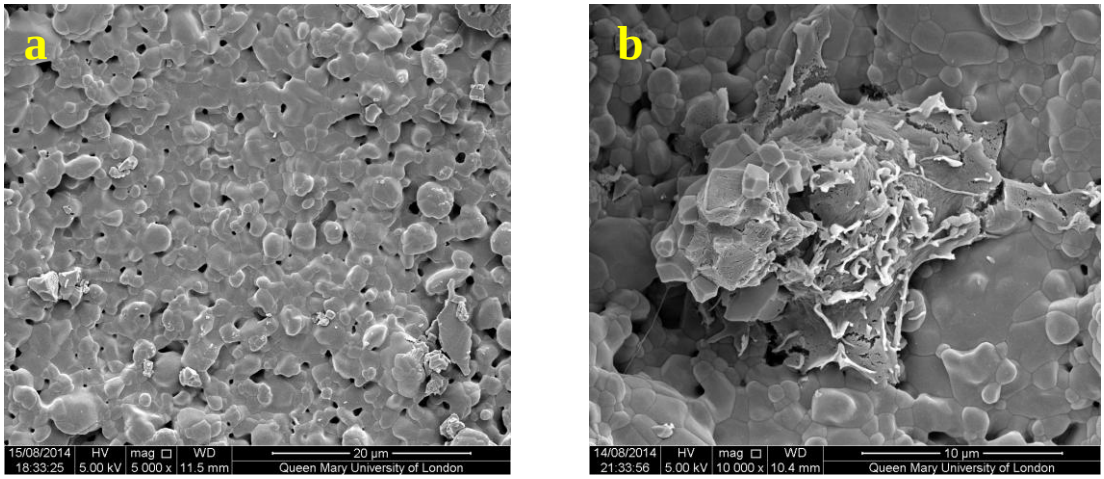

Figure 9.49: MG63 cells seeded at a cell conc. of 6x10^4 cells/ml at DAY 1 (MIDDLE)

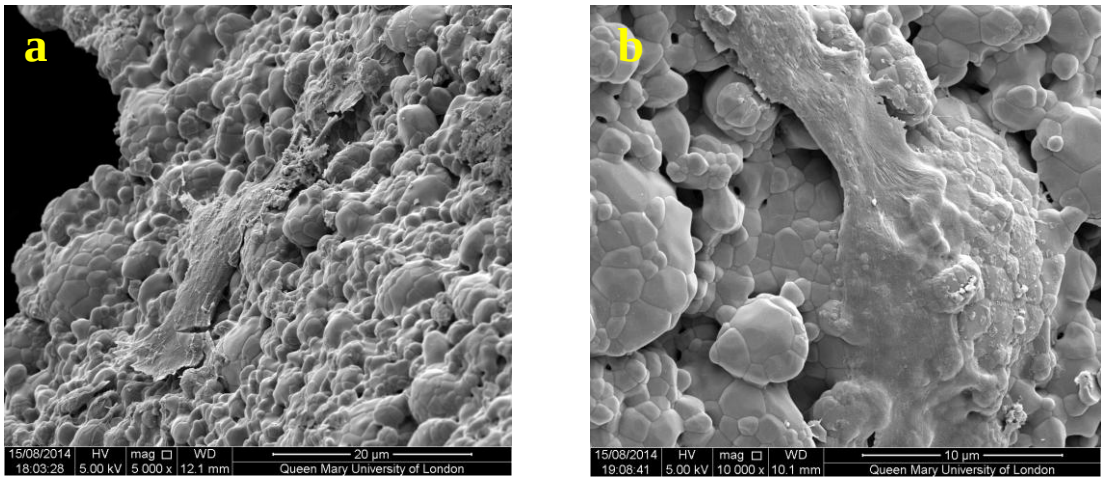

Figure 9.50: MG63 cells seeded at a cell conc. of 6x10^4 cells/ml at DAY 1 (BOTTOM)

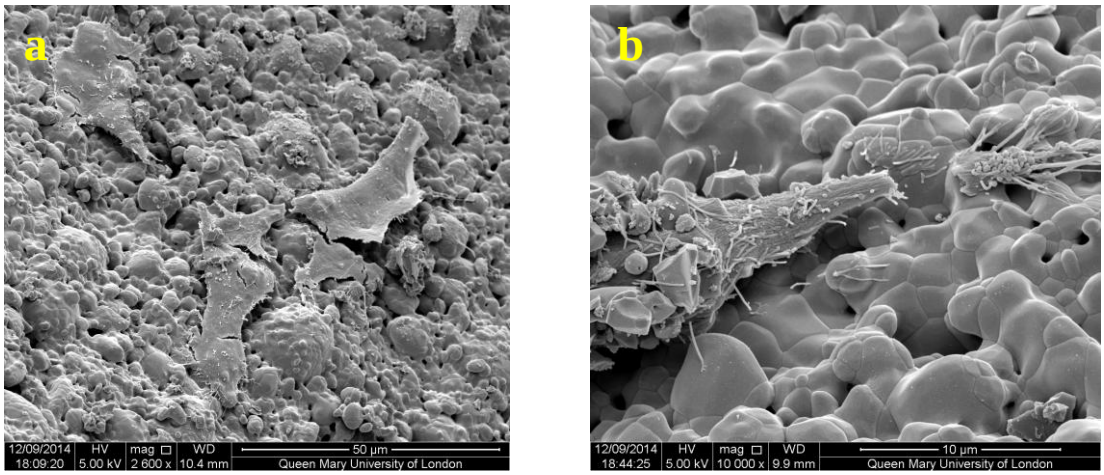

Figure 9.51: MG63 cells seeded at a cell conc. of 6x10^4 cells/ml at DAY 3 (TOP)

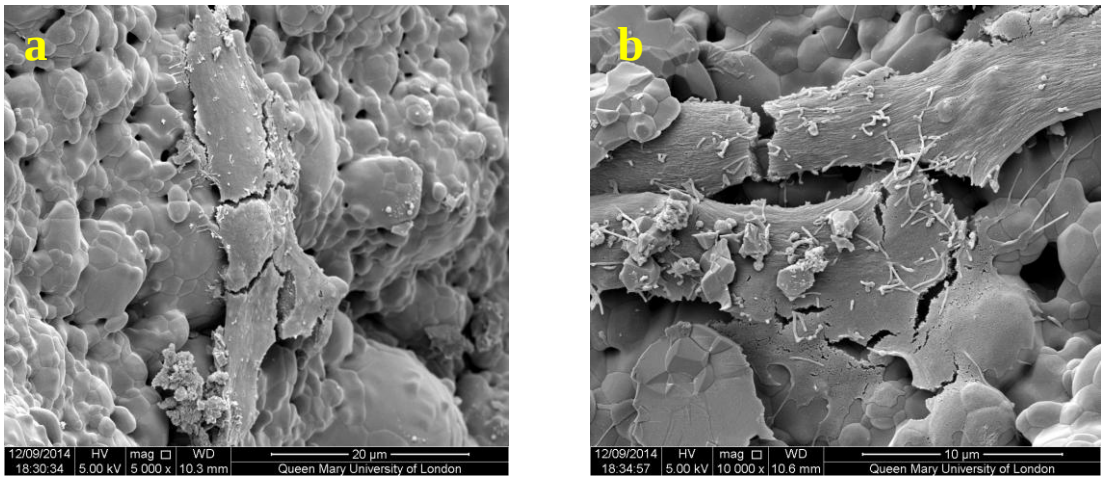

Figure 9.52: MG63 cells seeded at a cell conc. of 6x10^4 cells/ml at DAY 3 (MIDDLE)

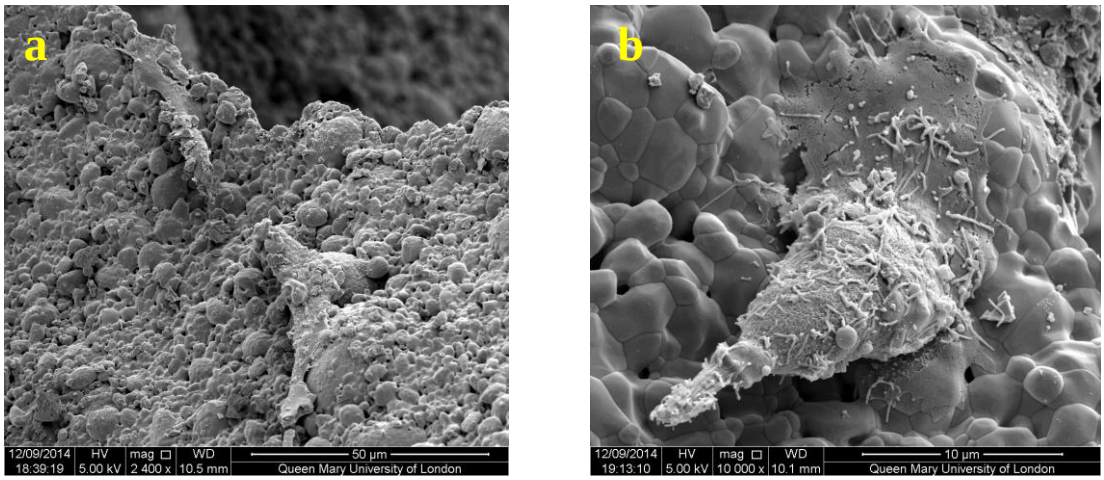

Figure 9.53: MG63 cells seeded at a cell conc. of 6x10^4 cells/ml at DAY 3 (BOTTOM)

8x10^4 cells/ml (a: 2400/5000 mag, b: 5000/10000 mag)

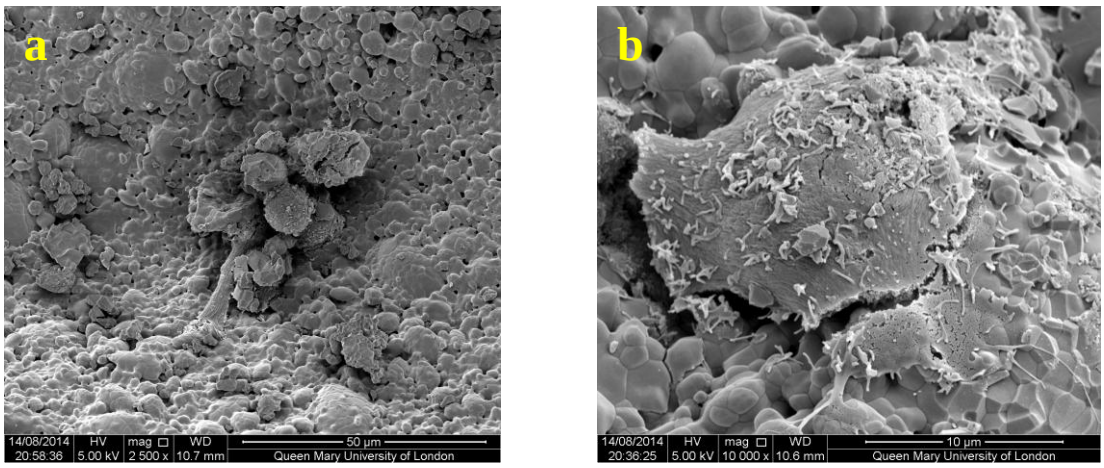

Figure 9.54: MG63 cells seeded at a cell conc. of 8x10^4 cells/ml at DAY 0 (TOP)

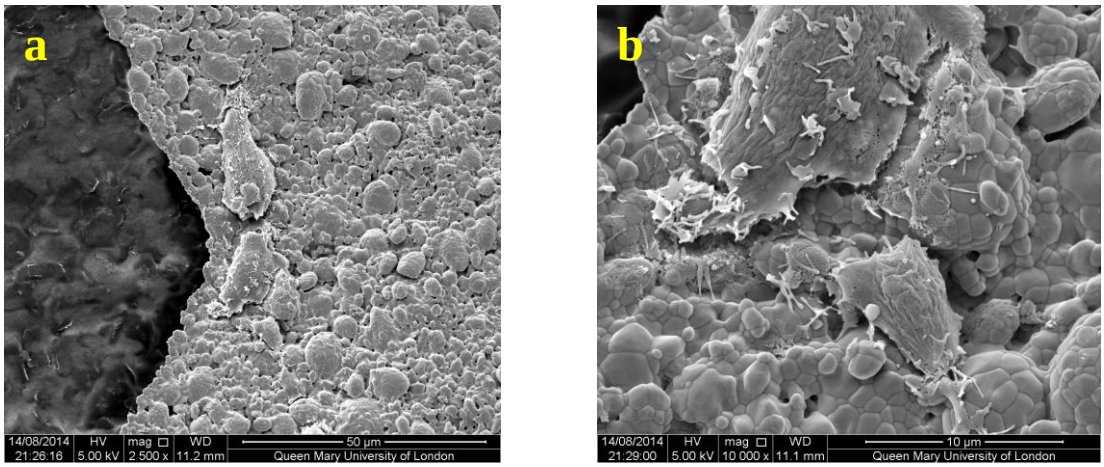

Figure 9.55: MG63 cells seeded at a cell conc. of 8x10^4 cells/ml at DAY 0 (MIDDLE)

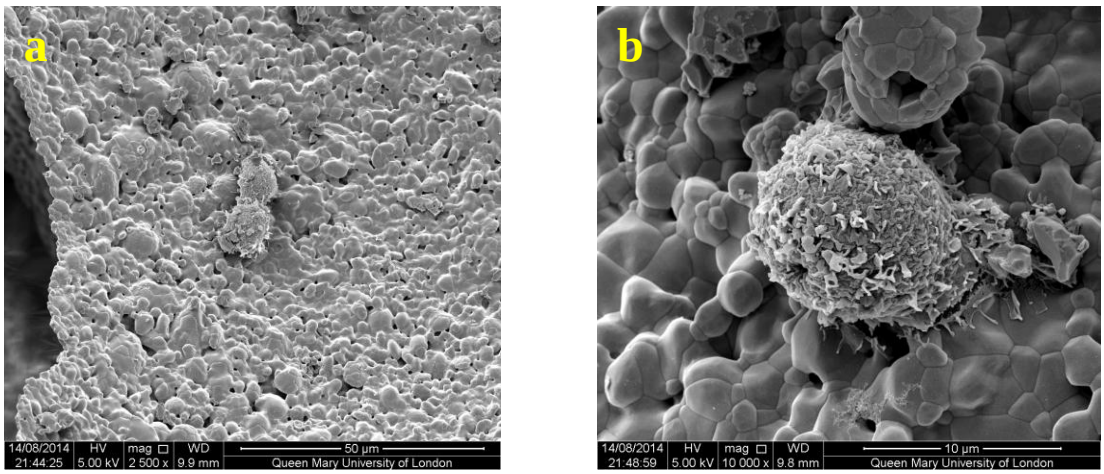

Figure 9.56: MG63 cells seeded at a cell conc. of 8x10^4 cells/ml at DAY 0 (BOTTOM)

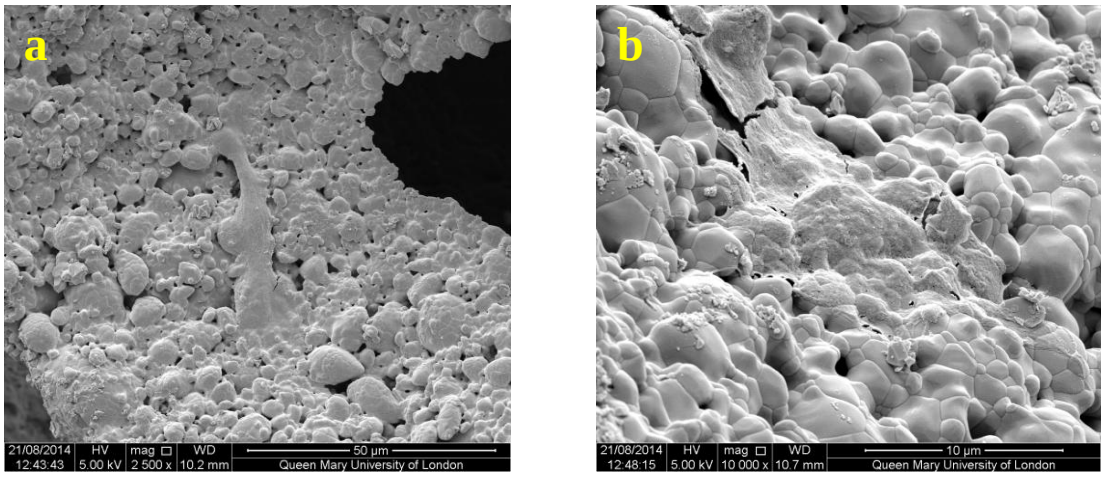

Figure 9.57: MG63 cells seeded at a cell conc. of 8x10^4 cells/ml at DAY 1 (TOP)

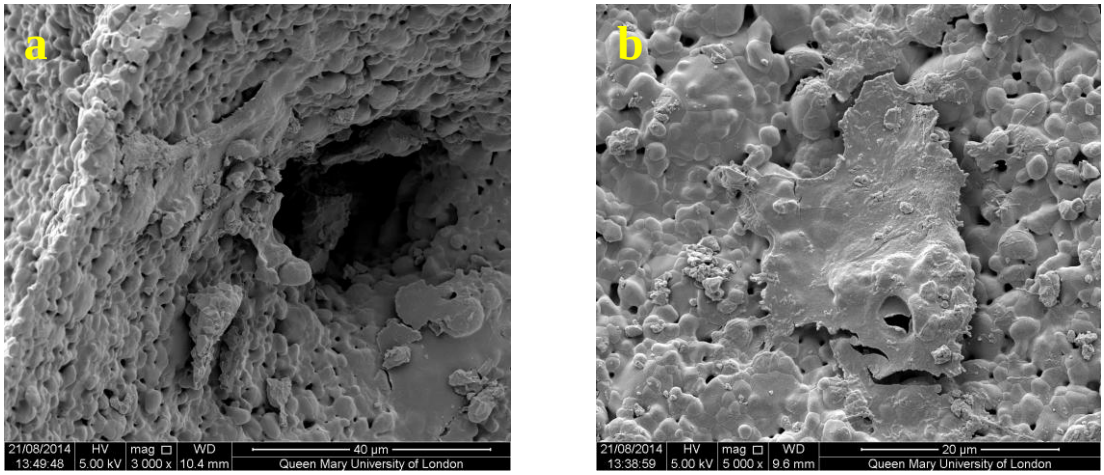

Figure 9.58: MG63 cells seeded at a cell conc. of 8x10^4 cells/ml at DAY 1 (MIDDLE)

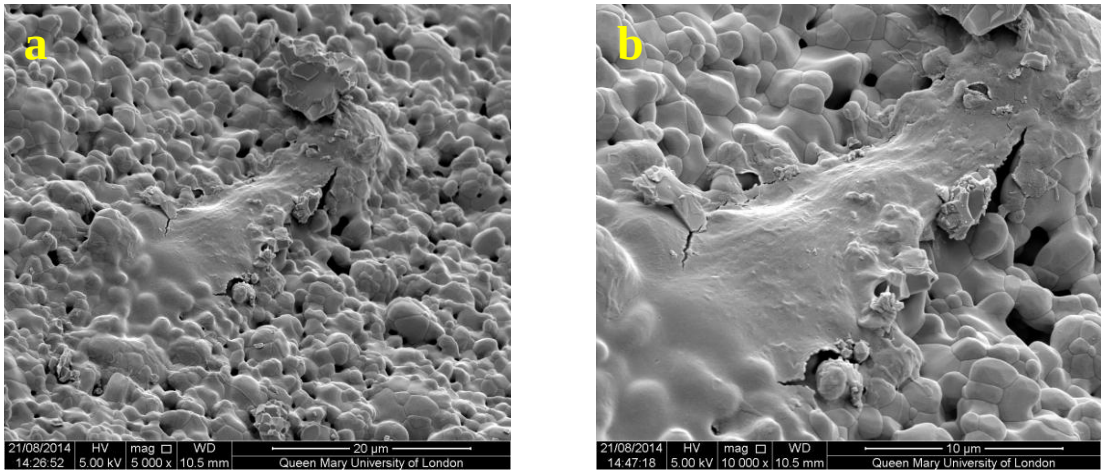

Figure 9.59: MG63 cells seeded at a cell conc. of 8x10^4 cells/ml at DAY 1 (BOTTOM)

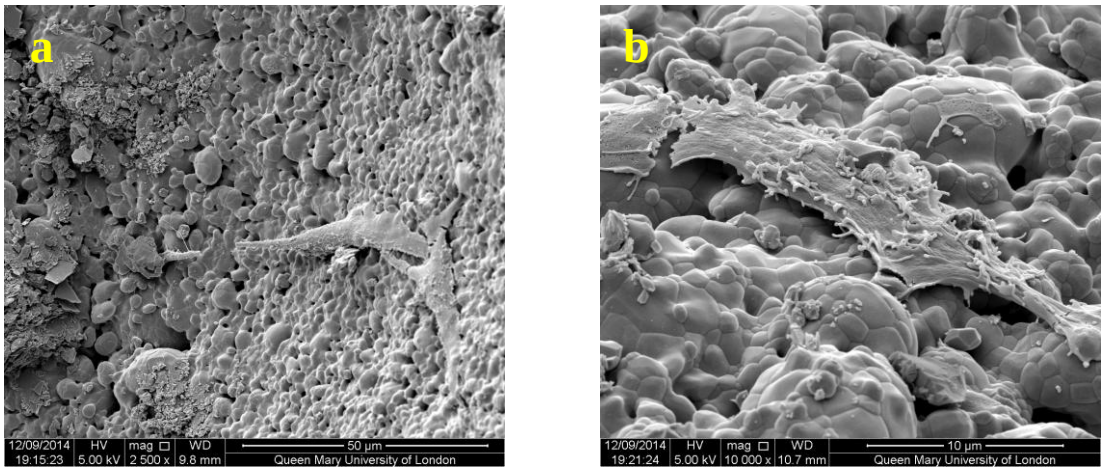

Figure 9.60: MG63 cells seeded at a cell conc. of 8x10^4 cells/ml at DAY 3 (TOP)

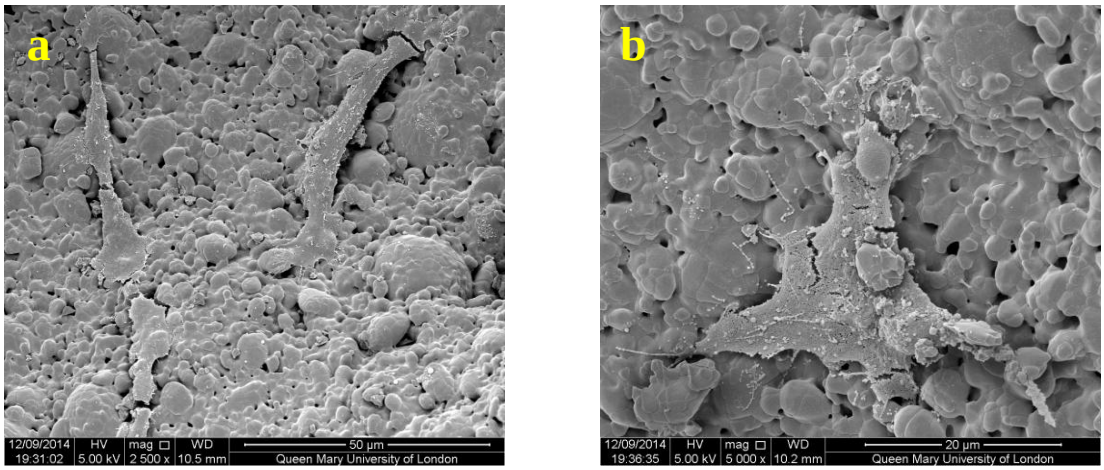

Figure 9.61: MG63 cells seeded at a cell conc. of 8x10^4 cells/ml at DAY 3 (MIDDLE)

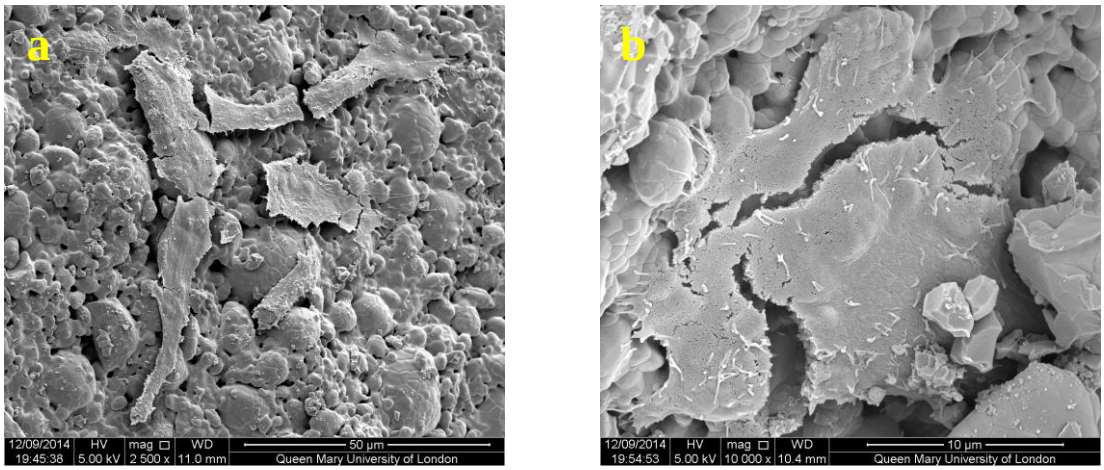

Figure 9.62: MG63 cells seeded at a cell conc. of 8x10^4 cells/ml at DAY 3 (BOTTOM)

The qualitative observations of the SEM analysis was corroborated by the quantitative analysis of total DNA detailed in Figure 9.63. From the DNA results, the highest cell concentration used had a significantly greater level of cell growth in comparison to the other two lower cell concentrations tested. The difference observed was significantly different between the lower cell concentrations and the highest cell concentration tested. Also the cell growth over the 3 days was seen to be significantly different (Figure 9.63)

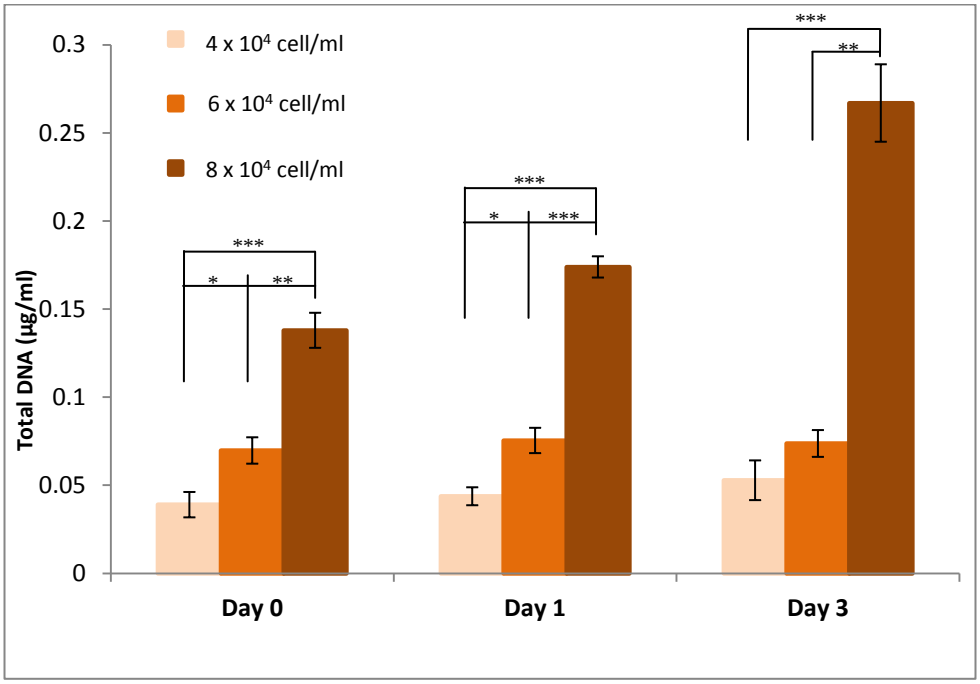

Figure 9.63: DNA conc. observed for all cell concentrations tested for 3 days using Method 2 (n=6)

9.4 Discussion

The cell and BGS interaction *in vitro* partially reflects the behaviour of a cell and BGS interaction *in vivo* and it is able to provide and insight in to the response of the specific cell type to these specific materials under controlled conditions. It has been shown that microscopy is a vital tool for biomaterial scientists to visualise the cellular response to many biomaterials including BGS. These studies have included the use of fibroblasts as well as osteoblasts (Folkman and Moscona 1978, Malik, Puleo et al. 1992, Vrouwenvelder, Groot et al. 1993, Schmidt, Kaspar et al. 2002). It has also been shown that the majority of the studies reported in literature, investigate cellular response to dense materials and therefore the cell response that is observed reflects their behaviour on flat surfaces. A study by Annaz et al looked in to investigating macro and microporosity in HA with osteoblast like cells. The study was successful in showing that microporosity plays a role in the initial cellular anchorage and attachment (Annaz, Hing et al. 2004).

When inserting the granules into a 3D dynamic perfusion environment, 0.45g of the granules are packed into 15mm long and 8mm diameter tubes (as previously described in earlier chapters). In order to study the cell response within this 3D environment, a suitable method needs to be found in order to seed the cells efficiently on to the granules without causing cell death. The seeding of cells on to the granules within these sample tubes was found to be a very delicate process and had to be handled with attention and precision. Therefore the aim of the work presented in this chapter was to establish a suitable cell concentration and cell seeding method of cells on to porous BGS, which in this case was SA80/20 granules.

From the result obtained it was evident that the type of method employed dictated the cell attachment to the surface of the granules. Method 1, involved the cells being seeded on to the granules in a 24 well plate first and then transferring the granules seeded with cells in to the sample tubes after allowing the cells to attach for 2 hours. In hindsight this particular method was an aggressive way to transfer the cell seeded granules in to the samples tubes. For this reason, the cell attachment to the granules was very poor despite increasing the cell concentration for the same volume. The lowest cell concentration tested saw no cell attachment throughout the sample tube (Figure 9.8 - Figure 9.16). The next cell concentration tested was $6x10^4$ cell/ml, where cell attachment was seen on the top and bottom sections taken of the granules from the sample tube, however no cells were seen in the middle section which suggests that this particular cell seeding method was unable to provide a homogeneous spread of cells along the whole sample tube (Figure 9.17 - Figure 9.25). Finally with the highest cell concentration tested, cell attachment was apparent on all

days within all sections however there was not many cells observed even at day 3 (Figure 9.26 - Figure 9.34). For both $6x10^4$ and $8x10^4$ cell concentrations, the cells were round in shape with a rough surface when viewed at higher magnifications. The DNA concentrations calculated supported the findings from the SEM images as cell proliferation was significantly low for the lower cell concentrations and was found to be greater with the highest cell concentration tested however, the difference was not statistically different. Overall the results showed a suppressed levels of DNA therefore confirming that this method did not support osteoblast-like cell growth and proliferation.

Method 2 involved the cells being seeded on to the SA80/20 granules whist already packed in to the 8mm diameter and 15mm long silicone tubes also preconditioned with SCM. In comparison to method 1, this particular method was a gentler way of seeding the cells on to the granules as they were already housed in the environment they would be used in the 3D dynamic perfusion flow system. Preconditioning the granules with 200µl of SCM allowed them to become 'wet' which in turn gave the cells a dose of nutrients as soon as they got pipetted on the granules. The cells were seeded on to the granules in such a way that 250µl of the cell suspension was pipetted in from the top and 250µl were pipetted from the bottom. This enabled a better spread of the cell solution throughout the length of the packed granules.

The lowest cell concentration tested did not show any cell attachment until day 3 whereby only a few cells were observed, which were round in shape. On this particular day the cells were on seen at the top and bottom sections suggesting the cells had not migrated into the centre of the sample tube holding the granules (Figure 9.36 - Figure 9.44). The next cell concentration that was tested was $6x10^4$ cell/ml which showed cell attachment on all days and on every section taken from the sample tubes. However the number of cells visually seen were not many even at day 3 of the culture (Figure 9.45 - Figure 9.53). By day 3 the cells had become flat in shape but not many were visible.

Finally the greatest cell concentration provided the most supportive results for cell growth and proliferation (Figure 9.54 - Figure 9.62).At day 0, cell attachment was observed and at higher magnifications the cells exhibited a rough texture due to the presences of numerous 'blebs' on their surface (Figure 9.54b - Figure 9.56b). There was also contact and anchorage of the cells on the surface of the granules as extending filopodia were evident which varied in length. This trend in cell shape and attachment was seen through all sections taken from the sample tube. This suggested that the cells had migrated to the centre of the sample tubes, providing a homogeneous spread of cells throughout the scaffold length. By day 1, it was clear that the cells had undergone cell division and the majority of the cells observed were

flat in nature and polygonal in morphology (Figure 9.57 - Figure 9.59). Furthermore these cells displayed a smoother surface (Figure 9.64) compared to the cells seen at day 0.

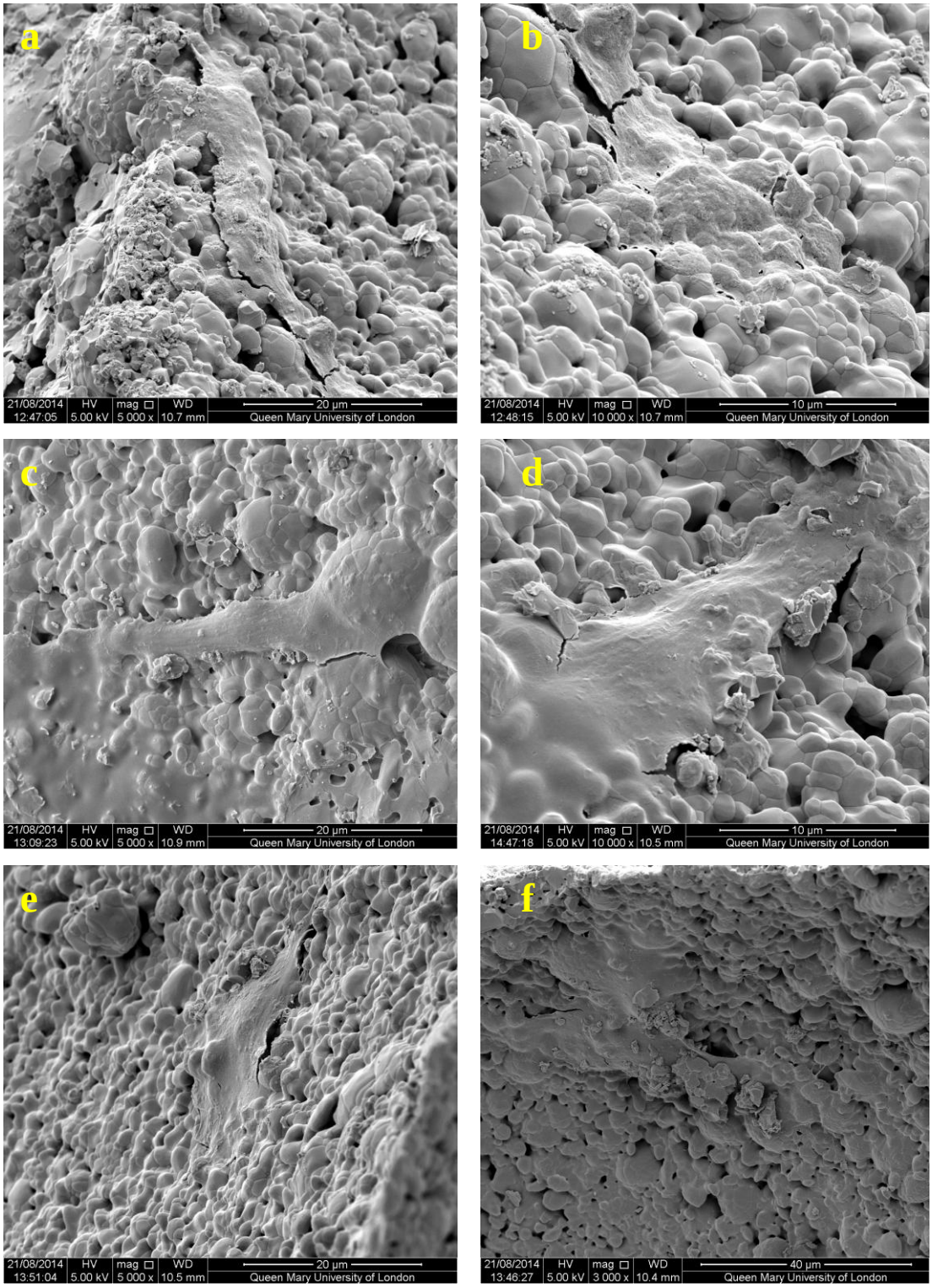

Figure 9.64: SEM images showing cell attachment at day 1 on SA80/20 surface using METHOD 2 at a cell concentration of $8x10^4$ cells/ml: a) & b) TOP section, c) & d) MIDDLE section and e) & f) BOTTOM section

Following 3 days static incubation, the cells had proliferated and spread covering a greater part of the surface of the SA80/20 granules in comparison to day 0 and day 1. The development of the filopodia extending from the cells was also observed, anchoring the cells more firmly to the surface of the granules (Figure 9.65).

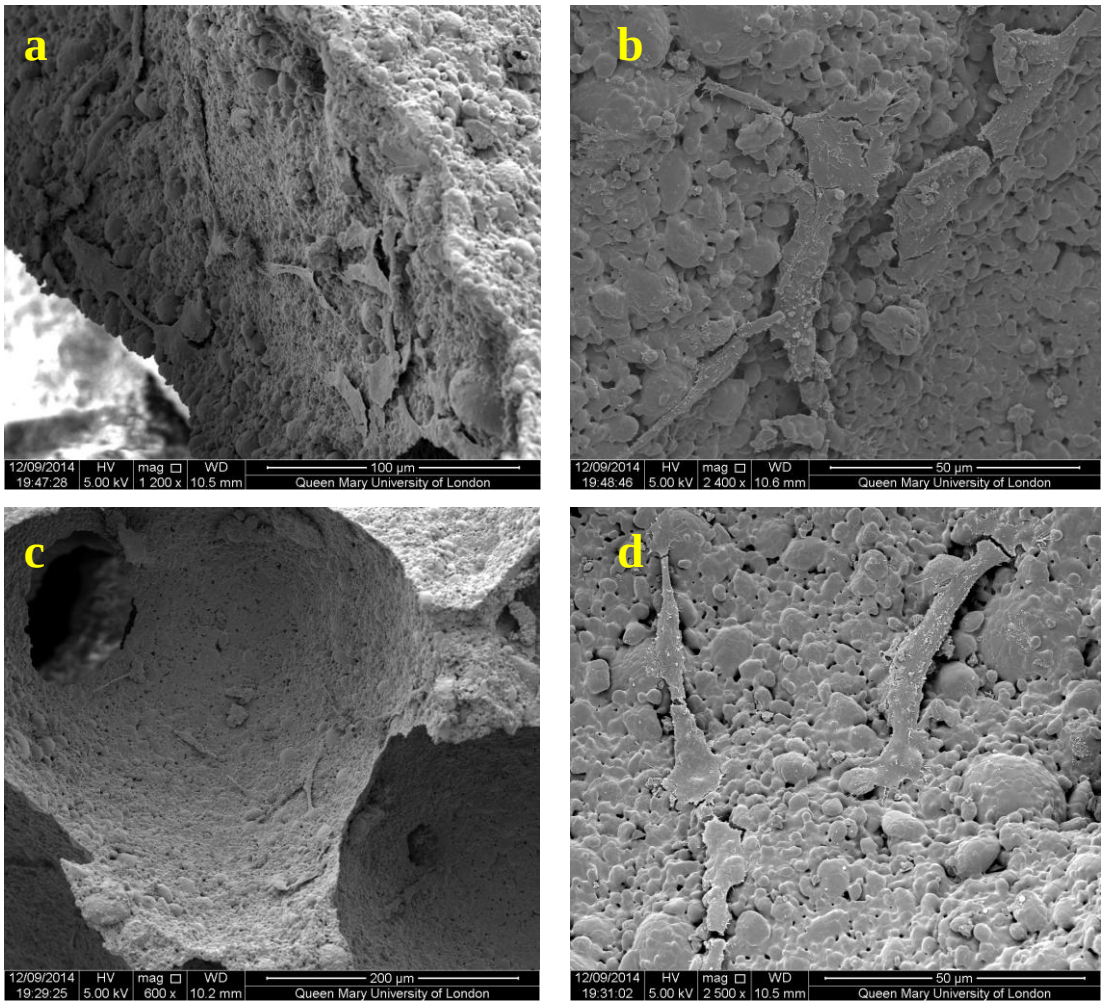

Figure 9.65: SEM images showing cell attachment at day 3 on SA80/20 surface using METHOD 2 at a cell concentration of $8x10^4$ cells/ml: a) TOP section, b) MIDDLE section and c) & d) BOTTOM section

From Figure 9.65 it is evident that cellular anchorage was observed with cells forming long and thin tapering extensions which had attached to the surface of the SA80/20 granules. It was also evident that there was a greater cell attachment on the inner sides of the macropores with the thin extensions appearing to penetrate the micropores of the granules.

Looking at the DNA results for Method 2, it is obvious that an increase in cell concentration was observed 24 hours following cell seeding of the granules (Figure 9.63). By day 3 there

was a greater cell proliferation seen with the greater concentration of cells in comparison to the other two lower cell concentrations tested. There was significant difference observed between the individual cell concentrations at day 3. In general the cells had a relatively flattened morphology by day 3 which suggests that the cells were positively dividing enabling surface coverage.

Rajarama et al claimed that the roughened surface of the cell morphology is because of the formation of 'blebs' and microvilli. This in turn is related to the increase in total surface area of the harvested cells as they round up from the flattened state when treated with trypsin. It is widely believe that blebs and microvilli form an intrinsic part of the anchorage dependent cell cycle and are linked to their morphology. This contributes to the roughened cell surface appearance when the cells are in a rounded morphology (Rajarama, Rounds et al. 1974). It has also been suggested that the spreading of cells is made possible by the use of surface membranes formed previously in the numerous blebs and microvilli present on the surface of a rounded cell. Erickson et al used hamster kidney cells to help demonstrate that newly mitotic cells have surfaces that are highly convoluted and are composed of blebs and microvilli whose presences decreases and finally disappears one the cells attains a flattened morphology (Erickson and Trinkaus 1976).

Work conducted from Chapter 3 to Chapter 8 detailed the development of the 3D perfusion system without seeding the porous granules in the perfusion system with cells. The validations made in this chapter were to explore the basic principles and operating parameters of the 3D perfusion system when cells would be seeded directly on the granules inside the silicon tube. The results from this chapter showed that method 2 and a cell density of $8x10^4$ cells/ml were the optimal seeding conditions and provides a better environment for cell growth allowing a better spread of cells over the materials surface.

9.5 Summary and Conclusions

In general it can be seen that method 1 was a far more abrasive approach in transferring the cell seeded granules to the sample tubes. In doing this there was a greater cell death and a decrease in cell number even when using a greater cell concentration. Once the cells had settled into the sample tube environment they did grow however due to the major loss of cells at the beginning, this method proved to be a less particle way of transferring the cell seeded granules to the sample tube.

Method 2 however was able to show the proliferation of cells with the greater concentrations of cells. It seemed like the lower concentration of cells did not provide enough cells in order to colonise the materials surface which would pose to be a problem as there would not be enough cells to interact with each other in order to proliferate and continue on to help bone repair. The highest cell concentration tested; $8x10^4$ cell/ml provided the most supportive environment for cell proliferation over time and with the SEM images, by day 3 there were greater number of cells observed covering a greater part of the granules surface.

From this work it can be concluded that Method 2 was a better way of seeding osteoblast-like cells on to the SA80/20 granules. Also it was concluded that the greater cell concentration tested, $8x10^4$ cell/ml made more cells available for cell on cell interaction. This in turn provides a better environment for cell growth and allows a better spread of cells covering a considerable part of the materials surface.

Chapter 10 Influence of Dynamic Fluid Flow on Ion Exchange and Cell Response within a 3D Perfusion Culture System

10.1 Background

In order to appreciate the incorporation of BGS *in vivo*, it is important to understand the development of osteoblast-like cells on BGS. BGS materials are being developed in order to stimulate the migration of osteoblast-like cells to the BGS material as well as to stimulate their differentiation in order to ultimately deposit increased amounts of bone in to the defective sites (Yang, Whitaker et al. 2004). Traditional 2D static *in vitro* studies have been useful screening tools to look at effects of changing substrate chemistry on osteoblast-like or even stem cell response when in either direct contact with substrate (Rashid, Buckland et al. 2005, Best, Zou et al. 2008, Guth, Campion et al. 2010, Botelho, Brooks et al. 2011, Castagna 2014) or when in indirect contact with a substrate via culture in media that has been preconditioned by contact with different substrates (Xynos, Edgar et al. 2000, Guth, Campion et al. 2011). Furthermore, given the importance of scaffold morphological characteristics on performance *in vivo*, these techniques have also been used to investigate the effect of changing scaffold porosity (Annaz, Hing et al. 2004, Castagna 2014). However, the ability of these studies to accurately screen for optimal scaffold characteristics has been limited and in no way predicted the significant enhancement observed *in vivo*, with increased level of strut porosity.

Ionic exchange between BGS and the surrounding media has been well documented in SBF testing however the effect of these findings have not been extensively explored within perfusion culture experiments (Kokubo, Kushitani et al. 1990, Kokubo and Takadama 2006, Gandolfi, Ciapetti et al. 2009, Campion, Ball et al. 2013). Cellular response is also found to be sensitive to ionic dissolution from BGS material surfaces to the surrounding media (Guth, Buckland et al. 2006, Guth, Campion et al. 2011). However these effects have not been studied extensively using a dynamic perfusion system in order to try and mimic the *in vivo* environment. Previous chapters in this work have demonstrated the sensitivity of cell response to dynamic ion exchange with changes in dynamic perfusion system variables and culture medium make up (chapter 4- chapter 8). Using a to waste perfusion system delays

the depletion calcium and phosphate ions and introducing serum proteins within the medium helps regulate ion release from the BGS to the surrounding media.

The ultimate aim of this thesis was to develop a 3D perfusion culture system to more accurately replicate the *in vivo* environment and investigate whether or not such a system would provide a better screening tool for bone graft scaffold optimisation studies and targeted investigation of the factors that influence bone graft performance *in vivo*. Having developed a flow to waste perfusion system that was able to maintain a stable media pH while undergoing dynamic ion exchange with real apatite-based bone graft substituted materials the next step was to validate the system through seeding osteoblast-like cells onto a range of scaffolds with well characterised differences in chemistry and structure that resulted in known variations *in vivo* behaviour to identify whether any correlation in subsequent osteoblast like response was observed or not.

10.2 Methodology

10.2.1 Media Preparation

The media used in the dynamic flow perfusion system was C-DMEM which was made up as previously described in Chapter 8 section 8.2.1. All of the media preparation was done under sterile conditions.

10.2.2 BGS Sample Preparation

All the BGS granules were sterilised for 4 hours at 500^{o}C in a furnace and left to cool overnight before preparing the sample tubes. Previous trial experiments showed that sterilising the granules for 2 hours under UV light was not a suitable method as it still resulted in bacterial or fungal contamination of the granules when seeded with cells. The sample tubes were prepared as previously described in Chapter 4 section 4.2.1.1 for all three BGS tested; HA80/20, SA80/20 and SA80/30. All sample preparation was done under sterile conditions.

10.2.3 Cell Seeded Sample Tube Preparation

MG63 cells were grown and expanded as described previously in Chapter 4 section 4.2.2.1. 500µl of a suspension containing 8x10^{4} MG63 osteoblast-like cells (P4) were seeded on to the granules within the sample tubes as previously described in Chapter 9 section 9.2.2. Once seeded the sample tubes, the tubes were left for 2 hours to allow for cell attachment.

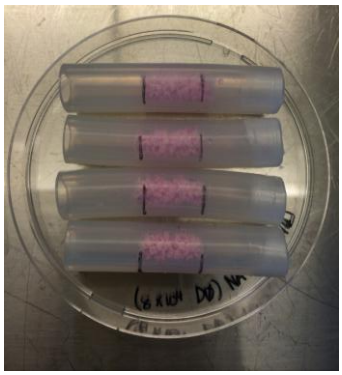

Figure 10.1: Sample tubes prepared with individual BGS seeded with MG63 cells ready for incubation for 2 hours to allow cell attachment

During these 2 hours the flow to waste perfusion apparatus was set up as described in Chapter 7, section 7.2.1.2. After the 2 hour cell attachment period, the large connectors were

connected to the sample tubes and then the sample tubes were connected to the flow perfusion system and the peristaltic pump was started. All of the samples were prepared and seeded with cells under sterile conditions.

10.2.4 Flow Perfusion System Set-up

The dynamic flow to waste perfusion experiments were conducted in a sterile incubator at 37^{o}C. All the equipment required for the set up for the perfusion experiments was autoclaved to ensure the sterility of all parts to avoid bacterial or fungal contamination during the experiments. All media delivery tubes were connected to the media bottles and collection containers and were sealed with parafilm to ensure an air tight connection. 500ml of C-DMEM was made up for each sample, connected to the delivery tubes and left in the incubator to allow the media to reach 37^{o}C before starting the experiments.

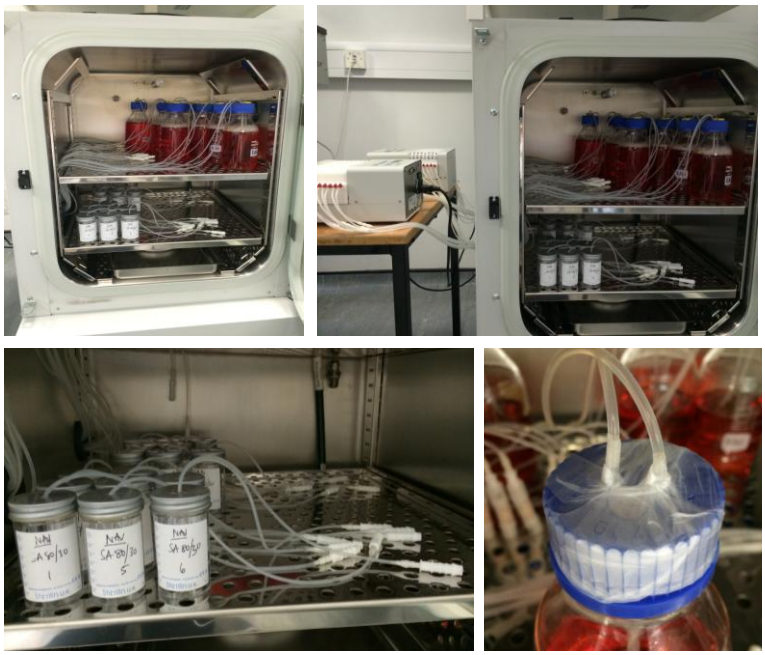

Figure 10.2: Dynamic flow perfusion set-up before connecting cell seeded sample tubes in to the system

C-DMEM was circulated at a flow rate of 0.1ml/min through the cell seeded sample tubes. Circulated C-DMEM was collected from the individual sample collection reservoirs at time intervals of 0.5, 1, 2 and 4 hours, 1, 3, 5, 6 and 7 days and the collected media was then analysed for calcium, phosphate and silicate ion concentrations using colorimetric assays as previously described in Chapter 4 section 4.2.1.2 The C-DMEM in the delivery reservoirs was refreshed every 24 hours.

Figure 10.3: Dynamic flow perfusion system set-up after connecting cell seeded sample tubes. Images showing sterile incubator housing all equipment with peristaltic pumps sitting outside incubator, connected sample tubes and media collection bottles

The 3 BGS granules were collected at day 0 (cell suspension just before being seeded on to the granules), day1, day3, day5 and day7. The collected granules at each time point were analysed for total DNA and ALP specific activity. The protocols followed for these assays can be found in Chapter 4 section 4.2.2.2 - 4.2.2.5. The specific ALP activity was also analysed from the media solutions collected at the same time intervals stated above.

SEM analysis was also conducted on the collected granules and the protocol followed for this can be found in Chapter 9 section 9.2.1.1. pH was also measured of fresh C-DMEM and at the individual collection time intervals during this study.

10.2.5 C-terminal Propeptide of Type I Collagen (CICP) Analysis

Collagen is a triple-helical molecule which forms the fibrous framework of all connective tissues and is synthesized as pro-collagen, a larger precursor molecule. Pro-collagen consists of mature collagen with extension peptides at both the amino and carboxy termini. The release of these peptides into the blood provides a stoichiometric representation of the production of collagen. The MicroVue CICP Kit (Quidel, USA) provides a quantitative method for determining levels of CICP. As the primary organic constituent of bone, Type I Collagen levels have been linked to bone growth and formation.

The quantification of CICP was determined both extracellularly and intracellularly at day0, day1, day3, day5 and day7. The kit provided 6 ready to use standards ranging from 0ng/ml to 82.2ng/ml. The concentrations of CICP present in the samples were calculated using the calibration curve (presented in APPENDIX 7) if the R^2 value was ≥ 0.99. Table 10.1 lists the standards used in triplicates.

Table 10.1: CICP standards used to plot calibration curve

Std	CICP conc. (ng/ml)	Vol. used (µl)
A	0	100
B	0.8	100
C	1.9	100
D	4.7	100
E	19.9	100
F	82.2	100

All solutions and samples had to be equilibrated to room temperature before use. Individual samples were tested at n=6 for accuracy. The assay procedure was as follows:

- Place desired number of coated strips in strip well frame just before use and label
- Pipette 100µl of each standard and sample in to the assay wells
- Incubate plate for 2 hours at room temperature
- Dilute 10X Wash Buffer 1:10 with dH_2O
- After 2 hours, manually invert/empty strips in plate and add 300µl of 1X Wash Buffer to each well and manually invert/empty the strips. Repeat this two more times, vigorously blotting the strips dry on paper towel after the last wash
- Add 100µl of Rabbit anti-CICP into each well
- Incubate plate for 45 minutes at room temperature
- Prepare Enzyme Conjugate with 7ml of 1X Wash Buffer
- After 45 minutes, manually invert/empty strips in plate and add 300µl of 1X Wash Buffer to each well and manually invert/empty the strips. Repeat this two more times, vigorously blotting the strips dry on paper towel after the last wash
- Pipette 100µl of Enzyme Conjugate to each well
- Incubate plate for 45 minutes at room temperature
- Prepare substrate solution by adding 1 pNPP tablet per bottle of substrate buffer

- After 45 minutes, manually invert/empty strips in plate and add 300µl of 1X Wash Buffer to each well and manually invert/empty the strips. Repeat this two more times, vigorously blotting the strips dry on paper towel after the last wash
- Pipette 100µl of Substrate Solution to each well
- Incubate plate for 30 minutes at room temperature
- After 30 minutes add 50µl of stop solution to each well
- Read optical density at 405nm using FLUOstar OPTIMA fluorometer and its associated software (BMG LABTECH, UK). Analyse results using a 4 parameter curve fit.

Upon gaining the results from the CICP assay, the amount of CICP found in each sample was then normalised by DNA content of the specific sample.

10.2.6 Osteocalcin (OCN) Analysis

OCN is found exclusively in bone tissue and is a protein produced by osteoblasts. OCN is thought to be involved in calcium ion and HA binding. It accounts for 10–20% of the non-collagenous protein in bone and it implies a role in bone formation. The MicroVue OCN immunoassay (Quidel, USA) quantitatively measures intact OCN and it is thought to be useful as a biochemical indicator of bone turnover. The quantification of OCN was determined extracellularly and intracellularly at day0, day1, day3, day5 and day7.

The kit provided 6 standards ranging from 0ng/ml to 27.1ng/ml. the standards provided needed to be reconstituted with 500µl of 1X Wash Buffer. The 1X Wash Buffer was prepared by diluting 10X Wash Buffer 1:10 with dH_2O. The concentrations of OCN present in the samples were calculated using the calibration curve (presented in APPENDIX 7) if the R^2 value was ≥ 0.99. Table 10.1 lists the standards used in triplicates.

Table 10.2: OCN standards used to plot calibration curve

Std	1X Wash Buffer (µl)	OCN conc. (ng/ml)	Vol. used (µl)
A	500	0	25
B	500	0.9	25
C	500	3.9	25
D	500	7.2	25
E	500	13.4	25
F	500	27.1	25

All solutions and samples had to be equilibrated to room temperature before use. Individual samples were tested at n=6 for repeatability. The assay procedure was as follows:

- Place desired number of coated strips in strip well frame just before use and label
- Pipette 25µl of each standard and sample in to the assay wells
- Add 125µl of anti-Osteocalcin to each well containing standards and samples
- Incubate plate for 2 hours at room temperature
- Prepare Enzyme Conjugate with 10ml of 1X Wash Buffer allowing pellet to dissolve
- After 2 hours, manually invert/empty strips in plate and add 300µl of 1X Wash Buffer to each well and manually invert/empty the strips. Repeat this two more times, vigorously blotting the strips dry on paper towel after the last wash
- Pipette 150µl of Enzyme Conjugate to each well
- Incubate plate for 1 hour at room temperature
- Prepare substrate solution by adding 1 substrate tablet per bottle of substrate buffer
- After 1 hour, manually invert/empty strips in plate and add 300µl of 1X Wash Buffer to each well and manually invert/empty the strips. Repeat this two more times, vigorously blotting the strips dry on paper towel after the last wash
- Pipette 150µl of Substrate Solution to each well
- Incubate plate for 45 minutes at room temperature
- After 45 minutes add 50µl of stop solution to each well
- Read optical density at 405nm using FLUOstar OPTIMA fluorometer and its associated software (BMG LABTECH, UK). Analyse results using a 4 parameter curve fit.

Upon gaining the results from the OCN assay, the amount of OCN found in each sample was then normalised by DNA content of the specific sample.

10.2.7 Statistical Analysis

All collected data was conducted at n=3 and analysed and expressed in terms of mean ± standard deviation. Statistical significance was evaluated using ANOVA, Post Hoc test: Tukey HSD with $\alpha=0.05$, (were *$p<0.05$, **$p<0.01$ and ***$p<0.005$).

10.3 Results

10.3.1 Ion Concentration Analysis and pH

Results of the ion concentration analysis can be seen in Figure 10.4 - Figure 10.6. As compared to the data obtained in Chapter 8 Figure 8.2, the calcium ion concentration in the media was initially significantly increased for SA80/20 BGS and the subsequent rate of ion depletion was significantly reduced, in contrast the pattern of behaviour for SA80/30 to that observed in Chapter 8. At day 6 (8640 mins) there is a significant depletion ($p<0.05$) in calcium ions from the media with SA80/20 in comparison to HA80/20 and SA80/30.

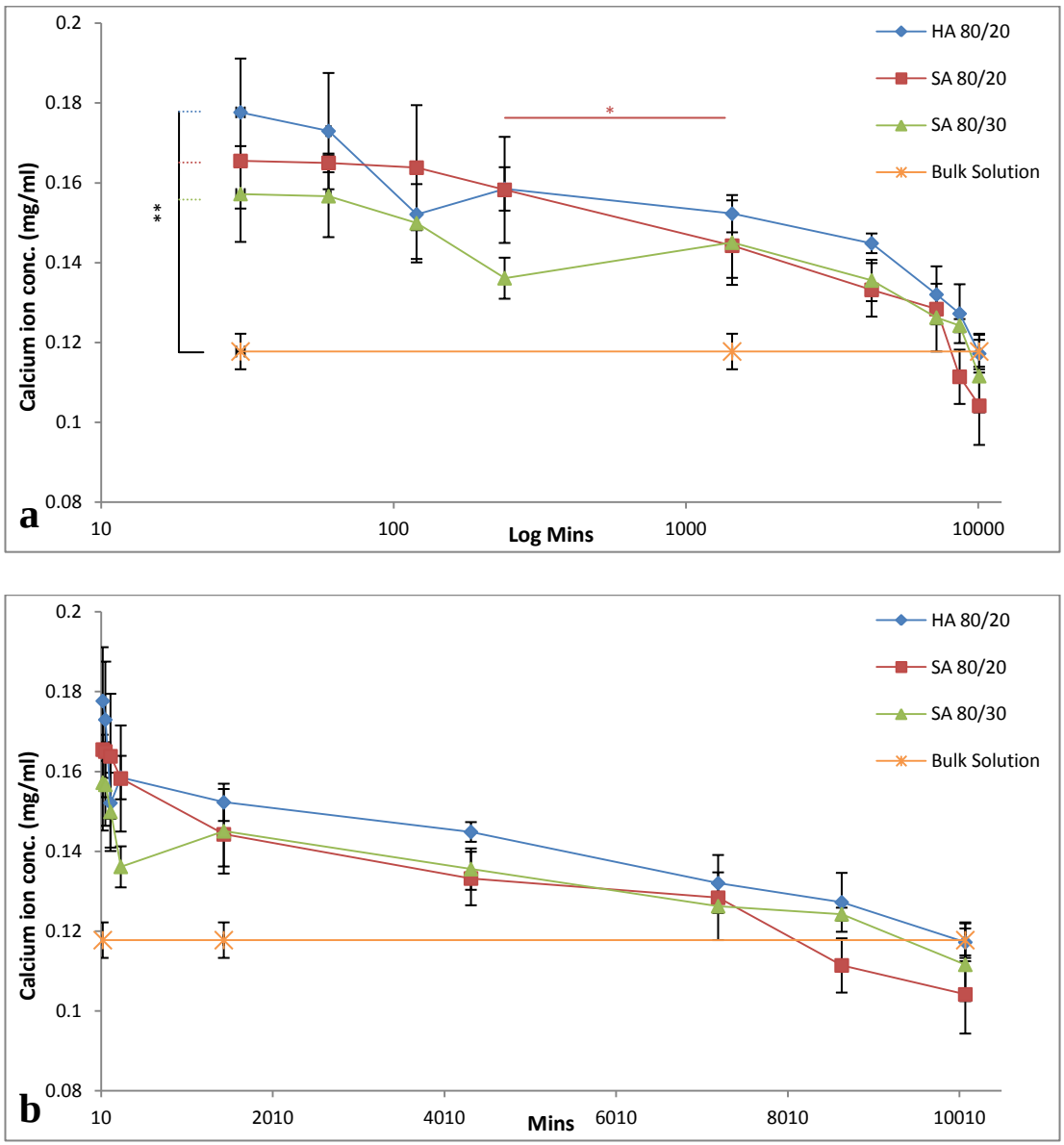

Figure 10.4: Calcium ion concentration of C-DMEM from HA80/20, SA80/20 & SA80/30 plotted against a) log minutes scale & b) minutes scale (n=6)

There was no significant difference in the temporal pattern of phosphate ion concentration with either graft chemistry or structure. With all BGS there was a significant increase in phosphate ion concentration ($P<0.05$) by 30 mins, which returned to basal levels between 1-3 days and was significantly lower than that of the bulk media by 5-6 days.

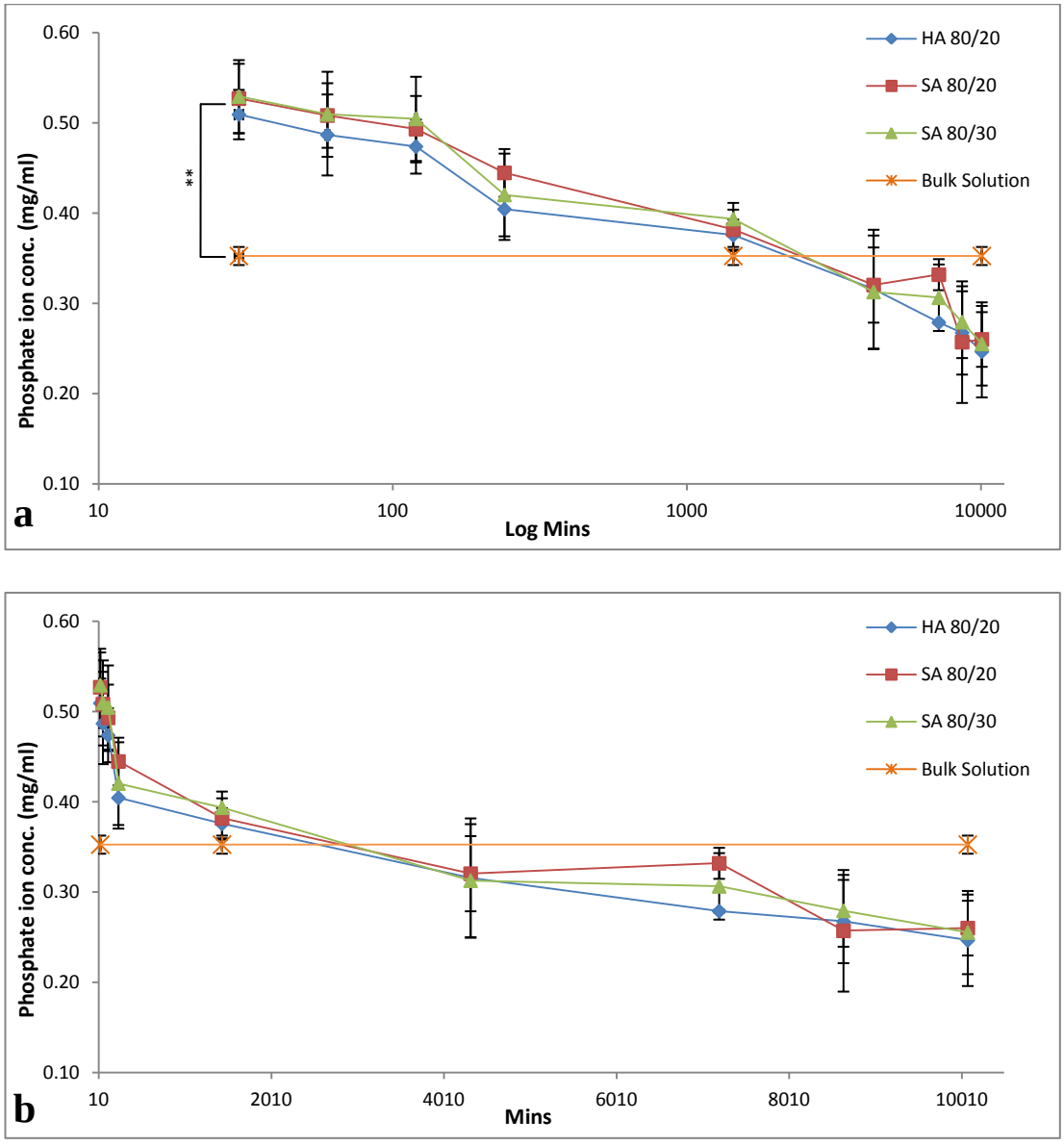

Figure 10.5: Phosphate ion concentration of C-DMEM from HA80/20, SA80/20 & SA80/30 plotted against a) log minutes scale & b) minutes scale (n=6)

Figure 10.6 shows a significantly greater ($p<0.005$) initial release of silicate ions from both SA80/20 and SA80/30 while HA80/20 shows a lesser release ($p<0.01$) in comparison to the bulk solution. With the significant initial increase in silicate ions from all BGS, the levels then returned to basal levels by day 1, with the silicate ion concentration levels for SA80/20 and SA80/30 being significantly higher than that of HA80/20 for the first 30-240 mins.

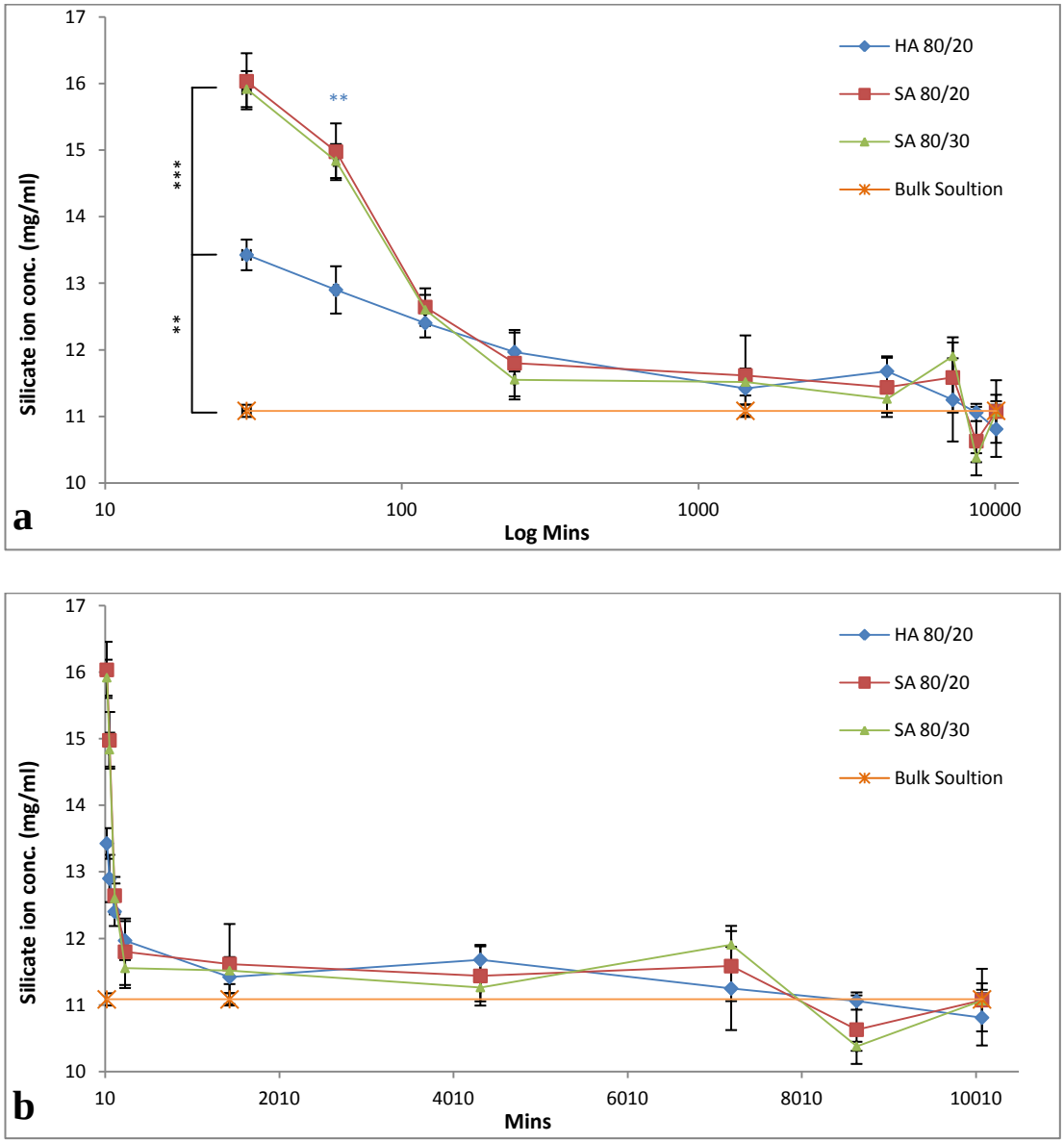

Figure 10.6: Silicate ion concentration of C-DMEM from HA80/20, SA80/20 & SA80/30 plotted against a) log minutes scale & b) minutes scale (n=6)

The pH levels (Figure 10.7) observed showed a significant initial increase in pH from all BGS ($p<0.05$). A gradual decrease in pH was observed with time from all three BGS. At 4 hours, the pH levels returned close to basal levels of 7.2 for the rest of the circulation study.

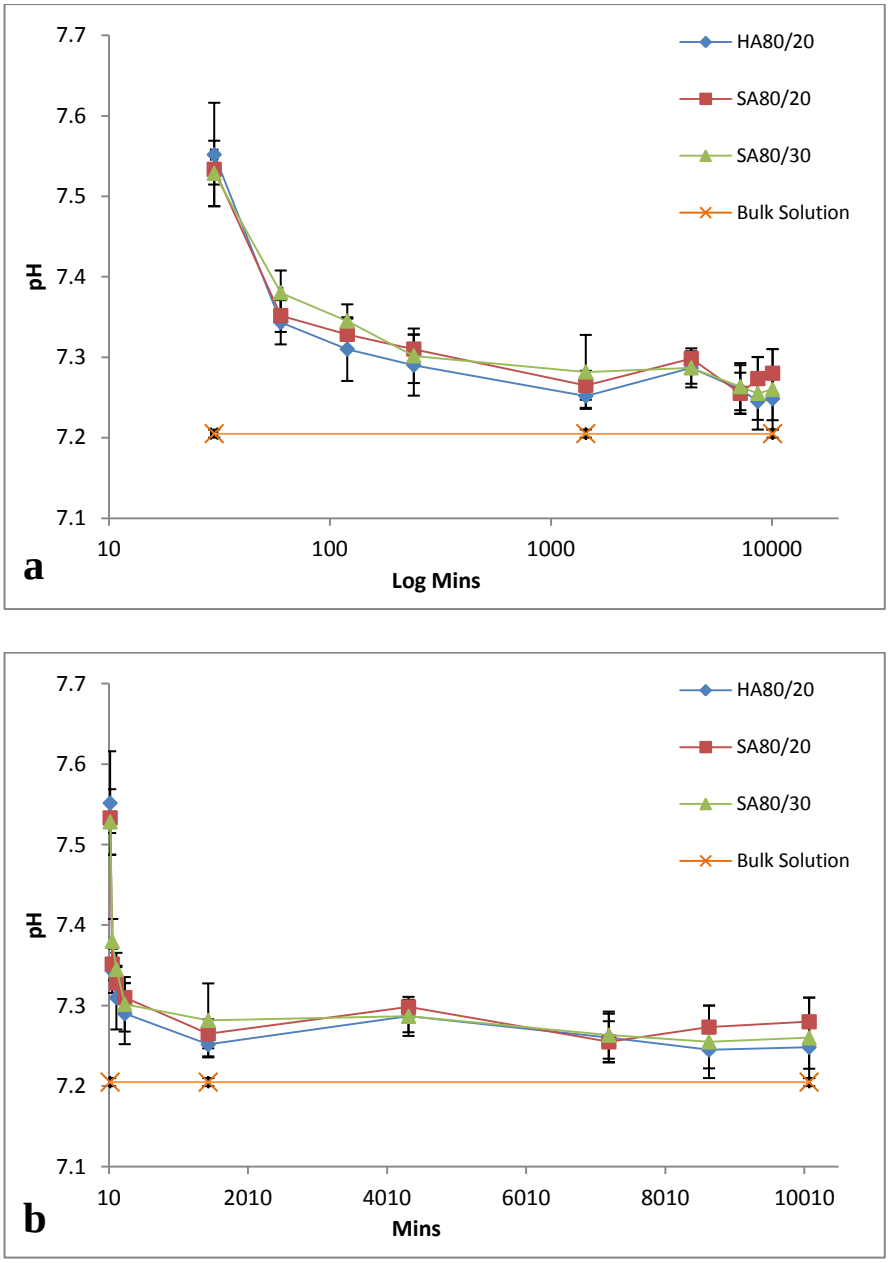

Figure 10.7: pH of C-DMEM from HA80/20, SA80/20 and SA80/30 plotted against a) log minutes scale & b) minutes scale (n=6)

10.3.2 Cell Assay Analysis

From the total DNA analysis (Fig 10.8) it was evident that there was an increase in cell number over time on all BGS used within this study. Significantly greater cell proliferation was seen with HA80/20 from day 3 to day 7 in comparison to SA80/20. There was a significant difference in total DNS between SA80/30 and SA80/20 at day 3 and 7 (Figure 10.8) with SA80/30 showing an increased total DNA. There was a significant drop in the value of Total DNA assayed from all BGS from day 0 (DNA content of cell suspension) to day 1. Comparing the two different chemistries tested, HA80/20 showed significantly greater cell proliferation with time compared to SA80/20. When comparing the two different strut porosities tested, SA80/30 showed a significantly greater proliferation on day 3 and day 7 in comparison to SA80/20.

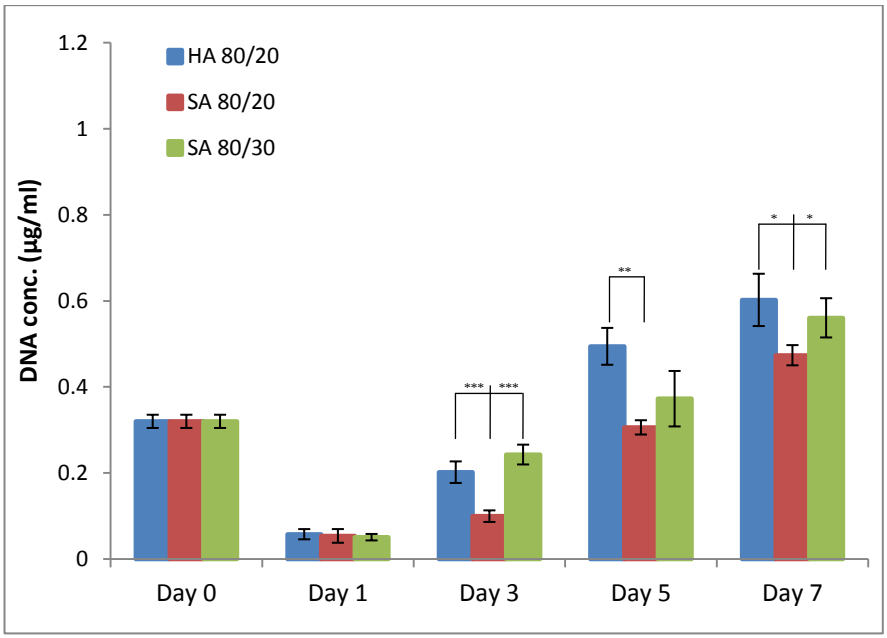

Figure 10.8: DNA concentration of MG63 cells cultured on HA80/20, SA80/20 and SA80/30 within a 3D dynamic perfusion system for 7 days (n=6)

Figure 10.9a shows the intracellular specific ALP activity. There was an initial decrease in ALP activity observed from day 0 to day 1with HA80/20 however with SA80/20 and SA80/30 there was an increase in ALP activity observed from day 0 to day 1 although this increase was significant. A greater ALP activity was observed on day 1 from SA80/30 however, this level of activity was not significantly different to that observed with SA80/20. A significantly increased peak of ALP was observed with HA80/20 and SA80/20 on day 3 with SA80/20 showing a significantly greater ALP activity. After day 3 there was a general decrease observed in ALP specific activity with all BGS with a significant difference still

being observed between HA80/20 & SA80/20 and SA80/20 & SA80/30. ALP specific activity was also measured in the media (extracellular) collected at each time (Figure 10.9b). It was interesting to see the difference in activity in the cells in comparison to the activity in media all in proximity to the granules. At all-time points there was significant difference in the extracellular release of ALP in the media from all BGS. At day 0 there was no ALP activity detected in the bulk media. From day 1 to day 7, media that had perfused through SA80/30 granules observed significantly increased levels of ALP activity in comparison to the media from HA80/20 and SA80/20. ALP activity was significantly increase at day 7 in the media collected from SA80/30 in comparison to the other two BGS tested.

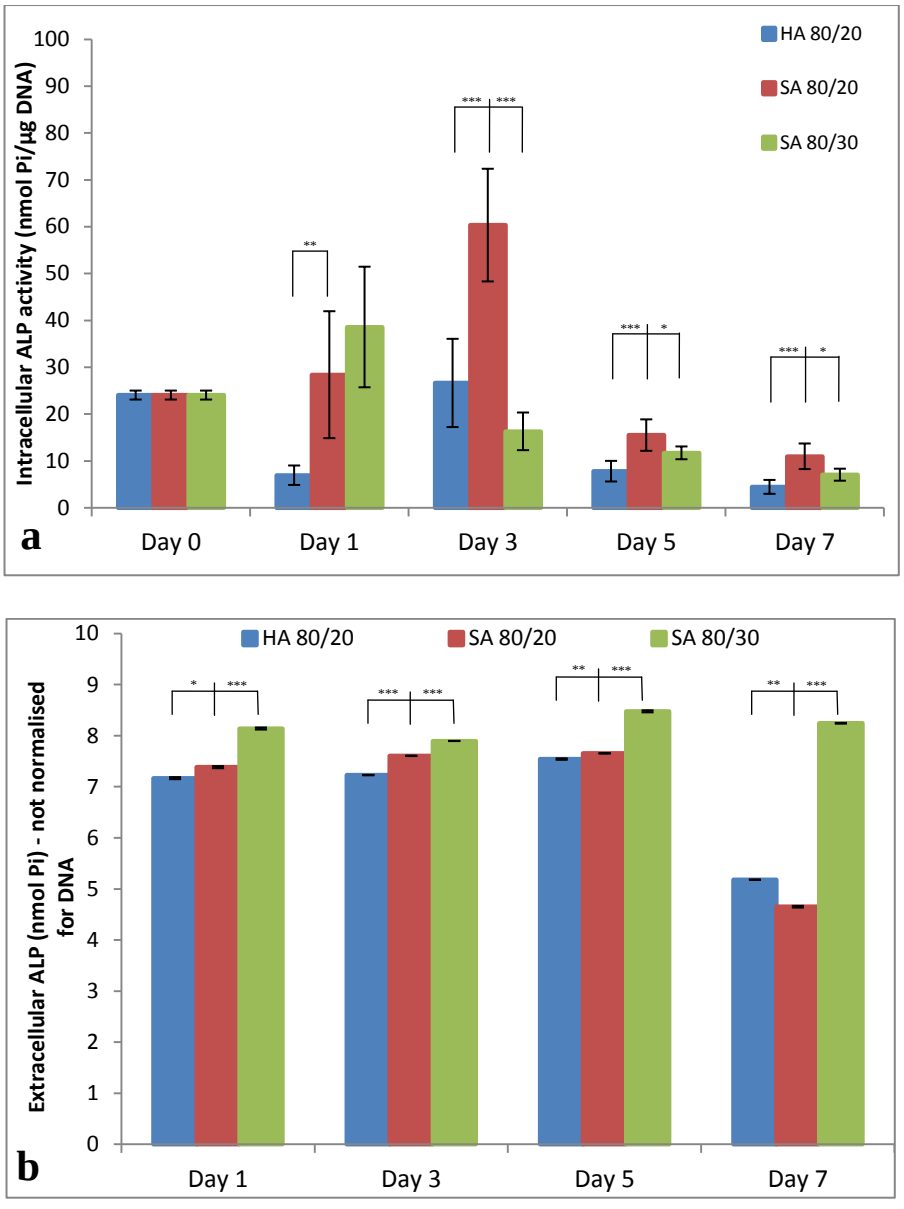

Figure 10.9: ALP activity investigated a) intracellular & b) extracellular (n=6)

Analysis of Procollagen-I (CICP) was conducted both on cell lysates (intracellular) and on the perfused media (extracellular) (Figure 10.10). There was a significant increase in intracellular CICP production with all BGS tested from day 0 to day 1. The CICP levels were significantly greater with both SA BGS in comparison to HA80/20 at day 1 however the CICP production between the SA BGS was not significantly different. From day 1, CICP production decreased with time with SA80/20 showing lesser drop compared to the other BGS although, at day 7 the difference became statistically similar between all BGS. No clear trend was with time for extracellular CICP release in to the media with all BGS. HA80/20 showed a significantly greater CICP release in to media on days 1, 3 and 7 in comparison the SA80/20. The media perfused through SA80/20 granules showed significantly greater CICP release in comparison to SA80/30 media on days 1 and 3 however SA80/30 media showed a significantly greater CICP release on days 5 and 7 in comparison to SA80/20 media.

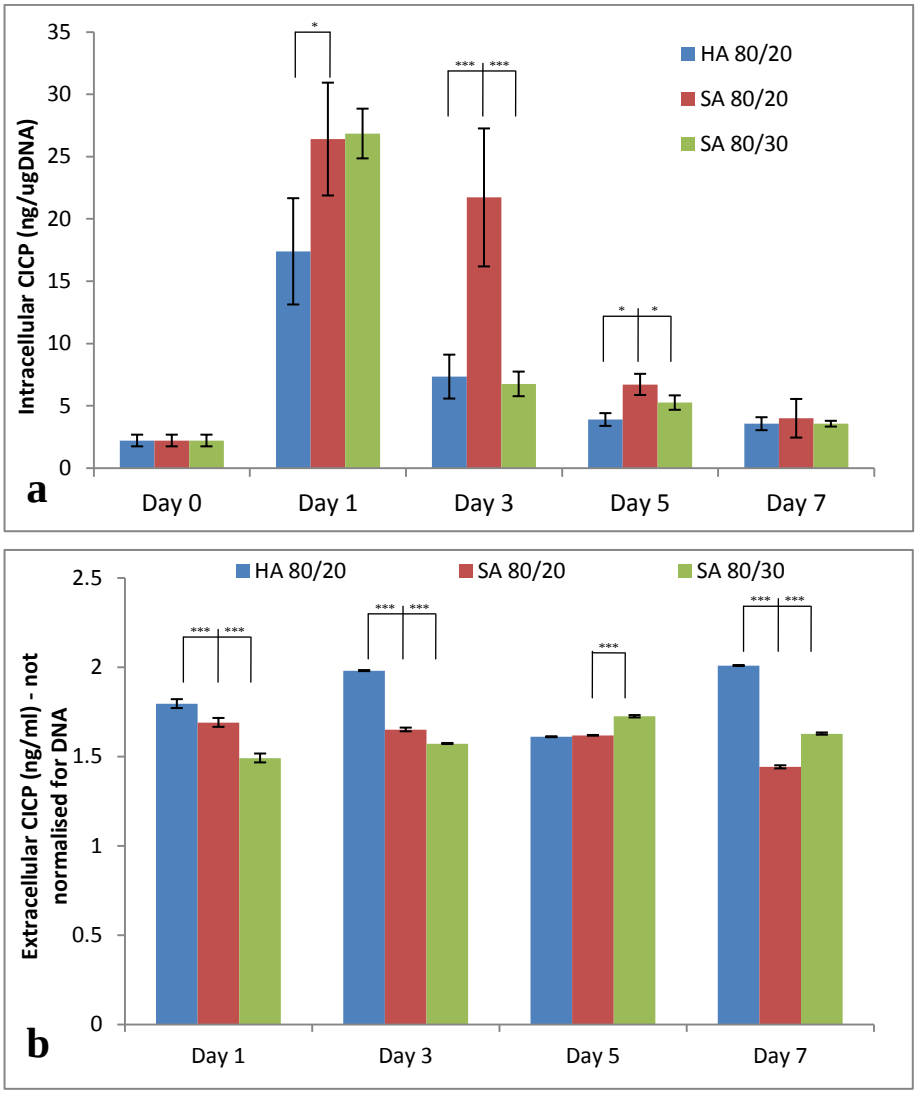

Figure 10.10: CICP levels investigated a) intracellular & b) extracellular (n=6)

OCN analysis was conducted both on cell lysates (intracellular) and on the perfused media (extracellular) (Figure 10.11). There was a significant increase in intracellular OCN production with all BGS tested from day 0 to day 3 however, the differences in OCN production were not significantly different between all BGS tested on all three days. Day 5 saw a significant drop in OCN production with all BGS with SA80/30 showing a lesser drop. Day 7 observed significantly lowers levels of OCN in comparison to day 5 across all BGS however the levels were not significantly different between the individual BGS tested. When investigating OCN release in media, over 7 days SA80/20 observed statistically increased levels of OCN in media in comparison to HA80/20 media and SA80/30 media.

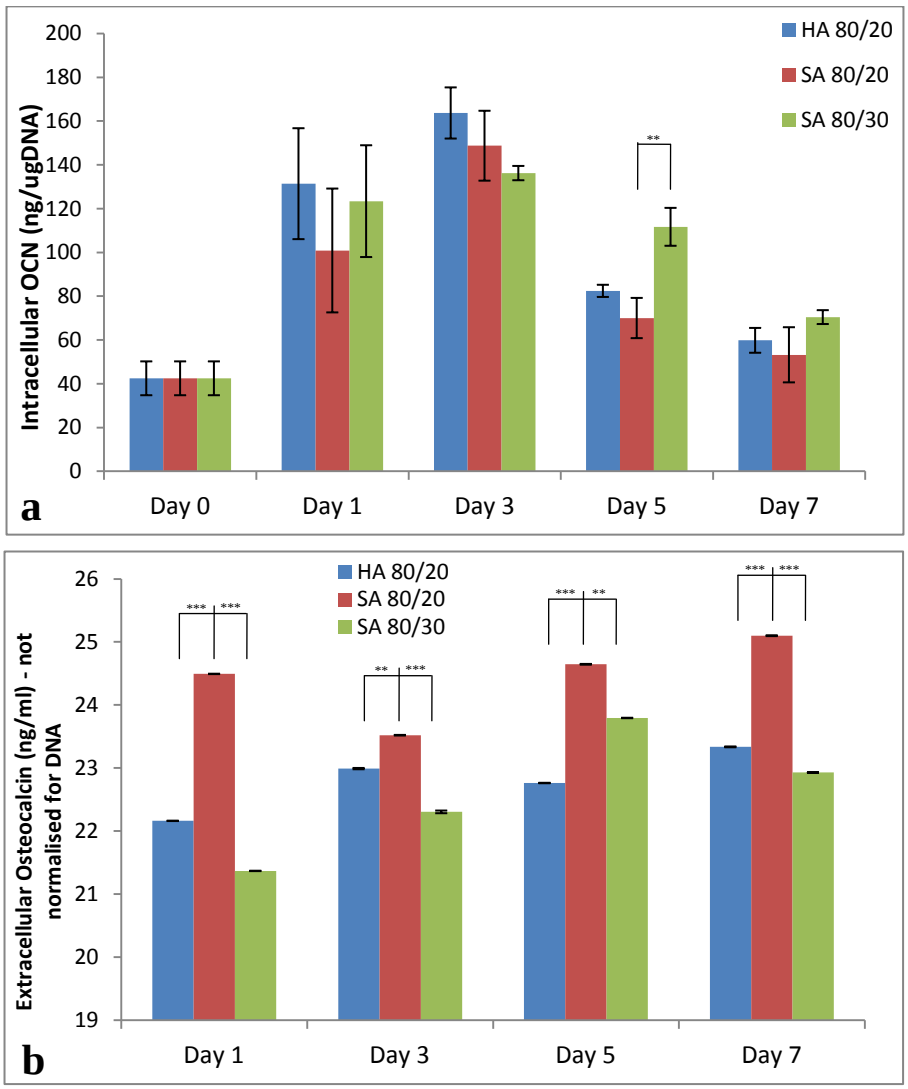

Figure 10.11: OCN levels investigated a) intracellular & b) extracellular (n=6)

From the SEM images it is evident that all three BGS supported cell proliferation during the course of the dynamic perfusion experiments. From the images there is a clear increase in cell proliferation on the surface of the BGS from day 3 to day 7, with day 7 showing the greater proliferation of cells on the surface of the BGS granules used. Generally from all the images taken it is also evident that there is cell growth on all sections taken from each BGS on each day during the study. Figure 10.12 - Figure 10.15 demonstrate that there was successful cell growth on all sections of the HA80/20 granules. With an increase in time the images show an increase in cell attachment. At day 0 and even day 1 the cells are found to be round in shape with blebs present on the surface of the cells. By day 3, the cells become flat in morphology and begin to spread over the surface of the granules. On Day 7, the SEM images show extensive cell growth with cells appearing in a sheet like nature. The cells become more visible at lower magnifications of 600x.

This is the general trend seen from all the BGS. Figure 10.16 - Figure 10.19 show cell attachment on SA80/20 granules surface on all days from all sections taken from the BGS sample tubes. Figure 10.20 - Figure 10.23 present cell attachment on SA80/30 granule surface. With these two BGS, there is again an increase in cell growth noticeable with time and by day 7 there is a vast amount of cells covering the surface of the granules. There are more cells visible within deeper pores of SA80/20 and SA80/30 at lower magnifications.

HA80/20

- DAY 1

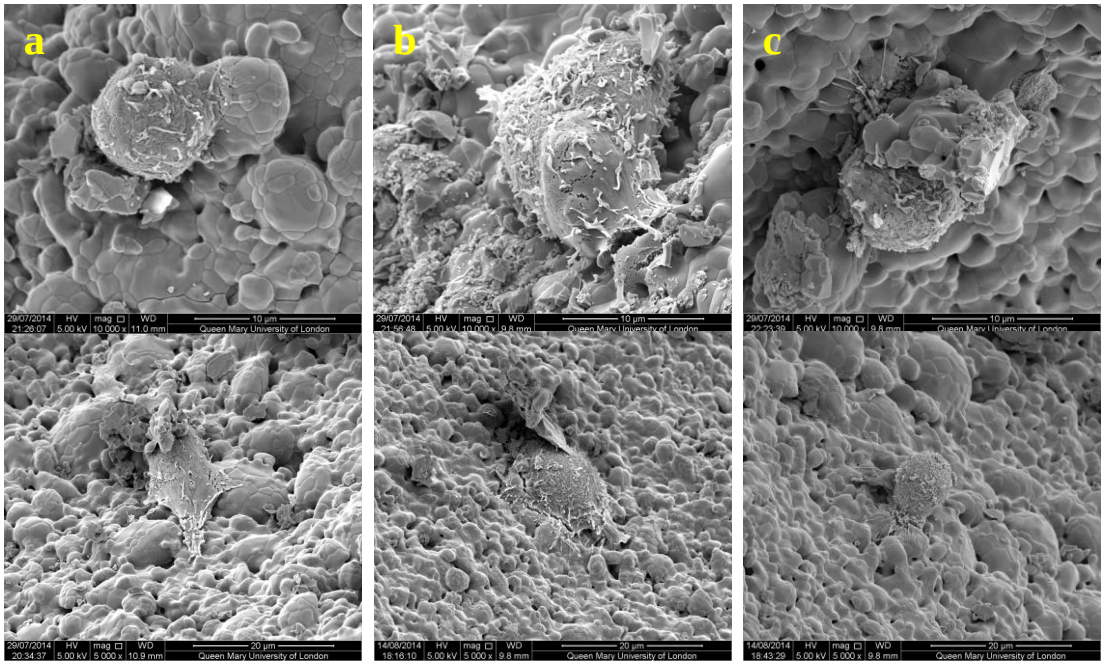

Figure 10.12: Day 1 cell attachment on HA80/20 surface from a) top section at 10000x & 5000x, b) middle section at 10000x & 5000x & c) bottom section at 10000x & 5000x

- DAY 3

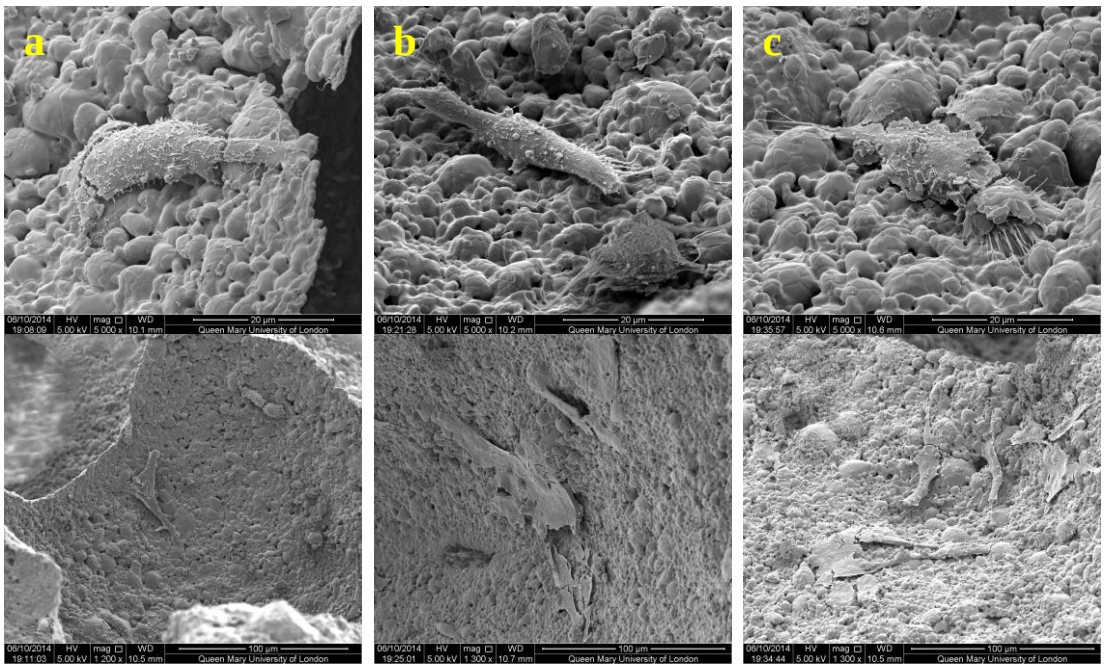

Figure 10.13: Day 3 cell attachment on HA80/20 surface from a) top section at 5000x & 1200x, b) middle section at 5000x & 1200x & c) bottom section at 5000x & 1200x

- DAY 5

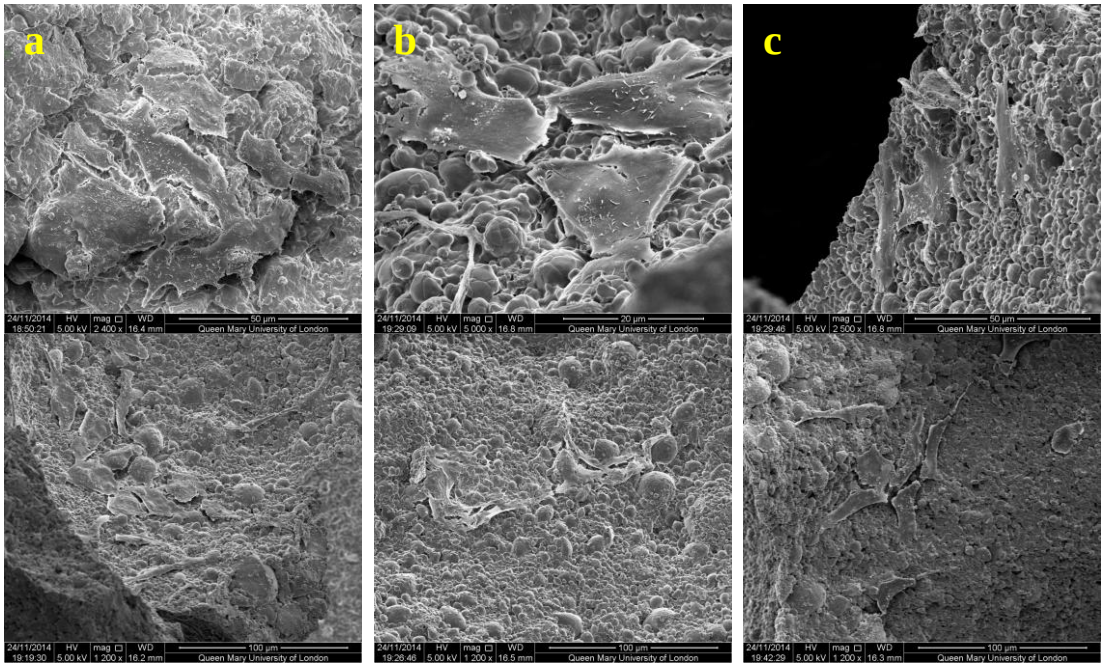

Figure 10.14: Day 5 cell attachment on HA80/20 surface from a) top section at 2500x & 1200x, b) middle section at 2500x & 1200x & c) bottom section at 2500x & 1200x

- DAY 7

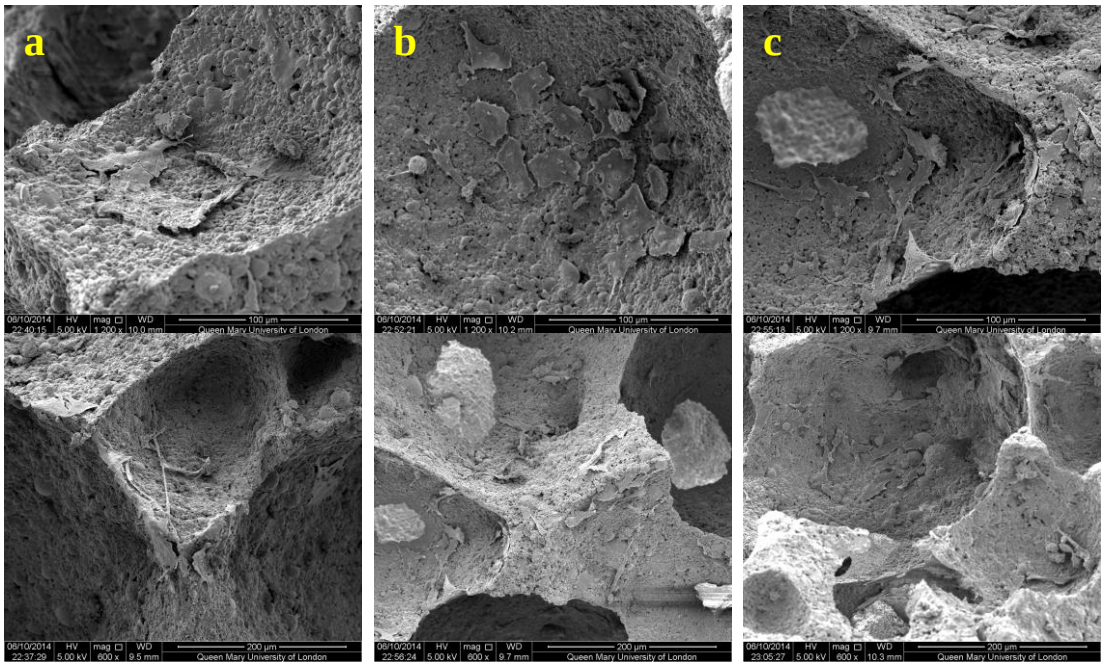

Figure 10.15: Day 7 cell attachment on HA80/20 surface from a) top section at 1200x & 600x, b) middle section at 1200x & 600x & c) bottom section at 1200x & 600x

SA80/20

- DAY 1

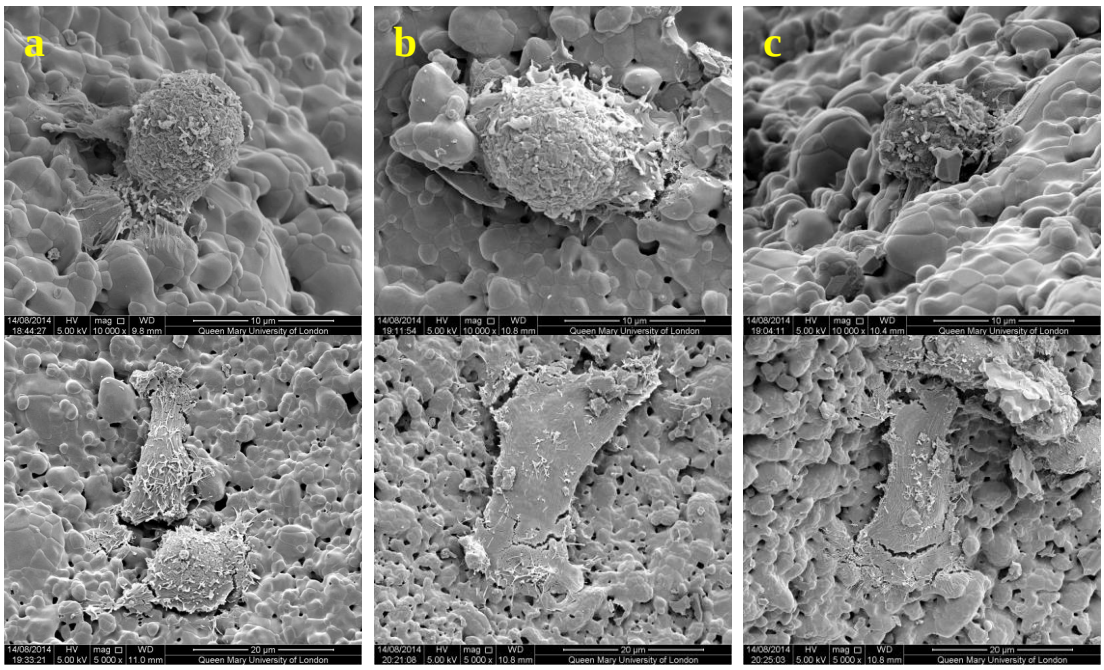

Figure 10.16: Day 1 cell attachment on SA80/20 surface from a) top section at 10000x & 5000x, b) middle section at 10000x & 5000x & c) bottom section at 10000x & 5000x

- DAY 3

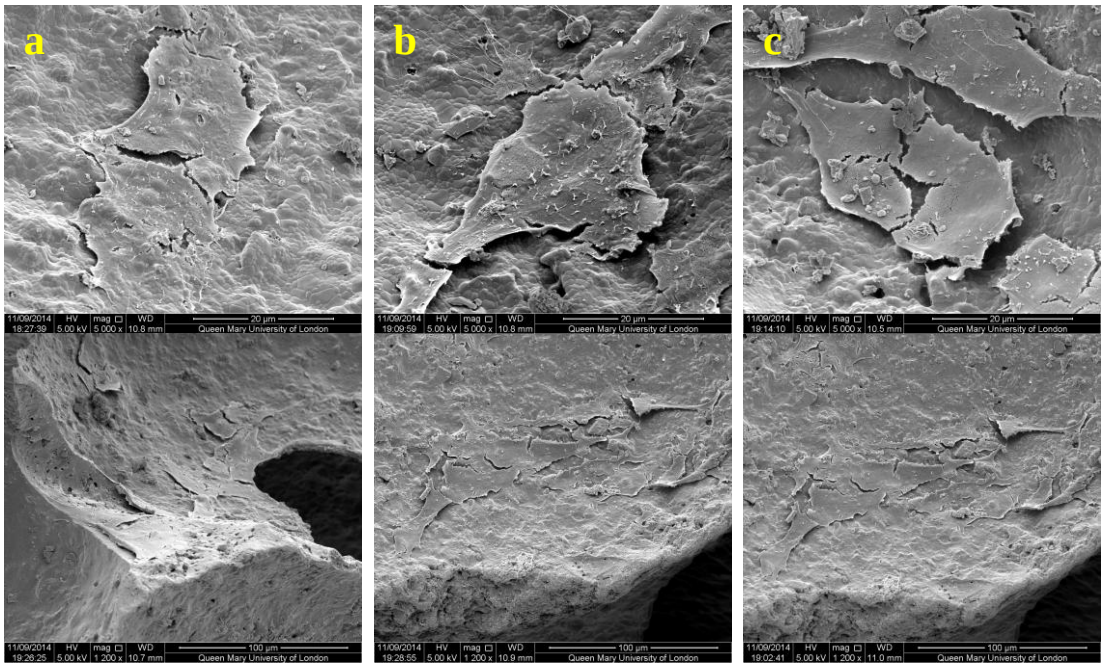

Figure 10.17: Day 3 cell attachment on SA80/20 surface from a) top section at 5000x & 1200x, b) middle section at 5000x & 1200x & c) bottom section at 5000x & 1200x

- DAY 5

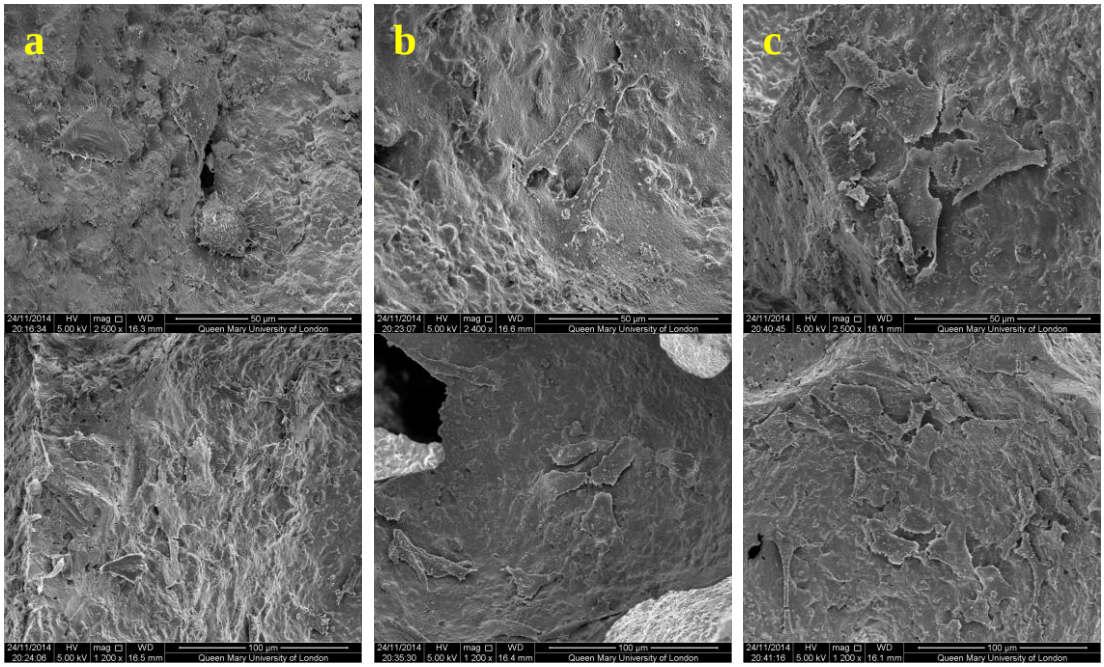

Figure 10.18: Day 5 cell attachment on SA80/20 surface from a) top section at 2500x & 1200x, b) middle section at 2500x & 1200x & c) bottom section at 2500x & 1200x

- DAY 7

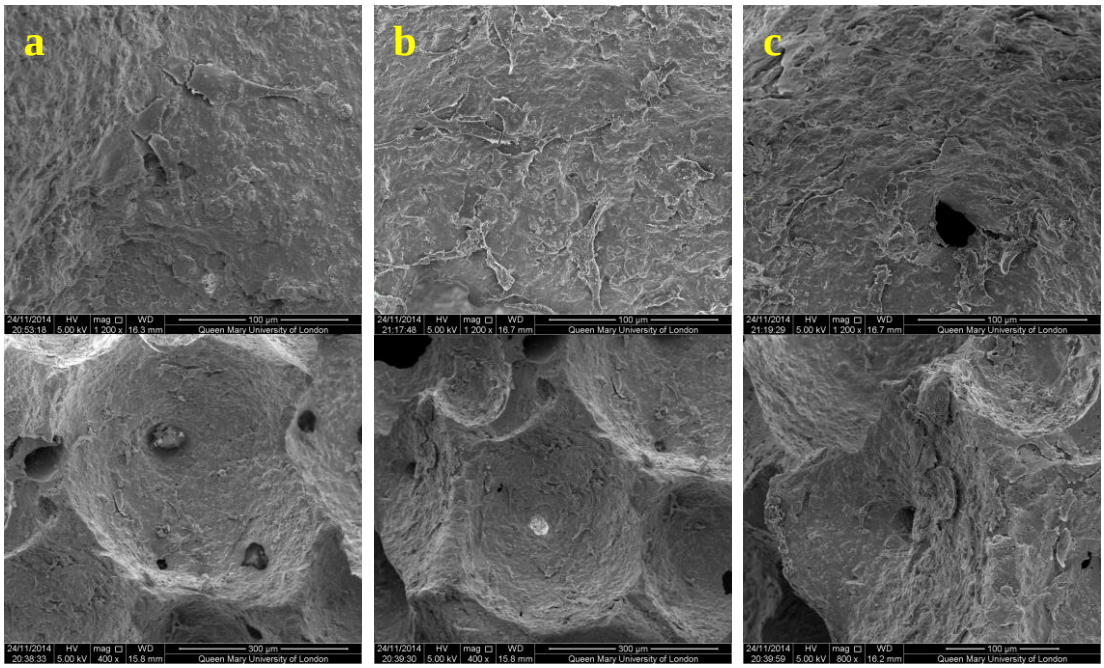

Figure 10.19: Day 7 cell attachment on SA80/20 surface from a) top section at 1200x & 600x, b) middle section at 1200x & 600x & c) bottom section at 1200x & 600x

SA80/30

- DAY 1

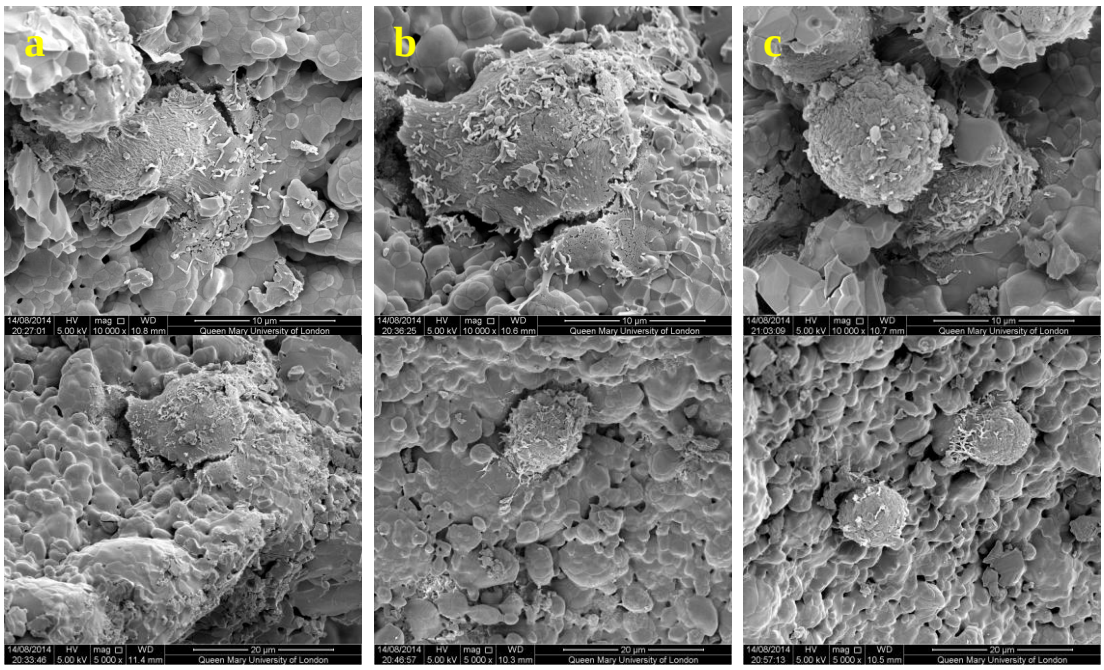

Figure 10.20: Day 1 cell attachment on SA80/30 surface from a) top section at 10000x & 5000x, b) middle section at 10000x & 5000x & c) bottom section at 10000x & 5000x

- DAY 3

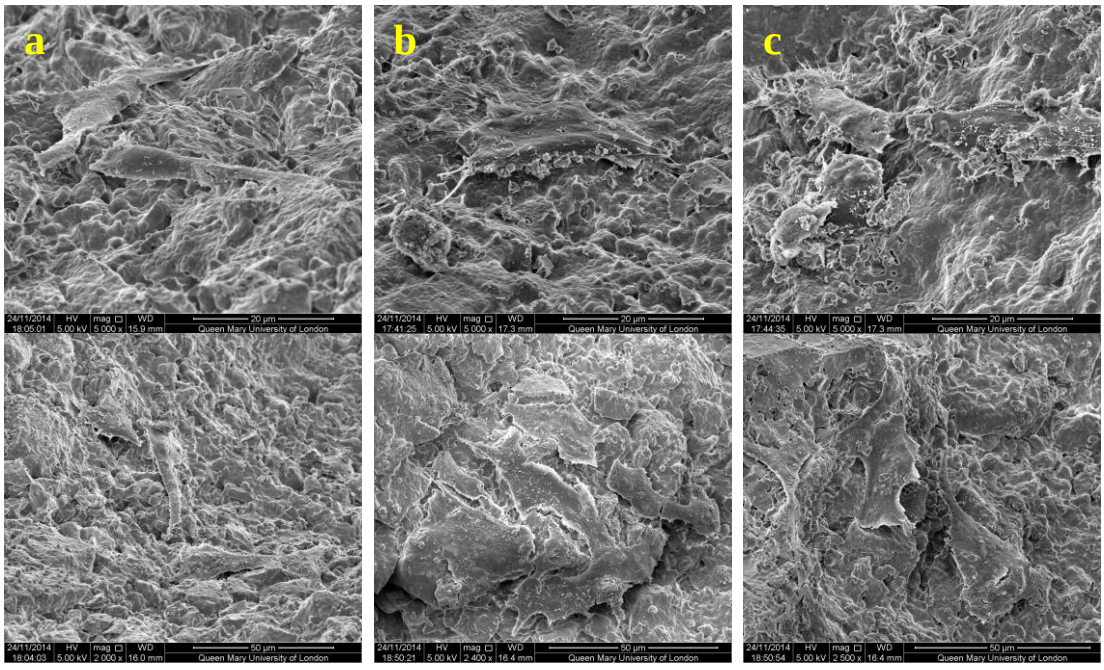

Figure 10.21: Day 3 cell attachment on SA80/30 surface from a) top section at 5000x & 2500x, b) middle section at 5000x & 2500x & c) bottom section at 5000x & 2500x

- DAY 5

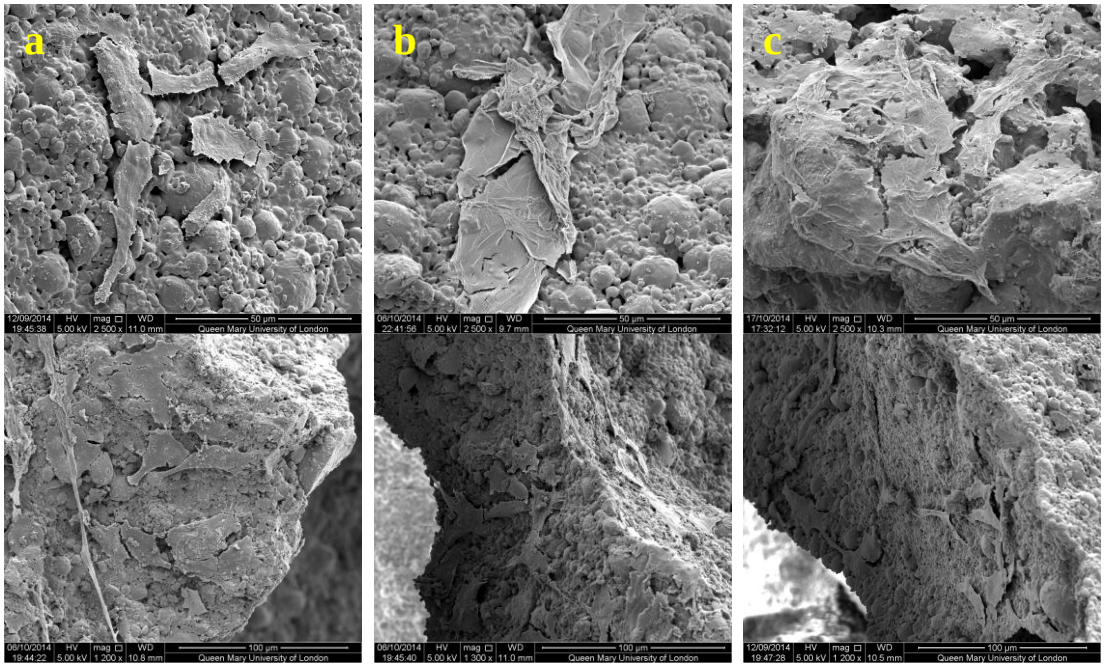

Figure 10.22: Day 5 cell attachment on SA80/30 surface from a) top section at 2500x & 1200x, b) middle section at 2500x & 1200x & c) bottom section at 2500x & 1200x

- DAY 7

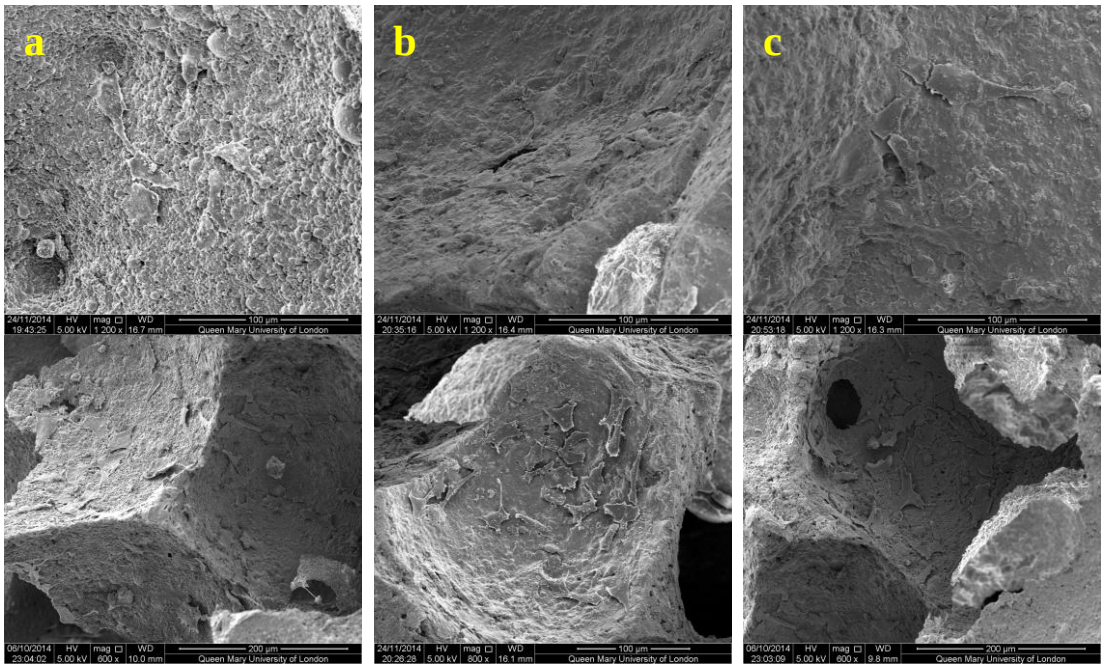

Figure 10.23: Day 7 cell attachment on SA80/20 surface from a) top section at 1200x & 600x, b) middle section at 1200x & 600x & c) bottom section at 1200x & 600x

10.4 Discussion

Previous chapters have concentrated on validating the 3D perfusion system by studying the dynamic ion exchange occurring in SA80/20 granules and then looking at subsequent static cell response to the PCM collected from the perfusion experiments. The results gained from this chapter looked into understand the relationship between dynamic ion exchange and osteoblast-like cell response within a 3D dynamic perfusion system using HA80/20, SA80/20 and SA80/30 porous granules. In essences the system would be able to demonstrate whether altering the chemistry and/or porosity of the BGS granules had an effect on ion release and what effect this had on cell response.

10.4.1 Influence of Chemistry

When investigating the influence of chemistry between HA80/20 and SA80/20, it was evident that the release of calcium ions was statistically different at day 1 whereby the media incubated in HA80/20 saw a statistically greater release in comparison to SA80/20 ($p<0.05$). A significant drop in calcium ion concentrations was seen from 4 hours to day1 from HA80/20 and S80/20 ($p<0.05$), however these levels were still significantly higher than the bulk solution at day 1 ($p<0.05$). By the end of the study (day 7) calcium ion levels had reached bulk solution levels with HA80/20 however with SA80/20 the levels were significantly lower than the bulk solution level ($p<0.05$). These findings would suggest that there was a greater precipitation of calcium ions back on to the surface of SA80/20 granules in comparison to HA80/20 as the levels of calcium ions were found to be statistically lower in the media from SA80/20. The initial release of phosphate ions were statistically similar between HA80/20 and SA80/20. Thereafter the phosphate levels began to drop at levels statistically similar to each other ($p<0.05$). By the end of the study (day 7), phosphate ion concentration levels in the surrounding media from HA80/20 and SA80/20 had reached statistically similar levels. This suggested that the phosphate ions had precipitated back on to the BGS surface. Significantly greater silicate ion release was observed from SA80/20. After the initial release, silicate ion concentration levels decreased in media from both BGS. At day 7 the silicate ion levels were statistically similar to the bulk solution levels.

From the results, it is evident that HA80/20 showed a significantly increase DNA concentration for the duration of the experiments in comparison to SA80/20 from day 3 to day 7. SA80/20 provided a significantly more supportive environment for cell differentiation over cell proliferation (Figure 10.9 and Figure 10.8 respectively). ALP is an ectoenzyme, produced by active osteoblasts which are involved in the early initiation of

mineralisation of newly formed bone tissue. Therefore, ALP is a useful marker for osteoblast activity (Wang, Duan et al. 2004). A study conducted by da Silva et al looked at investigating osteoblast-like cells seeded on to HA and SA under static and dynamic conditions. The study showed that there was a high activity of the ALP enzyme under dynamic conditions on both HA and SA in comparison to static conditions and that there was greater ALP activity seen with SA under dynamic conditions (da Silva, Mateescu et al. 2010). The findings in the current work are in agreement with these findings in that SA80/20 provided a statistically improved environment for cell differentiation with increased levels of ALP activity throughout the study. It is found that the organisation of acting fibres have a direct influence on cellular differentiation (Ehara, Ogata et al. 2003). It is also been found that stressed fibres change their biophysical properties which can generate several types of signalling molecules (Thian, Huang et al. 2006). Therefore it can be suggested that due to the presence of a dynamic environment, the higher ALP activity seen on the SA80/20 granules could be related to the modification of these acting fibres morphology exhibited by cells under dynamic fluid flow conditions. Also another reason for the increase ALP activity with SA80/20 could be due to the presence of silicon within the HA structure. Silicon is essential for the normal bone growth and development, because collagen and proteoglycans are cross-linked by this element. Moreover, silicon has also been shown to act directly in the bone mineralisation process (Pietak, Reid et al. 2007).

Recently, Castagna reported ALP activity being significantly higher on HA granules at earlier times points (days 1 - 5) and on SA at later time points (days 7-14). However this was only seen on samples that had not been pre-treated. With the addition of serum proteins, there was a significantly higher ALP activity seen on only the HA (Castagna 2014). These findings are in discordance with the current work as the perfusing media contained FBS and with this a significantly greater ALP activity was observed with SA80/20 especially on day 3 where ALP activity peaked intracellular. A study by Botelho et al, compared the cell behaviour of human osteoblast cells between HA and 0.8wt% and 1.5wt% SA. Greater ALP activity was observed at day 7 from the 0.8wt% SA compared to HA. However this particular study used dense discs. This change in form of the BGS compared to porous granules being used in this current study could play a role in the difference in results achieved as porous granules provide a greater surface area for cell attachment and growth in comparison to dense discs therefore, showing an increase in ALP activity earlier at day 3 in comparison to peaking at day 7 as it did in Botelho's study (Botelho, Brooks et al. 2006). Another aspect to consider is that the study by Castagna and Botelho et al conducted their experiments under static conditions with regular medium changes. In essence a static

environment does not provide an environment which represents physiological conditions in the body. Using a 3D dynamic perfusion system allows for efficient fluid flow to and within the porous granules allowing better mass transfer of nutrients to the cells seeded on the BGS (Martin, Wendt et al. 2004).

CICP was investigated extracellular and intracellular and both observed different trends. The deposition of extracellular matrix protein, collagen-I is well established to be directly proportional to the presence of CICP in medium (Kaspar, Seidl et al. 2000). The c-terminal end of the collagen molecule is cleaved off by the osteoblast once deposited in to the extracellular matrix. Guth found and increase in CICP concentration in medium on SA throughout the time analysed (Guth 2007). Although collagen-I is not exclusive to bone, the deposition of collagen-I is a marker for osteoblast matrix maturation but is also produced in tissues such as kidneys and skin (Maeno, Niki et al. 2005). The expression of collagen-I is known to be a marker of mature osteoblast-like cells. Botelho et al reported higher CICP production from osteoblast-like cells which were in contact with SA compared to HA at all the time points up to 25 days (Botelho, Brooks et al. 2006). Reffitt et al (Reffitt, Ogston et al. 2003) showed how orthosilicic acid stimulates collagen-I synthesis in human osteoblast-like cells and enhances osteoblastic differentiation. Castagna found that the presence of silicon significantly increased CICP production at day 4 with MSC's however, this was on granules that had not been pre-treated with proteins. Once pre-treated with serum proteins the CICP production was found to be statistically similar between HA and SA granules (Castagna 2014). Fielding et al was able to show the positive effect that silicate ions have when incorporated in TCP whereby it promoted greater collagen-I levels and blood vessels density compared to pure TCP *in vivo* (Fielding and Bose 2013). The findings in this current study corroborate with previous findings however, the CICP production intracellular was only statistically different on day 3 and day 5 of the experiments with the cells lysates from SA80/20 showing greater production. There was a distinctive increase in CICP production on day 1, but the current study is unable to clarify the positive effect of the incorporation of silicon in to the HA lattice at this particular time point. A difference between the previous studies and the current work is that previous work use static models with regular media changes to conduct their experiments in comparison to the a 3D dynamic perfusion system which has been used in the current study. There is a lack of literature available whereby collagen-I levels have not been investigated within perfusion bioreactor systems. The addition of fluid flow within direct perfusion bioreactor systems have shown to enhance growth, differentiation and mineralised matrix deposition by bone cells (Goldstein, Juarez et al. 2001, Bancroft, Sikavitsast et al. 2002). Therefore trying to maintain and mimic a

physiological environment is essential when trying to conduct experiments investigating cell response. The current study looked at CICP production intracellular and results obtained were different to what was seen extracellular with the differences in chemistry being significantly different from day 1 to day 5, again with SA80/20 observing a greater CICP production intracellular. Most studies conduct CICP analysis extracellular however, it was interesting to see that CICP levels are altered intracellular when tested.

OCN is a protein which plays an important role in the process of bone formation therefore it is widely used as a marker for osteoblast differentiation. Botelho reported high levels of OCN at day 7 from osteoblast-like cells seeded on HA and 0.8wt% SA and 1.5wt% SA with 0.8wt% SA showing a significantly increased amount of OCN expression (Botelho, Brooks et al. 2006). Castagna observed extracellular OCN production to be significantly higher on HA however, once pre-treated with fibronectin the SA granules supported greater OCN production (Castagna 2014). The current work did not show a clear trend with time with the extracellular OCN release in the surrounding collected media from all BGS however, a significant difference in intracellular OCN production at the earlier time point of day 1 with SA80/20 observing the greater production at this time point. Bancroft et al saw a peak release of OCN at day 13 of their experiments involving rat stromal osteoblast cells being seeded on titanium fiber mesh scaffolds (Bancroft, Sikavitsast et al. 2002). In 2003, Cartmell et al observed OCN to be upregulated at a flow rate of 0.2ml/min in the extracellular media normalised by RNA obtained by seeding osteoblast-like cells in to human trabecular bone scaffolds (Cartmell, Porter et al. 2003). Wang et al investigated cell viability within a perfusion system using bone marrow derived osteoblasts seeded on β-TCP scaffolds. OCN was detected within the first week in culture and increased significantly by 4 weeks in culture (Wang, Uemura et al. 2003). The current work saw a significant production of intracellular OCN at day 3 with HA80/20 and SA80/20. The important factor to consider is that the previous work involving perfusion systems used different scaffold materials to seed cells on and the extracellular OCN release in media was either normalised for DNA or RNA however, in the present study the extracellular OCN release was not normalised. Previous studies using perfusion systems have used TCP-HA, coralline HA or collagen-HA as the scaffold materials (Vance, Galley et al. 2005, Bjerre, Bunger et al. 2011, Antebi, Cheng et al. 2013). However stoichiometric HA along with SA have not been investigated within perfusion systems. This could be a reason for the differences in extracellular OCN release in to media seen especially at earlier time points. As SA80/20 showed a significantly greater OCN release for the duration of the 7 day study it can be suggested that this was due to the

presence of silicon within the HA lattice. However there was no distinctive trend that was observed with time with the release of OCN in media for all BGS tested.

10.4.2 Influence of Strut Porosity

For over 30 year, porous ceramics have been considered for use as synthetic BGS with many reporting greater and faster degree of bone penetration with increasing macroporosity (Klawitter and Hulbert 1972, Eggli, Muller et al. 1988, Kuehne, Bartl et al. 1994, Hing 2005). From previous *in vitro* and *in vivo* studies, the biological sensitivity to the level of microporosity within the ceramic struts has been demonstrated (Bignon, Chouteau et al. 2003, Annaz, Hing et al. 2004, Hing, Saeed et al. 2004). It has also been clearly demonstrated that microporosity significantly effects the post implantation response of porous HA scaffold (Hing, Annaz et al. 2005). Annaz et al showed that cells are able to sense the microporosity and respond to this by orienting protruded filipodia towards the micropores (Annaz, Hing et al. 2004). In the current study it was found that there was a significantly increased release ($p<0.05$) of calcium, phosphate and silicate ions from SA80/20 and SA80/30 in comparison to the bulk media. SA80/20 showed a significantly increased calcium ion release between 30 minutes and 4 hours of the experiments ($p<0.05$) with the greatest difference shown at 4 hours. From day 1 to day 7 calcium levels were statistically similar between SA80/20 and SA80/20. Phosphate and silicate ion release was statistically similar between the two BGS for the duration of the experiments. After 4 hours silicate ion levels dropped with both BGS and then remained statistically similar to the bulk solution levels until the end of the experiments. From these results it can be suggested that there was statistically similar levels of calcium and phosphate ions precipitated back on the individual BGS surfaces along with a statistically similar uptake of silicate ions.

When investigating the differences in the levels of microporosity, there have been some *in vivo* studies which have found that with a greater level of microporosity, osteointegration is enhanced (Hing, Saeed et al. 2004, Campion, Chander et al. 2011). From the current study the DNA concentrations results obtained showed that cell proliferation was favoured with SA80/30 with a significant difference observed on day 3 and day 7 of the experiments in comparison to SA80/20. At earlier time points (day 0 and day 1) the concentration of DNA seen were similar suggesting cell proliferation was statistically similar in both SA80/20 and SA80/30. A higher osteogenic potential of SA with a greater strut porosity has been previously demonstrated with *in vivo* studies (Hing, Saeed et al. 2004, Campion, Chander et al. 2011, Coathup, Samizadeh et al. 2011, Chan, Coathup et al. 2012, Coathup, Hing et al. 2012). Findings by Castagna showed that a change in strut porosity has a significant effect

on intracellular ALP activity. SA with 30% strut porosity showed increase cell differentiation irrespective of either being pre-treated with fibronectin or not being pre-treated (Castagna 2014). The current study was not able to corroborate with previous findings as SA80/20 observed a significantly greater intracellular ALP activity in comparison to SA80/30 from days 3 to 7. SA80/30 showed an increased release on day 1 however this release was not significantly different to SA80/20 on the same day.

CICP analysis conducted extracellular and intracellular observed varying results. SA80/20 saw significantly greater intracellular CICP production between days 1 and 7 in comparison to SA80/30 however this increase was only significant at day 3 and day 5. Extracellular CICP release in media observed CICP release to be significantly greater with SA80/20 at the earlier time points and CICP release with SA80/30 showed significant increase at the later time points when comparing strut porosities. There is very limited literature on the effects of microporosity on CICP production *in vitro* within static environments or even within perfusion system. However *in vivo* studies have showed that a dense collagenous cellular region is found in the centre of some micropores and it appeared that these specific regions gradually got replaced by bone (Coathup, Samizadeh et al. 2011, Coathup, Hing et al. 2012). However the study reported that this was occurring commonly on CaP specimens used in comparison to silicon containing CaP specimens with greater strut porosities.

OCN was again measured extracellular and intracellular. When tested intracellular, the result obtained showed a distinctive peak production of OCN with SA80/20 at day 3 which then significantly decreased by day 5 and a further decrease was observed at day 7. SA80/30 on the other hand saw an increased production at day 1 which began to decrease by the drop was not significant until day 7. On days 5 and 7 OCN production remained significantly increased in SA80/30 in comparison to SA80/20 however these levels were still lower than the levels that been observed earlier on in the experiments. There was no clear trend observed with time for the OCN release from the two BGS with time. Castagna was able to show greater OCN production from SA80/30 however once pre-treated with fibronectin, OCN production increased on SA80/20 (Castagna 2014). The result obtained from the CICP and OCN levels extracellular show no clear trend between the two different SA structures. This in turn suggests that maybe the cell concentration was low or the time points tested were too early in order for MG63 cells to show CICP or OCN release extracellular. These could be a reason as to why no net increase in CICP or OCN release was observed.

The results obtained in this particular experiment are not comparable to previous work as there are many differing factors which need to be considered. From the experiments it was

anticipated that the 3D perfusion system would be able to test the differences in cell response between different strut porosities in order to try and mimic *in vivo* responses but within an *in vitro* setting. However the results obtained were not able to corroborate with data observed *in vivo*. There was no clear trend seen which suggested that SA80/30 has an increase osteoinductivity when compared SA80/20. Previously it has been shown that when analysing BGS in orthotopic sites, it is often difficult to see significant differences between strut porosities (Campion, Chander et al. 2011). This may be due to the presences of both stem cells and pre differentiated cells. This is turn suggest that maybe to really test the osteoinductive potential of a BGS *in vitro* stem cells need to be used. Castagna saw a difference in cell response between pre differentiated MG63 cells and human stem cells with stem cells showing greater sensitivity to cell proliferation and cell differentiation between SA80/20 and SA80/30 (Castagna 2014). The findings by Castagna corroborate with previous work conducted at ectopic site whereby differences in strut porosity show a greater significance as only stem cells are present therefore the cells are driven to differentiate in to bone cells in order to help in bone regeneration (Coathup, Samizadeh et al. 2011, Coathup, Hing et al. 2012).

It has also been shown that the addition or exposure to growth factors stimulates differentiation of cells which in turn enhance bone growth. Bone morphogenic proteins (BMPs) have been demonstrated to stimulate differentiation of MSCs down the osteogenic lineage. BMP-2 and BMP-7 have shown positive results for their use in orthopaedic reconstruction and also show how silicate substitution increases affinity between BMPs and CaP (Alam, Asahina et al. 2001, Yang, Whitaker et al. 2004, Pluhar, Turner et al. 2006). From these findings it may be possible in the future to pre-condition the BGS granules with growth factors in order to enhance cell response which may result in differences between BGS structures and chemistry. Another factor to consider would be to add mechanical loading to the cell seeded BGS constructs in order to mimic the loading conditions which would occur on the granules when inserted in to the body. Increasing evidence has suggested the addition of mechanical forces increase the activity of the cells which in turn improve or accelerate the rate of bone tissue regeneration (Bjerre, Bunger et al. 2008). Bioreactors that are able to apply controlled mechanical forces, such as dynamic compression, to BGS constructs can be used as model systems of bone tissue development under physiological loading conditions, and to generate functional tissue grafts. Compressive deformation can be applied by a computer controlled micro-stepper motor, and the stress on the constructs can be measured using a load cell(Martin, Wendt et al. 2004).

10.4.3 Wall Shear Stress and Streaming Potential

The research behind bone tissue engineering aims to generate suitable BGS to ease the demands and reduce the potential risks which are associated with the traditional autograft and allograft bone replacement procedures. The work in this thesis established a 3D perfusion system which offers a more systematic investigation of how scaffold structure can impact on the local physiological environment and subsequent cell behaviour.

Consequently the setup of this current 3D perfusion system can further go on to provide a convenient way to deliver mechanical stimulation to the cells *in vitro*. Biomechanical stimuli play an important role in the normal formation, development and homeostasis of bone tissue. Removal of mechanical loading, such as bed rest, prolonged periods in low gravity (space travel) leads to disuse osteoporosis. It has been found that when bone is exposed to relatively brief periods of physiological levels of mechanical stimulation, with a different strain distribution new bone formation can be initiated. However, little is known of the cellular mechanisms underlying the osteogenic response and the nature of the mechanical signal that activates a sensor cell(s) within bone. There have been many suggestions, which include cell deformation as a result of direct strain on the bone surface, or loading-induced fluid flow through the lacunocanalicular network of bone (Smalt, Mitchell et al. 1997). This may be detected as wall shear stress or streaming potentials, which are two distinctive stimuli that could affect cells behaviour. The osteocyte response to mechanical strain is lost in the presence of gadolinium chloride a stretch/shear activated ion channel inhibitor, however in osteoblasts, the early responses to bone loading have been shown to be associated with ion channels that are sensitive to gadolinium (Rawlinson, Pitsillides et al. 1996). Increased flow rates too high levels is likely to lead to larger wall shear stresses which in turn can either wash away the attached cells, unfavourably alter cell metabolism or even cause cell death (Yan, Chen et al. 2011). Streaming potentials are generated when there is a movement of charged molecules in the fluid across the cell surface. When the fluid flows, a potential difference is generated across the cell membrane. These generated potential differences can lead to either changes in cellular ion balance or activate voltage-gated ion channels (Smalt, Mitchell et al. 1997). Osteoblast cells are known to have voltage-gated ion channels. If the streaming potential magnitude is changed, this could affect the gating levels allowing cells to respond more easily if these levels are bought closer to the threshold.

This model was established to replicate the possible situation in vivo, where BGS are implanted into a defect. It is important to note that highly porous scaffolds, as used in this study, have exceptionally irregular geometries as a result of their manufacturing processes.

This results in non-uniform flow patterns, making shear stress estimations extremely challenging. Additionally, the overall fluid dynamics would be highly complicated with many variables and boundary conditions, and so any computer aided modelling would ultimately be difficult to compute requiring extensive computational time and resources.

10.5 Summary and Conclusions

In summary, when comparing the results obtained from the different chemistries, it can be suggested that the presence of silicon within the HA lattice along with the increased levels of calcium ions on the SA80/20 surface made an environment more favourable for cell differentiation as the levels of ALP were significantly increased with SA80/20 from day 1 through to day 7. HA80/20 however showed a more favourable environment for cell proliferation from day 3 to day 7. CICP production was also significantly increased extracellular from day 1 to day 7 from SA80/20 along with significantly increased levels of OCN from day 1-5. The variation in cell response to the two different BGS used highlights the sensitivity of cellular behaviour to porous scaffold substrate chemistry even within a 3D dynamic environment where the media undergoes continuous replenishment throughout the 7 day period. This data corroborates the data obtained from clinically relevant *in vivo* models that slight changes in graft chemistry can have a significant effect on cell response.

When evaluating the differences in strut porosities with SA BGS, the 3D perfusion system was not able to show significant differences in cell response between SA80/20 and SA80/30 therefore the work did not corroborate with previous work conducted at *in vivo* ectopic sites which show a significant difference between increased strut porosities.

The work conducted in this thesis has successfully identified that porous apatite BGS granules interact significantly with the local aqueous environment. A 3D perfusion system has been set up that can be seeded with pre differentiated MG63 cells that can then be monitored as they colonise and respond to the various BGS while seemingly also having a significant effect on the way in which a BGS interacts with the local aqueous environment.

Chapter 11 Conclusions and Recommendations for Future Research

The purpose of this chapter is to bring together all the findings observed from the previous chapters and highlight the important conclusions obtained. The aim of this research was to develop a 3D *in vitro* perfusion system in order to monitor ion exchange and subsequent cell response to real granular synthetic bone graft substitute materials within a truly 3D environment. The purpose of the system was to more closely mimic the 3D environment *in vivo* which would allow a more efficient way to investigate how scaffold structure can impact on the local physiological environment and cell response.

11.1 Main Conclusions from Chapters

- In chapter 3, the experiments conducted found that a semi-dynamic system showed that material chemistry and strut porosity had an effect on ionic interactions between the surrounding media and the BGS surface by observing a successful CaP layer on the surface of the graft materials. From the experiments, through SEM imaging it was found that the formation of a CaP layer was not homogenously distributed on the granules. The layer was only seen on granules which were on the outer side of the mesh basket the granules were held in. Within the basket the granules did not have a CaP layer present as they were not exposed to as much, if any media which would have allowed for the exchange of ions hence developing a CaP layer on the granules, making this a limitation of the experimental setup. Therefore in order to understand the complexity of interactions between the BGS and surrounding *in vivo* environment, a semi-dynamic system was not a true representation of the dynamic ion exchange between the BGS and the surrounding environment which would be taking place *in vivo*.

- In response to the limitation of the work in Chapter 3, Chapter 4 endeavoured to set up a 3D perfusion system whereby the effect of media volume on the rate and extent of ion depletion on exposure to a fixed mass of granules was investigated. Additionally, cell culture experiments were performed to investigate any potentially confounding sensitivity to ion depletion under standard 2D and 3D static conditions with periodic refreshment of pre-conditioned media. The circulating study

demonstrated that there was a fluctuation in ion concentration with not only time but also volume of circulating media. The cell study demonstrated that variation in calcium, phosphate and silicate $_{ion}$ concentrations has a clear impact on osteoblast-like cell response. The depletion of phosphate ions from all PCM seemed to affect cell proliferation regardless of the volume of media being perfused. Therefore to investigate this further and to overcome this it was suggested that the 3D perfusion experiments should be partially or continuously refreshed in order to reflect more closely the *in vivo* environment if the mechanisms behind osteoinductivity are to be investigated *in vitro*.

- The work presented in chapter 5 showed that partially replenishing the bulk media within the 3D circulating system, unsurprisingly, delayed the depletion of calcium and phosphate ions. Cell response was sensitive to greater levels of these ions with increased cell proliferation and metabolism. However by day 7, ion levels were severely depleted which suppressed cell response with time. The work also showed that there was no significant difference in ion exchange and subsequent cell response when stirring or not stirring the circulating media. Having identified the severely depleted levels of ions by day 7 and the suppressed cell response, further development of the 3D perfusion system was needed to explore the effects of the increased levels of calcium and phosphate ions on cell response. Investigating a continuous media replenishment during the circulation study needed to be explored to see whether this had an effect on ion exchange and subsequent cell response on porous BGS in 3D.

- In chapter 6 for complete refreshment of media, day 1 and day 5 were chosen as the first and second time points. This was because at these specific time points there was a decrease in both calcium and phosphate ion concentrations (Chapter 5 section 5.3). From this work it was concluded that having complete media replenishments at 2 different time points would inevitably subject cells to fluctuating ion concentrations in the circulating medium which in turn may have confounding effects on their behaviour. Also it will not be possible to conclude whether the changes in cell behaviour are occurring due to the fluctuation in the dynamic ionic environment, the changes in structure or the changes in chemistry of the BGS granules being used. It was also found that there was an instability of the pH of the circulating media which could have been due to the formation of bone like apatite combined with the absence

of a positive CO_2 atmosphere. Therefore the results obtained necessitated the use of a fully 'perfused flow to waste system' testing different media types which would mimic the physiological environment.

- Chapter 7 investigated ionic concentration and pH behaviour of sodium bicarbonate buffered DMEM and HEPES buffered DMEM when perfused through porous silicate substituted granules, directly to waste, as opposed to into a fixed volume reservoir which was either maintained (Chapter 4), partially replenished (Chapter 5) or completely replenished (Chapter 6) over 7 days. Once the ionic behaviour was known the second objective was to investigate osteoblast-like cell response to the two types of collected pre-conditioned media. From this work it was concluded that the 'to waste' flow perfusion system is a better system to be working with as it provides an improved solution to investigate varying flow dynamics which can offer insight into sample response *in vivo*. It was also found that supplementing DMEM with HEPES buffer supports better ion exchange along with positive effects on cell response whilst maintaining physiological pH levels.

- The objective of the work conducted in chapter 8 was to investigate the effects of serum containing media on dynamic ion exchange within a flow to waste perfusion system between 3 grades of bone graft substitute granules, stoichiometric hydroxyapatite of 80% total porosity and 20% strut porosity (HA80/20) and 0.8wt% silicate substituted hydroxyapatite with 80% total porosity and 20% & 30% strut porosity (SA80/20 and SA80/30 respectively) and the surrounding media. Subsequent cell response was also determined by incubating MG63 cells on tissue culture plates with the PCM collected from the 'to waste' circulation experiment between HA80/20, SA80/20 and SA80/30 and the surrounding media. This work concluded that the addition of serum proteins to the bulk feeding media was able to regulate ion release from the BGS to the surrounding media however it was interesting to note that cell response was suppressed with there being no sign of cell differentiation by day 5. This would suggest the cell seeding concentration of $4x10^4$ cells/ml might have been too low.

- The work in Chapter 9 aimed to investigate two methods in order to seed cells on to the porous granules and also consider the cell concentration in order to find an optimum cell concentration and seeding method of the MG63 cells on to the porous

silicon substitute hydroxyapatite granules (SA80/20) without causing immense cell death before inserting the cell seeded scaffolds in to the 3D flow perfusion environment for periods of up to 7 days. The worked demonstrated that seeding the cells directly on the packed granules within the sample silicone tube of 8mm diameter and 15mm length was a more efficient way to seed the cells on to the scaffold material compared to seeding the cells on the porous granules in 24 well plates and after allowing 2 hours for cell attachment, transferring the granules into the silicone tubes which, showed greater cell death. Also it was concluded that the greater cell concentration tested, $8x10^4$ cell/ml made more cells available for cell on cell interaction. This in turn provides a better environment for cell attachment and growth and allows a better spread of cells covering a considerable part of the materials surface.

- Having developed a flow to waste perfusion system that was able to maintain a stable media pH while undergoing dynamic ion exchange with real apatite-based bone graft substituted materials, chapter 10 endeavoured to validate the system through seeding osteoblast-like cells onto a range of scaffolds with well characterised differences in chemistry and structure that resulted in known variations in *in vivo* behaviour to identify whether any correlation in subsequent osteoblast like response was observed or not. The work conducted in this chapter successfully identified that porous apatite BGS granules interact significantly with the local aqueous environment and that the system was sensitive in showing how changes in material chemistry can alter cell response. The 3D perfusion system can be seeded with pre differentiated MG63 cells that can then be monitored as they colonise and respond to the various BGS.

11.2 Future Research Work

From the results obtained in this research, there are some suggestions for future work in order to maximise the efficiency of the *in vitro* 3D perfusion system. This will then more closely mimic the 3D *in vivo* environment to enable a more systematic investigation of how scaffold chemistry and strut porosity can impact the local physiological environment and subsequent cell behaviour.

- Conducting the 3D perfusion system experiments with stem cells and not pre-differentiated osteoblast-like cells may make the system more sensitive, which in

turn would mean cell response to graft porosity would observe significant differences highlighting the enhanced osteoinductive nature of SA80/30 as previously done so in ectopic studies.

- Pre-conditioning the granules with BMPs growth factors may mediate greater cellular response to bone graft substitutes before seeding the grafts with cells as previous work has shown an increase in cell response once pre-treating the graft material with this particular growth factor. Once pre-conditioning the granules with BMPs and seeding them with cells, placing these loaded constructs in to the 3D perfusion system may then improve the results gained from the system by emphasising how changes in scaffold chemistry and porosity can dictate the osteoinductive nature of bone graft substitute materials.

- Another approach to look at the differences between scaffold chemistry and strut porosity would be to subject the scaffold to mechanical loading in order to test a BGSs osteoinductive potential *in vitro*. Increasing evidence has suggested that mechanical forces, which are known to be important modulators of cell physiology, might increase the activity of cells when seeded on synthetic scaffolds thus, possibly improve or accelerate the rate of bone tissue regeneration. Hing et al conducted a study showing how microporosity enhances bioactivity of synthetic bone graft substitutes using an ectopic model. It was found that graft materials with increased strut porosity had elevated bone volume. Mechanical testing results suggested that the difference in behaviour between the varying porosities may reflect the variations in scaffold mechanics *in vivo* (Hing, Annaz et al. 2005). Other authors have shown how increasing strains of up to 40% are provoked by the deflection osteotomy gap by the patello-femoral force during walking (Claes, Reusch et al. 2011). Despite numerous studies showing that mechanical conditioning can improve the structural and functional properties of synthetic scaffolds, little is known about the specific mechanical forces that are stimulatory for a particular tissue (Martin, Wendt et al. 2004). Long bones are normally subjected to mechanical strains up to 3000 microstrain (0.3% deformation) and thus very sensitive to the mechanical environment. An understanding of this highly complex field can be achieved by performing experiments aimed at explaining the mechanisms of processes for cellular response to well defined and specific mechanical stimuli. In this context, using the developed 3D perfusion system from this research can provide a controlled

environment for the reproducible and accurate application of specific mechanical forces to real bone graft substitutes in order to test the osteoinductive potential of these materials. Because of the bone anatomy, resident bone cells are exposed to many potential stimuli generated by mechanical loading (Liu, Liu et al. 2013) generating a number of potential regulators of cell activities:

- Direct mechanical strain – tension/compression/torsion
- Fluid shear through canaliculi
- Streaming potentials
- Calcium dissolution
- Strain energy density

However, the 'anatomy' of the granules is unlike that of bone, the potential for the exact stimuli is not expected. As stated previously, the design of the perfusion system is to try to replicate the BGS environment in vitro in order to test the suitability of novel particulate BGS formulations.

Notwithstanding, mechanical forces affect cellular differentiation pathways and are important in order to control tissue morphogenesis from stem cells. There have been many studies which have investigated the influence of substrate properties on the mechanostimulation of bone cell cultures, however, most of these studies have concentrated on single features of the material, such as; substrate chemistry, substrate roughness or pore size (Di Palma, Douet et al. 2003, Kilpadi, Sawyer et al. 2004, Di Palma, Guignandon et al. 2005). Research in this area has concentrated on the effects of fluid shear stress, direct strain or both on cell regulation by designing *in vitro* models that have mainly been based on experimental calculations for the expected fluid shear stress or direct strain within physiological bone. However, there have not been many studies, which have calculated the expected physical properties of biomaterial substrates when applied within a clinical setting and hence relate the data to *in vitro* or *in vivo* data for the same biomaterial, therefore an exact in vitro loading/strain protocol is difficult to devise. Mechanical testing in a previous study by Campion (2015) revealed silicate substituted calcium phosphate to have similar mechanical behaviour to morcellised cancellous bone, under similar test conditions. It was further proposed that regions within these bone graft masses, appear to be stress-shielded under the conditions presumed to occur in typical applications such

as, a tumour defect void or in a spinal fusion defect (Campion 2015). Therefore, mechanical deformation of the majority of the BGS mass was minimal, and fluid flow was presumed to be the dominant signal affecting resident cells.

Bioreactors have been developed to study the effects of mechanical stimulation on cell growth. Flow through the scaffold produces local shear stresses on the cell surface. The architecture of the scaffold can further control the transport of nutrients within the sample. The presence of flow within a bioreactor can also result in the production of extra cellular matrix elements (Lawrence 2008).

A preliminary model was adapted from a model previously used by Haj et al (Haj, Minter et al. 1990) and technical drawings were produced (see APPENDIX 8). The Bose ElectroForce 5500 Load Frame System (Figure 11.1) was used in order to allow for compression testing of the cell seeded scaffolds. However due to time constraints this model was not manufactured and tested. The schematic in Figure 11.2 shows the assembly of the parts. This assembly would fit in to the Bose load frame. The complete loading system would then be contained within a temperature, carbon dioxide and oxygen controlled Binder incubator. The Bose load frame together with a 444N (100lb) load cell would allow for the compressive force on the cell seeded scaffolds to be measured. The system would firstly allow for packing of the granules before any potential deformation could take place. Cell colonisation can be affected by loading from both external forces and fluid flow once the scaffold is placed in to the flow system. The scaffold will be subjected to most of the forces provided by the system and fluid flow, while the cells will experience the micromechanical properties and the local shear stresses within the porous scaffold structure. Under uniaxial compression conditions, there may be a stress-shielding effect, as reported by Campion (2015), where the central portion of the granule mass may see little direct loading or deformation. It is important to remember that in the physiological environment, there will never be uniaxial loading alone, there will always be a combination of fluid shear isostatic and multiple point shear, compression and tension because of muscle attachment and direct skeletal loading due to the occasional bit of bone to bone or inanimate object impingement, gravity and atmospheric pressure. The aim of the current work presented in this thesis was to set up a simple 3D system where we could look at the response of bone cells to granules exposed to a couple of the isolated factors as a possible mechanism to screen for structural as well as chemical factors in BGS design.

The cells are believed to be able to sense the porosity of scaffold grafts and the other cells which, are attached nearby (Lawrence 2008). The aim of this system would be to develop a 3D system that would closely mimic the physiological BGS environment in order to test the osteoinductivity of clinically relevant BGS seeded with osteoblast-like cells or stem cells that can then be monitored as they colonise and respond to the various BGS and to see whether changes in scaffold chemistry and porosity have an effect on cell response under mechanical loading conditions.

Figure 11.1: Bose ElectroForce 5500 Load Frame

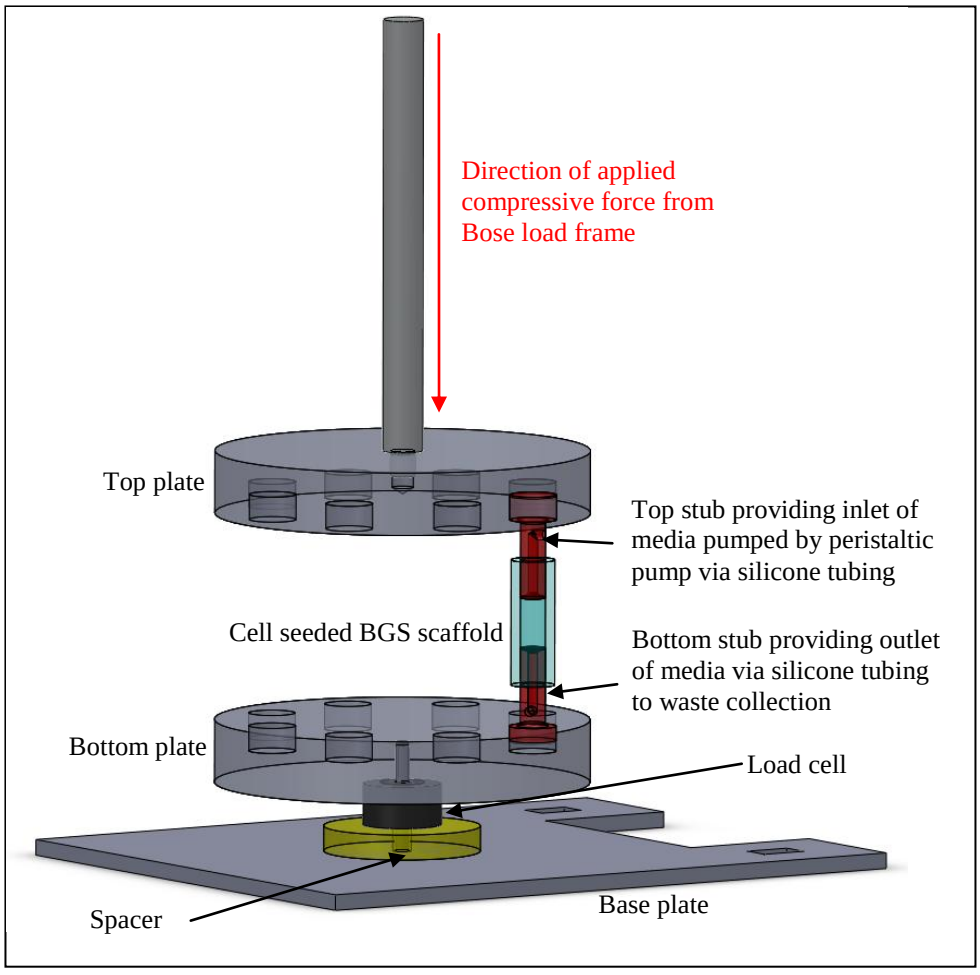

Figure 11.2: Schematic showing assembly parts of loading model

References

Adams, B. R., A. Mostafa, Z. Schwartz and B. D. Boyan (2014). "Osteoblast response to nanocrystalline calcium hydroxyapatite depends on carbonate content." Journal of Biomedical Materials Research Part A 102(9): 3237-3242.

Alam, M. I., I. Asahina, K. Ohmamiuda and S. Enomoto (2001). "Comparative study of biphasic calcium phosphate ceramics impregnated with rhBMP-2 as bone substitutes." Journal of Biomedical Materials Research 54(1): 129-138.

Albee, F. H. (1920). "Studies in Bone Growth: Triple Calcium Phosphate as a Stimulus to Osteogenesis." Annals of Surgery 71(1): 32-39.

Alberts, B., D. Bray, J. Lewis, M. Raff, K. Roberts and J. D. Watson (1994). Molecular Biology of the Cell, Garland Publishing, New York and London.

Anderson, H. C. (2003). "Matrix vesicles and calcification." Current rheumatology reports 5(3): 222-226.

Anderson, S. I., S. Downes, C. C. Perry and A. M. Caballero (1998). "Evaluation of the osteoblast response to a silica gel in vitro." Journal of Materials Science-Materials in Medicine 9(12): 731-735.

Annaz, B., K. A. Hing, M. Kayser, T. Buckland and L. Di Silvio (2004). "Porosity variation in hydroxyapatite and osteoblast morphology: a scanning electron microscopy study." Journal of Microscopy-Oxford 215: 100-110.

Antebi, B., X. G. Cheng, J. N. Harris, L. B. Gower, X. D. Chen and J. Ling (2013). "Biomimetic Collagen-Hydroxyapatite Composite Fabricated via a Novel Perfusion-Flow Mineralization Technique." Tissue Engineering Part C-Methods 19(7): 487-496.

Arcos, D., D. C. Greenspan and M. Vallet-Regi (2002). "Influence of the stabilization temperature on textural and structural features and ion release in SiO2-CaO-P2O5 sol-gel glasses." Chemistry of Materials 14(4): 1515-1522.

Arcos, D., D. C. Greenspan and M. Vallet-Regi (2003). "A new quantitative method to evaluate the in vitro bioactivity of melt and sol-gel-derived silicate glasses." Journal of Biomedical Materials Research Part A 65A(3): 344-351.

Areva, S., T. Peltola, E. Sailynoja, K. Laajalehto, M. Linden and J. B. Rosenholm (2002). "Effect of albumin and fibrinogen on calcium phosphate formation on sol-gel-derived titania coatings in vitro." Chemistry of Materials 14(4): 1614-1621.

Arinzeh, T. L., T. Tran, J. McAlary and G. Daculsi (2005). "A comparative study of biphasic calcium phosphate ceramics for human mesenchymal stem-cell-induced bone formation." Biomaterials 26(17): 3631-3638.

Athanasiou, K. A., C. F. Zhu, D. R. Lanctot, C. M. Agrawal and X. Wang (2000). "Fundamentals of biomechanics in tissue engineering of bone." Tissue Engineering 6(4): 361-381.

Aubin, J. E., F. Liu, L. Malaval and A. K. Gupta (1995). "Osteoblast and chondroblast differentiation." Bone 17(2): S77-S83.

Ayad, S., R. Boot-Handford, M. J. Humphires, K. L. Kadler and A. Shuttleworth (1998). The Extracellular Matrix FactsBook, San Diego, California, Academic Press.

Bagambisa, F. B., U. Joos and W. Schilli (1993). "Mechanisms and Structure of the Bond Between Bone and Hydroxyapatite Ceramics." Journal of Biomedical Materials Research 27(8): 1047-1055.

Balamurugan, A., A. H. S. Rebelo, A. F. Lemos, J. H. G. Rocha, J. M. G. Ventura and J. M. F. Ferreira (2008). "Suitability evaluation of sol-gel derived Si-substituted hydroxyapatite for dental and maxillofacial applications through in vitro osteoblasts response." Dental Materials 24(10): 1374-1380.

Balas, F., J. Perez-Pariente and M. Vallet-Regi (2003). "In vitro bioactivity of silicon-substituted hydroxyapatites." Journal of Biomedical Materials Research Part A 66A(2): 364-375.

Bancroft, G. N., V. I. Sikavitsas and A. G. Mikos (2003). "Design of a flow perfusion bioreactor system for bone tissue-engineering applications." Tissue Engineering 9(3): 549-554.

Bancroft, G. N., V. I. Sikavitsast, J. van den Dolder, T. L. Sheffield, C. G. Ambrose, J. A. Jansen and A. G. Mikos (2002). "Fluid flow increases mineralized matrix deposition in 3D perfusion culture of marrow stromal osteloblasts in a dose-dependent manner." Proceedings of the National Academy of Sciences of the United States of America 99(20): 12600-12605.

Barakat, A. I. and P. F. Davies (1998). "Mechanisms of Shear Stress Transmission and Transduction in Endothelial Cells." Chest 114(1, Supplement): 58S-63S.

Barradas, A. M. C., H. P. Yuan, C. A. van Blitterswijk and P. Habibovic (2011). "Osteoinductive Biomaterials; Current Knowledge of Porperties, Experimental Models and Biological Mechanisms." European Cells & Materials 21: 407-429.

Berger, C. E. M., H. Rathod, J. I. Gillespie, B. R. Horrocks and H. K. Datta (2001). "Scanning electrochemical microscopy at the surface of bone-resorbing osteoclasts: Evidence for steady-state disposal and intracellular functional compartmentalization of calcium." Journal of Bone and Mineral Research 16(11): 2092-2102.

Best, S. M., W. Bonfield, I. R. Gibson, L. J. Jha and J. D. D. Santos (2001). Silicon-Substituted Apatites and Process for the Preparation thereof. U. S. Patent. US. US 6312468B1.

Best, S. M., S. Zou, R. Brooks, J. Huang, N. Rushton and W. Bonfield (2008). The osteogenic behaviour of silicon substituted hydroxyapatite. Bioceramics, Vol 20, Pts 1 and 2. G. Daculsi and P. Layrolle. Stafa-Zurich, Trans Tech Publications Ltd. 361-363: 985-988.

Betz, R. R. (2002). "Limitations of autograft and allograft: New synthetic solutions." Orthopedics 25(5): S561-S570.

Bielby, R. C., I. S. Christodoulou, R. S. Pryce, W. J. P. Radford, L. L. Hench and J. M. Polak (2004). "Time- and concentration-dependent effects of dissolution products of 58S sol-gel bioactive glass on proliferation and differentiation of murine and human osteoblasts." Tissue Engineering 10(7-8): 1018-1026.

Bigi, A., G. Falini, E. Foresti, M. Gazzano, A. Ripamonti and N. Roveri (1996). "Rietveld structure refinements of calcium hydroxylapatite containing magnesium." Acta Crystallographica Section B-Structural Science 52: 87-92.

Bignon, A., J. Chouteau, J. Chevalier, G. Fantozzi, J. P. Carret, P. Chavassieux, G. Boivin, M. Melin and D. Hartmann (2003). "Effect of micro- and macroporosity of bone substitutes on their mechanical properties and cellular response." Journal of Materials Science-Materials in Medicine 14(12): 1089-1097.

Billiau, A., V. G. Edy, H. Heremans, D. J. Van, J. Desmyter and J. A. Geogiades (1977). " Human interferon: mass production in a newly established cell line, MG-63." Antimicrobial Agents Chemotherapy 12: 11-15.

BioMedGPS (2012). Bone-Market Overview. BioMedGPS, BioMedGPS LLC.

Bjerre, L., C. Bunger, A. Baatrup, M. Kassem and T. Mygind (2011). "Flow perfusion culture of human mesenchymal stem cells on coralline hydroxyapatite scaffolds with various pore sizes." Journal of Biomedical Materials Research Part A 97A(3): 251-263.

Bjerre, L., C. E. Bunger, M. Kassem and T. Mygind (2008). "Flow perfusion culture of human mesenchymal stem cells on silicate-substituted tricalcium phosphate scaffolds." Biomaterials 29(17): 2616-2627.

Bloebaum, R. D., B. M. Willie, B. S. Mitchell and A. A. Hofmann (2007). "Relationship between bone ingrowth, mineral apposition rate, and osteoblast activity." Journal of Biomedical Materials Research Part A 81A(2): 505-514.

Bobyn, J. D., R. M. Pilliar, H. U. Cameron and G. C. Weatherly (1980). "The Optimum Pore-Size for the Fixation Of Porous-Surfaced Metal Implants by the Ingrowth of Bone." Clinical Orthopaedics and Related Research(150): 263-270.

Botchwey, E. A., S. R. Pollack, E. M. Levine and C. T. Laurencin (2001). "Bone tissue engineering in a rotating bioreactor using a microcarrier matrix system." Journal of Biomedical Materials Research 55(2): 242-253.

Botelho, C. M. (2005). Silicon substituted Hydroxyapatite for Biomedical Applications.

Botelho, C. M., R. Brooks, M. Kanitakahara, C. Ohtsuki, S. M. Best, M. A. Lopers, N. Rushton, W. Bonfield and J. D. Santos (2011). "Effect of Protein Adsorption onto the Dissolution of Silicon-Substituted Hydroxyapatite." Journal of Encapsulation and Adsorption Sciences Vol.01No.04: 8.

Botelho, C. M., R. A. Brooks, S. M. Best, M. A. Lopes, J. D. Santos, N. Rushton and W. Bonfield (2006). "Human osteoblast response to silicon-substituted hydroxyapatite." Journal of Biomedical Materials Research Part A 79A(3): 723-730.

Botelho, C. M., R. A. Brooks, T. Kawai, S. Ogata, C. Ohtsuki, S. M. Best, M. A. Lopes, J. D. Santos, N. Rushton and W. Bonfield (2005). In vitro analysis of protein adhesion to phase pure hydroxyapatite and silicon substituted hydroxyapatite. Bioceramics, Vol 17. P. Li, K. Zhang and C. W. Colwell. Zurich-Uetikon, Trans Tech Publications Ltd. 284-286: 461-464.

Botelho, C. M., M. A. Lopes, I. R. Gibson, S. M. Best and J. D. Santos (2002). "Structural analysis of Si-substituted hydroxyapatite: zeta potential and X-ray photoelectron spectroscopy." Journal of Materials Science-Materials in Medicine 13(12): 1123-1127.

Boyer, L., J. Carpena and J. L. Lacout (1997). "Synthesis of phosphate silicate apatites at atmospheric pressure." Solid State Ionics 95(1-2): 121-129.

Boyer, L., J. M. Savariault, J. Carpena and J. L. Lacout (1998). "A neodymium-substituted britholite compound." Acta Crystallographica Section C-Crystal Structure Communications 54: 1057-1059.

Boyne, P. J. (1970). "Autogenous cancellous bone and marrow transplants." Clinical orthopaedics and related research 73: 199-209.

Brown, P. W. and B. Constantz (1994). Hydroxyapatite and Related Materials, CRC Press.

Buckwalter, J. A., T. A. Einhorn, M. E. Bolander and R. L. Cruess (1996). Healing of the musculoskeletal tissues.

Buckwalter, J. A., M. J. Glimcher, R. R. Cooper and R. Recker (1996). "Bone biology. I: Structure, blood supply, cells, matrix, and mineralization." Instructional course lectures 45: 371-386.

Bui, X. V., H. Oudadesse, Y. Le Gal, O. Merdrignac-Conanec and G. Cathelineau (2012). "Bioactivity behaviour of biodegradable material comprising bioactive glass." Korean Journal of Chemical Engineering 29(2): 215-220.

Burchardt, H. (1983). "The Biology of Bone-Graft Repair." Clinical Orthopaedics and Related Research(174): 28-42.

Burchardt, H. (1987). "Biology of Bone Transplantation." Orthopedic Clinics of North America 18(2): 187-196.

Campion, C. (2015). Role of Physiochemical Parameters in the Osteogenic Potential of Calcium Phosphate Biomaterials. PhD, Queen Mary University of London.

Campion, C. R., S. L. Ball, D. L. Clarke and K. A. Hing (2013). "Microstructure and chemistry affects apatite nucleation on calcium phosphate bone graft substitutes." Journal of Materials Science-Materials in Medicine 24(3): 597-610.

Campion, C. R., C. Chander, T. Buckland and K. Hing (2011). "Increasing strut porosity in silicate-substituted calcium-phosphate bone graft substitutes enhances osteogenesis." Journal of Biomedical Materials Research Part B-Applied Biomaterials 97B(2): 245-254.

Canham, L. T., C. L. Reeves, J. P. Newey, M. R. Houlton, T. I. Cox, J. M. Buriak and M. P. Stewart (1999). "Derivatized mesoporous silicon with dramatically improved stability in simulated human blood plasma." Advanced Materials 11(18): 1505-+.

Caplan, A. I. and S. P. Bruder (2001). "Mesenchymal stem cells: building blocks for molecular medicine in the 21st century." Trends in Molecular Medicine 7(6): 259-264.

Carlisle, E. M. (1970). "Silicon: A Possible Factor in Bone Calcification." Science 167(3916): 279-&.

Carlisle, E. M. (1972). "Silicon - essential element for chick." Science 178(4061): 619-&.

Carlisle, E. M. (1974). "Relationship between silicon, glycosaminoglycan and collagen formation." Federation Proceedings 33(3): 704-704.

Carlsson, L., L. Regner, C. Johansson, M. Gottlander and P. Herberts (1994). "Bone Response to Hydroxyapatite-Coated and Commercially Pure Titanium Implants in the Human Arthritic Knee." Journal of Orthopaedic Research 12(2): 274-285.

Cartmell, S. H., B. D. Porter, A. J. Garcia and R. E. Guldberg (2003). "Effects of medium perfusion rate on cell-seeded three-dimensional bone constructs in vitro." Tissue Engineering 9(6): 1197-1203.

Carvalho, R. S., P. J. Kostenuik, E. Salih, A. Bumann and L. C. Gerstenfeld (2003). "Selective adhesion of osteoblastic cells to different integrin ligands induces osteopontin gene expression." Matrix Biology 22(3): 241-249.

Castagna, V. (2014). The role of chemistry and strut porosity and the influence of serum proteins in modulating cellular response to Bone Graft Substitutes. PhD, Queen Mary University of London.

Chan, O., M. J. Coathup, A. Nesbitt, C. Y. Ho, K. A. Hing, T. Buckland, C. Campion and G. W. Blunn (2012). "The effects of microporosity on osteoinduction of calcium phosphate bone graft substitute biomaterials." Acta Biomaterialia 8(7): 2788-2794.

Chan, Y. H., Y. S. Chang, Y. D. Shen, T. S. Yang, S. F. Ou, Y. J. Hsu, M. S. Huang and K. L. Ou (2015). "Comparative In Vitro Osteoinductivity Study of HA and alpha-TCP/HA Bicalcium Phosphate." International Journal of Applied Ceramic Technology 12(1): 192-198.

Chana, N. K. (2010). Investigation of solute composition on the dissolution behaviour of stoichiometric and silicate substituted apatites. Postgraduate MSc Postgraduate MSc, Queen Mary University of London.

Chen, P. S., T. Y. Toribara and H. Warner (1956). "Microdetermination of Phosphorus." Analytical Chemistry 28(11): 1756-1758.

Chou, Y. F., W. B. Huang, J. C. Y. Dunn, T. A. Miller and B. M. Wu (2005). "The effect of biomimetic apatite structure on osteoblast viability, proliferation, and gene expression." Biomaterials 26(3): 285-295.

Claes, L., M. Reusch, M. Göckelmann, M. Ohnmacht, T. Wehner, M. Amling, F. T. Beil and A. Ignatius (2011). "Metaphyseal fracture healing follows similar biomechanical rules as diaphyseal healing." Journal of Orthopaedic Research 29(3): 425-432.

Clover, J., R. A. Dodds and M. Gowen (1992). " Integrin subunit expression by human osteoblasts and osteoclasts in situ and in culture." Journal of Cell Science 103: 267-271.

Coathup, M. J., K. A. Hing, S. Samizadeh, O. Chan, Y. S. Fang, C. Campion, T. Buckland and G. W. Blunn (2012). "Effect of increased strut porosity of calcium phosphate bone graft substitute biomaterials on osteoinduction." Journal of Biomedical Materials Research Part A 100A(6): 1550-1555.

Coathup, M. J., S. Samizadeh, Y. S. Fang, T. Buckland, K. A. Hing and G. W. Blunn (2011). "The Osteoinductivity of Silicate-Substituted Calcium Phosphate." Journal of Bone and Joint Surgery-American Volume 93A(23): 2219-2226.

Combes, C. and C. Rey (2002). "Adsorption of proteins and calcium phosphate materials bioactivity." Biomaterials 23(13): 2817-2823.

Cortes, D. A., A. Medina, J. C. Escobedo, S. Escobedo and M. A. Lopez (2004). "Effect of wollastonite ceramics and bioactive glass on the formation of a bonelike apatite layer on a cobalt base alloy." Journal of Biomedical Materials Research Part A 70A(2): 341-346.

Cowles, E. A., L. L. Brailey and G. A. Gronowicz (2000). "Integrin-mediated signaling regulates AP-1 transcription factors and proliferation in osteoblasts." Journal of Biomedical Materials Research 52(4): 725-737.

Cowles, E. A., M. E. DeRome, G. Pastizzo, L. L. Brailey and G. A. Gronowicz (1998). "Mineralization and the expression of matrix proteins during in vivo bone development." Calcified Tissue International 62(1): 74-82.

Currey, J. D. (2002). Bones: Structure and Mechanics, Princeton University Press.

Currey, J. D. (2012). "The structure and mechanics of bone." Journal of Materials Science 47(1): 41-54.

Cutler, S. M. and A. J. Garcia (2003). "Engineering cell adhesive surfaces that direct integrin alpha(5)beta(1) binding using a recombinant fragment of fibronectin." Biomaterials 24(10): 1759-1770.

Czekanska, E. M., M. J. Stoddart, R. G. Richards and J. S. Hayes (2012). "In Search of anOsteoblast Cell Model for In Vitro Research." European Cells & Materials 24: 1-17.

Da Silva, H. M., M. Mateescu, C. Damia, E. Champion, G. Soares and K. Anselme (2010). "Importance of dynamic culture for evaluating osteoblast activity on dense silicon-substituted hydroxyapatite." Colloids and Surfaces B-Biointerfaces 80(2): 138-144.

Daculsi, G., R. Z. Legeros, M. Heughebaert and I. Barbieux (1990). "Formation of carbonate-apatite crystals after implantation of calcium phosphate ceramics." Calcified Tissue International 46(1): 20-27.

Daculsi, G., R. Z. Legeros and D. Mitre (1989). "Crystal Dissolution of Biological and Ceramic Apatites." Calcified Tissue International 45(2): 95-103.

Daculsi, G., P. Pilet, M. Cottrel and G. Guicheux (1999). "Role of fibronectin during biological apatite crystal nucleation: Ultrastructural characterization." Journal of Biomedical Materials Research 47(2): 228-233.

Damien, E. and P. A. Revell (2004). "Coralline hydroxyapatite bone graft substitute: A review of experimental studies and biomedical applications." Journal of applied biomaterials & biomechanics : JABB 2(2): 65-73.

Danoux, C., D. C. Bassett, Z. Othman, A. I. Rodrigues, R. L. Reis, J. E. Barralet, C. A. van Blitterswijk and P. Habibovic (2015). "Elucidating the individual effects of calcium and phosphate ions on hMSCs by using composite materials." Acta Biomaterialia 17: 1-15.

Davies, P. F. (1995). "Flow-Mediated Endothelial Mechanotransduction." Physiological reviews 75(3): 519-560.

Davies, P. F. and R. O. Dull (1990). How Does the Arterial Endothelium Sense Flow? Hemodynamic Forces and Signal Transduction. Tobacco Smoking and Atherosclerosis: Pathogenesis and Cellular Mechanisms. J. N. Diana. Boston, MA, Springer US: 281-293.

Davies, P. F., A. Remuzzi, E. J. Gordon, C. F. Dewey and M. A. Gimbrone (1986). "Turbulent fluid shear stress induces vascular endothelial cell turnover in vitro." Proceedings of the National Academy of Sciences 83(7): 2114-2117.

Davies, P. F. and S. C. Tripathi (1993). "Mechanical Stress Mechanisms and the Cell - An Endothelial Paradigm." Circulation Research 72(3): 239-245.

De Long, W. G., Jr., T. A. Einhorn, K. Koval, M. McKee, W. Smith, R. Sanders and T. Watson (2007). "Bone, grafts and bone graft substitutes in orthopedic trauma surgery - A critical analysis." Journal of Bone and Joint Surgery-American Volume 89A(3): 649-658.

Deboer, B. G., A. Sakthivel, J. R. Cagle and R. A. Young (1991). "Determination of the Antimony Substitution Site in Calcium Fluorapatite from Powder X-Ray-Diffraction Data." Acta Crystallographica Section B-Structural Science 47: 683-692.

Demaeyer, E. A. P., R. M. H. Verbeeck and D. E. Naessens (1993). "Stoichiometry of Na+- And CO32--Containing Apatites Obtained by Hydrolysis of Monetite." Inorganic Chemistry 32(25): 5709-5714.

Demarteau, O., M. Jakob, D. Schafer, M. Heberer and I. Martin (2003). "Development and validation of a bioreactor for physical stimulation of engineered cartilage." Biorheology 40(1-3): 331-336.

Demarteau, O., D. Wendt, A. Braccini, M. Jakob, D. Schafer, M. Heberer and I. Martin (2003). "Dynamic compression of cartilage constructs engineered from expanded human articular chondrocytes." Biochemical and Biophysical Research Communications 310(2): 580-588.

Depprich, R., J. Handschel, H. P. Wiesmann, J. Jasche-Meyer and U. Meyer (2008). "Use of bioreactors in maxillofacial tissue engineering." British Journal of Oral & Maxillofacial Surgery 46(5): 349-354.

Di Palma, F., M. Douet, C. Boachon, A. Guignandon, S. Peyroche, B. Forest, C. Alexandre, A. Chamson and A. Rattner (2003). "Physiological strains induce differentiation in human osteoblasts cultured on orthopaedic biomaterial." Biomaterials 24(18): 3139-3151.

Di Palma, F., A. Guignandon, A. Chamson, M. H. Lafage-Proust, N. Laroche, S. Peyroche, L. Vico and A. Rattner (2005). "Modulation of the responses of human osteoblast-like cells to physiologic mechanical strains by biomaterial surfaces." Biomaterials 26(20): 4249-4257.

Dietrich, E., H. Oudadesse, M. Le Floch, B. Bureau and T. Gloriant (2009). "In vitro Chemical Reactivity of Doped Bioactive Glasses: an Original Approach by Solid-State NMR Spectroscopy." Advanced Engineering Materials 11(8): B98-B105.

Duan, Y. R., Z. R. Zhang, C. Y. Wang, J. Y. Chen and X. D. Zhang (2005). "Dynamic study of calcium phosphate formation on porous HA/TCP ceramics." Journal of Materials Science-Materials in Medicine 16(9): 795-801.

Ducheyne, P. and Q. Qiu (1999). "Bioactive ceramics: the effect of surface reactivity on bone formation and bone cell function." Biomaterials 20(23-24): 2287-2303.

Dvir, T., N. Benishti, M. Shachar and S. Cohen (2006). "A novel perfusion bioreactor providing a homogenous milieu for tissue regeneration." Tissue Engineering 12(10): 2843-2852.

Dvorak, M. M., A. Siddiqua, D. T. Ward, D. H. Carter, S. L. Dallas, E. F. Nemeth and D. Riccardi (2004). "Physiological changes in extracellular calcium concentration directly control osteoblast function in the absence of calciotropic hormones." Proceedings of the National Academy of Sciences of the United States of America 101(14): 5140-5145.

Eggli, P. S., W. Muller and R. K. Schenk (1988). "Porous hydroxyapatite and tricalcium phosphate cylinders with 2 different pore size ranges implanted in cancellous bone of rabbits - A comparative histomophometric and histologic study of bony in growth and implant substitution." Clinical Orthopaedics and Related Research(232): 127-138.

Ehara, A., K. Ogata, S. Imazato, S. Ebisu, T. Nakano and Y. Umakoshi (2003). "Effects of alpha-TCP and TetCP on MC3T3-E1 proliferation, differentiation and mineralization." Biomaterials 24(5): 831-836.

Ergun, C., T. J. Webster, R. Bizios and R. H. Doremus (2002). "Hydroxylapatite with substituted magnesium, zinc, cadmium, and yttrium. I. Structure and microstructure." Journal of Biomedical Materials Research 59(2): 305-311.

Erickson, C. A. and J. P. Trinkaus (1976). "Microvilli and blebs as sources of reserve surface membrane during cell spreading." Experimental Cell Research 99(2): 375-384.

Fabriziushoman, D. J. and S. L. Cooper (1991). "Competitive Adsorption of Vitronectin with Albumin, Fibrinogen, and Fibronectin on Polymeric Biomaterials." Journal of Biomedical Materials Research 25(8): 953-971.

Favus, M. J., D. A. Bushinsky and J. J. Lemann (2006). "Chapter 13. Regulation of Calcium, Magnesium and Phosphate metabolism." In: Favus M, ed. Primer on the metabolic bone diseases and disorders of mineral metabolism 6th Edition. Washington DC.

Ferrara, N. (2004). "Vascular endothelial growth factor: Basic science and clinical progress." Endocrine Reviews 25(4): 581-611.

Ferraz, M. P., M. H. Fernandes, A. T. Cabral, J. D. Santos and F. J. Monteiro (1999). "In vitro growth and differentiation of osteoblast-like human bone marrow cells on glass reinforced hydroxyapatite plasma-sprayed coatings." Journal of Materials Science-Materials in Medicine 10(9): 567-576.

Fielding, G. and S. Bose (2013). "SiO2 and ZnO dopants in three-dimensionally printed tricalcium phosphate bone tissue engineering scaffolds enhance osteogenesis and angiogenesis in vivo." Acta Biomaterialia 9(11): 9137-9148.

Folkman, J. and A. Moscona (1978). "Role of cell shape in growth control." Nature 273(5661): 345-349.

Frayssinet, P., J. L. Trouillet, N. Rouquet, E. Azimus and A. Autefage (1993). "Osseointergration of macroporous calcium-phosphate ceramics having a different chemical composition." Biomaterials 14(6): 423-429.

Fu, K., Q. G. Xu, J. Czernuszka, J. T. Triffitt and Z. D. Xia (2013). "Characterization of a biodegradable coralline hydroxyapatite/calcium carbonate composite and its clinical implementation." Biomedical Materials 8(6): 11.

Furlong, I. J., R. Ascaso, A. L. Rivas and M. K. L. Collins (1997). "Intracellular acidification induces apoptosis by stimulating ICE-like protease activity." Journal of Cell Science 110: 653-661.

Galante, J., W. Rostoker, R. Lueck and R. D. Ray (1971). "Sintered Fiber Metal Composites as a Basis for Attachment of Implants to Bone." Journal of Bone and Joint Surgery-American Volume A 53(1): 101-&.

Gandolfi, M. G., G. Ciapetti, F. Perut, P. Taddei, E. Modena, P. L. Rossi and C. Prati (2009). "Biomimetic calcium-silicate cements aged in simulated body solutions. Osteoblast response and analyses of apatite coating." Journal of Applied Biomaterials & Biomechanics 7(3): 160-170.

Garcia, A. J., P. Ducheyne and D. Boettiger (1998). "Effect of surface reaction stage on fibronectin-mediated adhesion of osteoblast-like cells to bioactive glass." Journal of Biomedical Materials Research 40(1): 48-56.

Gauthier, O., J. M. Bouler, E. Aguado, P. Pilet and G. Daculsi (1998). "Macroporous biphasic calcium phosphate ceramics: influence of macropore diameter and macroporosity percentage on bone ingrowth." Biomaterials 19(1-3): 133-139.

Giachelli, C. M., S. Jono, A. Shioi, Y. Nishizawa, K. Mori and H. Morii (2001). "Vascular calcification and inorganic phosphate." American Journal of Kidney Diseases 38(4): S34-S37.

Gibson, I. R., S. M. Best and W. Bonfield (1999). "Chemical characterization of silicon-substituted hydroxyapatite." Journal of Biomedical Materials Research 44(4): 422-428.

Gibson, I. R., S. M. Best and W. Bonfield (2002). "Effect of silicon substitution on the sintering and microstructure of hydroxyapatite." Journal of the American Ceramic Society 85(11): 2771-2777.

Gibson, I. R., J. Huang, S. M. Best and W. Bonfield (1999). "Enhanced in vitro cell activity and surface apatite formation of novel silicon-substituted hydroxyapatite " Bioceramics 12: 191-194.

Goldstein, A. S., T. M. Juarez, C. D. Helmke, M. C. Gustin and A. G. Mikos (2001). "Effect of convection on osteoblastic cell growth and function in biodegradable polymer foam scaffolds." Biomaterials 22(11): 1279-1288.

Goldstein, S. A. (2002). Tissue engineering - Functional assessment and clinical outcome. Reparative Medicine: Growing Tissues and Organs. J. D. Sipe, C. A. Kelley and L. A. McNicol. New York, New York Acad Sciences. 961: 183-192.

Gomes, M. E., H. L. Holtorf, R. L. Reis and A. G. Mikos (2006). "Influence of the porosity of starch-based fiber mesh scaffolds on the proliferation and osteogenic differentiation of bone marrow stromal cells cultured in a flow perfusion bioreactor." Tissue Engineering 12(4): 801-809.

Good, N. E., G. D. Winget, W. Winter, T. N. Connolly, S. Izawa and R. M. Singh (1966). "Hydrogen ion buffers for biological research." Biochemistry 5(2): 467-477.

Gough, J. E., J. R. Jones and L. L. Hench (2004). Osteoblast nodule formation and mineralisation on foamed 58S bioactive glass. Bioceramics, Vol 16. M. A. Barbosa, F. J. Monteiro, R. Correia and B. Leon. Zurich-Uetikon, Trans Tech Publications Ltd. 254-2: 985-988.

Green, R. J., M. C. Davies, C. J. Roberts and S. J. B. Tendler (1999). "Competitive protein adsorption as observed by surface plasmon resonance." Biomaterials 20(4): 385-391.

Gross, K. A. and C. C. Berndt (1998). "Thermal processing of hydroxyapatite for coating production." Journal of Biomedical Materials Research 39(4): 580-587.

Gugala, Z. and S. Gogolewski (2004). "Protein adsorption, attachment, growth and activity of primary rat osteoblasts on polylactide membranes with defined surface characteristics." Biomaterials 25(12): 2341-2351.

Gupta, G., S. Kirakodu and A. El-Ghannam (2007). "Dissolution kinetics of a Si-rich nanocomposite and its effect on osteoblast gene expression." Journal of Biomedical Materials Research Part A 80A(2): 486-496.

Guth, K. (2007). Mechanisms of the Improved Biological Response with Silicate Substitution in Hydroxyapatie. Doctoral, Queen Mary University of London.

Guth, K., T. Buckland and K. A. Hing (2006). Silicon dissolution from microporous silicon substituted hydroxyapatite and its effect on osteoblast behaviour. Bioceramics 18, Pts 1 and 2. T. Nakamura, K. Yamashita and M. Neo. Zurich-Uetikon, Trans Tech Publications Ltd. 309-311: 117-120.

Guth, K., C. Campion, T. Buckand and K. A. Hing (2010). "Surface Physiochemistry Affects Protein Adsorption to Stoichiometric and Silicate-Substituted Microporous Hydroxyapatites." Advanced Engineering Materials 12(4): B113-B121.

Guth, K., C. Campion, T. Buckland and K. A. Hing (2010). "Effect of Silicate-Substitution on Attachment and Early Development of Human Osteoblast-Like Cells Seeded on Microporous Hydroxyapatite Discs." Advanced Engineering Materials 12(1-2): B26-B36.

Guth, K., C. Campion, T. Buckland and K. A. Hing (2011). "Effects of serum protein on ionic exchange between culture medium and microporous hydroxyapatite and

silicate-substituted hydroxyapatite." Journal of Materials Science-Materials in Medicine 22(10): 2155-2164.

Gyorgyey, A., K. Ungvari, G. Kecskemeti, J. Kopniczky, B. Hopp, A. Oszko, I. Pelsoczi, Z. Rakonczay, K. Nagy and K. Turzo (2013). "Attachment and proliferation of human osteoblast-like cells (MG-63) on laser-ablated titanium implant material." Materials Science & Engineering C-Materials for Biological Applications 33(7): 4251-4259.

Habibovic, P., H. P. Yuan, C. M. van der Valk, G. Meijer, C. A. van Blitterswijk and K. de Groot (2005). "3D microenvironment as essential element for osteoinduction by biomaterials." Biomaterials 26(17): 3565-3575.

Haibo Wang, B. S. (2004). Hydroxyapatite Degradation and Biocompatibility. Degree of Philisopy, Ohio State University.

Haj, A. J. E., S. L. Minter, S. C. F. Rawlinson, R. Suswillo and L. E. Lanyon (1990). "Cellular responses to mechanical loading in vitro." Journal of Bone and Mineral Research 5(9): 923-932.

Harding, I. S., N. Rashid and K. A. Hing (2005). "Surface charge and the effect of excess calcium ions on the hydroxyapatite surface." Biomaterials 26(34): 6818-6826.

Heikkila, J. T., A. J. Aho, A. Yliurpo, O. H. Andersson, H. J. Aho and R. P. Happonen (1993). "Bioactive Glass Versus Hydroxylapatite in Reconstruction of Osteochondral Defects in the Rabbit." Acta Orthopaedica Scandinavica 64(6): 678-682.

Hench, L. L. (1991). "Bioceramics - From Concept to Clinic." Journal of the American Ceramic Society 74(7): 1487-1510.

Hench, L. L. (1998). "Biomaterials: a forecast for the future." Biomaterials 19(16): 1419-1423.

Hench, L. L. and J. Wilson (1993). Introduction. An Introduction to Bioceramics: 1-24.

Heremans, H., A. Billiau, J. J. Cassiman, J. C. Mulier and P. De Somer (1978). "In vitro cultivation of human tumor tissues. II. Morphological and virological characterization of three cell lines." Oncology 35: 246-252.

Hillsley, M. V. and J. A. Frangos (1994). "Bone tissue engineering - The role of interstitial fluid flow - Review." Biotechnology and Bioengineering 43(7): 573-581.

Hing, K., I. R. Gibson, L. Di-Silvio, S. M. Best and W. Bonfield (1998). "Effect on variation in CA:P ratio on cellular response of primary human osteoblast-like cells to hydroxyapatite-based ceramics." Bioceramics 11.

Hing, K., J. C. Merry, I. R. Gibson, L. Di Silvio, S. M. Best and W. Bonfield (1999). Effect of Carbonate content on the response of human osteoblast-like cells to carbonate substituted hydroxyapatite. 12th International Symposium on Ceramics in Medicine, Nara, Japan, 1999 World Scientific Publishing Co. Pte. Ltd.

Hing, K. A. (2004). "Bone repair in the twenty-first century: biology, chemistry or engineering?" Philosophical Transactions of the Royal Society of London Series a-Mathematical Physical and Engineering Sciences 362(1825): 2821-2850.

Hing, K. A. (2005). "Bioceramic bone graft substitutes: Influence of porosity and chemistry." International Journal of Applied Ceramic Technology 2(3): 184-199.

Hing, K. A., B. Annaz, S. Saeed, P. A. Revell and T. Buckland (2005). "Microporosity enhances bioactivity of synthetic bone graft substitutes." Journal of Materials Science-Materials in Medicine 16(5): 467-475.

Hing, K. A., S. M. Best and W. Bonfield (1999). "Characterization of porous hydroxyapatite." Journal of Materials Science-Materials in Medicine 10(3): 135-145.

Hing, K. A., S. M. Best, K. E. Tanner, W. Bonfield and P. A. Revell (1997). "Biomechanical assessment of bone ingrowth in porous hydroxyapatite." Journal of Materials Science: Materials in Medicine 8(12): 731-736.

Hing, K. A., S. M. Best, K. E. Tanner, W. Bonfield and P. A. Revell (2004). "Mediation of bone ingrowth in porous hydroxyapatite bone graft substitutes." Journal of Biomedical Materials Research Part A 68A(1): 187-200.

Hing, K. A., P. A. Revell, N. Smith and T. Buckland (2006). "Effect of silicon level on rate, quality and progression of bone healing within silicate-substituted porous hydroxyapatite scaffolds." Biomaterials 27(29): 5014-5026.

Hing, K. A., S. Saeed, B. Annaz, T. Buckland and P. A. Revell (2004). Microporosity affects bioactivity of macroporous hydroxyapatite bone graft substitutes. Bioceramics 16. M. A. Barbosa, F. J. Monteiro, R. Correia and B. Leon. Stafa-Zurich, Trans Tech Publications Ltd. 254-2: 273-276.

Hing, K. A., L. F. Wilson and T. Buckland (2007). "Comparative performance of three ceramic bone graft substitutes." The Spine Journal 7(4): 475-490.

Hoang, Q. Q., F. Sicheri, A. J. Howard and D. S. C. Yang (2003). "Bone recognition mechanism of porcine osteocalcin from crystal structure." Nature 425(6961): 977-980.

Hodgskinson, R. and J. D. Currey (1990). "The effect of variation in structure on the Young's modulus of cancellous bone: a comparison of human and non-human material." Proceedings of the Institution of Mechanical Engineers. Part H, Journal of engineering in medicine 204(2): 115-121.

Hofmann, A. A., R. D. Bloebaum and K. N. Bachus (1997). "Progression of human bone ingrowth into porous-coated implants - Rate of bone ingrowth in humans." Acta Orthopaedica Scandinavica 68(2): 161-166.

Holmes, R. and H. Hagler (1988). "Porous Hydroxyapatite as a Bone-Graft Substitute in Maxillary Augmentation - An Histometric Study." Journal of Cranio-Maxillofacial Surgery 16(5): 199-205.

Holtorf, H. L., T. L. Sheffield, C. G. Ambrose, J. A. Jansen and A. G. Mikos (2005). "Flow perfusion culture of marrow stromal cells seeded on porous biphasic calcium phosphate ceramics." Annals of Biomedical Engineering 33(9): 1238-1248.

Horbett, T. A. (2004). The role of Adsorbed Proteins in Tissue Response to Biomaterials. Biomaterials Science: An Introduction to Materials in Medicine. B. D. Ratner: 851.

Hunter, A., C. W. Archer, P. S. Walker and G. W. Blunn (1995). "Attachment and Proliferation of Osteoblasts and Fibroblasts on Biomaterials for Orthopedic Use." Biomaterials 16(4): 287-295.

Ikada, Y. (2006). Tissue Engineering: Fundamentals and Applications. Tissue Engineering: Fundamentals and Applications, Elsevier Science Bv, Sara Burgerhartstraat 25, Po Box 211, 1000 Ae Amsterdam, Netherlands. 8.

Im, G. I., S. A. Qureshi, J. Kenney, H. E. Rubash and A. S. Shanbhag (2004). "Osteoblast proliferation and maturation by bisphosphonates." Biomaterials 25(18): 4105-4115.

Janssen, F. W., J. Oostra, A. van Oorschot and C. A. van Blitterswijk (2006). "A perfusion bioreactor system capable of producing clinically relevant volumes of tissue-engineered bone: In vivo bone formation showing proof of concept." Biomaterials 27(3): 315-323.

Janssen, F. W., R. van Dijkhuizen-Radersma, A. Van Oorschot, J. Oostra, J. D. de Bruijn and C. A. Van Blitterswijk (2010). "Human tissue-engineered bone produced in clinically relevant amounts using a semi-automated perfusion bioreactor system: a preliminary study." Journal of Tissue Engineering and Regenerative Medicine 4(1): 12-24.

Jasmund, I. and A. Bader (2002). "Bioreactor developments for tissue engineering applications by the example of the bioartificial liver." Advances in biochemical engineering/biotechnology 74: 99-109.

Kale, S., S. Biermann, C. Edwards, C. Tarnowski, M. Morris and M. W. Long (2000). "Three-dimensional cellular development is essential for ex vivo formation of human bone." Nature Biotechnology 18(9): 954-958.

Kanatani, M., T. Sugimoto, M. Fukase and T. Fujita (1991). "Effect of elevated extracellular calcium on the proliferation of osteoblastic MC3T3-E1 cells: Its direct and indirect effects via monocytes." Biochemical and Biophysical Research Communications 181(3): 1425-1430.

Kanis, J. A. (2007). Assessment of Osteoporosis at the Primary Health Care Level, World Health Organization Scientific Group collaborating Centre for Metabolic Bone Diseases, University of Sheffield, UK. Techincal Report.

Kaspar, D., W. Seidl, C. Neidlinger-Wilke, A. Ignatius and L. Claes (2000). "Dynamic cell stretching increases human osteoblast proliferation and CICP synthesis but decreases osteocalcin synthesis and alkaline phosphatase activity." Journal of Biomechanics 33(1): 45-51.

Ketteler, M. and J. Floege (2006). "Calcification and the usual suspect phosphate: still guilty but there are other guys behind the scenes." Nephrology Dialysis Transplantation 21(1): 33-35.

Kilpadi, K. L., P. L. Chang and S. L. Bellis (2001). "Hydroxylapatite binds more serum proteins, purified integrins, and osteoblast precursor cells than titanium or steel." Journal of Biomedical Materials Research 57(2): 258-267.

Kilpadi, K. L., A. A. Sawyer, C. W. Prince, P. L. Chang and S. L. Bellis (2004). "Primary human marrow stromal cells and Saos-2 osteosarcoma cells use different mechanisms to adhere to hydroxylapatite." Journal of Biomedical Materials Research Part A 68A(2): 273-285.

Kim, H., H. Arakawa, T. Osada and A. Ikai (2003). "Quantification of cell adhesion force with AFM: distribution of vitronectin receptors on a living MC3T3-E1 cell." Ultramicroscopy 97(1-4): 359-363.

Kim, H. W., E. J. Lee, H. E. Kim, V. Salih and J. C. Knowles (2005). "Effect of fluoridation of hydroxyapatite in hydroxyapatite-polycaprolactone composites on osteoblast activity." Biomaterials 26(21): 4395-4404.

Kim, J. and T. Ma (2012). "Perfusion regulation of hMSC microenvironment and osteogenic differentiation in 3D scaffold." Biotechnology and Bioengineering 109(1): 252-261.

Kim, S. S., R. Penkala and P. Abrahimi (2007). "A perfusion bioreactor for intestinal tissue engineering." Journal of Surgical Research 142(2): 327-331.

Klawitter, J. J. and S. F. Hulbert (1972). Applications of porous ceramics for the attcahment of load bearing internal orthopedic applications.

Knowles, J. C. (2003). "Phosphate based glasses for biomedical applications." Journal of Materials Chemistry 13(10): 2395-2401.

Kobayashi, T., S. Shingaki, T. Nakajima and K. Hanada (1993). "Chin Augmentation with Porous Hydroxyapatite Blocks." Journal of Long-Term Effects of Medical Implants 3(4): 283-294.

Koch, H., J. A. Jadlowiec, J. D. Whalen, P. Robbins, C. Lattermann, F. H. Fu, H. R. Merk and J. O. Hollinger (2005). "Osteoblastic differentiation of human adult mesenchymal stem cells after Ad-BMP-2 in the absence of dexamethasone." Zeitschrift Fur Orthopadie Und Ihre Grenzgebiete 143(6): 684-690.

Kokubo, T., S. Ito, Z. T. Huang, T. Hayashi, S. Sakka, T. Kitsugi and T. Yamamuro (1990). "Ca, P-rich layer formed on High-Strength Bioactive Glass-Ceramic A-W." Journal of Biomedical Materials Research 24(3): 331-343.

Kokubo, T., H. Kushitani, S. Sakka, T. Kitsugi and T. Yamamuro (1990). "Solutions able to reproduce In Vivo Surface-Structure changes in Bioactive Glass-Ceramic A-W3." Journal of Biomedical Materials Research 24(6): 721-734.

Kokubo, T. and H. Takadama (2006). "How useful is SBF in predicting in vivo bone bioactivity?" Biomaterials 27(15): 2907-2915.

Kowalczynska, H. M., M. Nowak-Wyrzykowska, R. Kolos, J. Dobkowski and J. Kaminski (2005). "Fibronectin adsorption and arrangement on copolymer surfaces and their significance in cell adhesion." Journal of Biomedical Materials Research Part A 72A(2): 228-236.

Kruyt, M. C., W. J. A. Dhert, C. Oner, C. A. van Blitterswijk, A. J. Verbout and J. D. de Bruijn (2004). "Optimization of bone-tissue engineering in goats." Journal of Biomedical Materials Research Part B-Applied Biomaterials 69B(2): 113-120.

Kuehne, J.-H., R. Bartl, B. Frisch, C. Hammer, V. Jansson and M. Zimmer (1994). "Bone formation in coralline hydroxyapatite: Effects of pore size studied in rabbits." Acta Orthopaedica Scandinavica 65(3): 246-252.

Kumarasuriyar, A., S. Murali, V. Nurcombe and S. M. Cool (2009). " Glycosaminoglycan composition changes with MG-63 osteosarcoma osteogenesis in vitro and induces human mesenchymal stem cell aggregation." Journal of Cell Physiology 218: 501-511.

Landis, W. J. (1995). "The Strength of a Calcified Tissue Depends in Part on the Molecular-Structure and Organization of its Constituent Mineral Crystals in their Organic Matrix." Bone 16(5): 533-544.

Landis, W. J., K. J. Hodgens, M. J. Song, J. Arena, S. Kiyonaga, M. Marko, C. Owen and B. F. McEwen (1996). "Mineralization of collagen may occur on fibril surfaces: Evidence from conventional and high-voltage electron microscopy and three-dimensional imaging." Journal of Structural Biology 117(1): 24-35.

Lanza, R. P., R. Langer and J. Vacanti (2000). Principles of Tissue Engineering, Academic Press.

Lawrence, B. J. (2008). Mass Transfer in Porous Tissue Engineering Scaffolds, Oklahoma State University.

LeGeros, R. Z., J. R. Parsons, G. Daculsi, F. Driessens, D. Lee, S. T. Liu, S. Metsger, D. Peterson and M. Walker (1988). "Significance of the porosity and physical chemistry of calcium phosphate ceramics. Biodegradation-bioresorption." Annals of the New York Academy of Sciences 523: 268-271.

Leonor, I. B., E. T. Baran, M. Kawashita, R. L. Reis, T. Kokubo and T. Nakamura (2008). "Growth of a bonelike apatite on chitosan microparticles after a calcium silicate treatment." Acta Biomaterialia 4(5): 1349-1359.

Lin, Q., Y. B. Li, X. H. Lan, C. H. Lu, Y. X. Chen and Z. Z. Xu (2009). "The apatite formation ability of CaF2 doping tricalcium silicates in simulated body fluid." Biomedical Materials 4(4): 6.

Lin, S. J., R. Z. LeGeros, R. Rohanizadeh, D. Mijares and J. P. LeGeros (2003). Biphasic calcium phosphate (BCP) bioceramics: Preparation and properties. Bioceramics 15. B. BenNissan, D. Sher and W. Walsh. Zurich-Uetikon, Trans Tech Publications Ltd. 240-2: 473-476.

Lossdorfer, S., Z. Schwartz, C. H. Lohmann, D. C. Greenspan, D. M. Ranly and B. D. Boyan (2004). "Osteoblast response to bioactive glasses in vitro correlates with inorganic phosphate content." Biomaterials 25(13): 2547-2555.

Lu, J. X., M. C. Blary, S. Vavasseur, M. Descamps, K. Anselme and P. Hardouin (2004). "Relationship between bioceramics sintering and micro-particles-induced cellular damages." Journal of Materials Science-Materials in Medicine 15(4): 361-365.

Macewen, W. (1912). The Growth of Bone: Observations on Osteogenesis: An Experimental Inquiry Into the Development and Reproduction of Diaphyseal Bone. Glasgow, James Maclehose & Sons.

Maeno, S., Y. Niki, H. Matsumoto, H. Morioka, T. Yatabe, A. Funayama, Y. Toyama, T. Taguchi and J. Tanaka (2005). "The effect of calcium ion concentration on

osteoblast viability, proliferation and differentiation in monolayer and 3D culture." Biomaterials 26(23): 4847-4855.

Malik, M. A., D. A. Puleo, R. Bizios and R. H. Doremus (1992). "Osteoblasts on hydroxyapatite, alumina and bone surfaces in vitro- morphology during the 1st 2h of attachment." Biomaterials 13(2): 123-128.

Mami, M., A. Lucas-Girot, H. Oudadesse, R. Dorbez-Sridi, F. Mezahi and E. Dietrich (2008). "Investigation of the surface reactivity of a sol-gel derived glass in the ternary system SiO(2)-CaO-P(2)O(5)." Applied Surface Science 254(22): 7386-7393.

Martin, I., D. Wendt and M. Heberer (2004). "The role of bioreactors in tissue engineering." Trends in Biotechnology 22(2): 80-86.

Matsuoka, H., H. Akiyama, Y. Okada, H. Ito, C. Shigeno, J. Konishi, T. Kokubo and T. Nakamura (1999). "In vitro analysis of the stimulation of bone formation by highly bioactive apatite- and wollastonite-containing glass-ceramic: Released calcium ions promote osteogenic differentiation in osteoblastic ROS17/2.8 cells." Journal of Biomedical Materials Research 47(2): 176-188.

McKeownLongo, P. J. and T. S. Panetti (1996). "Structure and function of vitronectin." Trends in Glycoscience and Glycotechnology 8(43): 327-340.

Meinel, L., V. Karageorgiou, R. Fajardo, B. Snyder, V. Shinde-Patil, L. Zichner, D. Kaplan, R. Langer and G. Vunjak-Novakovic (2004). "Bone tissue engineering using human mesenchymal stem cells: Effects of scaffold material and medium flow." Annals of Biomedical Engineering 32(1): 112-122.

Meredith, J. and K. K. Mallick (2015). "High-strength scaffolds for bone regeneration." Bioinspired Biomimetic and Nanobiomaterials 4(1): 48-58.

Midy, V., M. Dard and E. Hollande (2001). "Evaluation of the effect of three calcium phosphate powders on osteoblast cells." Journal of Materials Science-Materials in Medicine 12(3): 259-265.

Miller, A. (1984). "Collagen - The Organic Matrix of Bone." Philosophical Transactions of the Royal Society of London Series B-Biological Sciences 304(1121): 455-477.

Miller, S. C., L. Saintgeorges, B. M. Bowman and W. S. S. Jee (1989). "Bone Lining Cells - Structure and Function." Scanning Microscopy 3(3): 953-961.

Monroe, E. A., W. Votava, D. B. Bass and J. McMullen (1971). "New calcium phosphate ceramic material for bone and tooth implants." Journal of Dental Restoration 50(4): 860-861.

Mygind, T., M. Stiehler, A. Baatrup, H. Li, X. Zoua, A. Flyvbjerg, M. Kassem and C. Bunger (2007). "Mesenchymal stem cell ingrowth and differentiation on coralline hydroxyapatite scaffolds." Biomaterials 28(6): 1036-1047.

Nelson, D. G. A., J. D. McLean and J. V. Sanders (1983). "A High-Resolution Electron Study of Synthetic and Biological Carbonated Apatites " Journal of Ultrastructure Research 84(1): 1-15.

Nesbitt, S. A. and M. A. Horton (1997). "Trafficking of matrix collagens through bone-resorbing osteoclasts." Science 276(5310): 266-269.

Nielsen, L. B., F. S. Pedersen and L. Pedersen (2001). "Expression of type III sodium-dependent phosphate transporters/retroviral receptors mRNAs during osteoblast differentiation." Bone 28(2): 160-166.

Ning, C. Q. and Y. Zhou (2002). "In vitro bioactivity of a biocomposite fabricated from HA and Ti powders by powder metallurgy method." Biomaterials 23(14): 2909-2915.

Noh, H., S. T. Yohe and E. A. Vogler (2008). "Volumetric interpretation of protein adsorption: Ion-exchange adsorbent capacity, protein pI, and interaction energetics." Biomaterials 29(13): 2033-2048.

Norde, W. (1995). "Adsorption of Proteins at Solid-Liquid Interfaces." Cells and Materials 5(1): 97-112.

Oonishi, H., L. L. Hench, J. Wilson, F. Sugihara, E. Tsuji, M. Matsuura, S. Kin, T. Yamamoto and S. Mizokawa (2000). "Quantitative comparison of bone growth behavior in granules of Bioglass (R), A-W glass-ceramic, and hydroxyapatite." Journal of Biomedical Materials Research 51(1): 37-46.

Ozawa, S. and S. Kasugai (1996). "Evaluation of implant materials (hydroxyapatite, glass-ceramics, titanium) in rat bone marrow stromal cell culture." Biomaterials 17(1): 23-29.

Patel, N., S. M. Best, W. Bonfield, I. R. Gibson, K. A. Hing, E. Damien and P. A. Revell (2002). "A comparative study on the in vivo behavior of hydroxyapatite and silicon substituted hydroxyapatite granules." Journal of Materials Science-Materials in Medicine 13(12): 1199-1206.

Patel, N., E. L. Follon, I. R. Gibson, S. M. Best and W. Bonfield (2003). Comparison of sintering and mechanical properties of hydroxyapatite and silicon-substituted hydroxyapatite. Bioceramics 15. B. BenNissan, D. Sher and W. Walsh. Zurich-Uetikon, Trans Tech Publications Ltd. 240-2: 919-922.

Pietak, A. M., J. W. Reid, M. J. Stott and M. Sayer (2007). "Silicon substitution in the calcium phosphate bioceramics." Biomaterials 28(28): 4023-4032.

Pirhonen, E., H. Niiranen, T. Niemela, M. Brink and P. Tormala (2006). "Manufacturing, mechanical characterization, and in vitro performance of bioactive glass 13-93 fibers." Journal of Biomedical Materials Research Part B-Applied Biomaterials 77B(2): 227-233.

Pluhar, G. E., A. S. Turner, A. R. Pierce, C. A. Toth and D. L. Wheeler (2006). "A comparison of two biomaterial carriers for osteogenic protein-1 (BMP-7) in an ovine critical defect model." Journal of Bone and Joint Surgery-British Volume 88B(7): 960-966.

Porter, A. E., C. M. Botelho, M. A. Lopes, J. D. Santos, S. M. Best and W. Bonfield (2004). "Ultrastructural comparison of dissolution and apatite precipitation on hydroxyapatite and silicon-substituted hydroxyapatite in vitro and in vivo." Journal of Biomedical Materials Research Part A 69A(4): 670-679.

Porter, A. E., T. Buckland, K. Hing, S. M. Best and W. Bonfield (2006). "The structure of the bond between silicon-substituted hydroxyapatite bone and porous bioceramic implants." Journal of Biomedical Materials Research Part A 78A(1): 25-33.

Porter, A. E., N. Patel, J. N. Skepper, S. M. Best and W. Bonfield (2003). "Comparison of in vivo dissolution processes in hydroxyapatite and silicon-substituted hydroxyapatite bioceramics." Biomaterials 24(25): 4609-4620.

Porter, A. E., N. Patel, J. N. Skepper, S. M. Best and W. Bonfield (2004). "Effect of sintered silicate-substituted hydroxyapatite on remodelling processes at the bone-implant interface." Biomaterials 25(16): 3303-3314.

Pountos, I., E. Jones, C. Tzioupis, D. McGonagle and P. V. Giannoudis (2006). "Growing bone and cartilage - The role of mesenchymal stem cells." Journal of Bone and Joint Surgery-British Volume 88B(4): 421-426.

Radin, S. and P. Ducheyne (1996). "Effect of serum proteins on solution-induced surface transformations of bioactive ceramics." Journal of Biomedical Materials Research 30(3): 273-279.

Raggi, M. A., C. Sabbioni, R. Mandrioli, Q. Zini and G. Varani (1999). "Spectrophotometric determination of silicate traces in hemodialysis solutions." Journal of Pharmaceutical and Biomedical Analysis 20(1-2): 335-342.

Raja, M. (2010). In vitro comparison of the effect of structural variation on the dissolution behaviour of silicon substituted hydroxyapatite. MEng, Queen Mary University of London.

Rajarama, R., D. E. Rounds, S. P. S. Yen and A. Rembaum (1974). "Scanning electron microscope study of cell adhesion and spreading in vitro." Experimental Cell Research 88(2): 327-339.

Rashid, N., T. Buckland and K. A. Hing (2005). Influence of Si substitutttion on Protein Adsorption and Early Cellural Response. 19th European Conference on Biomaterials Sorrento, Italy.

Rawlinson, S. C. F., A. A. Pitsillides and L. E. Lanyon (1996). "Involvement of different ion channels in osteoblasts' and osteocytes' early responses to mechanical strain." Bone 19(6): 609-614.

Reffitt, D. M., R. Jugdaohsingh, R. P. H. Thompson and J. J. Powell (1999). "Silicic acid: its gastrointestinal uptake and urinary excretion in man and effects on aluminium excretion." Journal of Inorganic Biochemistry 76(2): 141-147.

Reffitt, D. M., N. Ogston, R. Jugdaohsingh, H. F. J. Cheung, B. A. J. Evans, R. P. H. Thompson, J. J. Powell and G. N. Hampson (2003). "Orthosilicic acid stimulates

collagen type 1 synthesis and osteoblastic differentiation in human osteoblast-like cells in vitro." Bone 32(2): 127-135.

Robinson, R. A. (1952). "An electron-microscopic study of the crystalline inorganic component of bone and its relationship to the organic matrix." The Journal of bone and joint surgery. American volume 34-A(2): 389-passim.

Rohl, L., E. Larsen, F. Linde, A. Odgaard and J. Jorgensen (1991). "Tensile and Compressive Properties of Cancellous Bone." Journal of Biomechanics 24(12): 1143-1149.

Rouahi, M., O. Gallet, E. Champion, J. Dentzer, P. Hardouin and K. Anselme (2006). "Influence of hydroxyapatite microstructure on human bone cell response." Journal of Biomedical Materials Research Part A 78A(2): 222-235.

Rubin, P. A. D., J. K. Popham, J. R. Bilyk and J. W. Shore (1994). "Comparison of fibrovascular in growth in to hydroxyapatite and porous polyethylene orbital implants." Ophthalmic Plastic and Reconstructive Surgery 10(2): 96-103.

Rubin, P. A. D., J. K. Popham, J. R. Bilyk and J. W. Shore (1994). "Comparison of Fibrovascular Ingrowth into Hydroxyapatite and Porous Polyethylene Orbital Implants." Ophthalmic Plastic and Reconstructive Surgery 10(2): 96-103.

Ruys, A. (1993). "Silicon-doped hydroxyapatite." J. Australas. Ceram. Soc.(Switzerland) 29(1): 71-80.

Saldana, L., F. Bensiamar, A. Bore and N. Vilaboa (2011). " In search of representative models of human bone-forming cells for cytocompatibility studies." Acta Biomaterialia (7): 4210-4221.

Salgado, A. J., O. P. Coutinho and R. L. Reis (2004). "Bone tissue engineering: State of the art and future trends." Macromolecular Bioscience 4(8): 743-765.

Salo, J., P. Lehenkari, M. Mulari, K. Metsikko and H. K. Vaananen (1997). "Removal of osteoclast bone resorption products by transcytosis." Science 276(5310): 270-273.

Samy, M. (2011). Characterisation and in vitro dissolution behaviour of silicon substituted hydroxyapatite in the semi-dynamic biological environment. Intercalated BSc, Queen Mary University of London.

Sari, A., R. Yavuzer, S. Ayhan, S. Tuncer, O. Latifoglu, K. Atabay and M. C. Celebi (2003). "Hard tissue augmentation of the mandibular region with hydroxyapatite granules." Journal of Craniofacial Surgery 14(6): 919-923.

Sasaki, T., E. Hohenester, W. Gohring and R. Timpl (1998). "Crystal structure and mapping by site-directed mutagenesis of the collagen-binding epitope of an activated form of BM-40/SPARC/osteonectin." Embo Journal 17(6): 1625-1634.

Sawyer, A. A., K. M. Hennessy and S. L. Bellis (2005). "Regulation of mesenchymal stem cell attachment and spreading on hydroxyapatite by RGD peptides and adsorbed serum proteins." Biomaterials 26(13): 1467-1475.

Schepers, E., M. Declercq, P. Ducheyne and R. Kempeneers (1991). "Bioactive Glass Particulate Material as a Filler for Bone-Lesions." Journal of Oral Rehabilitation 18(5): 439-452.

Schmalzried, T. P., E. S. Szuszczewicz, M. R. Northfield, K. H. Akizuki, R. E. Frankel, G. Belcher and H. C. Amstutz (1998). "Quantitative assessment of walking activity after total hip or knee replacement." Journal of Bone and Joint Surgery-American Volume 80A(1): 54-59.

Schmelzer, E., A. Finoli, I. Nettleship and J. C. Gerlach (2015). "Long-Term Three-Dimensional Perfusion Culture of Human Adult Bone Marrow Mononuclear Cells in Bioreactors." Biotechnology and Bioengineering 112(4): 801-810.

Schmidt, C., D. Kaspar, M. R. Sarkar, L. E. Claes and A. A. Ignatius (2002). "A scanning electron microscopy study of human osteoblast morphology on five orthopedic metals." Journal of Biomedical Materials Research 63(3): 252-261.

Schwarz, K. (1978). Significance and Functions of Silicon in Warm-Blooded Animals. Review and Outlook. Biochemistry of Silicon and Related Problems. G. Bendz, I. Lindqvist and V. Runnström-Reio, Springer US. 40: 207-230.

Schwarz, K. and D. B. Milne (1972). "Growth-Promoting Effects of Silicon in Rats." Nature 239(5371): 333-&.

Serret, A., M. V. Cabanas and M. Vallet-Regi (2000). "Stabilization of calcium oxyapatites with lanthanum(III)-created anionic vacancies." Chemistry of Materials 12(12): 3836-3841.

Shah, F. A., D. S. Brauer, R. M. Wilson, R. G. Hill and K. A. Hing (2014). "Influence of cell culture medium composition on in vitro dissolution behavior of a fluoride-containing bioactive glass." Journal of Biomedical Materials Research Part A 102(3): 647-654.

Sharpe, J. R., R. L. Sammons and P. M. Marquis (1997). "Effect of pH on protein adsorption to hydroxyapatite and tricalcium phosphate ceramics." Biomaterials 18(6): 471-476.

Shors, E. C. and R. E. Holmes (2013). Porous Hydroxyapatite. An Introduction to Bioceramics: 287-304.

Sikavitsas, V. I., G. N. Bancroft, H. L. Holtorf, J. A. Jansen and A. G. Mikos (2003). "Mineralized matrix deposition by marrow stromal osteoblasts in 3D perfusion culture increases with increasing fluid shear forces." Proceedings of the National Academy of Sciences of the United States of America 100(25): 14683-14688.

Sikavitsas, V. I., G. N. Bancroft and A. G. Mikos (2002). "Formation of three-dimensional cell/polymer constructs for bone tissue engineering in a spinner flask and a rotating wall vessel bioreactor." Journal of Biomedical Materials Research 62(1): 136-148.

Smalt, R., F. T. Mitchell, R. L. Howard and T. J. Chambers (1997). "Induction of NO and prostaglandin E2 in osteoblasts by wall-shear stress but not mechanical strain." AMerican Journal of Physiology 273: E751 - E758.

Steele, J. G., B. A. Dalton, G. Johnson and P. A. Underwood (1995). "Adsorption of Fibronectin and Vitronectin Onto Primaria(TM) and Tissue-Culture Polystyrene and Relationship to the Mechanism of Initial Attachment of Human Vein Endothelial-Cells and BHK-21 Fibroblasts." Biomaterials 16(14): 1057-1067.

Stein, G. S., J. B. Lian and T. A. Owen (1990). "Relationship of cell growth to the regulation of tissue specific gene expression during osteoblast differentiation." Faseb Journal 4(13): 3111-3123.

Suchanek, W. and M. Yoshimura (1998). "Processing and properties of hydroxyapatite-based biomaterials for use as hard tissue replacement implants." Journal of Materials Research 13(1): 94-117.

Suzuki, T., T. Yamamoto, M. Toriyama, K. Nishizawa, Y. Yokogawa, M. R. Mucalo, Y. Kawamoto, F. Nagata and T. Kameyama (1997). "Surface instability of calcium phosphate ceramics in tissue culture medium and the effect on adhesion and growth

of anchorage-dependent animal cells." Journal of Biomedical Materials Research 34(4): 507-517.

Tanizawa, Y. and T. Suzuki (1995). "Effects of Silicate Ions on the Formation and Transformation of Calcium Phosphates in Neutral Aqueous-Solutions." Journal of the Chemical Society-Faraday Transactions 91(19): 3499-3503.

Thian, E. S., J. Huang, S. M. Best, Z. H. Barber, R. A. Brooks, N. Rushton and W. Bonfield (2006). "The response of osteoblasts to nanocrystalline silicon-substituted hydroxyapatite thin films." Biomaterials 27(13): 2692-2698.

Tortora, G. J. and B. Derrickson (2006). Principles of Anatomy and Physiology John Wiley & Sons Canada.

Tortora, G. J. and B. Derrickson (2008). Principles of Anatomy and Phyiology, John Wiley & Sons, Inc.

Uemura, T., A. Nemoto, Y. K. Liu, H. Kojima, J. Dong, T. Yabe, T. Yoshikawa, H. Ohgushi, T. Ushida and T. Tateishi (2001). "Osteopontin involvement in bone remodeling and its effects on in vivo osteogenic potential of bone marrow-derived osteoblasts/porous hydroxyapatite constructs." Materials Science & Engineering C-Biomimetic and Supramolecular Systems 17(1-2): 33-36.

Valerio, P., M. M. Pereira, A. M. Goes and M. F. Leite (2004). "The effect of ionic products from bioactive glass dissolution on osteoblast proliferation and collagen production." Biomaterials 25(15): 2941-2948.

Vallet-Regi, M. and D. Arcos (2005). "Silicon substituted hydroxyapatites. A method to upgrade calcium phosphate based implants." Journal of Materials Chemistry 15(15): 1509-1516.

Vanblitterswijk, C. A., D. Bakker, S. C. Hesseling and H. K. Koerten (1991). "Reactions of Cells at Implant Surfaces." Biomaterials 12(2): 187-193.

Vance, J., S. Galley, D. F. Liu and S. W. Donahue (2005). "Mechanical stimulation of MC3T3 osteoblastic cells in a bone tissue-engineering bioreactor enhances prostaglandin E-2 release." Tissue Engineering 11(11-12): 1832-1839.

Verbeeck, R. M. H., E. A. P. Demaeyer and F. C. M. Driessens (1995). "Stoichiometry of Potassium- and Carbonate-Containing Apatites Synthesized by Solid-State Reactions." Inorganic Chemistry 34(8): 2084-2088.

Vrouwenvelder, W. C. A., C. G. Groot and K. Degroot (1993). "Histological and biochemical evaluation of osteoblasts cultured on bioactive glass, hydroxylapatite, titanium-alloy and stainless steel." Journal of Biomedical Materials Research 27(4): 465-475.

VunjakNovakovic, G., L. E. Freed, R. J. Biron and R. Langer (1996). "Effects of mixing on the composition and morphology of tissue-engineered cartilage." Aiche Journal 42(3): 850-860.

Wang, C. Y., Y. R. Duan, B. Markovic, J. Barbara, C. R. Howlett, X. D. Zhang and H. Zreiqat (2004). "Phenotypic expression of bone-related genes in osteoblasts grown on calcium phosphate ceramics with different phase compositions." Biomaterials 25(13): 2507-2514.

Wang, J., L. Qu, X. Meng, J. Gao, H. Li and G. Wen (2008). "Preparation and biological properties of PLLA/beta-TCP composites reinforced by chitosan fibers." Biomedical Materials 3(2).

Wang, L., X. Y. Ma, Y. Zhang, Y. F. Feng, X. Li, Y. Y. Hu, Z. Wang, Z. S. Ma and W. Lei (2014). "Repair of Segmental Bone Defect Using Totally Vitalized Tissue Engineered Bone Graft by a Combined Perfusion Seeding and Culture System." Plos One 9(4): 10.

Wang, Y. C., T. Uemura, R. Dong, H. Kojima, J. Tanaka and T. Tateishi (2003). "Application of perfusion culture system improves in vitro and in vivo osteogenesis of bone marrow-derived osteoblastic cells in porous ceramic materials." Tissue Engineering 9(6): 1205-1214.

Wei, Z.-c., D.-z. Cai and J.-f. Zhang (2003). "Repair of bone defect with compound of coralline hydroxyapatite porous, fibrin sealant and Staphylococcus aureus injection." Zhongguo xiu fu chong jian wai ke za zhi = Zhongguo xiufu chongjian waike zazhi = Chinese journal of reparative and reconstructive surgery 17(5): 363-366.

Weiner, S. and H. D. Wagner (1998). "THE MATERIAL BONE: Structure-Mechanical Function Relations." Annual Review of Materials Science 28(1): 271-298.

Wen, S. L. and Q. A. Liu (1998). "High resolution electron microscopy investigations of interface and other structure defects in some ceramics." Microscopy Research and Technique 40(3): 177-186.

Weng, J., Q. Liu, J. G. C. Wolke, X. D. Zhang and K. deGroot (1997). "Formation and characteristics of the apatite layer on plasma-sprayed hydroxyapatite coatings in simulated body fluid." Biomaterials 18(15): 1027-1035.

Wiechelman, K. J., R. D. Braun and J. D. Fitzpatrick (1988). "Investigation of the Bicinchoninic Acid Assay - Identification of the groups responsible for color formation " Analytical Biochemistry 175(1): 231-237.

Wilson, C. J., R. E. Clegg, D. I. Leavesley and M. J. Pearcy (2005). "Mediation of biomaterial-cell interactions by adsorbed proteins: A review." Tissue Engineering 11(1-2): 1-18.

Wilson, R. M., J. C. Elliott and S. E. P. Dowker (1999). "Rietveld refinement of the crystallographic structure of human dental enamel apatites." American Mineralogist 84(9): 1406-1414.

Wozney, J. M. and V. Rosen (1998). "Bone morphogenetic protein and bone morphogenetic protein gene family in bone formation and repair." Clinical Orthopaedics and Related Research(346): 26-37.

Wuttke, M., S. Muller, D. P. Nitsche, M. Paulsson, F. G. Hanisch and P. Maurer (2001). "Structural characterization of human recombinant and bone-derived bone sialoprotein - Functional implications for cell attachment and hydroxyapatite binding." Journal of Biological Chemistry 276(39): 36839-36848.

Xu, S. L., P. G. Du, Y. Z. Xie and Y. Yue (2008). "Cell Distribution in a Scaffold with Random Architectures under the Influence of Fluid Dynamics." Journal of Biomaterials Applications 23(3): 229-245.

Xynos, I. D., A. J. Edgar, L. D. K. Buttery, L. L. Hench and J. M. Polak (2000). "Ionic products of bioactive glass dissolution increase proliferation of human osteoblasts and induce insulin-like growth factor II mRNA expression and protein synthesis." Biochemical and Biophysical Research Communications 276(2): 461-465.

Yan, X., X. B. Chen and D. J. Bergstrom (2011). "Modeling of the Flow within Scaffolds in Perfusion Bioreactors." American Journal of Biomedical Engineering 1(2): 72-77.

Yang, X. B. B., M. J. Whitaker, W. Sebald, N. Clarke, S. M. Howdle, K. M. Shakesheff and R. O. C. Oreffo (2004). "Human osteoprogenitor bone formation using encapsulated bone morphogenetic protein 2 in porous polymer scaffolds." Tissue Engineering 10(7-8): 1037-1045.

Yaszemski, M. J., R. G. Payne, W. C. Hayes, R. Langer and A. G. Mikos (1996). "Evolution of bone transplantation: Molecular, cellular and tissue strategies to engineer human bone." Biomaterials 17(2): 175-185.

Younger, E. M. and M. W. Chapman (1989). "Morbidity at bone graft donor sites." Journal of orthopaedic trauma 3(3): 192-195.

Yuan, H. P., Z. J. Yang, J. D. de Bruijn, K. de Groot and X. D. Zhang (2001). "Material-dependent bone induction by calcium phosphate ceramics: a 2.5-year study in dog." Biomaterials 22(19): 2617-2623.

Yuan, H. P., P. Zou, Z. J. Yang, X. D. Zhang, J. D. De Bruijn and K. De Groot (1998). "Bone morphogenetic protein and ceramic-induced osteogenesis." Journal of Materials Science-Materials in Medicine 9(12): 717-721.

Zaidi, M., B. S. Moonga and C. L. H. Huang (2004). "Calcium sensing and cell signaling processes in the local regulation of osteoclastic bone resorption." Biological Reviews 79(1): 79-100.

Zhao, F., R. Chella and T. Ma (2007). "Effects of shear stress on 3-D human mesenchymal stem cell construct development in a perfusion bioreactor system: Experiments and hydrodynamic modeling." Biotechnology and Bioengineering 96(3): 584-595.

Zhao, F. and T. Ma (2005). "Perfusion bioreactor system for human mesenchymal stem cell tissue engineering: Dynamic cell seeding and construct development." Biotechnology and Bioengineering 91(4): 482-493.

Zhong, J. P. and D. C. Greenspan (2000). "Processing and properties of sol-gel bioactive glasses." Journal of Biomedical Materials Research 53(6): 694-701.

Appendix 1: XRF Data

INORGANIC ANALYSIS REPORT

LUCIDEON
insight creating advantage

UKAS TESTING
0013

Queen Mary University of London
Mile End Road
London
E1 4NS

FAO: Dan Johnson/Karin Hing
Report of Tests on: Hydroxyapatite Powder
Your Reference: HA80/20 Dec 2014 A80XXB0473A
Lucideon Reference: (146095)-31086
Date Reported: 06-Jan-2015 **Order Number:** 9351254
Date Logged: 22-Dec-2014 **Date(s) of Test(s):** 05-Jan-2015 **to** 06-Jan-2015

XRF Analysis

Methods C201 based on BSEN ISO 12677:2011

Result(s)		Units	
Sample Basis			Dried 110 deg C
Silicon Dioxide	SiO_2	%	0.16
Titanium Dioxide	TiO_2	%	<0.01
Aluminium Oxide	Al_2O_3	%	<0.02
Iron (III) Oxide	Fe_2O_3	%	<0.01
Calcium Oxide	CaO	%	55.95
Magnesium Oxide	MgO	%	<0.02
Potassium Oxide	K_2O	%	<0.01
Sodium Oxide	Na_2O	%	<0.03
Phosphorus Pentoxide	P_2O_5	%	42.15
Chromium (III) Oxide	Cr_2O_3	%	<0.01
Manganese (II,III) Oxide	Mn_3O_4	%	<0.01
Zirconium Oxide	ZrO_2	%	<0.02
Hafnium (IV) Oxide	HfO_2	%	<0.01
Lead Oxide	PbO	%	<0.02
Zinc Oxide	ZnO	%	<0.01
Barium Oxide	BaO	%	<0.01
Strontium (II) Oxide	SrO	%	<0.01
Tin (IV) Oxide	SnO_2	%	<0.01
Loss on Ignition		%	0.76
Loss on Ignition Temperature		°C	1200
Total		%	99.02
Sulphur Trioxide	SO_3	%	<0.05
UKAS Accredited			Yes

The sulphur trioxide may not be a total sulphur figure but is the sulphur remaining after LOI and fusion. Results are quoted to 2 decimal places but are accurate to 3 significant figures or the number of figures given, whichever is the lesser.

Opinions and interpretations expressed herein are outside the scope of UKAS Accreditation.

End of Test Report

Mrs Sharon Mansfield
Author

Page 1 of 1

This report is issued in accordance with the Conditions of Business of Lucideon Limited and relates only to the sample(s) tested. No responsibility is taken for the accuracy of the sampling unless this is done under our own supervision. This report shall not be reproduced in part without the written approval of Lucideon Limited, nor used in any way as to lead to misrepresentation of the results or their implications.

Lucideon is the trading name of Lucideon Limited. Registered in England No. 1960455 Registered Office as above.

Lucideon Ltd
Queens Road, Penkhull
Stoke-on-Trent
Staffordshire ST4 7LQ, UK

T +44 (0)1782 764428
enquiries@lucideon.com
www.lucideon.com
Reg. England 1960455

INORGANIC ANALYSIS REPORT

LUCIDEON
insight creating advantage

UKAS TESTING
0013

Queen Mary University of London
Mile End Road
London
E1 4NS

FAO: Dan Johnson/Karin Hing

Report of Tests on: Hydroxyapatite Powder

Your Reference: Actifuse SA 80/20 Dec 2014 S80PPD1483E

Lucideon Reference: (146095)-31087

Date Reported: 06-Jan-2015 **Order Number:** 9351254

Date Logged: 22-Dec-2014 **Date(s) of Test(s):** 05-Jan-2015 **to** 06-Jan-2015

XRF Analysis

Methods C201 based on BSEN ISO 12677:2011

Result(s)		Units	
Sample Basis			Dried 110 deg C
Silicon Dioxide	SiO_2	%	1.84
Titanium Dioxide	TiO_2	%	<0.01
Aluminium Oxide	Al_2O_3	%	<0.02
Iron (III) Oxide	Fe_2O_3	%	<0.01
Calcium Oxide	CaO	%	56.23
Magnesium Oxide	MgO	%	0.02
Potassium Oxide	K_2O	%	<0.01
Sodium Oxide	Na_2O	%	<0.03
Phosphorus Pentoxide	P_2O_5	%	40.33
Chromium (III) Oxide	Cr_2O_3	%	<0.01
Manganese (II,III) Oxide	Mn_3O_4	%	<0.01
Zirconium Oxide	ZrO_2	%	<0.02
Hafnium (IV) Oxide	HfO_2	%	<0.01
Lead Oxide	PbO	%	<0.02
Zinc Oxide	ZnO	%	<0.01
Barium Oxide	BaO	%	<0.01
Strontium (II) Oxide	SrO	%	<0.01
Tin (IV) Oxide	SnO_2	%	<0.01
Loss on Ignition		%	0.66
Loss on Ignition Temperature		°C	1200
Total		%	99.08
Sulphur Trioxide	SO_3	%	<0.05
UKAS Accredited			Yes

The sulphur trioxide may not be a total sulphur figure but is the sulphur remaining after LOI and fusion. Results are quoted to 2 decimal places but are accurate to 3 significant figures or the number of figures given, whichever is the lesser.

Opinions and interpretations expressed herein are outside the scope of UKAS Accreditation.

End of Test Report

Mrs Sharon Mansfield
Author

This report is issued in accordance with the Conditions of Business of Lucideon Limited and relates only to the sample(s) tested. No responsibility is taken for the accuracy of the sampling unless this is done under our own supervision. This report shall not be reproduced in part without the written approval of Lucideon Limited, nor used in any way as to lead to misrepresentation of the results or their implications.

Lucideon is the trading name of Lucideon Limited. Registered in England No. 1960455 Registered Office as above.

Lucideon Ltd
Queens Road, Penkhull
Stoke-on-Trent
Staffordshire ST4 7LQ, UK

T +44 (0)1782 764428
enquiries@lucideon.com
www.lucideon.com
Reg. England 1960455

INORGANIC ANALYSIS REPORT

LUCIDEON
insight creating advantage

UKAS TESTING
0013

Queen Mary University of London
Mile End Road
London
E1 4NS

FAO: Dan Johnson/Karin Hing

Report of Tests on: Hydroxyapatite Powder

Your Reference: Inductigraft SA 80/30 Dec 2014 N83PPF1676JF

Lucideon Reference: (146095)-31088

Date Reported: 06-Jan-2015 **Order Number:** 9351254

Date Logged: 22-Dec-2014 **Date(s) of Test(s):** 05-Jan-2015 **to** 06-Jan-2015

XRF Analysis

Methods C201 based on BSEN ISO 12677:2011

Result(s)		Units	
Sample Basis			Dried 110 deg C
Silicon Dioxide	SiO_2	%	1.75
Titanium Dioxide	TiO_2	%	<0.01
Aluminium Oxide	Al_2O_3	%	<0.02
Iron (III) Oxide	Fe_2O_3	%	<0.01
Calcium Oxide	CaO	%	56.20
Magnesium Oxide	MgO	%	<0.02
Potassium Oxide	K_2O	%	<0.01
Sodium Oxide	Na_2O	%	<0.03
Phosphorus Pentoxide	P_2O_5	%	40.40
Chromium (III) Oxide	Cr_2O_3	%	<0.01
Manganese (II,III) Oxide	Mn_3O_4	%	<0.01
Zirconium Oxide	ZrO_2	%	<0.02
Hafnium (IV) Oxide	HfO_2	%	<0.01
Lead Oxide	PbO	%	<0.02
Zinc Oxide	ZnO	%	<0.01
Barium Oxide	BaO	%	<0.01
Strontium (II) Oxide	SrO	%	<0.01
Tin (IV) Oxide	SnO_2	%	<0.01
Loss on Ignition		%	0.67
Loss on Ignition Temperature		°C	1200
Total		%	99.02
Sulphur Trioxide	SO_3	%	<0.05
UKAS Accredited			Yes

The sulphur trioxide may not be a total sulphur figure but is the sulphur remaining after LOI and fusion. Results are quoted to 2 decimal places but are accurate to 3 significant figures or the number of figures given, whichever is the lesser.

Opinions and interpretations expressed herein are outside the scope of UKAS Accreditation.

End of Test Report

Mrs Sharon Mansfield
Author

This report is issued in accordance with the Conditions of Business of Lucideon Limited and relates only to the sample(s) tested. No responsibility is taken for the accuracy of the sampling unless this is done under our own supervision. This report shall not be reproduced in part without the written approval of Lucideon Limited, nor used in any way as to lead to misrepresentation of the results or their implications.

Lucideon is the trading name of Lucideon Limited. Registered in England No. 1960455 Registered Office as above.

Lucideon Ltd
Queens Road, Penkhull
Stoke-on-Trent
Staffordshire ST4 7LQ, UK

T +44 (0)1782 764428
enquiries@lucideon.com
www.lucideon.com
Reg. England 1960455

Appendix 2: Calibration curves for Calcium, Phosphate and Silicate ion concentrations

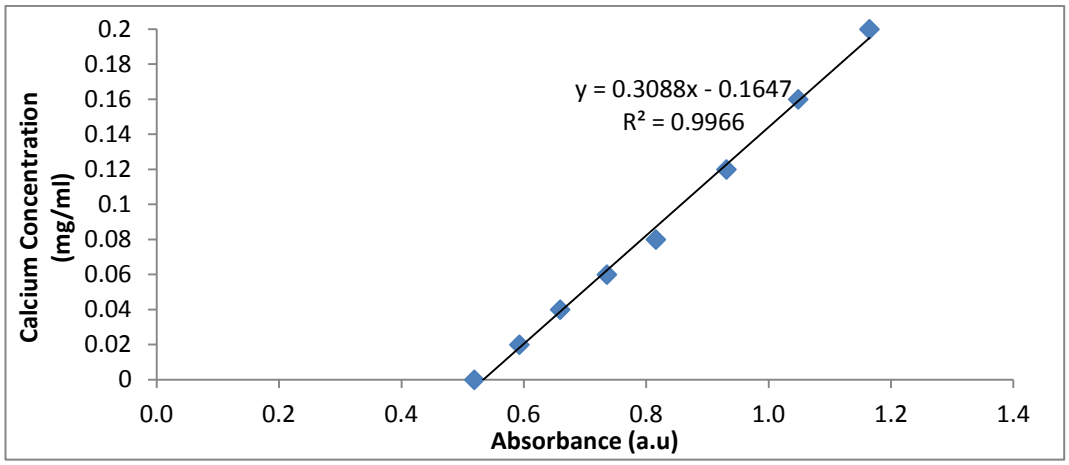

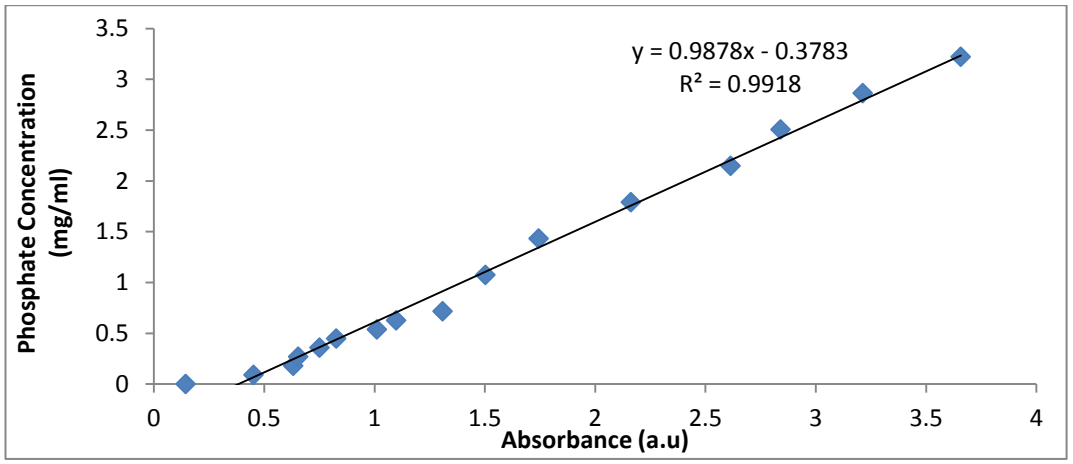

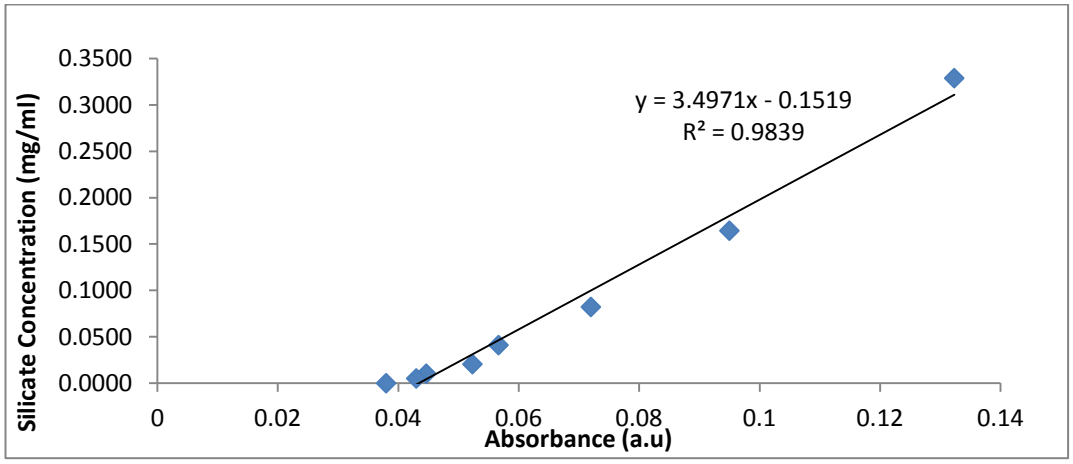

Appendix 3: Total DNA and ALP Activity of MG63 Cells at Varying Cell Concentrations

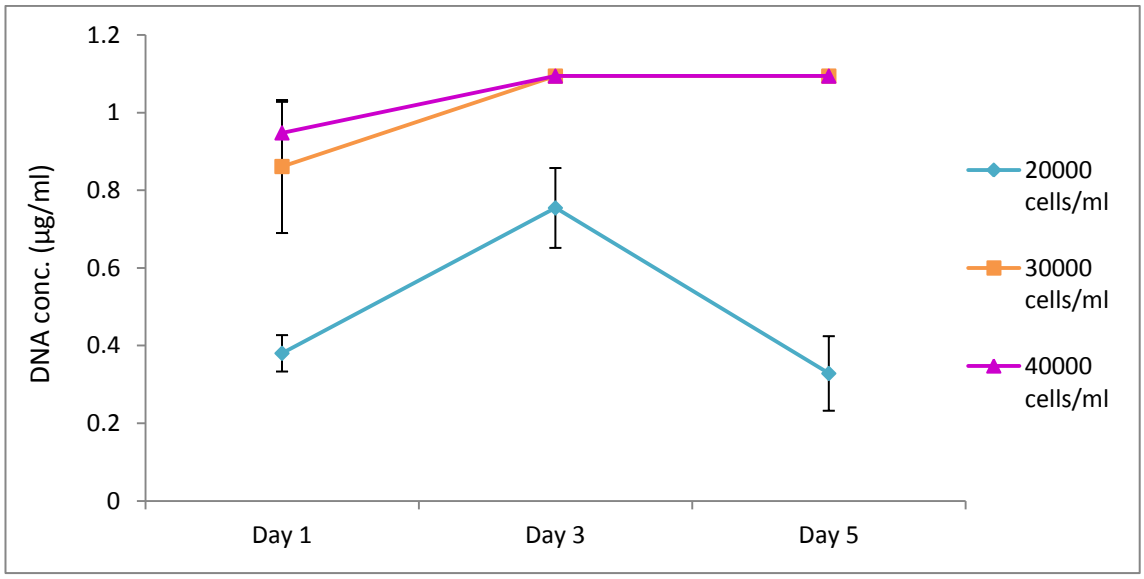

DNA concentration of MG63 cells at different cell concentrations over 5 days cultured in 24 well plates

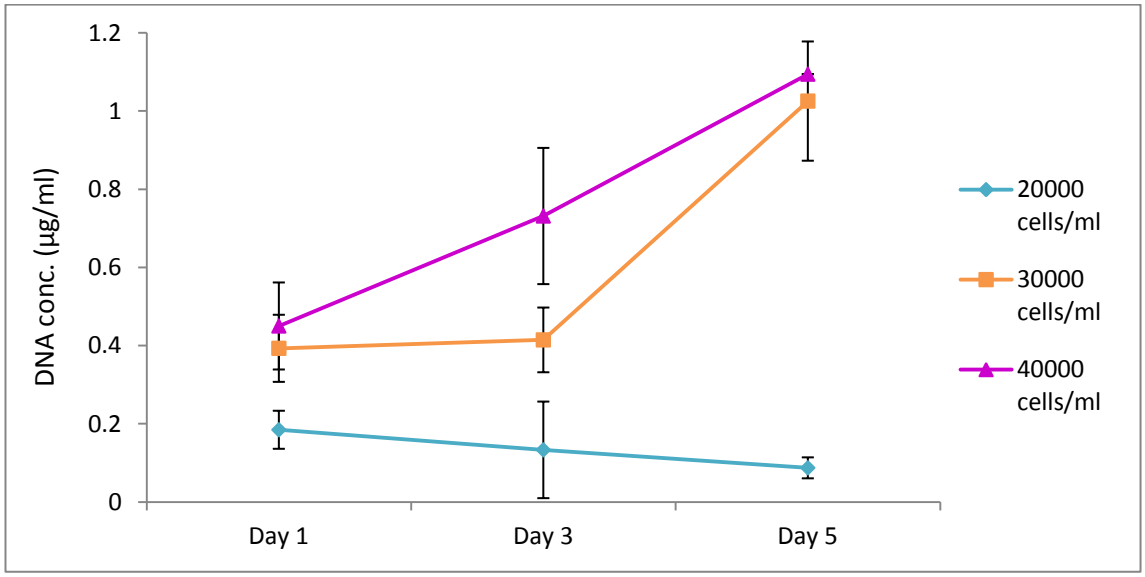

DNA concentration of MG63 cells at different cell concentrations over 5 days cultured on 0.45g HA80/20 granules

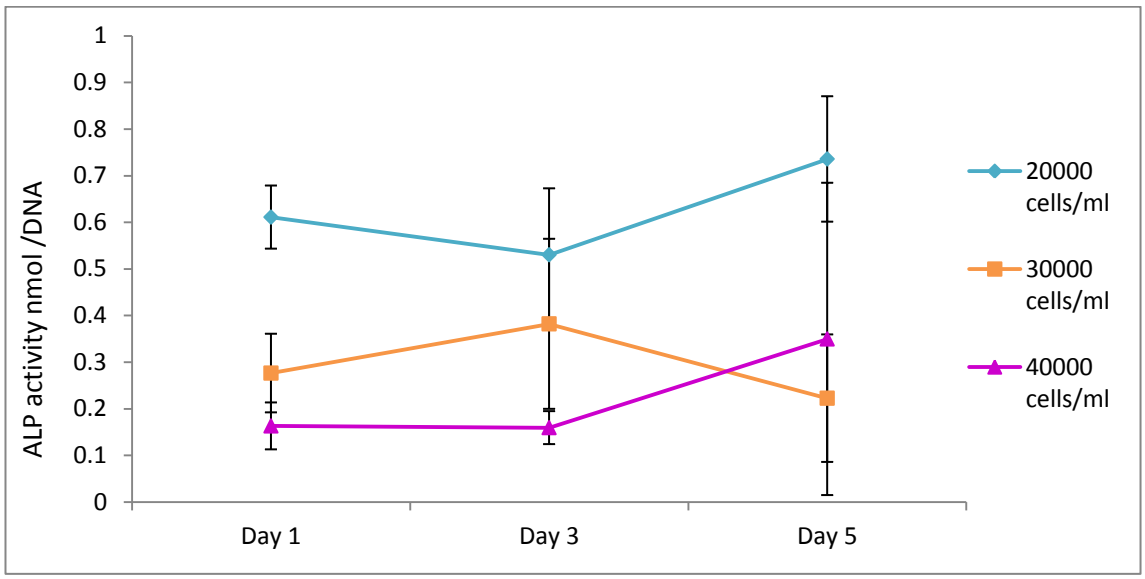

ALP activity of MG63 cells at different cell concentrations over 5 days cultured in 24 well plates

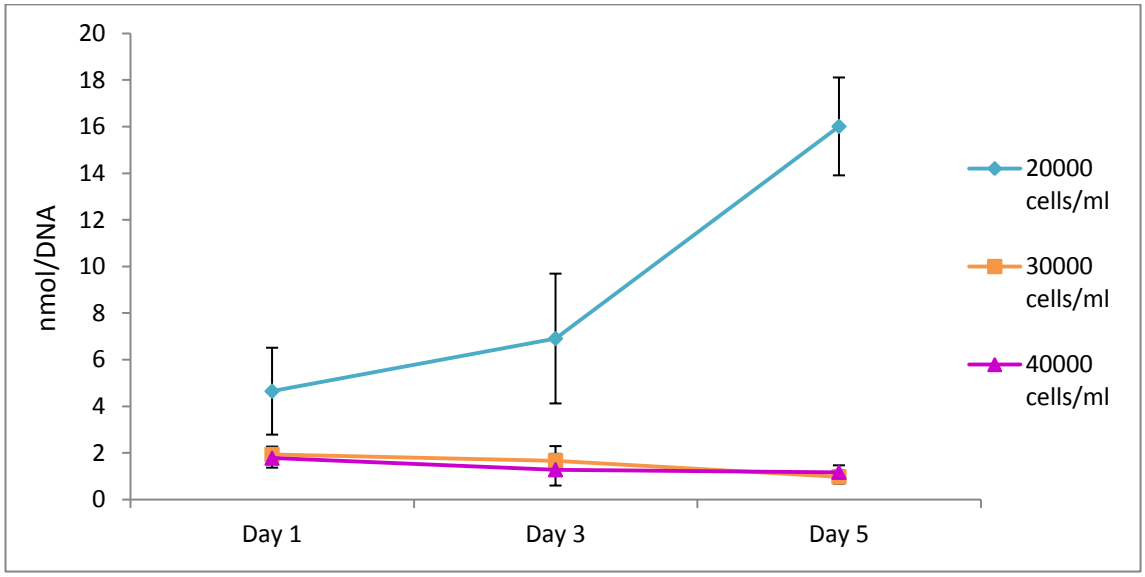

ALP activity of MG63 cells at different cell concentrations over 5 days cultured on 0.45g HA80/20 granules

Appendix 4: Calibration Curves for DNA, ALP and Total Protein Concentrations

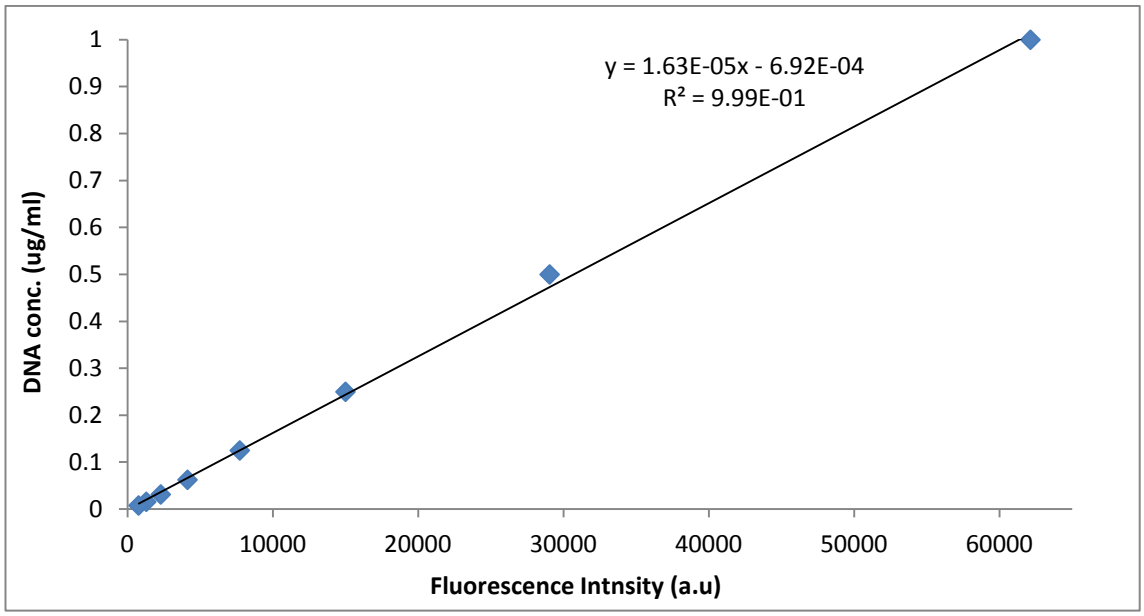

Calibration curve for DNA concentration

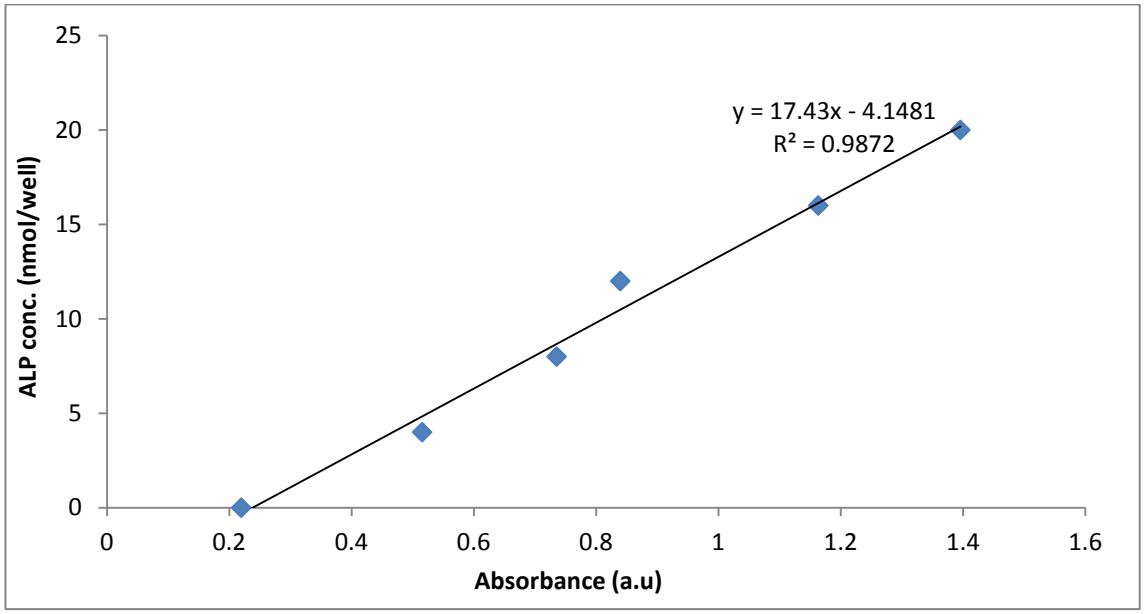

Calibration curve for ALP concentration

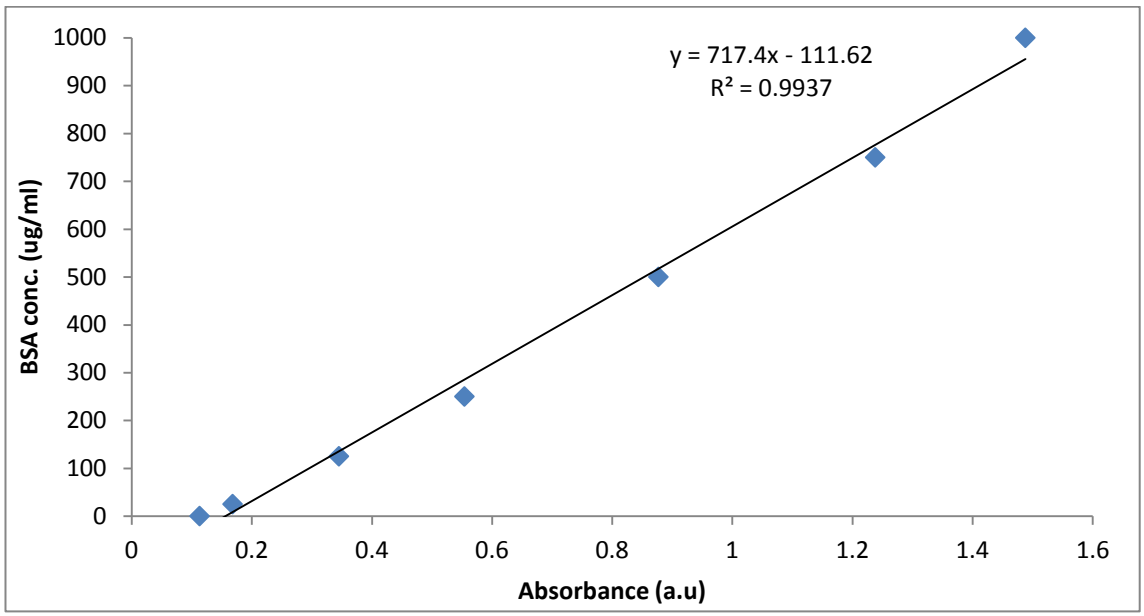

Calibration curve for BSA concentration for Total Protein BCA assay (High calibration - granules)

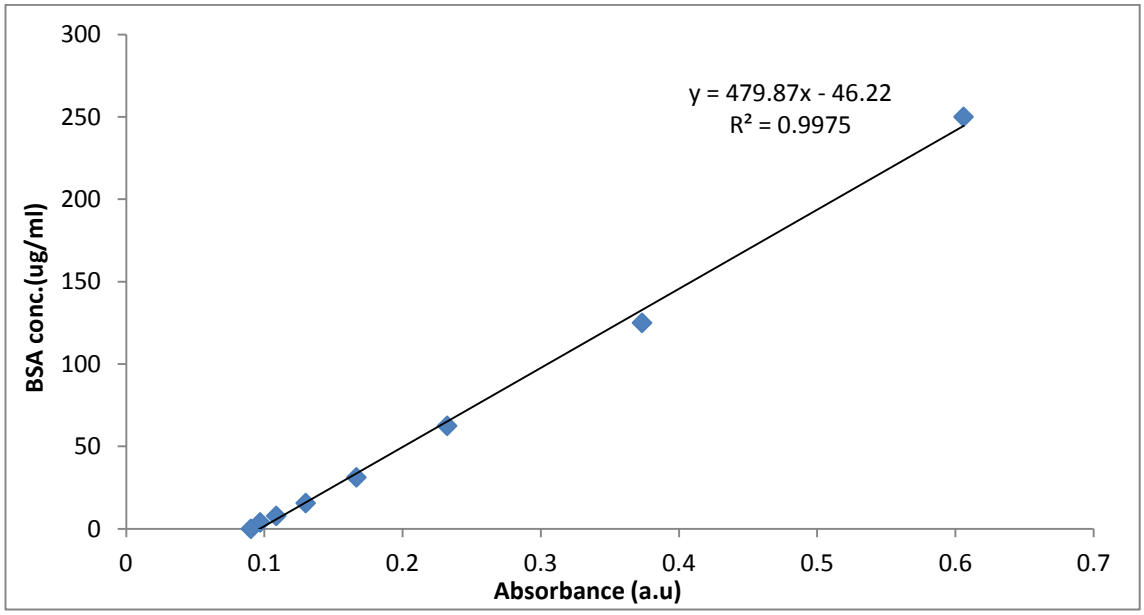

Calibration curve for BSA concentration for Total Protein BCA assay (Low calibration - 24 well plate)

Appendix 5: Alamar Blue Incubation Optimisation under 2D and 3D Static Conditions

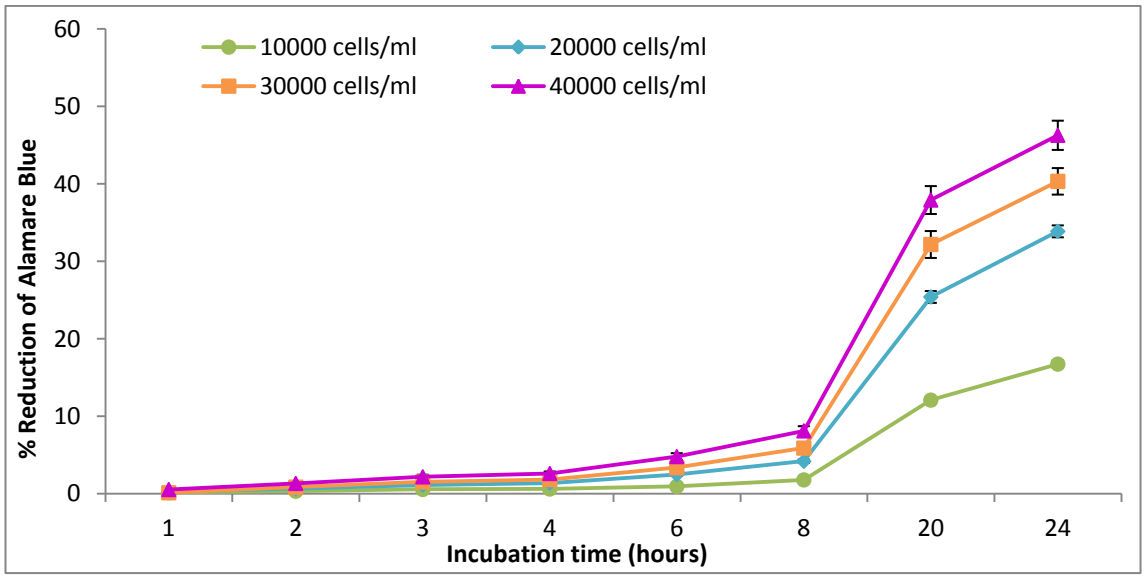

% Reduction of Alamar Blue over 24 hours with varying cell concentrations. MG63 cells cultured on 24 well plate

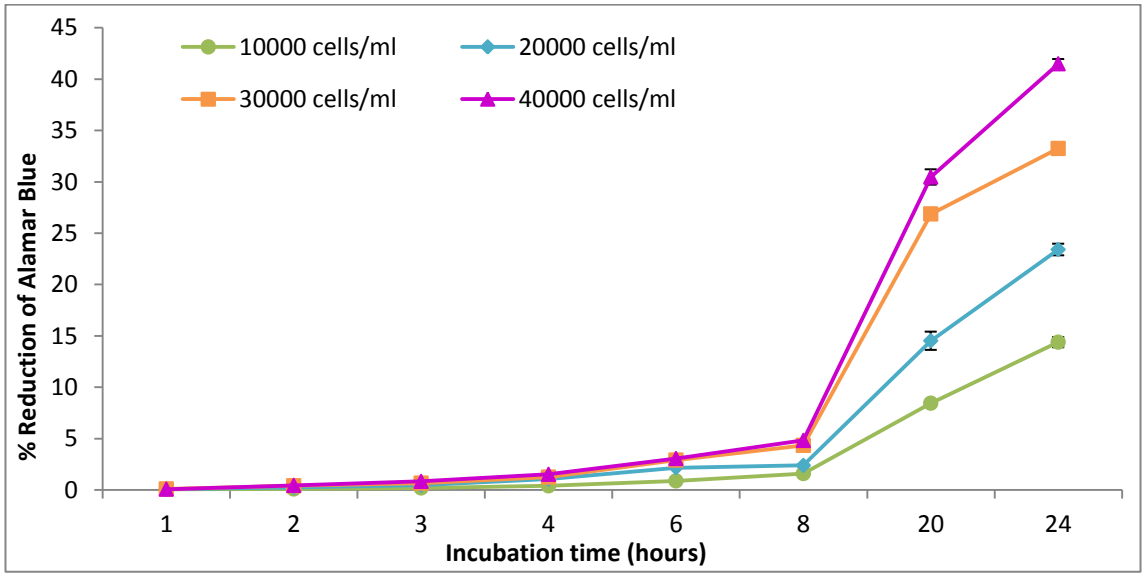

% Reduction of Alamar Blue over 24 hours with varying cell concentrations. MG63 cells cultured on 0.45g HA80/20 granules

Appendix 6: DMEM Formulations (D6429 and D7777)

SIGMA-ALDRICH®

sigma-aldrich.com

3050 Spruce Street, St. Louis, MO 63103 USA
Tel: (800) 521-8956 (314) 771-5765 Fax: (800) 325-5052 (314) 771-5757
email: techservice@sial.com sigma-aldrich.com

Product Information

Dulbecco's Modified Eagle's Medium (DME)

Many modifications of Eagle's Medium have been developed since the original formulation appeared in the literature. Among the most widely used of these modifications is Dulbecco's Modified Eagle's Medium (DME).

DME is a modification of Basal Medium Eagle (BME) that contains a 4-fold higher concentration of amino acids and vitamins, as well as additional supplementary components. The original DME formula, first reported for culturing embryonic mouse cells, contained 1,000 mg/L of glucose. An alteration with 4,500 mg/L glucose is optimal in cultivating certain cell types.

	D0422	D1145	D0819	D1152	D2429	D2902	D5030	D5523
	[1×]	[1×]	[1×]	[powder]	[10×]	[powder]	[powder]	[powder]
COMPONENT	g/L	g/L	g/L	g/L	g/L	g/L	g/L	g/L
Inorganic Salts								
$CaCl_2$	0.265	0.265	0.2	0.2	2.65	0.2	0.2	0.2
$Fe(NO_3)_3 \cdot 9H_2O$	0.0001	0.0001	0.0001	0.0001	0.001	0.0001	0.0001	0.0001
$MgSO_4$	0.09767	0.09767	0.09767	0.09767	0.9767	0.09767	0.09767	0.09767
KCl	0.4	0.4	0.4	0.4	4	0.4	0.4	0.4
$NaHCO_3$	3.7	3.7	3.7	—	—	—	—	—
NaCl	6.4	6.4	6.4	4.4	64	6.4	6.4	6.4
NaH_2PO_4	0.109	0.109	0.109	0.109	1.09	0.109	0.109	0.109
Amino Acids								
L-Alanyl-L-Glutamine	—	—	0.869	—	—	—	—	—
L-Arginine • HCl	0.084	0.084	0.084	0.084	0.84	0.084	0.084	0.084
L-Cysteine • 2HCl	—	0.0626	0.0626	0.0626	0.626	0.0626	0.0626	0.0626
L-Glutamine	—	—	—	0.584	—	0.584	—	0.584
Glycine	0.03	0.03	0.03	0.03	0.3	0.03	0.03	0.03
L-Histidine • HCl • H_2O	0.042	0.042	0.042	0.042	0.42	0.042	0.042	0.042
L-Isoleucine	0.105	0.105	0.105	0.105	1.05	0.105	0.105	0.105
L-Leucine	0.105	0.105	0.105	0.105	1.05	0.105	0.105	0.105
L-Lysine • HCl	0.146	0.146	0.146	0.146	1.46	0.146	0.146	0.146
L-Methionine	—	0.03	0.03	0.03	0.3	0.03	0.03	0.03
L-Phenylalanine	0.066	0.066	0.066	0.066	0.66	0.066	0.066	0.066
L-Serine	0.042	0.042	0.042	0.042	0.42	0.042	0.042	0.042
L-Threonine	0.095	0.095	0.095	0.095	0.95	0.095	0.095	0.095
L-Tryptophan	0.016	0.016	0.016	0.016	0.16	0.016	0.016	0.016
L-Tyrosine • 2Na • $2H_2O$	0.12037	0.12037	0.10379	0.10379	—	0.10379	0.10379	0.10379
L-Tyrosine	—	—	—	—	1.13033	—	—	—
L-Valine	0.094	0.094	0.094	0.094	0.94	0.094	0.094	0.094
Vitamins								
Choline Chloride	0.004	0.004	0.004	0.004	0.04	0.004	0.004	0.004
Folic Acid	0.004	0.004	0.004	0.004	-	0.004	0.004	0.004
myo-Inositol	0.0072	0.0072	0.0072	0.0072	0.072	0.0072	0.0072	0.0072
Niacinamide	0.004	0.004	0.004	0.004	0.04	0.004	0.004	0.004
D-Pantothenic Acid • ½Ca	0.004	0.004	0.004	0.004	0.04	0.004	0.004	0.004
Pyridoxal • HCl	—	—	—	0.004	—	0.004	0.004	0.004
Pyridoxine • HCl	0.00404	0.00404	0.00404	—	0.04	—	—	—
Riboflavin	0.0004	0.0004	0.0004	0.0004	0.004	0.0004	0.0004	0.0004
Thiamine • HCl	0.004	0.004	0.004	0.004	0.04	0.004	0.004	0.004
Other								
D-Glucose	4.5	4.5	4.5	4.5	10	1.0	—	1.0
HEPES	—	—	—	5.958	—	—	—	—
Phenol Red • Na	0.0159	—	0.0159	0.0159	0.159	—	—	0.0159
Pyruvic Acid • Na	0.11	—	0.11	—	1.1	0.11	—	0.11
ADD								
Glucose	—	—	—	—	—	—	1.0	—
L-Glutamine	0.584	0.584	—	—	0.584 at 1×	—	0.584	—
$NaHCO_3$	—	—	—	3.7	3.7 at 1×	3.7	3.7	3.7

	D5546	D5648	D5671	D5796	D5921	D6046	D6171	D6429
	[1×]	[powder]	[1×]	[1×]	[1×]	[1×]	[1×]	[1×]
COMPONENT	g/L	g/L	g/L	g/L	g/L	g/L	g/L	g/L
Inorganic Salts								
$CaCl_2$	0.2	0.2	0.2	0.2	0.265	0.2	0.0265	0.2
$Fe(NO_3)_3 \cdot 9H_2O$	0.0001	0.0001	0.0001	0.0001	0.0001	0.0001	0.0001	0.0001
$MgSO_4$	0.09767	0.09767	0.09767	0.09767	0.09767	0.09767	0.09767	0.09767
KCl	0.4	0.4	0.4	0.4	0.4	0.4	0.4	0.4
$NaHCO_3$	3.7	—	3.7	3.7	3.7	3.7	3.7	3.7
NaCl	6.4	6.4	6.4	6.4	6.4	6.4	4.4	6.4
NaH_2PO_4	0.109	0.109	0.109	0.109	0.109	0.109	0.109	0.109
Amino Acids								
L-Alanyl-L-Glutamine	—	—	—	—	—	—	—	—
L-Arginine • HCl	0.084	0.084	0.084	0.084	0.084	0.084	0.084	0.084
L-Cysteine • 2HCl	0.0626	0.0626	0.0626	0.0626	0.0626	0.0626	0.0626	0.0626
L-Glutamine	—	0.584	—	0.584	—	0.584	—	0.584
Glycine	0.03	0.03	0.03	0.03	0.03	0.03	0.03	0.03
L-Histidine • HCl • H_2O	0.042	0.042	0.042	0.042	0.042	0.042	0.042	0.042
L-Isoleucine	0.105	0.105	0.105	0.105	0.105	0.105	0.105	0.105
L-Leucine	0.105	0.105	0.105	0.105	0.105	0.105	0.105	0.105
L-Lysine • HCl	0.146	0.146	0.146	0.146	0.146	0.146	0.146	0.146
L-Methionine	0.03	0.03	0.03	0.03	0.03	0.03	0.03	0.03
L-Phenylalanine	0.066	0.066	0.066	0.066	0.066	0.066	0.066	0.066
L-Serine	0.042	0.042	0.042	0.042	0.042	0.042	0.042	0.042
L-Threonine	0.095	0.095	0.095	0.095	0.095	0.095	0.095	0.095
L-Tryptophan	0.016	0.016	0.016	0.016	0.016	0.016	0.016	0.016
L-Tyrosine • 2Na • $2H_2O$	0.10379	0.10379	0.10379	0.10379	0.12037	0.10379	0.10379	0.10379
L-Valine	0.094	0.094	0.094	0.094	0.094	0.094	0.094	0.094
Vitamins								
Choline Chloride	0.004	0.004	0.004	0.004	0.004	0.004	0.004	0.004
Folic Acid	0.004	0.004	0.004	0.004	0.004	0.004	0.004	0.004
myo-Inositol	0.0072	0.0072	0.0072	0.0072	0.0072	0.0072	0.0072	0.0072
Niacinamide	0.004	0.004	0.004	0.004	0.004	0.004	0.004	0.004
D-Pantothenic Acid • ½Ca	0.004	0.004	0.004	0.004	0.004	0.004	0.004	0.004
Pyridoxal • HCl	—	0.004	—	—	—	—	—	—
Pyridoxine • HCl	0.00404	—	0.00404	0.00404	0.00404	0.00404	0.00404	0.00404
Riboflavin	0.0004	0.0004	0.0004	0.0004	0.0004	0.0004	0.0004	0.0004
Thiamine • HCl	0.004	0.004	0.004	0.004	0.004	0.004	0.004	0.004
Other								
D-Glucose	1.0	4.5	4.5	4.5	1.0	1.0	4.5	4.5
HEPES	—	—	—	—	—	—	5.958	—
Phenol Red • Na	0.0159	0.0159	0.0159	0.0159	—	0.0159	0.0159	0.0159
Pyruvic Acid • Na	0.11	—	—	—	—	0.11	—	0.11
ADD								
Glucose	—	—	—	—	—	—	—	—
L-Glutamine	0.584	—	0.584	—	0.584	—	0.584	—
$NaHCO_3$	—	3.7	—	—	—	—	—	—

	D6546	D7777	D9443	D0572	D0822
	[1×]	[powder]	[1×]	[1×]	[1×]
COMPONENT	g/L	g/L	g/L	g/L	g/L
Inorganic Salts					
$CaCl_2$	0.2	0.2	0.2	0.265	0.2
$Fe(NO_3)_3 \cdot 9H_2O$	0.0001	0.0001	0.0001	0.0001	0.0001
$MgSO_4$	0.09767	0.09767	0.09767	0.09767	0.09767
KCl	0.4	0.4	0.4	0.4	0.4
$NaHCO_3$	3.7	—	3.7	3.7	3.7
NaCl	6.4	6.4	6.4	4.4	6.4
NaH_2PO_4	0.109	0.109	0.109	0.109	0.109
Amino Acids					
L-Alanyl-L-Glutamine	—	—	—	0.869	0.868
L-Arginine • HCl	0.084	0.084	—	0.084	0.084
L-Cysteine • 2HCl	0.0626	0.0626	0.0626	0.0626	0.0626
L-Glutamine	—	0.584	0.584	—	—
Glycine	0.03	0.03	0.03	0.03	0.03
L-Histidine • HCl • H_2O	0.042	0.042	0.042	0.042	0.042
L-Isoleucine	0.105	0.105	0.105	0.105	0.105
L-Leucine	0.105	0.105	—	0.105	0.105
L-Lysine • HCl	0.146	0.146	—	0.146	0.146
L-Methionine	0.03	0.03	0.03	0.03	0.03
L-Phenylalanine	0.066	0.066	0.066	0.066	0.066
L-Serine	0.042	0.042	0.042	0.042	0.042
L-Threonine	0.095	0.095	0.095	0.095	0.095
L-Tryptophan	0.016	0.016	0.016	0.016	0.016
L-Tyrosine • 2Na • $2H_2O$	0.10379	0.10379	—	0.10379	0.10379
L-Tyrosine	—	—	0.10379	—	—
L-Valine	0.094	0.094	0.094	0.094	0.094
Vitamins					
Choline Chloride	0.004	0.004	0.004	0.004	0.004
Folic Acid	0.004	0.004	0.004	0.004	0.004
myo-Inositol	0.0072	0.0072	0.0072	0.0072	0.0072
Niacinamide	0.004	0.004	0.004	0.004	0.004
D-Pantothenic Acid • ½Ca	0.004	0.004	0.004	0.004	0.004
Pyridoxal • HCl	—	0.004	—	—	—
Pyridoxine • HCl	0.004	—	0.004	0.004	0.004
Riboflavin	0.0004	0.0004	0.0004	0.0004	0.0004
Thiamine • HCl	0.004	0.004	0.004	0.004	0.004
Other					
D-Glucose	4.5	4.5	1.0	4.5	4.5
HEPES	—	—	—	5.958	—
Phenol Red • Na	0.0159	0.0159	—	0.0159	0.0159
Pyruvic Acid • Na	0.11	0.11	—	—	0.11
ADD					
$NaHCO_3$	—	3.7	—	—	—
L-Glutamine	0.584	—	—	0.584	—
Glucose	—	—	—	—	—

References

1. Dulbecco, R., and Freeman, G., Plaque Production by the Polyoma Virus. Virology, **8**, 396-397 (1959).
2. Smith, J.D., Freeman, G., Vogt, M., and Dulbecco, R., The Nucleic Acid of Polyoma. Virus, **12**, 185-196 (1960).
3. Morton, H.J., A Survey of Commercially Available Tissue Culture Media. In Vitro, **6**, 89 (1970).
4. Rutzky, L.P., and Pumper, R.W., Supplement to a Survey of Commercially Available Tissue Culture Media (1970). In Vitro, **9**, 468 (1974).

JG,GS,PD,JF,MAM 08/13-1

Appendix 7: Calibration Curves for CICP and OCN Concentrations

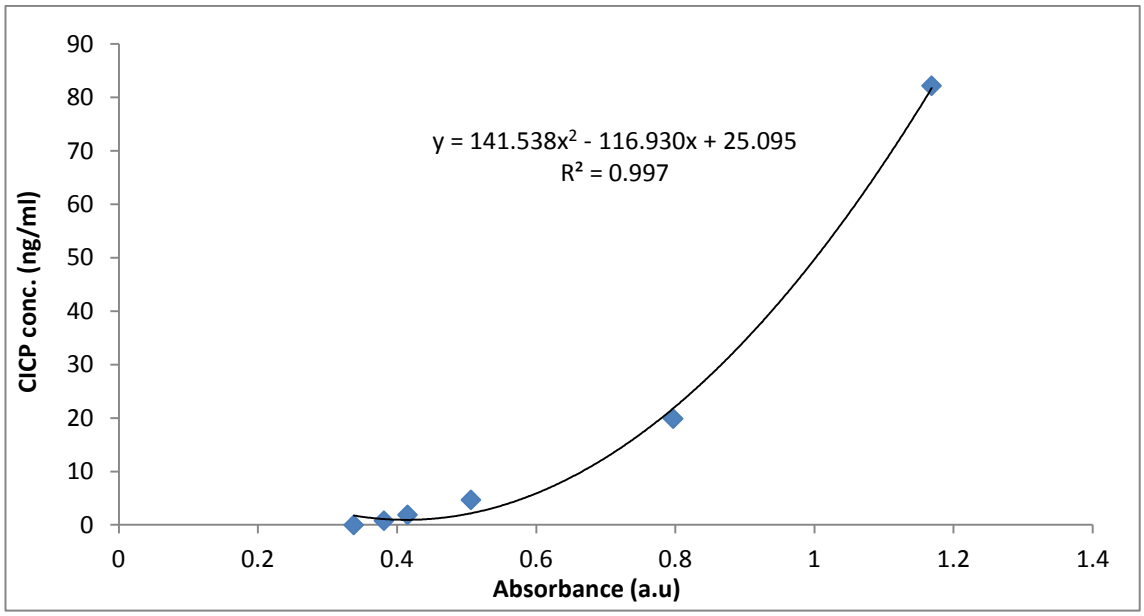

Calibration curve for CICP concentration

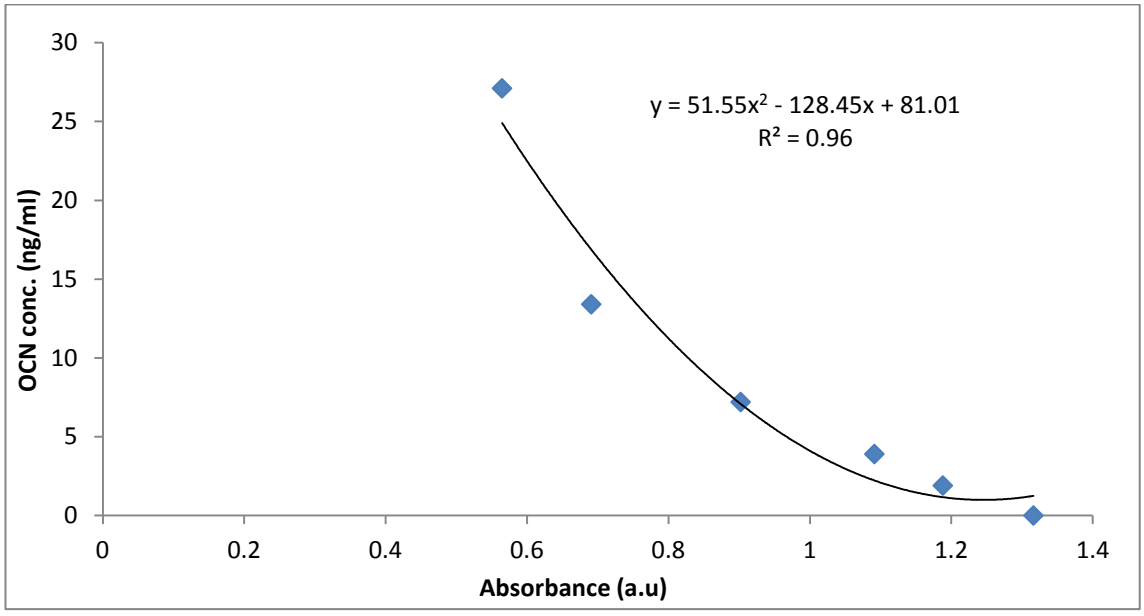

Calibration curve for OCN concentration

Appendix 8: Technical Drawings for Loading Model

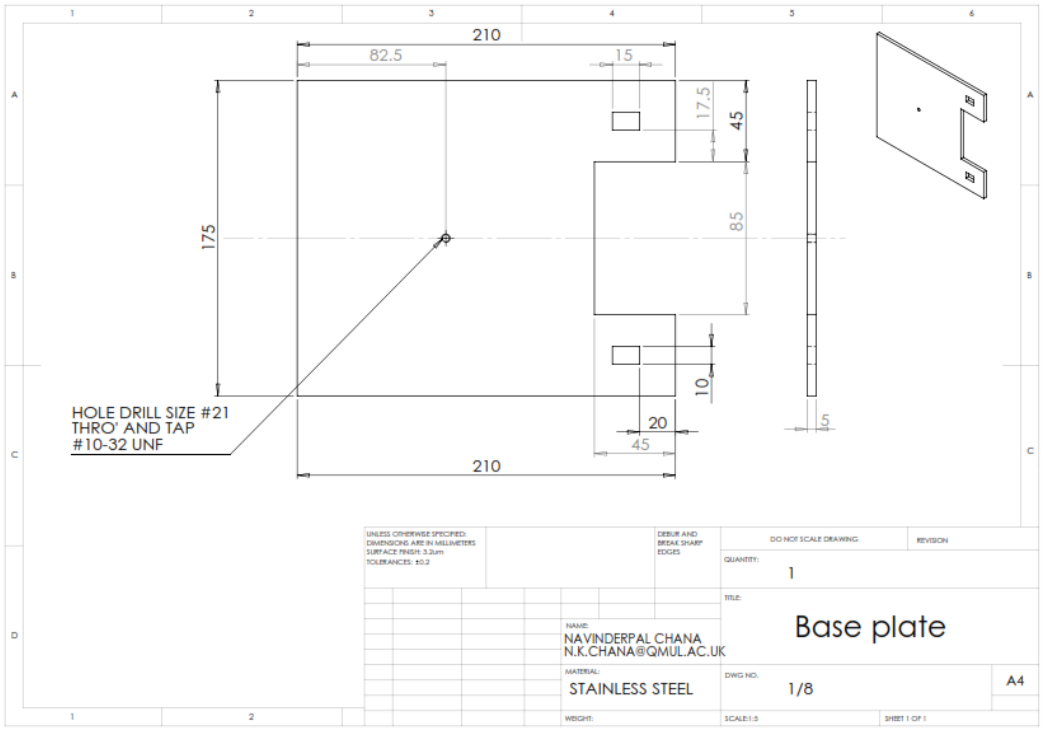

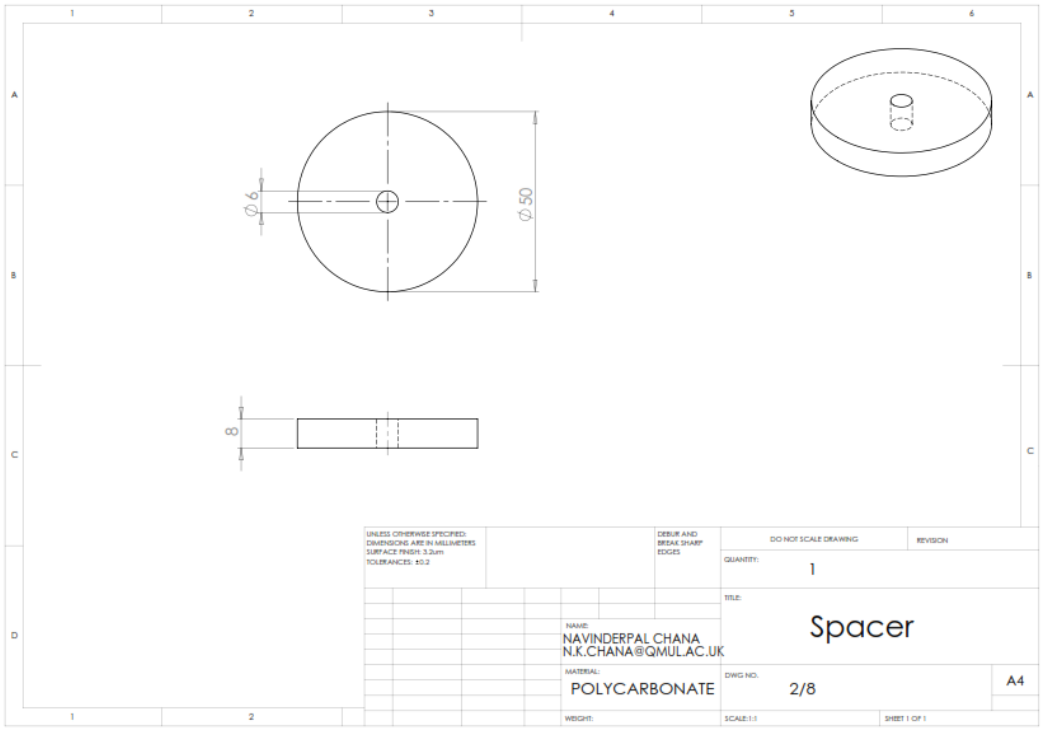

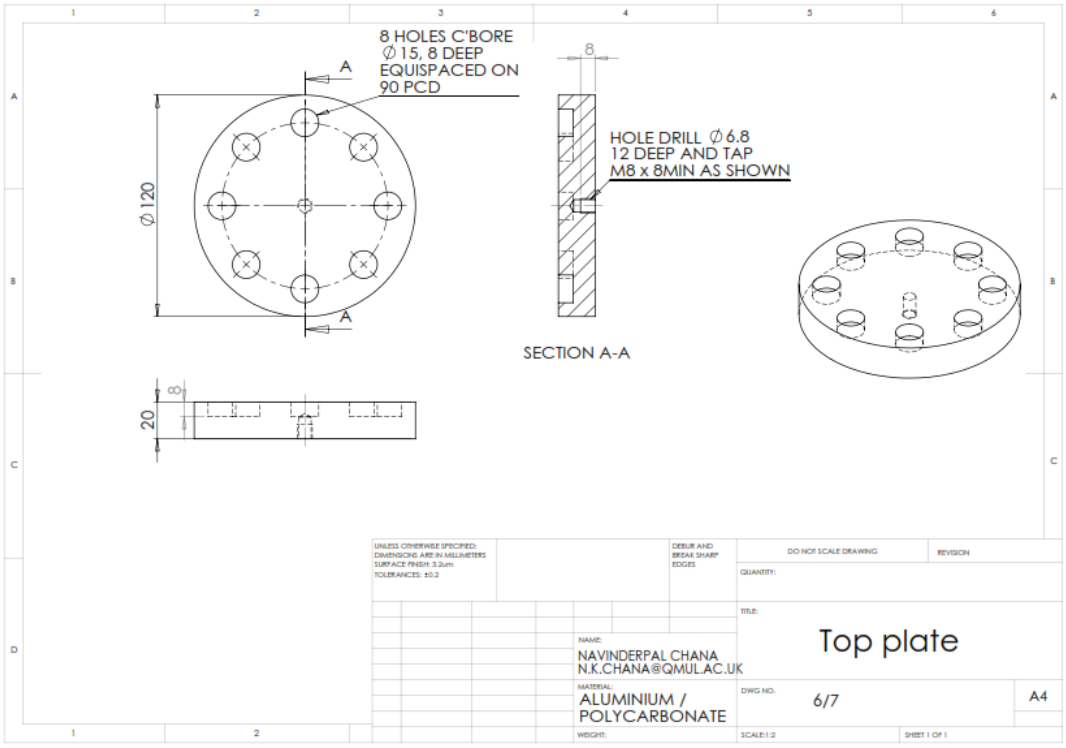
8 HOLES C'BORE
∅15, 8 DEEP
EQUISPACED ON
90 PCD
A
A
∅120
8
HOLE DRILL ∅6.8
12 DEEP AND TAP
M8 x 8MIN AS SHOWN
SECTION A-A
8
20
UNLESS OTHERWISE SPECIFIED:
DIMENSIONS ARE IN MILLIMETERS
SURFACE FINISH: 3.2um
TOLERANCES: ±0.2
DEBUR AND
BREAK SHARP
EDGES
DO NOT SCALE DRAWING
REVISION
QUANTITY:
TITLE:
Top plate
NAME:
NAVINDERPAL CHANA
N.K.CHANA@QMUL.AC.UK
MATERIAL:
ALUMINIUM /
POLYCARBONATE
DWG NO.
6/7
A4
WEIGHT:
SCALE:1:2
SHEET 1 OF 1

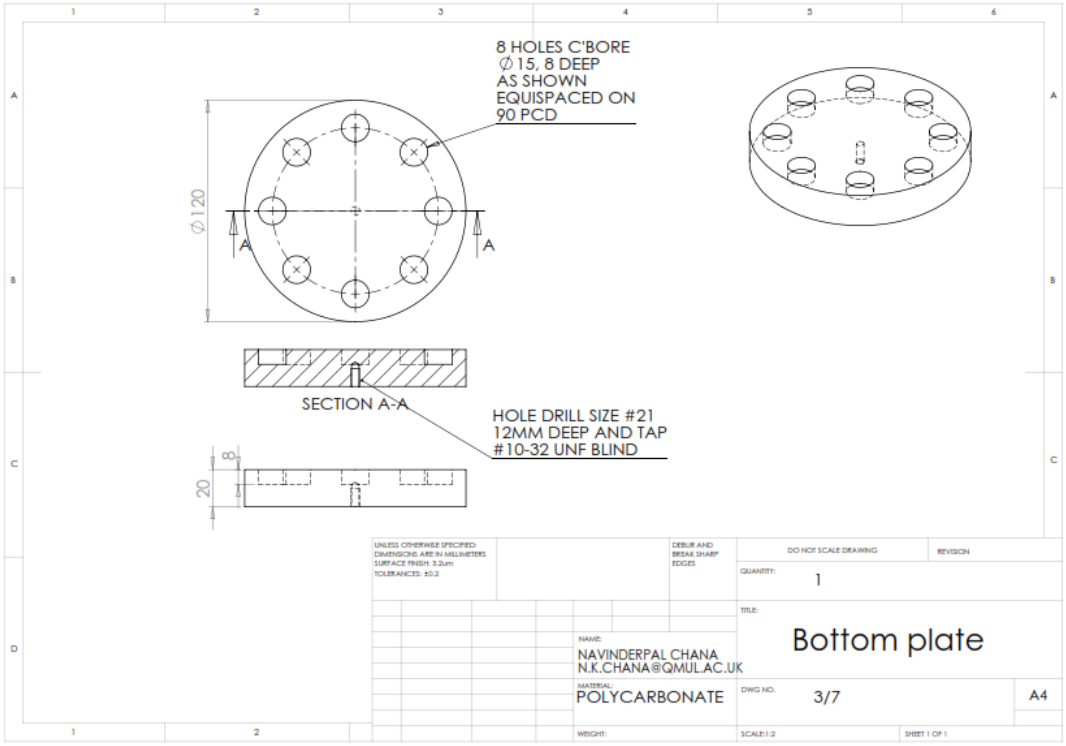
8 HOLES C'BORE
∅15, 8 DEEP
AS SHOWN
EQUISPACED ON
90 PCD
∅120
A
A
SECTION A-A
HOLE DRILL SIZE #21
12MM DEEP AND TAP
#10-32 UNF BLIND
8
20
UNLESS OTHERWISE SPECIFIED:
DIMENSIONS ARE IN MILLIMETERS
SURFACE FINISH: 3.2um
TOLERANCES: ±0.2
DEBUR AND
BREAK SHARP
EDGES
DO NOT SCALE DRAWING
REVISION
QUANTITY:
1
TITLE:
Bottom plate
NAME:
NAVINDERPAL CHANA
N.K.CHANA@QMUL.AC.UK
MATERIAL:
POLYCARBONATE
DWG NO.
3/7
A4
WEIGHT:
SCALE:1:2
SHEET 1 OF 1

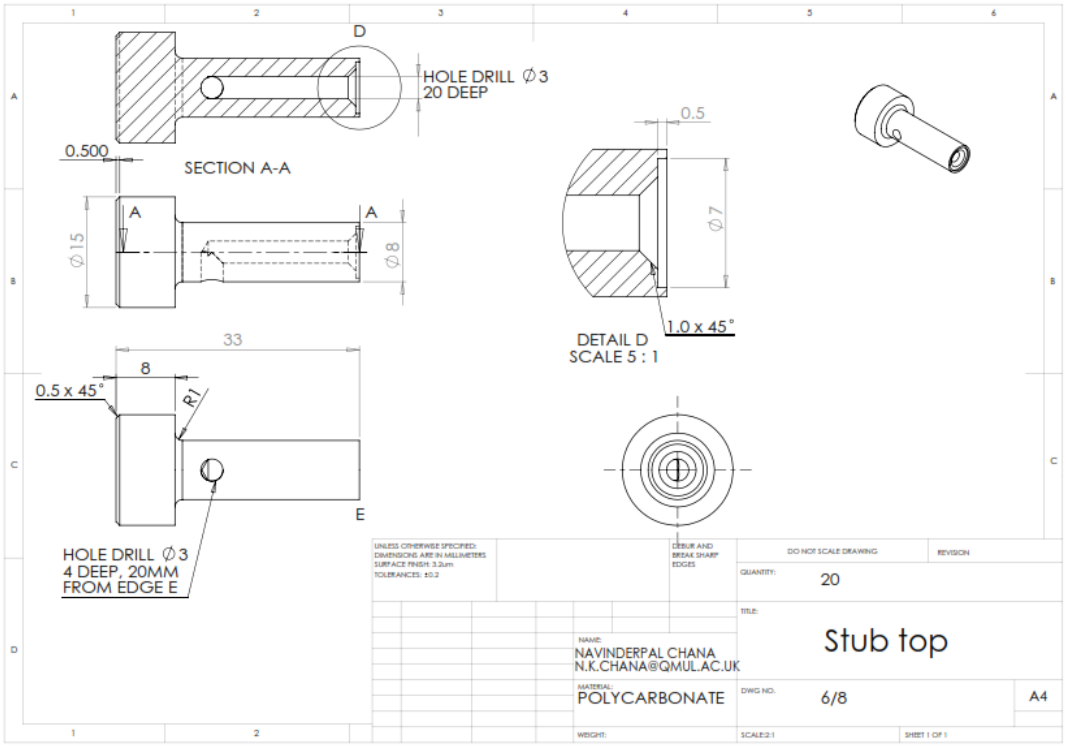
D
HOLE DRILL ∅3
20 DEEP
0.500
SECTION A-A
A
A
∅15
∅8
0.5
∅7
1.0 x 45°
DETAIL D
SCALE 5 : 1
33
8
0.5 x 45°
R1
E
HOLE DRILL ∅3
4 DEEP, 20MM
FROM EDGE E
UNLESS OTHERWISE SPECIFIED:
DIMENSIONS ARE IN MILLIMETERS
SURFACE FINISH: 3.2um
TOLERANCES: ±0.2
DEBUR AND
BREAK SHARP
EDGES
DO NOT SCALE DRAWING
REVISION
QUANTITY:
20
TITLE:
Stub top
NAME:
NAVINDERPAL CHANA
N.K.CHANA@QMUL.AC.UK
MATERIAL:
POLYCARBONATE
DWG NO.
6/8
A4
WEIGHT:
SCALE:2:1
SHEET 1 OF 1

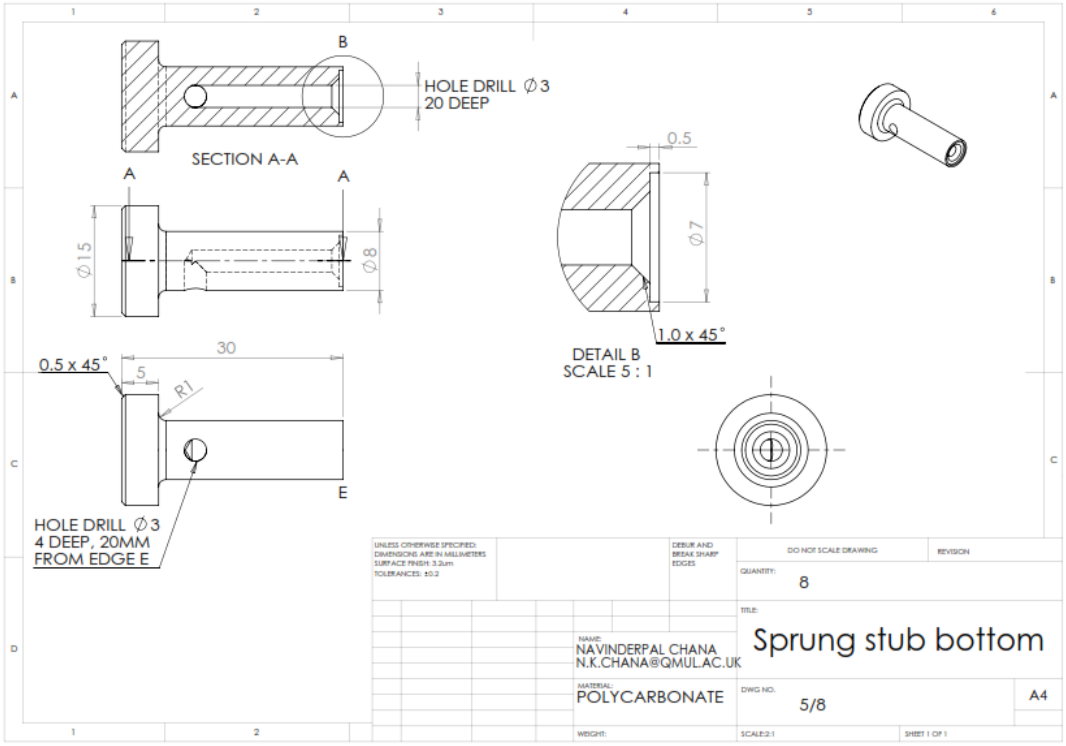
B
HOLE DRILL ∅3
20 DEEP
SECTION A-A
A
A
∅15
∅8
0.5
∅7
1.0 x 45°
DETAIL B
SCALE 5 : 1
30
0.5 x 45°
5
R1
E
HOLE DRILL ∅3
4 DEEP, 20MM
FROM EDGE E
UNLESS OTHERWISE SPECIFIED:
DIMENSIONS ARE IN MILLIMETERS
SURFACE FINISH: 3.2um
TOLERANCES: ±0.2
DEBUR AND
BREAK SHARP
EDGES
DO NOT SCALE DRAWING
REVISION
QUANTITY:
8
TITLE:
Sprung stub bottom
NAME:
NAVINDERPAL CHANA
N.K.CHANA@QMUL.AC.UK
MATERIAL:
POLYCARBONATE
DWG NO.
5/8
A4
WEIGHT:
SCALE:2:1
SHEET 1 OF 1

Appendix 9: List of Presentations

[1] Chana, N. K., Rawlinson, S. C. F. and Hing, K. A. (2013). *Investigation of Solute Composition on the Dissolution Behaviour of Stoichiometric and Silicate Substituted Apatites*. **Poster presentation**. Orthopaedic Research Society Conference, San Antonio, Texas, USA. January 2013.

[2] Chana, N. K., Rawlinson, S. C. F. and Hing, K. A. (2013). *Investigating the Dissolution Behaviour of Stoichiometric and Silicate Substituted Apatites with Varied Strut Porosity*. **Poster presentation**. UK Society for Biomaterials Conference, Birmingham, UK. June 2013.

[3] Chana, N. K., Rawlinson, S. C. F. and Hing, K. A. (2014). *Dynamic Ion Exchange Between SA Bone Graft Substitutes Affects Osteoblast-like Cell Response*. **Poster presentation**. Orthopaedic Research Society Conference, New Orleans, Louisiana, USA. March 2014.

[4] Chana, N. K., Rawlinson, S. C. F. and Hing, K. A. (2014). *Osteoblast-like Cells Incubated on Porous Stoichiometric HA Scaffolds are Sensitive to Dynamic Ion Exchange with Silicate-substituted Bone Graft Materials.* **Oral presentation**. European Orthopaedic Research Society Conference, Nantes, France. July 2014

[5] Chana, N. K., Rawlinson, S. C. F. and Hing, K. A. (2014). *Influence of Media Replenishment on Dynamic Ion Exchange with Silicate-substituted Bone Graft Substitute and Subsequent Osteoblast-like Cell Response.* **Oral presentation**. European Orthopaedic Research Society Conference, Nantes, France. July 2014

[6] Chana, N. K., Rawlinson, S. C. F. and Hing, K. A. (2014). *Investigation of Ion Exchange between Silicate-substituted Bone Graft Substitutes and Cell Culture Media and the effect on Osteoblast-like Cell Response.* **Poster presentation and rapid fire round**. 26th European Conference on Biomaterials, Liverpool, August 2014.